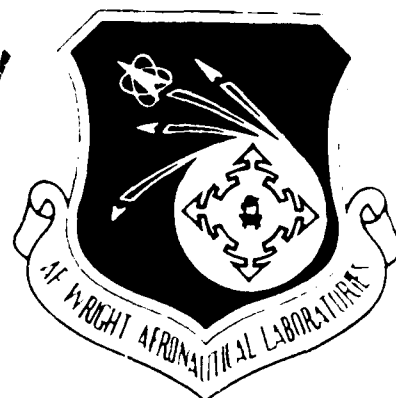


AD-A219 123

DTIC FILE COPY

AFWAL-TR-88-3089

**MODELING FLEXIBLE
AIRCRAFT FOR FLIGHT
CONTROL DESIGN**



**E.C. Bekir
W.J. Davis, A. Goforth, H. Hassig,
E.J. Horowitz, R.N. Moon, G.A. Watts**

**Lockheed Aeronautical Systems Company
Burbank, CA 91520**

January 1989

**DTIC
ELECTRONIC
MAR 07 1990
S B D**

Interim Report for the Period September 1986 to March 1988

Approved for public release; distribution unlimited.

**FLIGHT DYNAMICS LABORATORY
AIR FORCE WRIGHT AERONAUTICAL LABORATORIES
AIR FORCE SYSTEMS COMMAND
WRIGHT-PATTERSON AIR FORCE BASE, OHIO 45433-6553**


90 03 06 023

NOTICE

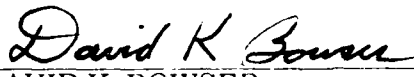
When Government drawings, specifications, or other data are used for any purpose other than in connection with a definitely Government-related procurement, the United States Government incurs no responsibility or any obligation whatsoever. The fact that the Government may have formulated or in any way supplied the said drawings, specifications, or other data, is not to be regarded by implication or otherwise as in any manner construed, as licensing the holder or any other person or corporation; or as conveying any rights or permission to manufacture, use, or sell any patented invention that may in any way be related thereto.

This report is releasable to the National Technical Information Service (NTIS). At NTIS, it will be available to the general public, including foreign nations.

This technical report has been reviewed and is approved for publication.

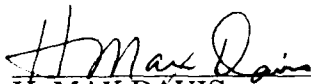


ANDREW G. SPARKS, 1st Lt, USAF
Project Engineer
Control Dynamics Branch
Flight Control Division



DAVID K. BOWSER
Chief, Control Dynamics Branch
Flight Control Division

FOR THE COMMANDER



H. MAX DAVIS,
Assistant for Research and Technology
Flight Control Division
Flight Dynamics Laboratory

"If your address has changed, if you wish to be removed from our mailing list, our mailing list, or if the addressee is no longer employed by your organization please notify WRDC/FIGC, Wright-Patterson AFB, OH 45433-6553 to help us maintain a current mailing list."

Copies of this report should not be returned unless return is required by security considerations, contractual obligations, or notice on a specific document.

REPORT DOCUMENTATION PAGE

1a. REPORT SECURITY CLASSIFICATION Unclassified		1b. RESTRICTIVE MARKINGS N/A										
2a. SECURITY CLASSIFICATION AUTHORITY N/A		3. DISTRIBUTION/AVAILABILITY OF REPORT Approved for public release; distribution unlimited										
2b. DECLASSIFICATION/DOWNGRADING SCHEDULE N/A												
4. PERFORMING ORGANIZATION REPORT NUMBER(S)		5. MONITORING ORGANIZATION REPORT NUMBER(S) AFWAL-TR-88-3089										
6a. NAME OF PERFORMING ORGANIZATION Lockheed Aeronautical Systems Company	6b. OFFICE SYMBOL <i>(If applicable)</i>	7a. NAME OF MONITORING ORGANIZATION Air Force Wright Aeronautical Laboratories Flight Dynamics Laboratory (AFWAL/FDCC)										
6c. ADDRESS (City, State and ZIP Code) Burbank, CA 91520		7b. ADDRESS (City, State and ZIP Code) Wright Patterson Air Force Base, OH 45433-6553										
8a. NAME OF FUNDING/SPONSORING ORGANIZATION N/A	8b. OFFICE SYMBOL <i>(If applicable)</i>	9. PROCUREMENT INSTRUMENT IDENTIFICATION NUMBER F33615-86-C-3625										
8c. ADDRESS (City, State and ZIP Code) N/A		10. SOURCE OF FUNDING NOS. <table border="1" style="width: 100%; border-collapse: collapse; margin-top: 5px;"> <thead> <tr> <th style="width: 25%;">PROGRAM ELEMENT NO.</th> <th style="width: 25%;">PROJECT NO.</th> <th style="width: 25%;">TASK NO.</th> <th style="width: 25%;">WORK UNIT NO.</th> </tr> </thead> <tbody> <tr> <td style="text-align: center;">62201F</td> <td style="text-align: center;">2403</td> <td style="text-align: center;">05</td> <td style="text-align: center;">66</td> </tr> </tbody> </table>		PROGRAM ELEMENT NO.	PROJECT NO.	TASK NO.	WORK UNIT NO.	62201F	2403	05	66	
PROGRAM ELEMENT NO.	PROJECT NO.	TASK NO.	WORK UNIT NO.									
62201F	2403	05	66									
11. TITLE (Include Security Classification) Modeling Flexible Aircraft for Flight Control Design												
12. PERSONAL AUTHOR(S) E.C. Bekir, W.J. Davis, A. Goforth, N. Hassig, E.J. Horowitz, R.N. Moon, G.A. Watts												
13a. TYPE OF REPORT Interim	13b. TIME COVERED FROM Sep 86 to Mar 88	14. DATE OF REPORT (Yr., Mo., Day) January 1989	15. PAGE COUNT 433									
16. SUPPLEMENTARY NOTATION												
17. COSATI CODES <table border="1" style="width: 100%; border-collapse: collapse; margin-top: 5px;"> <thead> <tr> <th style="width: 33%;">FIELD</th> <th style="width: 33%;">GROUP</th> <th style="width: 33%;">SUB. GR.</th> </tr> </thead> <tbody> <tr> <td style="text-align: center;">01</td> <td style="text-align: center;">03</td> <td></td> </tr> <tr> <td style="text-align: center;">01</td> <td style="text-align: center;">01</td> <td></td> </tr> </tbody> </table>		FIELD	GROUP	SUB. GR.	01	03		01	01		18. SUBJECT TERMS (Continue on reverse if necessary and identify by block number) Aeroelasticity, Aeroservoelasticity, Aerodynamics, Structures, Model Order Reduction, Servos	
FIELD	GROUP	SUB. GR.										
01	03											
01	01											
19. ABSTRACT (Continue on reverse if necessary and identify by block number) <p>Trends to lower structural fraction of aircraft increase flexibility effects. Higher bandwidth control systems combined with these more flexible structures cause more aero-servoelastic interactions. Active, closed-loop control systems allow greater flexibility. To take advantage of this design possibility, an integrated ASE model is needed for conceptual and preliminary design stages of aircraft.</p> <p>The purpose of this report is to define the equations of motion of a flexible aircraft from first principles to aid future discussions between experts in the specialties which make up ASE: aerodynamics, controls, and structures. This theoretical report documents the development of the equations, and states under what conditions the assumptions and approximations are accurate.</p> <p>This report consists of five sections on different technical areas and a summary section: The five technical sections are: 1) Linearization of Flexible Aircraft Hybrid-Coordinate Dynamic Equations and Inclusion of Aerodynamic and Gravitational Loads, (over)</p>												
20. DISTRIBUTION/AVAILABILITY OF ABSTRACT UNCLASSIFIED/UNLIMITED <input checked="" type="checkbox"/> SAME AS RPT. <input type="checkbox"/> DTIC USERS <input type="checkbox"/>		21. ABSTRACT SECURITY CLASSIFICATION Unclassified										
22a. NAME OF RESPONSIBLE INDIVIDUAL Lt. Andrew Sparks		22b. TELEPHONE NUMBER <i>(Include Area Code)</i> (513) 255-8686	22c. OFFICE SYMBOL AFWAL/FDCCA									

19. ABSTRACT (continued)

2) Derivation of Equations of Motion and Stability Derivatives for a Flexible Aircraft Vehicle; 3) Aerodynamics for Aeroservoelasticity, 4) Model-Order Reduction for Linear Systems, and 5) Hydraulic Actuator Equations for Aeroservoelastic Modeling.

FOREWORD

This report was prepared by the Lockheed Aeronautical Systems Company, Burbank, California under the requirements of Air Force Contract F33615-86-C-3625. Dr. Hussein Youssef was the Program Manager and Dr. Nick Radovcich was the principal investigator. The work was sponsored by the Air Force Wright Aeronautical Laboratories, Flight Dynamics Laboratory, Aeronautical; Systems Division (AFSC), United States Air Force, Wright-Patterson AFB, OH. The contract was monitored first by Air Force Captain Mike Dunbar and later by Air Force Lieutenant Andrew Sparks.

This report consists of five sections on different technical areas and an introduction section. The six sections and their authors are: 1) Introduction: W. J. Davis; 2) Linearization of Flexible Aircraft Hybrid-Coordinate Dynamic Equations and Inclusion of Aerodynamic and Gravitational Loads: E. J. Horowitz; 3) Derivation of Equations of Motion and Stability Derivatives for a Flexible Aircraft Vehicle: R. N. Moon; 4) Aerodynamics for Aeroservoelasticity: A. Goforth, H. Hassig, and G. A. Watts; 5) Model-Order Reduction for Linear Systems: W. J. Davis (with subcontracted work by Dr. Edmond Jonkheere of the University of Southern California); and 6) Hydraulic Actuator Equations for Aeroservoelastic Modeling: W. J. Davis.

Dr. Esmat Bekir was responsible for reviewing and editing the textual and equation contents of these sections, and compiling all sections of the report.



Accession For	
NTIS GRA&I	<input checked="" type="checkbox"/>
DTIC TAB	<input type="checkbox"/>
Unannounced	<input type="checkbox"/>
Justification	
By _____	
Distribution/	
Availability Codes	
Dist	Avail and/or Special
A-1	

TABLE OF CONTENTS

Section		Page
1	INTRODUCTION	1-1
1.1	SUMMARY OF DISCIPLINES	1-3
1.2	INTEGRATION OF THE TECHNICAL DISCIPLINES	1-7
1.2.1	Structural Dynamics	1-7
1.2.2	Aerodynamics	1-9
1.2.3	Flight Dynamics	1-10
1.2.4	Aeroelastic Modeling	1-12
1.3	SUMMARY OF COORDINATE SYSTEM METHODS	1-13
1.3.1	Hybrid Coordinates	1-14
1.3.2	Stability Coordinates	1-17
1.4	CONTRIBUTION FROM THE TECHNICAL DISCIPLINES	1-22
1.4.1	Structural Modeling	1-25
1.4.2	Aerodynamics	1-35
1.4.3	Flight Dynamics	1-36
1.4.4	Aeroelastic Modeling	1-40
2	LINEARIZATION OF FLEXIBLE AIRCRAFT HYBRID-COORDINATE DYNAMIC EQUATIONS AND INCLUSION OF AERODYNAMIC AND GRAVITATIONAL LOADS	2-1
2.1	INTRODUCTION	2-1
2.1.1	Scope	2-1
2.1.2	Development Overview	2-1
2.1.3	Hybrid-Coordinate Definition	2-4
2.1.4	Operators	2-12
2.1.5	Development of Hybrid-Coordinate Dynamic Equations	2-14
2.2	LINEARIZATION OF THE DYNAMIC EQUATIONS	2-36
2.2.1	Variable Linearization	2-36
2.2.2	Quasi-static Equations	2-37
2.2.3	Perturbation Equations	2-41
2.3	AERODYNAMIC AND GRAVITATIONAL LOADS	2-50
2.3.1	Aerodynamic Loads	2-50
2.3.2	Gravitational Loads	2-80

TABLE OF CONTENTS (Continued)

Section	Page
2.4	SPECIAL CASES 2-83
2.4.1	Rigid Body Stability and Control Dynamics 2-83
2.4.2	Simple Test Case 2-88
2.5	SUMMARY 2-96
2.5.1	Review of Assumptions 2-96
2.5.2	Review of Hybrid-Coordinate Dynamic Equations Development 2-97
2.5.3	Linearization of Hybrid-Coordinate Dynamic Equations 2-98
2.5.4	Inclusion of Aerodynamic and Gravitational Loads 2-98
2.5.5	Special Cases 2-99
3	DERIVATION OF EQUATIONS OF MOTION AND STABILITY DERIVATIVES FOR A FLEXIBLE AIRCRAFT VEHICLE 3-1
3.1	INTRODUCTION 3-1
3.2	RIGID BODY EQUATIONS OF MOTION 3-2
3.3	LONGITUDINAL EQUATION OF MOTION 3-7
3.4	AERODYNAMIC FORCES AND MOMENTS 3-8
3.4.1	Solution of the Equations of Motion for α 3-11
3.4.2	Solution of the Equations of Motion for q 3-12
3.5	AERODYNAMIC DERIVATIVES OF A FLEXIBLE AIRPLANE 3-13
3.5.1	Inertial Reference Axis 3-13
3.6	FLEXIBLE STABILITY DERIVATIVES 3-19
3.6.1	Longitudinal Stability Derivatives 3-22
3.6.2	Concept of Flexible Longitudinal Stability Derivatives 3-23
3.6.3	Concept of Free Longitudinal Stability Derivatives 3-28
3.6.4	Effect of Flexibility on α_0 and C_{m0} 3-29
3.6.5	Horizontal Stabilizer Downwash Contributions 3-31
3.6.6	Determinations of α Contributions 3-33
3.7	LATERAL/DIRECTIONAL STABILITY DERIVATIVES 3-34
3.7.1	Lateral/Directional Equations of Motion 3-34
3.7.2	Equations of Motion in a Panel Point Load System 3-36

TABLE OF CONTENTS (Continued)

Section	Page	
3.7.3	Concept of Fixed Lateral/Directional Stability Derivatives	3-40
3.7.4	Concept of Free Lateral/Directional Stability Derivatives	3-41
4	AERODYNAMICS FOR AEROSERVOELASTICITY	4-1
4.1	INTRODUCTION	4-1
4.2	EQUATIONS OF FLUID MOTION	4-4
4.2.1	Linearized Potential Equation (Unsteady Prantl-Glauert)	4-9
4.2.2	The Linearized Unsteady, Bernoulli Equations	4-10
4.3	BOUNDARY CONDITIONS	4-10
4.4	METHODS OF THE EQUATIONS SOLUTION	4-12
4.4.1	Incompressible Equation (Laplace)	4-13
4.4.2	2-D Vortex Lattice Method	4-21
4.4.3	Linearized Potential Equation	4-31
4.5	DERIVATION OF THE STATE SPACE EQUATION	4-42
4.5.1	Introduction	4-42
4.5.2	The Force Equation	4-44
4.5.3	Formulation of the Aerodynamics	4-45
4.5.4	The Dynamics Equation	4-49
4.6	STATE SPACE EQUATIONS FOR AEROSERVOELASTICITY SYMMETRIC AIRPLANE	4-53
4.6.1	Gust Equations	4-53
4.6.2	Servoactuator Model	4-56
4.6.3	Phugoid Mode	4-59
4.6.4	Equations of Motion	4-64
5	MODEL-ORDER REDUCTION FOR LINEAR SYSTEMS	5-1
5.1	MODEL-ORDER REDUCTION FOR LINEAR SYSTEMS	5-1
5.1.1	Introduction	5-1
5.1.2	Background	5-1
5.1.3	Summary of Two Model Reduction Approaches	5-4
5.2	THE MATH MODEL - FROM FIRST PRINCIPLES	5-6

TABLE OF CONTENTS (Continued)

Section	Page
5.2.1	Solutions of the State-Space Equation 5-8
5.3	MODEL-ORDER REDUCTION APPROACHES 5-10
5.3.1	The Balanced Approximation Approach 5-10
5.3.2	Model-Order Reduction by Spectral Decomposition 5-31
5.4	EXAMPLES: AST LONGITUDINAL FLEXIBLE-BODY MODEL 5-50
5.4.1	AST Flexible-Body Model 5-50
5.4.2	Spectral Decomposition 5-53
5.4.3	Balancing 5-60
5.4.4	Comparison of Methods 5-65
6	HYDRAULIC ACTUATOR EQUATIONS FOR AEROSERVOELASTIC MODELING 6-1
6.1	INTRODUCTION 6-3
6.2.1	Hydraulic Model 6-4
6.3	FOUR-WAY HYDRAULIC VALVE 6-9
6.4	DIFFERENTIAL PRESSURE MODULATOR (DPM) 6-12
6.5	DYNAMIC INERTIAL LOAD MODEL 6-14
6.6	LINEARIZED SYSTEM MODEL 6-15
6.6.1	Dynamic Stability 6-19
6.7	STATIC STIFFNESS 6-21
6.8	AEROSERVOELASTIC INTEGRATION 6-22
6.8.1	Required Representation of Servo Nonlinearities 6-23
	REFERENCES R-1
	GLOSSARY G-1
	ACRONYMS S-1
	SYMBOLS S-2
APPENDIX	
A	AERODYNAMIC SIGN CONVENTION AND MEANINGS OF STABILITY DERIVATIVES A-1
B	DEFINITION OF AXIS SYSTEMS B-1
C	AERODYNAMIC EQUATIONS FIXED LONGITUDINAL FLEXIBLE STABILITY C-1
D	FIXED LONGITUDINAL FLEXIBLE STABILITY DERIVATIVE PROGRAM (P-10) D-1

TABLE OF CONTENTS (Concluded)

Section		Page
D.1	FIXED STABILITY DERIVATIVES DUE TO AIRLOAD ONLY	D-1
D.2	FREE LONGITUDINAL FLEXIBLE STABILITY DERIVATIVE PROGRAM (P-137)	D-10
D.3	FIXED AND FREE LATERAL/DIRECTIONAL FLEXIBLE, STABILITY DERIVATIVES PROGRAM - DRSD F-72	D-17

LIST OF FIGURES

<u>Figure</u>		<u>Page</u>
1-1	Interfaces between the Technical Disciplines	1-8
1-2	Axis Systems	1-19
1-3	Simplified FEM Model	1-26
1-4	Simplified Structural Model Program Flowchart	1-28
1-5	Simplified Load Dynamics Model - Actuator Interface	1-47
2-1	Basic Symbol Notation Used	2-2
2-2	Vectors and Bases Summary	2-3
2-3	Discrete-Parameter Aircraft Element Coordinates	2-5
2-4	Rigid Sub-Body Local Coordinates	2-7
2-5	Aircraft Inertial Coordinates	2-8
2-6	Differential Element Coordinates	2-11
2-7	Relative Coordinate Motion	2-26
2-8	Discretized Aircraft	2-51
2-9	Aerodynamic Panel	2-52
2-10	Aerodynamic Panel Rotation	2-58
2-11	Aerodynamic Panel Relative Velocity	2-62
2-12	Aerodynamic Panel Angle-of-Attack	2-63
2-13	Perturbation Aerodynamic Panel Rotation	2-76
2-14	Rigid Aircraft Coordinates	2-87
2-15	One-Dimensional Three Mass Model	2-89
3-1	Definition of Euler Angles	3-4
3-2	Axis Systems	3-4
3-3	Explanation of Distances Appearing in the Longitudinal Equations	3-11
3-4	Flight in Plane of Symmetry	3-14
3-5	Inertial Reference and Body Axis	3-14
4-1	Euler Equation Solution Volumetric Element Grid	4-6
4-2	Body Defined by the Function $F(r,t) = 0$	4-11
4-3	Incompressible, Steady, 2-D, Airfoil	4-22
4-4	Chordwise Lift Distribution Due to Unit Angle-of-Attack	4-24
4-5	Surface and Wake Representation	4-25

LIST OF FIGURES (Continued)

<u>Figure</u>		<u>Page</u>
4-6	Ring vortex Geometric Specification	4-26
4-7	Typical Wing and Wake Model	4-27
4-8	Pressure Distribution versus Time for the Indicial Response of a Wing of Aspect Ratio 3.33 and Taper Ratio 2.43	4-28
4-9	Indicial Lift versus Aspect Ratio	4-29
4-10	Upwash Induced at a Control Point by a Loaded Acceleration Potential Doublet Traveling at Subsonic Mach Numbers	4-41
5-1	Time-Variant (A, B, C) Model with Anticipated Feedback	5-8
5-2	Bijective Mapping between RHP and Disk D	5-28
5-3	Advanced Supersonic Transport (AST)	5-51
5-4	AST Longitudinal Flexible-Body Model	5-51
5-5	Frequency Response of u/δ_e	5-66
5-6	Frequency Response of α/δ_e	5-66
5-7	Frequency Response of θ/δ_e	5-67
5-8	Frequency Response of q/δ_e	5-67
6-1	Hydraulic Servo-Dynamic Model	6-4
6-2	Hydraulic Component Interface	6-5
6-3	Hydraulic System Analog	6-6
6-4	Valve Characteristics - Flow versus Load Pressure	6-10
6-5	Flow versus Valve Stroke	6-11
6-6	Load Pressure versus Valve Stroke	6-11
6-7	Load Dynamics - Flying Tail	6-16
6-8	Hydraulic Servo System	6-16
6-9	Velocity Feedback Models	6-20
D-1	Fixed Longitudinal Stability Derivative Program	D-3
D-2	Flow chart for Lateral/Directional Stability Derivative Program	D-12
D-3	Flow Chart for Longitudinal Free Stability Derivative Program	D-20

LIST OF TABLES

<u>Table</u>		<u>Page</u>
1-1	Relation between Euler Angles and Axis Systems	1-20

SECTION 1
INTRODUCTION

In the past, the effect of structural flexibility of an airplane has been accounted for by modifying the rigid-body stability derivatives. However, modern highly maneuverable fighters like F-15, F-16, F-18, and high performance large transport airplanes, operating at subsonic, transonic, and supersonic Mach number, have the frequencies of their structural motion sufficiently reduced by increase in both airplane flexibility and dynamic pressure. This has caused an ever increasing interaction between aerodynamics, structural dynamics, flight dynamics, and control disciplines. This necessitates the development of a theoretical foundation for synthesizing an aeroservoelastic (ASE) model to be used in the stability and control (S&C) analysis.

The objectives of this study are:

- To develop a theoretical foundation for synthesizing an ASE model to be used in the stability and control analysis of a flexible airplane.
- To provide a better understanding of the equations, underlying assumptions and interactions among different disciplines from first principles.

The report is divided into six sections including a summary for the reader to gain an overall understanding of the subject. The report has achieved these objectives by accomplishing the following tasks:

- Formulation of the equations used in each discipline from first principles whenever convenient.
- Integration of the equations into a set of governing nonlinear equations and definition of bounds for the assumptions and linearization effects associated with each step.
- Linearization of the nonlinear equations.
- Provision for time domain and frequency domain representation of the flexible aircraft.

- Provision for model order reduction methods that are compatible with control synthesis.
- Approach for computing the quasi-static and higher order static and dynamic stability and control (S&C) derivatives of flexible aircraft.
- Method of state space formulation for the design of active controls.
- Adequate documentation for the theoretical formulation and analysis.

Completion of these tasks resulted in:

- Enhancement of the analytical capability to deal with the active aeroservoelastic (AASE) problem by means of improved models and computer programs.
- Development of a method for obtaining stability derivatives of a flexible airplane, such that "rigid-body" techniques can be applied.
- Inclusion of the complete six degrees of freedom motion, the flexible modes and the actuator dynamics to account for coupling effects.
- Provision for the effect of simplification on the accuracy of the results.
- Accommodation of different levels of detail and definition of the structure, aerodynamics and servos, especially during the preliminary design.
- Provision for means of grid and coordinate transformations used in different disciplines.
- Provision for different levels of frequency content in calculating the S&C derivatives (e.g., flexibility effects derived from steady or unsteady aerodynamics).
- Provision for obtaining ASE modeling data suitable for designing flight control systems.

The scope of the investigation included consideration of flexible airplanes operating in the low subsonic to high supersonic flight conditions. Only "clean" configurations are studied; landing, takeoff, ground effects, stability augmentation are not included. The dynamic equations are developed for a flexible airplane having arbitrary configuration and undergoing arbitrary maneuvers, utilizing a hybrid coordinate system to describe the

motion of the airplane. The development of the equations of motion follows the approach suggested by P. W. Likins in his paper entitled, "Dynamics and Control of Flexible Space Vehicles" (Reference 1).

Two mathematical models of an elastic airplane are considered; "rigid model" and "three lumped mass one dimensional model." The "rigid model" admits no structural deflections from the shape in the reference motion. The "three lumped mass model" idealizes the aircraft as a collection of linear-elastically, interconnected, and discrete rigid subbodies.

The notations employed for stability derivatives in Section 3 follow the standard pattern. A list of airplane stability derivatives with their meanings is given in Appendix A. Appendix B covers the definition of the axis systems used in the derivation of equations of motion. Appendix C deals with the aerodynamic equations in the three degree-of-freedom longitudinal maneuver. Appendix D contains the listing of computer programs P-107, P-137 and DRSD F-72 for the fixed longitudinal stability derivatives, free longitudinal stability derivatives, and the fixed and free lateral-directional flexible stability derivatives, respectively.

Matrix notations and methods have been used in developing and presenting many equations. A glossary of the terminology used is provided on Page G-1.

1.1 SUMMARY OF DISCIPLINES

The task of the flight control system has been traditionally to provide control for the vehicle motion with improved stability and handling qualities. In the past, it was proper to design the system using rigid-body equations of motion with the stability derivatives adjusted for the effects of structural flexibility. Lower airframe weight is now made possible by the application of active control technology to compensate for more structural flexibility. Because the simply adjusted stability derivatives are no longer adequate, it is necessary to analyze much larger systems of equations to accomplish that traditional role. Furthermore, with the advent of new technologies aimed at controlling the structural modes of large flexible airframes, a synergism of

integrated disciplines is needed to expand the control theory domain to combine rigid body and flexible body modes.

When control engineers first recognized the need for an expanded control theory domain, they adopted a more extensive use of linear algebra - vectors and matrices - the basic analytical tools for structural dynamics. Adoption of these methods in control theory led naturally to the development of multi-loop optimization processes which utilize state-space models and which are covered under the broad discipline known as "modern control theory." Powerful digital computers are essential tools for this work because of the large matrix sizes.

The state-space approach is little more than a method of accounting. It is equally applicable to time-domain (differential equation) or frequency domain (Fourier/Laplace transform) models of dynamic systems. Some advantages of state-space models approach are:

- A large number of scalar equations can be expressed as a small number of vector-matrix equations.
- First-order differential equations, for which mathematical techniques are highly developed, represent the entire system.
- The linearization of aircraft equations, which are inherently nonlinear, is straight forward via computation of Jacobians.
- Appropriate reduced-order models can be generated easily.

In order to benefit from the above advantages, in addition to those of the classical methods, control theory applied to the design of airplanes is based primarily on linear analyses. Traditionally, rigid-body data in the form of stability derivatives from the wind-tunnel curves are used to compute response to small perturbations, the related output data characterizing the flight dynamics. A set of these linear models, each representing a particular flight condition, is used to study airplane control in the total flight envelope. The rigid body input data may also include stability derivative corrections to represent airframe flexure influences upon the aerodynamic

forces. This is, however, not sufficient when the dynamics of the lowest structural mode couple with the short period of the rigid body model. Similarly, the lowest structural mode will couple with the next higher mode, ad infinitum; so that the correct model for some handling quality studies must include the dynamics of rigid body and several structural modes.

In case the model (designed for flutter analysis) does not include accurate rigid-body characteristics, a good representation can usually be obtained by inserting rigid-body coefficients in the appropriate aerodynamic matrix locations. This approach "estimates" the coupling between the short-period and the lowest structural mode. If this is not acceptable, then the original model must include accurate representation of the rigid-body modes.

A large aeroelastic model of the type commonly used for loads or flutter analyses must be reduced to relatively low order before it can be used in a practical setting for control system studies; e.g., a real-time flight simulator. Since structural dynamics models are practically time invariant, the required simplifications can be done conveniently by exploiting the fundamental attributes of linear algebra: eigenvalues, eigenvectors, and superposition. After the aeroelastic model has been reduced to an appropriate order, it can then be superimposed upon a rigid-body total-force model if desired. An alternative to the total-force model, sometimes used for "take-off" or "landing", is one which utilizes time-variable interpolation of stability derivative increments between sets of stability derivatives. In most cases, however, linear models with constant coefficients are adequate for the study of stability and control characteristics, including handling qualities.

The methods required to develop and evaluate an aeroservoelastic (ASE) modeling capability necessitate the integration of many disciplines that are difficult to tie together and hence have been neglected in the early design of an aircraft. The difficulty of implementation is usually attributable to technical and organizational reasons. Another obstacle lies in the nature of the organization including the different disciplines which employ rigid

compartmentalized boundaries. As a result of these difficulties, there has been no universally accepted approach to develop a comprehensive ASE methodology.

Thus, ASE itself must now become a new discipline. It involves nonlinear partial differential and integral equations which require a great deal of computer power to solve even simple cases.

The aeroservoelastic equations can be divided into four categories:

- Flexible Airplane Equation: This is a matrix equation in terms of degrees of freedom that describe the overall motion of the airplane and its deformation due to flexibility.
- Actuator Equation: This equation relates control command input to a control surface deflection; i.e., it provides the relation between control command, actuator force and actuator extension.
- Control System Equation: This is the equation that generates control commands from the stick force and sensor outputs. The task of the control system designer is to synthesize physically realizable equations such that the airplane has the desired characteristics.
- Output Equation (Sensor Equation): This equation relates detected motions (e.g., acceleration, rate of rotation, angle-of-attack) to the degrees of freedom in the airplane equation.

The chairman of a typical ASE project might assign a sequence of tasks in terms of the required equations:

Flexible Airplane and Actuator Equations

- Represent the structure of the model in sufficient detail to obtain the desired objectives.
- Write the set of differential equations defining the structural dynamics of the system.
- Modalize the set of equations, thus reducing its number to selected dynamic modes.
- Write the expressions for the forcing functions, including the aerodynamics and actuator dynamics, and convert them to generalized loads corresponding to the modalized structural model.

- Convert the model to a state-space format for application of digitally computed optimal control techniques.
- Reduce the order of the state-space model to one that is sufficiently accurate and amenable for control-law synthesis and laboratory simulation.

Actuator and Control System Equation

- Define the control system actuator models and interfaces.
- Define the criteria for an optimal control law.
- Compute the control law.
- Reduce the complexity of the control law to one that is sufficient and compatible with the original model.

Output Equation

- Transform the output state back to the original coordinate system, thus locating the sensor positions.
- Evaluate and iterate the improvement obtained (as indicated by the simplified synthesis model) on more detailed loads and flutter analysis models.

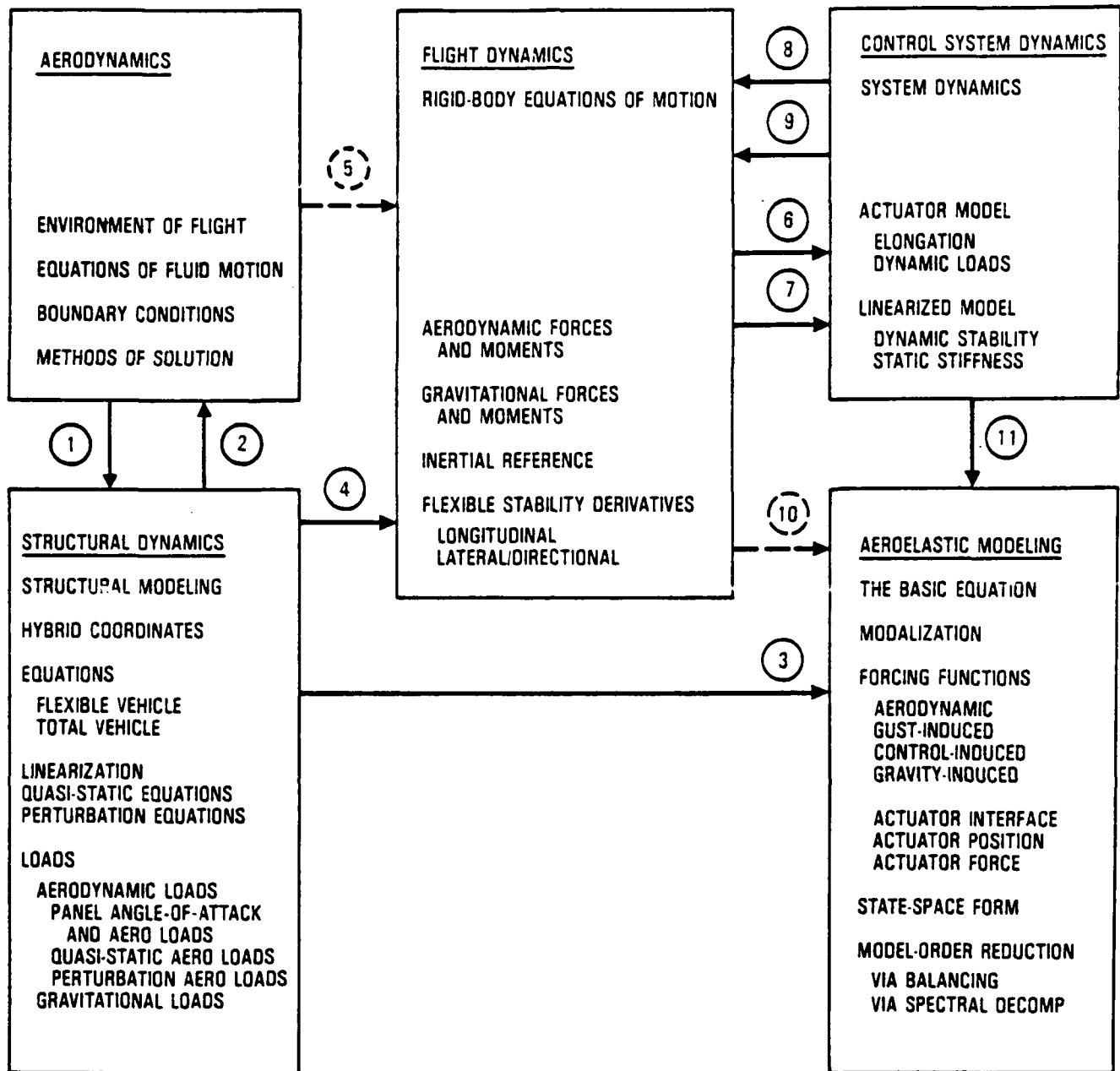
An overview of the interfaces between the technical disciplines is presented in Section 1.2. Amplification of detail follows in the subsequent sections. Topics concerning the control-law equations are omitted, because the scope of this program is limited to open-loop systems.

1.2 INTEGRATION OF THE TECHNICAL DISCIPLINES

Figure 1-1 is a flowchart of various theoretical topics included in the documents resulting from this study. The legend points to topics that comprise the interfaces among the technical disciplines. The development and flow of information leading to the ASE model is described in the following paragraphs.

1.2.1 Structural Dynamics

Translation and rotation of each sub-body is described relative to a hybrid-coordinate system. This set of sub-bodies are defined as discrete representation conforming to the stiffness and mass distribution of the



LEGEND:

- | | |
|---|---|
| 1. AERODYNAMIC PRESSURE DISTRIBUTION | 7. CONTROL SYSTEM REQUIREMENTS |
| 2. PANEL INFLUENCES ON AERODYNAMIC FLOW | 8. CONTROL CONFIGURED VEHICLE REQUIREMENTS |
| 3. STRUCTURAL AND AERODYNAMIC PARAMETERS | 9. CONTROL SURFACE INFLUENCES |
| 4. INFLUENCES ON STABILITY DERIVATIVES | 10. RIGID BODY COEFFICIENTS IN STATE-SPACE MATRIX |
| 5. AERODYNAMIC FORCES ON RIGID BODY MODEL | 11. ACTUATOR ELONGATIONS AND FORCES |
| 6. STABILITY DERIVATIVES | |

Figure 1-1. Interfaces Between the Technical Disciplines

flexible body. Mathematical operators allow translational and rotational displacements, velocities, and accelerations of the set of the force and moment equations to be represented in matrix form.

The orientations of the coordinate references are selected to minimize resulting products of inertia; nevertheless, some do exist even in fixed coordinate systems. These, along with the gyroscopic effects resulting from rotating coordinate systems, introduce significant nonlinearities.

The aerodynamic forces are generated by the airflow over the deformed structure which in turn affects the deformation of the structure. This closed loop is represented by an Arrow 2 from the structural dynamics discipline into the aerodynamics discipline indicating that each individual panel influences the airflow, and Arrow 1 from the aerodynamics discipline into the structural discipline representing the aerodynamic force that drives the deformation activity among the discrete elements of the structural model.

Small perturbations are universally accepted in structural dynamics, thus permitting linear approximations at an appropriate stage in the procedure. The corresponding arrow from the structural dynamics discipline into the aeroelastic modeling discipline represents the structural and aerodynamic influence coefficients that are used to formulate the basic equation of the aeroelastic model.

Arrow 4 from the structural dynamics discipline into the flight dynamics discipline indicates the effects of dynamic pressure, downwash, and others that produce the flexible-airplane stability derivatives. Under the traditional approach, this arrow would represent only those influences which add flexibility increments to the rigid-body stability derivatives.

1.2.2 Aerodynamics

The physical characteristics of the atmosphere and the airflow relative to the aerodynamic surfaces results in the aerodynamic forces and moments

applied to the airplane. Conservation principles are applied to determine the equations of the motion of the fluid particles comprising the airstream.

Various approaches to the formulation of these equations are described in Section 1.4. The Laplace equations which describe the kinematics of incompressible flow and the Bernoulli's equation, which converts the kinematics in to pressure distribution over the aerodynamic surfaces yield the resultant surface loads.

These loads act on the corresponding individual elements in the discrete system (structural dynamics model) or at the center of lift and drag on the airplane surfaces (rigid-body model).

1.2.3 Flight Dynamics

The rigid-body equations of motion are written traditionally in the stability coordinate system (moments defined relative to body axes and forces defined relative to wind axes). These axis systems are defined on page 1-17, Section 1.3.2. The motion of the airframe is defined in terms of body axes: translational velocities u , v , and w in the directions of x , y , and z respectively; and angular velocities p , q , and r about the x , y , and z axes respectively. Although the reference coordinate system is instantaneously aligned with the body axes with its origin at the airframe center of gravity, it does not move with the airframe.

The body axes fixed to the body are related to an inertial coordinate system fixed to the earth by a sequence of body axis rotations. This sequence, called the Euler coordinate system, is first in yaw (rotation about the z axis), then in pitch (rotation about the y axis), and finally in roll (rotation about the x axis). The corresponding product of the three transformation matrices defines the Euler coordinate system in terms of trigonometric functions of the three rotation angles: Ψ (psi), Θ (theta), and Φ (phi).

The wind axes are obtained from the body axes by a sequence of two rotations: first in pitch with angle " α " about the y axis, and then in yaw with angle " β " about the z axis. The corresponding product of the two transformation matrices defines the wind coordinate system relative to body axes in terms of trigonometric functions of α and β .

Even though the trigonometric functions are nonlinear, small perturbation angles in sine-cosine products permit linear approximations at an appropriate stage in the procedure. Flexibility increments due to steady loads have an influence on the static angle-of-attack and on the static moments, which in turn influence the stability derivatives. The arrow from the structural dynamics discipline into the flight dynamics discipline in Figure 1-1 represents these influences. The corresponding stability derivatives and state-space formulations are used in the linear analysis and synthesis of the flight control systems. This interface is represented by Arrow 6 from the flight dynamics discipline into the control system discipline.

Obviously the stability and control requirements determine the control system design; and, in control-configured vehicles, the control system capability influences the airframe design. This loop is represented by Arrows 7 and 8 from the flight dynamics discipline into the control system discipline and visa versa.

The dashed Arrow 5 from the aerodynamics discipline into the flight dynamics discipline represents the aerodynamic forces which are generated by the air flowing over the surfaces of the rigid-body model of the airplane. This interface does not exist under the ASE approach to modeling. Typically, it would indicate the aerodynamic effects on the rigid-body: dynamic pressure, downwash, stability derivatives, etc. The stability derivatives are usually derived from the wind-tunnel data fitted-polynomials.

Arrow 9 from the control system discipline into the flight dynamics discipline represents the effect of the control surfaces on aircraft dynamics.

Arrow 10 from the flight dynamics discipline into the aeroelastic modeling discipline is dashed because it does not exist under the ASE approach to modeling. Under the traditional approach it would represent rigid-body coefficients in the state-space model where the structural dynamics model does not contain accurate rigid-body mode representation (short period, phugoid, etc.).

Arrow 7 (control system requirements) from the flight dynamics discipline into the control system discipline includes the loads on the actuators. Usually these loads are small compared with the actuator capability, thus permitting the actuators to be represented by linear models. There are, however, designs (e.g., spoiler blowback) where, under heavy load, the actuator operates in its nonlinear region. Furthermore, with large control surfaces, the surface dynamics might be reflected back into the control valve, thus creating a dynamic instability.

1.2.4 Aeroelastic Modeling

The development of a reduced-order aeroelastic model begins with an intermediate sized model having more modes than those intended for the actual analysis; then it is reduced in such a manner as to preserve certain residual effects of the eliminated modes. The intermediate model results from modalizing and truncating a larger model.

The initial equations define the larger system in terms of the structural composition and the aerodynamic forces which act upon it. The structural part of the model represents all main airframe components (wing, fuselage, tail, et cetera). Discrete elements of these airframe parts are represented by Arrow 3 from the structural dynamics discipline into the aeroelastic modeling discipline.

Standard procedures, using small perturbation dynamics lead to the linear state space equation. Its state includes the rigid body variables, control surface deflections, or gust variables as well as structural mode shapes.

As indicated by Arrows 3 and 11 in Figure 1-1, elements in the equations of dynamics are obtained mainly from two of the technical disciplines: Mathematical models representing structural deflections and total airframe motions are from the structural dynamics discipline, and models representing actuator elongations and forces are from the control systems discipline. If the traditional approach is used, then rigid-body elements of the state vector (e.g., the six degrees of freedom of the c.g. - incremental pitch angle, pitch rate, angle-of-attack, air speed) might be obtained from the flight dynamics disciplines. The influence coefficient matrices, Aerodynamic Influence Coefficient (AIC) and Structural Influence Coefficient (SIC), are from the aero and structural dynamics disciplines. Likewise the mass and stiffness matrices and the modalization matrices are from the structural dynamics discipline.

Arrow 11 from the control system discipline to the aeroelastic modeling discipline represents either or both of two types of interface: actuator displacements and actuator forces. Where the actuator loading is negligible as compared to its capability, the displacement transfer function is used; but where the surface dynamics significantly load the actuator, the actuator-force interface is used.

1.3 SUMMARY OF COORDINATE SYSTEM METHODS

The motion of a body is described by considering the translation of its center of mass under the sum of the forces acting on the body and the rotation about its center of mass under the sum of the moments. Traditionally, the motion of a flexible airplane, under suitable assumptions, can be defined as the translation and rotation of an axis system for inertial reference, and the deformations relative to that inertial reference. Current assumptions are: the deformations must be relatively small and, if the overall motions of the airplane are large, they must be relatively slow compared to the first natural structural frequency.

The airframe, in an inertial reference system, moves under the influence of total aerodynamic force and moment, and the force of gravity, as if it were

rigidized in its zero external load shape (no elastic deformation). For the deformations relative to the inertial reference, the small perturbation theory equations for stability and flutter apply.

Thus, the equations of motion can be categorized as follows:

- **Maneuvering equations**

These equations relate the total aerodynamic force and moment on the flexible airplane, and the force of gravity, to the overall motion of the airplane, defined by the inertial reference. The flexibility effects will include that of a maneuver load alleviation system, if present.

- **Stability equations**

These equations describe the small deflections of the airplane relative to the inertial reference. They cover stability in the flight mechanics sense and flutter. The effects of stability augmentation, flutter suppression, gust load alleviation, and ride control are included.

1.3.1 Hybrid Coordinates

The complete dynamic equations of motion for flexible aircraft (of arbitrary configuration undergoing arbitrary motion and experiencing an arbitrary load) using hybrid-coordinate system are derived in Section 2. The approach utilizes two reference frames: one inertial and one vehicle fixed. This permits the assumption of small elastic deformation while allowing large vehicle motion. Thus, the total and flexible body dynamics are linear in structural deformation variables, but nonlinear in rotational parameters, e.g., θ and ω .

1.3.1.1 The Hybrid-Coordinate Assumptions

The use of hybrid coordinates begins with the following assumptions relative to Figure 2-3.

- The aircraft, Body A, is composed of finite rigid sub-bodies, A_S , that are interconnected by linearly elastic members. Therefore, the deflection of any of these elastic members yields a restoring force that is proportional only to the corresponding deflection (K is

constant). Thus, q is limited to deflections which do not produce any cross-coupling stiffness effects due to the geometry changes.

- The aircraft, Body A, is attached to a massless Body B for all six degrees of freedom at one Point Q. The sum of the loads at Q is zero. This auxiliary relationship is used to define the stiffness matrix of the flexible aircraft. Prior to deformation, when u_s and β_s are zero, and origin of Body B, Point O, is coincident with the vehicle mass center.
- The overall matrix equations of motion are written in terms of the sub-body deformations. However, the coefficients of these equations are in terms of the overall vehicle motion and the direction cosine matrices all of which are also unknown. Thus, $3n + 9$ additional auxiliary equations are required to uniquely describe the matrix equations of motion.

1.3.1.2 Review of Hybrid-Coordinate Dynamic Equations Development

The work by P. W. Likins for flexible spacecraft was rederived for an aircraft of arbitrary configuration undergoing an arbitrary maneuver using a hybrid-coordinate system. Vector bases are defined relative to an inertially fixed reference frame, the vehicle, and each rigid subbody. Direction cosine matrices are defined describing the rotation of the vector bases to each other. Vehicle deformation is defined by the motion of the rigid subbodies relative to the vehicle center of mass. The motion of each subbody is described as a series of vectors which are resolved relative to the appropriate vector bases.

Special operators are defined to facilitate the matrix algebra necessary in using a hybrid-coordinate system. Translational vehicle deformation is considered first. The motion of the vehicle mass center relative to the massless body reference point is described in terms of the rigid subbody translational deformations. Separate Newton-Euler equations of motion are written for translation and rotation for each rigid subbody in terms of the hybrid-coordinates. The resulting equations are combined into two sets of $3n$ equations, which are then written as one matrix equation of order $6n$. The Newton-Euler equations are then developed for the vehicle, which yields two sets of three equations each; for translation and rotation.

These $6n+6$ equations have $9n+15$ unknowns. Auxiliary equations are developed to uniquely specify the problem. $6n$ equations describe the n subbody direction cosines matrices as a function of the subbody's rotational deformation. Six more equations result from the vehicle's rotation: three associated with defining the direction cosine matrix and three defining rotational as a function of rotational velocity. For a free-free vehicle, the vehicle stiffness matrix allows the motion of the massless Body B to be described in terms of the deformation variables. This allows the deformation variables to be reduced to $6n-6$. The remaining three degrees-of-freedom result from the choice of hybrid-coordinates: The vector base associated with the massless body is defined to always be coincident with the vehicle vector base.

1.3.1.3 Linearization of Hybrid-Coordinate Dynamic Equations

All time dependent variables are assumed to be composed of quasi-static and perturbation components. The quasi-static component allows for large amplitude, but slowly time varying deformations. The perturbation component allows for small amplitude rapid fluctuations about the quasi-static solution.

All variables are expressed in terms of their quasi-static and perturbation components. The resulting equations are expanded. All purely quasi-static terms are collected into a set of quasi-static equations. All first order perturbation terms are collected into a set of perturbation equations. All higher order perturbation terms are assumed negligible. The resulting quasi-static equations are non-linear zero order (with respect to time). The resulting perturbation equation is linear second order (with respect to the perturbation variables).

1.3.1.4 Inclusion of Aerodynamic and Gravitational Loads

For the aerodynamic loads, a deformable panel method is assumed that allows for large vehicle deformation. The deformation of the panels is a function of the deformation of rigid subbodies. Aerodynamic loads are assumed to act normal to the panel surface at the panel load points and are functions of the angle-of-attack at the panel normal wash points. The specific

relationship between load and angle-of-attack is discussed in Section 4. A vector base is defined at each load point and each normal wash point. The orientation of these vector bases relative to the vehicle's vector base is derived as a function of the vehicle deformation. The angle-of-attack is defined as the angle between the relative velocity and the plane of the panel at the normal wash point.

The results are linearized using the above described procedure. The perturbation components are highly non-linear. To facilitate the description of the perturbation angle-of-attack, an additional vector base is defined that has one base coincident with the quasi-static relative velocity, and one base remaining in the plane of the panel. Perturbation aerodynamic loads become linear functions of the perturbation angle-of-attack, which become a linear function of the perturbation relative velocity, which become a linear function of the structural deformations.

Since gravitational acceleration acts in a constant direction with respect to the inertial vector base, gravitational loads are directly implemented into the hybrid-coordinate dynamic equations.

1.3.2 Stability Coordinates

The equations of motion commonly used for analysis of transient maneuvers involving all six degrees of freedom of the rigid airplane, employ four different axes systems; these axes systems are designated ground axes, body axes, stability axes and wind axes. The definition of these axes and their functions are as follows:

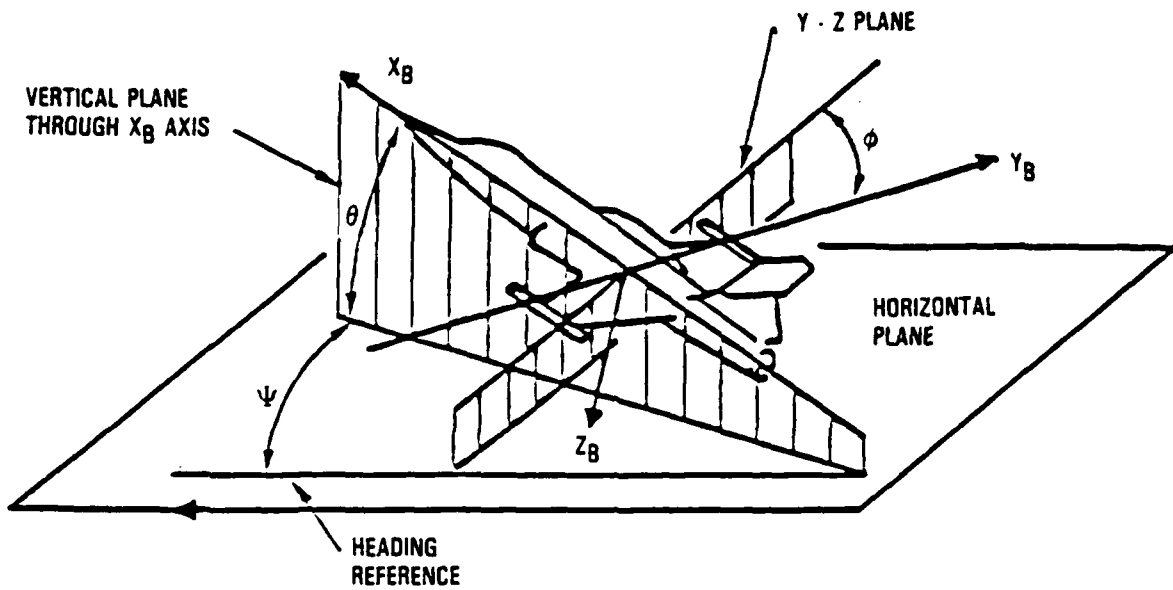
- Ground Axes - Ground axes are a set of orthogonal axes fixed with respect to the ground. The z axis is coincident with the weight vector. The x and y axes are arbitrary but the equations are simplified if either the x and y axis is chosen to coincide with the horizontal component of the wind relative to the ground. Ground axes are required to define components of weight and ground winds in the other axes systems.

- Body Axes - Body axes are a set of orthogonal axes through the airplane c.g. which remain fixed relative to the body. The y axis is chosen normal to the plane of symmetry (for most airplanes there is a plane of symmetry and this plane is designated the xz plane). The x axis is usually the horizontal reference axis. The moment equations are in the body axes system because inertia properties remain fixed with respect to these axes.
- Stability Axes System - Stability axes system is nothing but a special case of a body fixed system where the orientation with respect to the body has been selected with respect to a steady state flight condition. With origin at the center of gravity, x-axis points in to the direction of the relative wind. y-axis is orthogonal to the x-axis and z axis is defined in such a manner that right hand rule holds.
- Wind Axes - Wind axes are a set of orthogonal axes through the airplane c.g., the z axis of which is coincident with the z axis of the stability axis system. The x axis is coincident with the airplane velocity vector. Again, the velocity is the airplane velocity relative to the air. The force equations are simplest when written in the wind axes system.

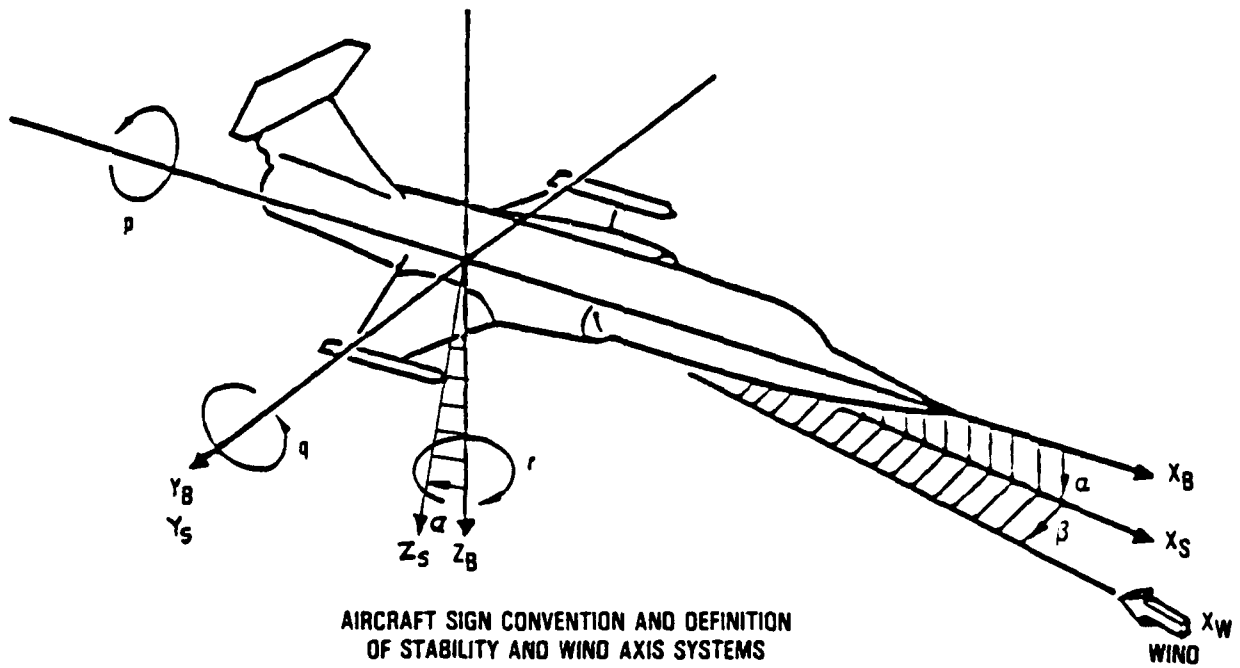
The relationships between ground, body, stability, and wind axes, are shown in Figure 1-2.

In each set of axes, the x, y, z axes are orthogonal; i.e, mutually perpendicular. One set of axes can be made to coincide with another set of axes by rotating through Euler angles. Since the axes about which Euler rotations take place are not orthogonal, the order in which the rotations take place must be specified. The Euler angles and their order for transferring from one axis system to another are specified in Table 1-1.

Vector components in one axis system can be related to vector components in another system through the use of transformation matrices which are functions of the Euler angles. Transformation matrices applicable to the four axes systems used in transient maneuver loads analysis are presented below:



DEFINITION OF EULER ANGLES



AIRCRAFT SIGN CONVENTION AND DEFINITION OF STABILITY AND WIND AXIS SYSTEMS

Figure 1-2. Axis Systems

TABLE 1-1. RELATION BETWEEN EULER ANGLES AND AXES SYSTEMS

Rotating		Order of Rotation	Euler Angle	Rotation Axis
From	To			
Wind Axes	Stability Axes	1	$-\beta$	$z_{\text{Wind}} = z_{\text{Stab}}$
Stability Axes	Wind Axes	1	β	$z_{\text{Wind}} = z_{\text{Stab}}$
Stability Axes	Body Axes	1	$-\alpha$	$y_{\text{Stab}} = y_{\text{Body}}$
Body Axes	Stability Axes	1	α	$y_{\text{Stab}} = y_{\text{Body}}$
Wind Axes	Body Axes	1 2	$-\beta$ $-\alpha$	$z_{\text{Wind}} = z_{\text{Stab}}$ $y_{\text{Stab}} = y_{\text{Body}}$
Body Axes	Wind Axes	1 2	α β	$y_{\text{Stab}} = y_{\text{Body}}$ $z_{\text{Wind}} = z_{\text{Stab}}$
Ground Axes	Body Axes	1 2 3	ψ θ ϕ	z_G y'_G $x''_G = x_B$
Body Axes	Ground Axes	1 2 3	$-\phi$ $-\theta$ $-\psi$	$x''_G = x_B$ y'_G z_G

Transformation Matrices

- Wind Axes to Stability Axes

$$\begin{pmatrix} x_S \\ y_S \\ z_S \end{pmatrix} = \begin{bmatrix} \cos \beta & -\sin \beta & 0 \\ \sin \beta & \cos \beta & 0 \\ 0 & 0 & 1 \end{bmatrix} \begin{pmatrix} x_W \\ y_W \\ z_W \end{pmatrix}$$

- Stability Axes to Wind Axes

$$\begin{pmatrix} x_W \\ y_W \\ z_W \end{pmatrix} = \begin{bmatrix} \cos \beta & \sin \beta & 0 \\ -\sin \beta & \cos \beta & 0 \\ 0 & 0 & 1 \end{bmatrix} \begin{pmatrix} x_S \\ y_S \\ z_S \end{pmatrix}$$

- Stability Axes to Body Axes

$$\begin{pmatrix} x_B \\ y_B \\ z_B \end{pmatrix} = \begin{bmatrix} \cos \alpha & 0 & -\sin \alpha \\ 0 & 1 & 0 \\ \sin \alpha & 0 & \cos \alpha \end{bmatrix} \begin{pmatrix} x_S \\ y_S \\ z_S \end{pmatrix}$$

- Body Axes to Stability Axes

$$\begin{pmatrix} x_S \\ y_S \\ z_S \end{pmatrix} = \begin{bmatrix} \cos \alpha & 0 & \sin \alpha \\ 0 & 1 & 0 \\ -\sin \alpha & 0 & \cos \alpha \end{bmatrix} \begin{pmatrix} x_B \\ y_B \\ z_B \end{pmatrix}$$

- Wind Axes to Body Axes

$$\begin{pmatrix} x_B \\ y_B \\ z_B \end{pmatrix} = \begin{bmatrix} \cos \alpha \cos \beta & -\cos \alpha \sin \beta & -\sin \alpha \\ \sin \beta & \cos \beta & 0 \\ \sin \alpha \cos \beta & -\sin \alpha \sin \beta & \cos \alpha \end{bmatrix} \begin{pmatrix} x_W \\ y_W \\ z_W \end{pmatrix}$$

- Body Axes to Wind Axes

$$\begin{pmatrix} x_W \\ y_W \\ z_W \end{pmatrix} = \begin{bmatrix} \cos \beta \cos \alpha & \sin \beta & \cos \beta \sin \alpha \\ -\sin \beta \cos \alpha & \cos \beta & -\sin \beta \sin \alpha \\ -\sin \alpha & 0 & \cos \alpha \end{bmatrix} \begin{pmatrix} x_B \\ y_B \\ z_B \end{pmatrix}$$

- Ground Axes to Body Axes

$$\begin{pmatrix} x_B \\ y_B \\ z_B \end{pmatrix} = \begin{bmatrix} \cos \psi \cos \theta & \sin \psi \cos \theta & \sin \theta \\ \cos \psi \sin \theta \sin \phi & \cos \psi \cos \phi & \cos \theta \sin \phi \\ -\sin \psi \cos \theta & +\sin \psi \sin \theta \sin \phi & \\ \sin \psi \sin \phi & \sin \psi \sin \theta \cos \phi & \cos \theta \cos \phi \\ +\cos \psi \sin \theta \cos \phi & -\cos \psi \sin \phi & \end{bmatrix} \begin{pmatrix} x_G \\ y_G \\ z_G \end{pmatrix}$$

- Euler Axes (z_G, y'_G, x''_G) to Body Axes

$$\begin{pmatrix} p \\ q \\ r \end{pmatrix} = \begin{bmatrix} 1 & 0 & -\sin \theta \\ 0 & \cos \phi & \cos \theta \sin \phi \\ 0 & -\sin \phi & \cos \theta \cos \phi \end{bmatrix} \begin{pmatrix} \dot{\phi} \\ \dot{\theta} \\ \dot{\psi} \end{pmatrix}$$

- Body Axes to Euler Axes (x''_G, y'_G, z_G)

$$\begin{pmatrix} \dot{\phi} \\ \dot{\theta} \\ \dot{\psi} \end{pmatrix} = \begin{bmatrix} 1 & \tan \theta \sin \phi & \tan \theta \cos \phi \\ 0 & \cos \phi & -\sin \phi \\ 0 & \sec \theta \sin \phi & \sec \theta \cos \phi \end{bmatrix} \begin{pmatrix} p \\ q \\ r \end{pmatrix}$$

1.4 CONTRIBUTIONS FROM THE TECHNICAL DISCIPLINES

In the following, development of each discipline is discussed as it evolved from first principles. The goal is to state clearly the simplifying assumptions required to resolve the complete nonlinear system into a set of equations that satisfy a predefined level of accuracy in the computation of flexible airplane characteristics.

The formulation of equations for each discipline leads to a statement of the complete nonlinear equations. Nonlinear terms are resolved without explicit line, surface or volume integrals. After linearization, the unsteady aerodynamics is converted from frequency to time domain representation. The quasi-static flexible aircraft stability and control derivatives, with the option of including higher order terms, are obtained from the linearized equations.

Equations from First Principles

The basic principles governing the dynamics equations of a flexible airplane, the equations that lead to a formulation of the flexibility characteristics, and the forcing functions are discussed.

Analyses concerning the motion of a continuous system begin with the statement of four basic physical laws: conservation of matter, Newton's second law of motion, first law of thermodynamics, and second law of thermodynamics.

Additional equations such as equation of state, etc., are necessary to form a complete set upon which the complete analysis of airplane dynamics in particular, and dynamics in general, may be constructed.

The formalism of describing a dynamic system in the lumped parameter representation is most demanding when the system contains body and inertially fixed reference coordinates. It is identified as the hybrid coordinate approach. The key to describing dynamic systems is the retention of the full nonlinear terms during the development of the equations. This approach

permits the complete accounting of the second order terms during the linearizing process.

Nonlinear terms are retained in the equations for those disciplines that successfully resolve the volume and surface integrals from first principles without the need to linearize. There are closed-form solutions of some force terms, such as unsteady aerodynamics, which require the dropping of the nonlinear terms early in the development from first principles.

The following sections outline the procedures that were followed in developing the aeroservoelastic equations for synthesizing the ASE model. The presentation is based on the assumption that the external forces in Newton's second law of motion are only functions of the state variables, their derivatives and history. This assumption permits the independent derivation of the internal structural forces, the aerodynamic forces, the thrust and drag forces, and the control surface actuator forces.

The governing equations for a flexible vehicle can be formulated by Newtonian methods using a framework advanced by Likins. A feature of the approach which sets it apart from many approaches in current use is the introduction of two reference frames: one inertial and one vehicle fixed. This permits the assumption of small elastic deformations while allowing large vehicle motions. The resulting equations are nonlinear. Several of the coefficient matrices multiplying the displacement q and its derivatives in the rotational equation are functions of rigid body rotation ω and $\dot{\omega}$. Also since the direction cosine matrix H is nonlinear, the translational equations are nonlinear, as are the kinematical equations. The equations are, however, linear in the deformation variables. This permits modal descriptions of q which will be important for subsequent coordinate reductions.

The nonlinearities in the structural dynamics are mainly due to the interaction of flexible dynamics and the rotational motion. If rotational rates are small, these nonlinearities can be neglected. For further development (i.e., flutter, stability derivatives, state space equations) these nonlinear terms are neglected.

Grid and Coordinate Transformations

Several coordinate systems are generated as a matter of convenience and expediency. In unsteady aerodynamics, the downwash is measured at an aft collocation point on the aerodynamic panel chord while the aerodynamic force is placed at the quarter chord or centroid of the panel. The stiffness grid is usually different from these and the mass grid. To compound the problem, different disciplines view the analysis grid and the number and type of degrees of freedom differently. The solution to the problem of different grids is called grid transformations.

There are two types of grid transformation procedures commonly used. The first is based on a simple interpolation procedure. This procedure is based on a rigid plate of 3 or 4 points for surface interpolations. The 3 point plate is a unique solution while the four point plate (washed) is really a sequence of two point interpolations.

The second type is a multi-interpolation where a beam, plate, etc., is used to interpolate for points once the deflection of the plate (here it is a continuous plate) is known at all the known grid points. This is called the spline technique and there are many numerical procedures which do this type of interpolation.

The primary difference between the first and second type of grid transformation is the number of nonzero elements of the transformation matrix.

When applied to an actual vehicle, the developed dynamic equations would result in hundreds of second-order scalar differential equations which are nonlinear and highly coupled. If these equations are to be of any practical value to synthesizing the aeroservoelastic model for use in the controls analysis, transformations must be generated that will provide some relief by uncoupling the equations and reducing the number of differential equations.

There are two distinct and different objectives that will drive the resolution of the equations of motion into manageable sets. The first is the reduction of the equations of motion into a set of linear, constant coefficient differential equations that may be used in the flight control synthesis and linear analysis.

The second is the reduction of the full set of nonlinear equations to a form that is suitable for time domain solutions. Within this set are two other objectives, time solutions in real time (like motion simulators), and time solutions in non-real time.

The practical mechanization constraints associated with the final use of the set of equations will force the analyst to estimate the most significant terms. Currently there is no one transformation that will address the best solution of all possible numerical forms that the full nonlinear equations will assume.

The objective of the full nonlinear system of equations, then, is not so much to include all nonlinear terms in the equations for analysis and time domain solutions, but to offer a reference to the analyst for numerically evaluating the consequences of one transformation over another, or to establish the domain of application for a transformation or linearizing procedure.

1.4.1 Structural Modeling

The step from a rigid airplane to a flexible airplane is made by the introduction of the flexibility of the structure depicted symbolically in Figure 1-3. The flexibility of a given structure is defined by means of structural influence coefficient (SIC) or a stiffness matrix.

1.4.1.1 Simplified Structural Model

The Simplified Structural Modeling Program (SSMP) developed under Task 2 of this contract is an interactive program with the sole purpose of helping the user create a simplified finite element model of an aircraft.

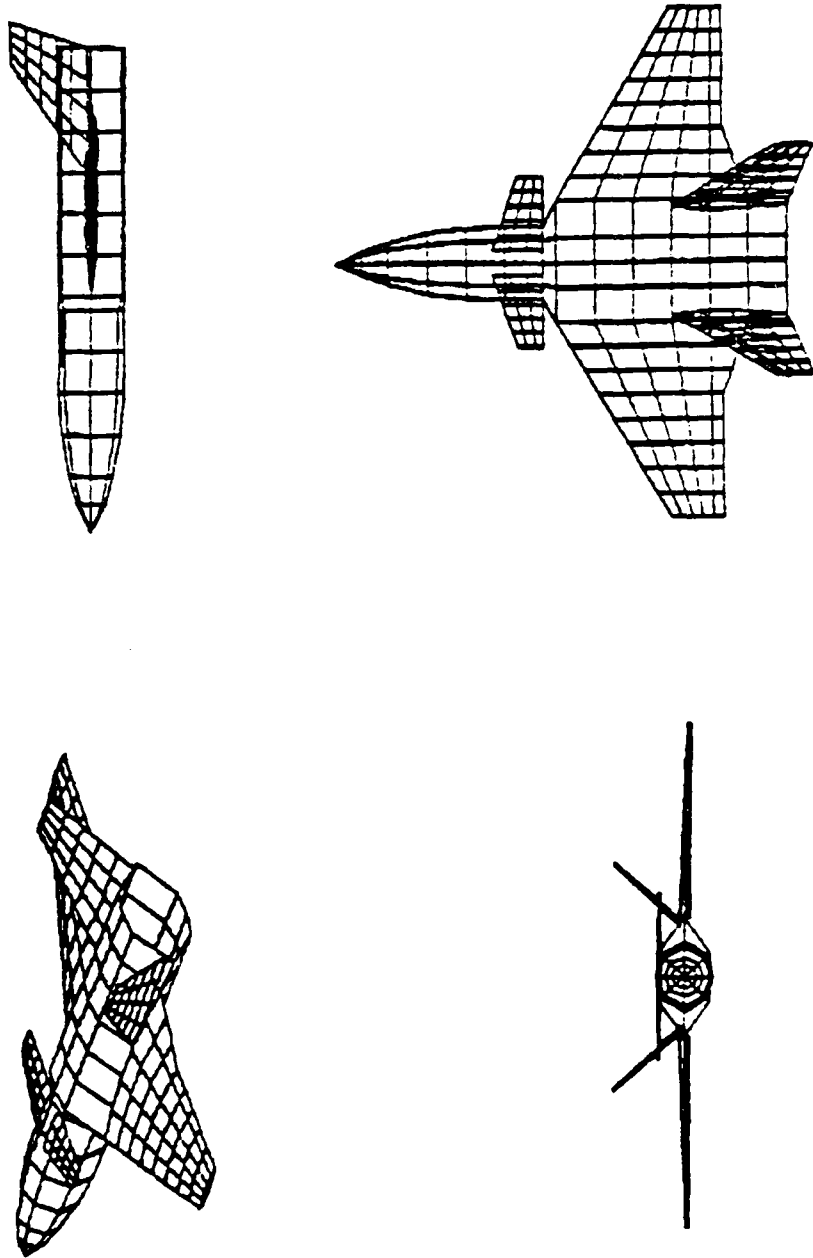


Figure 1-3. Simplified FEM Model

configuration. The model will be analyzed using the ASTROS program. All interactive input is entered in an "input steering file" that can be re-run in a batch mode enabling the user to edit the FEM model while rerunning the program. When used under the Modeling Flexible Aircraft Program operating system, the SSM program will usually be operated in the batch mode.

Figure 1-4 shows a flowchart of program interaction. Aircraft configurations are described by several components (i.e., wing, fuselage, engine, etc.). The planform geometry and cross-sectional shape are defined in either the SSMP or the CDMS program. The grid points for each component are also defined in either one of these programs. The user must then define how each component is connected to the others. He must also define the structural and mass properties of each component. Information for running CADS is entered and the output of CADS is processed to get the data into the correct format for ASTROS. The executive control deck for ASTROS is then defined and ASTROS is run. ASTROS input and output may be plotted using CADS, but the documentation for doing this is not described under this contract.

1.4.1.2 Structural Static Analysis

In the case of the flexibility matrix the basic equation is:

$$\{u\} = [E] \{P\}$$

where:

$\{u\}$ = structural degrees of freedom: discrete structural deflection, translations and rotations

$\{P\}$ = concentrated external forces and moments corresponding to the structural degrees of freedom

$[E]$ = a symmetric matrix of structural influence coefficients.

Although there are ways to define an "effective" flexibility matrix for a free structure, when the flexibility matrix is used, it is most practicable to define it for a structure that is supported in a statically determinate way.

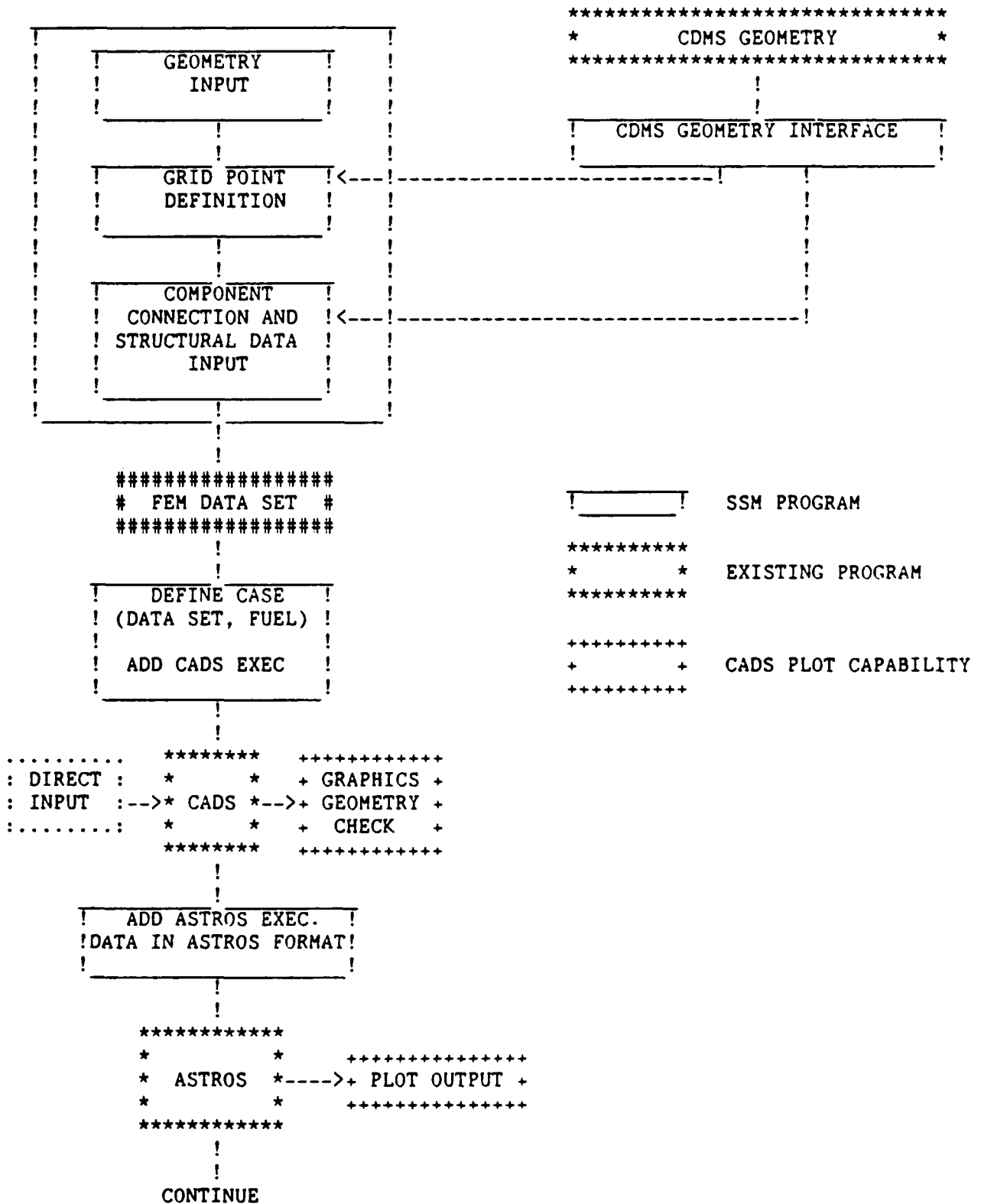


Figure 1-4. Simplified Structural Model Program Flowchart

The deflections are then measured relative to a structural reference defined by the support.

In the case of the stiffness matrix the basic equation is:

$$[K] \{u\} = \{P\}$$

The stiffness matrix, [K], can be defined for either a supported structure or an unsupported structure. In the case of the unsupported structure, the rank of [K] is its size minus the number of rigid body degrees of freedom. In contrast, for a supported structure, [E] and [K] are positive definite, in which case [K] is the inverse of [E], and K has full rank.

Two main approaches to modeling the structure for computing [E] or [K] are recognized: finite element theory and simple beam theory. In the finite element approach the structure is divided into many small structural elements, that interact with each other at the nodes of a structural grid where internal and external forces are defined, and where deflections are continuous. In the simple beam approach a lifting surface, or a fuselage, is represented by a simple beam with bending flexibility in two perpendicular planes, and torsional flexibility.

With the advent of powerful finite element programs (e.g., NASTRAN), finite element models have become commonplace. They are needed for accurate prediction of the internal stresses. The finite element model is also used for the calculation of [E] or [K]. Typically, a finite element model for a complete airplane contains a thousand or more finite elements and associated degrees of freedom; usually more degrees of freedom than are practical from a dynamics analysis point of view. Reduction of the number of structural degrees of freedom number is the first model reduction the airplane dynamicist must apply. It should be noted that in the case of a finite element model, the dynamicist chooses as his reduced set of degrees of freedom mostly translational deflections along the major axes of the structure: e.g., on a wing, perpendicular to the wing surface.

In the early design stages, a finite element model may not be available. In that case major airplane components are idealized as beams with a bending stiffness defined by EI and a torsion stiffness defined by GJ. The resulting degrees of freedom are translational and rotational deflections at selected nodes on the beams. Typically, on a wing, a structural axis is defined and the degrees of freedom are: translations perpendicular to the wing surface and in the plane of the wing perpendicular to the structural axis, and rotations about the structural axis. The number of degrees of freedom associated with a simple beam model is usually small enough to be acceptable for dynamic analyses.

Both approaches to structural modeling assume a linear stress strain relation when the airplane is represented in a normal flying condition. In addition, deformations are assumed to be sufficiently small, such that one geometry defines the structural characteristics under all load conditions. This means that in the above equation, [E] and [K] are independent of {u}. (Nonlinear force-deflection relations are considered only for crash conditions).

The structural analysis consists of obtaining internal loads, internal stresses and displacements for a set of external loads. To obtain these in a finite element model, which consists of many discrete finite element members representing the load carrying structure, the principle of minimum value of the total potential energy is used to obtain basic displacement equations. This principle may be stated as follows:

Of all the sets of displacements, that satisfy prescribed constraint conditions, the correct set is that which makes the total potential energy a minimum.

The total potential energy consists of external work and internal strain energy.

$$PI = U_{\text{internal}} - W_{\text{external}}$$

For any linear system the total potential energy for one element(i) can be expressed in terms of displacement degrees of freedom associated with that element as:

$$PI_i = \frac{1}{2} \{u\}^T [k] \{u\} + \{u\}^T \{q\} \quad (1.1)$$

Where $\{u\}$ displacement matrix, $[K]$ is the stiffness matrix and q is the external load. PI_i is expressed in a convenient local coordinate system.

The strain energy comprises potential due to thermal effects and distributed loads applied to the elements.

The following assumptions are made to obtain Equation (1.1).

- The material properties are assumed to produce linear and elastic stress-strain behavior.
- The "small" displacement theory is applied.
- The external loads do not change directions while undergoing displacements.
- The superposition principle is valid throughout the analysis.

The adequacy of these assumptions have been tested by deflection analyses of typical military aircraft to limit load.

Equation (1.1) can be transformed into a reference coordinate system using transformation matrix $[t]$.

$$\{u\} = [t] \{ur\} \quad (1.2)$$

where $\{ur\}$ is matrix of displacements at the reference coordinate system.

Substituting Equation (1.2) into (1.1) yields:

$$PI_i = \frac{1}{2} \{ur\}^T [t]^T [k] [t] \{ur\} + \{ur\}^T [t]^T \{q\}$$

The total potential energy of the complete system of M elements and N degrees of freedoms can be written as follows:

$$PI = \frac{1}{2} \sum_{i=1}^M \{ur\}^T [t]^T [k] [t] \{ur\} + \sum_{i=1}^M \{ur\}^T [t]^T \{q\} - \sum_{j=1}^N \{ur\}^T \{P\} \quad (1.3)$$

Where {P} is a vector of concentrated applied loads and moments.

Equation (1.3) can be reduced to the following form:

$$PI = \frac{1}{2} \{U\}^T [K] \{U\} - \{U\}^T \{Q\}$$

Variations of PI with respect to the reference degrees of freedom will yield:

$$PI = \frac{1}{2} \{U\}^T \{[K] \{U\} - \{Q\}\} = 0 \quad (1.4)$$

From Equation (1.4), the following well known finite element equation is obtained for the unconstrained structure.

$$[K] \{U\} = \{Q\}$$

After application of prescribed displacement boundary conditions, the constrained stiffness matrix is inverted and post-multiplied by the external load vector to obtain unknown displacements as follows.

$$\{U_a\} = [K_{aa}]^{-1} \{Q_a - K_{ab} \{U_b\}\} \quad (1.5)$$

Where

$\{U_a\}$ is a vector of unknown displacements.

$[K_{aa}]$ is a constrained stiffness matrix.

Element internal stresses and forces can be obtained from $\{U_a\}$.

1.4.1.3 Mass Distribution

In the classical analysis of beams and plates, the mass is considered to be a continuous quantity, expressible in term of pounds per unit length or pounds per unit area. In the early analyses of practical airplane structures the mass was still considered a continuous quantity. In the typical Lagrange's equations/Rayleigh-Ritz approach to vibration analysis the product of assumed deflection shapes and the mass was integrated along the span of a wing. With the advent of the digital computer around 1950, new computational techniques emerged, based on matrix notation and matrix algebra. The description of airplane structures became discretized: the deformation is defined only at discrete points. The flexibility of the structure is defined by force-deflection relations only at discrete points. A natural step was to define the mass at the same discrete points. Although there is a mathematical approach to replacing a continuous mass distribution by discrete (lumped) masses at these points, usually a heuristic approach is followed. The heuristic approach is justified, because the accuracy implied by the mathematical approach exceeds the accuracy of the data available.

Although for the vibration analysis it is necessary that the mass characteristics of the structure are described by a matrix based on the same degrees of freedom as the structural model, it is often convenient to do the basic mass discretization in a different grid system. This is especially the case when a finite element model is used. To avoid the need of having to carry along moments of inertia of the discrete masses, the mass grid is rather dense. To avoid computational singularities, there must be at least as many

mass points as there are structural grid points. By expressing the deflection of the mass points in terms of the deflections at the structural grid points, a transformation is obtained that generates a mass matrix consistent with the structural grid.

In the case of a simple beam model, the same mass discretization may be used as for a finite element model. In early design stages, however, it may be more expedient to define the mass, chordwise center of mass position, and radius of gyration of strips of the wing, in a direction perpendicular to the beam.

In addition to the distributed masses, discussed so far, large masses of "rigid" bodies are recognized. A rigid body, in this context, is a body, such as an engine, or a store, of which its own lowest natural frequency is considerably higher than the highest frequency of interest in the flight dynamics analysis to be performed. Such rigid bodies are represented by their total mass, center of mass position and radii of gyration about three axes. Correspondingly, in the structural degrees of freedom, such masses are given three translational and three rotational degrees of freedom.

With the subset of displacement equations established in its particular reference frame in accordance with Equation (1.5), it can be related to other subsets, which might be rotating, by use of the hybrid coordinate approach.

1.4.1.4 Dynamic Degrees-of-Freedom

The usual approach to a flutter analysis is that the dynamics equations are formulated in dynamics degrees of freedom. The dynamics degrees of freedom are discrete displacements in which the flexibility of the airplane can be expressed by a suitable reduction of the stiffness matrix derived for all structural degrees of freedom. Typically the number of dynamics degrees of freedom for half an airplane is 100 to 500. The structural degrees of freedom may number several thousand. The dynamics degrees of freedom are used in a vibration analysis to determine the lowest 10 to 50 natural frequencies and natural modes. The natural modes are used to "modalize" the flutter

equation, i.e., the number of degrees of freedom is reduced from the original 100 to 500 discrete displacements to 10 to 50 modal coefficients. The solution of the flutter equation at a selected speed consists of damping and frequency of in-flight vibration modes and associated eigenvectors of modal coefficients. The modal coefficients determine how much of each vibration mode participates in the flutter solution.

Because flutter may occur at frequencies considerably above the lowest one or two vibration modes, the modalized flutter equation must include several modes above the lowest structural modes. For control system synthesis, however, a reduced order model may be sufficient. Obviously, the control system designer would like to reduce the number of degrees of freedom; he must include to a minimum and include only those modes that affect his design.

1.4.2 Aerodynamics

The emphasis in this study is on low angle-of-attack, high dynamic pressure flight, the region of greatest aeroelastic effect. The scope of the work includes methodology applicable to Mach numbers from low subsonic to high supersonic, and dynamic pressures up to the "never exceed" speed.

Fighter aircraft have experienced stability and control problems in the high dynamic pressure range due to the fading of controls effectiveness as aeroelastic reversal approached with increasing equivalent airspeed. This phenomenon can be accompanied by an opposite effect: increased sensitivity to disturbances, measured by lift curve slope amplification as surface divergence simultaneously approaches. So severe can problems associated with these phenomena become that even robust controls techniques may be ineffective. This situation has been exacerbated by the use of aerodynamic methods that did not correctly model the physical flow.

Section 4 discusses currently employed aerodynamic methodology. This should make the effect of aerodynamics on static aeroelasticity and stability derivatives clearer. Improved understanding should permit control system

designers and aeroelasticians to jointly make more efficient solutions to control system-structural design problems and effect these earlier in the aircraft design cycle.

1.4.3 Control Systems

Except for the use of nonlinear equations in simulations, most control theory applications (modern and classical) are restricted to linear systems. This is justified, because a linearized representation of system dynamics can be considered to be a superimposed small amplitude part of a more accurate model which would include the important nonlinearities of the system. For example, an airplane flying through changing flight conditions is described mathematically by a set of nonlinear aerodynamic curves from which linear stability derivatives are normally derived. A simulation of the exact equations would not include the stability derivatives per se; nevertheless, the derivatives would be represented in the simulation by the slopes of the aerodynamic curves. The resultant dynamics of the simulation would closely approximate those of a linear model, for small motions.

The nonlinear equations of motion can be written as a single vector differential equation

$$\dot{\underline{x}} = \underline{f}(\underline{x}(t), \underline{u}(t))$$

where $\underline{x}(t)$ is the state vector, and $\underline{u}(t)$ is the control vector. The aircraft is trimmed in unaccelerated flight if the state is unchanging, such that:

$$\underline{0} = \underline{f}(\underline{x}_0(t), \underline{u}_0(t))$$

Perturbations from this trimmed condition are characterized by a linear model which is obtained by a Taylor series expansion of the original nonlinear equation about the trimmed state values. The linearized dynamic equation is:

$$\dot{\underline{d}}\underline{x}(t) = \underline{A}(t) \underline{d}\underline{x}(t) + \underline{B}(t) \underline{d}\underline{u}(t)$$

where $A(t)$ and $B(t)$ are Jacobian matrices of derivatives evaluated at the trim condition. All elements of these Jacobian matrices are real scalar variables.

In general, the matrices are time varying; but, in keeping with the assumption that the aircraft is trimmed, the matrices are usually assumed to be constant (over the time scale of the dynamics). Any incremental equations of the above form will hereafter be written with the increment indicator d deleted.

The desired input from the aerodynamic and structural disciplines to the control system engineer are the A and B matrices for all trim conditions representative of the entire flight envelope. If relaxed static stability (RSS) applications are intended, then variations in speed/altitude/weight conditions are expanded to include variations in center-of-gravity conditions to be used in the control law synthesis process.

The elements of the state vector \underline{x} include all of the variables of the flexible model and of the control system, including the actuators and sensors. Those of the control vector \underline{u} contain all of the control commands. If the model is reduced from a larger one, then the extraneous variables of the state vector are removed and the A and B matrices are modified accordingly.

Control Law Synthesis

Although the feedback system, per se, is not a part of the basic airplane, the nature of the control laws in a modern airplane has an important impact on the airframe configuration design.

For example, an airplane with extreme relaxed static stability and an automatic control system can fly successfully with the center of gravity as far aft as 60 percent mean aerodynamic chord (mac), thus permitting a very small tail. The specifications require that the longitudinal control characteristics fall within certain demanding specified boundaries on the appropriate plots: (1) short-period and phugoid frequency and damping, (2)

column-force gradients, and (3) blended normal-acceleration/pitch-rate response histories.

The math model is the state-space equation of the system, including servo and sensor dynamics. A reference eigenstructure (prescribed eigenvalues and eigenvectors) is used for each flight condition to specify the control law by application of the modern control technique called eigenstructure placement. A reference-model for each baseline flight condition (the one with the c.g. at 25 percent \bar{c}) is used to define the desired eigenstructure for each of the other corresponding c.g. conditions.

The control math model in state-space form is shown in Figure 5-1. With the feedback loop closed, the control synthesis method produces the set of feedback gains. The closed-loop state-space equation becomes:

$$\dot{\underline{x}} = (A + BFC) \underline{x}$$

The eigenstructure placement procedure produces the feedback matrix F for each c.g. condition, such that the eigenstructure of the matrix (A + BFC) approximates that of the corresponding A for each baseline condition.

The feedback gains are adjusted to compensate for the nonlinearities in the mechanical part of the control system which is designed to match feel characteristics to the flight condition.

After obtaining the feedback control laws, the synthesis procedure closes the feed-forward paths (Figure 5-1) to obtain a force-gradient transfer function. This is combined with the feel-spring characteristics to obtain the resulting set of feed-forward gains.

Servo and Sensor Dynamics

The behavior of a typical single-stage hydraulic servo operating within its linear range (lightly loaded) can be represented as having a first-order-lag response characteristic. Although the transfer function of a power servo

and its corresponding input series servo should be expected to have real poles, they are sometimes coupled such as to yield a complex pair of poles (damping less than critical). Representation of the higher frequency characteristics (second-order) of electro-hydraulic valves are typically neglected, but might be required when used to control structural modes.

The frequency characteristic of an accelerometer is typically first-order because of a first-order filter inside a high-bandpass force-balancing servo loop which attenuates the response of the seismic element. The servo loop constrains the seismic element within a very small range of displacement. The seismic natural frequency can be neglected because it is well above any of the control modes, including those for controlling structural vibrations.

Rate gyros are second-order at frequencies that can be neglected when controlling the lower structural modes, but must be included for the higher ones.

Actuator Force Equations

The structural dynamics of a control surface couples into the main structure as a function of the applied actuator forces. If the surface is comparatively flexible, then special equations which reflect the servo load must be represented as:

$$F_a = H_c(s) x_c - H_a(s) x_a$$

where F_a is the actuator force; x_a is the elongation of the actuator; and x_c is the commanded elongation. The above expression takes into account all static and dynamic loads applied by the actuator to the connecting points between the airframe and the control surface. These points are included in the state vector of the structural model.

The computation of the above force includes effects due to the hydraulic flow and pressure characteristics of the control valve and of any load stability compensating device. For example, the linearized actuator model used for the analysis of the L-1011 horizontal stabilizer was:

$$F_a = \frac{(a_1s + b_1) x_c - (s^2 + a_2s + b_2) x_a}{(d_2s^2 + d_1s + d_0)}$$

where the coefficients (a's, b's, and d's) are computed from the servo characteristics.

Servo Nonlinearities

As mentioned previously, the hydraulic servos can usually be represented with linear models. In order for this assumption to be acceptable, however, care must be taken that excessive flow rates not be commanded such as to exceed the saturation level corresponding to the maximum valve stroke. If rate saturation does occur, it sharply lowers the rolloff frequency of the linearized first-order model.

Other nonlinear valve effects are due to the parabolic characteristic (flow versus pressure) of an orifice. A trim condition with the quiescent design load near stall is unusual. It occurs only in cases where load limiting is required, such as for spoiler or rudder blowback, or in cases where parallel systems have failed. If operation requires high inertial loads at high frequencies, then the valve's parabolic characteristic becomes very significant; and the model must include some linearized representation, such as a describing function, whereby frequency and phase characteristics are functions of actuator displacement amplitudes.

1.4.4 Aeroelastic Modeling

In this section, a summary of the derivation of a simplified aeroelastic model will illustrate how the equations (structural, aerodynamic, and actuator) are interfaced. Simplifying assumptions are stated as needed; e.g., a particular lumped parameter representation of the structure is assumed.

The development of a reduced-order aeroelastic model begins with an intermediate sized model having more modes than those finally intended; then it is reduced in such a manner as to preserve certain residual effects of the

eliminated modes. The intermediate model results from modalizing and truncating a larger model.

The initial equations define the larger system in terms of the structural composition and the aerodynamic forces which act upon it. The structural part of the model represents all of the main airframe components (wing, fuselage, tail, etc.).

1.4.4.1 The Modalized Equation

Standard procedures, in which the small perturbation dynamics of the airplane are defined in terms of rigid body displacements and natural vibration modes, lead to equations of the following type:

$$\begin{aligned}
 [T^T] \left([M]s^2 + [K] - \frac{\rho V^2}{2} [A] \right) [T] \{q\} = \\
 [T^T] \left((-[M]s^2 + \frac{\rho V^2}{2} [A]) [D] \{d\} + \frac{\rho V^2}{2} [B] \{\alpha\} \right) \quad (1.6)
 \end{aligned}$$

The mass matrix [M], the stiffness matrix [K], and the aerodynamic matrices [A] and [B] are coefficients of displacements of discrete structural nodes.

By means of the modalization matrix [T] and its transpose [T^T], the rigid-body degrees of freedom and the natural vibration modes are accounted for by the modal coefficients of {z}. Control surface deflections are shown separately as {d} and each column of [D] defines a shape corresponding to the associated element of {d}.

1.4.4.2 Modalization

In anticipation of modalizing the system equations, the differential equation of the structural model with n degrees of freedom are written in the matrix form:

$$[M] \{\ddot{z}\} = -[K] \{z\} + \sum_k \{Z_k\} \quad (1.7)$$

where $\sum_k \{Z_k\}$ includes all forces, except the inertial and stiffness forces, which are shown separately.

Modalization begins by finding the n eigenvalues of $[M^{-1}] [K]$, which are all real and positive. The m eigenvectors corresponding to those m frequencies which are considered essential to the intermediate model are computed, and an $n \times m$ modal transformation matrix $[T]$ is formed from the set of eigenvectors. The equations are then transformed to modalized form, having m generalized coordinates of mode shapes $\{q\}$, which are the new variables. The transformation is:

$$\{z\} = [T] \{q\} \quad (1.8)$$

Substituting Equation (1.8) into Equation (1.7) and premultiplying by the transpose of $[T]$:

$$[T^T] [M] [T] \{\ddot{q}\} = -[T^T] [K] [T] \{q\} + [T^T] \sum_k \{Z_k\} \quad (1.9)$$

In a passive flexible system, the inertia and stiffness matrices each are symmetrical; so, with appropriate scaling of its columns, $[T]$ is scaled such that $[T^T] [M] [T] = [I]$. Then $[T^T] [K] [T] = [\Lambda]$ is a diagonal matrix of eigenvalues. This reduces Equation (1.9) to:

$$\{\ddot{q}\} + [\Lambda] \{q\} = \{Q\} \quad (1.10)$$

where:

$$\{Q\} = [T^T] \sum_k \{Z_k\} \quad (1.11)$$

is the generalized force.

1.4.4.3 Forcing Functions

The expression for the forcing functions $\sum_k \{Z_k\}$ includes steady and unsteady forces due to mode dynamics in smooth air, aerodynamic forces in turbulent air, aerodynamic and inertial forces due to the control surface dynamics, and mechanical forces due to the actuator coupling between the control surface and airframe structure.

Aerodynamic Forces

Steady and unsteady aerodynamic forces due to mode dynamics are:

$$\{Z_1\} = \frac{\rho V^2}{2} [A] \{z\} \quad (1.12)$$

where:

$$[A] = [AIC(ik)] \left(\frac{d}{dx} + \frac{1}{V} \frac{d}{dt} \right)$$

$[AIC(ik)]$ is a matrix of aerodynamic influence coefficients, functions of the reduced frequency $k = \omega/V$.

The derivatives represent the set of element angles at each mode and the set of angle-of-attack increments due to the vertical velocities at each mode.

The operator $[A]$ is sometimes denoted as $[A(p)]$, where $p (= sc/V)$ is the nondimensional equivalent of the Laplace operator, $s = \sigma + i\omega$.

Gust Induced Forces

Forces in turbulent air are:

$$\{Z_2\} = \frac{\rho V^2}{2} [B] \{\bar{\alpha}\}$$

where:

$$\{\bar{\alpha}\} = \left[\frac{\bar{v}}{V} \right] \{e^{-ik FS/c}\} \quad (1.13)$$

and, [B] , sometimes denoted as [AIC (ik)], is a matrix of aerodynamic influence coefficients, functions of the reduced frequency $k = \omega c/V$.

Control Forces

Forces due to control surface deflections include both inertial and aerodynamic forces. The revised set of aerodynamic forces is denoted as:

$$\frac{\rho V^2}{2} [A] \{z\} + \{Z_3\} = \frac{\rho V^2}{2} [A] \begin{bmatrix} \{z_1\} \\ \{z_d\} + [R] \{d\} \end{bmatrix} \quad (1.14)$$

where $\{z_d\}$ is the subvector of state variables in $\{z\}$, at whose locations the control surfaces $\{d\}$ are located. The set of deflections $[R] \{d\}$ are superimposed on the motions corresponding to $\{z_d\}$. $[R]$ is a diagonal matrix of radii from the surface hinge lines to the nodes on the surfaces. In the above equation, if the aerodynamic matrix $[A]$ is partitioned, the equation leads to an expression which separates $\{z_3\}$, the control surface aerodynamic forces, from those of the main body:

$$\begin{bmatrix} [A_{11}] & [A_{12}] \\ [A_{21}] & [A_{22}] \end{bmatrix} \begin{bmatrix} \{z_1\} \\ \{z_d\} + [R] \{d\} \end{bmatrix} = [A] \{z\} + [A] [D] \{d\}$$

where:

$$[D] = \begin{bmatrix} [O] \\ [R] \end{bmatrix}$$

Therefore,

$$\{Z_3\} = \frac{\rho V^2}{2} [A] [D] \{d\} \quad (1.15)$$

Similarly, the inertial forces due to the control surface accelerations are separated from those due to other accelerations by partitioning the mass matrix.

$$[M] \{\ddot{z}\} - \{Z\} = [M] \begin{bmatrix} \{\ddot{z}_1\} \\ \{z_d\} + [R] \{d\} \end{bmatrix} = [M] \{\ddot{z}\} + [M] [D] \{\ddot{d}\}$$

$$\{Z_d\} = - [M] [D] \{\ddot{d}\} \quad (1.16)$$

Collecting the forces in the summation from Equations (1.12) through (1.16), and transposing such that the terms which are functions of $\{z\}$ are on the left hand side; then modalizing in accordance with Equation (1.9), yields Equation (1.6).

1.4.4.4 Actuator Interface

The control surface interface in Equation (1.6) is based upon the assumption that loading effects do not delay any actuator, i.e., actuators provide whatever force is required to generate $\{d\}$. If this assumption does not hold for any actuator, then that particular actuator is excluded from $\{d\}$ and an additional force expression instead is added to the right-hand side of Equation (1.6).

A lightly loaded hydraulic actuator can usually be represented by one pole (first-order transfer function) per servo stage. This is not so in the case of a heavily loaded actuator. Both interface types are explained in the following subsections.

Actuator Position Coupling

A particular control surface angle d_i (an element of $\{d\}$ in Equation (1.12)) usually is related to the corresponding command signal d_{ci} as a first-order transfer function:

$$d_i = \frac{1}{\tau_i s + 1} d_{ci} \quad , \quad 1 \leq i \leq k \quad (1.17)$$

With the load force on the hydraulic actuator negligible, the motion of the piston is simply the integral of the servo error; so the transfer function

is a first-order lag with its time constant equal to the loop gain of the servo.

Actuator Force Coupling

The actuator force driving a control surface is computed from a hydraulic servo model which includes the dynamic loading from the aeroelastic model of the surface. The actuator force F_a is related to the actuator displacement X_a and the actuator command x_c by:

$$F_a = H_c(s) x_c - H_a(s) x_a \quad (1.18)$$

Equation (1.18) makes it possible to account for the static and dynamic loads on the control surface due to its own motion and also due to the motion of the main surface to which it is attached. The transfer functions $H_c(s)$ and $H_a(s)$ are computed from the servo characteristics. The force F_a is applied by the actuator to the connecting points z_f and z_s on the fuselage and control surface respectively. The points are included in the degrees of freedom $\{z\}$ of the structural model and are related to Equation (1.18) through the actuator displacement:

$$x_a = z_s - z_f \quad (1.19)$$

Figure 1-5 illustrates the meaning of the above equation. The figure shows interface between one of four activators and the dynamic inertial load model of a symmetric flexible control surface.

The vector $\{z_1\}$ is partitioned further, such that:

$$\{z_1\} = \begin{bmatrix} \{z_2\} \\ \{z_a\} \end{bmatrix} \quad \text{where} \quad \{z_a\} = \begin{bmatrix} z_f \\ z_s \end{bmatrix} \quad (1.20)$$

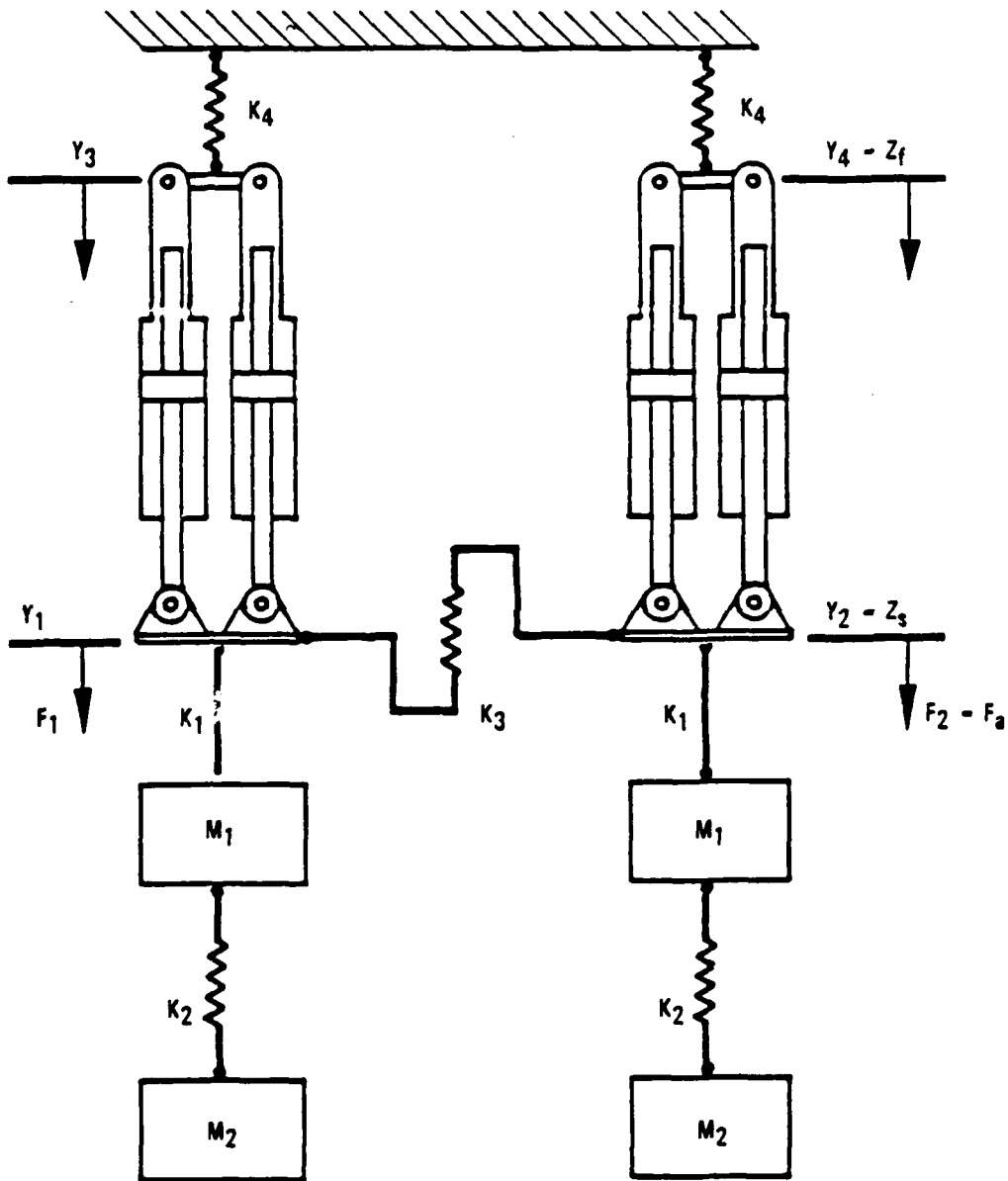


Figure 1-5. Simplified Load Dynamics Model - Actuator Interface

1.4.4.5 Equations in State-Space Form

When Equation (1.6) is changed to the state space format, it is necessary that $[A(p)]$ and $[AIC(ik)] \{e^{-ik FS/c}\}$ be approximated by algebraic functions of p . A third-degree polynomial approximation might be adequate for the lower part of the frequency range of interest. The usual approximation, however, recognizes the presence of aerodynamic lag by the inclusion of $p/(p+b)$ terms.

Real and imaginary values at discrete frequencies of all terms which include $[AIC(ik)]$ are used to determine the coefficients of each third-order polynomial approximation.

Applying the third-order polynomial approximation, the aerodynamic force and gust force in Equations (1.12) and (1.13) reduce respectively to:

$$\frac{\rho V^2}{2} [A] \{z\} = ([A_0] + [A_1]s + [A_2]s^2 + [A_3]s^3) \{z\} \quad (1.21)$$

and

$$\frac{\rho V^2}{2} [B] \{\bar{\alpha}\} = ([B_0] + [B_1]s + [B_2]s^2 + [B_3]s^3) \{\bar{\alpha}\} \quad (1.22)$$

The $[A_i]$'s and $[B_i]$'s are computed least-square fits to the desired functions.

Dryden Gust Representation

In this illustration a 2-D gust is assumed. It has a Dryden power spectral density. Then the expression for the gust angle $\{\bar{\alpha}\}$ is obtained by considering white noise $n(t)$ with a unit power spectral density to pass through a second-order filter whose transfer function corresponds to the Dryden power spectral density for vertical gusts.

In Equation (1.13), $\{\bar{\alpha}\}$ is defined as $[\frac{\bar{w}}{\bar{v}}] \{e^{-ik FS/c}\}$. Here the definition is changed to:

$$\{\bar{\alpha}\} = \{e^{-ik} FS/c\} \varpi/V$$

where ϖ is the scalar RMS intensity of the gust.

The transfer function of the second-order filter is converted to state-space form by the same method that will be shown to convert that of the heavily-loaded actuator. The resulting state-space equation is:

$$s\{\varpi\} = [W] \{\varpi\} + [N] n \quad (1.23)$$

The vector $\{\varpi\}$ is included in the force expression Equation (1.22) as

$$\frac{\rho V^2}{2} [B] \{\bar{\alpha}\} = ([B_0] + [B_1]s + [B_2]s^2 + [B_3]s^3) [G] \{\bar{w}\} \quad (1.24)$$

where $[G]$ is an $n \times 2$ matrix whose first column is all 1's and whose second column is all 0's, because the two elements of $\{\varpi\}$ are $\bar{\alpha}$ and a dummy variable.

Lightly-Loaded Actuator Displacements

The state-space equation for the set of control-surface transfer functions, Equation (1.17), is obtained by cross multiplying each individual transfer function and forming the k-vector.

$$s\{d\} = [\tau_d^{-1}] (-\{d\} + \{d_c\}) \quad (1.25)$$

where $[\tau_d]$ is the diagonal matrix of time constants.

Heavily Loaded Actuator Forces

The expression for the actuator force coupling is expressed in state-space form using the coefficients of the expanded versions of the transfer functions in Equation (1.18).

$$F_a = \frac{(a_1 s + b_1) x_c - (s^2 + a_2 s + b_2) x_a}{d_2 s^2 + d_1 s + d_0}$$

Cross multiplying and separating out the zero-derivative terms, let:

$$d_2 \dot{F}_b = -d F_a + b_1 x_c - b_2 x_a$$

After integrating the remaining terms,

$$d_2 \dot{F}_a = d_1 F_a + a_1 x_c - \dot{x}_a - a_2 x_a + d_2 F_b$$

Recalling from Equations (1.19) and (1.20) that $x_a = [-1 \ 1] \{z_a\}$, then the actuator force is represented by the state-space equation:

$$\{\dot{f}\} = [F_1] \{f\} + [\hat{F}_2] \{\dot{z}_a\} + [F_3] \{\hat{z}_a\} + \{F_4\} x_c \quad (1.26)$$

where:

$$\{f\} = \begin{bmatrix} F_a \\ F_b \end{bmatrix}, \quad [F_1] = \begin{bmatrix} -d_1 & d_2 \\ -d_0 & 0 \end{bmatrix} / d_2, \quad [\hat{F}_2] = \begin{bmatrix} 1 & -1 \\ 0 & 0 \end{bmatrix} / d_2$$

$$[\hat{F}_3] = \begin{bmatrix} a_2 & -a_2 \\ b_2 & -b_2 \end{bmatrix} / d_2, \quad \text{and } \{F_4\} = \begin{bmatrix} a_1 \\ b_1 \end{bmatrix} / d_2$$

The matrices in Equation (1.26) are made compatible with the rest of the system by fitting them into matrix coefficients of the n vector $\{z\}$ as follows:

$$\{\dot{f}\} = [F_1] \{f\} + [F_2] \{\dot{z}\} + [F_3] \{z\} + \{F_4\} x_c \quad (1.27)$$

where:

$$\{z\} = \begin{bmatrix} \{z_2\} \\ \{z_a\} \\ \{z_d\} \end{bmatrix}, \quad [F_2] = \begin{bmatrix} [0] & [\hat{F}_2] & [0] \\ [0] & [\hat{F}_3] & [0] \end{bmatrix}$$

The force acting on points $\{z_a\}$ in $\{z\} = \begin{bmatrix} \{z_2\} \\ z_f \\ z_s \\ \{z_d\} \end{bmatrix}$ is $[F_a] \{f\}$.

where:

$$[F_a] = \begin{bmatrix} \{0\} & \{0\} \\ 1 & 0 \\ -1 & 0 \\ \{0\} & \{0\} \end{bmatrix}; \quad \text{so } [F_a] \{f\} = \begin{bmatrix} \{0\} \\ F_a \\ F_a \\ \{0\} \end{bmatrix} \quad (1.28)$$

This force is added into Equation (1.6) which then becomes:

$$\begin{aligned} [T^T] [M] \{T\} \{q\} + [T^T] [K] \{T\} \{q\} - [T^T] \frac{\rho V^2}{2} [A] \{T\} \{q\} = \\ [T^T] \left(\frac{\rho V^2}{2} ([B] \{\bar{\alpha}\} + [A] [D] \{d\}) - [M] [D] \{d\} \right) + [T^T] [F_a] \{f\} \end{aligned} \quad (1.29)$$

Control Surface Deflection in Expanded State-Space Form

In a form similar to that of Equations (1.21) and (1.22), the polynomial representation of the actuator forces due to the surface deflections is:

$$\frac{\rho V^2}{2} [A] [D] \{d\} = ([C_0] + [C_1]s + [C_2]s^2 + [C_3]s^3) \{d\} \quad (1.30)$$

Then from Equations (1.29), (1.9), (1.11), (1.21), (1.24), (1.28), and (1.30), the generalized force is:

$$\begin{aligned}
\{Q\} &= [T^T] ([A_0] + [A_1]s + [A_2]s^2 + [A_3]s^3) [T] \{q\} \\
&+ [T^T] ([B_0] + [B_1]s + [B_2]s^2 + [B_3]s^3) [G] \{w\} \\
&+ [T^T] ([C_0] + [C_1]s + [C_2]s^2 + [C_3]s^3) \{d\} - [T^T] [M] [D]s^2 \{d\} \\
&+ [T^T] [F_a] \{f\}
\end{aligned}$$

where from Equation (1.27), with $[T^T] [M] [T] = I$, (1.31)

$$\{\dot{f}\} = [F_1] \{f\} + [F_2] [T] \{\dot{q}\} + [F_3] [T] \{q\} + \{F_4\} x_c$$

The notation is simplified by:

$$[T^T] [A_0] [T] = [\bar{A}_0], [T^T] [B_0] = [\bar{B}_0], [F_2] [T] = [\bar{F}_2], \text{ etc.}$$

Substituting Equation (1.31) into Equation (1.10), then transposing and collecting some of the coefficients of $\{q\}$ yields:

$$\begin{aligned}
&(-[\bar{A}_3]s^3 + ([I] - [\bar{A}_2])s^2 - [\bar{A}_1]s + [\Lambda] - [\bar{A}_0]) \{q\} = [F_a] \{f\} \\
&+ ([\bar{B}_3]s^3 + [\bar{B}_2]s^2 + [\bar{B}_1]s + [\bar{B}_0]) [G] \{w\} \\
&+ ([\bar{C}_3]s^3 + [\bar{C}_2]s^2 + [\bar{D}]s^2 + [\bar{C}_1]s + [\bar{C}_0]) \{d\}
\end{aligned} \tag{1.32}$$

and

$$s\{f\} = [\bar{F}_2] s\{q\} + [\bar{F}_3] \{q\} + [F_1] \{f\} + \{F_4\} x_c \tag{1.33}$$

The complete set of equations describing the system in state-space form comprises Equations (1.32), (1.33), (1.25), and (1.33).

With each of the above equations written with only the highest order of s , along with its coefficient, on the left hand side, the set is expressed as:

$$\hat{C}\{\dot{x}\} = [\hat{A}]\{x\} + [\hat{B}]\{u\} \quad (1.34)$$

where $\{x\}$ is the vector of state variables and $\{u\}$ is the vector of control variables.

Since the matrix coefficient on the left-hand side must be inverted, it is necessary that it be nonsingular. Therefore, an expression must be found to define higher derivatives of $\{w\}$ and $\{\bar{\alpha}\}$. This is accomplished by adding additional lag terms in the transfer function for $\bar{\alpha}/n$. Additional lag terms need not be physically justified but can be chosen easily if it is desired to represent any known characteristics in the higher frequency ranges.

The third-order polynomial representation of unsteady aerodynamic influences permits good accuracy only through a certain frequency band; but at higher frequencies, the model is not correct. Indeed, some of the extraneous poles resulting from the polynomial might be on the right-hand-side of the s plan (unstable). These must be removed from the transfer functions in a manner that will retain their residual influences in the lower frequency range where the model is considered to be accurate.

1.4.4.6 The Output System

Any control law which is based upon a modalized system must be reflected back to the original coordinate system. Assuming that "sensors" of the dynamic modes (q) are the only signal sources in the control law, then the vector of feedback signals $[F]$ (q) would be computed as follows. Let $[H]$ be an $m \times n$ matrix of 1's and 0's used to select the $\{z\}$ elements at which the sensors will be placed.

Now since:

$$[H] \{z\} = [H] [T] \{q\}$$

then,

$$[F] \{q\} = [F] ([H] [T])^{-1} [H] \{z\}$$

In the matrix of feedback gains, $([F] ([H] [T])^{-1} [H])$ all the elements are zero except from the selected sensors. The best locations of the sensors is determined by observation of the mode shapes.

1.4.4.7 Model Order Reduction

It is common practice to reduce the order of Equation (1.6) by excluding the high frequency modes from $\{q\}$. Usually the required accuracy of flutter related analyses dictates the number of modal degrees of freedom to be retained.

The state-space model, if obtained directly from a structural dynamics equation of sufficiently large order to properly represent flutter modes, usually is of very large order, say 100 or more. Once the large-order model is available, it can be reduced to a significantly smaller order by one of several available methods.

Two entirely different approaches to model reduction of linear time-invariant systems are summarized here. They are: 1) balanced approximation, and 2) spectral decomposition. The balanced approximation approach is better known, having been thoroughly developed and discussed in the technical literature since about 1979, at which time the importance of model reduction, as applied to multi-input/multi-output systems, had barely been recognized [10]. The spectral decomposition approach was developed and used by Lockheed, beginning in 1974, during studies that led to the development of the L-1011 Active Control System [5], [6].

More recently, Lockheed has been examining two forms of frequency compensation which supplement the balanced approximation approach: but these topics are beyond the scope of this report. The first of the frequency compensation methods, developed by Honeywell, applies a balancing algorithm to

a full model which includes frequency-dependent weighting. The second method, developed by the University of Southern California, truncates the model using approximate balancing; then applies the balancing algorithm to the truncated after bilinear frequency weighting.

SECTION 2
LINEARIZATION OF FLEXIBLE AIRCRAFT HYBRID-COORDINATE
DYNAMIC EQUATIONS AND INCLUSION OF AERODYNAMIC
AND GRAVITATION LOADS

2.1 INTRODUCTION

2.1.1 Scope

The complete dynamic equations of motion for a flexible aircraft (of arbitrary configuration undergoing arbitrary motion and experiencing an arbitrary load) using a hybrid-coordinate system has been derived by this author. The effort here is to examine these results in light of practical applications.

Specifically, the complete hybrid-dynamic coordinate equations will be linearized and expanded to include the effects of aerodynamic and gravitational forces. The former is done by keeping track of a judicious choice of assumptions. The latter is not a detailed aerodynamic development, but rather a relatively general method in which aerodynamic forces (which are functions of the structural motion) may be directly accounted for. Gravitational forces are accounted for directly and completely. In addition, several examples are investigated to test the validity of these results.

2.1.2 Development Overview

Since the development herein is a continuation of that of Reference 1 the variable notation used is followed as closely as possible. Figure 2-1 summarizes the notation used in this report. Specific variables and operators unique to this report are defined as needed in the text (mostly in Paragraph 2.1.4). A summary of the basic symbol notation used is listed in Figure 2-1; and summary of the vectors and vector bases used is listed in Figure 2-2. For a complete list of symbols see "List of Symbols" at the end of this report.

This section will present a summary of the development of the complete hybrid-coordinate dynamic equations. The first part is a detailed description

- V Capital or lower case: scalar quantity, or identifies a point or body.
- V_j Subscripted: matrix element, or identifies a point or sub-body.
- V Underlined: vector.
- V_j Underlined and subscripted: vector component.
- D Double underlined: dyadic.
- {e} Underlined and braced: unit orthogonal vector base.
- V** Bold: column or square matrix.
- { } Braces: column matrix, or additional parentheses.
- [] Brackets: square matrix, or additional parentheses.
- \mathbf{A}^T Superscript T: matrix transpose.
- \mathbf{A}^{-1} Superscript -1: matrix inverse.
- \mathbf{A}' Prime: Matrix expanded to j partitions of \mathbf{A} ($j=n, n-1$).
- $\bar{\mathbf{A}}$ Over-bar: Matrix associated with reduced variable.
- \mathbf{A}_{jk} Double subscript: Matrix representing result on j due to input at k.
- \mathbf{A}_0 Subscript 0: quasi-static component of variable.
- $\Delta \mathbf{A}$ Leading Δ : perturbation component of variable.
- \mathbf{A}_a Pre-superscript a: variable associated with aerodynamic model.

Any operator superscripting a closing parenthesis acts on the contents of the parentheses as a whole.

Figure 2-1. Basic Symbol Notation Used

FOR THE STRUCTURAL MODEL:

- (i) inertial reference frame.
- (\underline{b}) reference frame fixed to body B.
- (\underline{a}) reference frame fixed to body A.
- (\underline{a}_s) reference frame fixed to rigid sub-body A_s .
- θ direction cosine relating (\underline{b}) relative to (i).
- C direction cosine relating (\underline{a}) relative to (\underline{b}).
- C_s direction cosine relating (\underline{a}_s) relative to (\underline{a}).
- Γ rotation of (\underline{b}) relative to (i): defined in (\underline{b}).
- $\underline{\Gamma}_B$ rotation of (\underline{a}) relative to (\underline{b}): defined in (\underline{a}).
- $\underline{\Gamma}_s$ rotation of (\underline{a}_s) relative to (\underline{a}): defined in (\underline{a}_s).
- \underline{x} defined in (i).
- \underline{r} defined in (\underline{b}).
- \underline{r}_s defined in (\underline{b}).
- \underline{u}_s defined in (\underline{a}).
- \underline{r}_s defined in (\underline{a}).

FOR THE AERODYNAMIC MODEL:

- $^a(\underline{a}_{s0})$ reference frame fixed to panel load point.
- $^a(\underline{a}_{s1})$ reference frame fixed to panel normal wash point.
- $^a C_{s0}$ direction cosine matrix relating $^a(\underline{a}_{s0})$ to (\underline{b}).
- $^a C_{s1}$ direction cosine matrix relating $^a(\underline{a}_{s1})$ to (\underline{b}).
- $^a C_{s\infty}$ direction cosine matrix relating relative velocity to $^a(\underline{a}_{s0})$.
- $^a \underline{\beta}_{s0}$ rotation of $^a(\underline{a}_{s0})$ relative to (\underline{b}): defined in $^a(\underline{a}_{s0})$.
- $^a \underline{\beta}_{s1}$ rotation of $^a(\underline{a}_{s1})$ relative to (\underline{b}): defined in $^a(\underline{a}_{s1})$.
- $^a \underline{\beta}_{s\infty}$ rotation of relative velocity relative to $^a(\underline{a}_{s0})$: defined relative to relative velocity.
- $^a \underline{u}_s$ defined in (\underline{b}).
- $^a \underline{r}_s$ defined in (\underline{b}).

Figure 2-2. Vectors and Bases Summary

of the vehicle model. The second part is a list of the important steps in the developed of the equations.

Linearization of the general dynamic equations of motion is considered first. This will be done in two steps: First, the coordinate transformations are examined more closely and approximated (Paragraph 2.2.1). Then, the independent variables are broken down into two parts: quasi-static and perturbation components (Paragraphs 2.2.2 and 2.2.3 respectively).

In Paragraph 2.3 two external loads are investigated. The aerodynamic forces are considered in Paragraph 2.3.1. First, a generic aerodynamic element model is conceived. Then, this model is set up so as to be incorporated into the dynamic equations of motion. A similar procedure is used in Paragraph 2.3.2 for the incorporation of the gravitational forces into the dynamic equations of motion.

In the first part of Paragraph 2.4.2 the hybrid-coordinate equations are evaluated under rigid body assumptions. The simplified results are then compared to classical developments for the rigid body stability derivatives. In the second part of Paragraph 2.4.2 a simple test case is evaluated. Each variable is tracked so as to bring a better understanding of how they affect the hybrid-coordinate equations. Dynamic equations are also developed relative to a Newtonian reference frame for the same model using classical techniques and these results are compared with the hybrid-coordinate results.

2.1.3 Hybrid-Coordinate Definition

Consider a flexible aircraft, Body A, attached to a massless rigid Body B at a Point Q (See Figure 2-3). The aircraft is idealized as a collection of linear-elastically inter-connected (such that the component internal restoring force, stress, is proportional to the component structural deformation, strain), discrete rigid sub-bodies, A_s , $s=1, \dots, n$. Body B, being massless, can be any arbitrary shape - internal and/or external to Body A.

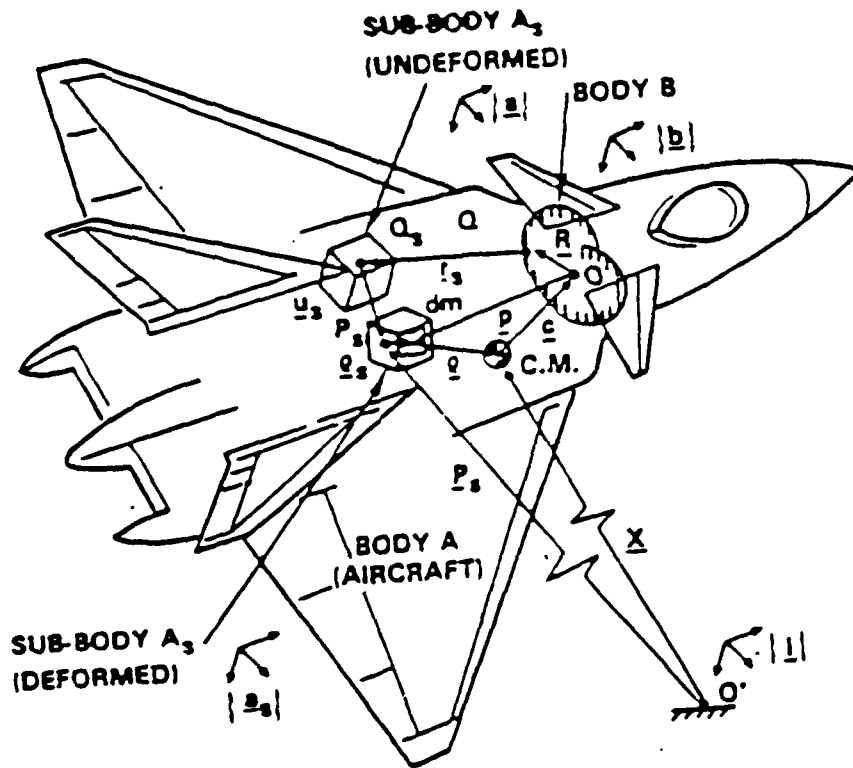


Figure 2-3. Discrete-Parameter Aircraft Element Coordinates

It is convenient to describe the motion of each rigid sub-body, element, A_S , relative to a set of dextral orthogonal unit vectors \underline{a}_1 , \underline{a}_2 , and \underline{a}_3 fixed in reference to Body A prior to deformation. Likewise \underline{b}_1 , \underline{b}_2 , and \underline{b}_3 are fixed to Body B and \underline{i}_1 , \underline{i}_2 , and \underline{i}_3 are fixed to the inertial reference frame. These unit vectors are written as:

$$\{\underline{a}\} = \begin{Bmatrix} \underline{a}_1 \\ \underline{a}_2 \\ \underline{a}_3 \end{Bmatrix} \quad \{\underline{b}\} = \begin{Bmatrix} \underline{b}_1 \\ \underline{b}_2 \\ \underline{b}_3 \end{Bmatrix} \quad \{\underline{i}\} = \begin{Bmatrix} \underline{i}_1 \\ \underline{i}_2 \\ \underline{i}_3 \end{Bmatrix} \quad (2.1)$$

These arrays are related to each other by direction cosine matrices \mathbf{C} and $\mathbf{\Theta}$ such that:

$$\begin{aligned} \{\underline{b}\} &= \mathbf{\Theta}\{\underline{i}\} \quad \text{or} \quad \{\underline{i}\}^T = \{\underline{b}\}^T \mathbf{\Theta} \\ \{\underline{a}\} &= \mathbf{C}\{\underline{b}\} \quad \text{or} \quad \{\underline{b}\}^T = \{\underline{a}\}^T \mathbf{C} \quad \text{and} \quad \{\underline{i}\}^T = \{\underline{a}\}^T \mathbf{C} \mathbf{\Theta} \end{aligned} \quad (2.2)$$

where

$$C_{kl} = (\underline{a}_{k-1}^T \underline{b}_l) / |\underline{a}_k| |\underline{b}_l| \quad k, l = 1, 2, 3$$

and,

$$\Theta_{kl} = (\underline{b}_{k-1}^T \underline{i}_l) / |\underline{b}_k| |\underline{i}_l| \quad k, l = 1, 2, 3$$

The inertial position vector, \underline{P}_S , of element A_S (the translation from Point Q_S to Point P_S) can be described as a summation of the deflection from the undeformed state, \underline{u}_S ; the undeformed position relative to the constraint Point Q, \underline{r}_S (See Figure 2-4); Point Q's position relative to the reference Point O of Body B, \underline{R} ; Body B's position relative to the center of mass (CM) of the vehicle, \underline{c} ; and the vehicle's CM inertial position, \underline{X} (See Figure 2-5). As shown in Figure 2-4 the inertial position vector, \underline{P}_S , may be written as:

$$\underline{P}_S = \underline{X} + \underline{c} + \underline{R} + \underline{r}_S + \underline{u}_S \quad (2.3)$$

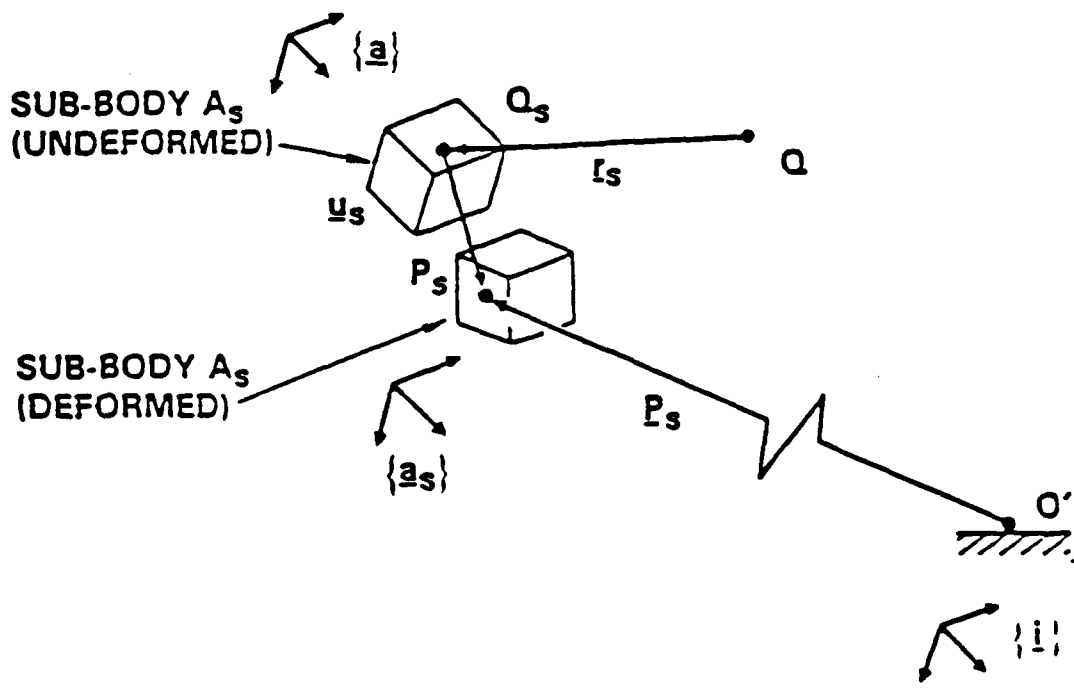


Figure 2-4. Rigid Sub-Body Local Coordinates

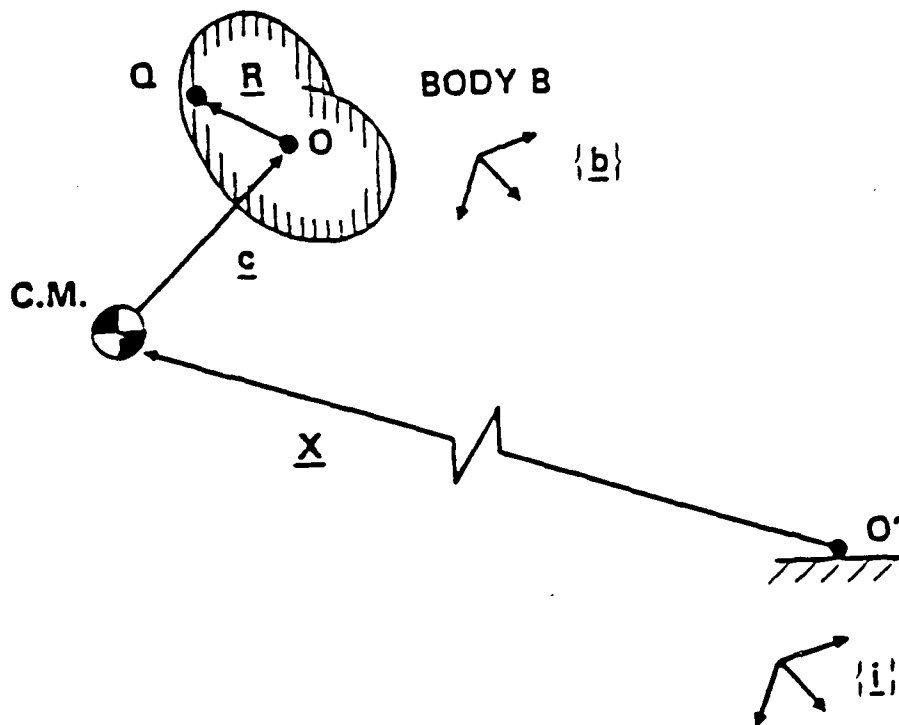


Figure 2-5. Aircraft Inertial Coordinates

where it is obvious to describe \underline{X} in terms of $\{\underline{i}\}$, \underline{c} and \underline{R} in terms of $\{\underline{b}\}$, and \underline{r}_S and \underline{u}_S in terms of $\{\underline{a}\}$. This series of position vectors can now be represented as column matrices premultiplied by the transpose of the appropriate vector base:

$$\underline{X} = \{\underline{i}_1, \underline{i}_2, \underline{i}_3\} \begin{Bmatrix} X_1 \\ X_2 \\ X_3 \end{Bmatrix} = \{\underline{i}\}^T \underline{X} \quad (2.4a)$$

$$\underline{c} = \{\underline{b}_1, \underline{b}_2, \underline{b}_3\} \begin{Bmatrix} c_1 \\ c_2 \\ c_3 \end{Bmatrix} = \{\underline{b}\}^T \underline{c} \quad (2.4b)$$

$$\underline{R} = \{\underline{b}_1, \underline{b}_2, \underline{b}_3\} \begin{Bmatrix} R_1 \\ R_2 \\ R_3 \end{Bmatrix} = \{\underline{b}\}^T \underline{R} \quad (2.4c)$$

$$\underline{r}_S = \{\underline{a}_1, \underline{a}_2, \underline{a}_3\} \begin{Bmatrix} r_{S1} \\ r_{S2} \\ r_{S3} \end{Bmatrix} = \{\underline{a}\}^T \underline{r}_S \quad (2.4d)$$

$$\underline{u}_S = \{\underline{a}_1, \underline{a}_2, \underline{a}_3\} \begin{Bmatrix} u_{S1} \\ u_{S2} \\ u_{S3} \end{Bmatrix} = \{\underline{a}\}^T \underline{u}_S \quad (2.4e)$$

In addition, a set of dextral orthogonal unit vectors \underline{a}_{S1} , \underline{a}_{S2} , and \underline{a}_{S3} are defined fixed relative to its corresponding rigid sub-body, A_S . As was done for $\{\underline{a}\}$, $\{\underline{b}\}$, and $\{\underline{i}\}$ in Equation (2.1), write this new vector base is written as:

$$\{\underline{a}_S\} = \begin{Bmatrix} \underline{a}_{S1} \\ \underline{a}_{S2} \\ \underline{a}_{S3} \end{Bmatrix} \quad (2.5)$$

This new vector base, $\{\underline{a}_S\}$, is related to the $\{\underline{a}\}$ vector base via direction cosine matrices, C_S ; as are $\{\underline{a}\}$ to $\{\underline{b}\}$ and $\{\underline{b}\}$ to $\{\underline{i}\}$ via C and Θ respectively:

$$\{\underline{a}_S\} = C_S \{\underline{a}\} \quad (2.6)$$

The rotational deformation of each element, $\underline{\beta}_S$, can be defined relative to $\{\underline{a}_S\}$ and be represented as a column matrix of $\underline{\beta}_S$ component magnitudes premultiplied by the transpose of $\{\underline{a}_S\}$; as was done for the vectors defined in Equations (2.4):

$$\underline{\beta}_S = \{\underline{a}_{S1}, \underline{a}_{S2}, \underline{a}_{S3}\} \begin{Bmatrix} \beta_{S1} \\ \beta_{S2} \\ \beta_{S3} \end{Bmatrix} = \{\underline{a}_S\}^T \underline{\beta}_S \quad (2.7)$$

The position of any differential mass element, dm , relative to the vehicle center of mass, \underline{p} , is expanded as (See Figure 2-6):

$$\begin{aligned} \underline{p} &= \underline{c} + \underline{R} + \underline{r}_S + \underline{u}_S + \underline{\rho}_S \\ &= \underline{c} + \underline{p} \end{aligned} \quad (2.8)$$

where \underline{c} , \underline{R} , \underline{r}_S , and \underline{u}_S are as before and $\underline{\rho}_S$ is the vector from the center of mass of sub-body A_S to the differential mass, dm , in A_S .

Likewise, the inertial rotational velocity of each sub-body, $\underline{\omega}_S$, is expanded as:

$$\underline{\omega}_S = \underline{\omega}^S + \underline{\omega}^a + \underline{\omega} \quad (2.9)$$

where $\underline{\omega}^S = \{\underline{a}_S\}^T \underline{\omega}^S$ is the angular velocity of the $\{\underline{a}_S\}$ reference frame with respect to the $\{\underline{a}\}$ reference frame, $\underline{\omega}^a = \{\underline{a}\}^T \underline{\omega}^a$ is the angular velocity of the $\{\underline{a}\}$ reference frame with respect to the $\{\underline{b}\}$ reference frame, and $\underline{\omega} = \{\underline{b}\}^T \underline{\omega}$ is the inertial angular velocity of the $\{\underline{b}\}$ reference frame. The angular sub-body deformation, $\underline{\beta}_S$, and the angular element velocity are defined relative to the same vector base, $\{\underline{a}_S\}$. Thus:

$$\underline{\omega}^S = \frac{d}{dt} \underline{\beta}_S = \{\underline{a}_S\}^T \dot{\underline{\beta}}_S \quad (2.10)$$

where the superscript on the derivative operator implies differentiation with respect to the $\{\underline{a}_S\}$ reference frame (See Paragraph 2.1.4)

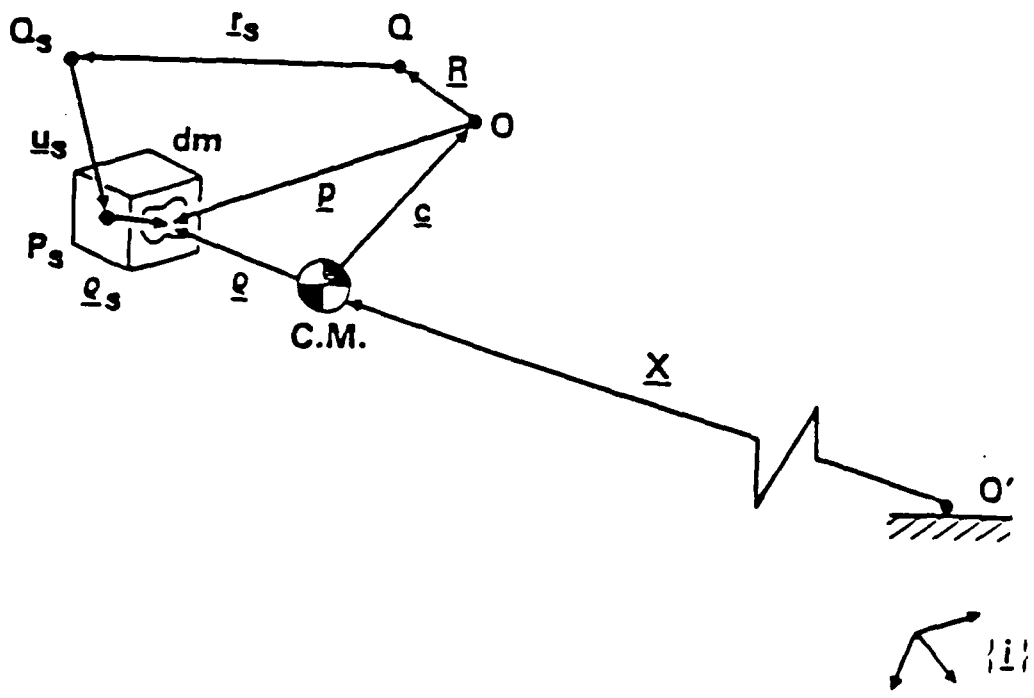


Figure 2-6. Differential Element Coordinates

2.1.4 Operators

Before summarizing the development of the dynamic equations it is necessary to define the operators and operations that were used. The most common fundamental identity used is that of the vector/dyadic differential calculus identity:

$$\frac{f1}{dt} \underset{-}{d} \underset{-}{V} = \frac{f2}{dt} \underset{-}{d} \underset{-}{V} + \underset{-}{\omega} \underset{-}{X} \underset{-}{V} \quad (2.11)$$

$$\frac{f1}{dt} \underset{=}{d} \underset{=}{D} = \frac{f2}{dt} \underset{=}{d} \underset{=}{D} + \underset{=}{\omega} \underset{=}{X} \underset{=}{D} - \underset{=}{D} \underset{=}{X} \underset{=}{\omega} \quad (2.12)$$

where $\underset{-}{V}$ is any vector, $\underset{=}{D}$ is any dyadic, $\underset{-}{\omega} \underset{-}{X} \underset{-}{f2}$ is the angular velocity of any reference frame $f2$ relative to any other reference frame $f1$, and the superscript preceding the derivative operator indicates the reference frame of differentiation. Equations (2.11) and (2.12) require the cross product of two arbitrary vectors, $\underset{-}{V}$ and $\underset{-}{W}$, be expressed in matrix terms:

$$\underset{-}{V} \underset{-}{X} \underset{-}{W} = \{e\}^T \underset{-}{V} \underset{-}{X} \{e\}^T \underset{-}{W} = \{e\}^T \underset{-}{\tilde{V}} \underset{-}{W} \quad (2.13)$$

where:

$$\underset{-}{V} \equiv \begin{Bmatrix} V_1 \\ V_2 \\ V_3 \end{Bmatrix} \quad \underset{-}{W} \equiv \begin{Bmatrix} W_1 \\ W_2 \\ W_3 \end{Bmatrix} \quad \underset{-}{\tilde{V}} \equiv \begin{bmatrix} 0 & -V_3 & V_2 \\ V_3 & 0 & -V_1 \\ -V_2 & V_1 & 0 \end{bmatrix} \quad (2.14)$$

where the tilde operator ($\tilde{\quad}$) over a three by one matrix represents the corresponding skew-symmetric three by three matrix, as expanded in Equation (2.14). A tilde operator over a closing parenthesis implies the tilde operation on the contents of the parenthesis as a whole.

Next, a set of Boolean operator matrices are defined to facilitate combining all the degrees-of-freedom into a single matrix equation. These are the carrot operator ($\hat{\quad}$), the sigma operator (Σ_n), and the pi operator (Π_n) defined as:

$$\begin{pmatrix} A_S \end{pmatrix}^n \equiv \begin{bmatrix} A_1 & 0 & \dots & 0 \\ 0 & A_2 & \dots & 0 \\ \vdots & \vdots & & \vdots \\ 0 & 0 & \dots & A_n \end{bmatrix} \quad \text{note} \quad \begin{pmatrix} A \end{pmatrix}^n = \begin{bmatrix} A & 0 & \dots & 0 \\ 0 & A & \dots & 0 \\ \vdots & \vdots & & \vdots \\ 0 & 0 & \dots & A \end{bmatrix} \quad (2.15)$$

$i \times i$ $i \times i$ $i \times i$ $i \times i$

and,

$$\begin{pmatrix} E(i) \end{pmatrix}^n \equiv \begin{bmatrix} E(i) & E(i) & \dots & E(i) \\ E(i) & E(i) & \dots & E(i) \\ \vdots & \vdots & & \vdots \\ E(i) & E(i) & \dots & E(i) \end{bmatrix} \quad (2.16)$$

$i \times i$ $i \times i$ $i \times i$ $i \times i$

$$= \begin{Bmatrix} E(i) \\ E(i) \\ \vdots \\ E(i) \end{Bmatrix} \{ E(i) \ E(i) \ \dots \ E(i) \} \equiv \begin{pmatrix} E(i) \end{pmatrix}^n \begin{pmatrix} E(i) \end{pmatrix}^{nT}$$

$i \times i$ $i \times i$ $i \times i$

where

$$E(i) = \begin{bmatrix} 1 & & 0 \\ & \ddots & \\ 0 & & 1 \end{bmatrix}_{i \times i}$$

is an $i \times i$ unit matrix.

Finally, vector components (including that of the independent variables) may be combined in a manner similar to the Boolean operator matrices. These column matrices are denoted by a superscript ':

$$\begin{matrix} q' \\ 3n \times 1 \end{matrix} = \begin{Bmatrix} q'_1 \\ q'_2 \\ \vdots \\ q'_n \end{Bmatrix} = \begin{Bmatrix} q'_{11} \\ q'_{12} \\ q'_{13} \\ q'_{21} \\ \vdots \\ q'_{n2} \\ q'_{n3} \end{Bmatrix} \quad (2.17)$$

q'_k is 3×1 q'_{ki} is the i^{th} component of q'_k

2.1.5 Development of Hybrid-Coordinate Dynamic Equations

The development of the dynamic equations is in four parts: First, the flexible vehicle equations; Next, the total vehicle equations; Then, the auxiliary equations; And finally, the complete dynamic equations. In the first two parts the development begins from first principles - the Newton-Euler equations:

$$\begin{aligned} \underline{F}_S = \frac{d}{dt} (m_S \dot{\underline{P}}_S) = m_S \ddot{\underline{P}}_S \quad \text{and} \quad \underline{F} = \frac{d}{dt} (M_A \underline{V}) = M_A \underline{a} \\ \underline{T}_S = \frac{d}{dt} \underline{H}_S = \underline{I}_S \frac{d\omega_S}{dt} \quad \text{and} \quad \underline{T} = \frac{d}{dt} \underline{H} = \underline{I} \dot{\omega} \end{aligned} \quad (2.18)$$

where m_S is the mass of the s rigid sub-body, M_A is the vehicle mass, \underline{I}_S and \underline{I} are the s rigid sub-body and the vehicle moments of inertia matrices respectively; $\underline{F}_S = \{\underline{a}\}^T \underline{F}_S$ and $\underline{T}_S = \{\underline{a}\}^T \underline{T}_S$ are the resultant external force and torque applied to the s subbody; $\underline{F} = \{\underline{b}\}^T \underline{F}$ and $\underline{T} = \{\underline{b}\}^T \underline{T}$ are the resultant external force and torque applied to the vehicle; and \underline{P}_S , \underline{V} , \underline{a} , \underline{H}_S , and \underline{H} are the inertial sub-body location, total vehicle velocity, total vehicle acceleration, and angular momentum of the s sub-body and total vehicle, respectively; all with respect to the corresponding body's center of mass.

By allowing the origin of Body B to coincide with the vehicle center of mass prior to deformation, (\underline{c} is initially zero) \underline{c} may be expressed as a function of \underline{u} :

$$\underline{c} = - \sum_{S=1}^n \underline{C}^T \mu_S \underline{u}_S \quad (2.19)$$

where

$$\mu_S = m_S / M_A$$

is the sub-body mass ratio.

It is desirable to express time derivatives of c such that the direction cosine matrix C does not need to be differentiated with respect to time. It can be shown that:

$$\dot{c} = - \sum_{s=1}^n C^T \mu_s \dot{u}_s - C^T \dot{\bar{q}}^a \sum_{s=1}^n \mu_s u_s \quad (2.20)$$

and:

$$\ddot{c} = -C^T \left[\sum_{s=1}^n \mu_s \ddot{u}_s + \dot{\bar{q}}^a \sum_{s=1}^n \mu_s u_s + 2 \bar{q}^a \sum_{s=1}^n \mu_s \dot{u}_s + \dot{\bar{q}}^a \dot{\bar{q}}^a \sum_{s=1}^n \mu_s u_s \right] \quad (2.21)$$

2.1.5.1 Flexible Vehicle Equations

For any rigid sub-body the translational and rotational equations of motion are developed independently. From Equations (2.3) and (2.18), the translational vector equation becomes:

$$\underline{F}_S = m_S \frac{d^2}{dt^2} (\underline{X} + \underline{c} + \underline{R} + \underline{r}_S + \underline{u}_S) \quad (2.22)$$

or, expressing all variables with respect to the $\{a\}$ vector base yields the following matrix form:

$$\begin{aligned} \underline{F}_S = m_S & \left\{ \ddot{\underline{u}}_S - \sum_{k=1}^n \mu_k \ddot{u}_k \right\} + m_S \left\{ 2 \left(\bar{q}^a + C\bar{\omega} \right) \dot{\underline{u}}_S - 2 \left(C\bar{\omega}C^T + \dot{\bar{q}}^a \right) \sum_{k=1}^n \mu_k \dot{u}_k \right\} \\ & + m_S \left\{ \left[\left(\dot{\bar{q}}^a + C\dot{\bar{\omega}} \right) + (C\bar{\omega})(C\bar{\omega}) + 2(C\bar{\omega})\bar{q}^a + \bar{q}^a\bar{q}^a \right] \underline{u}_S \right. \\ & \quad \left. - \left(C\bar{\omega}C^T + \bar{q}^a + 2C\bar{\omega}C^T\bar{q}^a + \bar{q}^a\bar{q}^a + C\bar{\omega}\bar{\omega}C^T \right) \sum_{k=1}^n \mu_k u_k \right\} \\ & + m_S \left\{ \left(C\bar{\omega}\ddot{\underline{X}} - C\bar{R}\dot{\bar{\omega}} + C\bar{\omega}\ddot{\underline{R}} \right) + \left[\left(C\dot{\bar{\omega}} + \dot{\bar{q}}^a \right) + (C\bar{\omega})(C\bar{\omega}) + 2(C\bar{\omega})\bar{q}^a + \bar{q}^a\bar{q}^a \right] \underline{r}_S \right\} \quad (2.23) \end{aligned}$$

From Equations (2.9), and (2.18), the rotational vector equation becomes:

$$\underline{T}_S = \underline{I}_S \cdot \frac{d}{dt} (\underline{\omega} + \underline{\omega}^a + \underline{\omega}^S) + (\underline{\omega} + \underline{\omega}^a + \underline{\omega}^S) \times \underline{I}_S \cdot (\underline{\omega} + \underline{\omega}^a + \underline{\omega}^S) \quad (2.24)$$

where $\underline{\omega}^S = d(\underline{\beta}_S)/dt$. Or, in matrix form relative to the $\{a\}$ vector base:

$$\begin{aligned} \underline{T}_S = & C_S^T I_S \ddot{\underline{\beta}}_S + \left\{ C_S^T I_S C_S \left((C\omega + \omega^a \tilde{\cdot}) + ((C\omega + \omega^a + C_S^T \dot{\beta}_S \tilde{\cdot})) C_S^T I_S C_S - (C_S^T I_S C_S (C\omega + \omega^a \tilde{\cdot})) \right) \right\} C_S^T \dot{\beta}' \\ & + C_S^T I_S C_S \left(C\dot{\omega} + \dot{\omega}^a + (C\omega \tilde{\cdot}) \omega^a \right) + (C\omega + \omega^a \tilde{\cdot}) C_S^T I_S C_S (C\omega + \omega^a \tilde{\cdot}) \end{aligned} \quad (2.25)$$

Using the Boolean operator matrices defined in Equations (2.15) and (2.16), the n sets of Equations (2.23) and (2.25) are combined into a single matrix equation of motion for the flexible aircraft.

$$M\ddot{q} + D\dot{q} + Gq + Kq + Aq = L \quad (2.26)$$

where:

$$q = \begin{Bmatrix} u' \\ \beta' \end{Bmatrix} \quad (2.26a)$$

$$M = \begin{bmatrix} M'_T & [0] \\ [0] & M'_R \end{bmatrix} = \begin{bmatrix} M_T \left[E(3n) - \frac{1}{M_A} (E(3)) \tilde{E}^n M_T \right] & [0] \\ [0] & (C_S^T)^n M_R \end{bmatrix} \quad (2.26b)$$

$$D = \begin{bmatrix} D'_T & D'_{TR} \\ D'_{RT} & D'_R \end{bmatrix} \quad \text{note: } D'_{RT} = D'_{TR}{}^T \quad (2.26c)$$

$$G = \begin{bmatrix} G'_T & [0] \\ [0] & G'_R \end{bmatrix} \quad (2.26d)$$

$$= \begin{bmatrix} 2M_T \left([\dot{\varphi}^a + C\dot{\omega}] \right)^n \left[E(3n) - \frac{1}{M_A} \left(E(3) \right)^n M_T \right] & [0] \\ [0] & \left(C_S^T \right)^n M_R \left(C_S (C\omega + \dot{\varphi}^a) C_S^T \right)^n + \left((C\omega + \dot{\varphi}^a + C_S^T \dot{\beta}_S) C_S^T \right)^n M_R - \left([C_S^T I_S C_S (C\omega + \dot{\varphi}^a)] C_S^T \right)^n \end{bmatrix}$$

$$K = \begin{bmatrix} K'_T & K'_{TR} \\ K'_{RT} & K'_R \end{bmatrix} \quad \text{note: } K'_{RT} = K'^T_{TR} \quad (2.26e)$$

$$A = \begin{bmatrix} A'_T & [0] \\ [0] & A'_R \end{bmatrix} \quad (2.26f)$$

$$= \begin{bmatrix} M_T \left(\ddot{\varphi}^a + (C\dot{\omega}) + (C\omega)(C\dot{\omega}) + 2(C\omega)\dot{\varphi}^a + \dot{\varphi}^a \dot{\varphi}^a \right)^n \left[E(3n) - \frac{1}{M_A} \left(E(3) \right)^n M_T \right] & [0] \\ [0] & [0] \end{bmatrix}$$

$$L = \begin{bmatrix} L'_T \\ L'_R \end{bmatrix} \quad (2.26g)$$

$$= \begin{bmatrix} -M_T \left[(C\theta)^n \ddot{X}' + (C\dot{\omega} + C\dot{\omega})^n R' + (C\dot{\omega}) + \dot{\varphi}^a + (C\omega)(C\dot{\omega}) + 2(C\omega)\dot{\varphi}^a + \dot{\varphi}^a \dot{\varphi}^a \right)^n r' \right] + f \\ - \left(C_S^T \right)^n M_R \left(C_S \right)^n \left[\left(C \right)^n \dot{\omega}' + \dot{\varphi}^a - \left(\dot{\varphi}^a C \right)^n \omega' \right] \\ - \left([C\omega + \dot{\varphi}^a] \right)^n \left(C_S^T \right)^n M_R \left(C_S \right)^n \left[\left(C \right)^n \omega' + \varphi^a \right] + t \end{bmatrix}$$

In the above equations, note:

D and K are the free-free structural damping and stiffness matrices for the flexible vehicle.

f and t are column matrices of load components applied externally to the sub-bodies, resolved relative to the {a} reference frame.

Subscripts T and R refer to translation and rotation, respectively.

$$M_T = \begin{bmatrix} m_1 & 0 & \dots & 0 \\ 0 & m_2 & \dots & 0 \\ \vdots & \vdots & & \vdots \\ 0 & 0 & \dots & m_n \end{bmatrix} \quad \text{and} \quad m_j = \begin{bmatrix} m_j & 0 & 0 \\ 0 & m_j & 0 \\ 0 & 0 & m_j \end{bmatrix} \quad (2.27)$$

$$M_R = \begin{bmatrix} I_1 & 0 & \dots & 0 \\ 0 & I_2 & \dots & 0 \\ \vdots & \vdots & & \vdots \\ 0 & 0 & \dots & I_n \end{bmatrix} \quad \text{and} \quad I_j = \begin{bmatrix} I_{j11} & 0 & 0 \\ 0 & I_{j22} & 0 \\ 0 & 0 & I_{j33} \end{bmatrix} \quad (2.28)$$

2.1.5.2 Total Vehicle Equations

In the previous section, equations of motion were presented that relate the motion of all the rigid subbodies to each other. In this section, equations of motion for the total vehicle are presented. As was done for the flexible vehicle equations, the total vehicle equations were derived from first principles, the Newton-Euler equations (Equation (2.18), rewritten here for convenience):

$$\begin{aligned} \underline{F} &= \frac{d}{dt} (M_A \underline{V}) \\ &= M_A \ddot{\underline{X}} \end{aligned} \quad (2.29)$$

and:

$$\begin{aligned} \underline{T} &= \frac{d}{dt} \underline{H} \\ &= \left(\frac{d}{dt} \underline{I} \cdot \underline{\omega} + \underline{\omega} \times \underline{I} \cdot \underline{\omega} + \underline{I} \cdot \dot{\underline{\omega}} \right) + M_A \ddot{\underline{X}}_c + \frac{d}{dt} \int \frac{d}{dt} \underline{p} \times \underline{p} \, dm \end{aligned} \quad (2.30)$$

The final form of the total vehicle equations is written in terms of the (b) reference frame. Also, use is made of the sigma and pi operators. Equation (2.16), to obtain:

$$\underline{F} = M_A \Theta \ddot{\underline{X}} \quad (2.31)$$

and:

$$\left(\mathbf{E}(3)\right)^{\mathbf{n}} \left\{ \left[\mathbf{M}_{V_T} \quad \mathbf{M}_{V_R} \right] \ddot{\mathbf{q}} + \left[\mathbf{G}_{V_T} \quad \mathbf{G}_{V_R} \right] \dot{\mathbf{q}} + \left[\mathbf{A}_{V_T} \quad \mathbf{A}_{V_R} \right] \mathbf{q} \right\} = \mathbf{T} - \left(\mathbf{E}(3)\right)^{\mathbf{n}} \left\{ \mathbf{L}_{V_T} + \mathbf{L}_{V_R} \right\} \quad (2.32)$$

where:

$$\mathbf{M}_{V_T} = \mathbf{M}_T \left\{ \left[\left[\mathbf{R} + \mathbf{C}^T (\mathbf{u}_S + \mathbf{r}_S) \right] \right]^{\mathbf{n}} - \frac{1}{M_A} \left(\mathbf{E}(3)\right)^{\mathbf{n}} \mathbf{M}_T \left[\left(\mathbf{C}^T \mathbf{u}_S \right) \right]^{\mathbf{n}} \right\} \left(\mathbf{C}^T \right)^{\mathbf{n}} \quad (2.32a)$$

$$\mathbf{M}_{V_R} = \left(\mathbf{C}^T \mathbf{C}_S^T \right)^{\mathbf{n}} \mathbf{M}_R \quad (2.32b)$$

$$\begin{aligned} \mathbf{G}_{V_T} = \mathbf{M}_T \left\{ \left[2\omega \left(\mathbf{R}^T + \mathbf{r}_S^T \mathbf{C} + \mathbf{u}_S^T \mathbf{C} \right) - 2\omega^T \left(\mathbf{R} + \mathbf{C}^T \mathbf{r}_S + \mathbf{C}^T \mathbf{u}_S \right) \mathbf{E}(3) + \left(\tilde{\omega} \left[\mathbf{R} + \mathbf{C}^T (\mathbf{u}_S + \mathbf{r}_S) \right] \right) \right]^{\mathbf{n}} \right. \\ \left. + \left[\mathbf{R} + \mathbf{C}^T (\mathbf{u}_S + \mathbf{r}_S) \right] \left(\omega + 2\mathbf{C}^T \mathbf{Q}^a \right) \right]^{\mathbf{n}} - \frac{2}{M_A} \left(\mathbf{E}(3)\right)^{\mathbf{n}} \mathbf{M}_T \left[\left(\mathbf{C}^T \mathbf{u}_S \right) \mathbf{C}^T \mathbf{Q}^a \mathbf{C} \right]^{\mathbf{n}} \right\} \left(\mathbf{C}^T \right)^{\mathbf{n}} \end{aligned} \quad (2.32c)$$

$$\begin{aligned} \mathbf{G}_{V_R} = \left\{ - \left[\left[\mathbf{C}^T \mathbf{C}_S^T \mathbf{I}_S \mathbf{C}_S \mathbf{C} \left(\omega + \mathbf{C}^T \mathbf{Q}^a \right) \right] \right]^{\mathbf{n}} + \left(\mathbf{C}^T \mathbf{C}_S^T \right)^{\mathbf{n}} \mathbf{M}_R \left[\mathbf{C}_S \mathbf{C} \left(\omega - \mathbf{C}^T \mathbf{Q}^a + \mathbf{C}^T \mathbf{C}_S^T \dot{\beta}_S \right) \right]^{\mathbf{n}} \right. \\ \left. + \left[\left(\omega + \mathbf{C}^T \mathbf{Q}^a + \mathbf{C}^T \mathbf{C}_S^T \dot{\beta}_S \right) \mathbf{C}^T \mathbf{C}_S^T \right]^{\mathbf{n}} \mathbf{M}_R \left(\mathbf{C}_S \mathbf{C} \right)^{\mathbf{n}} \right\} \left(\mathbf{C}^T \mathbf{C}_S^T \right)^{\mathbf{n}} \end{aligned} \quad (2.32d)$$

$$\begin{aligned}
A_{V_T} = M_T \left\{ \right. & \left[2\omega (R^T + 2r_S^T C + u_S^T C) (C^T \tilde{Q}^a) - [\omega^T (R + C^T r_S + C^T u_S)] (C^T \tilde{Q}^a) - (C^T \tilde{Q}^a) C^T r_S \omega^T \right. \\
& - (R + C^T r_S + C^T u_S) \omega^T (C^T \tilde{Q}^a) - [\omega^T (C^T \tilde{Q}^a) C^T r_S] E(3) - \tilde{\omega} (R + C^T r_S + C^T u_S) \omega^T \\
& - \tilde{\omega} [\omega^T (R + C^T r_S)] + \dot{\tilde{\omega}} (2R^T + 2r_S^T C + u_S^T C) - (R + C^T r_S + C^T u_S) \dot{\tilde{\omega}}^T - [\dot{\tilde{\omega}}^T (R + C^T r_S)] E(3) \\
& + (\tilde{\omega} [R + C^T (u_S + r_S)]) (C^T \tilde{Q}^a) + [R + C^T (u_S + r_S)] [(C^T \dot{\tilde{Q}}^a + \tilde{\omega} C^T \tilde{Q}^a) \\
& + (C^T \tilde{Q}^a) (\omega + C^T \tilde{Q}^a)] - [(C^T \tilde{Q}^a) C^T r_S] \tilde{\omega} - \{ [(C^T \dot{\tilde{Q}}^a + \tilde{\omega} C^T \tilde{Q}^a) \\
& + (C^T \tilde{Q}^a) (\omega + C^T \tilde{Q}^a)] C^T r_S \} + \{ [(C^T \tilde{Q}^a) C^T u_S] (C^T \tilde{Q}^a) \}^n \\
& \left. + \frac{1}{M_A} (E(3))^n M_T \{ [C^T (\tilde{Q}^a + \tilde{Q}^a \tilde{Q}^a) u_S] \}^n \right\} (C^T)^n
\end{aligned} \tag{2.32e}$$

$$A_{V_R} = [0] \tag{2.32f}$$

$$\begin{aligned}
L_{V_T} = M_T \left\{ \right. & -\tilde{\omega} [(R^T + r_S^T C) \omega] + \dot{\tilde{\omega}} (R^T + r_S^T C) - (R + C^T r_S) \dot{\tilde{\omega}}^T \}^n [R' + (C^T)^n r'] \\
& + M_T \left\{ \right. 2\omega (R^T + r_S^T C) (C^T \tilde{Q}^a) - [\omega^T (R + C^T r_S)] (C^T \tilde{Q}^a) - (R + C^T r_S) \omega^T (C^T \tilde{Q}^a) \\
& + [\tilde{\omega} (R + C^T r_S)] (C^T \tilde{Q}^a) + (R + C^T r_S) [(C^T \dot{\tilde{Q}}^a + \tilde{\omega} C^T \tilde{Q}^a) + (C^T \tilde{Q}^a) (\omega + C^T \tilde{Q}^a)] \\
& \left. + \{ [(C^T \tilde{Q}^a) C^T r_S] (C^T \tilde{Q}^a) \}^n (C^T)^n r' \right\}
\end{aligned} \tag{2.32g}$$

$$\begin{aligned}
L_{V_R} = & \left\{ (C^T C_S^T)^n M_R (C_S C)^n \right\} [\dot{\omega}' + (C^T)^n \dot{Q}^a'] \\
& + \left\{ \left[(\omega + C^T \tilde{Q}^a) C^T C_S^T \right]^n M_R (C_S C)^n + (C^T C_S^T)^n M_R [C_S C (C^T \tilde{Q}^a)]^n \right\} [\omega' + (C^T)^n Q^a'] \\
& + \left\{ (C^T C_S^T)^n M_R (C_S C \tilde{\omega})^n \right\} (C^T)^n Q^a'
\end{aligned} \tag{2.32h}$$

These dynamic equations, Equations (2.26), (2.31), and (2.32), parallel the work of P. W. Likins in his treatment of flexible spacecraft (Reference 1). However, this is not sufficient to be used for practical applications as will be discussed in more detail in the next section.

2.1.5.3 Auxiliary Equations

The overall matrix equations of motion, (Equations (2.26), (2.31), and (2.32), of dimension $6n$, 3 , and 3 respectively), are written in terms of the sub-body deformations, q . However, the coefficients of these equations are in terms of the overall vehicle motion (ω , α , and X ; 3 unknowns each) and the direction cosine matrices (θ , C , and C_s ; 3, 3, and $3n$ unknowns, respectively); also q represents $6n$ unknowns. Thus, there are $9n+15$ unknowns with only $6n+6$ equations. Hence, $3n+9$ auxiliary equations are required to uniquely describe the system.

There are three auxiliary equations associated with each C_s , which is a function of β_s . This is best shown by expanding C_s into its component Euler angles:

$$\{a_s\} = C_{s3} C_{s2} C_{s1} \{a\} \quad (2.33)$$

These Euler angle components are expressed in terms of the rotational deformation components of β_s :

$$C_{s3} C_{s2} C_{s1} = \begin{bmatrix} c\beta_{s3} & s\beta_{s3} & 0 \\ -s\beta_{s3} & c\beta_{s3} & 0 \\ 0 & 0 & 1 \end{bmatrix} \begin{bmatrix} c\beta_{s2} & 0 & -s\beta_{s2} \\ 0 & 1 & 0 \\ s\beta_{s2} & 0 & c\beta_{s2} \end{bmatrix} \begin{bmatrix} 1 & 0 & 0 \\ 0 & c\beta_{s1} & s\beta_{s1} \\ 0 & -s\beta_{s1} & c\beta_{s1} \end{bmatrix}$$

$$= \begin{bmatrix} c\beta_{s3}c\beta_{s2} & c\beta_{s3}s\beta_{s2}s\beta_{s1} + s\beta_{s3}c\beta_{s1} & -c\beta_{s3}s\beta_{s2}c\beta_{s1} + s\beta_{s3}s\beta_{s1} \\ -s\beta_{s3}c\beta_{s2} & -s\beta_{s3}s\beta_{s2}s\beta_{s1} + c\beta_{s1}c\beta_{s3} & -s\beta_{s3}s\beta_{s2}c\beta_{s1} + c\beta_{s3}s\beta_{s1} \\ s\beta_{s2} & -c\beta_{s2}s\beta_{s1} & c\beta_{s2}c\beta_{s1} \end{bmatrix} \quad (2.34)$$

where $c(*)$ and $s(*)$ are abbreviations for the cosine(*) and sine(*), respectively. Thus, C_s is now resolved in terms of the desired $6n+6$ unknown: specifically, β_s .

There are six auxiliary equations associated with θ and C , which are functions of ω and Ω^a , respectively. New angular vectors are defined: β_B which relates the rotation of reference frame $\{b\}$ relative to reference frame $\{a\}$, and Γ which relates the rotation of the inertial reference frame $\{i\}$ relative to reference frame $\{b\}$. β_B is resolved relative to the $\{a\}$ reference frame and Γ is resolved relative to the $\{b\}$ reference frame. C and θ are expressed in terms of β_B and Γ , respectively, by expanding the Euler angle components as was done for C_s in Equation (2.33):

$$C = \begin{bmatrix} c\beta_{B3}c\beta_{B2} & c\beta_{B3}s\beta_{B2}s\beta_{B1} & -c\beta_{B3}s\beta_{B2}c\beta_{B1} \\ & +s\beta_{B3}c\beta_{B1} & +s\beta_{B3}s\beta_{B1} \\ -s\beta_{B3}c\beta_{B2} & -s\beta_{B3}s\beta_{B2}s\beta_{B1} & -s\beta_{B3}s\beta_{B2}c\beta_{B1} \\ & +c\beta_{B1}c\beta_{B3} & +c\beta_{B3}s\beta_{B1} \\ s\beta_{B2} & -c\beta_{B2}s\beta_{B1} & c\beta_{B2}c\beta_{B1} \end{bmatrix} \quad (2.35)$$

and:

$$\theta = \begin{bmatrix} c\Gamma_3c\Gamma_2 & c\Gamma_3s\Gamma_2s\Gamma_1+s\Gamma_3c\Gamma_1 & -c\Gamma_3s\Gamma_2c\Gamma_1+s\Gamma_3s\Gamma_1 \\ -s\Gamma_3c\Gamma_2 & -s\Gamma_3s\Gamma_2s\Gamma_1+c\Gamma_1c\Gamma_3 & -s\Gamma_3s\Gamma_2c\Gamma_1+c\Gamma_3s\Gamma_1 \\ s\Gamma_2 & -c\Gamma_2s\Gamma_1 & c\Gamma_2c\Gamma_1 \end{bmatrix} \quad (2.36)$$

C and θ have been accounted for, but there are six new unknowns: β_B and Γ .

The composite internal force applied at all nodes, \underline{L}_A , due to the structural stiffness, K_A (Note: this is not the same K as in the flexible vehicle equations), Equation (2.26) is written as:

$$\underline{L}_A = \begin{Bmatrix} \underline{L}_q \\ \underline{F}_B \\ \underline{T}_B \end{Bmatrix} = \begin{bmatrix} K_{Lq} & K_{Lq''B} & K_{Lq}\beta_B \\ K_{FBq} & K_{FBuB} & K_{FB}\beta_B \\ K_{TBq} & K_{TBuB} & K_{TB}\beta_B \end{bmatrix} \begin{Bmatrix} q \\ u_B \\ \beta_B \end{Bmatrix} = K_A q_A \quad (2.37)$$

where L_q represents all $6n$ loads acting on all n rigid sub-bodies due to the vehicle's structural stiffness, F_B and T_B are the forces and torques acting on Body B due to the vehicle's structural stiffness, and K_A has been partitioned relative to these three variables.

Since Body B is massless, the sum of the loads acting at Point O must be zero. With F_B and T_B zero u_B and β_B are extracted from the lower two rows of Equation (2.37), resolved relative to the $\{a\}$ reference frame:

$$\begin{Bmatrix} u_B \\ \beta_B \end{Bmatrix} = \begin{bmatrix} -E(3) & K_{F_B u_B}^{-1} & K_{F_B \beta_B} \\ K_{T_B \beta_B}^{-1} & K_{T_B u_B} & -E(3) \end{bmatrix} \begin{bmatrix} [K_{F_B u_B} & -K_{F_B \beta_B} & K_{T_B \beta_B}^{-1} & K_{T_B u_B}]^{-1} & K_{F_B q} \\ [K_{T_B \beta_B} & -K_{T_B u_B} & K_{F_B u_B}^{-1} & K_{F_B \beta_B}]^{-1} & K_{T_B q} \end{bmatrix} q \quad (2.38)$$

Thus, u_B and β_B are now functions of q . Equation (2.38) is substituted back into Equation (2.37), solved for $L_q = Kq$, and extracting K (this is the K in Equation (2.26) yields:

$$\begin{aligned} K = & K_{L_q q} - K_{L_q u_B} \left([K_{F_B u_B} & -K_{F_B \beta_B} & K_{T_B \beta_B}^{-1} & K_{T_B u_B}]^{-1} K_{F_B q} \right. \\ & \left. - K_{F_B u_B}^{-1} K_{F_B \beta_B} [K_{T_B \beta_B} & -K_{T_B u_B} & K_{F_B u_B}^{-1} & K_{F_B \beta_B}]^{-1} K_{T_B q} \right) \\ & + K_{L_q \beta_B} \left(K_{T_B \beta_B}^{-1} K_{T_B u_B} [K_{F_B u_B} & -K_{F_B \beta_B} & K_{T_B \beta_B}^{-1} & K_{T_B u_B}]^{-1} K_{F_B q} \right. \\ & \left. - [K_{T_B \beta_B} & -K_{T_B u_B} & K_{F_B u_B}^{-1} & K_{F_B \beta_B}]^{-1} K_{T_B q} \right) \end{aligned} \quad (2.39)$$

Now $\dot{\beta}_B$ (the first time derivative of β_B) can also be expressed as a function of q by taking the first time derivative of the lower portion of Equation (2.38) (note: β_B was chosen to be resolved into the $\{a\}$ reference frame):

$$\begin{aligned}
\underline{\{a\}}^T \underline{\dot{\varphi}}^a &= -\underline{\{a\}}^T \frac{d}{dt} \underline{\beta}_B \\
&= \underline{\{a\}}^T \left(\begin{array}{c} -K_{TB\beta_B}^{-1} K_{TBu_B} \left[K_{FBu_B} - K_{FB\beta_B} K_{TB\beta_B}^{-1} K_{TBu_B} \right]^{-1} K_{FBq} \\ + \left[K_{TB\beta_B} - K_{TBu_B} K_{FBu_B}^{-1} K_{FB\beta_B} \right]^{-1} K_{TBq} \end{array} \right) \dot{q}
\end{aligned} \tag{2.40}$$

The vehicle is not attached to ground. By definition, $\underline{\omega}$ is the time derivative of $\underline{\Gamma}$. However, it is preferable to express $\underline{\Gamma}$ in terms of $\underline{\omega}$ (note: $\underline{\Gamma}$ and $\underline{\omega}$ are resolved relative to the $\underline{\{b\}}$ reference frame):

$$\underline{\Gamma} = \int_0^t \underline{\omega} dt + \underline{\Gamma}^* \tag{2.41}$$

where $\underline{\Gamma}^*$ is the initial rotational orientation of the $\underline{\{b\}}$ reference frame relative to the inertial reference frame, $\underline{\{i\}}$

In summary: C_S has been expressed in terms of $\underline{\beta}_S$; C and $\underline{\varphi}^a$ have been expressed in terms of $\underline{\beta}_B$; \underline{u}_B and $\underline{\beta}_B$ has been expressed in terms of q ; and $\underline{\theta}$ has been expressed in terms of $\underline{\Gamma}$, which has been expressed in terms of $\underline{\omega}$. Thus, the $3n+9$ additional auxiliary equations required to describe the system have been produced.

There are only n nodes ($6n$ degrees-of-freedom) with mass being described by $6n+6$ equations. $\underline{\beta}_B$ describes the rotation of the $\underline{\{b\}}$ reference frame relative to the $\underline{\{a\}}$ reference frame. All the undeformed sub-body position vectors, \underline{r}_S , are time invariant with respect to the $\underline{\{a\}}$ reference frame and must rotate as a rigid body relative to the $\underline{\{b\}}$ reference frame. With \underline{r}_S as a reference for the sub-bodies it is apparent that this "rigid body" rotation, $\underline{\beta}_B$, can be arbitrarily defined.

As the vehicle deforms, for a finite β_B , r_S rotates about Point Q from its initial position, r_S^0 (See Figure 2-7). Subsequently, the rigid sub-bodies deform from this new position u_S . Therefore, u_S is a function of r_S . If β_B is set to zero, then r_S^0 is always coincident with r_S , the reference for u_S (Shown as u_S^0 in Figure 2-7). This also implies that $\{a\} \equiv \{b\}$ and that $C = E(3)$. Point Q is treated as a node that can deform u_B relative to the $\{a\}$ reference frame. For this point r_B is zero. Since all r_S traverse with Point Q, including r_B , u_B is always zero. These observations are substituted into Equation (2.38), which defines u_B and β_B (now set to zero) as a function of q :

$$\begin{aligned} \{0\} &= K_{qBq} q \\ &= \begin{bmatrix} K_{qB\bar{q}} & K_{qBq_n} \end{bmatrix} \begin{Bmatrix} \bar{q} \\ q_n \end{Bmatrix} \end{aligned} \quad (2.42)$$

or:

$$q_n = -K_{qBq_n}^{-1} K_{qB\bar{q}} \bar{q} \quad (2.43)$$

where q_n can be any six deformation degrees-of-freedom associated with Point Q through the stiffness matrix, and \bar{q} is the remaining $6n-6$ deformations. This leaves only $6n$ unknowns for $6n$ rigid sub-bodies (the other six being X and ω).

2.1.5.4 Complete Dynamic Equations

In the previous section auxiliary equations were developed which reduced the total number of independent unknowns to the number of inertially possible degrees-of-freedom. In this section these auxiliary equations are incorporated into the dynamic equations. Specifically, the inclusion of two sets of auxiliary equations will be presented:

First, the dynamic equations will be simplified using the observation that u_B and β_B are zero. And then, the resultant dynamic equations will be rewritten in terms of the reduced deformation variable, \bar{q} .

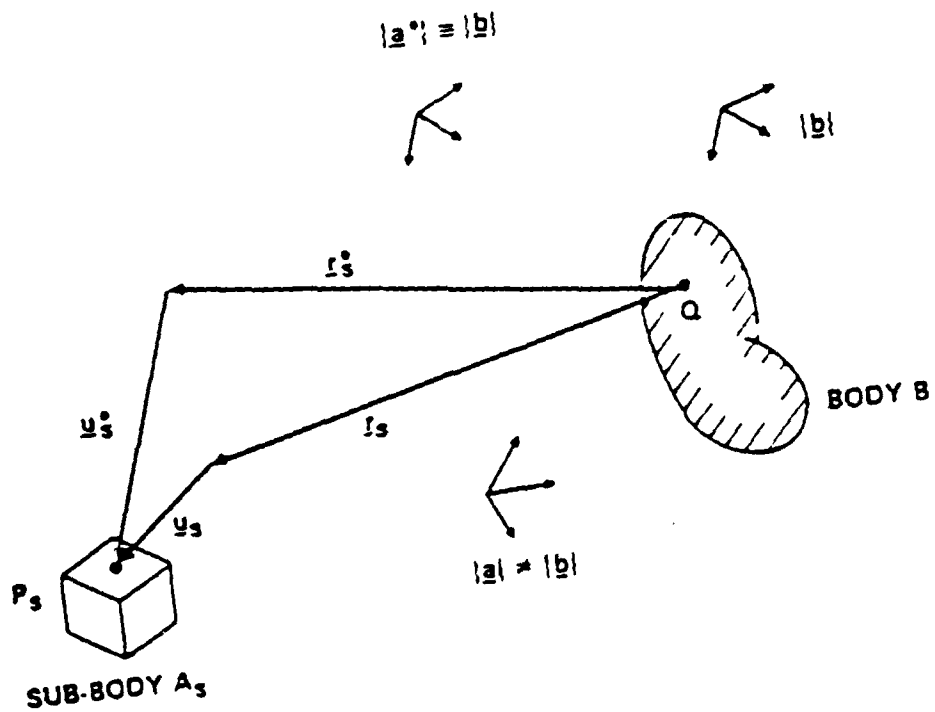


Figure 2-7. Relative Coordinate Motion

It was shown in the previous section that {a} being unique from {b} was unnecessary. The development is equally general under this observation. Fortunately, this greatly simplifies the results: $\mathbf{q}^a = \{0\}$ and $\mathbf{C} = \mathbf{E}^{(3)}$. This is substituted into the flexible vehicle equations, Equation (2.26), to yield:

$$\mathbf{M}\ddot{\mathbf{q}} + \mathbf{D}\dot{\mathbf{q}} + \mathbf{K}\mathbf{q} + \mathbf{A}\mathbf{q} = \mathbf{L} \quad (2.44)$$

where:

$$\mathbf{G} = \begin{bmatrix} \mathbf{G}'_{\mathbf{T}} & [0] \\ [0] & \mathbf{G}'_{\mathbf{R}} \end{bmatrix} = \begin{bmatrix} 2\mathbf{M}_{\mathbf{T}} (\hat{\omega})^{\mathbf{n}} \left[\mathbf{E}^{(3\mathbf{n})} - \frac{1}{\mathbf{M}_{\mathbf{A}}} (\mathbf{E}^{(3)})^{\mathbf{n}} \mathbf{M}_{\mathbf{T}} \right] & [0] \\ [0] & (\mathbf{C}_{\mathbf{S}}^{\mathbf{T}})^{\mathbf{n}} \mathbf{M}_{\mathbf{R}} (\mathbf{C}_{\mathbf{S}} \hat{\omega} \mathbf{C}_{\mathbf{S}}^{\mathbf{T}})^{\mathbf{n}} + ((\hat{\omega} + \mathbf{C}_{\mathbf{S}}^{\mathbf{T}} \dot{\beta}_{\mathbf{S}}) \mathbf{C}_{\mathbf{S}}^{\mathbf{T}})^{\mathbf{n}} \mathbf{M}_{\mathbf{R}} \\ & - [(\mathbf{C}_{\mathbf{S}}^{\mathbf{T}} \mathbf{I}_{\mathbf{S}} \mathbf{C}_{\mathbf{S}} \hat{\omega})] \mathbf{C}_{\mathbf{S}}^{\mathbf{T}})^{\mathbf{n}} \end{bmatrix} \quad (2.44a)$$

$$\mathbf{A} = \begin{bmatrix} \mathbf{A}'_{\mathbf{T}} & [0] \\ [0] & \mathbf{A}'_{\mathbf{R}} \end{bmatrix} = \begin{bmatrix} \mathbf{M}_{\mathbf{T}} (\hat{\omega} + \tilde{\omega})^{\mathbf{n}} \left[\mathbf{E}^{(3\mathbf{n})} - \frac{1}{\mathbf{M}_{\mathbf{A}}} (\mathbf{E}^{(3)})^{\mathbf{n}} \mathbf{M}_{\mathbf{T}} \right] & [0] \\ [0] & [0] \end{bmatrix} \quad (2.44b)$$

$$\mathbf{L} = \begin{bmatrix} \mathbf{L}'_{\mathbf{T}} \\ \mathbf{L}'_{\mathbf{R}} \end{bmatrix} = \begin{bmatrix} -\mathbf{M}_{\mathbf{T}} \left[(\hat{\theta})^{\mathbf{n}} \ddot{\mathbf{x}}' + (\hat{\omega} + \tilde{\omega})^{\mathbf{n}} (\mathbf{R}' + \mathbf{r}') \right] + \mathbf{f} \\ -(\mathbf{C}_{\mathbf{S}}^{\mathbf{T}})^{\mathbf{n}} \mathbf{M}_{\mathbf{R}} (\mathbf{C}_{\mathbf{S}})^{\mathbf{n}} \dot{\omega}' - (\tilde{\omega} \mathbf{C}_{\mathbf{S}}^{\mathbf{T}})^{\mathbf{n}} \mathbf{M}_{\mathbf{R}} (\mathbf{C}_{\mathbf{S}})^{\mathbf{n}} \omega' + \mathbf{t} \end{bmatrix} \quad (2.44c)$$

and \mathbf{q} , \mathbf{M} , \mathbf{D} , and \mathbf{K} are as defined in Equations (2.26a), (2.26b), (2.26c), and (2.26e), respectively.

Similarly, the total vehicle equations, Equations (2.31), and (2.32), become:

$$\mathbf{F} = \mathbf{M}_{\mathbf{A}} \ddot{\boldsymbol{\theta}} \quad (2.45)$$

and:

$$\left(E(3)\right)^n \left\{ \left[M_{VT} \ M_{VR} \right] \ddot{q} + \left[G_{VT} \ G_{VR} \right] \dot{q} + \left[A_{VT} \ A_{VR} \right] q \right\} = - \left(E(3)\right)^n \left\{ L_{VT} + L_{VR} \right\} \quad (2.46)$$

where:

$$M_{VT} = M_T \left\{ \left[\left(R + u_S + r_S \right) \right]^n - \frac{1}{M_A} \left(E(3) \right)^n M_T \left(\tilde{u}_S \right)^n \right\} \quad (2.46a)$$

$$M_{VR} = \left(C_S^T \right)^n M_R \quad (2.46b)$$

$$G_{VT} = M_T \left\{ 2\omega \left(R^T + r_S^T + u_S^T \right) - 2\omega^T \left(R + r_S + u_S \right) E(3) + \left[\tilde{\omega} \left(R + u_S + r_S \right) \right] + \left(R + u_S + r_S \right) \tilde{\omega} \right\}^n \quad (2.46c)$$

$$G_{VR} = \left\{ - \left[\left(C_S^T I_S C_S \omega \right) \right]^n + \left(C_S^T \right)^n M_R \left[C_S \left(\omega + C_S^T \dot{\beta}_S \right) \right]^n + \left[\left(\omega + C_S^T \dot{\beta}_S \right) C_S^T \right]^n M_R \left(C_S \right)^n \right\} \left(C_S^T \right)^n \quad (2.46d)$$

$$A_{VT} = M_T \left\{ -\tilde{\omega} \left(R + r_S + u_S \right) \omega^T - \tilde{\omega} \left[\omega^T \left(R + r_S \right) \right] + \dot{\omega} \left(2R^T + 2r_S^T + u_S^T \right) - \left(R + r_S + u_S \right) \dot{\omega}^T - \left[\dot{\omega}^T \left(R + r_S \right) \right] E(3) \right\}^n \quad (2.46e)$$

$$A_{VR} = \{ 0 \} \quad (2.46f)$$

$$L_{VT} = M_T \left\{ -\tilde{\omega} \left[\left(R^T + r_S^T \right) \omega \right] + \dot{\omega} \left(R^T + r_S^T \right) - \left(R + r_S \right) \dot{\omega}^T \right\}^n \left(R' + r' \right) \quad (2.46g)$$

$$L_{VR} = \left(C_S^T \right)^n M_R \left(C_S \right)^n \dot{\omega}' + \left(\tilde{\omega} C_S^T \right)^n M_R \left(C_S \right)^n \omega' \quad (2.46h)$$

From Equation (2.43), six deformation variables, q_n , can be determined in terms of the remaining $6n-6$ deformation variables, \bar{q} . For purposes of discussion, it will be assumed that these six variables are the last three u_s and β_s ($s=n$). Specifically, Equation (2.43) becomes:

$$\begin{Bmatrix} u_n \\ \beta_n \end{Bmatrix} = q_n = -K_{QB}^{-1} K_{BQ} \bar{q} = \begin{bmatrix} K_{u_n \bar{u}} & K_{u_n \bar{\beta}} \\ K_{\beta_n \bar{u}} & K_{\beta_n \bar{\beta}} \end{bmatrix} \begin{Bmatrix} \bar{u} \\ \bar{\beta} \end{Bmatrix} \quad (2.47)$$

where the overbar is used to denote a concatenation of $(n-1)$ 3×1 columns.

The variables and coefficients of Equation (2.44) are partitioned accordingly and the notation of Equation (2.47) is employed; for example, the second derivative coefficient becomes:

$$M_{\bar{q}\bar{q}} = \begin{bmatrix} M_{\bar{u}\bar{u}} & M_{\bar{u}u_n} & M_{\bar{u}\bar{\beta}} & M_{\bar{u}\beta_n} \\ M_{u_n\bar{u}} & M_{u_n u_n} & M_{u_n\bar{\beta}} & M_{u_n\beta_n} \\ M_{\bar{\beta}\bar{u}} & M_{\bar{\beta}u_n} & M_{\bar{\beta}\bar{\beta}} & M_{\bar{\beta}\beta_n} \\ M_{\beta_n\bar{u}} & M_{\beta_n u_n} & M_{\beta_n\bar{\beta}} & M_{\beta_n\beta_n} \end{bmatrix} \begin{Bmatrix} \ddot{\bar{u}} \\ K_{u_n\bar{u}}\ddot{\bar{u}} + K_{u_n\bar{\beta}}\ddot{\bar{\beta}} \\ \ddot{\bar{\beta}} \\ K_{\beta_n\bar{u}}\ddot{\bar{u}} + K_{\beta_n\bar{\beta}}\ddot{\bar{\beta}} \end{Bmatrix} \quad (2.48)$$

where, from Equation (2.26b):

$$\begin{aligned} \begin{bmatrix} M_{\bar{u}\bar{u}} & M_{\bar{u}u_n} \\ M_{u_n\bar{u}} & M_{u_n u_n} \end{bmatrix} &= M_T \left[E(3n) - \frac{1}{M_A} (E(3))^{\bar{I}_n} M_T \right] \\ &= \begin{bmatrix} \bar{M}_T \left[E(3n-3) - \frac{1}{M_A} (E(3))^{\bar{I}_{n-1}} \bar{M}_T \right] - \frac{1}{M_A} \bar{M}_T (E(3))^{\bar{I}_{n-1}} m_n \\ \left[-\frac{1}{M_A} \bar{M}_T (E(3))^{\bar{I}_{n-1}} m_n \right]^T & m_n \left[E(3) - \frac{1}{M_A} m_n \right] \end{bmatrix} \end{aligned} \quad (2.48a)$$

$$\begin{bmatrix} M_{\bar{u}\bar{\beta}} & M_{\bar{u}\beta_n} \\ M_{u_n\bar{\beta}} & M_{u_n\beta_n} \end{bmatrix} = \begin{bmatrix} M_{\bar{\beta}\bar{u}} & M_{\bar{\beta}u_n} \\ M_{\beta_n\bar{u}} & M_{\beta_n u_n} \end{bmatrix} = [0] \quad (2.48b)$$

$$\begin{bmatrix} \overline{M_{\beta\beta}} & \overline{M_{\beta\beta_n}} \\ \overline{M_{\beta_n\beta}} & \overline{M_{\beta_n\beta_n}} \end{bmatrix} = (\overline{C_S^T})^n \overline{M_R} = \begin{bmatrix} (\overline{C_S^T})^{n-1} \overline{M_R} & [0] \\ [0] & \overline{C_n^T I_n} \end{bmatrix} \quad (2.48c)$$

and:

$$\overline{M_T} = \begin{bmatrix} m_1 & 0 & \dots & 0 \\ 0 & m_2 & \dots & 0 \\ \vdots & \vdots & & \vdots \\ 0 & 0 & \dots & m_{n-1} \end{bmatrix} \quad \text{and} \quad m_j = \begin{bmatrix} m_j & 0 & 0 \\ 0 & m_j & 0 \\ 0 & 0 & m_j \end{bmatrix} \quad (2.48d)$$

$$\overline{M_R} = \begin{bmatrix} I_1 & 0 & \dots & 0 \\ 0 & I_2 & \dots & 0 \\ \vdots & \vdots & & \vdots \\ 0 & 0 & \dots & I_{n-1} \end{bmatrix} \quad \text{and} \quad I_j = \begin{bmatrix} I_{j11} & 0 & 0 \\ 0 & I_{j22} & 0 \\ 0 & 0 & I_{j33} \end{bmatrix} \quad (2.48e)$$

The same procedure is repeated for the remaining coefficients. Partitioning accordingly and using the same subscript notation yields:

from Equation (2.44a):

$$\begin{aligned} \begin{bmatrix} \overline{G_{uu}} & \overline{G_{uu_n}} \\ \overline{G_{u_n\bar{u}}} & \overline{G_{u_n u_n}} \end{bmatrix} &= 2\overline{M_T}(\tilde{\omega})^n \left[\overline{E(3n)} - \frac{1}{\overline{M_A}} (\overline{E(3)})^n \overline{M_T} \right] \\ &= \begin{bmatrix} 2\overline{M_T}(\tilde{\omega})^{n-1} \left[\overline{E(3n-3)} - \frac{1}{\overline{M_A}} (\overline{E(3)})^{n-1} \overline{M_T} \right] & - \frac{2\overline{M_T}}{\overline{M_A}} (\overline{E(3)})^{n-1} \frac{1}{\omega m_n} \\ \left[- \frac{2\overline{M_T}}{\overline{M_A}} (\overline{E(3)})^{n-1} \frac{1}{\omega m_n} \right]^T & 2m_n \tilde{\omega} \left[\overline{E(3)} - \frac{1}{\overline{M_A}} m_n \right] \end{bmatrix} \end{aligned} \quad (2.49a)$$

$$\begin{bmatrix} \overline{G_{u\beta}} & \overline{G_{u\beta_n}} \\ \overline{G_{u_n\beta}} & \overline{G_{u_n\beta_n}} \end{bmatrix} = \begin{bmatrix} \overline{G_{\beta u}} & \overline{G_{\beta u_n}} \\ \overline{G_{\beta_n \bar{u}}} & \overline{G_{\beta_n u_n}} \end{bmatrix} = [0] \quad (2.49b)$$

$$\begin{aligned} \begin{bmatrix} \overline{G_{\beta\beta}} & \overline{G_{\beta\beta_n}} \\ \overline{G_{\beta_n\beta}} & \overline{G_{\beta_n\beta_n}} \end{bmatrix} &= (\overline{C_S^T})^n \overline{M_R} (\overline{C_S} \tilde{\omega} \overline{C_S^T})^n + ((\omega + \overline{C_S^T} \tilde{\beta}_S) \tilde{C_S^T})^n \overline{M_R} - \left[(\overline{C_S^T} I_S \overline{C_S} \omega) \tilde{C_S^T} \right]^n \\ &= \begin{bmatrix} (\overline{C_S^T})^{n-1} \overline{M_R} (\overline{C_S} \tilde{\omega} \overline{C_S^T})^{n-1} + ((\omega + \overline{C_S^T} \tilde{\beta}_S) \tilde{C_S^T})^{n-1} \overline{M_R} - \left[(\overline{C_S^T} I_S \overline{C_S} \omega) \tilde{C_S^T} \right]^{n-1} & [0] \\ [0] & \overline{C_n^T} I_n \overline{C_n} \tilde{\omega} \overline{C_n^T} + (\omega + \overline{C_n^T} \tilde{\beta}_n) \tilde{C_n^T} I_n - \left[\overline{C_n^T} I_n \overline{C_n} \omega \right] \tilde{C_n^T} \end{bmatrix} \end{aligned} \quad (2.49c)$$

from Equation (2.44b):

$$\begin{bmatrix} \overline{A_{uu}} & \overline{A_{uu_n}} \\ \overline{A_{u_n\bar{u}}} & \overline{A_{u_n u_n}} \end{bmatrix} = \overline{M_T} (\dot{\omega} + \ddot{\omega})^n \left[E(3n) - \frac{1}{M_A} (E(3))^n \overline{M_T} \right] \\ = \begin{bmatrix} \overline{M_T} (\dot{\omega} + \ddot{\omega})^{n-1} \left[E(3n-3) - \frac{1}{M_A} (E(3))^{n-1} \overline{M_T} \right] & \frac{1}{M_A} \overline{M_T} (E(3))^{n-1} (\dot{\omega} + \ddot{\omega}) m_n \\ \left[\frac{1}{M_A} \overline{M_T} (E(3))^{n-1} (\dot{\omega} + \ddot{\omega}) m_n \right]^T & m_n (\dot{\omega} + \ddot{\omega}) \left[E(3) - \frac{1}{M_A} m_n \right] \end{bmatrix} \quad (2.50a)$$

$$\begin{bmatrix} \overline{A_{u\beta}} & \overline{A_{u\beta_n}} \\ \overline{A_{u_n\beta}} & \overline{A_{u_n\beta_n}} \end{bmatrix} = \begin{bmatrix} \overline{A_{\beta u}} & \overline{A_{\beta u_n}} \\ \overline{A_{\beta_n\bar{u}}} & \overline{A_{\beta_n u_n}} \end{bmatrix} = \begin{bmatrix} \overline{A_{\beta\beta}} & \overline{A_{\beta\beta_n}} \\ \overline{A_{\beta_n\beta}} & \overline{A_{\beta_n\beta_n}} \end{bmatrix} = [0] \quad (2.50b)$$

and, from Equation (2.44c)

$$L = \begin{bmatrix} \overline{L_{\bar{u}}} \\ \overline{L_{u_n}} \\ \overline{L_{\beta}} \\ \overline{L_{\beta_n}} \end{bmatrix} = \begin{bmatrix} -\overline{M_T} \left[(\ddot{\theta})^{n-1} \ddot{X}' + (\dot{\omega} + \ddot{\omega})^{n-1} (\ddot{R}' + \ddot{r}') \right] + \ddot{f} \\ -m_n \left[\ddot{\theta} \ddot{X} + (\dot{\omega} + \ddot{\omega}) (\ddot{R} + \ddot{r}) \right] + \ddot{f}_n \\ - \left(\overline{C_S^T} \right)^{n-1} \overline{M_R} \left(\overline{C_S} \right)^{n-1} \dot{\omega}' - \left(\overline{\omega C_S^T} \right)^{n-1} \overline{M_R} \left(\overline{C_S} \right)^{n-1} \dot{\omega}' + \ddot{t} \\ - \overline{C_n^T} \overline{I_n} \overline{C_n} \dot{\omega} - \overline{\omega C_n^T} \overline{I_n} \overline{C_n} \omega + \ddot{t}_n \end{bmatrix} \quad (2.51)$$

The first and third rows of these coefficients are multiplied through and combined into one matrix equation, the complete flexible vehicle equations:

$$\overline{M}\ddot{q} + \overline{D}\dot{q} + \overline{G}q + \overline{K}q + \overline{A}q = \overline{L} \quad (2.52)$$

where:

$$\overline{M} = \begin{bmatrix} \overline{M_{uu}} + \overline{M_{uu_n}} \overline{K_{u_n\bar{u}}} & \overline{M_{uu_n}} \overline{K_{u_n\beta}} \\ [0] & \overline{M_{\beta\beta}} \end{bmatrix} \quad (2.52a)$$

$$\overline{D} = \begin{bmatrix} \overline{D_{uu}} + \overline{D_{uu_n}} \overline{K_{u_n\bar{u}}} + \overline{D_{u\beta_n}} \overline{K_{\beta_n\bar{u}}} & \overline{D_{u\beta}} + \overline{D_{uu_n}} \overline{K_{u_n\beta}} + \overline{D_{u\beta_n}} \overline{K_{\beta_n\beta}} \\ \overline{D_{\beta u}} + \overline{D_{\beta u_n}} \overline{K_{u_n\bar{u}}} + \overline{D_{\beta\beta_n}} \overline{K_{\beta_n\bar{u}}} & \overline{D_{\beta\beta}} + \overline{D_{\beta u_n}} \overline{K_{u_n\beta}} + \overline{D_{\beta\beta_n}} \overline{K_{\beta_n\beta}} \end{bmatrix} \quad (2.52b)$$

$$\bar{G} = \begin{bmatrix} \bar{G}_{uu} + \bar{G}_{uu_n} K_{u_n \bar{u}} & \bar{G}_{uu_n} K_{u_n \bar{\beta}} \\ [0] & \bar{G}_{\beta\beta} \end{bmatrix} \quad (2.52c)$$

$$\bar{K} = \begin{bmatrix} \bar{K}_{uu} + \bar{K}_{uu_n} K_{u_n \bar{u}} + \bar{K}_{u\beta_n} K_{\beta_n \bar{u}} & \bar{K}_{u\beta} + \bar{K}_{uu_n} K_{u_n \bar{\beta}} + \bar{K}_{u\beta_n} K_{\beta_n \bar{\beta}} \\ \bar{K}_{\beta u} + \bar{K}_{\beta u_n} K_{u_n \bar{u}} + \bar{K}_{\beta\beta_n} K_{\beta_n \bar{u}} & \bar{K}_{\beta\beta} + \bar{K}_{\beta u_n} K_{u_n \bar{\beta}} + \bar{K}_{\beta\beta_n} K_{\beta_n \bar{\beta}} \end{bmatrix} \quad (2.52d)$$

$$\bar{A} = \begin{bmatrix} \bar{A}_{uu} + \bar{A}_{uu_n} K_{u_n \bar{u}} & \bar{A}_{uu_n} K_{u_n \bar{\beta}} \\ [0] & [0] \end{bmatrix} \quad (2.52e)$$

$$\bar{L} = \begin{Bmatrix} L_u \\ L_\beta \end{Bmatrix} \quad (2.52f)$$

and \bar{q} is as defined before.

It is important to note that through this variable reduction the resulting flexible vehicle equations, Equation (2.52), does not contain any rigid body modes.

For the total vehicle equations the variables and coefficients of Equation (2.44) are partitioned accordingly and the notation of Equation (2.47) is employed; for example, the second derivative coefficient becomes:

$$[M_{V_T} \ M_{V_R}] \ddot{q} = \begin{bmatrix} M_{V_{uu}} & M_{V_{uu_n}} & M_{V_{\beta\beta}} & M_{V_{\beta\beta_n}} \\ M_{V_{u_n \bar{u}}} & M_{V_{u_n u_n}} & M_{V_{\beta_n \bar{\beta}}} & M_{V_{\beta_n \beta_n}} \end{bmatrix} \begin{Bmatrix} \ddot{u} \\ K_{u_n \bar{u}} \ddot{u} + K_{u_n \bar{\beta}} \ddot{\beta} \\ \ddot{\beta} \\ K_{\beta_n \bar{u}} \ddot{u} + K_{\beta_n \bar{\beta}} \ddot{\beta} \end{Bmatrix} \quad (2.53)$$

where, from Equation (2.46a):

$$\begin{bmatrix} M_{V_{uu}} & M_{V_{uu_n}} \\ M_{V_{u_n \bar{u}}} & M_{V_{u_n u_n}} \end{bmatrix} = M_T \left\{ \left[(R+r_s+u_s) \right]^n - \frac{1}{M_A} (E^{(3)}) \right\}^T M_T (\bar{u}_s)^n \quad (2.54)$$

$$M_{\underline{V}_{UU}} = \bar{M}_T \left\{ \left[(R+r_S+u_S) \right]^{n-1} - \frac{1}{M_A} (E(3))^{n-1} \bar{M}_T (\tilde{u}_S)^{n-1} \right\} \quad (2.54a)$$

$$M_{\underline{V}_{UU_n}} = - \frac{1}{M_A} \bar{M}_T (\tilde{u}_S)^{n-1} (E(3))^{n-1} m_n \quad (2.54b)$$

$$M_{\underline{V}_{U_n U}} = \left[- \frac{1}{M_A} \bar{M}_T (\tilde{u}_S)^{n-1} (E(3))^{n-1} m_n \right]^T \quad (2.54c)$$

$$M_{\underline{V}_{U_n U_n}} = m_n \left[R+r_S+u_S - \frac{1}{M_A} m_n \tilde{u}_n \right] \quad (2.54d)$$

and, from Equation (2.42b):

$$\begin{bmatrix} M_{\underline{V}_{\beta\beta}} & M_{\underline{V}_{\beta\beta_n}} \\ M_{\underline{V}_{\beta_n\beta}} & M_{\underline{V}_{\beta_n\beta_n}} \end{bmatrix} = (C_S^T)^n M_R = \begin{bmatrix} (C_S^T)^{n-1} \bar{M}_R & [0] \\ [0] & C_n^T I_n \end{bmatrix} \quad (2.55)$$

The same procedure is repeated for the remaining coefficients. Partitioning accordingly and using the same subscript notation yields:

from Equation (2.46c):

$$G_{\underline{V}_{UU}} = \bar{M}_T \left\{ 2\omega (R^T + r_S^T + u_S^T) - 2\omega^T (R+r_S+u_S) E(3) \right. \\ \left. + \left[\tilde{\omega} (R+u_S+r_S) \right] + (R+u_S+r_S) \tilde{\omega} \right\}^{n-1} \quad (2.56a)$$

$$G_{\underline{V}_{UU_n}} = G_{\underline{V}_{U_n U}} = [0] \quad (2.56b)$$

$$G_{\underline{V}_{U_n U_n}} = m_n \left\{ 2\omega (R^T + r_S^T + u_S^T) - 2\omega^T (R+r_S+u_S) E(3) \right. \\ \left. + \left[\tilde{\omega} (R+u_S+r_S) \right] + (R+u_S+r_S) \tilde{\omega} \right\} \quad (2.56c)$$

from Equation (2.46d):

$$G_{V\bar{\beta}\bar{\beta}} = \left\{ - \left[\left(C_S^T I_S C_S \tilde{\omega} \right)^{n-1} + \left(C_S^T \right)^{n-1} \bar{H}_R \left[C_S \left(\tilde{\omega} + C_S^T \dot{\tilde{\beta}}_S \right) \right]^{n-1} \right. \right. \\ \left. \left. + \left[\left(\tilde{\omega} + C_S^T \dot{\tilde{\beta}}_S \right) C_S^T \right]^{n-1} \bar{H}_R \left(C_S \right)^{n-1} \right\} \left(C_S^T \right)^{n-1} \quad (2.57a)$$

$$G_{V\bar{\beta}\beta_n} = G_{V\beta_n\bar{\beta}} = [0] \quad (2.57b)$$

$$G_{V\beta_n\beta_n} = \left\{ - \left(C_n^T I_n C_n \tilde{\omega} \right) + C_n^T I_n C_n \left(\tilde{\omega} + C_n^T \dot{\tilde{\beta}}_n \right) + \left(\tilde{\omega} + C_n^T \dot{\tilde{\beta}}_n \right) C_n^T I_n C_n \right\} C_n^T \quad (2.57c)$$

from Equation (2.46e):

$$A_{V\bar{u}\bar{u}} = \bar{H}_T \left\{ - \tilde{\omega} \left(R + r_S + u_S \right) \omega^T - \tilde{\omega} \left[\omega^T \left(R + r_S \right) \right] + \dot{\omega} \left(2R^T + 2r_S^T + u_S^T \right) \right. \\ \left. - \left(R + r_S + u_S \right) \dot{\omega}^T - \left[\dot{\omega}^T \left(R + r_S \right) \right] E(3) \right\}^{n-1} \quad (2.58a)$$

$$A_{V\bar{u}u_n} = A_{V u_n \bar{u}} = [0] \quad (2.58b)$$

$$A_{V u_n u_n} = \bar{H}_T \left\{ - \tilde{\omega} \left(R + r_n + u_n \right) \omega^T - \tilde{\omega} \left[\omega^T \left(R + r_n \right) \right] + \dot{\omega} \left(2R^T + 2r_n^T + u_n^T \right) \right. \\ \left. - \left(R + r_n + u_n \right) \dot{\omega}^T - \left[\dot{\omega}^T \left(R + r_n \right) \right] E(3) \right\} \quad (2.58c)$$

and, from Equation (2.42f):

$$\begin{bmatrix} A_{V\bar{\beta}\bar{\beta}} & A_{V\bar{\beta}\beta_n} \\ A_{V\beta_n\bar{\beta}} & A_{V\beta_n\beta_n} \end{bmatrix} = [0] \quad (2.59)$$

Since q_n does not appear on the right hand side of Equation (2.46) this part of the total vehicle equation will remain as is. The left hand side of the equation is multiplied through making use of the coefficient partitioning

in Equations (2.53), (2.56), (2.57), (2.58), and (2.59) and combined into matrix coefficients for \bar{q} . This results in the complete total vehicle equations:

$$\bar{M}_V \ddot{\bar{q}} + \bar{G}_V \dot{\bar{q}} + \bar{A}_V \bar{q} = \bar{L}_V \quad (2.60)$$

where:

$$\begin{aligned} \bar{M}_V = \left(E(3) \right)^{n-1 T} & \left[M_{V_{UU}} + M_{V_{U_n U_n}} K_{U_n \bar{u}} \mid M_{V_{\beta\beta}} + M_{V_{U_n U_n}} K_{U_n \bar{\beta}} \right] \\ & + \left[\begin{array}{c} M_{V_{U_n \bar{u}}} + M_{V_{U_n U_n}} K_{U_n \bar{u}} \mid M_{V_{U_n U_n}} K_{U_n \bar{\beta}} \\ + M_{V_{\beta_n \beta_n}} K_{\beta_n \bar{u}} \mid + M_{V_{\beta_n \beta_n}} K_{\beta_n \bar{\beta}} \end{array} \right] \end{aligned} \quad (2.60a)$$

$$\begin{aligned} \bar{G}_V = \left(E(3) \right)^{n-1 T} & \left[G_{V_{UU}} \mid G_{V_{\beta\beta}} \right] \\ & + \left[G_{V_{U_n U_n}} K_{U_n \bar{u}} + G_{V_{\beta_n \beta_n}} K_{\beta_n \bar{u}} \mid G_{V_{U_n U_n}} K_{U_n \bar{\beta}} + G_{V_{\beta_n \beta_n}} K_{\beta_n \bar{\beta}} \right] \end{aligned} \quad (2.60b)$$

$$\bar{A}_V = \left(E(3) \right)^{n-1 T} \left[A_{V_{UU}} \mid [0] \right] + \left[A_{V_{U_n U_n}} K_{U_n \bar{u}} \mid A_{V_{U_n U_n}} K_{U_n \bar{\beta}} \right] \quad (2.60c)$$

$$\bar{L}_V = T - \left(E(3) \right)^n \left\{ L_{V_T} + L_{V_R} \right\} \quad (2.60d)$$

and, for completeness:

$$M_A \ddot{\Theta X} = F \quad (2.61)$$

By substituting $\Gamma(\omega)$, Equation (2.41), into $\Theta(\Gamma)$ in Equation (2.31), and substituting this and $C_S(\beta_S)$, Equation (2.30), into Equations (2.52), (2.60), and (2.61) these complete dynamic equations represent $6n$ equations in $6n$ unknowns (\bar{q} , X , and ω), for $6n$ rigid sub-bodies. These equations are nonlinear with respect to the unknowns.

2.2 LINEARIZATION OF THE DYNAMIC EQUATIONS

2.2.1 Variable Linearization

The resulting dynamic equations presented in Paragraph 2.1.5 are nonlinear in \bar{q} . Worse off, the coefficients are also a function of \underline{X} , $\underline{\omega}$, $\underline{\theta}$, and C_S which are also time varying (most being somewhat a function of \bar{q}). The dynamic equations have been formulated such that \bar{q} is to be solved for assuming that the coefficients are known. With this in mind, the dynamic equations will be linearized in \bar{q} .

It is reasonable to assume that there will not be any large amplitude high frequency deformations. Thus, the motion of the vehicle can be divided into two components: quasi-static and perturbation. The quasi-static corresponds to motions that vary relatively slowly. The perturbation corresponds to small amplitude fluctuations about the quasi-static position. Thus, \bar{q} is approximated as:

$$\bar{q} \approx \bar{q}_0 + \Delta\bar{q} \quad (2.62)$$

where:

\bar{q}_0 = quasi-static deformation. It is, the part of the deformation for which time rate of change of the deformation is negligible, i.e.,

$$(\bar{K} + \bar{A})^{-1} \bar{M} \ddot{\bar{q}}_0 \ll \bar{q}_0 \quad \text{and} \quad (\bar{K} + \bar{A})^{-1} (\bar{D} + \bar{G}) \dot{\bar{q}}_0 \ll \bar{q}_0 \quad (2.63)$$

$\Delta\bar{q}$ = perturbation deformation. It is, the part of the deformation for which amplitudes are small; thus nonlinear terms are negligible, i.e.,

$$\begin{aligned} & (\bar{K} + \bar{A})^{-1} \bar{M} \Delta\ddot{\bar{q}}, (\bar{K} + \bar{A})^{-1} (\bar{D} + \bar{G}) \Delta\dot{\bar{q}}, \text{ and } \Delta\bar{q} \Delta\bar{q} \\ & \ll (\bar{K} + \bar{A})^{-1} \bar{M} \ddot{\Delta\bar{q}}, (\bar{K} + \bar{A})^{-1} (\bar{D} + \bar{G}) \dot{\Delta\bar{q}}, \text{ and } \Delta\dot{\bar{q}} \end{aligned} \quad (2.64)$$

Likewise, the coefficients of \bar{q} can also be decomposed into quasi-static and perturbation components. As was done for \bar{q} , quasi-static components will

be denoted with a subscript o and perturbation components will be denoted with a leading Δ . These components will be expanded as needed in the following sections.

The total vehicle variables, \mathbf{X} and ω , will take exception to the quasi-static definition; the time derivatives of \mathbf{X}_o and ω_o are not zero. The quasi-static motion of the vehicle is such that at any instant of time the maneuver is maintained such that the vehicle does not translate or rotate, but has total vehicle velocity and acceleration; about which only the transient deformations are allowed to subside.

2.2.2 Quasi-static Equations

For the quasi-static equations all terms that are "highly" time dependant and of small amplitude (See Paragraph 2.2.1) will be eliminated. Therefore, the coordinate approximations developed in the previous section will not be used here. In the following sections the auxiliary equations, Equations (2.34) and (2.36), flexible vehicle equations, Equation (2.52), and total vehicle equations, Equations (2.60) and (2.61), will be approximated, in this order, with respect to the quasi-static assumptions.

2.2.2.1 Auxiliary Equations

With the full nonlinear nature of the dynamic equations being retained, the auxiliary equations change very little. The coordinate transformation matrices, \mathbf{C}_s and Θ , Equations (2.34) and (2.36), respectively, are rewritten using a subscript o to indicate that they are evaluated under the quasi-static assumptions (See Equation (2.63)):

$$\mathbf{C}_{s_o} = \begin{bmatrix} c\beta_{s_{o3}} & c\beta_{s_{o2}} & c\beta_{s_{o3}} s\beta_{s_{o2}} s\beta_{s_{o1}} & -c\beta_{s_{o3}} s\beta_{s_{o2}} c\beta_{s_{o1}} \\ & & +s\beta_{s_{o3}} c\beta_{s_{o1}} & +s\beta_{s_{o3}} s\beta_{s_{o1}} \\ -s\beta_{s_{o3}} & c\beta_{s_{o2}} & -s\beta_{s_{o3}} s\beta_{s_{o2}} s\beta_{s_{o1}} & -s\beta_{s_{o3}} s\beta_{s_{o2}} c\beta_{s_{o1}} \\ & & +c\beta_{s_{o3}} c\beta_{s_{o1}} & +c\beta_{s_{o3}} s\beta_{s_{o1}} \\ & s\beta_{s_{o2}} & -c\beta_{s_{o2}} s\beta_{s_{o1}} & c\beta_{s_{o2}} c\beta_{s_{o1}} \end{bmatrix} \quad (2.65)$$

and:

$$\Theta_0 = \begin{bmatrix} c\Gamma_{03} c\Gamma_{02} & c\Gamma_{03} s\Gamma_{02} s\Gamma_{01} + s\Gamma_{03} c\Gamma_{01} & -c\Gamma_{03} s\Gamma_{02} c\Gamma_{01} + s\Gamma_{03} s\Gamma_{01} \\ -s\Gamma_{03} c\Gamma_{02} & -s\Gamma_{03} s\Gamma_{02} s\Gamma_{01} + c\Gamma_{03} c\Gamma_{01} & -s\Gamma_{03} s\Gamma_{02} c\Gamma_{01} + c\Gamma_{03} s\Gamma_{01} \\ s\Gamma_{02} & -c\Gamma_{02} s\Gamma_{01} & c\Gamma_{02} c\Gamma_{01} \end{bmatrix} \quad (2.66)$$

Likewise, Γ is expressed as a function of ω in Equation (2.41). Under the quasi-static assumptions Γ^* does not change. Thus, Equation (2.41) becomes:

$$\Gamma_0 = \int_0^t \omega_0 dt + \Gamma^* \quad (2.67)$$

Θ_0 is found by substituting Equation (2.67) into Equation (2.66). For many applications Γ_0 and Θ_0 may be input as a known initial condition: $t=0$, thus eliminating the integral in Equation (2.67).

2.2.2.2 Flexible Vehicle Equations

Without the time derivative \bar{q} terms, Equation (2.52) reduces to:

$$\bar{K}q_0 + \bar{A}_0 \bar{q}_0 = \bar{L}_0 \quad (2.68)$$

where:

$$A_0 = \begin{bmatrix} A_{0uu} & +A_{0uu_n} K_{u_n \bar{u}} & A_{0uu_n} K_{u_n \bar{\beta}} \\ [0] & & [0] \end{bmatrix} \quad (2.68a)$$

$$L_0 = \begin{bmatrix} L_{0\bar{u}} \\ L_{0\bar{\beta}} \end{bmatrix} = \begin{bmatrix} -\bar{M}_T \left[(\Theta_0)^{n-1} \ddot{\bar{X}}_0 + (\omega_0 + \tilde{\omega}_0 \tilde{\omega}_0)^{n-1} (\bar{R}' + \bar{r}') \right] + \bar{f}_0 \\ - (C_{S_0}^T)^{n-1} \bar{M}_R (C_{S_0})^{n-1} \dot{\omega}_0 - (\tilde{\omega}_0 C_{S_0}^T)^{n-1} \bar{M}_R (C_{S_0})^{n-1} \omega_0 + \bar{t}_0 \end{bmatrix} \quad (2.68b)$$

and:

$$A_{0UU} = \bar{M}_T (\bar{\omega}_0 + \tilde{\omega}_0 \tilde{\omega}_0)^{n-1} \left[E(3n-3) - \frac{1}{M_A} (E(3))^{n-1} \bar{M}_T \right] \quad (2.68c)$$

$$A_{0UU_n} = \frac{1}{M_A} \bar{M}_T (E(3))^{n-1} (\bar{\omega}_0 + \tilde{\omega}_0 \tilde{\omega}_0) m_n \quad (2.68d)$$

note:

\bar{F}_0 and \bar{T}_0 are column matrices of quasi-static load components applied externally to the n-1 subbodies, resolved relative to the {a} reference frame.

X_0 is the quasi-static inertial position of the vehicle center of mass.

ω_0 is the quasi-static angular velocity of {b} relative to {i}.

\bar{M}_T , \bar{M}_R , K , and \bar{q}_0 are as before.

2.2.2.3 Total Vehicle Equations

The quasi-static component of the total vehicle equations are also simplified. The time derivative \bar{q} terms in Equation (2.60) are neglected as stipulated by the assumptions imposed in Equation (2.63). In keeping with the quasi-static assumption, the total vehicle acceleration terms are not neglected: that is, the first time derivative of ω_0 and the second time derivative of X_0 are retained. All that remains of the total vehicle equations, Equations (2.61) and (2.60), are:

$$F_0 = M_A \Theta_0 \ddot{X}_0 \quad (2.69)$$

and,

$$\bar{A}_{V_0} \bar{q}_0 = \bar{L}_{V_0} \quad (2.70)$$

where:

$$\bar{A}_{V_O} = (E(3))^{n-1} \left[A_{V_O \bar{U}U} | [0] \right] + \left[A_{V_O u_n u_n} K_{u_n \bar{u}} | A_{V_O u_n u_n} K_{u_n \bar{\beta}} \right] \quad (2.70a)$$

$$\bar{L}_{V_O} = T_O - (E(3))^{n-1} \left\{ L_{V_O T} + L_{V_O R} \right\} \quad (2.70b)$$

and from Equations (2.58a), (2.58c), (2.46g), and (2.46h) respectively:

$$A_{V_O \bar{U}U} = \bar{M}_T \left\{ -\tilde{\omega}_O (R+r_S+u_{S_O}) \omega_O^T - \tilde{\omega}_O \left[\omega_O^T (R+r_S) \right] + \dot{\omega}_O (2R^T + 2r_S^T + u_{S_O}^T) - (R+r_S+u_{S_O}) \dot{\omega}_O^T - \left[\dot{\omega}_O^T (R+r_S) \right] E(3) \right\}^{n-1} \quad (2.70c)$$

$$A_{V_O u_n u_n} = \bar{M}_n \left\{ -\tilde{\omega}_O (R+r_n+u_{n_O}) \omega_O^T - \tilde{\omega}_O \left[\omega_O^T (R+r_n) \right] + \dot{\omega}_O (2R^T + 2r_n^T + u_{n_O}^T) - (R+r_n+u_{n_O}) \dot{\omega}_O^T - \left[\dot{\omega}_O^T (R+r_n) \right] E(3) \right\} \quad (2.70d)$$

$$L_{V_O T} = \bar{M}_T \left\{ -\tilde{\omega}_O \left[(R^T + r_S^T) \omega_O \right] + \dot{\omega}_O (R^T + r_S^T) - (R+r_S) \dot{\omega}_O^T \right\}^n (R' + r') \quad (2.70e)$$

$$L_{V_O R} = (C_{S_O}^T)^n \bar{M}_R (C_{S_O})^n \omega_O' + (\tilde{\omega}_O C_{S_O}^T)^n \bar{M}_R (C_{S_O})^n \omega_O' \quad (2.70f)$$

note:

F_O and T_O are column matrices of the quasi-static load components applied to the vehicle relative to the vehicle center of mass, resolved relative to the {b} reference frame.

2.2.3 Perturbation Equations

In the previous section (Paragraph 2.2.2) the quasi-static dynamic equations were developed. In this section the corresponding perturbation equations will be developed. Here, the aircraft deformations are assumed small in amplitude, thus the equations will be linearized (See Equation (2.64)). As was done for the quasi-static equations in Section 2.63, the perturbation dynamic equations will be presented in three parts: auxiliary equations, flexible vehicle equations, and total vehicle equations.

2.2.3.1 Auxiliary Equations

In keeping with the perturbation assumptions it is assumed that the deformation of the structure is limited, that is $\Delta \underline{\omega}_S$ and $\Delta \underline{\beta}_S$ are limited. Specifically, $\Delta \underline{\beta}_S$ will never achieve magnitudes greater than 10 to 15 degrees. With this assumption some of the auxiliary equations are reduced.

By making the above assumption and assuming that $\{\underline{a}_S\}$ for the perturbation analysis coincides with $\{\underline{a}\}$ prior to perturbation deformation, $\Delta \underline{\beta}_S$ is approximately represented in the $\{\underline{a}\}$ reference frame. In so doing, however, note that \underline{I}_S (the inertial element dyadic) will not, in general, be diagonal. With $\Delta \underline{\beta}_S$ redefined, $\Delta \underline{\omega}_S$ becomes (See Equation (2.9)):

$$\begin{aligned} \Delta \underline{\omega}_S &= \Delta \underline{\omega} + \Delta \underline{\Omega}^a + \Delta \underline{\Omega}^S \\ &= \Delta \underline{\omega} + \Delta \underline{\Omega}^a + \Delta \dot{\underline{\beta}}_S \\ &\cong \Delta \underline{\omega} + \Delta \underline{\Omega}^a + \{\underline{a}_S\}^T \dot{\Delta \underline{\beta}}_S \end{aligned} \quad (2.71)$$

Likewise, the element mass inertial dyadic, $\underline{\underline{I}}_S$, is now defined as (See Equation (2.28)):

$$\begin{aligned} \underline{\underline{I}}_S &\cong \underline{I}_S \alpha \beta \underline{a}_S \alpha \underline{a}_S \beta \\ &= \{\underline{a}_{S1} \quad \underline{a}_{S2} \quad \underline{a}_{S3}\} \begin{bmatrix} I_{S11} & I_{S12} & I_{S13} \\ I_{S21} & I_{S22} & I_{S23} \\ I_{S31} & I_{S32} & I_{S33} \end{bmatrix} \begin{Bmatrix} \underline{a}_{S1} \\ \underline{a}_{S2} \\ \underline{a}_{S3} \end{Bmatrix} \\ &= \{\underline{a}_S\}^T \underline{I}_S \{\underline{a}_S\} \end{aligned} \quad (2.72)$$

It is desirable to keep I_s time independent. This is done by allowing $\{\underline{a}_s\}$ to rotate with the rigid sub-body. The direction cosine, ΔC_s , relating $\{\underline{a}_s\}$ and $\{\underline{a}\}$, is expressed in terms of $\Delta\beta_s$. With the small $\Delta\beta_s$ assumption, this relationship between $\{\underline{a}_s\}$ and $\{\underline{a}\}$, Equation (2.33), is approximated as:

$$\begin{aligned} \{\underline{a}_s\} &\cong \begin{bmatrix} 1 & \Delta\beta_{s3} & -\Delta\beta_{s2} \\ -\Delta\beta_{s3} & 1 & \Delta\beta_{s1} \\ \Delta\beta_{s2} & -\Delta\beta_{s1} & 1 \end{bmatrix} C_{s_0}^T \{\underline{a}\} \\ &= \left\{ \begin{bmatrix} 1 & 0 & 0 \\ 0 & 1 & 0 \\ 0 & 0 & 1 \end{bmatrix} - \begin{bmatrix} 0 & -\Delta\beta_{s3} & \Delta\beta_{s2} \\ \Delta\beta_{s3} & 0 & -\Delta\beta_{s1} \\ -\Delta\beta_{s2} & \Delta\beta_{s1} & 0 \end{bmatrix} \right\} C_{s_0}^T \{\underline{a}\} \\ &= [E(3) - \Delta\tilde{\beta}_s] C_{s_0}^T \{\underline{a}\} = \Delta C_s C_{s_0}^T \{\underline{a}\} \end{aligned} \quad (2.73)$$

Note also:

$$\begin{aligned} \{\underline{a}_s\}^T &= \left([E(3) - \Delta\tilde{\beta}_s] C_{s_0}^T \{\underline{a}\} \right)^T \\ &= \{\underline{a}\}^T C_{s_0} [E(3) - \Delta\tilde{\beta}_s]^T \\ &= \{\underline{a}\}^T C_{s_0} [E(3) + \Delta\tilde{\beta}_s] = \{\underline{a}\}^T C_{s_0} \Delta C_s^T \end{aligned} \quad (2.73a)$$

$$(\Delta C_s)^n \cong E(3n) - (\Delta\tilde{\beta}_s)^n \quad (2.73b)$$

$$(\Delta C_s^T)^n \cong E(3n) + (\Delta\tilde{\beta}_s)^n \quad (2.73c)$$

Likewise, the perturbation coordinate transformation relating the vehicle's inertial orientation, $\Delta\theta$, is expressed in terms of $\Delta\Gamma$ (See Equation (2.36)). The same approximation used for ΔC_s in Equation (2.73) is used for $\Delta\theta$:

$$\Delta\theta \begin{bmatrix} 1 & \Delta\Gamma_3 & -\Delta\Gamma_2 \\ -\Delta\Gamma_3 & 1 & \Delta\Gamma_1 \\ \Delta\Gamma_2 & -\Delta\Gamma_1 & 1 \end{bmatrix} = \begin{bmatrix} 1 & 0 & 0 \\ 0 & 1 & 0 \\ 0 & 0 & 1 \end{bmatrix} - \begin{bmatrix} 0 & -\Delta\Gamma_3 & \Delta\Gamma_2 \\ \Delta\Gamma_3 & 0 & -\Delta\Gamma_1 \\ -\Delta\Gamma_2 & \Delta\Gamma_1 & 0 \end{bmatrix} = E(3) - \Delta\tilde{\Gamma} \quad (2.74)$$

also:

$$\Delta\theta^T \cong E(3) + \Delta\bar{\Gamma} \quad (2.74a)$$

$$(\Delta\theta)^n \cong E(3n) - (\Delta\bar{\Gamma})^n \quad (2.74b)$$

$$(\Delta\theta^T)^n \cong E(3n) + (\Delta\bar{\Gamma})^n \quad (2.74c)$$

Finally, $\Delta\Gamma$ is found by substituting $\Delta\omega$ for the perturbation component in Equation (2.41):

$$\Delta\Gamma = \int_0^t \Delta\omega dt \quad (2.75)$$

For $\Delta\Gamma$ to be expressed as a linear function of $\Delta\omega$, and hence $\Delta\theta$ also to be expressed as a linear function of $\Delta\omega$, then $\Delta\omega$ as a function of time must be known, the integration of Equation (2.75) performed, and the result linearized. The functional form of $\Delta\omega$ will not be assumed here. Instead, all $\Delta\Gamma$ terms will remain on the right-hand side of the dynamic equations as an apparent forcing term.

2.2.3.2 Flexible Vehicle Equations

All the previous approximations are implemented into the nonlinear flexible vehicle equations (Equation (2.52)). The following rational is utilized: any linear terms in ΔC_S , $\Delta\theta$, and $\Delta\omega$ are retained; any time derivative quasi-static deformation terms are neglected (See Paragraph 2.2.2). Using the quasi-static/perturbation notation of Equations (2.63) and (2.64), the perturbation flexible vehicle equation is written as:

$$\bar{H}_0 \Delta\ddot{q} + \bar{D} \Delta\dot{q} + \bar{G}_0 \Delta\dot{q} + \bar{K} \Delta q + \Delta\bar{A}_0 \Delta\bar{q} = \Delta\bar{L} - \Delta\bar{A}q_0 \quad (2.76)$$

where:

$$\Delta \bar{q} = \begin{Bmatrix} \Delta \bar{u}' \\ \Delta \bar{\beta}' \end{Bmatrix} \quad (2.76a)$$

$$\bar{H}_0 = \begin{bmatrix} M_{0\bar{u}\bar{u}} + M_{0\bar{u}u_n} K_{u_n\bar{u}} & M_{0\bar{u}u_n} K_{u_n\bar{\beta}} \\ [0] & M_{0\bar{\beta}\bar{\beta}} \end{bmatrix} \quad (2.76b)$$

$$\bar{G}_0 = \begin{bmatrix} G_{0\bar{u}\bar{u}} + G_{0\bar{u}u_n} K_{u_n\bar{u}} & G_{0\bar{u}u_n} K_{u_n\bar{\beta}} \\ [0] & G_{0\bar{\beta}\bar{\beta}} \end{bmatrix} \quad (2.76c)$$

$$\Delta \bar{A}_0 = \begin{bmatrix} \Delta A_{0\bar{u}\bar{u}} + \Delta A_{0\bar{u}u_n} K_{u_n\bar{u}} & \Delta A_{0\bar{u}u_n} K_{u_n\bar{\beta}} \\ \Delta A_{0\bar{\beta}\bar{\beta}} K_{\beta_n\bar{u}} & \Delta A_{0\bar{\beta}\bar{\beta}} + \Delta A_{0\bar{\beta}\beta_n} K_{\beta_n\bar{\beta}} \end{bmatrix} \quad (2.76d)$$

$$\Delta \bar{L} = \begin{Bmatrix} \Delta L_{\bar{u}} \\ \Delta L_{\bar{\beta}} \end{Bmatrix} = \begin{Bmatrix} -\bar{H}_T \left[(\Delta \theta)^{n-1} \ddot{\bar{x}}_0 + (\theta_0)^{n-1} \ddot{\Delta \bar{x}}' + (\Delta \dot{\omega} + \Delta \ddot{\omega} \tilde{\omega}_0 + \tilde{\omega}_0 \Delta \ddot{\omega})^{n-1} (\bar{R}' + \bar{r}') + \Delta \bar{f} \right] \\ - (C_{S_0}^T)^{n-1} \bar{H}_R (C_{S_0})^{n-1} \Delta \dot{\omega}' - (\Delta \tilde{\omega} C_{S_0}^T)^{n-1} \bar{H}_R (C_{S_0} \omega_0)^{n-1} \\ - (\tilde{\omega}_0 C_{S_0}^T)^{n-1} \bar{H}_R (C_{S_0} \Delta \omega)^{n-1} + \Delta \bar{t} \end{Bmatrix} \quad (2.76e)$$

$$\Delta \bar{A} = \begin{bmatrix} \Delta A_{\bar{u}\bar{u}} + \Delta A_{\bar{u}u_n} K_{u_n\bar{u}} & \Delta A_{\bar{u}u_n} K_{u_n\bar{\beta}} \\ [0] & [0] \end{bmatrix} \quad (2.76f)$$

and, from Equations (2.48):

$$\begin{aligned} \begin{bmatrix} M_{0\bar{u}\bar{u}} & M_{0\bar{u}u_n} \\ M_{0u_n\bar{u}} & M_{0u_nu_n} \end{bmatrix} &= \bar{H}_T \left[E(3n) - \frac{1}{M_A} (E(3))^n \right] \bar{H}_T \\ &= \begin{bmatrix} \bar{H}_T \left[E(3n-3) - \frac{1}{M_A} (E(3))^{n-1} \bar{H}_T \right] - \frac{1}{M_A} \bar{H}_T (E(3))^{n-1} m_n \\ \left[-\frac{1}{M_A} \bar{H}_T (E(3))^{n-1} m_n \right]^T & m_n \left[E(3) - \frac{1}{M_A} m_n \right] \end{bmatrix} \\ &= \begin{bmatrix} M_{\bar{u}\bar{u}} & M_{\bar{u}u_n} \\ M_{u_n\bar{u}} & M_{u_nu_n} \end{bmatrix} \end{aligned} \quad (2.77a)$$

$$\begin{aligned} \begin{bmatrix} M_{0\bar{\beta}\bar{\beta}} & M_{0\bar{\beta}\beta_n} \\ M_{0\beta_n\bar{\beta}} & M_{0\beta_n\beta_n} \end{bmatrix} &= (C_{S_0}^T)^n M_R \\ &= \begin{bmatrix} (C_{S_0}^T)^{n-1} M_R & [0] \\ [0] & C_{nI_n}^T \end{bmatrix} = \begin{bmatrix} \bar{M}_{\bar{\beta}\bar{\beta}} & \bar{M}_{\bar{\beta}\beta_n} \\ \bar{M}_{\beta_n\bar{\beta}} & \bar{M}_{\beta_n\beta_n} \end{bmatrix} \end{aligned} \quad (2.77b)$$

from Equations (2.49):

$$\begin{aligned} \begin{bmatrix} G_{0\bar{u}\bar{u}} & G_{0\bar{u}u_n} \\ G_{0u_n\bar{u}} & G_{0u_nu_n} \end{bmatrix} &= 2\bar{M}_T (\tilde{\omega}_0)^n \left[E(3n) - \frac{1}{M_A} (E(3))^n \bar{M}_T \right] \\ &= \begin{bmatrix} 2\bar{M}_T (\tilde{\omega}_0)^{n-1} \left[E(3n-3) - \frac{1}{M_A} (E(3))^{n-1} \bar{M}_T \right] - \frac{2}{M_A} \bar{M}_T (E(3))^{n-1} \tilde{\omega}_0^{m_n} & \\ \left[-\frac{2}{M_A} \bar{M}_T (E(3))^{n-1} \tilde{\omega}_0^{m_n} \right]^T & 2m_n \tilde{\omega}_0 \left[E(3) - \frac{1}{M_A} m_n \right] \end{bmatrix} \end{aligned} \quad (2.77c)$$

$$\begin{aligned} \begin{bmatrix} G_{0\bar{\beta}\bar{\beta}} & G_{0\bar{\beta}\beta_n} \\ G_{0\beta_n\bar{\beta}} & G_{0\beta_n\beta_n} \end{bmatrix} &= (C_{S_0}^T)^n M_R (C_{S_0} \tilde{\omega}_0 C_{S_0}^T)^n + (\tilde{\omega}_0 C_{S_0}^T)^n M_R - \left[(C_{S_0}^T I_S C_{S_0} \omega_0) \right] C_{S_0}^T \hat{C}_{S_0}^T \hat{C}_{S_0}^T \\ &= \begin{bmatrix} (C_{S_0}^T)^{n-1} \bar{M}_R (C_{S_0} \tilde{\omega}_0 C_{S_0}^T)^{n-1} + (\tilde{\omega}_0 C_{S_0}^T)^{n-1} \bar{M}_R & [0] \\ - \left[(C_{S_0}^T I_S C_{S_0} \omega_0) \right] C_{S_0}^T \hat{C}_{S_0}^T \hat{C}_{S_0}^T & \\ [0] & C_{n_0}^T I_n C_{n_0} \tilde{\omega}_0 C_{n_0}^T + \tilde{\omega}_0 C_{n_0}^T I_n - \left[C_{n_0}^T I_n C_{n_0} \omega_0 \right] \hat{C}_{n_0}^T \hat{C}_{n_0}^T \end{bmatrix} \end{aligned} \quad (2.77d)$$

from Equations (2.50) and (2.51):

$$\begin{aligned} \begin{bmatrix} \Delta A_{0\bar{u}\bar{u}} & \Delta A_{0\bar{u}u_n} \\ \Delta A_{0u_n\bar{u}} & \Delta A_{0u_nu_n} \end{bmatrix} &= \bar{M}_T (\tilde{\omega}_0 + \tilde{\omega}_0 \tilde{\omega}_0)^n \left[E(3n) - \frac{1}{M_A} (E(3))^n \bar{M}_T \right] \\ &= \begin{bmatrix} \bar{M}_T (\tilde{\omega}_0 + \tilde{\omega}_0 \tilde{\omega}_0)^{n-1} \left[E(3n-3) - \frac{1}{M_A} (E(3))^{n-1} \bar{M}_T \right] & \frac{1}{M_A} \bar{M}_T (E(3))^{n-1} (\tilde{\omega}_0 + \tilde{\omega}_0 \tilde{\omega}_0)^{m_n} \\ \left[\frac{1}{M_A} \bar{M}_T (E(3))^{n-1} (\tilde{\omega}_0 + \tilde{\omega}_0 \tilde{\omega}_0)^{m_n} \right]^T & m_n (\tilde{\omega}_0 + \tilde{\omega}_0 \tilde{\omega}_0) \left[E(3) - \frac{1}{M_A} m_n \right] \end{bmatrix} \end{aligned} \quad (2.77e)$$

$$\begin{aligned}
\begin{bmatrix} \Delta A_{o\bar{\beta}\bar{\beta}} & \Delta A_{o\bar{\beta}\beta_n} \\ \Delta A_{o\beta_n\bar{\beta}} & \Delta A_{o\beta_n\beta_n} \end{bmatrix} &= (C_{S_o}^T)^n M_R (C_{S_o} \bar{\omega}_o)^n - \left[(C_{S_o}^T I_S C_{S_o} \bar{\omega}_o) \right]^n + (\bar{\omega}_o C_{S_o}^T)^n M_R (C_{S_o} \bar{\omega}_o)^n \\
&\quad - \left[\bar{\omega}_o (C_{S_o}^T I_S C_{S_o} \bar{\omega}_o) \right]^n \\
&= \begin{bmatrix} (C_{S_o}^T)^{n-1} M_R (C_{S_o} \bar{\omega}_o)^{n-1} - \left[(C_{S_o}^T I_S C_{S_o} \bar{\omega}_o) \right]^{n-1} & [0] \\ + (\bar{\omega}_o C_{S_o}^T)^{n-1} M_R (C_{S_o} \bar{\omega}_o)^{n-1} - \left[\bar{\omega}_o (C_{S_o}^T I_S C_{S_o} \bar{\omega}_o) \right]^{n-1} & \\ [0] & C_{n_o}^T I_n C_{n_o} \bar{\omega}_o - (C_{n_o}^T I_n C_{n_o} \bar{\omega}_o) + \bar{\omega}_o C_{n_o}^T I_n C_{n_o} \bar{\omega}_o - \bar{\omega}_o (C_{n_o}^T I_n C_{n_o} \bar{\omega}_o) \end{bmatrix} \quad (2.77f)
\end{aligned}$$

$$\begin{aligned}
\begin{bmatrix} \Delta A_{u\bar{u}} & \Delta A_{u\bar{u}u_n} \\ \Delta A_{u_n\bar{u}} & \Delta A_{u_n u_n} \end{bmatrix} &= M_T (\Delta \bar{\omega} + \Delta \bar{\omega} \bar{\omega}_o + \bar{\omega}_o \Delta \bar{\omega})^n \left[E(3n) - \frac{1}{M_A} (E(3))^n M_T \right] \\
&= \begin{bmatrix} M_T (\Delta \bar{\omega} + \Delta \bar{\omega} \bar{\omega}_o + \bar{\omega}_o \Delta \bar{\omega})^{n-1} & \frac{1}{M_A} M_T (E(3))^{n-1} (\Delta \bar{\omega} + \Delta \bar{\omega} \bar{\omega}_o + \bar{\omega}_o \Delta \bar{\omega}) m_n \\ \cdot \left[E(3n-3) - \frac{1}{M_A} (E(3))^{n-1} M_T \right] & \\ \left[\frac{1}{M_A} M_T (E(3))^{n-1} (\Delta \bar{\omega} + \Delta \bar{\omega} \bar{\omega}_o + \bar{\omega}_o \Delta \bar{\omega}) m_n \right]^T & m_n (\Delta \bar{\omega} + \Delta \bar{\omega} \bar{\omega}_o + \bar{\omega}_o \Delta \bar{\omega}) \left[E(3) - \frac{1}{M_A} m_n \right] \end{bmatrix} \quad (2.77g)
\end{aligned}$$

Remarks:

1. $\Delta \bar{F}$ and $\Delta \bar{f}$ are column matrices of perturbation load components applied externally to the sub-bodies, resolved relative to the $\{a\}$ reference frame.
2. M_T , M_R , H_T , H_R , D , and K are as defined before.

2.2.3.3 Total Vehicle Equations

The perturbation total vehicle equations are developed in a manner similar to the development of the perturbation flexible vehicle in the previous subsection: The approximations derived in Paragraph 2.2.3.1 are implemented into the nonlinear total vehicle equations, Equation (2.60) and (2.61). Only first order perturbation terms are retained; zero order terms

having been accounted for in the quasi-static total vehicle equations, Equations (2.69) and (2.70), and higher order terms assumed negligible (See Equation (2.64)). This yields:

$$M_A \theta_0 \Delta \ddot{x} = \Delta F - M_A \Delta \theta \ddot{x}_0 \quad (2.78)$$

and:

$$\bar{M}_{V_0} \Delta \ddot{q} + \bar{G}_{V_0} \dot{\Delta q} + \Delta \bar{A}_{V_0} \Delta \bar{q} = \Delta \bar{L}_V - \Delta \bar{A} \bar{q}_0 \quad (2.79)$$

where:

$$\begin{aligned} \bar{M}_{V_0} = & \left(E(3) \right)^{n-1 T} \left[M_{V_0 \bar{u}\bar{u}} + M_{V_0 \bar{u}u_n} K_{u_n \bar{u}} \mid M_{V_0 \bar{\beta}\bar{\beta}} + M_{V_0 \bar{u}u_n} K_{u_n \bar{\beta}} \right] \\ & + \left[M_{V_0 u_n \bar{u}} + M_{V_0 u_n u_n} K_{u_n \bar{u}} \mid M_{V_0 u_n u_n} K_{u_n \bar{\beta}} \right] \\ & \quad + \left[M_{V_0 \beta_n \beta_n} K_{\beta_n \bar{u}} \mid M_{V_0 \beta_n \beta_n} K_{\beta_n \bar{\beta}} \right] \end{aligned} \quad (2.79a)$$

$$\begin{aligned} \bar{G}_{V_0} = & \left(E(3) \right)^{n-1 T} \left[G_{V_0 \bar{u}\bar{u}} \mid G_{V_0 \bar{\beta}\bar{\beta}} \right] \\ & + \left[G_{V_0 u_n u_n} K_{u_n \bar{u}} + G_{V_0 \beta_n \beta_n} K_{\beta_n \bar{u}} \mid G_{V_0 u_n u_n} K_{u_n \bar{\beta}} + G_{V_0 \beta_n \beta_n} K_{\beta_n \bar{\beta}} \right] \end{aligned} \quad (2.79b)$$

$$\begin{aligned} \Delta \bar{A}_{V_0} = & \left(E(3) \right)^{n-1 T} \left[\Delta A_{V_0 \bar{u}\bar{u}} \mid \Delta A_{V_0 \bar{\beta}\bar{\beta}} \right] \\ & + \left[\Delta A_{V_0 u_n u_n} K_{u_n \bar{u}} + \Delta A_{V_0 \beta_n \beta_n} K_{\beta_n \bar{u}} \mid \Delta A_{V_0 u_n u_n} K_{u_n \bar{\beta}} + \Delta A_{V_0 \beta_n \beta_n} K_{\beta_n \bar{\beta}} \right] \end{aligned} \quad (2.79c)$$

$$\Delta \bar{L}_{V_0} = T - \left(E(3) \right)^n \left\{ \Delta L_{V_0 T} + \Delta L_{V_0 R} \right\} \quad (2.79d)$$

$$\Delta \bar{A}_V = \left(E(3) \right)^{n-1 T} \left[\Delta A_{V \bar{u}\bar{u}} \mid [0] \right] + \left[\Delta A_{V u_n u_n} K_{u_n \bar{u}} \mid \Delta A_{V u_n u_n} K_{u_n \bar{\beta}} \right] \quad (2.79e)$$

and, from Equations (2.54) and (2.55):

$$M_{V_{OUU}} = \bar{M}_T \left\{ \left[(R+r_S+u_{S_0}) \right]^{n-1} - \frac{1}{M_A} (E(3))^{n-1} \bar{M}_T (\tilde{u}_{S_0})^{n-1} \right\} \quad (2.80a)$$

$$M_{V_{OUu_n}} = - \frac{1}{M_A} \bar{M}_T (\tilde{u}_{S_0})^{n-1} (E(3))^{n-1} m_n \quad (2.80b)$$

$$M_{V_{OU_n \bar{u}}} = \left[- \frac{1}{M_A} \bar{M}_T (\tilde{u}_{S_0})^{n-1} (E(3))^{n-1} m_n \right]^T \quad (2.80c)$$

$$M_{V_{OU_n u_n}} = m_n \left[R+r_S+u_{S_0} - \frac{1}{M_A} m_n \tilde{u}_{n_0} \right] \quad (2.80d)$$

$$M_{V_{O\beta\beta}} = (C_{S_0}^T)^{n-1} \bar{M}_R \quad (2.80e)$$

$$M_{V_{O\beta_n \beta}} = C_{n_0}^T I_n \quad (2.80f)$$

From Equations (2.56) and (2.57):

$$G_{V_{OUU}} = \bar{M}_T \left\{ 2\omega_0 (R^T + r_S^T + u_{S_0}^T) - 2\omega_0^T (R+r_S+u_{S_0}) E(3) + \left[\tilde{\omega}_0 (R+r_S+u_{S_0}) \right] + (R+r_S+u_{S_0}) \tilde{\omega}_0 \right\}^{n-1} \quad (2.81a)$$

$$G_{V_{OU_n u_n}} = m_n \left\{ 2\omega_0 (R^T + r_S^T + u_{S_0}^T) - 2\omega_0^T (R+r_S+u_{S_0}) E(3) + \left[\tilde{\omega}_0 (R+r_S+u_{S_0}) \right] + (R+r_S+u_{S_0}) \tilde{\omega}_0 \right\} \quad (2.81b)$$

$$G_{V_{O\beta\beta}} = \left\{ - \left[(C_{S_0}^T I_S C_{S_0} \omega_0) \right]^{n-1} + (C_{S_0}^T)^{n-1} \bar{M}_R (C_{S_0} \tilde{\omega}_0)^{n-1} + (\tilde{\omega}_0 C_{S_0}^T)^{n-1} \bar{M}_R (C_{S_0})^{n-1} \right\} (C_{S_0}^T)^n \quad (2.81c)$$

$$G_{V_0 \beta_n \beta_n} = \left\{ - \left(C_{n_0}^T I_n C_{n_0} \dot{\omega}_0 \right) + C_{n_0}^T I_n C_{n_0} \ddot{\omega}_0 + \ddot{\omega}_0 C_{n_0}^T I_n C_{n_0} \right\} C_{n_0}^T \quad (2.81d)$$

From Equations (2.58a), (2.58c) and (2.77f):

$$\Delta A_{V_{0uu}} = \bar{M}_T \left\{ - \ddot{\omega}_0 (R+r_S+u_{S_0}) \omega_0^T - \ddot{\omega}_0 \left[\omega_0^T u_{S_0} \right] - \ddot{\omega}_0 \left[\omega_0^T (R+r_S) \right] + 2 \dot{\omega}_0 (R^T+r_S^T+u_{S_0}^T) \right. \\ \left. - (R+r_S+u_{S_0}) \dot{\omega}_0^T - \left[\dot{\omega}_0^T u_{S_0} \right] - \left[\dot{\omega}_0^T (R+r_S) \right] E(3) \right\}^{n-1} \quad (2.82a)$$

$$\Delta A_{V_{0u_n u_n}} = \bar{M}_n \left\{ - \ddot{\omega}_0 (R+r_n+u_{n_0}) \omega_0^T - \ddot{\omega}_0 \left[\omega_0^T u_{n_0} \right] - \ddot{\omega}_0 \left[\omega_0^T (R+r_n) \right] + 2 \dot{\omega}_0 (R^T+r_n^T+u_{n_0}^T) \right. \\ \left. - (R+r_n+u_{n_0}) \dot{\omega}_0^T - \left[\dot{\omega}_0^T u_{n_0} \right] - \left[\dot{\omega}_0^T (R+r_n) \right] E(3) \right\} \quad (2.82b)$$

$$\Delta A_{V_{0\beta\beta}} = \left[\left(C_{S_0}^T I_S C_{S_0} \dot{\omega}_0 \right) \right]^{n-1} - \left(C_{S_0}^T \right)^{n-1} \bar{M}_R \left(C_{S_0}^T \dot{\omega}_0 \right)^{n-1} \\ + \left[\ddot{\omega}_0 \left(C_{S_0}^T I_S C_{S_0} \omega_0 \right) \right]^{n-1} - \left(\ddot{\omega}_0 C_{S_0}^T \right)^{n-1} \bar{M}_R \left(C_{S_0} \ddot{\omega}_0 \right)^{n-1} \quad (2.82c)$$

$$\Delta A_{V_{0\beta_n \beta_n}} = \left(C_{n_0}^T I_n C_{n_0} \dot{\omega}_0 \right) - C_{n_0}^T I_n C_{n_0} \ddot{\omega}_0 + \ddot{\omega}_0 \left(C_{n_0}^T I_n C_{n_0} \omega_0 \right) - \ddot{\omega}_0 C_{n_0}^T I_n C_{n_0} \ddot{\omega}_0 \quad (2.82d)$$

From Equations (2.46g) and (2.46h):

$$\Delta L_{V_T} = \bar{M}_T \left\{ - \Delta \ddot{\omega} \left[\left(R^T+r_S^T \right) \omega_0 \right] - \Delta \ddot{\omega} \left[\left(R^T+r_S^T \right) \Delta \omega \right] \right. \\ \left. + \Delta \dot{\omega} \left(R^T+r_S^T \right) - \left(R+r_S \right) \Delta \dot{\omega}^T \right\}^n \left(R'+r' \right) \quad (2.83a)$$

$$\Delta L_{V_R} = \left(C_{S_0}^T \right)^n \bar{M}_R \left(C_{S_0} \right)^n \Delta \dot{\omega}' + \left(\Delta \ddot{\omega} C_{S_0}^T \right)^n \bar{M}_R \left(C_{S_0} \right)^n \omega_0' + \left(\ddot{\omega}_0 C_{S_0}^T \right)^n \bar{M}_R \left(C_{S_0} \right)^n \Delta \omega' \quad (2.83b)$$

From Equations (2.58):

$$\Delta A_{V_{uu}} = \bar{H}_T \left\{ -\Delta \tilde{\omega} (R+r_S+u_{S_0}) \omega_0^T - \tilde{\omega}_0 (R+r_S+u_{S_0}) \Delta \omega^T - \Delta \tilde{\omega} [\omega_0^T (R+r_S)] - \tilde{\omega}_0 [\Delta \omega^T (R+r_S)] \right. \\ \left. + \Delta \dot{\omega} (2R^T + 2r_S^T + u_{S_0}^T) - (R+r_S+u_{S_0}) \Delta \dot{\omega}^T - [\Delta \dot{\omega}^T (R+r_S)] E(3) \right\}^{n-1} \quad (2.84a)$$

$$\Delta A_{V_{u_n u_n}} = \bar{m}_n \left\{ -\Delta \tilde{\omega} (R+r_n+u_{n_0}) \omega_0^T - \tilde{\omega}_0 (R+r_n+u_{n_0}) \Delta \omega^T - \Delta \tilde{\omega} [\omega_0^T (R+r_n)] - \tilde{\omega}_0 [\Delta \omega^T (R+r_n)] \right. \\ \left. + \Delta \dot{\omega} (2R^T + 2r_n^T + u_{n_0}^T) - (R+r_n+u_{n_0}) \Delta \dot{\omega}^T - [\Delta \dot{\omega}^T (R+r_n)] E(3) \right\} \quad (2.84b)$$

2.3 AERODYNAMIC AND GRAVITATIONAL LOADS

2.3.1 Aerodynamic Loads

2.3.1.1 Introduction

In the preceding analysis, all non-structural and non-inertial loads acting on the structure have been assumed to act as an external forcing function, independent of structural motion. Aerodynamic loads, however, are dependant upon the movement of the structure. This interaction of aerodynamics and structural dynamics - more commonly known as aeroelasticity - encompasses much more than will be considered here.

Usually, aerodynamicists calculate aerodynamic forces for the rigid body motion of the aircraft. These forces are then put into the equations of motion as external loads. The resultant structural motion (time dependant) is then fed back to the aerodynamicists. They, in turn, calculate a new set of aerodynamic loads. And the cycle continues (hopefully to convergence).

If the aerodynamic loads can be expressed as functions of the structural variables, then a more empirical solution is possible. Many assumptions are needed in order to account for the aerodynamics directly. The aerodynamic force acting on a panel is assumed to be a function of the angle of attack of

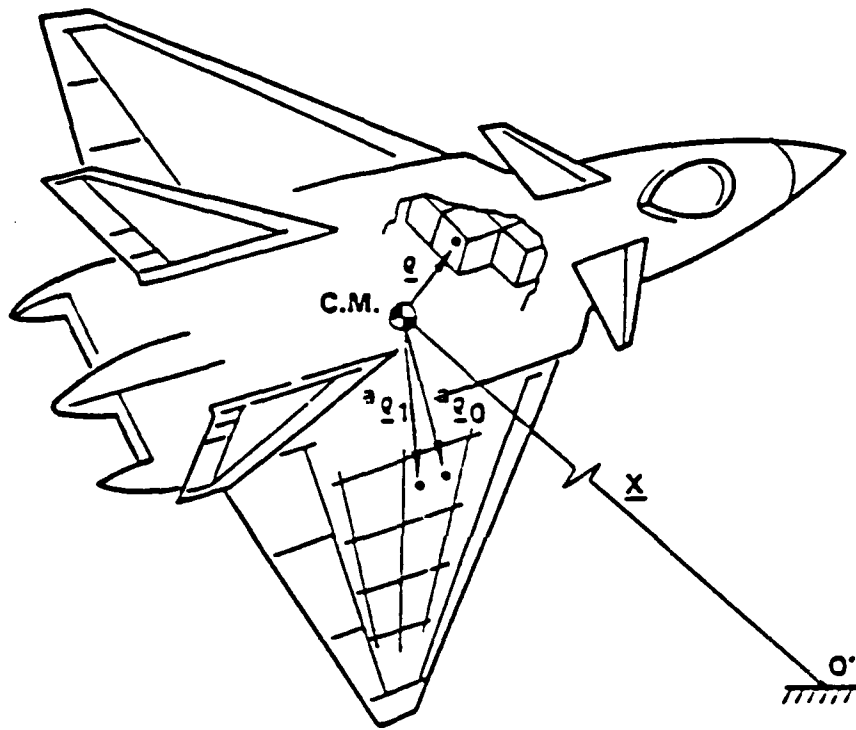


Figure 2-8. Discretized Aircraft

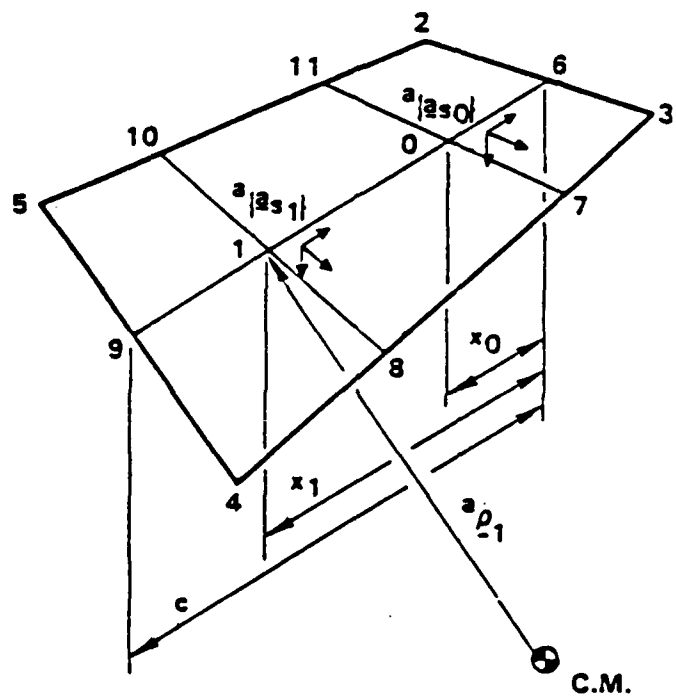


Figure 2-9. Aerodynamic Panel

all panels; α_s , $s=1, \dots, m$. The angle-of-attack is a function of the relative panel velocity, \underline{V}_s , and the orientation of that panel. The next sections will detail one possible approach for modeling the aerodynamic forces.

2.3.1.2 Aerodynamic Panel Orientation

For an aerodynamic analysis, it is assumed that the surface of the aircraft is modeled using a panel method (See Figure 2-8). One such panel is shown in Figure 2-9. In general, this panel is curved. The curvature of the panel is approximated as a surface which connects all four vertices with straight lines and linearly varies in both directions. This allows the modeled surface to remain continuous, even for large vehicle deformations.

The mean span chord line is defined as the straight line which connects the mid points of the leading and trailing edges. Points 0 and 1 are defined along the mean span chord line. These points are chosen anticipating that the resultant aerodynamic force will be expressed at Point 0, and that the angle-of-attack is defined, and the downwash boundary condition will be satisfied at Point 1. Both points are expressed in terms of the vectors which locate the vertices of the panel by using weighted averages:

$${}^a \underline{r}_{s0} + {}^a \underline{u}_{s0} = \frac{1}{2} \left[(1-x_0) ({}^a \underline{r}_{s2} + {}^a \underline{u}_{s2} + {}^a \underline{r}_{s3} + {}^a \underline{u}_{s3}) + x_0 ({}^a \underline{r}_{s4} + {}^a \underline{u}_{s4} + {}^a \underline{r}_{s5} + {}^a \underline{u}_{s5}) \right] \quad (2.85)$$

and:

$${}^a \underline{r}_{s1} + {}^a \underline{u}_{s1} = \frac{1}{2} \left[(1-x_1) ({}^a \underline{r}_{s2} + {}^a \underline{u}_{s2} + {}^a \underline{r}_{s3} + {}^a \underline{u}_{s3}) + x_1 ({}^a \underline{r}_{s4} + {}^a \underline{u}_{s4} + {}^a \underline{r}_{s5} + {}^a \underline{u}_{s5}) \right] \quad (2.86)$$

where a pre-superscript a indicates that the variable is associated with the aerodynamic model, and x_0 and x_1 are the percent distances aft of the leading edge of the panel for Points 0 and 1, respectively.

Associated with each of Points 0 and 1 is a vector base ${}^a \{ \underline{a}_{s0} \}$ and ${}^a \{ \underline{a}_{s1} \}$, respectively. The orientation of these dextral orthogonal vector bases will follow standard flutter sign convention: the first unit vector lies

along the mean chord line from trailing edge to leading edge (this unit vector is same for both points), the second unit vector lies in the plane of the panel "out the right wing," and the third vector is perpendicular to the other two "down" or away from the wetted surface. These vector bases are related to the $\{b\}$ vector base through direction cosine matrices:

$${}^a_{\{a_{s0}\}} = {}^a C_{s0} \{b\} \quad \text{and} \quad {}^a_{\{a_{s1}\}} = {}^a C_{s1} \{b\} \quad (2.87)$$

Since the orientation of the aerodynamic panels is a function of q these direction cosine matrices are also functions of q . This functionality will be discussed in Paragraph 2.3.1.3.

The location of the panel vertices relative to Point Q , ${}^a_{p_s} = {}^a_{r_{sj}} + {}^a_{q_{sj}}$ ($j=2, \dots, 5$; $s=1, \dots, m$), are related to the structural degrees-of-freedom via a grid transformation matrix, D_Q :

$${}^a_{p'} = {}^a_{r'} + {}^a_{u'} = {}^a_{r'} + D_Q q' \quad (2.88)$$

where ${}^a_{p'}$ is a column of all non-redundant panel vertex locations, D_Q is dimensioned accordingly (in general not square).

Likewise, the resultant aerodynamic loads acting on the rigid sub-bodies at Points Q_s are related to forces acting at the panel vertex points via a grid transformation matrix, D_f :

$$\begin{Bmatrix} \underline{f}_{aero} \\ \underline{t}_{aero} \end{Bmatrix} = D_f \begin{Bmatrix} {}^a \underline{f}_v \end{Bmatrix} \quad (2.89)$$

where \underline{f}_{aero} and \underline{t}_{aero} are the resultant aerodynamic forces and moments, respectively, acting on the rigid sub-bodies, ${}^a \underline{f}_v$ is a column of all non-redundant forces acting at the panel vertices, and D_f is dimensioned accordingly (in general not square).

The weighted averages in Equations (2.85) and (2.86) are incorporated into the transformations in Equations (2.88) and (2.89) to yield two new matrices, D_q and D_L , relating the deformation of all panels at Point 1 to q , and sub-body f_{aero} and t_{aero} to forces acting at all Points 0:

$$a_{u_1}' = D_u(\bar{u}') + D_\beta (C_S^T)^{n-1} (\bar{\beta}') = D_q q = \begin{bmatrix} D_{\bar{q}} & -D_{q_n} K_{qBq_n}^{-1} K_{qBq} \end{bmatrix} \bar{q} \quad (2.90)$$

and:

$$\begin{Bmatrix} f_{aero} \\ t_{aero} \end{Bmatrix} = D_L (a_{C_{S0}}^T)^m a_f \quad (2.91)$$

where D_q is $3m \times 6n$, $D_{\bar{q}}$ and D_{q_n} are the appropriate extractions of D_q (See Equation (2.51)), D_L is $6n - 6 \times 3m$, and a_f is a column of all m resultant aerodynamic forces at Point 0.

2.3.1.3 Panel Coordinate Transformations

In Paragraph 2.1.5.3 auxiliary equations were developed which expressed the direction cosine matrices, C_S , as a function of q : specifically, a unique function of only the corresponding β_S (See Equation (2.34)). This was possible because each rigid sub-body has its own β_S which are independent degrees of freedom. Such is not the case here with $a_{C_{S0}}$ and $a_{C_{S1}}$ for the aerodynamic panels. The motion of each panel, and hence the direction cosines defining the rotation of the related hybrid-coordinates, is a function of all a_{u_S} . In this section the direction cosines will be defined.

The direction cosines are order dependant. In Paragraph 2.3.1.2 this order was defined as: 1 forward, 2 out the right wing, and 3 down (or away from the wetted surface). The three successive rotations of each and the intermediate coordinates generated are shown in Figure 2-10. Since the motion of the panel (in three-space) is defined by the translation of the vertices of the panels, the rotation of the panel at Points 0 and 1 will be defined by the relative difference in motion of these points. To demonstrate this procedure

additional points are identified which lie on the edges of the panels (See Figure 2-9). Points 6 and 9 define the leading and trailing edges of the mid-span of the panel. Points 7 and 11, and 8 and 10 define the x_0 and x_1 percent-chord lines of the panel, respectively. As was done for Points 2 through 5, the location of Points 6 through 11 may be expressed as weighted averages of Points 2 through 5:

$$a_{r_{s6}} + a_{u_{s6}} = \frac{1}{2} (a_{r_{s2}} + a_{u_{s2}} + a_{r_{s3}} + a_{u_{s3}}) \quad (2.92a)$$

$$a_{r_{s7}} + a_{u_{s7}} = (1-x_0) (a_{r_{s3}} + a_{u_{s3}}) + x_0 (a_{r_{s4}} + a_{u_{s4}}) \quad (2.92b)$$

$$a_{r_{s8}} + a_{u_{s8}} = (1-x_1) (a_{r_{s3}} + a_{u_{s3}}) + x_0 (a_{r_{s4}} + a_{u_{s4}}) \quad (2.92c)$$

$$a_{r_{s9}} + a_{u_{s9}} = \frac{1}{2} (a_{r_{s4}} + a_{u_{s4}} + a_{r_{s5}} + a_{u_{s5}}) \quad (2.92d)$$

$$a_{r_{s10}} + a_{u_{s10}} = (1-x_1) (a_{r_{s2}} + a_{u_{s2}}) + x_0 (a_{r_{s5}} + a_{u_{s5}}) \quad (2.92e)$$

$$a_{r_{s11}} + a_{u_{s11}} = (1-x_0) (a_{r_{s2}} + a_{u_{s2}}) + x_0 (a_{r_{s5}} + a_{u_{s5}}) \quad (2.92f)$$

For the first direction of rotation the deformations are resolved into the y-z plane (Directions 2 and 3, respectively) as shown in Figure 2-10. Points 8 and 10 translate to induce rotation of the x_1 chord line about Point 1. This direction cosine angle, $a_{\beta_{s1}}$, is defined as the arctangent of the difference in the vertical deformations divided by the initial chord length plus the difference in the horizontal deformations:

$$a_{\beta_{s1}} = \tan^{-1} \frac{a_{u_{83}} - a_{u_{103}}}{a_{r_{82}} + a_{u_{82}} - a_{r_{102}} - a_{u_{102}}} \quad (2.93)$$

The direction cosine matrix, $a_{C'_{s1}}$, associated with the angle defined in Equation (2.93), defines the first rotation with respect to the $a_{\{a_{s1}\}}$ vector base. The new axis is identified with a superscript '. The second direction cosine matrix is found using the same procedure: the deformations are resolved into the $z'-x'$ plane (Directions 3 and 1, respectively) as shown in Figure 2-10. Points 6 and 9 translate to induce rotation of the mid-span line about Point 1:

$${}^a\beta_{s12} = \tan^{-1} \frac{-(a'_{u63} - a'_{u93})}{a'_{r61} + a'_{u61} - a'_{r91} - a'_{u91}} = \tan^{-1} \frac{-(a''_{u63} - a''_{u93})}{a''_{r61} + a''_{u61} - a''_{r91} - a''_{u91}} \quad (2.94)$$

Since the previous rotation was about the x axis the prime and no-prime values for the x direction are equal. The new axis defined by this rotation is identified with a superscript ". The final direction cosine matrix is found using the same procedure: the deformations are resolved into the x"-y" plane (Directions 1 and 2, respectively) as shown in Figure 2-10. Points 6 and 9 translate to induce rotation of the mid-span line about Point 1:

$${}^a\beta_{s13} = \tan^{-1} \frac{a''_{u62} - a''_{u92}}{a''_{r61} + a''_{u61} - a''_{r91} - a''_{u91}} = \tan^{-1} \frac{a'_{u62} - a'_{u92}}{a'_{r61} + a'_{u61} - a'_{r91} - a'_{u91}} \quad (2.95)$$

Since the previous rotation was about the y axis the double prime and single prime values for the y direction are equal. With all direction cosine angles defined, the direction cosine matrix for Point 1 is evaluated as:

$${}^aC_{s1} = {}^aC_{s13} {}^aC_{s12} {}^aC_{s11}$$

$$= \begin{bmatrix} c^a\beta_{s13} & s^a\beta_{s13} & 0 \\ -s^a\beta_{s13} & c^a\beta_{s13} & 0 \\ 0 & 0 & 1 \end{bmatrix} \begin{bmatrix} c^a\beta_{s12} & 0 & -s^a\beta_{s12} \\ 0 & 1 & 0 \\ s^a\beta_{s12} & 0 & c^a\beta_{s12} \end{bmatrix} \begin{bmatrix} 1 & 0 & 0 \\ 0 & c^a\beta_{s11} & s^a\beta_{s11} \\ 0 & -s^a\beta_{s11} & c^a\beta_{s11} \end{bmatrix}$$

$$= \begin{bmatrix} c^a\beta_{s13} c^a\beta_{s12} & c^a\beta_{s13} s^a\beta_{s12} & c^a\beta_{s13} s^a\beta_{s11} & -c^a\beta_{s13} s^a\beta_{s12} c^a\beta_{s11} \\ +s^a\beta_{s13} c^a\beta_{s11} & +s^a\beta_{s13} s^a\beta_{s11} & +s^a\beta_{s13} s^a\beta_{s11} & +s^a\beta_{s13} s^a\beta_{s11} \\ -s^a\beta_{s13} c^a\beta_{s12} & -s^a\beta_{s13} s^a\beta_{s12} & -s^a\beta_{s13} s^a\beta_{s11} & -s^a\beta_{s13} s^a\beta_{s12} c^a\beta_{s11} \\ +c^a\beta_{s11} c^a\beta_{s13} & +c^a\beta_{s11} s^a\beta_{s13} & +c^a\beta_{s11} s^a\beta_{s11} & +c^a\beta_{s11} s^a\beta_{s11} \\ s^a\beta_{s12} & -c^a\beta_{s12} s^a\beta_{s11} & c^a\beta_{s12} c^a\beta_{s11} & c^a\beta_{s12} c^a\beta_{s11} \end{bmatrix} \quad (2.96)$$

In a similar manner the direction cosine angles are formulated and used to define the direction cosine matrix for the ${}^a\{a_{s0}\}$ vector base.

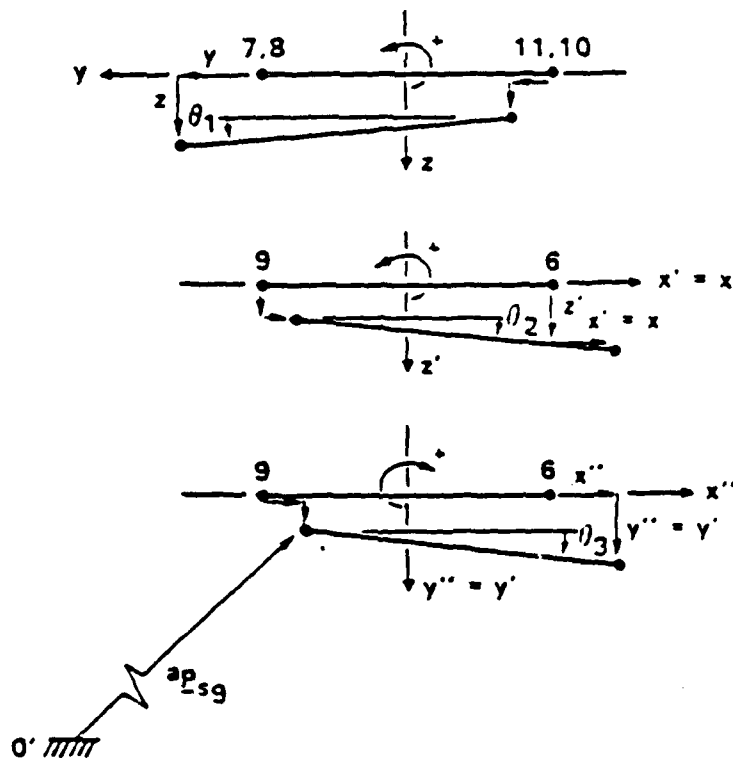


Figure 2-10. Aerodynamic Panel Rotation

$${}^a\beta_{s01} = \tan^{-1} \frac{{}^a u_{73} - {}^a u_{113}}{{}^a r_{72} + {}^a u_{72} - {}^a r_{112} - {}^a u_{112}} \quad (2.97)$$

$${}^a\beta_{s02} = \tan^{-1} \frac{-(a'_{u63} - a'_{u93})}{a'_{r61} + a'_{u61} - a'_{r91} - a'_{u91}} = \tan^{-1} \frac{-(a''_{u63} - a''_{u93})}{a''_{r61} + a''_{u61} - a''_{r91} - a''_{u91}} \quad (2.98)$$

$${}^a\beta_{s03} = \tan^{-1} \frac{a''_{u62} - a''_{u92}}{a''_{r61} + a''_{u61} - a''_{r91} - a''_{u91}} = \tan^{-1} \frac{a'_{u62} - a'_{u92}}{a'_{r61} + a'_{u61} - a'_{r91} - a'_{u91}} \quad (2.99)$$

Equations (2.98) and (2.99) look identical to Equations (2.94) and (2.95), however the prime and double prime quantities are dependent upon the first rotation which, in general, is not equal at both points. The deformation angles described by Equations (2.97) through (2.99) are now used to formulate the direction cosine matrix for Point 0:

$$\begin{aligned} {}^a C_{s0} &= {}^a C_{s03} {}^a C_{s02} {}^a C_{s01} \\ &= \begin{bmatrix} c^a\beta_{s03} & s^a\beta_{s03} & 0 \\ -s^a\beta_{s03} & c^a\beta_{s03} & 0 \\ 0 & 0 & 1 \end{bmatrix} \begin{bmatrix} c^a\beta_{s02} & 0 & -s^a\beta_{s02} \\ 0 & 1 & 0 \\ s^a\beta_{s02} & 0 & c^a\beta_{s02} \end{bmatrix} \begin{bmatrix} 1 & 0 & 0 \\ 0 & c^a\beta_{s01} & s^a\beta_{s01} \\ 0 & -s^a\beta_{s01} & c^a\beta_{s01} \end{bmatrix} \\ &= \begin{bmatrix} c^a\beta_{s03} c^a\beta_{s02} & c^a\beta_{s03} s^a\beta_{s02} s^a\beta_{s01} & -c^a\beta_{s03} s^a\beta_{s02} c^a\beta_{s01} \\ -s^a\beta_{s03} c^a\beta_{s02} & -s^a\beta_{s03} s^a\beta_{s02} s^a\beta_{s01} & -s^a\beta_{s03} s^a\beta_{s02} c^a\beta_{s01} \\ s^a\beta_{s02} & -c^a\beta_{s02} s^a\beta_{s01} & c^a\beta_{s02} c^a\beta_{s01} \end{bmatrix} \quad (2.100) \end{aligned}$$

For completeness, the following relationships define the location vectors for Points 6 through 9 in the intermediate reference frames as a function of their values relative to the initial panel reference frame:

$$\begin{aligned}
{}^a r_{sjk} + {}^a u_{sjk} &= {}^a C_{sj3} ({}^a r_{sk}'' + {}^a u_{sk}'') \\
&= {}^a C_{sj3} {}^a C_{sj2} ({}^a r_{sk}' + {}^a u_{sk}') \\
&= {}^a C_{sj3} {}^a C_{sj2} {}^a C_{sj1} ({}^a r_{sk}^* + {}^a u_{sk}^*) = {}^a C_{sj} ({}^a r_{sk}^* + {}^a u_{sk}^*) \quad (2.101)
\end{aligned}$$

where $j=0$ or 1 ; $k=6, \dots, 11$, and the asterisk indicates the initial value (before transformation) which is the value evaluated with respect to the $\{b\}$ vector base.

2.3.1.4 Panel Relative Velocity

Each panel may be subjected to a gust, \underline{V}_{gs} . Other than the gust velocity there is no contribution to the panel relative velocity other than the motion of the panel (See Figure 2-11). Relative velocity of the panel will reduce the velocity of the panel, \underline{V}_s . The velocity of the panel at Point 1 is found by using the vector differential calculus identity in Equation (2.11) on the inertial position vector of Point 1:

$$\frac{d}{dt} (\underline{X} + \underline{c} + \underline{R} + {}^a \underline{r}_{s1} + {}^a \underline{u}_{s1}) = \frac{d}{dt} \underline{X} + \frac{d}{dt} \underline{c} + \frac{d}{dt} \underline{R} + \underline{\omega} \times (\underline{c} + \underline{R} + {}^a \underline{r}_{s1} + {}^a \underline{u}_{s1}) \quad (2.102)$$

If Equation (2.102) and the gust velocity, \underline{V}_{gs} , are expressed in terms of the $\{a_{s1}\}$ vector base then the relative velocity, \underline{V}_s , of the panel vehicle becomes:

$$\underline{V}_s = \underline{V}_{gs} - {}^a C_{s1} \left[\underline{\dot{X}} + \underline{\dot{c}} + \underline{\dot{a}}_{s1} + \underline{\omega} \times (\underline{c} + \underline{R} + {}^a \underline{r}_{s1} + {}^a \underline{u}_{s1}) \right] \quad (2.103)$$

The expressions for \underline{c} and its time derivative, given by Equations (2.19) and (2.20), are repeated here for convenience (recalling that C is $E^{(3)}$):

$$\underline{c} = - \frac{1}{M} \sum_{A_s=1}^n m_s \underline{u}_s \quad (2.104)$$

and (recalling that $\dot{\mathbf{q}}^a$ is zero):

$$\dot{\mathbf{c}} = - \frac{1}{M_{A_{S=1}}} \sum_{m_S=1}^n \dot{m}_S \dot{\mathbf{u}}_S \quad (2.105)$$

Equations (2.104) and (2.105) are substituted into Equation (2.103):

$$\mathbf{v}_S = \mathbf{v}_{g_S} - {}^a C_{S1} \left[\dot{\boldsymbol{\theta}} \dot{\mathbf{x}} - \frac{1}{M_{A_{S=1}}} \sum_{m_S=1}^n \dot{m}_S \dot{\mathbf{u}}_S + \dot{\mathbf{u}}_{S1} + \tilde{\boldsymbol{\omega}} \left(- \frac{1}{M_{A_{S=1}}} \sum_{m_S=1}^n m_S \mathbf{u}_S + \mathbf{R} + {}^a \mathbf{r}_{S1} + {}^a \mathbf{u}_{S1} \right) \right] \quad (2.106)$$

Substituting for ${}^a \mathbf{u}'_1$ from Equation (2.90) into Equation (2.106) yields,

$$\mathbf{v}_S = \mathbf{v}_{g_S} - {}^a C_{S1} \left[\dot{\boldsymbol{\theta}} \dot{\mathbf{x}} - \frac{1}{M_{A_{S=1}}} \sum_{m_S=1}^n \dot{m}_S \dot{\mathbf{u}}_S + \mathbf{d}_{\bar{q}_S} \dot{\bar{q}} + \tilde{\boldsymbol{\omega}} \left(- \frac{1}{M_{A_{S=1}}} \sum_{m_S=1}^n m_S \mathbf{u}_S + \mathbf{R} + {}^a \mathbf{r}_{S1} + \mathbf{d}_{\bar{q}_S} \bar{q} \right) \right] \quad (2.107)$$

where $\mathbf{d}_{\bar{q}_S}$ is a $3 \times 6n-6$ extraction of \mathbf{D}_q beginning at row 3s. Using the pi operator of Equation (2.16) and the auxiliary equation expressing \mathbf{u}_n as a function of \bar{q} , Equation (2.47), the terms in Equation (2.107) are rearranged and combined according to the order of the unknown:

$$\begin{aligned} \mathbf{v}_S &= \mathbf{v}_{g_S} - {}^a C_{S1} \left[\dot{\boldsymbol{\theta}} \dot{\mathbf{x}} + \tilde{\boldsymbol{\omega}} \left(\mathbf{R} + {}^a \mathbf{r}_{S1} \right) + \tilde{\boldsymbol{\omega}} \left(- \frac{1}{M_{A_{S=1}}} \sum_{m_S=1}^n m_S \mathbf{u}_S + \mathbf{d}_{\bar{q}_S} \bar{q} \right) - \frac{1}{M_{A_{S=1}}} \sum_{m_S=1}^n \dot{m}_S \dot{\mathbf{u}}_S + \mathbf{d}_{\bar{q}_S} \dot{\bar{q}} \right] \\ &= \mathbf{v}_{g_S} - {}^a C_{S1} \left[\dot{\boldsymbol{\theta}} \dot{\mathbf{x}} + \tilde{\boldsymbol{\omega}} \left(\mathbf{R} + {}^a \mathbf{r}_{S1} \right) - \tilde{\boldsymbol{\omega}} \left(\frac{1}{M_A} \left(\mathbf{E}(3) \right)^{n-1} \left[\bar{\mathbf{M}}_T | [0] \right] + \frac{m_n}{M_A} \left[\mathbf{K}_{u_n \bar{u}} | \mathbf{K}_{u_n \bar{\beta}} \right] - \mathbf{d}_{\bar{q}_S} \right) \bar{q} \right. \\ &\quad \left. - \left(\frac{1}{M_A} \left(\mathbf{E}(3) \right)^{n-1} \left[\bar{\mathbf{M}}_T | [0] \right] + \frac{m_n}{M_A} \left[\mathbf{K}_{u_n \bar{u}} | \mathbf{K}_{u_n \bar{\beta}} \right] - \mathbf{d}_{\bar{q}_S} \right) \dot{\bar{q}} \right] \quad (2.108) \end{aligned}$$

2.3.1.5 Panel Angle-of-Attack and Aerodynamic Loads

Angle-of-attack, α_S , is defined as the angle between the relative velocity and the projection of the relative velocity that lies in the plane of the panel at Point 1 (See Figure 2-12):

$$\alpha_S = \tan^{-1} \frac{v_{S3}}{\sqrt{v_{S1}^2 + v_{S2}^2}} \quad (2.109)$$

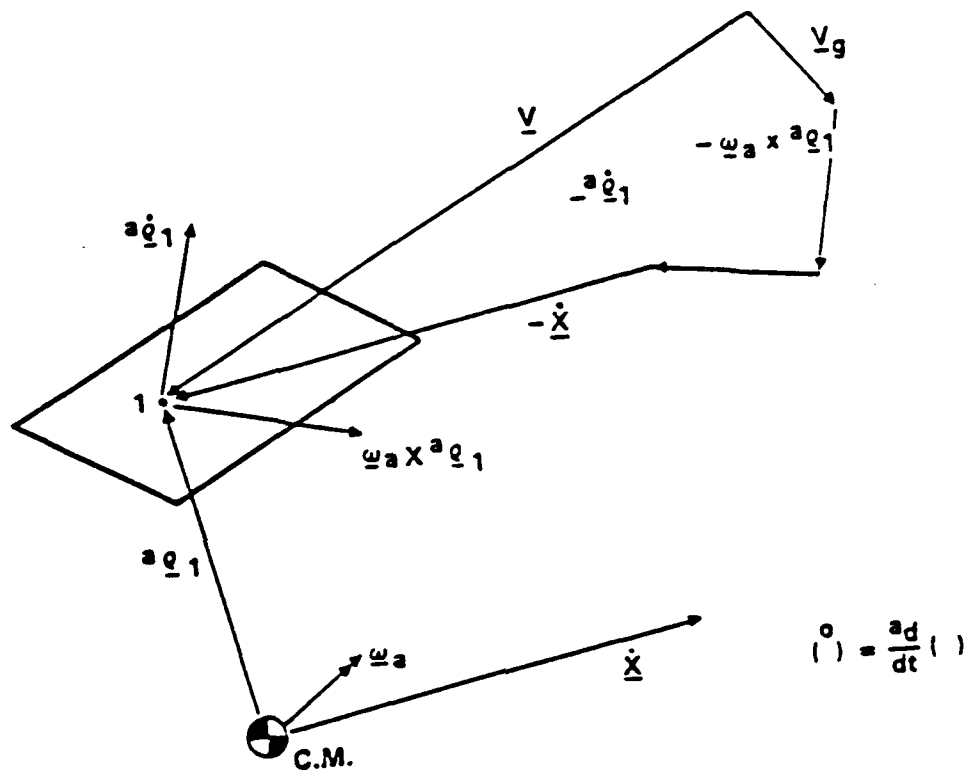


Figure 2-11. Aerodynamic Panel Relative Velocity

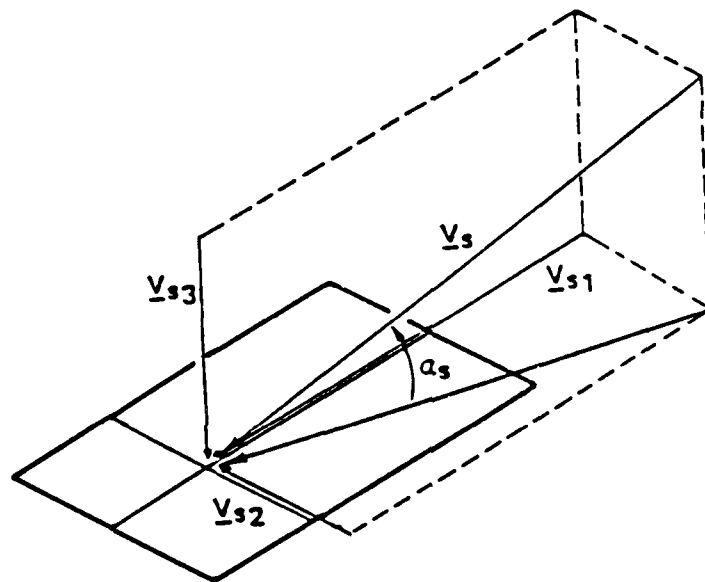


Figure 2-12. Aerodynamic Panel Angle-of-Attack

It is assumed that an aerodynamic force, $a_{f_{sk}}$, proportional to the angle-of-attack of the k panel, α_k , is induced on the s panel, and acts orthogonal to the s panel surface at Point 0. This proportionality is expressed as:

$$a_{f_{sk}} = \text{GAM}_{sk} \alpha_k \quad (2.110)$$

where GAM_{sk} is the s,k element of a General Aerodynamic Matrix: a function of the panel areas, panel chord, relative panel position, singularity type and strength of the k panel, and the local dynamic pressure of the k panel, $1/2 \rho V_k \cdot V_k$.

The total aerodynamic force acting on the s panel, a_{f_s} , is the sum of all $a_{f_{sk}}$; $k=1, \dots, m$. These total panel forces are arranged into a single column: occupying every third element, the other two being zero, by premultiplying each row by a 3X1 shuffle matrix, $C_{shuf} = \{0 \ 0 \ 1\}^T$. This results in a_f (See Equation (2.91)):

$$a_f = \left(C_{shuf} \right)^m [GAM] \alpha' \quad (2.111)$$

where $[GAM]$ is a $m \times m$ matrix of all GAM_{sk} and α' is a $m \times 1$ of all α_k .

Now the aerodynamic loads, f_{aero} and t_{aero} , can be expressed as an explicit function of the independent structural variables X , ω , and \bar{q} : Equations (2.97) through (2.101), and Equation (2.111) are substituted into Equation (2.91) to express $a_{C_{S0}}$ as a function of X , ω , and \bar{q} , and a_f' as a function of α' ; Equation (2.119) is substituted into Equation (2.111) to express α' as a function of V_s ($s=1, \dots, m$); Equation (2.108) is substituted into Equation (2.109) to express V_s as a function of \bar{q} ; and Equations (2.93) through (2.96) and (2.101) are substituted into Equation (2.108) to express $a_{C_{S1}}$ as a function of X , ω , and \bar{q} .

This form of the aerodynamic loads is consistent with the assumptions in Paragraph 2.1 and is suitable for use in the flexible and total vehicle

equations, provided by Equations (2.52f), (2.60d), and (2.61). For the reduced flexible vehicle equations, \bar{f}_{aero} and \bar{t}_{aero} are the upper $3n-3 \times 1$ sub-columns of f_{aero} and t_{aero} , respectively. For the translational total vehicle equations, F_{aero} is the sum of all f_{aero_s} ; $s=1, \dots, n$:

$$F_{aero} = \left(E(3) \right)^n \bar{f}_{aero} \quad (2.112)$$

And, for the rotational total vehicle equations, T_{aero} is the sum of all t_{aero_s} and the matrix components of the cross products of $r_s + u_s$ with f_{aero_s} , $s=1, \dots, n$:

$$T_{aero} = \left(E(3) \right)^n \left[t_{aero} + \left((r_s + u_s) \right)^n \bar{f}_{aero} \right] \quad (2.113)$$

In the next sections the aerodynamic loads formulated above will be simplified using the assumptions in Paragraph 2.2 for quasi-static and perturbation (linear) analysis.

2.3.1.6 Quasi-static Aerodynamic Loads

To formulate the quasi-static aerodynamic loads: first, all time dependent variables are expanded into the quasi-static and perturbation approximation of Equation (2.62); then, all terms negligible with respect to the purely quasi-static terms are dropped (See Equation (2.63)). The resultant quasi-static aerodynamic loads as functions of the quasi-static aerodynamic panel forces are extracted from Equation (2.91):

$$\begin{Bmatrix} f_{aero_0} \\ t_{aero_0} \end{Bmatrix} = D_{L_0} \left(a_{C_{S_0}}^T \right)^m a_{f_0} \quad (2.114)$$

Quasi-static deformations may be large enough to warrant a re-evaluation of the grid transformation matrices D_L and D_q . For the direction cosine

matrices associated with Points 1 and 0, the quasi-static components are extracted out of Equations (2.93) through (2.96) and Equations (2.97) through (2.100), respectively:

$$\begin{aligned}
 & \begin{matrix} a_{Cs10} & a_{Cs130} & a_{Cs120} & a_{Cs110} \end{matrix} \\
 & = \begin{bmatrix} c^{\alpha\beta s_{130}} & s^{\alpha\beta s_{130}} & 0 \\ -s^{\alpha\beta s_{130}} & c^{\alpha\beta s_{130}} & 0 \\ 0 & 0 & 1 \end{bmatrix} \begin{bmatrix} c^{\alpha\beta s_{120}} & 0 & -s^{\alpha\beta s_{120}} \\ 0 & 1 & 0 \\ s^{\alpha\beta s_{120}} & 0 & c^{\alpha\beta s_{120}} \end{bmatrix} \begin{bmatrix} 1 & 0 & 0 \\ 0 & c^{\alpha\beta s_{110}} & s^{\alpha\beta s_{110}} \\ 0 & -s^{\alpha\beta s_{110}} & c^{\alpha\beta s_{110}} \end{bmatrix} \\
 & = \begin{bmatrix} c^{\alpha\beta s_{130}} c^{\alpha\beta s_{120}} c^{\alpha\beta s_{110}} & c^{\alpha\beta s_{130}} s^{\alpha\beta s_{120}} c^{\alpha\beta s_{110}} & c^{\alpha\beta s_{130}} c^{\alpha\beta s_{110}} & -s^{\alpha\beta s_{130}} s^{\alpha\beta s_{120}} c^{\alpha\beta s_{110}} \\ -s^{\alpha\beta s_{130}} c^{\alpha\beta s_{120}} c^{\alpha\beta s_{110}} & -s^{\alpha\beta s_{130}} s^{\alpha\beta s_{120}} c^{\alpha\beta s_{110}} & -s^{\alpha\beta s_{130}} c^{\alpha\beta s_{110}} & s^{\alpha\beta s_{130}} s^{\alpha\beta s_{120}} c^{\alpha\beta s_{110}} \\ s^{\alpha\beta s_{120}} c^{\alpha\beta s_{110}} & -c^{\alpha\beta s_{120}} s^{\alpha\beta s_{110}} & c^{\alpha\beta s_{120}} c^{\alpha\beta s_{110}} & -s^{\alpha\beta s_{120}} s^{\alpha\beta s_{110}} \\ \dots & \dots & \dots & \dots \end{bmatrix} \quad (2.115)
 \end{aligned}$$

where:

$$a_{\beta s_{110}} = \tan^{-1} \frac{a_{u83_0} - a_{u103_0}}{a_{r82_0} + a_{u82_0} - a_{r102_0} - a_{u102_0}} \quad (2.115a)$$

$$a_{\beta s_{120}} = \tan^{-1} \frac{-(a'_{u63_0} - a'_{u93_0})}{a'_{r61_0} + a'_{u61_0} - a'_{r91_0} - a'_{u91_0}} = \tan^{-1} \frac{-(a'_{u63_0} - a'_{u93_0})}{a'_{r61_0} + a'_{u61_0} - a'_{r91_0} - a'_{u91_0}} \quad (2.115b)$$

$$a_{\beta s_{130}} = \tan^{-1} \frac{a''_{u62_0} - a''_{u92_0}}{a''_{r61_0} + a''_{u61_0} - a''_{r91_0} - a''_{u91_0}} = \tan^{-1} \frac{a'_{u62_0} - a'_{u92_0}}{a''_{r61_0} + a''_{u61_0} - a''_{r91_0} - a''_{u91_0}} \quad (2.115c)$$

and:

$$\begin{aligned}
 {}^a C_{s0_0} &= {}^a C_{s0_3_0} \quad {}^a C_{s0_2_0} \quad {}^a C_{s0_1_0} \\
 &= \begin{bmatrix} c^{a\beta_{s0_3_0}} & s^{a\beta_{s0_3_0}} & 0 \\ -s^{a\beta_{s0_3_0}} & c^{a\beta_{s0_3_0}} & 0 \\ 0 & 0 & 1 \end{bmatrix} \begin{bmatrix} c^{a\beta_{s0_2_0}} & 0 & -s^{a\beta_{s0_2_0}} \\ 0 & 1 & 0 \\ s^{a\beta_{s0_2_0}} & 0 & c^{a\beta_{s0_2_0}} \end{bmatrix} \begin{bmatrix} 1 & 0 & 0 \\ 0 & c^{a\beta_{s0_1_0}} & s^{a\beta_{s0_1_0}} \\ 0 & -s^{a\beta_{s0_1_0}} & c^{a\beta_{s0_1_0}} \end{bmatrix} \\
 &= \begin{bmatrix} c^{a\beta_{s0_3_0}} c^{a\beta_{s0_2_0}} c^{a\beta_{s0_1_0}} & c^{a\beta_{s0_3_0}} s^{a\beta_{s0_2_0}} c^{a\beta_{s0_1_0}} & c^{a\beta_{s0_3_0}} (-s^{a\beta_{s0_2_0}}) c^{a\beta_{s0_1_0}} & s^{a\beta_{s0_3_0}} c^{a\beta_{s0_2_0}} c^{a\beta_{s0_1_0}} & s^{a\beta_{s0_3_0}} c^{a\beta_{s0_2_0}} s^{a\beta_{s0_1_0}} & s^{a\beta_{s0_3_0}} (-s^{a\beta_{s0_2_0}}) s^{a\beta_{s0_1_0}} & s^{a\beta_{s0_3_0}} c^{a\beta_{s0_2_0}} c^{a\beta_{s0_1_0}} \\ -s^{a\beta_{s0_3_0}} c^{a\beta_{s0_2_0}} c^{a\beta_{s0_1_0}} & -s^{a\beta_{s0_3_0}} s^{a\beta_{s0_2_0}} c^{a\beta_{s0_1_0}} & -s^{a\beta_{s0_3_0}} (-s^{a\beta_{s0_2_0}}) c^{a\beta_{s0_1_0}} & -s^{a\beta_{s0_3_0}} c^{a\beta_{s0_2_0}} s^{a\beta_{s0_1_0}} & -s^{a\beta_{s0_3_0}} c^{a\beta_{s0_2_0}} (-s^{a\beta_{s0_1_0}}) & -s^{a\beta_{s0_3_0}} (-s^{a\beta_{s0_2_0}}) (-s^{a\beta_{s0_1_0}}) & -s^{a\beta_{s0_3_0}} c^{a\beta_{s0_2_0}} (-s^{a\beta_{s0_1_0}}) \\ s^{a\beta_{s0_3_0}} c^{a\beta_{s0_2_0}} s^{a\beta_{s0_1_0}} & s^{a\beta_{s0_3_0}} s^{a\beta_{s0_2_0}} s^{a\beta_{s0_1_0}} & s^{a\beta_{s0_3_0}} (-s^{a\beta_{s0_2_0}}) s^{a\beta_{s0_1_0}} & s^{a\beta_{s0_3_0}} c^{a\beta_{s0_2_0}} c^{a\beta_{s0_1_0}} & s^{a\beta_{s0_3_0}} c^{a\beta_{s0_2_0}} s^{a\beta_{s0_1_0}} & s^{a\beta_{s0_3_0}} (-s^{a\beta_{s0_2_0}}) c^{a\beta_{s0_1_0}} & s^{a\beta_{s0_3_0}} c^{a\beta_{s0_2_0}} s^{a\beta_{s0_1_0}} \\ -s^{a\beta_{s0_3_0}} c^{a\beta_{s0_2_0}} c^{a\beta_{s0_1_0}} & -s^{a\beta_{s0_3_0}} s^{a\beta_{s0_2_0}} c^{a\beta_{s0_1_0}} & -s^{a\beta_{s0_3_0}} (-s^{a\beta_{s0_2_0}}) c^{a\beta_{s0_1_0}} & -s^{a\beta_{s0_3_0}} c^{a\beta_{s0_2_0}} s^{a\beta_{s0_1_0}} & -s^{a\beta_{s0_3_0}} c^{a\beta_{s0_2_0}} (-s^{a\beta_{s0_1_0}}) & -s^{a\beta_{s0_3_0}} (-s^{a\beta_{s0_2_0}}) (-s^{a\beta_{s0_1_0}}) & -s^{a\beta_{s0_3_0}} c^{a\beta_{s0_2_0}} (-s^{a\beta_{s0_1_0}}) \\ s^{a\beta_{s0_3_0}} c^{a\beta_{s0_2_0}} s^{a\beta_{s0_1_0}} & s^{a\beta_{s0_3_0}} s^{a\beta_{s0_2_0}} s^{a\beta_{s0_1_0}} & s^{a\beta_{s0_3_0}} (-s^{a\beta_{s0_2_0}}) s^{a\beta_{s0_1_0}} & s^{a\beta_{s0_3_0}} c^{a\beta_{s0_2_0}} c^{a\beta_{s0_1_0}} & s^{a\beta_{s0_3_0}} c^{a\beta_{s0_2_0}} s^{a\beta_{s0_1_0}} & s^{a\beta_{s0_3_0}} (-s^{a\beta_{s0_2_0}}) c^{a\beta_{s0_1_0}} & s^{a\beta_{s0_3_0}} c^{a\beta_{s0_2_0}} s^{a\beta_{s0_1_0}} \end{bmatrix} \quad (2.116)
 \end{aligned}$$

where:

$$a_{\beta_{s0_1_0}} = \tan^{-1} \frac{a_{u7_3_0} - a_{u11_3_0}}{a_{r7_2_0} + a_{u7_2_0} - a_{r11_2_0} - a_{u11_2_0}} \quad (2.116a)$$

$$a_{\beta_{s0_2_0}} = \tan^{-1} \frac{-(a'_{u6_3_0} - a'_{u9_3_0})}{a'_{r6_1_0} + a'_{u6_1_0} - a'_{r9_1_0} - a'_{u9_1_0}} = \tan^{-1} \frac{-(a'_{u6_3_0} - a'_{u9_3_0})}{a'_{r6_1_0} + a'_{u6_1_0} - a'_{r9_1_0} - a'_{u9_1_0}} \quad (2.116b)$$

$$a_{\beta_{s0_3_0}} = \tan^{-1} \frac{a''_{u6_2_0} - a''_{u9_2_0}}{a''_{r6_1_0} + a''_{u6_1_0} - a''_{r9_1_0} - a''_{u9_1_0}} = \tan^{-1} \frac{a'_{u6_2_0} - a'_{u9_2_0}}{a''_{r6_1_0} + a''_{u6_1_0} - a''_{r9_1_0} - a''_{u9_1_0}} \quad (2.116c)$$

For completeness, the following relationships define the quasi-static location vectors for Points 6 through 9 in the intermediate reference frames as a function of their values relative to the initial panel reference frame:

$$\begin{aligned}
a_{r_{sk}} + a_{u_{sk_0}} &= a_{C_{sj3_0}} (a_{r_{sk}}'' + a_{u_{sk_0}}'') \\
&= a_{C_{sj3_0}} a_{C_{sj2_0}} (a_{r_{sk}}' + a_{u_{sk_0}}') \\
&= a_{C_{sj3_0}} a_{C_{sj2_0}} a_{C_{sj1_0}} (a_{r_{sk}}^* + a_{u_{sk_0}}^*) = a_{C_{s0_0}} (a_{r_{sk}}^* + a_{u_{sk_0}}^*) \quad (2.117)
\end{aligned}$$

where $j=0$ or 1 ; $k=6, \dots, 11$, and the asterisk indicates the initial value (before transformation) which is the value evaluated with respect to the $\underline{[b]}$ vector base. Specifically:

$$a_{r_{s6}} + a_{u_{s6_0}} = \frac{1}{2} (a_{r_{s2}} + a_{u_{s2_0}} + a_{r_{s3}} + a_{u_{s3_0}}) \quad (2.118a)$$

$$a_{r_{s7}} + a_{u_{s7_0}} = (1-x_0) (a_{r_{s3}} + a_{u_{s3_0}}) + x_0 (a_{r_{s4}} + a_{u_{s4_0}}) \quad (2.118b)$$

$$a_{r_{s8}} + a_{u_{s8_0}} = (1-x_1) (a_{r_{s3}} + a_{u_{s3_0}}) + x_0 (a_{r_{s4}} + a_{u_{s4_0}}) \quad (2.118c)$$

$$a_{r_{s9}} + a_{u_{s9_0}} = \frac{1}{2} (a_{r_{s4}} + a_{u_{s4_0}} + a_{r_{s5}} + a_{u_{s5_0}}) \quad (2.118d)$$

$$a_{r_{s10}} + a_{u_{s10_0}} = (1-x_1) (a_{r_{s2}} + a_{u_{s2_0}}) + x_0 (a_{r_{s5}} + a_{u_{s5_0}}) \quad (2.118e)$$

$$a_{r_{s11}} + a_{u_{s11_0}} = (1-x_0) (a_{r_{s2}} + a_{u_{s2_0}}) + x_0 (a_{r_{s5}} + a_{u_{s5_0}}) \quad (2.118f)$$

The quasi-static aerodynamic panel loads are extracted from Equation (2.111):

$$a_{f_0} = (C_{shuf})^m [GAM_0] \alpha_0' \quad (2.119)$$

where C_{shuf} is as before, $[GAM_0]$ is updated to account for large quasi-static deformations, and each α_{s_0} in α_0' is found from the quasi-static form of Equation (2.109):

$$\alpha_{s_0} = \tan^{-1} \frac{v_{s3_0}}{\sqrt{v_{s1_0}^2 + v_{s2_0}^2}} \quad (2.120)$$

and the quasi-static components of the panel relative velocity, V_S , are extracted from Equation (2.108):

$$V_{S0} = V_{GS0} - {}^a C_{S10} \left[\theta_0 \dot{x}_0 + \tilde{\omega}_0 (R^a r_{S1}) - \tilde{\omega}_0 \left(\frac{1}{M_A} (E(3))^{\mathbb{H}_{n-1}^T} \left[\bar{M}_T | [0] \right] + \frac{m_n}{M_A} [K_{u_n \bar{u}} | K_{u_n \bar{\beta}}] - d_{q_{S0}} \right) \bar{q}_0 \right] \quad (2.121)$$

For the reduced quasi-static flexible vehicle equations, Equation (2.68b), F_0 and T_0 due to quasi-static aerodynamic loads are the upper $3n-3X1$ sub-columns of quasi-static aerodynamic forces and torques in Equation (2.114), respectively. For the translational quasi-static total vehicle equations, Equation (2.69), F_0 due to quasi-static aerodynamic loads is the sum of all the quasi-static aerodynamic forces in Equation (2.114):

$$F_{aero0} = (E(3))^{\mathbb{H}_n^T} f_{aero0} \quad (2.122)$$

And, for the rotational quasi-static total vehicle equations, Equation (2.68b), T_0 due to quasi-static aerodynamic loads is the sum of all quasi-static aerodynamic torques plus all the cross products of $r_S + u_{S0}$ with the corresponding quasi-static aerodynamic force:

$$T_{aero0} = (E(3))^{\mathbb{H}_n^T} \left[t_{aero0} + (\tilde{r}_S)^{\wedge n} f_{aero0} \right] + (E(3))^{\mathbb{H}_{n-1}^T} (\tilde{u}_{S0})^{\wedge n-1} - [K_{u_n \bar{u}} | K_{u_n \bar{\beta}}] \bar{q}_0 f_{aero_{n0}} \quad (2.123)$$

2 3.1.7 Perturbation Aerodynamic Loads

To formulate the perturbation aerodynamic loads: first, all time dependent variables are expanded into the quasi-static and perturbation approximation of Equation (2.62), the purely quasi-static terms have been accounted for in the

previous section; then, all terms negligible with respect to the first order perturbation terms are dropped (See Equation (2.64)). The resultant perturbation aerodynamic loads as a function of the perturbation aerodynamic panel forces is extracted from Equation (2.91):

$$\begin{Bmatrix} \Delta \bar{f}_{aero} \\ \Delta \bar{t}_{aero} \end{Bmatrix} = D_{L0} \left[\left(\Delta^a C_{S0}^T \ a C_{S0}^T \right)^m a_{f0} + \left(a C_{S0}^T \right)^m \Delta^a f \right] - \begin{Bmatrix} f_{aero0} \\ t_{aero0} \end{Bmatrix} \quad (2.124)$$

The grid transformation matrices, D_{L0} and D_{q0} , define a linear relationship between the structural and aerodynamic degrees-of-freedom ($\Delta \bar{f}_{aero}$ and $\Delta \bar{t}_{aero}$ to $\Delta^a f$, and $\Delta^a u'$ to $\Delta \bar{q}$): that is, D_{L0} and D_{q0} are constant under the perturbation assumptions. Furthermore, the perturbation rotation of the aerodynamic panel vector bases beyond the quasi-static position is assumed small: therefore the prime, double prime, and triple prime perturbation vector bases will be assumed coincident with the quasi-static vector base. Also, small angle assumptions will be employed in the evaluation of the perturbation direction cosine matrices, $\Delta^a C_{S1}$ and $\Delta^a C_{S0}$ (Equations (2.96), and (2.100), respectively). For $\Delta^a C_{S1}$:

$$\Delta^a C_{S1} \cong \begin{bmatrix} 1 & \Delta^a \beta_{S13} & -\Delta^a \beta_{S12} \\ -\Delta^a \beta_{S13} & 1 & \Delta^a \beta_{S11} \\ \Delta^a \beta_{S12} & -\Delta^a \beta_{S11} & 1 \end{bmatrix} = E^{(3)} - \Delta^a \tilde{\beta}_{S1} \quad (2.125)$$

where:

$$\begin{aligned} \Delta^a \beta_{S11} &= \tan^{-1} \frac{\Delta^a u_{83} - \Delta^a u_{103}}{a_{r82} + a_{u82_0} + \Delta^a u_{83} - a_{r102} - a_{u102_0} - \Delta^a u_{102}} \\ &\cong \frac{\Delta^a u_{83} - \Delta^a u_{103}}{a_{r82} + a_{u82_0} - a_{r102} - a_{u102_0}} \cong \frac{\Delta^a b_{S11}}{a_{bS11_0}} \end{aligned} \quad (2.126a)$$

$$\begin{aligned} \Delta^a \beta_{s12} &= \tan^{-1} \frac{-(\Delta^a u'_{63} - \Delta^a u'_{93})}{a_{r61} + a_{u61_0} + \Delta^a u'_{61} - a_{r91} - a_{u91_0} - \Delta^a u'_{91}} \\ &\equiv \frac{-(\Delta^a u_{63} - \Delta^a u_{93})}{a_{r61} + a_{u61_0} - a_{r91} - a_{u91_0}} \equiv \frac{\Delta^a b_{s12}}{a_{b s12_0}} \end{aligned} \quad (2.126b)$$

$$\begin{aligned} \Delta^a \beta_{s13} &= \tan^{-1} \frac{\Delta^a u''_{62} - \Delta^a u''_{92}}{a_{r61} + a_{u61_0} + \Delta^a u''_{61} - a_{r91} - a_{u91_0} - \Delta^a u''_{91_0}} \\ &\equiv \frac{\Delta^a u_{62} - \Delta^a u_{92}}{a_{r61} + a_{u61_0} - a_{r91} - a_{u91_0}} \equiv \frac{\Delta^a b_{s13}}{a_{b s13_0}} \end{aligned} \quad (2.126c)$$

Substituting Equations (2.126a), (2.126b), and (2.126c) into Equation (2.125) gives:

$$\Delta^a C_{s1} \equiv E(3) - a_{b s1_0} \Delta^a \bar{b}_{s1} = E(3) - a_{b s1_0} (d_{b s1_0} \Delta \bar{q}) \quad (2.127)$$

where $d_{b s1_0}$ is a 3X6n-6 grid transformation matrix which combines the appropriate weighted averages of all $\Delta \bar{q}$ to yield $\Delta^a \bar{b}_{s1}$ (the subscript 0 indicates that this matrix is evaluated for the quasi-statically deformed vehicle), and:

$$a_{b s1_0} = \begin{bmatrix} \frac{1}{a_{b s11_0}} & 0 & 0 \\ 0 & \frac{1}{a_{b s12_0}} & 0 \\ 0 & 0 & \frac{1}{a_{b s13_0}} \end{bmatrix} = \left(\frac{1}{a_{b s1k_0}} \right)^3 \quad (2.128)$$

The procedure above to define $\Delta^a C_{S1}$ is repeated to define $\Delta^a C_{S0}$:

$$\Delta^a C_{S0} \approx \begin{bmatrix} 1 & \Delta^a \beta_{S03} & -\Delta^a \beta_{S02} \\ -\Delta^a \beta_{S03} & 1 & \Delta^a \beta_{S01} \\ \Delta^a \beta_{S02} & -\Delta^a \beta_{S01} & 1 \end{bmatrix} = E(3) - \Delta^a \tilde{\beta}_{S0} \quad (2.129)$$

where:

$$\begin{aligned} \Delta^a \beta_{S01} &= \tan^{-1} \frac{\Delta^a u_{73} - \Delta^a u_{113}}{a_{r72} + a_{u72_0} + \Delta^a u_{72} - a_{r112} - a_{u112_0} - \Delta^a u_{112}} \\ &\approx \frac{\Delta^a u_{73} - \Delta^a u_{113}}{a_{r72} + a_{u72_0} - a_{r112} - a_{u112_0}} \approx \frac{\Delta^a b_{S01}}{a_{bS01_0}} \end{aligned} \quad (2.130a)$$

$$\begin{aligned} \Delta^a \beta_{S02} &= \tan^{-1} \frac{-(\Delta^a u'_{63} - \Delta^a u'_{93})}{a_{r'61} + a_{u'61_0} + \Delta^a u'_{61} - a_{r'91} - a_{u'91_0} - \Delta^a u'_{91}} \\ &\approx \frac{-(\Delta^a u_{63} - \Delta^a u_{93})}{a_{r61} + a_{u61_0} - a_{r91} - a_{u91_0}} \approx \frac{\Delta^a b_{S02}}{a_{bS02_0}} \end{aligned} \quad (2.130b)$$

$$\begin{aligned} \Delta^a \beta_{S03} &= \tan^{-1} \frac{\Delta^a u''_{62} - \Delta^a u''_{92}}{a_{r''61} + a_{u''61_0} + \Delta^a u''_{61} - a_{r''91} - a_{u''91_0} - \Delta^a u''_{91}} \\ &\approx \frac{\Delta^a u_{62} - \Delta^a u_{92}}{a_{r61} + a_{u61_0} - a_{r91} - a_{u91_0}} \approx \frac{\Delta^a b_{S03}}{a_{bS03_0}} \end{aligned} \quad (2.130c)$$

Substituting Equations (2.130) into Equation (2.129) results in:

$$\Delta^a C_{S0} \approx E(3) - a_{bS0_0} \Delta^a \tilde{\beta}_{S0} = E(3) - a_{bS0_0} \left(db_{S0_0} \Delta \tilde{a} \right) \quad (2.131)$$

where d_{bs0} is a $3 \times 6n-6$ grid transformation matrix which combines the appropriate weighted averages of all Δq to yield $\Delta^a b_{s0}$, and:

$${}^a b_{s0} = \begin{bmatrix} 1 & & \\ \frac{1}{a_{bs01_0}} & 0 & 0 \\ 0 & \frac{1}{a_{bs02_0}} & \\ 0 & 0 & \frac{1}{a_{bs03_0}} \end{bmatrix} = \left(\frac{1}{a_{bs0k_0}} \right)^3 \quad (2.132)$$

Equation (2.131) is substituted into the first term of Equation (2.124) to yield:

$$\begin{aligned} D_{L_0} \left(\Delta^a C_{s0}^T a_{C_{s0}}^T \right)^m a_{f_0} &\cong D_{L_0} \left\{ \left[E^{(3)} + {}^a b_{s0_0} (d_{bs0_0} \Delta \bar{q}) \right] a_{C_{s0_0}}^T \right\}^m a_{f_0} \\ &= D_{L_0} \left\{ \left(a_{C_{s0_0}}^T \right)^m a_{f_0} - \left[{}^a b_{s0_0} \left(a_{C_{s0_0}}^T a_{f_{s0}} \right) \right]^m d_{bs0_0} \right\}^m \Delta \bar{q} \\ &= \left\{ \begin{matrix} f_{aero_0} \\ t_{aero_0} \end{matrix} \right\} D_{L_0} \left[{}^a b_{s0_0} \left(a_{C_{s0_0}}^T a_{f_{s0}} \right) \right]^m d_{bs0_0} \Delta \bar{q} \end{aligned} \quad (2.133)$$

The second term in Equation (2.124) contains the coordinate transformation $a_{C_{s1}}$ (See Equation (2.106)). When expanded into quasi-static and perturbation components, the perturbation component is $E^{(3)}$ minus a perturbation on the deformation variables (See Equation (2.125)). The unity matrix will yield what appears to be an additional quasi-static aerodynamic panel force. However, this has already been accounted for in the first term. To see this more clearly a_f is assumed to be a function of $a_{C_{s1}}$ only. Equation (2.91) is expanded as:

$$\begin{aligned}
D_L^a C_{S0}^T C_{S1}^T &\approx D_{L0} \left(E^{(3)} + \Delta^a \tilde{\beta}_{S0} \right) C_{S0}^T \left(E^{(3)} + \Delta^a \tilde{\beta}_{S1} \right) C_{S1}^T \\
&\approx D_{L0} \left(C_{S0}^T C_{S1}^T + \Delta^a \tilde{\beta}_{S0} C_{S0}^T C_{S1}^T + C_{S0}^T \Delta^a \tilde{\beta}_{S1} C_{S1}^T \right) \quad (2.134)
\end{aligned}$$

The second order perturbation term in Equation (2.134) is neglected (See Equation (2.64)). The second term comes from the perturbation of the first coordinate transformation and the quasi-static of the second. The first term comes from the quasi-static of both coordinate transformations. Likewise, the first term in Equation (2.124) contains the quasi-static component of the aerodynamic panel forces including any pure quasi-static terms generated under the perturbation assumptions due to a coordinate transformation.

In light of the preceding discussion the second term of Equation (2.124) is expanded. It is assumed that [GAM] is only a function of the quasi-static variables. Therefore, the perturbation aerodynamic panel forces are linear functions of the perturbation angle-of-attacks, $\Delta\alpha'$, (See Equation (2.111)) and the second term of Equation (2.124) yields:

$$D_{L0} \left(C_{S0}^T \right)^m \Delta^a f = D_{L0} \left(C_{S0}^T C_{shuf} \right)^m [GAM] \Delta\alpha' \quad (2.135)$$

To find $\Delta\alpha_s$ an additional coordinate transformation, ${}^a C_{S00}$, is developed to rotate the ${}^a \{a_{s1}\}$ vector base such that the first axis is coincident with the quasi-static relative velocity and the second axis is still in the plane of the first and second components of ${}^a \{a_{s1}\}$ (See Figure 2-13). Only two rotations are needed: the first rotation is in the plane of the panel, about the third axis, such that the first axis coincides with the projection of V_{S0} in the plane of the panel, the second rotation is about the primed second axis:

$$\begin{aligned}
{}^a C_{S\alpha_0} &= \begin{bmatrix} 1 & 0 & 0 \\ 0 & 1 & 0 \\ 0 & 0 & 1 \end{bmatrix} \begin{bmatrix} c^a \beta_{S\alpha_2_0} & 0 & -s^a \beta_{S\alpha_2_0} \\ 0 & 1 & 0 \\ s^a \beta_{S\alpha_2_0} & 0 & c^a \beta_{S\alpha_2_0} \end{bmatrix} \begin{bmatrix} c^a \beta_{S\alpha_3_0} & s^a \beta_{S\alpha_3_0} & 0 \\ -s^a \beta_{S\alpha_3_0} & c^a \beta_{S\alpha_3_0} & 0 \\ 0 & 0 & 1 \end{bmatrix} \\
&= \begin{bmatrix} c^a \beta_{S\alpha_2_0} & c^a \beta_{S\alpha_3_0} & c^a \beta_{S\alpha_2_0} & s^a \beta_{S\alpha_3_0} & -s^a \beta_{S\alpha_2_0} \\ -s^a \beta_{S\alpha_3_0} & & c^a \beta_{S\alpha_3_0} & & 0 \\ s^a \beta_{S\alpha_2_0} & c^a \beta_{S\alpha_3_0} & c^a \beta_{S\alpha_2_0} & s^a \beta_{S\alpha_3_0} & c^a \beta_{S\alpha_2_0} \end{bmatrix} \quad (2.136)
\end{aligned}$$

where:

$${}^a \beta_{S\alpha_3_0} = \tan^{-1} \frac{V_{S1_0}}{V_{S2_0}} \quad (2.137a)$$

$${}^a \beta_{S\alpha_2_0} = \alpha_{S_0} \quad (2.137b)$$

$${}^a \beta_{S\alpha_1_0} = 0 \quad (2.137c)$$

$\Delta\alpha_S$ is defined as the arctangent of the magnitude of the vertical perturbation relative velocity divided by the magnitude of the total relative velocity. In the denominator the perturbation terms are negligible with respect to the quasi-static terms. The numerator is a perturbation term and is small compared to the denominator and hence allows a small angle approximation (Note, the magnitude of the denominator may be evaluated with respect to any reference frame):

$$\begin{aligned}
\Delta\alpha_S &= \tan^{-1} \frac{\Delta V_{S\alpha_3}}{\sqrt{(V_{S1_0} + \Delta V_{S1})^2 + (V_{S2_0} + \Delta V_{S2})^2 + (V_{S3_0} + \Delta V_{S3})^2}} \\
&\approx \frac{\Delta V_{S\alpha_3}}{\sqrt{V_{S1_0}^2 + V_{S2_0}^2 + V_{S3_0}^2}} \quad (2.138)
\end{aligned}$$

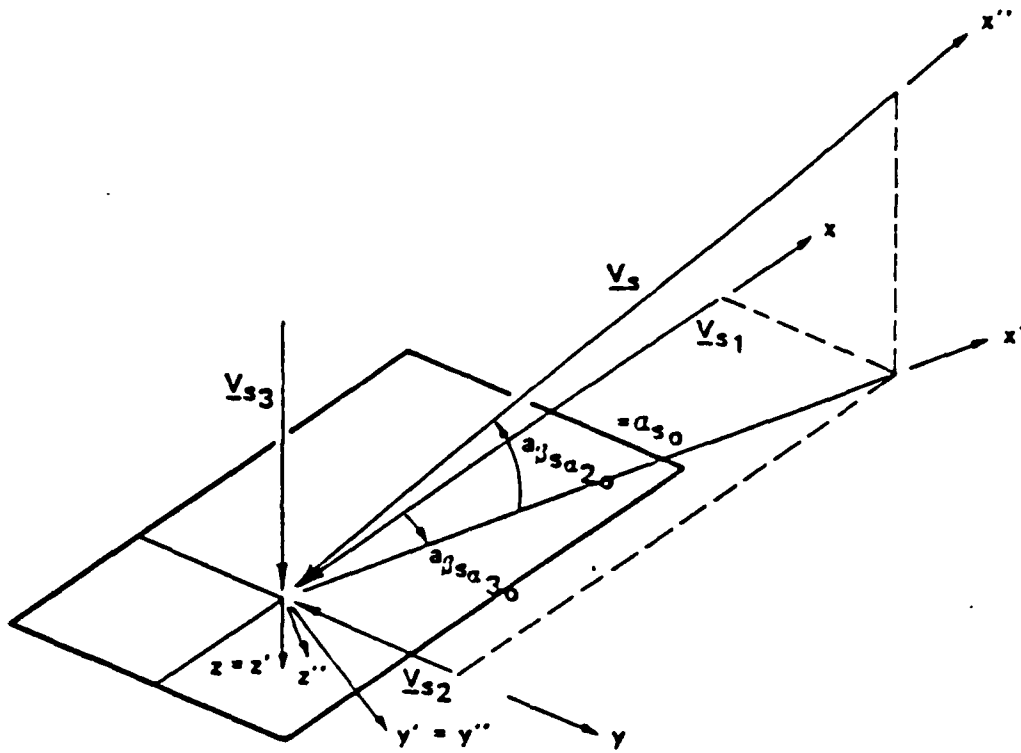


Figure 2-13. Perturbation Aerodynamic Panel Rotation

Equation (2.136) is expanded into quasi-static and perturbation components under the assumptions of Equation (2.62). This expansion and the shuffle matrix in Equation (2.111) are substituted into Equation (2.138) to yield $\Delta\alpha_S$ as a linear function of ΔV_S :

$$\Delta\alpha_S \approx \frac{C_{shuf}^T \Delta^a C_{S\alpha} C_{S\alpha_0} \Delta V_S}{\sqrt{V_{S1_0}^2 + V_{S2_0}^2 + V_{S3_0}^2}} \approx \frac{C_{shuf}^T C_{S\alpha_0} \Delta V_S}{\sqrt{V_{S1_0}^2 + V_{S2_0}^2 + V_{S3_0}^2}} \quad (2.139)$$

where the final approximation is made noting that $\Delta^a C_{S\alpha}$ is approximately $E(3)$ minus a skew-symmetric perturbation matrix.

ΔV_S is found by expanding Equation (2.108) under the perturbation assumptions. It is important to note that Equation (2.108) contains coordinate transformations, and any purely quasi-static terms that result from the expansion of these transformations have already been accounted for in Equation (2.133). Therefore, the perturbation approximation of ΔV_S is:

$$\begin{aligned} \Delta V_S = & \Delta V_{G_S} - \left(\Delta^a C_{S1} - E(3) \right) C_{S1_0} \left[\theta_0 \dot{x}_0 + \tilde{\omega}_0 (R + {}^a r_{S1}) - \tilde{\omega}_0 \left(\frac{1}{M_A} (E(3))^{n-1} \left[\bar{M}_T | 0 \right] \right) \right. \\ & + \frac{M_D}{M_A} \left[K_{u_n \bar{u}} | K_{u_n \bar{\beta}} \right] - d_{q_S} \bar{q}_0 \left. \right] - {}^a C_{S1_0} \left[\left(\Delta\theta - E(3) \right) \dot{x}_0 + \theta_0 \Delta \dot{x} + \Delta \tilde{\omega} (R + {}^a r_{S1}) \right. \\ & - \Delta \tilde{\omega} \left(\frac{1}{M_A} (E(3))^{n-1} \left[\bar{M}_T | 0 \right] \right) + \frac{M_D}{M_A} \left[K_{u_n \bar{u}} | K_{u_n \bar{\beta}} \right] - d_{q_S} \bar{q}_0 \\ & - \tilde{\omega}_0 \left(\frac{1}{M_A} (E(3))^{n-1} \left[\bar{M}_T | 0 \right] \right) + \frac{M_D}{M_A} \left[K_{u_n \bar{u}} | K_{u_n \bar{\beta}} \right] - d_{q_S} \Delta \bar{q} \\ & \left. - \left(\frac{1}{M_A} (E(3))^{n-1} \left[\bar{M}_T | 0 \right] \right) + \frac{M_D}{M_A} \left[K_{u_n \bar{u}} | K_{u_n \bar{\beta}} \right] - d_{q_S} \dot{\Delta \bar{q}} \right] \end{aligned} \quad (2.140)$$

Equations (2.127) and (2.97) are substituted into Equation (2.140) to replace $\Delta^a C_{S1}$ and $\Delta\theta$, respectively:

$$\begin{aligned}
\Delta V_S = & \Delta V_{G_S} + {}^a b_{S1_0} (d_{b_{S1_0}} \bar{\Delta q}) {}^a c_{S1_0} \left[\theta_0 \dot{x}_0 + \tilde{\omega}_0 (R + {}^a r_{S1}) - \tilde{\omega}_0 \left(\frac{1}{M_A} (E(3))^{n-1} \left[\bar{M}_T | [0] \right] \right) \right. \\
& + \left. \frac{m_n}{M_A} \left[K_{u_n \bar{u}} | K_{u_n \bar{\beta}} \right] - d_{\bar{q}_S} \right] \bar{q}_0 - {}^a c_{S1_0} \left[\Delta \tilde{\Gamma} \dot{x}_0 + \theta_0 \Delta \dot{x} + \Delta \tilde{\omega} (R + {}^a r_{S1}) \right. \\
& - \Delta \tilde{\omega} \left(\frac{1}{M_A} (E(3))^{n-1} \left[\bar{M}_T | [0] \right] + \frac{m_n}{M_A} \left[K_{u_n \bar{u}} | K_{u_n \bar{\beta}} \right] - d_{\bar{q}_S} \right) \bar{q}_0 \\
& - \tilde{\omega}_0 \left(\frac{1}{M_A} (E(3))^{n-1} \left[\bar{M}_T | [0] \right] + \frac{m_n}{M_A} \left[K_{u_n \bar{u}} | K_{u_n \bar{\beta}} \right] - d_{\bar{q}_S} \right) \Delta \bar{q} \\
& \left. - \left(\frac{1}{M_A} (E(3))^{n-1} \left[\bar{M}_T | [0] \right] + \frac{m_n}{M_A} \left[K_{u_n \bar{u}} | K_{u_n \bar{\beta}} \right] - d_{\bar{q}_S} \right) \Delta \dot{\bar{q}} \right] \quad (2.141)
\end{aligned}$$

The terms in Equation (2.141) are rewritten and regrouped so as to extract and combine according to the order of the independent quasi-static variables:

$$\begin{aligned}
\Delta V_S = & \Delta V_{G_S} + {}^a c_{S1_0} \left\{ \tilde{x}_0 \Delta \Gamma - \theta_0 \Delta \dot{x} + \left[R + {}^a r_{S1} + \left(\frac{1}{M_A} (E(3))^{n-1} \left[\bar{M}_T | [0] \right] \right) \right. \right. \\
& + \left. \left. \frac{m_n}{M_A} \left[K_{u_n \bar{u}} | K_{u_n \bar{\beta}} \right] - d_{\bar{q}_S} \right] \bar{q}_0 \right\} \Delta \omega - \left[{}^a b_{S1_0} \left\{ {}^a c_{S1_0} \left[\theta_0 \dot{x}_0 + \tilde{\omega}_0 (R + {}^a r_{S1}) \right. \right. \right. \\
& - \left. \left. \tilde{\omega}_0 \left(\frac{1}{M_A} (E(3))^{n-1} \left[\bar{M}_T | [0] \right] + \frac{m_n}{M_A} \left[K_{u_n \bar{u}} | K_{u_n \bar{\beta}} \right] - d_{\bar{q}_S} \right) \bar{q}_0 \right\} \right] d_{b_{S1_0}} \\
& + {}^a c_{S1_0} \left\{ \tilde{\omega}_0 \left(\frac{1}{M_A} (E(3))^{n-1} \left[\bar{M}_T | [0] \right] + \frac{m_n}{M_A} \left[K_{u_n \bar{u}} | K_{u_n \bar{\beta}} \right] - d_{\bar{q}_S} \right) \right\} \Delta \bar{q} \\
& - {}^a c_{S1_0} \left\{ \frac{1}{M_A} (E(3))^{n-1} \left[\bar{M}_T | [0] \right] + \frac{m_n}{M_A} \left[K_{u_n \bar{u}} | K_{u_n \bar{\beta}} \right] - d_{\bar{q}_S} \right\} \Delta \dot{\bar{q}} \quad (2.142)
\end{aligned}$$

The following short hand notation will be used to simplify Equation (2.142):

$$\Delta V_S = \Delta V_{G_S} + d_{V_S} \Delta \Gamma \Delta \Gamma + d_{V_S} \Delta \dot{x} \Delta \dot{x} + d_{V_S} \Delta \omega \Delta \omega + d_{V_S} \Delta \bar{q} \Delta \bar{q} + d_{V_S} \Delta \dot{\bar{q}} \Delta \dot{\bar{q}} \quad (2.143)$$

where the first three coefficients are 3X3 and the last two are 3X6n-6.

Equation (2.143) is substituted into Equation (2.139) to obtain α_s as a function of the structural perturbation variables. The Boolean operator matrices are used to substitute this result into Equation (2.135), which is the second term in Equation (2.124):

$$D_{L_0} \left(a_{CS_0}^T \right)^m \Delta^a f = D_{L_0} \left(a_{CS_0}^T C_{shuf} \right)^m [GAM] \left(\frac{C_{shuf}^a C_s \alpha_0}{\sqrt{V_{S1_0}^2 + V_{S2_0}^2 + V_{S3_0}^2}} \right)^m \cdot \left[\Delta V_g^n + \left(d_{V_S \Delta \Gamma} \right)^m \Delta \Gamma^n + \left(d_{V_S \Delta \dot{X}} \right)^m \Delta \dot{X}^n + \left(d_{V_S \Delta \omega} \right)^m \Delta \omega^n + d_{V_S \Delta \bar{q}}^n \Delta \bar{q} + d_{V_S \Delta \dot{\bar{q}}}^n \Delta \dot{\bar{q}} \right] \quad (2.144)$$

where the double prime represents a column matrix of m sub-matrices of the operand.

Finally, Equations (2.133) and (2.144) are substituted into (2.124) to yield the perturbation structural aerodynamic loads for all 6n rigid sub-bodies:

$$\begin{aligned} \begin{Bmatrix} \Delta f_{aero} \\ \Delta t_{aero} \end{Bmatrix} = D_{L_0} \left\{ \left(a_{CS_0}^T C_{shuf} \right)^m [GAM] \left(\frac{C_{shuf}^a C_s \alpha_0}{\sqrt{V_{S1_0}^2 + V_{S2_0}^2 + V_{S3_0}^2}} \right)^m \left[\Delta V_g^n + \left(d_{V_S \Delta \Gamma} \right)^m \Delta \Gamma^n \right. \right. \\ \left. \left. + \left(d_{V_S \Delta \dot{X}} \right)^m \Delta \dot{X}^n + \left(d_{V_S \Delta \omega} \right)^m \Delta \omega^n + d_{V_S \Delta \bar{q}}^n \Delta \bar{q} + d_{V_S \Delta \dot{\bar{q}}}^n \Delta \dot{\bar{q}} \right] \right. \\ \left. + \left[a_{bs_0} \left(a_{CS_0}^T a_{fs_0} \right)^m D_{bs_0} \Delta \bar{q} \right] \right\} \quad (2.145) \end{aligned}$$

For the reduced perturbation flexible vehicle equations. Equation (2.76e), ΔF and $\Delta \bar{F}$ due to perturbation aerodynamic loads are the upper 3n 3X1 sub-columns of perturbation aerodynamic panel forces and torques in Equation (2.145), respectively. For the translational perturbation total vehicle equations, Equation (2.78), ΔF due to perturbation aerodynamic panel loads is the sum of all the perturbation aerodynamic forces in Equation (2.145):

$$\Delta F_{aero} = \left(E(3) \right)^n \Delta f_{aero} \quad (2.146)$$

And, for the rotational quasi-static total vehicle equations, Equation (2.79), ΔT due to quasi-static aerodynamic panel loads is the sum of all perturbation aerodynamic torques plus all the cross products of $r_s + u_{s0}$ with the corresponding perturbation aerodynamic force and Δu_s with the corresponding quasi-static aerodynamic force:

$$\begin{aligned} \Delta T_{aero} = & \left(E(3) \right)^n \left[\Delta t_{aero} + \left(\tilde{r}_s \right)^n \Delta f_{aero} \right] \\ & + \left(E(3) \right)^{n-1} \left\{ \left(\tilde{u}_{s0} \right)^{n-1} \Delta \tilde{f}_{aero} - \left[\left(\tilde{f}_{aero s_0} \right)^{n-1} \mid [0] \right] \Delta \bar{q} \right\} \\ & - \left(\left[K_{u_n \bar{u}} \mid K_{u_n \bar{\beta}} \right] \bar{q}_0 \right) \Delta f_{aero n} + \tilde{f}_{aero n_0} \left[K_{u_n \bar{u}} \mid K_{u_n \bar{\beta}} \right] \Delta \bar{q} \end{aligned} \quad (2.147)$$

2.3.2 Gravitational Loads

2.3.2.1 Sub-body Gravitational Load

Forces due to the Earth's gravitational attraction are body forces, proportional only to the mass of the sub-body and always in a "downward" direction. It may be convenient to define the inertial reference frame at an arbitrary angle. Thus, although the direction of the gravitational acceleration does not change with respect to the inertial reference frame, it may not be coincident with any one base vector component of the inertial reference frame.

In order to incorporate gravitational effects into the hybrid-coordinate dynamic equations it is necessary to define the direction of the gravitational acceleration in term of the inertial vector base, $\{i\}$:

$$\underline{g} = \{i\}^T g \quad (2.148)$$

where \underline{g} is a 3×1 coefficient matrix in which all elements, in general, are not zero (depending on the choice of $\{\underline{i}\}$).

The gravity forces, to be included in Equations (2.52f), (2.60), and (2.61), should be expressed in the $\{\underline{b}\}$ vector base. Recall the base vector relationship of Equation (2.2):

$$\{\underline{i}\}^T = \{\underline{b}\}^T \underline{\theta} \quad (2.149)$$

This is substituted into the definition of the gravitational acceleration in Equation (2.148):

$$\underline{g} = \{\underline{b}\}^T \underline{\theta} \underline{g} \quad (2.150)$$

Therefore, the time dependent ($\underline{\theta}$ being a function of time) force due to gravitational acceleration, $\underline{f}_{\text{grav}_s}$ (a component of \underline{f} only, Equation (2.26g)), is:

$$\underline{f}_{\text{grav}_s} = m_s \underline{\theta} \underline{g} \quad (2.151)$$

2.3.2.2 Vehicle Gravitational Loads

For the reduced flexible vehicle equations, Equation (2.52f), $\underline{T}_{\text{grav}}$ and $\underline{f}_{\text{grav}}$ are a column of $\underline{f}_{\text{grav}_s}$ ($s=1, \dots, n-1$) and a $3n-3 \times 1$ column of zeros, respectively. For the translational total vehicle equations, Equation (2.61), $\underline{F}_{\text{grav}}$ is the sum of all $\underline{f}_{\text{grav}_s}$ ($s=1, \dots, n$):

$$\underline{F}_{\text{grav}} = \left(\underline{E}(3) \right)_n^T \underline{f}_{\text{grav}} \quad (2.152)$$

where $\underline{f}_{\text{grav}}$ is a $3n \times 1$ column matrix of all $\underline{f}_{\text{grav}_s}$. The total vehicle equations were developed with respect to the vehicle center-of-mass. Therefore, $\underline{T}_{\text{grav}}$ is zero.

2.3.2.3 Quasi-static Gravitational Loads

For the reduced quasi-static flexible vehicle equations, Equation (2.68b), the quasi-static assumptions defined in Paragraph 2.2, Equation (2.63), are imposed upon the n-1 column matrix of Equation (2.151):

$$\bar{f}_{\text{grav}_0} = \bar{H}_T (\theta_0)^{n-1} \bar{g}' \quad (2.153)$$

where \bar{g}' is a 3n-3x1 column matrix of g .

For the quasi-static total vehicle equations, Equation (2.69), the quasi-static assumptions are imposed upon Equation (2.152):

$$F_{\text{grav}_0} = (E(3))^n \bar{H}_T (\theta_0)^n \bar{g}' \quad (2.154)$$

where g' is a 3n x 1 column matrix of g .

2.3.2.4 Perturbation Gravitational Loads

For the reduced perturbation flexible vehicle equations, Equation (2.76e), the perturbation assumptions defined in Paragraph 2.2, Equation (2.64), are imposed upon the n-1 column matrix of Equation (2.151):

$$\Delta \bar{f}_{\text{grav}} = \bar{H}_T (\Delta \theta \theta_0)^{n-1} \bar{g}' - \bar{f}_{\text{grav}_0} = -\bar{H}_T (\Delta \bar{\Gamma} \theta_0)^{n-1} \bar{g}' \quad (2.155)$$

where the final equality makes use of Equation (2.74) which expresses $\Delta \theta$ as an approximate linear function of $\Delta \Gamma$.

For the perturbation total vehicle equations, Equation (2.78), the perturbation assumptions are imposed upon Equation (2.152):

$$\Delta F_{\text{grav}} = (E(3))^n \bar{H}_T (\Delta \theta \theta_0)^n \bar{g}' - F_{\text{grav}_0} = - (E(3))^n \bar{H}_T (\Delta \bar{\Gamma} \theta_0)^n \bar{g}' \quad (2.156)$$

2.4 SPECIAL CASES

In the first part of this section, the results of the previous sections will be examined under rigid body assumptions and compared to the rigid body stability derivatives. In the second part of this section a simple test case is evaluated to illustrate the use and significance of the hybrid-coordinate dynamic equations of motion.

2.4.1 Rigid Body Stability and Control Dynamics

2.4.1.1 Purpose

The purpose of this section is to demonstrate that the hybrid-coordinate dynamic equations summarized in Paragraph 2.1 will yield the classical special cases when the corresponding additional assumptions are applied. Specifically, the aircraft will be assumed rigid. The flexible vehicle equations will be shown to yield the total vehicle equations under this assumption. Then the resulting simplified total vehicle equations will be compared with those found in Reference 8.

2.4.1.2 Rigid Body Hybrid-Coordinate Equations

The aircraft is assumed to be rigid. This implies that the stiffness matrix, K_A , is infinite and that the aircraft does not deform (i.e. q is zero). This also implies that C_S is unity. With q zero, the right-hand side of the complete flexible vehicle equations, Equation (2.44c), is equated to zero and solved for the externally applied loads, f and t :

$$\begin{Bmatrix} f \\ t \end{Bmatrix} = \begin{Bmatrix} M_T \left[\left(\hat{\Theta} \right)^n \ddot{X}' + \left(\hat{\omega} + \hat{\omega}\hat{\omega} \right)^n (R' + r') \right] \\ M_R \dot{\omega}' + \left(\hat{\omega} \right)^n M_R \omega' \end{Bmatrix} \quad (2.157)$$

Likewise, the complete total vehicle equations, Equations (2.45) and (2.46), are also greatly simplified:

$$F = M_A \ddot{\Theta X} \quad (2.158)$$

and:

$$\begin{aligned}
 T &= \left(E(3) \right)^n \left\{ M_T \left[-\ddot{\omega} \left(R^T + r_S^T \right) \omega + \dot{\omega} \left(R^T + r_S^T \right) - \left(R + r_S \right) \dot{\omega}^T \right]^n \left(R' + r' \right) + M_R \dot{\omega}' + \left(\ddot{\omega} \right)^n M_R \omega' \right\} \\
 &= \left(\bar{E}(3) \right)^n \left\{ L_{V_T} + L_{V_R} \right\} = \{ \underline{b} \} \cdot \frac{d}{dt} \left(\underline{I} \cdot \omega \right) \quad (2.159)
 \end{aligned}$$

With q equal to zero there remains only six unknowns (X and ω) in $6n+6$ equations. It can be shown that Equation (2.157) is contained in Equations (2.158) and (2.159) by summing the flexible vehicle loads for all rigid sub-bodies to obtain the resultant total vehicle loads. The total vehicle force is f pre-multiplied by the pi operator:

$$\begin{aligned}
 F &= \left(E(3) \right)^n f \\
 &= \left(E(3) \right)^n M_T \left[\left(\Theta \right)^n \ddot{X}' + \left(\ddot{\omega} + \ddot{\omega} \right)^n \left(R' + r' \right) \right]
 \end{aligned}$$

The second term contains the sum of the first mass moments of each rigid sub-body about the vehicle center of mass and hence is zero. The first term is the sum of all mass pre-multiplying the total vehicle acceleration. Therefore

$$F = \left(E(3) \right)^n M_T (\Theta \ddot{X})' = M_A \Theta \ddot{X} \quad (2.160)$$

The total vehicle torque, T , is the sum of t and f weighted by its moment arm, $R+r_S$, pre-multiplied by the pi operator, thus,

$$\begin{aligned}
T &= (\mathbf{E}(3))^{\mathbb{H}_n^T} \left\{ \left[(\mathbf{R} + \mathbf{r}_S) \right]^{\mathbb{H}_n} \dot{\mathbf{f}} + \mathbf{t} \right\} \\
&= (\mathbf{E}(3))^{\mathbb{H}_n^T} \left\{ \left[(\mathbf{R} + \mathbf{r}_S) \right]^{\mathbb{H}_n} \mathbf{M}_T \left[(\Theta) \ddot{\mathbf{X}}' + (\tilde{\omega} + \tilde{\omega} \tilde{\omega})^{\mathbb{H}_n} (\mathbf{R}' + \mathbf{r}') \right] + \mathbf{M}_R \dot{\omega}' + (\tilde{\omega})^{\mathbb{H}_n} \mathbf{M}_R \omega' \right\} \\
&= (\mathbf{E}(3))^{\mathbb{H}_n^T} \left\{ \mathbf{M}_T \left[-\tilde{\omega} (\mathbf{R} + \mathbf{r}_S) \omega^{\mathbb{T}} + \dot{\omega} (\mathbf{R}^{\mathbb{T}} + \mathbf{r}_S^{\mathbb{T}}) - (\mathbf{R} + \mathbf{r}_S) \dot{\omega}^{\mathbb{T}} \right]^{\mathbb{H}_n} (\mathbf{R}' + \mathbf{r}') + \mathbf{M}_R \dot{\omega}' + (\tilde{\omega})^{\mathbb{H}_n} \mathbf{M}_R \omega' \right\} \\
&= (\mathbf{E}(3))^{\mathbb{H}_n^T} \left\{ \mathbf{L}_{V_T} + \mathbf{L}_{V_R} \right\} \tag{2.161}
\end{aligned}$$

In the above equation, getting from the second line to the third line is done by noting that: the $\Theta \mathbf{X}$ term is a constant post-multiplying the sum of the first mass moment of inertia for each rigid sub-body about the vehicle center of mass, which is zero; and the next two ω terms make use of the following skew-symmetric matrix identities:

$$\begin{aligned}
\tilde{\mathbf{v}} \tilde{\mathbf{v}} \mathbf{v} &= -(\tilde{\mathbf{v}} \mathbf{v}) \mathbf{v} = - \left(\begin{bmatrix} 0 & -w_3 & w_2 \\ w_3 & 0 & -w_1 \\ -w_2 & w_1 & 0 \end{bmatrix} \begin{Bmatrix} v_1 \\ v_2 \\ v_3 \end{Bmatrix} \right) \begin{Bmatrix} v_1 \\ v_2 \\ v_3 \end{Bmatrix} = - \begin{Bmatrix} -w_3 v_2 + w_2 v_3 \\ w_3 v_1 - w_1 v_3 \\ -w_2 v_1 + w_1 v_2 \end{Bmatrix} \begin{Bmatrix} v_1 \\ v_2 \\ v_3 \end{Bmatrix} \\
&= - \begin{bmatrix} 0 & w_2 v_1 + w_1 v_2 & w_3 v_1 + w_1 v_3 \\ -w_2 v_1 + w_1 v_2 & 0 & w_3 v_2 + w_2 v_3 \\ -w_3 v_1 + w_1 v_3 & -w_3 v_2 + w_2 v_3 & 0 \end{bmatrix} \begin{Bmatrix} v_1 \\ v_2 \\ v_3 \end{Bmatrix} \\
&= \left(\begin{bmatrix} w_1 v_1 & w_1 v_2 & w_1 v_3 \\ w_2 v_1 & w_2 v_2 & w_2 v_3 \\ w_3 v_1 & w_3 v_2 & w_3 v_3 \end{bmatrix} - \begin{bmatrix} w_1 v_1 & w_2 v_1 & w_3 v_1 \\ w_1 v_2 & w_2 v_2 & w_3 v_2 \\ w_1 v_3 & w_2 v_3 & w_3 v_3 \end{bmatrix} \right) \begin{Bmatrix} v_1 \\ v_2 \\ v_3 \end{Bmatrix} = (\mathbf{w} \mathbf{v}^{\mathbb{T}} - \mathbf{v} \mathbf{w}^{\mathbb{T}}) \mathbf{v} \tag{2.162}
\end{aligned}$$

and:

$$\begin{aligned}
(\tilde{\mathbf{v}} \tilde{\mathbf{v}} \tilde{\mathbf{v}}) \mathbf{v} &= \begin{bmatrix} 0 & -v_3 & v_2 \\ v_3 & 0 & -v_1 \\ -v_2 & v_1 & 0 \end{bmatrix} \begin{bmatrix} 0 & -w_3 & w_2 \\ w_3 & 0 & -w_1 \\ -w_2 & w_1 & 0 \end{bmatrix} \begin{bmatrix} 0 & -w_3 & w_2 \\ w_3 & 0 & -w_1 \\ -w_2 & w_1 & 0 \end{bmatrix} \begin{Bmatrix} v_1 \\ v_2 \\ v_3 \end{Bmatrix} \\
&= \begin{Bmatrix} v_1 v_2 w_1 w_3 - v_1 v_3 w_1 w_2 + v_2 v_2 w_2 w_3 - v_2 v_3 w_2 w_2 + v_2 v_3 w_3 w_3 - v_3 v_3 w_2 w_1 \\ -v_1 v_1 w_1 w_3 + v_1 v_3 w_1 w_1 - v_1 v_2 w_2 w_3 + v_2 v_3 w_1 w_2 - v_1 v_2 w_3 w_3 + v_1 v_3 w_3 w_1 \\ v_1 v_1 w_1 w_2 - v_1 v_2 w_1 w_1 + v_1 v_2 w_2 w_2 - v_2 v_2 w_1 w_2 + v_1 v_3 w_2 w_3 - v_2 v_3 w_1 w_1 \end{Bmatrix} \\
&= \{w_1 \ w_2 \ w_3\} \begin{Bmatrix} v_1 \\ v_2 \\ v_3 \end{Bmatrix} \begin{bmatrix} 0 & -w_3 & w_2 \\ w_3 & 0 & -w_1 \\ -w_2 & w_1 & 0 \end{bmatrix} \begin{Bmatrix} v_1 \\ v_2 \\ v_3 \end{Bmatrix} = \mathbf{w}^{\mathbb{T}} \tilde{\mathbf{v}} \tilde{\mathbf{v}} \mathbf{v} \tag{2.163}
\end{aligned}$$

2.4.1.3 Comparison of Results with Classical Development

The results of Equations (2.160) and (2.161) can be compared to other published results by appropriately renaming variables. Figure 2-14 shows the variable notation used in Reference 7. These variables are defined relative to a body fixed axis; $\{b\}$. Velocity components are U , V , and W ; first time derivative of \underline{X} resolved in the $\{b\}$ reference frame:

$$\theta \dot{\underline{X}} = \begin{Bmatrix} U \\ V \\ W \end{Bmatrix} \quad \text{therefore:} \quad \theta \ddot{\underline{X}} = \begin{Bmatrix} \frac{dU}{dt} \\ \frac{dV}{dt} \\ \frac{dW}{dt} \end{Bmatrix} \quad (2.164)$$

Forces acting at the vehicle center of mass are described as ΣF_s , where s is x , y , and z ; total vehicle force, F :

$$F = \begin{Bmatrix} \Sigma F_x \\ \Sigma F_y \\ \Sigma F_z \end{Bmatrix} \quad (2.165)$$

The total vehicle mass is m ; M_A . This mass multiplied by the vehicle acceleration, Equation (2.164), equals the vehicle force, Equation (2.165):

$$F = \begin{Bmatrix} \Sigma F_x = m \frac{dU}{dt} \\ \Sigma F_y = m \frac{dV}{dt} \\ \Sigma F_z = m \frac{dW}{dt} \end{Bmatrix} = M_A \theta \ddot{\underline{X}} \quad (2.166)$$

The same procedure is repeated to confirm the comparison of the total vehicle rotational equations. Rotational velocity components are P , Q , and R ; ω . The inertial dyadic elements are identified as I_{jk} , where j and k are x , y , and z . Thus:

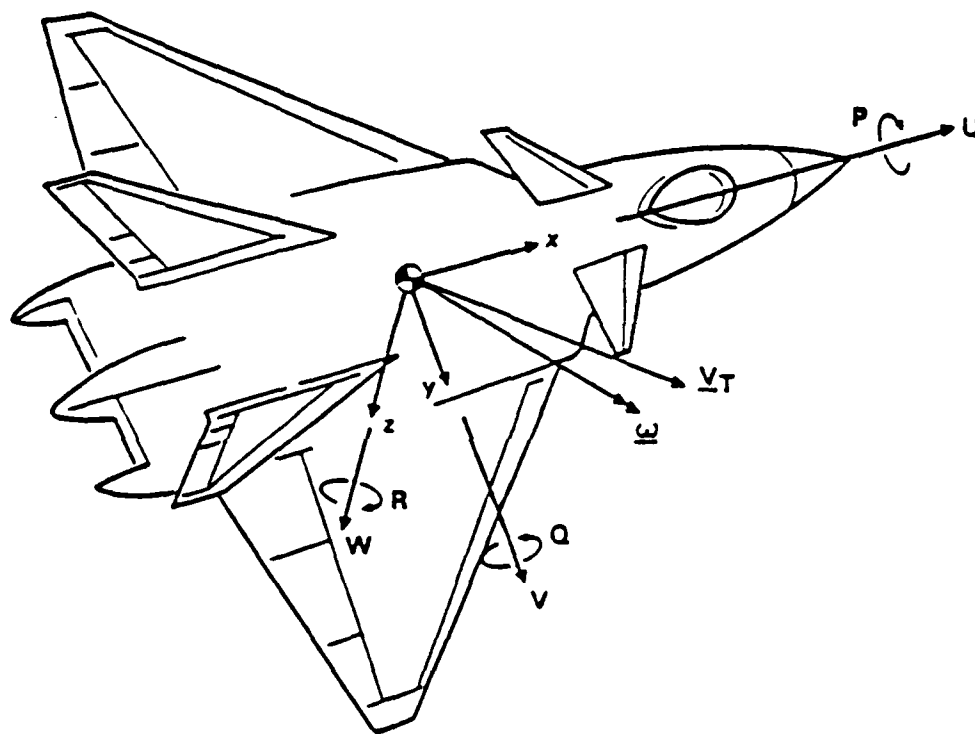


Figure 2-14. Rigid Aircraft Coordinates

$$\mathbf{I} \cdot \boldsymbol{\omega} = \begin{bmatrix} I_{xx} & -I_{xy} & -I_{xz} \\ -I_{yx} & I_{yy} & -I_{yz} \\ -I_{zx} & -I_{zy} & I_{zz} \end{bmatrix} \begin{Bmatrix} P \\ Q \\ R \end{Bmatrix} \quad (2.167)$$

Component torques acting at the vehicle center of mass are L, M, and N; total vehicle torque, T becomes:

$$\mathbf{T} = \begin{Bmatrix} \sum L \\ \sum M \\ \sum N \end{Bmatrix} \quad (2.168)$$

The time derivative of Equation (2.167) is equal to Equation (2.168):

$$\mathbf{T} = \begin{Bmatrix} \sum L = \dot{P}I_{xx} + P\dot{I}_{xx} - \dot{Q}I_{xy} - Q\dot{I}_{xy} - \dot{R}I_{xz} - R\dot{I}_{xz} \\ \sum M = \dot{Q}I_{yy} + Q\dot{I}_{yy} - \dot{R}I_{yz} - R\dot{I}_{yz} - \dot{P}I_{xy} - P\dot{I}_{xy} \\ \sum N = \dot{R}I_{zz} + R\dot{I}_{zz} - \dot{P}I_{xz} - P\dot{I}_{xz} - \dot{Q}I_{yz} - Q\dot{I}_{yz} \end{Bmatrix} = \frac{d}{dt} (\mathbf{I} \cdot \boldsymbol{\omega}) \quad (2.169)$$

Thus, it has been shown that the hybrid-coordinate dynamic equations for flexible aircraft reduce to the classical dynamic equations for a rigid body. Equations (2.166) and (2.169) are called the Euler equations of motion of the aircraft. Quod erat demonstrandum.

2.4.2 Simple Test Case

2.4.2.1 Purpose

The purpose of this section is to use a simple test case to demonstrate that the hybrid-coordinate dynamic equations do produce the same results as those derived relative to a Newtonian reference frame. The model being considered is one dimensional with four lump masses (See Figure 2.15). Body B is one of the center sub-bodies and is massless. The coordinate immediately

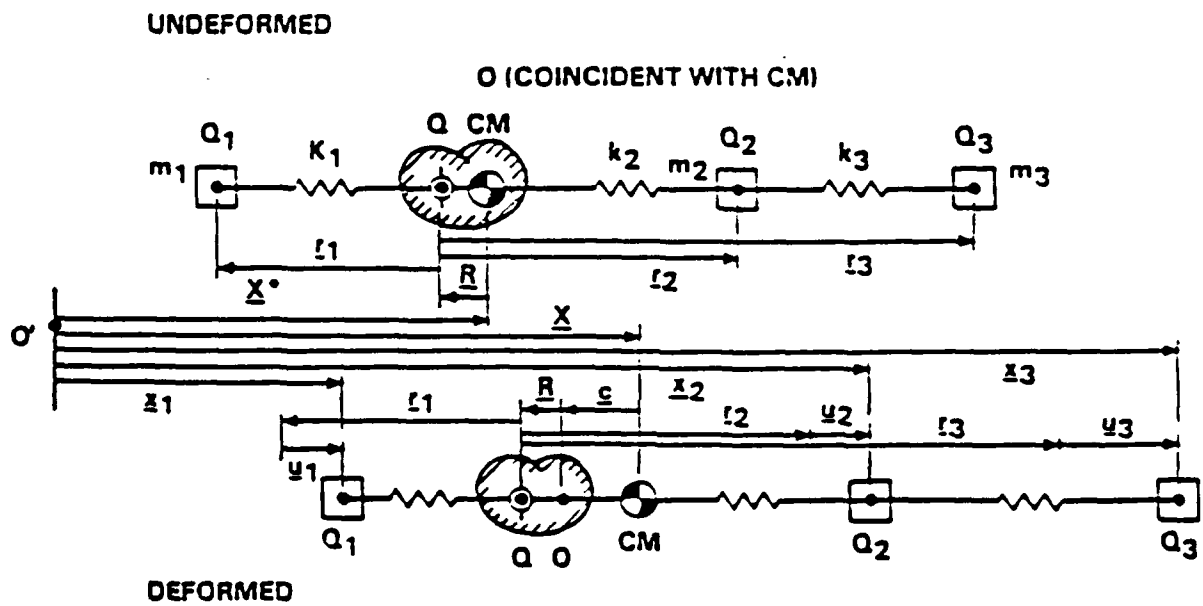


Figure 2-15. One-Dimensional Three-Mass Model

beneath the model in Figure 2-15 correspond to hybrid-coordinates, while the lower coordinates refer to inertial-coordinates. This model has only four degrees of freedom: u_1 , u_2 , u_3 , and X . For simplicity, this model has no structural damping; that is, D is zero. Also, the stiffness matrix will consist of the linear springs connecting only the neighboring sub-bodies as illustrated in Figure 2-15.

2.4.2.2 Hybrid-Coordinate Dynamic Equations Approach

The reduced flexible vehicle equations, Equation (2.52), are of dimension two; a one less the number of unknown deformations (this being only a linear problem). For this example u_2 will be resolved into the remaining degrees-of-freedom according to Equation (2.43). The independent degrees-of-freedom of Equation (2.52) become:

$$\bar{q} = \bar{u} = \begin{Bmatrix} u_1 \\ u_3 \end{Bmatrix}, \quad (2.170)$$

the dependant degrees-of-freedom become:

$$q_n = u_n = u_2, \quad (2.171)$$

and the coefficients become:

$$\bar{N} = N_{uu} + N_{uu_n} K_{u_n \bar{u}}, \quad (2.172)$$

where N is M , G , K , and A . Also:

$$\bar{L} = L_{\bar{u}} = \begin{Bmatrix} F_1 \\ F_3 \end{Bmatrix} \quad (2.173)$$

The stiffness matrix in the second term in Equation (2.172), $K_{u_n \bar{u}}$, is defined in Equation (2.47). For this example, Equation (2.47) is equivalent to Equation (2.43), which is short hand notation of Equation (2.38) where u_B is set to zero and solved for u_n . The elements of the stiffness matrix in Equation (2.38) are defined in Equation (2.37) which contains the free-free stiffness matrix of the vehicle, K_A :

$$\mathbf{L}_A = \begin{Bmatrix} F_1 \\ F_3 \\ F_2 \\ F_B \end{Bmatrix} = \begin{bmatrix} -k_1 & 0 & 0 & k_1 \\ 0 & -k_3 & k_3 & 0 \\ 0 & k_3 & -k_2 - k_3 & k_2 \\ k_1 & 0 & -k_2 & -k_1 - k_2 \end{bmatrix} \begin{Bmatrix} u_1 \\ u_3 \\ u_2 \\ u_B \end{Bmatrix} = \begin{bmatrix} K_{Lq} & K_{Lq} u_B \\ K_{FBq} & K_{FB} u_B \end{bmatrix} \begin{Bmatrix} q \\ u_B \end{Bmatrix} \quad (2.174)$$

The lower partition of Equation (2.174) is set equal to zero and solved for u_B :

$$u_B = -K_{FB}^{-1} K_{FBq} q = \frac{1}{k_1 + k_2} \begin{bmatrix} k_1 & 0 & k_2 \end{bmatrix} \begin{Bmatrix} u_1 \\ u_3 \\ u_2 \end{Bmatrix} \quad (2.175)$$

It is now apparent that the motion of m_3 can not be resolved in terms of the other degrees-of-freedom using this hybrid-coordinate method: m_3 is not being directly connected to Point Q. u_B is defined as zero for the hybrid-coordinate equations, thus u_1 can be expressed as a function of u_2 , or vice-versa:

$$q_n = u_2 = \begin{bmatrix} -k_1 & | & 0 \\ k_2 & | & 0 \end{bmatrix} \begin{Bmatrix} u_1 \\ u_3 \end{Bmatrix} = K_{un} \bar{u} \quad (2.176)$$

K_{un} as defined in Equation (2.176) is substituted into Equation (2.172). The reduced coefficient matrices, \mathbf{N} , are found as follows: the elements of \mathbf{H} are defined in Equation (2.48a):

$$\begin{aligned} \mathbf{H}_{uu} &= \bar{\mathbf{H}}_T \left[\mathbf{E}(2) - \frac{1}{M_A} (\mathbf{E}(1))^T \bar{\mathbf{H}}_T \right] \\ &= \begin{bmatrix} m_1 & 0 \\ 0 & m_3 \end{bmatrix} \left\{ \begin{bmatrix} 1 & 0 \\ 0 & 1 \end{bmatrix} - \frac{1}{m_1 + m_2 + m_3} \begin{bmatrix} 1 & 1 \\ 1 & 1 \end{bmatrix} \begin{bmatrix} m_1 & 0 \\ 0 & m_3 \end{bmatrix} \right\} \\ &= \frac{1}{m_1 + m_2 + m_3} \begin{bmatrix} m_1 m_2 + m_1 m_3 & -m_1 m_3 \\ -m_1 m_3 & m_1 m_3 + m_2 m_3 \end{bmatrix} \quad (2.177a) \end{aligned}$$

and:

$$\begin{aligned}
 M_{uu_n} &= -\frac{1}{M_A} \bar{M}_T (E(1)) \bar{I}_2 m_n \\
 &= -\frac{1}{m_1+m_2+m_3} \begin{bmatrix} m_1 & 0 \\ 0 & m_3 \end{bmatrix} \begin{bmatrix} 1 \\ 1 \end{bmatrix} m_2 \\
 &= -\frac{1}{m_1+m_2+m_3} \begin{bmatrix} m_1 m_2 \\ m_2 m_3 \end{bmatrix} \quad (2.177b)
 \end{aligned}$$

Similarly, the elements of \bar{G} are defined in Equation (2.49a); however, this is a linear problem with no rotation: ω is zero. Therefore, \bar{G} is zero. The same reasoning applies to \bar{A} being zero (See Equation (2.50a)). The appropriate elements for \bar{K} are extracted from the definition of K , Equation (2.39), which for this problem is found by setting F_B in Equation (2.174) to zero, solving for u_B as a function of q , Equation (2.176), and substituting back into Equation (2.174) to express the remaining loads as a function of q only:

$$\begin{aligned}
 L &= \begin{bmatrix} K_{Lq} & -K_{Lq} u_B & K_{F_B}^{-1} & K_{F_B} q \end{bmatrix} q = Kq \\
 &= \begin{bmatrix} -k_1 & 0 & 0 \\ 0 & -k_3 & k_3 \\ 0 & k_3 & -k_2 - k_3 \end{bmatrix} \begin{bmatrix} k_1 \\ 0 \\ k_2 \end{bmatrix} \begin{bmatrix} 1 \\ k_1+k_2 \end{bmatrix} \begin{bmatrix} k_1 & 0 & k_2 \end{bmatrix} \begin{Bmatrix} u_1 \\ u_3 \\ u_2 \end{Bmatrix} \\
 &= \frac{1}{k_1+k_2} \begin{bmatrix} -k_1 k_2 & 0 & k_1 k_2 \\ 0 & -k_1 k_3 - k_2 k_3 & -k_1 k_3 + k_2 k_3 \\ k_1 k_2 & k_1 k_3 + k_2 k_3 & -k_1 k_2 - k_1 k_3 - k_2 k_3 \end{bmatrix} \begin{Bmatrix} u_1 \\ u_3 \\ u_2 \end{Bmatrix} = \begin{bmatrix} K_{uu} & K_{uu_n} \\ K_{u_n u} & K_{u_n u_n} \end{bmatrix} q \quad (2.178)
 \end{aligned}$$

On the right hand side of Equation (2.52f) is $L_{\bar{u}}$, which is defined in Equation (2.51). For this one-dimensional example θ is unity. Equation (2.52f) becomes:

$$L_{\bar{u}} = -\bar{M} \ddot{X}' + \bar{F} = -\begin{Bmatrix} m_1 \ddot{X} \\ m_3 \ddot{X} \end{Bmatrix} + \begin{Bmatrix} F_1 \\ F_2 \end{Bmatrix} \quad (2.179)$$

The preceding development is substituted into Equation (2.52) to yield the reduced flexible vehicle equations for this model:

$$\frac{1}{m_1+m_2+m_3} \begin{bmatrix} m_1 m_2 + m_1 m_3 + m_1 m_2 \frac{k_1}{k_2} & -m_1 m_3 \\ -m_1 m_3 + m_2 m_3 \frac{k_1}{k_2} & m_1 m_3 + m_2 m_3 \end{bmatrix} \begin{Bmatrix} \ddot{u}_1 \\ \ddot{u}_3 \end{Bmatrix} - \frac{1}{k_1+k_2} \begin{bmatrix} k_1 k_1 + k_1 k_2 & 0 \\ \left(1 + \frac{k_1}{k_2}\right) k_1 k_3 & k_1 k_3 + k_2 k_3 \end{bmatrix} \begin{Bmatrix} u_1 \\ u_3 \end{Bmatrix} = - \begin{Bmatrix} m_1 \ddot{X} \\ m_3 \ddot{X} \end{Bmatrix} + \begin{Bmatrix} F_1 \\ F_3 \end{Bmatrix} \quad (2.180)$$

The reduced total vehicle equations, Equation (2.61), are of dimension one; the number of total vehicle degrees-of-freedom relative to the inertial reference frame (this being only a linear problem). For this example, Equation (2.60) becomes:

$$M_A \ddot{\Theta X} = (m_1 + m_2 + m_3) \ddot{X} = F_1 + F_2 + F_3 = F \quad (2.181)$$

Equations (2.180) and (2.181) are now combined into the three dimensional equation :

$$\frac{1}{m_1+m_2+m_3} \begin{bmatrix} m_1 m_2 + m_1 m_3 + m_1 m_2 \frac{k_1}{k_2} & -m_1 m_3 & (m_1+m_2+m_3)m_1 \\ -m_1 m_3 + m_2 m_3 \frac{k_1}{k_2} & m_1 m_3 + m_2 m_3 & (m_1+m_2+m_3)m_3 \\ 0 & 0 & (m_1+m_2+m_3)^2 \end{bmatrix} \begin{Bmatrix} \ddot{u}_1 \\ \ddot{u}_3 \\ \ddot{X} \end{Bmatrix} - \frac{1}{k_1+k_2} \begin{bmatrix} k_1 k_1 + k_1 k_2 & 0 & 0 \\ \left(1 + \frac{k_1}{k_2}\right) k_1 k_3 & k_1 k_3 + k_2 k_3 & 0 \\ 0 & 0 & 0 \end{bmatrix} \begin{Bmatrix} u_1 \\ u_3 \\ X \end{Bmatrix} = \begin{Bmatrix} F_1 \\ F_3 \\ F_1 + F_2 + F_3 \end{Bmatrix} \quad (2.182)$$

2.4.2.3 Newtonian Physics Approach

In this section the Newton-Euler dynamic equations of motion (See Equation (2.18)) is applied to the same one-dimensional three lumped mass model. This time, all motion will be expressed relative to the inertially fixed Point 0'. A free body equation is written for the translation of each rigid sub-body:

$$\text{For } m_1: \quad F_1 - k_{eq}(x_1 - x_1^*) + k_{eq}(x_2 - x_2^*) = m_1 \ddot{x}_1 \quad (2.183a)$$

$$\text{For } m_2: \quad F_2 + k_{eq}(x_1 - x_1^*) - (k_{eq} + k_3)(x_2 - x_2^*) + k_3(x_3 - x_3^*) = m_2 \ddot{x}_2 \quad (2.183b)$$

$$\text{For } m_3: \quad F_3 + k_3(x_2 - x_2^*) - k_3(x_3 - x_3^*) = m_3 \ddot{x}_3 \quad (2.183c)$$

where a superscript asterisk indicates the initial ($t=0$) position of the rigid sub-bodies, and the equivalent spring constant, k_{eq} , is expressed in terms of k_1 and k_2 by the series spring formulation:

$$\frac{1}{k_{eq}} = \frac{1}{k_1} + \frac{1}{k_2} \quad (2.184)$$

This implies:

$$k_{eq} = \frac{k_1 k_2}{k_1 + k_2} \quad (2.185)$$

Equation (2.185) is substituted into Equations (2.183a) and (2.183b). All Equations (2.183) are then combined into a single matrix equation of dimension three, expressed in terms of x_1 , x_2 , and x_3 :

$$\begin{bmatrix} m_1 & 0 & 0 \\ 0 & m_2 & 0 \\ 0 & 0 & m_3 \end{bmatrix} \begin{Bmatrix} \ddot{x}_1 \\ \ddot{x}_2 \\ \ddot{x}_3 \end{Bmatrix} + \begin{bmatrix} \frac{k_1 k_2}{k_1 + k_2} & -\frac{k_1 k_2}{k_1 + k_2} & 0 \\ -\frac{k_1 k_2}{k_1 + k_2} & \frac{k_1 k_2}{k_1 + k_2} + k_3 & -k_3 \\ 0 & -k_3 & k_3 \end{bmatrix} \begin{Bmatrix} x_1 - x_1^* \\ x_2 - x_2^* \\ x_3 - x_3^* \end{Bmatrix} = \begin{Bmatrix} F_1 \\ F_2 \\ F_3 \end{Bmatrix} \quad (2.186)$$

The results in Equation (2.186) may seem simpler than those obtained in Equation (2.182). However, each of the three modes of vibration obtained from these results will contain a weighted portion of the total vehicle motion and both flexible modes; whereas, the hybrid-coordinate dynamic equations yield these three modes directly. In the case of free vibration ($F_1 = F_2 = F_3 = 0$) Equation (2.186) may be reduced to two equations in two unknowns, say x_1 and x_3 . The coordinate x_2 is found in terms of x_1 and x_3 by using the Newton-Euler equation for the total vehicle:

$$m_1 x_1 + m_2 x_2 + m_3 x_3 = 0 \quad (2.187)$$

or:

$$x_2 = - \frac{m_1 x_1 + m_3 x_3}{m_2} \quad (2.188)$$

Equation (2.188) is substituted into the first and third partitions of Equation (2.186), which is then rewritten so as to be expressed as a function of x_1 and x_3 :

$$\begin{bmatrix} m_1 & 0 \\ 0 & m_3 \end{bmatrix} \begin{Bmatrix} \ddot{x}_1 \\ \ddot{x}_3 \end{Bmatrix} + \begin{bmatrix} -\frac{k_1 k_2}{k_1 + k_2} \left(1 + \frac{m_1}{m_2}\right) & -\frac{k_1 k_2 m_3}{(k_1 + k_2) m_2} \\ -k_3 \frac{m_1}{m_2} & -k_3 \left(1 + \frac{m_3}{m_2}\right) \end{bmatrix} \begin{Bmatrix} x_1 - x_1^* \\ x_3 - x_1^* \end{Bmatrix} = \begin{Bmatrix} 0 \\ 0 \end{Bmatrix} \quad (2.189)$$

2.4.2.4 Comparison of Results

Finally, in this section the results of the previous two sections will be compared. Specifically, Equation (2.189) will be shown to yield exactly Equation (2.181) by making the appropriate transformation of variables (x_1 and x_3 to u_1 and u_3). From Figure 2-15, the vector addition relating the two sets of variables is:

$$\begin{Bmatrix} x_1 \\ x_2 \\ x_3 \end{Bmatrix} = \begin{Bmatrix} X - R - c - r_1 + u_1 \\ X - R - c + r_2 + u_2 \\ X - R - c + r_3 + u_3 \end{Bmatrix} \quad \text{also} \quad \begin{Bmatrix} x_1^* \\ x_2^* \\ x_3^* \end{Bmatrix} = \begin{Bmatrix} X^* - R - r_1 \\ X^* - R + r_2 \\ X^* - R + r_3 \end{Bmatrix} \quad (2.190)$$

The definition for c in terms of u_g is in Equation (2.19). For this test case, Equation (2.19) yields (also, making use of Equation (2.176)):

$$c = \frac{1}{M_A} \left(m_1 u_1 - m_2 \frac{k_1}{k_2} u_1 + m_3 u_3 \right) \quad (2.191)$$

For the case of free vibration, $X = X^*$ and time derivatives of X are zero. Equation (2.191) is substituted into Equation (2.190), which is then substituted into Equation (2.189) to yield:

$$\begin{aligned}
& \begin{bmatrix} m_1 & 0 \\ 0 & m_3 \end{bmatrix} \begin{Bmatrix} \ddot{u}_1 - \frac{1}{M_A} (m_1 \ddot{u}_1 - m_2 \frac{k_1}{k_2} \ddot{u}_1 + m_3 \ddot{u}_3) \\ \ddot{u}_3 - \frac{1}{M_A} (m_1 \ddot{u}_1 - m_2 \frac{k_1}{k_2} \ddot{u}_1 + m_3 \ddot{u}_3) \end{Bmatrix} \\
& + \begin{bmatrix} -\frac{k_1 k_2}{k_1 + k_2} \left(1 + \frac{m_1}{m_2}\right) & -\frac{k_1 k_2 m_3}{(k_1 + k_2) m_2} \\ -k_3 \frac{m_1}{m_2} & -k_3 \left(1 + \frac{m_3}{m_2}\right) \end{bmatrix} \begin{Bmatrix} u_1 - \frac{1}{M_A} (m_1 u_1 - m_2 \frac{k_1}{k_2} u_1 + m_3 u_3) \\ u_3 - \frac{1}{M_A} (m_1 u_1 - m_2 \frac{k_1}{k_2} u_1 + m_3 u_3) \end{Bmatrix} = \begin{Bmatrix} 0 \\ 0 \end{Bmatrix} \quad (2.192)
\end{aligned}$$

which, upon regrouping, becomes:

$$\frac{1}{m_1 + m_2 + m_3} \begin{bmatrix} m_1 m_2 + m_1 m_3 + m_1 m_2 \frac{k_1}{k_2} & -m_1 m_3 \\ -m_1 m_3 + m_2 m_3 \frac{k_1}{k_2} & m_1 m_3 + m_2 m_3 \end{bmatrix} \begin{Bmatrix} \ddot{u}_1 \\ \ddot{u}_3 \end{Bmatrix} - \frac{1}{k_1 + k_2} \begin{bmatrix} k_1 k_1 + k_1 k_2 & 0 \\ \left(1 + \frac{k_1}{k_2}\right) k_1 k_3 & k_1 k_3 + k_2 k_3 \end{bmatrix} \begin{Bmatrix} u_1 \\ u_3 \end{Bmatrix} = \begin{Bmatrix} 0 \\ 0 \end{Bmatrix} \quad (2.193)$$

This is exactly the results obtained by using the Hybrid-coordinate dynamic equations approach, Equation (2.180), for the free vibration case. Quod erat demonstrandum.

2.5 SUMMARY

2.5.1 Review of Assumptions

The aircraft, Body A, is composed of finite rigid sub-bodies, A_s , that are inter-connected by linearly elastic members. Therefore, the deflection of any of these elastic members yields a restoring force that is proportional only to the corresponding deflection (K is constant). Thus q is limited to deflections which do not produce any cross-coupling stiffness effects due to the geometry changes.

The aircraft, Body A, is attached to a massless Body B for all six degrees of freedom at one Point O. The sum of the loads at O is zero. This auxiliary relationship is used to define the stiffness matrix of the flexible aircraft. Prior to deformation, when u_s and β_s are zero, the origin of Body B, Point O, is coincident with the vehicle mass center: therefore, q is initially zero.

The overall matrix equations of motion, Equations (2.62) and (2.113), are written in terms of the sub-body deformations. However, the coefficients of these equations are in terms of the overall vehicle motion (ω , Ω^a , and X) and the direction cosine matrices (Θ , C , and C_S); all of which are also unknown (mostly a function of q). Thus, $3n+9$ additional auxiliary equations are required to uniquely describe the matrix equations of motion.

2.5.2 Review of Hybrid-Coordinate Dynamic Equations Development

The work by P. W. Likins for flexible spacecraft was rederived for an aircraft of arbitrary configuration undergoing an arbitrary maneuver using a hybrid-coordinate system. Vector bases are defined relative to an inertially fixed reference frame, the vehicle, and each rigid sub-body. Direction cosine matrices are defined describing the rotation of the vector bases to each other. Vehicle deformation is defined by the motion of the rigid sub-bodies relative to the vehicle center of mass. The motion of each sub-body is described as a series of vectors which are resolved relative to the appropriate vector bases.

Special operators are defined to facilitate the matrix algebra necessary in using a hybrid-coordinate system. Translational vehicle deformation is considered first. The motion of the vehicle mass center relative to the massless body reference point is described in terms of the rigid sub-body translational deformations. Separate Newton-Euler equations of motion are written for translation and rotation for each rigid sub-body in terms of the hybrid-coordinates. The resulting equations are combined into two sets of $3n$ equations, which are then written as one matrix equation of order $6n$. The Newton-Euler equations are then developed for the vehicle, which yields two sets of three equations each; for translation and rotation.

These $6n+6$ equations have $9n+15$ unknowns. Auxiliary equations are developed to uniquely specify the problem. $6n$ equations describe the n sub-body direction cosines matrices as a function of the sub-body's rotational deformation. Six more equations result from the vehicle's rotation: three associated with defining the direction cosine matrix and three defining

rotational as a function of rotational velocity. For a free-free vehicle, the vehicle stiffness matrix allows the motion of the massless Body B to be described in terms of the deformation variables. This allows the deformation variables to be reduced to $6n-6$. The remaining three degrees-of-freedom result from the choice of hybrid-coordinates: The vector base associated with the massless body is defined to always be coincident with the vehicle vector base.

2.5.3 Linearization of Hybrid-Coordinate Dynamic Equations

All time dependent variables are assumed to be composed of quasi-static and perturbation components. The quasi-static component allows for large amplitude, but slowly time varying deformations. The perturbation component allows for small amplitude rapid fluctuations about the quasi-static solution.

All variables are expressed in terms of their quasi-static and perturbation components. The resulting equations are expanded. All purely quasi-static terms are collected into a set of quasi-static equations. All first order perturbation terms are collected into a set of perturbation equations. All higher order perturbation terms are assumed negligible. The resulting quasi-static equations are non-linear zero order (with respect to time). The resulting perturbation equation is linear second order (with respect to the perturbation variables).

2.5.4 Inclusion of Aerodynamic and Gravitational Loads

For the aerodynamic loads, a deformable panel method is assumed that allows for large vehicle deformation. The deformation of the panels is a function of the deformation of rigid sub-bodies. Aerodynamic loads are assumed to act normal to the panel surface at the panel load points and are a function of the angle-of-attack at the panel normal wash points. The specific relationship between load and angle-of-attack is beyond the scope of this report. A vector base is defined at each load point and each normal wash point. The orientation of these vector bases relative to the vehicle's vector base is derived as a function of the vehicle deformation. The angle-of-attack is defined as the angle between the relative velocity and the plane of the panel at the normal wash point.

The results are linearized using the same procedure before. The perturbation components are highly non-linear. To facilitate the description of the perturbation angle-of-attack, an additional vector base is defined that has one base coincident with the quasi-static relative velocity, and one base remaining in the plane of the panel. Perturbation aerodynamic loads become a linear function of the perturbation angle-of-attack, which become a linear function of the perturbation relative velocity, which become a linear function of the structural deformations.

Since gravitational acceleration acts in a constant direction with respect to the inertial vector base, gravitational loads are directly implemented into the hybrid-coordinate dynamic equations.

2.5.5 Special Cases

The hybrid-coordinate dynamic equations summarized in Paragraph 2.1 are evaluated under the assumption of a rigid vehicle. It was shown that for a rigid vehicle, the flexible vehicle equations reduce to the total vehicle equations. The resulting total vehicle equations were then compared to a classical derivation reference publication by simply renaming variables appropriately. This showed that the results are identical.

A simple one-dimensional three lumped mass model was evaluated. This provided a more tangible perspective on the application of the hybrid-coordinate dynamic equations, and particularly on the variable reduction. Equations of motion were derived for the same model using inertial position vectors. The two results were compared: most notably, the hybrid-coordinate approach results in the total vehicle equations being separated from the flexible modes, whereas the latter approach does not. By implementing a variable transformation, the two approaches were shown to be equivalent. nonlinear with respect to the unknowns.

SECTION 3
DERIVATION OF EQUATIONS OF MOTION AND
STABILITY DERIVATIVES FOR A FLEXIBLE AIRCRAFT VEHICLE

3.1 INTRODUCTION

This Section presents the development of the maneuvering and control equations from first principles. The derivation is based on ASE modeling methodology for the stability and control analysis of a flexible airplane that includes the synthesis of active control systems. In Section 2, Likins' method was used to derive these equations and is not used any further.

The stability and control equations are derived by defining the translation and rotation of an axis system relative to the inertial reference frame. The structural deformations and rigid body perturbations are defined relative to the inertial reference frame as well. The equations are categorized as follows:

- Maneuvering Equations - These equations relate the total aerodynamic forces and moments, including the force of gravity, to the overall motion of the airplane relative to the inertial reference frame. The flexibility effects, that account for the effect of a maneuver load alleviation system, are included.
- Stability Equations - These equations describe the rigid-body perturbations of the airplane relative to the inertial reference frame. The development of the equations covers stability augmentation, flutter suppression, gust load alleviation, and ride quality aspects. The resulting equations are developed further to the extent that "small angles" assumption is no longer valid.

3.2 RIGID BODY EQUATIONS OF MOTION

The six degrees of freedom equations of motion, that provide a time history of a rigid airplane during maneuvers, are developed.

Force Equation:

$$\underline{F} = m \frac{d \underline{V}}{dt} \quad (3.1)$$

Moment Equation:

$$\underline{T} = \frac{d}{dt} \underline{H} \quad (3.2)$$

where \underline{V} is the aircraft inertial velocity, \underline{H} is the inertial angular momentum, and m is aircraft mass. It is implicit in the above equations that the force, F , the moment, T , and the time derivatives are all expressed in the inertial reference system, the ground system in our case. It is impractical nor desirable to use that reference system for simulations. Experience has shown that six degrees-of-freedom aircraft simulation can be much simplified by solving the above equations in the body axes system.

In the following, it is shown how the force equation is derived further to be useful for simulation purposes. This derivation makes extensive use of the Ground, Body, Stability, and Wind axes systems, and therefore vectors in these systems will be subscribed with G, B, S, and W respectively. The definitions of the axes systems and the transformations from system to another are given in Section 1 of this report.

The R.H.S. of Equation (3.1) represents the total force, F ; the vector sum of the gravity force, the aerodynamic force, and the propulsive force. These forces, expressed in the proper reference systems, are:

Gravity Force:

$$\underline{F}_g = (0, 0, mg)_G \quad (3.3a)$$

Aerodynamic Force:

$$\underline{F}_A = (F_i, F_j, F_k)_S \quad (3.3b)$$

Propulsive Force:

$$\underline{F}_P = (P_x, P_y, P_z)_B \quad (3.3c)$$

The transformation matrices from axes system x to axes system y will be denoted by T_{xy} . Hence,

$$T_{SB} = [A] = \begin{bmatrix} \cos\alpha & 0 & \sin\alpha \\ 0 & 1 & 0 \\ \sin\alpha & 0 & \cos\alpha \end{bmatrix} \quad (3.4a)$$

$$T_{WS} = [B] = \begin{bmatrix} \cos\beta & -\sin\beta & 0 \\ \sin\beta & \cos\beta & 0 \\ 0 & 0 & 1 \end{bmatrix} \quad (3.4b)$$

$$T_{GB} = [T] = \begin{bmatrix} \cos\theta \cos\psi & \cos\theta \sin\psi & -\sin\theta \\ \cos\psi \sin\phi \sin\theta & \cos\psi \cos\phi & \cos\theta \sin\phi \\ -\cos\phi \sin\psi & +\sin\psi \sin\phi \sin\theta & \\ \sin\phi \sin\psi & -\cos\psi \sin\phi & \cos\theta \cos\phi \\ +\cos\phi \cos\psi \sin\theta & +\sin\psi \cos\phi \sin\theta & \end{bmatrix} \quad (3.4c)$$

will denote the transformation matrices from Stability to Body, Wind to Stability, and Ground to Body axes systems, respectively. In the above equations, α is the angle of attack between the Stability axis and the Body axis system, β is the sideslip angle of the Wind axis to the Stability axis, and ϕ, θ, ψ are the Euler angles between Body and Ground axes systems.

Since the Body axes system is adopted for deriving the force equation, then

$$\underline{F} = T_{GB} \underline{F}_G + T_{SB} \underline{F}_A + \underline{F}_P$$

Substituting from Equations (3.3) and (3.4) in the above equation gives

$$\underline{F} = \begin{bmatrix} T_{31} \\ T_{32} \\ T_{33} \end{bmatrix} mg + [A] \begin{bmatrix} F_i \\ F_j \\ F_k \end{bmatrix} + \begin{bmatrix} P_x \\ P_y \\ P_z \end{bmatrix} \quad (3.5)$$

where T_{31} , T_{32} , and T_{33} are the components of the third column of T_{GB} in Equation (3.4c).

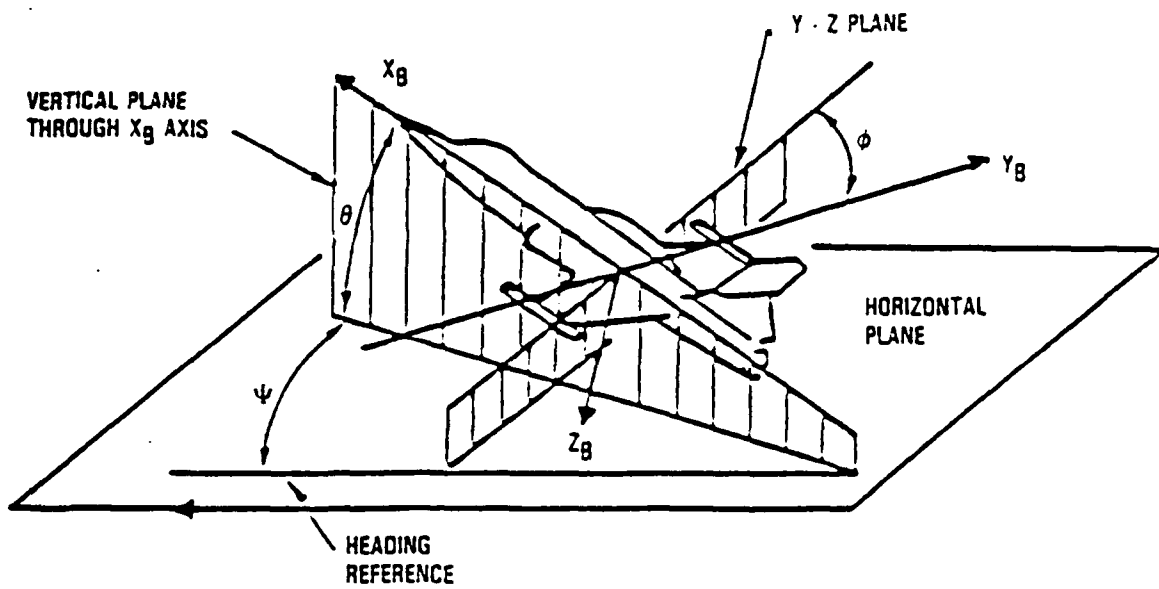


Figure 3-1. Definition of Euler Angles

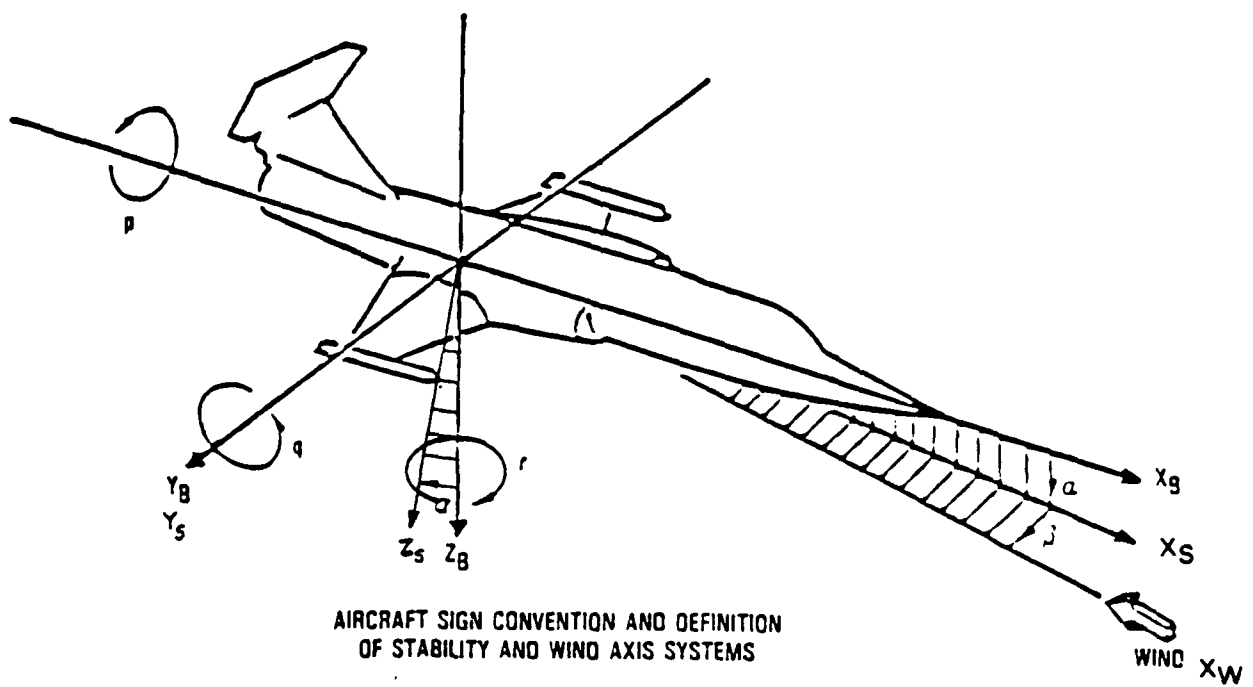


Figure 3-2. Axis Systems

Now, the L.H.S. of Equation (3.1) is proportional to the time derivative of the aircraft velocity relative to ground. Since aerodynamic loads are proportional to the aircraft velocity relative to the wind, $\underline{V}_{A/W}$, the velocity relative to the ground is decomposed into,

$$\underline{V}_{A/G} = \underline{V}_{A/W} + \underline{V}_{W/G} \quad (3.6)$$

where $\underline{V}_{W/G}$ is the wind velocity relative to the ground. Hence the time derivatives of both sides of Equation (3.6) is given by,

$$\frac{G_d}{dt} \underline{V}_{A/G}_B = \frac{G_d}{dt} \underline{V}_{A/W}_B + \frac{G_d}{dt} \underline{V}_{W/G}_B$$

where the subscript B is indicative of evaluation of the above terms in the Body axes system (for consistency with the force terms). Now,

$$\frac{G_d}{dt} \underline{V}_{A/W}_B = \frac{B_d}{dt} \underline{V}_{A/W}_B + \underline{\omega} \times \underline{V}_{A/W}_B$$

and

$$\frac{G_d}{dt} \underline{V}_{W/G}_B = T_{GB} \underline{\dot{V}}_{W/G} = \begin{bmatrix} \dot{v}_x \\ \dot{v}_y \\ \dot{v}_z \end{bmatrix}$$

where $\underline{\omega} = (p, q, r)$. But,

$$\frac{B_d}{dt} \underline{V}_{A/W}_B = \frac{B_d}{dt} [A] [B] \underline{V}_{A/W}_W = \frac{B_d}{dt} [A] [B] \begin{bmatrix} V \\ 0 \\ 0 \end{bmatrix}$$

This implies that,

$$\begin{aligned} \frac{B_d}{dt} \underline{V}_{A/W}_B &= \frac{d}{dt} \begin{bmatrix} V \cos \alpha \cos \beta \\ V \sin \beta \\ V \sin \alpha \cos \beta \end{bmatrix} \\ &= \dot{V} \begin{bmatrix} \cos \alpha \cos \beta \\ \sin \beta \\ \sin \alpha \cos \beta \end{bmatrix} + V \begin{bmatrix} -\sin \alpha \cos \beta \dot{\alpha} - \cos \alpha \sin \beta \dot{\beta} \\ \cos \beta \dot{\beta} \\ \cos \alpha \cos \beta \dot{\alpha} - \sin \alpha \sin \beta \dot{\beta} \end{bmatrix} \end{aligned}$$

Combining the above equations yields

$$\frac{d}{dt} \frac{V_{A/G}}{B} = \begin{bmatrix} \cos\alpha\cos\beta & -\sin\alpha\cos\beta & -\cos\alpha\sin\beta \\ \sin\beta & 0 & \cos\beta \\ \sin\alpha\cos\beta & \cos\alpha\cos\beta & -\sin\alpha\sin\beta \end{bmatrix} \begin{bmatrix} \dot{V} \\ V\dot{\alpha} \\ V\dot{\beta} \end{bmatrix} + \begin{bmatrix} \dot{v}_x \\ \dot{v}_y \\ \dot{v}_z \end{bmatrix} + V \begin{bmatrix} q\sin\alpha\cos\beta - r\sin\beta \\ r\cos\alpha\cos\beta - p\sin\alpha\cos\beta \\ p\sin\beta - q\cos\alpha\cos\beta \end{bmatrix} \quad (3.7)$$

In the above equations $\dot{v}_x, \dot{v}_y, \dot{v}_z$ are the components of wind acceleration in the Body axes system, V is the aircraft speed relative to wind. Equating the R.H.S.'s of Equations (3.5) and (3.7) and premultiplying both sides by the inverse of the 3x3 matrix in the later equation gives,

$$\begin{aligned} \dot{V} = & (T_{13} g + \frac{P_x}{m} - \dot{v}_x)\cos\alpha \cos\beta + (T_{23} g + \frac{P_y}{m} - \dot{v}_y)\sin\beta \\ & + (T_{33} g + \frac{P_z}{m} - \dot{v}_z)\sin\alpha \cos\beta + \frac{1}{m}(F_i \cos\beta + F_j \sin\beta) \end{aligned} \quad (3.8a)$$

$$\begin{aligned} \dot{\beta} = & \frac{1}{V} \left\{ (-T_{13} g - \frac{P_x}{m} + \dot{v}_x)\cos\alpha \sin\beta + (T_{23} g + \frac{P_y}{m} - \dot{v}_y)\cos\beta \right. \\ & \left. - (T_{33} g + \frac{P_z}{m} - \dot{v}_z)\sin\alpha \sin\beta + \frac{1}{m}(-F_i \sin\beta + F_j \cos\beta) \right\} - (r\cos\alpha - p\sin\alpha) \end{aligned} \quad (3.8b)$$

$$\begin{aligned} \dot{\alpha} = & \frac{1}{V\cos\beta} \left\{ -(T_{13} g + \frac{P_x}{m} - \dot{v}_x)\sin\alpha + (T_{33} g + \frac{P_z}{m} - \dot{v}_z)\cos\alpha + \frac{F_k}{m} \right\} \\ & - (r\sin\alpha + p\cos\alpha)\tan\beta + q \end{aligned} \quad (3.8c)$$

In body axes system, the Moment Equation (3.2) becomes:

$$\underline{T} = I \underline{\dot{\omega}} + \underline{\omega} \times (I\underline{\omega})$$

where,

$$I = \begin{bmatrix} I_{xx} & -I_{xy} & -I_{xz} \\ -I_{xy} & I_{yy} & -I_{yz} \\ -I_{xz} & -I_{yz} & I_{zz} \end{bmatrix}$$

is the moment of inertia matrix; I_{xx}, I_{yy}, I_{zz} are the mass moment of inertia about the longitudinal, lateral, and normal axes respectively, and I_{xy}, I_{yz}, I_{xz} are the products of inertia. Expanding the moment equation results in:

$$L = I_{xx}\dot{p} - I_{xz}\dot{r} + (I_{zz}-I_{yy})qr - I_{xz}pq + I_{xy}(\dot{q} - pr) - I_{yz}(q^2 - r^2) \quad (3.9a)$$

$$M = I_{yy}\dot{q} - (I_{zz}-I_{xx})pr + I_{xz}(p^2 - r^2) - I_{xy}(\dot{p} + qr) - I_{yz}(\dot{r} - pq) \quad (3.9b)$$

$$N = I_{zz}\dot{r} - I_{xz}\dot{p} + (I_{yy}-I_{xx})pq + I_{xz}qr - I_{xy}(p^2 - q^2) - I_{yz}(\dot{q} + pr) \quad (3.9c)$$

where L, M, and N are the sum of the external moments about the x, y, and z body axes respectively.

Equations (3.8) and (3.9) fully describe the motion of a rigid airplane in the six degrees of freedom system. Simplified sets of reduced degree of freedom equations can be readily obtained from these six equations.

3.3 LONGITUDINAL EQUATIONS OF MOTION

The longitudinal equations of motion are obtained from the six-degrees of freedom equations by setting all lateral and directional components to zero. The resulting equations are as follows:

$$\dot{V} = (T_{13} g + \frac{P_x}{m} - \dot{v}_x)\cos\alpha + (T_{33} g + \frac{P_z}{m} - \dot{v}_z)\sin\alpha + \frac{F_i}{m} \quad (3.10a)$$

$$\dot{\alpha} = \frac{1}{V} \left(-(T_{13} g + \frac{P_x}{m} - \dot{v}_x)\sin\alpha + (T_{33} g + \frac{P_z}{m} - \dot{v}_z)\cos\alpha + \frac{F_k}{m} \right) + q \quad (3.10b)$$

$$M_{cg} = I_{yy}\dot{q} \quad (3.10c)$$

$$\dot{\beta} = 0 ; \text{ and } L = N = 0$$

3.4 AERODYNAMIC FORCES AND MOMENTS

In Equations (3.10), the aerodynamic lift and drag forces, F_k , and, F_i and pitching moment, M_{cg} , have been, traditionally, expressed in nondimensional terms, i.e.,

$$F_i = - \bar{q} S C_{DT} \quad (3.11a)$$

$$F_k = - \bar{q} S C_{LT} \quad (3.11b)$$

$$M_{cg} = \bar{q} S \bar{c} C_{mT} \quad (3.11c)$$

where C_{DT} , C_{LT} , C_{mT} are the total drag, total lift, and total pitching moment coefficients, \bar{q} is the dynamic pressure, S is the surface area, and \bar{c} is the mean aerodynamic chord. The parameters that influence those aerodynamic coefficients are discussed in the following.

The total drag coefficient is expressed as,

$$C_{DT} = (C_D)_\alpha + (\Delta C_D)_{cg} + (\Delta C_D)_{\delta SP} + (\Delta C_D)_h$$

where $(C_D)_\alpha$, $(\Delta C_D)_{cg}$, $(\Delta C_D)_{\delta SP}$, $(\Delta C_D)_h$, are the drag coefficients due to angle of attack, α , trim correction for center of gravity shift from $\bar{c}/4$, spoiler deflections and, the Reynold Number correction for profile drag, respectively. These coefficients are determined as follows,

$$(C_D)_\alpha = C_D @ C_{LBasic}$$

$$C_{LBasic} = (C_L)_\alpha + (C_L)_{\delta H} + (C_L)_{\delta e}$$

$$(C_D)_{\delta SP} = \sum_{i=1}^n C_{D\delta SP_i} \delta SP_i$$

$$(\Delta C_D)_h = (30,000 - h) 4.5 \cdot 10^{-8}$$

The variables that influence the total lift coefficient are angle of attack, α , the horizontal stabilizer deflection, δH , the elevator deflection, δe , the pitch rate, q , the angle of attack rate, $\dot{\alpha}$, the pitch angular acceleration, \dot{q} , the normal load factor, n_z , and the spoiler deflections, δSP .

The normal load, n_z , is the load component along the normal axis of the aircraft body normalized by the aircraft weight. Equivalently, n_z is the projection of the sum of the aircraft acceleration and the gravity vector along the normal body axis normalized by the gravity constant. It can be determined from Equations (3.5) and (3.7) that,

$$n_z = -(\sin\alpha\cos\beta\dot{V} + \cos\alpha\cos\beta V\dot{\alpha} - \sin\alpha\sin\beta V\dot{\beta} + (p\sin\beta - q\cos\alpha\cos\beta)V + \dot{v}_z)/g + T_{33} \quad (3.12)$$

The total lift coefficient, C_{LT} , is expressed as,

$$C_{LT} = (C_L)_{\alpha} + (C_L)_{\delta H} + (C_L)_{\delta e} + (C_L)_q + (\Delta C_L)_{\delta SP} + (C_L)_{\dot{\alpha}} + (C_L)_{\dot{q}} + (C_L)_{n_z}$$

For small perturbations in the aforementioned parameters, the total lift coefficient is represented as

$$C_{LT} = C_{L1} + C_{L2} \frac{\bar{c}\dot{\alpha}}{2V} + C_{L3}\dot{q} - C_{L4}n_z$$

where,

$$C_{L1} = f(\alpha, \delta H, \delta e, q, \delta SP)$$

$$C_{L2} = \partial C_L / \partial (\bar{c}\dot{\alpha}/2V)$$

$$C_{L3} = \partial C_L / \partial \dot{q}$$

$$C_{L4} = \partial C_L / \partial n_z$$

Similarly, the total moment coefficient is represented as,

$$C_{mT} = C_{m1} + C_{m2} \frac{\bar{c}\dot{\alpha}}{2V} + C_{m3}\dot{q} - C_{m4}n_z$$

$$C_{m1} = f(\alpha, \delta H, \delta e, q, \delta SP)$$

$$C_{m2} = \partial C_m / \partial (\bar{c} \dot{\alpha} / 2V)$$

$$C_{m3} = \partial C_m / \partial \dot{q}$$

$$C_{m4} = \partial C_m / \partial nz$$

For detailed derivation of C_{LT} , C_{DT} and, C_{mT} , refer to Appendix C.

Considering the longitudinal motion ($\beta=0$), the normal load factor, nz , from Equation (3.12) is given by,

$$nz = nz_1 + nz_2 \dot{\alpha}$$

where

$$nz_1 = (-\dot{V} \sin \alpha + V q \cos \alpha + T_{33} g - \dot{v}_z) / g$$

$$nz_2 = -\dot{V} \cos \alpha / g$$

Now, the aerodynamic lift and moment equations (about the c.g.) become,

$$F_k = -\bar{q} S \left[C_{L1} + \left(\frac{\bar{c}}{2V} C_{L2} - C_{L4} nz_2 \right) \dot{\alpha} + C_{L3} \dot{q} - C_{L4} nz_1 \right] \quad (3.13)$$

$$M_{cg} = \bar{q} S \bar{c} \left[C_{m1} + \left(\frac{\bar{c}}{2V} C_{m2} - C_{m4} nz_2 \right) \dot{\alpha} + C_{m3} \dot{q} - C_{m4} nz_1 \right] \\ - F_k \bar{c} XZCG1 - F_i \bar{c} XZCG2 + MP \quad (3.14)$$

where,

$$XZCG1 = \left[\cos \alpha (x_{cg} - x_{REF}) + \sin \alpha (WL_{cg} - WL_{REF}) \right] / \bar{c}$$

$$XZCG2 = \left[\sin \alpha (x_{cg} - x_{REF}) - \cos \alpha (WL_{cg} - WL_{REF}) \right] / \bar{c}$$

MP = Moment due to thrust about the center of gravity (c.g.)

x_{cg} = The fuselage station (F.S.) at the c.g. of the aircraft

WL_{cg} = The waterline (W.L.) at the aircraft c.g.

X_{REF} = The F.S. at wing MAC
 WL_{REF} = The W.L. at wing MAC

The wing a.c. $XZCG1$ and $XZCG2$ represent the moment transfer arms that account for the changes in aerodynamic moments resulting from the forces determined at a moment reference point other than the aircraft center of gravity.

The sign convention here is such that the distance x is positive aft and WL is positive up. Figure 3-3 depicts the distances used in the above equation.

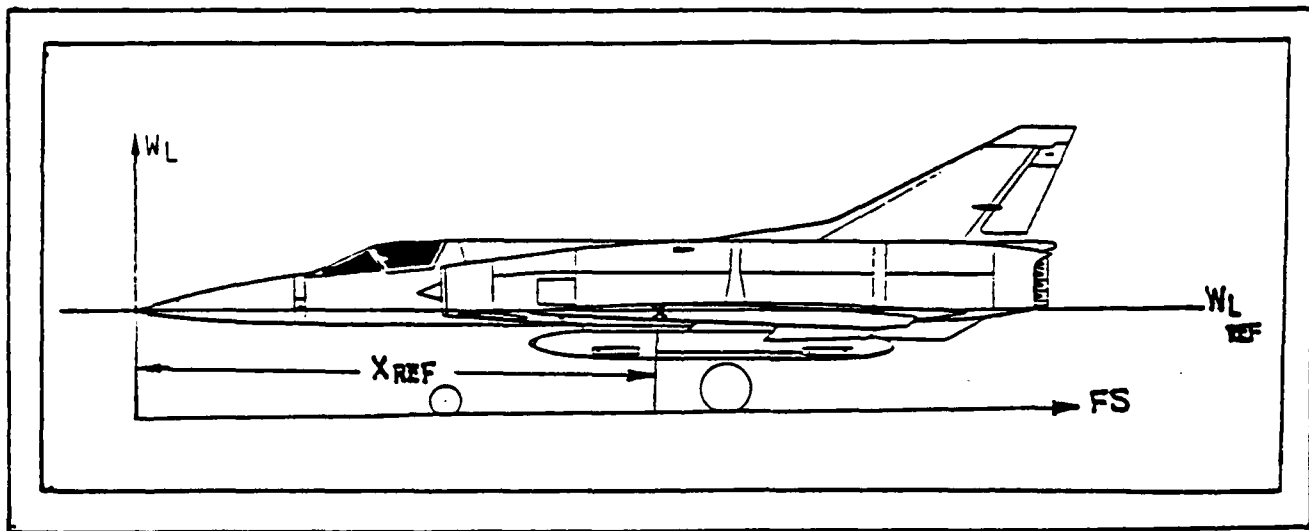


Figure 3-3. Explanation of Distances Appearing in the Longitudinal Equations

3.4.1 Solution of the Equations of Motion for $\dot{\alpha}$

The CSMP 90 computer graphics programs used for the time history analysis initiates solutions of the equations of motion by performing solutions for α and q at discrete intervals of time. Substituting for F_k from Equation (3.13) into Equation (3.10b) gives,

$$\begin{aligned}\dot{\alpha} = & \frac{1}{V} \left((-T_{13} \sin\alpha + T_{33} \cos\alpha) g + (\dot{v}_x \sin\alpha - \dot{v}_z \cos\alpha) \right. \\ & \left. + \frac{1}{m} [P_z \cos\alpha - P_x \sin\alpha + \bar{q} S (C_{L1} - C_{L4} n_{z1})] \right) \\ & + \frac{\bar{q} S}{m V} \left(\frac{\bar{c}}{2V} C_{L2} - C_{L4} n_{z2} \right) \dot{\alpha} + \frac{\bar{q} S}{m V} C_{L3} \dot{q} + q\end{aligned}$$

and rearranging yields,

$$\dot{\alpha} = (A_3 + A_2 \dot{q}) / A_1 \quad (3.15)$$

Where:

$$A_1 = 1.0 - \frac{\bar{q} S}{m V} \left(\frac{\bar{c}}{2V} C_{L2} - C_{L4} n_{z2} \right)$$

$$A_2 = \frac{\bar{q} S}{m V} C_{L3}$$

$$\begin{aligned}A_3 = & \frac{1}{V} \left\{ (-T_{13} \sin\alpha + T_{33} \cos\alpha) g + (\dot{v}_x \sin\alpha - \dot{v}_z \cos\alpha) \right. \\ & \left. + \frac{1}{m} [P_z \cos\alpha - P_x \sin\alpha + \bar{q} S (C_{L1} - C_{L4} n_{z1})] \right\} + q\end{aligned}$$

3.4.2 Solutions of the Equations of Motion for \dot{q}

The second phase of the solution of the longitudinal equations of motion is solving for the moment equation. Substituting for M_{cg} from Equation (3.10c) and F_k from Equation (3.13) into Equation (3.14) gives,

$$\begin{aligned}I_{yy} \dot{q} = & \bar{q} S \bar{c} \left[C_{m1} + \left(\frac{\bar{c}}{2V} C_{m2} - C_{m4} n_{z2} \right) \dot{\alpha} + C_{m3} \dot{q} - C_{m4} n_{z1} \right] + \bar{q} S \bar{c} C_{DT} XZCG2 \\ & + \bar{q} S \bar{c} \left[C_{L1} + \left(\frac{\bar{c}}{2V} C_{L2} - C_{L4} n_{z2} \right) \dot{\alpha} + C_{L3} \dot{q} - C_{L4} n_{z1} \right] XZCG1 + MP\end{aligned}$$

and rearranging yields,

$$\dot{q} = (M_3 - M_2 \dot{\alpha}) / M_1 \quad (3.16)$$

Where,

$$M_1 = I_{yy} - \bar{q} S \bar{c} (C_{m3} + C_{L3} XZCG1)$$

$$M_2 = -\bar{q} S \bar{c} \left[\frac{\bar{c}}{2V} C_{m2} - C_{m4} nz_2 + \left(\frac{\bar{c}}{2V} C_{L2} - C_{L4} nz_2 \right) XZCG1 \right]$$

$$M_3 = \bar{q} S \bar{c} [C_{m1} - C_{m4} nz_1 + (C_{L1} - C_{L4} nz_1) XZCG1 + C_{DT} XZCG2] + MP$$

From Equations (3.15) and (3.16) $\dot{\alpha}$ and \dot{q} can now be determined completely

3.5 AERODYNAMIC DERIVATIVES OF A FLEXIBLE AIRPLANE

3.5.1 Inertial Reference Axis

The aerodynamic derivatives for a flexible airplane are defined relative to an inertial reference axis. Definition of the inertial reference axis is essential.

The concept of an inertial reference system is illustrated for airplane flight in the plane of symmetry, omitting considerations of the fore-and-aft degree of freedom. The airplane is assumed to be flattened into the x-y plane to more easily demonstrate the principle. Figure 3-4 shows an arbitrary flight condition.

The aerodynamic force and moment, controlling the motion of the inertial reference, and thus the flight path are in coefficient form, Reference (6).

$$C_L = C_{L\alpha}(\alpha - \alpha_0) + C_{L\delta_e} \delta_e + C_{L\dot{\theta}} \frac{\dot{\theta}}{2V} + C_{L\dot{\alpha}} \frac{\dot{\alpha}}{2V} \quad (3.18)$$

$$C_m = C_{m0} + C_{m\alpha}(\alpha - \alpha_0) + C_{m\delta_e} \delta_e + C_{m\dot{\theta}} \frac{\dot{\theta}}{2V} + C_{m\dot{\alpha}} \frac{\dot{\alpha}}{2V} + C_{L\dot{\alpha}} \left(\frac{XZCG1}{V} \right) \frac{\dot{\alpha}}{2V} \quad (3.19)$$

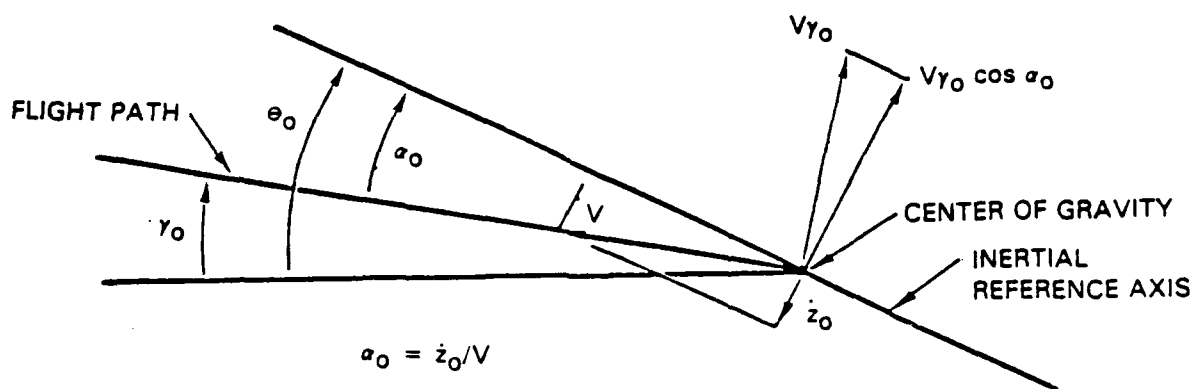


Figure 3-4. Flight in Plane of Symmetry

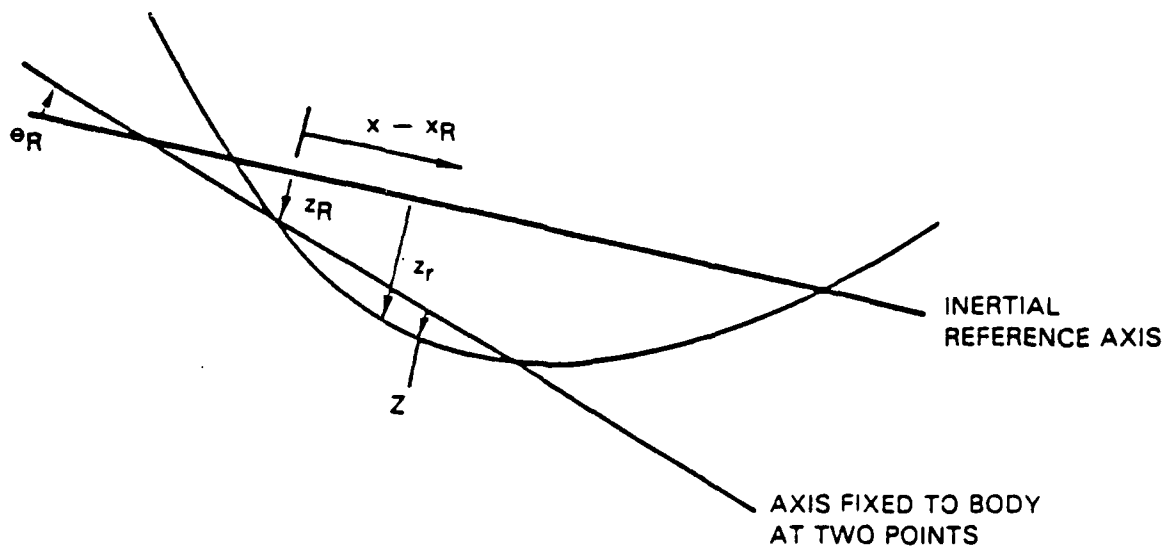


Figure 3-5. Inertial Reference and Body Axis

where α_0 is the angle of attack at zero lift, and δ_e is the longitudinal control surface deflection angle.

The derivatives on the right hand side of the equations must be computed for the flexible airplane. The computer codes used to generate these stability derivatives appear in Appendix D of this report. Figure 3-5 shows the inertial reference axis and an axis fixed to the body. In this figure the position of the body axis relative to the inertial reference is defined by z_R and θ_R . This distinction must be made because the inertial reference is not fixed to any point of the body. If the flexibility of the airplane is defined in terms of structural influence coefficients (flexibility coefficients), a reference fixed to the body in a statically determinate way must be defined. Elastic deformations are defined relative to this reference.

The inertial reference defines the overall motion of the airplane if the following conditions are satisfied:

$$[1] [M] \{z_r\} = 0 \quad (3.20)$$

$$[x-x_0] [M] \{z_r\} = 0 \quad (3.21)$$

where x_0 is the structural influence coefficient reference point, z_r is the displacement relative to the inertial reference axis and $[M]$ is the mass matrix.

These equations imply that the momentum and moment of momentum relative to the inertial axis are zero, thus; the motion of the aircraft in the inertial axis defines the total momentum and moment of momentum of the deforming airplane.

The deformation of the body relative to the inertial axis system, $\{z_r\}$, is defined by the following equation:

$$\{z_r\} = \{1\} z_R + \{x-x_R\} \theta_R + \{z\} \quad (3.22)$$

where $\{z\}$ defines the deformation relative to the body fixed axis. Figure 3-5.

Denoting the aerodynamic forces by $\{Z_a\}$ and the inertial forces by $\{Z_{in}\}$, then the total distributed force is:

$$\{Z\} = \{Z_{in}\} + \{Z_a\} \quad (3.23)$$

The key step in this procedure is that the vertical force and moment equilibrium are imposed before $\{Z_a\}$ is computed. As a result, the equilibrium between aerodynamic, elastic and inertial forces is automatically assured in the final answer. It also follows that the results are only applicable to free flight conditions and hence are not applicable to a supported model in a wind tunnel.

The forces-and-moments equilibrium is determined by the following two equations:

$$0 = [1]\{Z\} = [1]\{Z_{in}\} + [1]\{Z_a\} \quad (3.24)$$

$$0 = [x-x_0]\{Z\} = [x-x_0]\{Z_{in}\} + [x-x_0]\{Z_a\} \quad (3.25)$$

The total distributed force is written in the form:

$$\{Z\} = \left\{ [1] - (1/\bar{M})[M]\{1\}[1] - (1/I_0)[M]\{x-x_0\}[x-x_0] \right\} \{Z_a\} \quad (3.26)$$

where,

$$\bar{M} = [1][M]\{1\}$$

$$I_0 = [x-x_0][M]\{x-x_0\}$$

This equation expresses the total force distribution, in terms of aerodynamic forces, under the assumption of equilibrium between inertia forces and aerodynamic forces.

The aerodynamic forces, $\{Z_a\}$, can be expressed in terms of the dynamic pressure, aerodynamic influence coefficients, $[Q_{Z\alpha}]$, and local angle-of-attack distribution. The local angle of attack is the sum of angle of attack of the inertial reference axis; the built-in (zero load) angle-of-attack distribution $\{\theta_a\}$; an angle-of-attack distribution associated with a control surface deflection; an angle-of-attack distribution due to pitch rate of the reference; and angle-of-attack distribution due to elastic deformation. Aerodynamic lag effects are included by adding an α term, or by higher order approximations derived from unsteady aerodynamic theory.

In order to formulate aerodynamic derivatives that correctly describe the overall motions of the flexible airplane when used in the rigid airplane equations associated with Equations (3.18) and (3.19), the derivatives must be related to the inertial reference axis, and thus to α_0 and θ_0 .

In mathematical terms:

$$\{Z_a\} = \bar{q}[Q_{Z\alpha}]\left\{\{1\}\alpha_0 + \{\theta_a\} + (1/V)(x - x_0)\dot{\theta}_0 + [D_\theta]\{z_r\}\right\} + \bar{q}[Q_{Z\dot{\alpha}}]\{1\}\dot{\alpha}_0 \quad (3.27)$$

In this equation $[D_\theta]$ is a differentiating matrix, that is $[D_\theta]\{z_r\}$ defines the slope in the direction of the free stream. Alternatively, $[D_\theta]_{ij}$ is the streamwise angle of attack at point i due to a unit structural deflection at point j .

The deformation $\{z_r\}$ is given by,

$$\{z_r\} = \{z\} + \{z_\delta\}\delta$$

where $\{z\}$ is the elastic deformation, and $\{z_\delta\}\delta$ is the displacement due to control surface deflection.

Let

$$\begin{aligned}
 [B] &= [1] - \bar{q}[Q_{Z\alpha}] \left\{ (-1/I_{OR}) \{1\} [x - x_0] [M] + [D_\theta] \right\} [E] \quad (3.28) \\
 &\cdot \left\{ [1] - (1/M) [M] \{1\} [1] - (1/I_0) [M] [x - x_0] [x - x_0] \right\} \\
 I_{OR} &= [x - x_0] [M] [x - x_r]
 \end{aligned}$$

where [E] is the square matrix of structural influence coefficients with E_{ij} is the deflection at point i due to a unit load Z applied at point j, i.e.

$$\{z\} = [E]\{Z\}$$

Then it can be shown that:

$$\begin{aligned}
 [B] \{Z_a\} &= \bar{q}[Q_{Z\alpha}] \left\{ (-1/I_{OR}) \{1\} [x - x_0] [M] + [D_\theta] \right\} \{z_\delta\} \delta \\
 &+ \bar{q}[Q_{Z\alpha}] \left\{ \{1\} \alpha_0 + \{\theta_a\} + (1/V) [x - x_0] \dot{\theta}_0 \right\} + \bar{q}[Q_{Z\dot{\alpha}}] \{1\} \dot{\alpha}_0 \quad (3.29)
 \end{aligned}$$

The matrix [B] is constant for a given configuration and Mach number. This implies that all aerodynamic lag is accounted for in $[Q_{Z\alpha}]$. This may not be a valid assumption for fast maneuvers, because the above derivation is based on $[Q_{Z\alpha}]$ being constant.

From Equation (3.29) it follows:

$$\begin{aligned}
 \{Z_a\} &= \bar{q}[B]^{-1} [Q_{Z\alpha}] \left\{ \{1\} \alpha_0 + \{\theta_a\} + (1/V) [x - x_0] \dot{\theta}_0 \right. \\
 &+ \left. \left[(-1/I_{OR}) \{1\} [x - x_0] [M] + [D_\theta] \right] \{z_\delta\} \delta \right\} \\
 &+ \bar{q}[B]^{-1} [Q_{Z\dot{\alpha}}] \{1\} \dot{\alpha}_0 \quad (3.30)
 \end{aligned}$$

The above equation defines the distributed aerodynamic forces on the flexible airplane corresponding to an equilibrium between aerodynamic forces,

elastic forces, gravity forces, and inertial forces in terms of the motion of the inertial reference axis, built-in angle-of-attack distribution and control surface deflections. An implied assumption is that the inertial effects due to z_r can be neglected; that is, $[1][M]\{z_r\}$ and $[x-x_0][M]\{z_r\}$ can be neglected. Equations (3.20) and (3.21) satisfy these assumptions.

From Equation (3.30), all derivatives used in Equations (3.18) and (3.19) can be derived. In addition, the deflections relative to the inertial reference can be determined for any point on the flight path, and, therefore, the total motion of each point on the airplane can be determined. This includes the motion of the pilot seat and the motion of the sensors (acceleration and pitch rate).

The effect of airplane flexibility in the aerodynamic derivatives that determine the out-of-plane-symmetry motion is included in a manner similar to that outlined above. The effect of fore-and-aft force in the derivatives will also be included.

The technique under which the aerodynamic derivatives of the flexible airplane are derived imply that they are valid for use in the usual airplane stability equations, if the first structural frequency is sufficiently above the short period and Dutch roll frequencies. If there is a possibility of the dynamics of airplane flexibility entering into the stability characteristics, the complete dynamics equations of the flexible airplane will be used.

3.6 FLEXIBLE STABILITY DERIVATIVES

A stability derivative is defined as the rate of change of a force coefficient or moment coefficient with respect to some independent variable. The theoretical methods used to obtain the desired stability derivatives are outlined in the following sub-sections using simplified expressions for illustration.

Both rigid and flexible parts of the stability derivatives are determined as functions of dynamic pressure, Mach number and weight case. The flexible

derivatives are calculated in two distinct and independent sets. The distinction between the two is their frame of reference. One set is designated fixed airplane stability derivatives and the other as the free airplane stability derivatives. Although the magnitudes of the individual derivatives are different for each set, when all of the derivatives are applied to a \vec{a} time history problem for one set, the resulting accelerations and velocities versus time are identical to those that result from applying all of the derivatives from the other set to the same problem. A short physical description of the stability derivatives used in this report is given in Appendix A.

Lift and moment coefficients are defined by,

$$C_L = \text{LIFT}/(\bar{q} S_{\text{REF}}) \quad (3.31)$$

$$C_m = \text{MOMENT}/(\bar{q} S_{\text{REF}} \bar{c}) \quad (3.32)$$

$$\text{LIFT} = \sum_{i=1}^m P_i \quad ; \quad \text{MOMENT} = \sum_{i=1}^m P_i \text{ ARM}_i$$

$$\text{ARM}_i = x_{\text{REF}} - x_i \quad (3.33)$$

or in matrix form,

$$\begin{bmatrix} C_L \\ C_m \end{bmatrix} = \begin{bmatrix} k/\bar{q}S & 0 \\ 0 & k/\bar{q}S\bar{c} \end{bmatrix} \begin{bmatrix} [1] \\ [\text{ARM}] \end{bmatrix} \begin{bmatrix} \text{AIC} \end{bmatrix} \{\alpha\} \quad (3.34)$$

Where:

- P_i = The lift acting on the i^{th} panel
- x_{REF} = The F.S. where the wing mean aerodynamic center is located
- x_i = The a.c. of the i^{th} panel
- AIC_{ij} = Incremental lift on panel i due to downwash applied at point j
- k = 1 for full aircraft model
- = 2 for half aircraft model

Aerodynamic influence coefficient (AIC) matrices will be obtained using a number of theoretical aerodynamic programs, such as VORLAX, QUADPAN, FRE. TEAM and TRANSAM.

Higher order derivatives, coupling terms, relating rolling, pitching and yawing moments to aircraft rotational velocities are also considered as illustrated below:

<u>MOMENT</u>	<u>ROTATIONAL VELOCITIES</u>		
	p	q	r
ROLLING MOMENT	C_{l_p}		C_{l_r}
PITCHING MOMENT		C_{m_q}	
YAWING MOMENT	C_{n_p}		C_{n_r}

The total load acting on a balanced flexible airplane is then represented as the summation of rigid and flexible airloads and the inertia loads, that is:

$$[P] = \text{RIGID AIRLOADS} + \text{INERTIA LOADS} + \text{FLEXIBLE AIRLOADS} \quad (3.35)$$

Where:

$$\text{RIGID AIRLOADS} = [\Delta L/Q] = F[\alpha, \delta_{eREF}] \quad (3.36)$$

$$\text{INERTIA LOADS} = [W] = F[n_i, \ddot{\theta}_i] \quad (3.37)$$

$$\text{FLEXIBLE AIRLOADS} = [\Delta P/A] = F[\Delta\alpha_{flex}] \quad (3.38)$$

$$Q = \bar{q} S$$

3.6.1 Longitudinal Stability Derivatives

For the purposes of illustration, derivation of the longitudinal stability derivatives of a rigid airplane with $\alpha = 0$ will be dealt with in the following. Using Equations (3.18) and (3.19),

$$C_{L\alpha}(\alpha - \alpha_0) \bar{q} S + C_{L\delta_e} \delta_e \bar{q} S + C_{L\dot{\theta}} \frac{\dot{\theta}}{2V} \bar{q} S + nz W = 0 \quad (3.39)$$

$$C_{m\alpha}(\alpha - \alpha_0) \bar{q} S \bar{c} + C_{m\delta_e}(\delta_e) \bar{q} S \bar{c} + C_{m\dot{\theta}} \left(\frac{\dot{\theta}}{2V} \right) \bar{q} S \bar{c} + C_{m_0} \bar{q} S \bar{c} - \ddot{\theta} I_0 + nz W (x_{REF} - x_{cg}) = 0 \quad (3.40)$$

where:

$$I_0 = [x - x_0] [M] (x - x_0)$$

and, x_{REF} is the reference point about which the moment coefficients are taken. In this subsection if x_{REF} is taken at x_{cg} then the last term in Equation (3.40) becomes zero.

In matrix form, these equations become,

$$\begin{bmatrix} 1 \\ x_{cg} - x_j \end{bmatrix} \left\{ [A_S] \begin{Bmatrix} 1 \\ \alpha - \alpha_0 \end{Bmatrix} + [A_S] \begin{Bmatrix} \alpha_{\delta_e} \\ \delta_e \end{Bmatrix} + [A_S] \left\{ \frac{x_{cp} - x_{cg}}{\bar{c}/2} \right\} \left(\frac{\dot{\theta}}{2V} \right) + [A_S] \begin{Bmatrix} \alpha_0 \\ nz \end{Bmatrix} + \begin{Bmatrix} W \\ P_{Z:\ddot{\theta}} \end{Bmatrix} \begin{Bmatrix} \ddot{\theta} \end{Bmatrix} \right\} = \begin{Bmatrix} 0 \\ 0 \end{Bmatrix} \quad (3.41)$$

$$C_{L\alpha} = (\bar{q} S / 2)^{-1} \begin{bmatrix} 1 \\ 1 \end{bmatrix} [A_S] \begin{Bmatrix} 1 \\ \alpha \end{Bmatrix} \quad (3.42)$$

$$C_{m\alpha} = (\bar{q} S \bar{c} / 2)^{-1} \begin{bmatrix} 1 \\ x_{cg} - x_j \end{bmatrix} [A_S] \begin{Bmatrix} 1 \\ \alpha \end{Bmatrix} \quad (3.43)$$

where

$$[AIC_S] = .5([AIC] + [AIC]^T)$$

$$[A_S] = [AIC_S] \bar{q}$$

Collecting the terms that multiply $[A_S]$ and defining their sum as the rigid airplane angle of attack distribution yields:

$$\{\alpha_R\} = \begin{Bmatrix} 1 \end{Bmatrix} (\alpha - \alpha_0) + \{\alpha_{\delta_e}\} (\delta_e) + \left\{ \frac{x_{cp} - x_{cg}}{\bar{c} / 2} \right\} \left(\frac{\dot{\theta} \bar{c}}{2V} \right) + \{\alpha_0\} \quad (3.44)$$

3.6.2 Concept of Flexible Longitudinal Stability Derivatives

The incremental change in local panel angle of attack due to airframe flexibility is:

$$[\alpha_e] = [D_\theta] [E_S] \{P_{Z_{NET}}\} \quad (3.45)$$

where,

$$[E_S] = .5([E] + [E]^T)$$

The net vertical panel loads for a flexible airplane are:

$$\{P_{Z_{NET}}\} = [A_S] \{ \{\alpha_R\} + \{\alpha_e\} \} + \{W\} (nz) + \{P_{Z_{\ddot{\theta}}}\} (\ddot{\theta}) \quad (3.46)$$

Substituting for $\{\alpha_e\}$ from Equation (3.45) into Equation (3.46) yields,

$$\left(\begin{bmatrix} 1 \end{bmatrix} - [A_S] [D_\theta] [E_S] \right) \{P_{Z_{NET}}\} = [A_S] \{\alpha_R\} + \{W\} (nz) + \{P_{Z_{\ddot{\theta}}}\} (\ddot{\theta}) \quad (3.47)$$

Let,

$$[D] = \begin{bmatrix} 1 \end{bmatrix} - [A_S] [D_\theta] [E_S] \quad (3.48)$$

Then,

$$\left\{ \begin{matrix} P \\ Z_{NET} \end{matrix} \right\} = [D]^{-1} [A_S] \{ \alpha_R \} + [D]^{-1} \{ W \} (nz) + [D]^{-1} \left\{ \begin{matrix} P \\ Z_{\ddot{\theta}} \end{matrix} \right\} (\ddot{\theta}) \quad (3.49)$$

For steady maneuvers at specified load factors $\ddot{\theta} = 0$ and the $\dot{\theta}$ and nz terms are fixed so that a solution can be obtained for $(\alpha - \alpha_0)$ and (δ_e) such that:

$$\begin{bmatrix} [1] & [] \\ [x_{cg}^{-x}] & [] \end{bmatrix} \left\{ \begin{matrix} P \\ Z_{NET} \end{matrix} \right\} = \left\{ \begin{matrix} 0 \end{matrix} \right\} \quad (3.50)$$

Expanding $\{ \alpha_R \}$ in Equation (3.49), yields:

$$\begin{aligned} \left\{ \begin{matrix} P \\ Z_{NET} \end{matrix} \right\} = & [D^{-1}] [A_S] \{ 1 \} (\alpha - \alpha_0) + [D^{-1}] [A_S] \{ \alpha_0 \} + [D^{-1}] [A_S] \{ \alpha_{\delta_e} \} (\delta_e) \\ & + [D^{-1}] [A_S] \left[\frac{x_{cp} - x_{cg}}{\bar{c}/2} \right] \left(\frac{\dot{\theta} \bar{c}}{2V} \right) + [D^{-1}] \{ W \} (nz) + [D^{-1}] \left\{ \begin{matrix} P \\ Z_{\ddot{\theta}} \end{matrix} \right\} (\ddot{\theta}) \end{aligned} \quad (3.51)$$

Each of the terms in the above equation represents a constant times the parameter for which it is desired to have a flexible stability derivative. Formulation of flexible stability derivatives from this equation are given as follows:

$$C_{L\alpha}^{fixed} = \frac{[1] [D^{-1}] [A_S] \{ 1 \}}{\bar{q}S/2}$$

$$C_{m\alpha}^{fixed} = \frac{[x_{cg}^{-x}] [D^{-1}] [A_S] \{ 1 \}}{\bar{q}\bar{c}S/2}$$

$$C_{L\delta_e}^{fixed} = \frac{[1] [D^{-1}] [A_S] \{ \alpha_{\delta_e} \}}{\bar{q}S/2}$$

$$C_{m\delta_e}^{fixed} = \frac{[x_{cg}^{-x}] [D^{-1}] [A_S] \{ \alpha_{\delta_e} \}}{\bar{q}\bar{c}S/2}$$

$$C_{L\dot{\theta}}^{fixed} = \frac{[1] [D^{-1}] [A_S] \left\{ \frac{x_{cp} - x_{cg}}{\bar{c}/2} \right\}}{\bar{q}S/2}$$

$$C_{m\dot{\theta}}^{fixed} = \frac{[x_{cg}^{-x}] [D^{-1}] [A_S] \left\{ \frac{x_{cp} - x_{cg}}{\bar{c}/2} \right\}}{\bar{q}\bar{c}S/2}$$

$$\alpha_{0 \text{ flex}}^{\text{fixed}} = \frac{- [1] [D^{-1}] [A_S] \{\alpha_0\}}{[1] [D^{-1}] [A_S] \{1\}} \quad \{\alpha_{0 \text{ flex}}^{\text{fixed}}\} = \{\alpha_{0 \text{ rigid}}\} + \{1\} \{\alpha_{0 \text{ flex}}^{\text{fixed}}\}_{\text{rigid}}$$

$$C_{m0 \text{ flex}}^{\text{fixed}} = \frac{[x_{cg} - x] [A_S] \{\alpha_{0 \text{ flex}}^{\text{fixed}}\}}{\bar{q} \bar{c} S / 2}$$

$$C_{L \text{ flex}}^{\text{fixed}} = \frac{[1] [D^{-1}] \{W\} - [1] \{W\}}{q S / 2}$$

$$C_{m \text{ flex}}^{\text{fixed}} = \frac{[x_{cg} - x] [D^{-1}] \{W\} - [x_{cg} - x] \{W\}}{q \bar{c} S / 2}$$

$$C_{L \ddot{\theta} \text{ flex}}^{\text{fixed}} = \frac{[1] [D^{-1}] \{^P Z \ddot{\theta}\} - [1] \{^P Z \ddot{\theta}\}}{\bar{q} S / 2}$$

$$C_{m \ddot{\theta} \text{ flex}}^{\text{fixed}} = \frac{[x_{cg} - x] [D^{-1}] \{^P Z \ddot{\theta}\} - [x_{cg} - x] \{^P Z \ddot{\theta}\}}{\bar{q} \bar{c} S / 2} \quad (3.52)$$

The flexible stability derivative defined above can be used to define the flexible/rigid ratios and increments required to correct the equations in Appendix C (Aerodynamic Equations).

The preceding derivatives will be the same as those for the rigid airplane when [D] equals [1]. It is seen from Equation (3.48) that [D] equals [1] when the dynamic pressure equals zero, since [A_S] = (q̄)[AIC_S], or when [E_S] = [0].

3.6.2.1 Concept of Fixed Longitudinal Stability Derivatives

The stability derivatives derived in the previous section include the superscript "fixed" in their definition. This designation pertains to the assumption that physically speaking the airplane is constrained at two fixed points. These are the points in the [E_S] matrix that show zero deflection for all load conditions and from which all elastic deflections are referenced.

By examining the individual stability derivatives of Equation (3.50) it is apparent that the force system represented is a series of airload distributions due to unit changes in angles of attack in balance with concentrated loads at the constraint points. The entire system is in static balance.

Equation (3.52) may be used to generate a consistent set of "fixed" flexible stability derivatives suitable for use in time history balanced flight maneuver analysis. Two types of stability derivative output are required for a fixed airframe concept. The first type is the ratio of the flexible to rigid stability derivatives associated with the applied angles of attack, α , δ_e , and $\dot{\theta}\bar{c}/2V$. The second type consists of the inertia derivatives associate with nz and $\ddot{\theta}$. The inertia derivatives represent the incremental flexible airload.

The method of solution is illustrated by writing Equations (3.31) and (3.32) in coefficient form as follows:

$$\Sigma P_Z = \left[C_{L_{\sigma_T}}^{\sigma_{TOT}} + C_{L_{nz}} nz + C_{L_{\dot{\theta}}} \ddot{\theta} \right] (\bar{q}S) = -W nz \quad (3.53)$$

$$\Sigma M_y = \left[C_{m_{\sigma_T}}^{\sigma_{TOT}} + C_{m_{nz}} nz + C_{m_{\ddot{\theta}}} \ddot{\theta} \right] (\bar{q}S\bar{c}) = -W nz(x_{REF} - x_{cg}) + I_{yy}\ddot{\theta} \quad (3.54)$$

where:

$$C_{L_{\sigma_T}}^{\sigma_{TOT}} = C_{L_{\alpha}}(\alpha - \alpha_0) + C_{L_{\delta_e}} \delta_e + C_{L_{\dot{\theta}\bar{c}}} \frac{\dot{\theta}\bar{c}}{2V}$$

$$C_{m_{\sigma_T}}^{\sigma_{TOT}} = C_{m_{\alpha}}(\alpha - \alpha_0) + C_{m_{\delta_e}} \delta_e + C_{m_{\dot{\theta}\bar{c}}} \frac{\dot{\theta}\bar{c}}{2V} + C_{m_0}$$

The equations are then combined and expressed in matrix notation as:

$$\begin{bmatrix} C_{L_{\alpha}}^{fix} \end{bmatrix} \begin{Bmatrix} (\alpha - \alpha_0) \\ \delta_e \\ \dot{\theta}\bar{c}/2V \\ 1 \end{Bmatrix} + \begin{bmatrix} C_{nz} \end{bmatrix} \begin{Bmatrix} nz \\ \ddot{\theta} \end{Bmatrix} = (1/\bar{q}) \begin{bmatrix} W \\ - \\ S \end{bmatrix} \begin{Bmatrix} nz \\ \ddot{\theta} \end{Bmatrix}$$

where

$$\begin{bmatrix} C_{L_{\alpha}}^{fix} \end{bmatrix} = \begin{bmatrix} C_{L_{\alpha}} & C_{L_{\delta_e}} & C_{L_{\dot{\theta}\bar{c}}/2V} & 1 \\ C_{m_{\alpha}} & C_{m_{\delta_e}} & C_{m_{\dot{\theta}\bar{c}}/2V} & C_{m_0} \end{bmatrix}$$

is the normal force and pitching moment coefficients due to an applied angle of attack distribution for $(\alpha - \alpha_0)$, δ_e , $\dot{\theta}c/2V$ and C_{m0} ,

$$\begin{bmatrix} C_{nz} \end{bmatrix} = \begin{bmatrix} C_{Lnz} & C_{L\ddot{\theta}} \\ C_{m_{nz}} & C_{m\ddot{\theta}} \end{bmatrix}$$

is the flexible incremental normal force and pitching moment coefficients due to vertical and rotational accelerations (incremental airloads only),

$$\begin{bmatrix} W \\ - \\ S \end{bmatrix} = \begin{bmatrix} -\frac{W}{S/2} & 0 \\ -\frac{W}{S/2}(x_{REF} - x_{cg}) & \frac{I_{yy}}{\bar{c}S/2} \end{bmatrix}$$

is the normal force and pitching moment due to balancing inertia reactions,

$$\begin{Bmatrix} n_z \\ \ddot{\theta} \end{Bmatrix}$$

is the balancing inertia load factor and rotational acceleration at the reference point, and

$$\begin{Bmatrix} (\alpha - \alpha_0) \\ \delta_e \\ \dot{\theta}c/2V \\ 1 \end{Bmatrix}$$

is the applied external angle of attack distributions.

The required flexible ratios and inertia increments are obtained through independent solution of the terms of Equation (3.55). The required stability derivatives may be obtained by solution of $[C_{L\alpha}]$ for unit values of $\alpha - \alpha_0$, δ_e , and $\dot{\theta}c/2V$. The required inertia derivatives are obtained by solution of $[C_{Lnz}]$ for unit values of n_z and $\ddot{\theta}$. The required rigid values may be obtained by repeating the solutions with $[E_S] = [0]$. Flexible/rigid ratios are obtained by division of the above two solutions.

3.6.3 Concept of Free Longitudinal Stability Derivatives

The stability derivatives derived in the previous section are for the so-called "fixed" airframe consideration. The following discussion presents a method of generating stability derivatives for an unrestrained or "free" airplane system. These stability derivatives reflect the effects of the simultaneous application of airload distribution and the required balancing inertia load distributions. They provide greater insight into the physical significance of each parameter.

The solution of the equations of motion for a "free" airframe is illustrated by examining the "fixed" equations of motion for the single parameter $(\alpha - \alpha_0)$. Equation (3.55) may be rewritten as follows:

$$\begin{bmatrix} \text{fix} \\ C_L \\ \alpha \end{bmatrix} \begin{Bmatrix} (\alpha - \alpha_0) \\ 0 \\ 0 \\ 0 \end{Bmatrix} + \begin{bmatrix} C_{nz} \end{bmatrix} \begin{Bmatrix} nz \\ \ddot{\theta} \end{Bmatrix} = (1/\bar{q}) \begin{bmatrix} W \\ - \\ S \end{bmatrix} \begin{Bmatrix} nz \\ \ddot{\theta} \end{Bmatrix} \quad (3.56)$$

The "free" stability derivatives incorporating both airload distributions due to the applied angles of attack and the balancing inertia contributions are expressed as follows:

$$\begin{bmatrix} \text{free} \\ C_L \\ \alpha \end{bmatrix} \begin{Bmatrix} (\alpha - \alpha_0) \\ 0 \\ 0 \\ 0 \end{Bmatrix} + \begin{bmatrix} \text{fix} \\ C_L \\ \alpha \end{bmatrix} \begin{Bmatrix} (\alpha - \alpha_0) \\ 0 \\ 0 \\ 0 \end{Bmatrix} + \begin{bmatrix} C_{nz} \end{bmatrix} \begin{Bmatrix} nz \\ \ddot{\theta} \end{Bmatrix} \text{BALANCE} = 0 \quad (3.57)$$

If a solution is performed for a unit value of $(\alpha - \alpha_0)$, Equation (3.56) becomes:

$$\begin{Bmatrix} C_{L\alpha} \\ C_{m\alpha} \end{Bmatrix}^{\text{fix}} = \left\{ - \begin{bmatrix} C_{nz} \end{bmatrix} + (1/\bar{q}) \begin{bmatrix} W \\ - \\ S \end{bmatrix} \right\} \begin{Bmatrix} nz \\ \ddot{\theta} \end{Bmatrix} \text{BALANCE} \quad (3.58)$$

from which,

$$\begin{Bmatrix} nz \\ \ddot{\theta} \end{Bmatrix} \text{BALANCE} = \left\{ - \begin{bmatrix} C_{nz} \end{bmatrix} + (1/\bar{q}) \begin{bmatrix} W \\ - \\ S \end{bmatrix} \right\}^{-1} \begin{Bmatrix} C_{L\alpha} \\ C_{m\alpha} \end{Bmatrix}^{\text{fix}} \quad (3.59)$$

Thus the n_z and $\ddot{\theta}$ required to balance the "free" airframe may be obtained through the solution of Equation (3.59) and the final value for the "free" derivative can be obtained from Equation (3.57). The elements of $[C_{nz}]$, $[W/S]$, and $[C_{L\alpha}^{fix}]$ are the same as the "fixed" derivatives given in the previous section. The above solution can obviously be repeated for each type of arbitrary angle of attack distribution.

The solution represents an airplane force system in which the airframe is in equilibrium, where the airloads are in balance with the inertia loads, and the airframe is no longer "fixed" in space, but is free to accelerate in the z direction and rotate about the y axis. However, Equation (3.57) contains no allowance for the z translation or rotation about the y axis. The above equations are shown to present the concept of "free" derivatives. The particular solution for free derivatives encompassing the z translation and y rotation is developed in Subsection 3.5.

3.6.4 Effect of Flexibility on α_0 and C_{m0}

If the airframe under analysis has a design wing with a null camber and twist (C&T) distribution, then the aerodynamic load distributions at zero angle of attack, $\alpha_0 = 0^\circ$, will be equal to zero, and the zero lift angle, α_0 , will also equal zero. Similarly, the pitch moment coefficient, C_{m0} will also be zero.

If the design wing has a non-null camber and twist distribution, then the flexible body aerodynamic load distribution of Equation (3.52) at $\alpha = 0^\circ$ may be expressed as:

$$\left\{ P_{zC\&T}^{flex} \right\} = (\bar{q}) \left[D^{-1} \right] \left[A \right] \left\{ \alpha_0 \right\}$$

where $\left\{ \alpha_0 \right\}$ is the camber and twist distribution at $\alpha = 0^\circ$. The lift and moment coefficients due to camber and twist are then defined as:

$$\left\{ C_{LC\&T}^{flex} \right\} = (2/\bar{q}S) \left[1 \right] \left\{ P_{zC\&T}^{flex} \right\} \quad (3.61)$$

$$\left\{ C_{mC\&T}^{flex} \right\} = (2/\bar{q}S) \left[\Delta X \right] \left\{ P_{zC\&T}^{flex} \right\} \quad (3.62)$$

$$\left\{ C_{L\alpha}^{flex} \right\} = (2/\bar{q}S) \left[1 \right] \left[D^{-1} \right] \left[A \right] \left\{ 1 \right\} \quad (3.63)$$

$$\left\{ C_{m\alpha}^{flex} \right\} = (2/\bar{q}S\bar{c}) \left[\Delta X \right] \left[D^{-1} \right] \left[A \right] \left\{ 1 \right\} \quad (3.64)$$

Substituting the above expressions for lift and moment coefficient slopes into Equation (3.52) yields the following equations for the effect of flexibility on α_0 and C_{m0} .

$$\alpha_0^{flex} = - C_{L_{C\&T}}^{flex} / C_{L\alpha}^{flex} \quad (3.65)$$

$$C_{m0}^{flex} = - (C_{m_{C\&T}}^{flex} / C_{m\alpha}^{flex}) \alpha_0^{flex} \quad (3.66)$$

Values of α_0 and C_{m0} for the rigid body can be obtained by repeating the above calculations for $[D^{-1}] = [I]$. Flexible increments for α_0 and C_{m0} may then be expressed as follows:

$$\Delta\alpha_0^{flex} = \alpha_0^{flex} - \alpha_0^{rigid} \quad (3.67)$$

$$\Delta C_{m0}^{flex} = C_{m0}^{flex} - C_{m0}^{rigid} \quad (3.68)$$

The above flexible increments for α_0 and C_{m0} may be included in the rigid body equations of motion.

The total flexible lift and pitching moment coefficients of Equations (3.39) and (3.40) due to angle of attack α and α_0 are expressed as follows:

$$(C_L)_\alpha = C_{L\alpha} * R_{C_{L\alpha}} (\alpha - \alpha_0 + \Delta\alpha_0^{flex}) \quad (3.69)$$

$$(C_m)_\alpha = C_{m\alpha} * R_{C_{m\alpha}} (\alpha - \alpha_0 + \Delta\alpha_0^{flex}) + (C_{m0} + \Delta C_{m0}^{flex}) \quad (3.70)$$

Note that in a typical 2-DOF time history analysis $C_{L\alpha}$, $C_{m\alpha}$, α_0 , and C_{m0} are generally obtained from measured wind tunnel force data. The terms $R_{C_{L\alpha}}$, $R_{C_{m\alpha}}$, $\Delta\alpha_0^{flex}$, and ΔC_{m0}^{flex} represent theoretical flexible corrections as obtained from the type of analysis presented in this report.

3.6.5 Horizontal Stabilizer Downwash Contributions

The lift coefficient acting on the horizontal stabilizer may be expressed as follows:

$$(C_L)_{TAIL} = C_{L_{\alpha_T}} \alpha + (C_{L_{C\&T}})_T + C_{L_{\delta_{HT}}} \delta_H \quad (3.71)$$

or;

$$(C_L)_{TAIL} = C_{L_{\alpha_{HT}}} \left[\left(1 + \frac{\partial \epsilon}{\partial \alpha} \right) \alpha + \epsilon_0 \right] + C_{L_{\delta_{HT}}} \delta_H \quad (3.72)$$

where

$C_{L_{\alpha_T}}$ = stabilizer lift coefficient slope $dC_L/d\alpha$
in the presence of the wing.

$C_{L_{\alpha_{HT}}}$ = stabilizer lift coefficient slope $dC_L/d\alpha$
out of the presence of the wing.

ϵ_0 = downwash angle at $\alpha = 0^\circ$

$d\epsilon / d\alpha$ = slope of the downwash angle at $\alpha = 0^\circ$

$(C_{L_{C\&T}})_T$ = stabilizer lift coefficient due to wing camber
and twist at $\alpha = 0^\circ$

$(C_{L_{\delta_{HT}}})_T$ = stabilizer lift coefficient slope $dC_L/d\alpha$
in the presence of the wing.

The above stabilizer derivatives may be expressed as the summation of the load distribution on the tail plane only, as follows:

$$\left\{ C_{L\alpha_T} \right\} = (2/S) \left[1_T \right] \left[D^{-1} \right] \left[A_S \right] \left\{ 1 \right\} \quad (3.73)$$

$$\left\{ C_{L\alpha_{HT}} \right\} = (2/S) \left[1_T \right] \left[D^{-1} \right] \left[A_S \right] \left\{ \begin{matrix} 0 \\ 1_T \end{matrix} \right\} \quad (3.74)$$

$$\left\{ C_{LC\&T} \right\} = (2/S) \left[1_T \right] \left[D^{-1} \right] \left[A_S \right] \left\{ \alpha_0 \right\} \quad (3.75)$$

$$\left\{ C_{L\delta_{HT}} \right\} = (2/S) \left[1_T \right] \left[D^{-1} \right] \left[A_S \right] \left\{ \begin{matrix} 0 \\ 1_{\delta_H} \end{matrix} \right\} \quad (3.76)$$

where

$\left[1_T \right]$ = summation matrix for tail load distribution only

$\left\{ 1 \right\}$ = unit angle distribution for total airplane control points.

$\left\{ \begin{matrix} 0 \\ 1_T \end{matrix} \right\}$ = unit angle distribution for tail plane only.

$\left\{ \alpha_0 \right\}$ = camber and twist distribution at $\alpha = 0^\circ$.

$\left\{ \begin{matrix} 0 \\ 1_{\delta_H} \end{matrix} \right\}$ = unit angle distribution for tail plane moveable control surface only.

Reviewing Equation (3.72) indicates that the downwash terms at $\alpha = 0^\circ$ may be defined as follows:

$$\epsilon_0^{flex} = (C_{LC\&T}^{flex})_T / C_{L\alpha_{HT}}^{flex} \quad (3.77)$$

$$(d\epsilon/d\alpha)^{flex} = (C_{L\alpha_T}^{flex} - C_{L\alpha_{HT}}^{flex}) / C_{L\alpha_{HT}}^{flex} \quad (3.78)$$

Values of $C_{L\alpha_T}$, $C_{L\alpha_{HT}}$, $(C_{LC\&T})_T$, ϵ_0 and $d\epsilon/d\alpha$ may be generated in a manner similar to that for $\Delta\alpha_0$ and ΔC_{m_0} in Equations (3.67) and (3.68). Thus by repeating the above calculations for $[D^{-1}] = [1]$, flexible effects for $C_{L\alpha_{HT}}$, $(C_{L\delta_{HT}})_T$, ϵ_0 and $d\epsilon/d\alpha$ may then be expressed as follows:

$$\Delta\epsilon_0^{flex} = \epsilon_0^{flex} - \epsilon_0^{RIGID} \quad (3.79)$$

$$\Delta(d\epsilon/d\alpha)^{flex} = (d\epsilon/d\alpha)^{flex} - (d\epsilon/d\alpha)^{RIGID} \quad (3.80)$$

$$R_{CL_{\alpha HT}} = C_{L_{\alpha HT}}^{flex} / C_{L_{\alpha HT}}^{RIGID}$$

$$R_{CL_{\delta HT}} = (C_{L_{\delta HT}}^{flex})_T / (C_{L_{\delta HT}}^{RIGID})_T$$

Thus the horizontal stabilizer lift coefficient of Equation (3.72) may be rewritten to incorporate the above flexible effects as follows:

$$\begin{aligned} (C_L)_{TAIL} = & C_{L_{\alpha HT}} R_{CL_{\alpha HT}} \left[\left(1 + \frac{d\varepsilon}{d\alpha} + \Delta \left(\frac{d\varepsilon}{d\alpha} \right)^{flex} \right) \alpha + (\varepsilon_0 + \Delta \varepsilon_0^{flex}) \right] \\ & + C_{L_{\delta HT}} R_{CL_{\delta HT}} \delta_H \end{aligned} \quad (3.81)$$

Note that in a typical time history analysis $C_{L_{\alpha HT}}$, $C_{L_{\delta HT}}$, $\Delta d\varepsilon/d\alpha$ and $\Delta \varepsilon_0$ may be obtained from either experimental data or from theoretical aerodynamic codes. The terms $R_{CL_{\alpha HT}}$, $\Delta \varepsilon_0^{flex}$ and $\Delta(d\varepsilon/d\alpha)^{flex}$ represent the theoretical flexible corrections as obtained from the type analysis presented herein. The independent real time parameters are α and δ_H .

3.6.6 Determinations of α contributions

The change in lift coefficient with variation in the rate of change of angle of attack, α , arises essentially from an aerodynamic time lag effect. It comes from a so-called plunging type of motion along the z axis, in which the angle of attack, α , remains constant during the disturbance.

The horizontal tail of a conventional airplane is immersed in the downwash field of the wing and whenever the wing undergoes a change of angle of attack, the downwash field is altered. Thus the change in stabilizer lift may be expressed as a function of incremental downwash angle as follows:

$$(\Delta C_L)_{tail} = C_{L_{\alpha HT}} \Delta \varepsilon \quad (3.82)$$

where

$$\Delta \varepsilon = (d\varepsilon/d\alpha) \dot{\alpha} \Delta t \quad (3.83)$$

and Δt is the time lag from the wing to the tail. This lag can be expressed in terms of the tail length, (distance from wing $c/4$ to tail $c/4$), l_t , and the free stream velocity. Thus, Equation (3.82) may be expressed as:

$$(\Delta C_L)_{\text{tail}} = C_{L\alpha_{HT}} (d\varepsilon/d\alpha) \dot{\alpha} (l_t/V) \quad (3.84)$$

By definition, the incremental stabilizer lift may also be expressed as

$$C_{L(\dot{\alpha}\bar{c}/2V)} (\dot{\alpha}\bar{c}/2V) = C_{L\alpha_{HT}} (\dot{\alpha}\bar{c}/2)(2/\bar{c})(d\varepsilon/d\alpha)(l_t/V) \quad (3.85)$$

Thus

$$C_{L(\dot{\alpha}\bar{c}/2V)} = C_{L\alpha_{HT}} (2l_t/\bar{c})(d\varepsilon/d\alpha) \quad (3.86)$$

Similarly, it can be shown that

$$C_{m(\dot{\alpha}\bar{c}/2V)} = C_{m\alpha_{HT}} (2l_t/\bar{c})(d\varepsilon/d\alpha) \quad (3.87)$$

Using rigid and flexible values for $C_{L\alpha_{HT}}$, $C_{m\alpha_{HT}}$, and $d\varepsilon/d\alpha$ obtained from the above analysis, the theoretical flexible/rigid ratios $R_{C_{L\alpha}}$ and $R_{C_{m\alpha}}$ may be generated and included in time history analysis.

3.7 LATERAL/DIRECTIONAL STABILITY DERIVATIVES

The approach used for the longitudinal stability derivatives is similarly employed for the solution of the lateral/directional stability derivatives, except that anti-symmetric aeroinduction, inertia, and structural influence coefficients are utilized.

3.7.1 Lateral/Directional Equations of Motion

For simplicity, the applied aerodynamic forces used in the development of the equations of motion will be limited to the side force due to an applied sideslip angle. It will be shown later how to expand the applied aerodynamic forces to include all contributions due to the full set of lateral stability derivatives.

$$\Sigma P_Y = -W n_Y \quad (3.88)$$

$$\Sigma N = W(x_{cg} - x_{REF})n_Y + I_{zz}^{REF} \ddot{\Psi} - I_{xz}^{REF} \ddot{\Phi} \quad (3.89)$$

$$\Sigma L = W(z_{REF} - z_{cg})n_Y - I_{xz}^{REF} \ddot{\Psi} + I_{xx}^{REF} \ddot{\Phi} \quad (3.90)$$

where n_Y is the inertial load factor, and $\ddot{\Phi}$ and $\ddot{\Psi}$ are angular accelerations about the x and z axes respectively. The aerodynamic forces and moments may be expressed as follows:

$$\Sigma P_Y = (C_{Y\beta} \beta + C_{Yn_Y} n_Y + C_{Y\ddot{\Psi}} \ddot{\Psi} + C_{Y\ddot{\Phi}} \ddot{\Phi}) \bar{q} S \quad (3.91)$$

$$\Sigma N = (C_{n\beta} \beta + C_{nn_Y} n_Y + C_{n\ddot{\Psi}} \ddot{\Psi} + C_{n\ddot{\Phi}} \ddot{\Phi}) \bar{q} S b \quad (3.92)$$

$$\Sigma L = (C_{l\beta} \beta + C_{ln_Y} n_Y + C_{l\ddot{\Psi}} \ddot{\Psi} + C_{l\ddot{\Phi}} \ddot{\Phi}) \bar{q} S b \quad (3.93)$$

where β is the applied sideslip angle and,

$$C_{Y(\)} = \partial C_Y / \partial(\)$$

$$C_{n(\)} = \partial C_n / \partial(\)$$

$$C_{l(\)} = \partial C_l / \partial(\)$$

In matrix notations the above equations become:

$$\begin{Bmatrix} C_{Y\beta}^{fix} \\ C_{Yn} \end{Bmatrix}_{3 \times 1} \beta + \begin{bmatrix} C_{Y\ddot{\Psi}} \\ C_{Y\ddot{\Phi}} \end{bmatrix}_{3 \times 3} \begin{Bmatrix} n_Y \\ \ddot{\Psi} \\ \ddot{\Phi} \end{Bmatrix}_{3 \times 1} = \bar{q}^{-1} \begin{bmatrix} W \\ - \\ S \end{bmatrix}_{3 \times 3} \begin{Bmatrix} n_Y \\ \ddot{\Psi} \\ \ddot{\Phi} \end{Bmatrix} \quad (3.94)$$

where

$$\begin{Bmatrix} C_{Y\beta}^{FIX} \end{Bmatrix} = \begin{Bmatrix} C_{Y\beta} \\ C_{n\beta} \\ C_{l\beta} \end{Bmatrix}$$

is the flexible side force, yawing moment and rolling moment coefficients due to an applied sideslip distribution.

$$\begin{bmatrix} C_{Y n_Y} \\ C_{n_Y} \\ C_{l n_Y} \end{bmatrix}_{3 \times 3} = \begin{bmatrix} C_{Y \ddot{\psi}} & C_{Y \ddot{\phi}} \\ C_{n \ddot{\psi}} & C_{n \ddot{\phi}} \\ C_{l \ddot{\psi}} & C_{l \ddot{\phi}} \end{bmatrix}_{3 \times 3}$$

is the flexible incremental side force, yawing moments and rolling moment coefficients due to lateral and rotational accelerations. (incremental airloads only)

$$\begin{bmatrix} W \\ - \\ S \end{bmatrix}_{3 \times 3} = \frac{1}{bS} \begin{bmatrix} -bW & 0 & 0 \\ W(x_{cg} - x_{REF}) & I_{zz} & -I_{xz} \\ W(z_{REF} - z_{cg}) & -I_{xz} & I_{xx} \end{bmatrix}_{3 \times 3}$$

is the side force, yawing moment and rolling moments due to balancing inertia reactions, and

$$\begin{Bmatrix} n_Y \\ \ddot{\psi} \\ \ddot{\phi} \end{Bmatrix}$$

is the balancing inertia load factor and rotational accelerations at the reference point.

3.7.2 Equations of Motion in a Panel Point Load System

The preceding equations may be represented as the sum of a net panel load point system and expressed in matrix notation as follows

$$\begin{Bmatrix} P_Y \\ N_Y \\ L \end{Bmatrix} = \begin{Bmatrix} 0 \end{Bmatrix} = \begin{bmatrix} \Sigma \end{bmatrix} \begin{Bmatrix} P_{RIGID}^{NET} \end{Bmatrix} \quad (3.95)$$

where:

$$\begin{Bmatrix} P_{RIGID}^{NET} \end{Bmatrix} = \begin{Bmatrix} P_{Y,Z}^{AIR} \end{Bmatrix} + \begin{Bmatrix} P_{X,Y,Z}^{INERTIA} \end{Bmatrix} \quad (3.96)$$

and

$\left[\varepsilon \right] \rightarrow$ Summation matrix for total Y load, yawing moment and rolling moment.

This shows that the net loads acting at the panel points consist of anti-symmetric Y and Z airloads, and anti-symmetric X,Y and Z inertia loads.

The rigid body airloads are defined as follows:

$$\left\{ P_{Y,Z}^{AIR} \right\}_{RIGID} = \bar{q} \left[A_{Y,Z} \right] \left\{ \alpha\beta \right\} \beta \quad (3.97)$$

where

$$\left[A_{Y,Z} \right] = \left[Q_Y \right] + \left[Q_Z^{AS} \right]$$

and

$\left[Q_Z^{AS} \right] \rightarrow$ Theoretical aerodynamic induction matrix, relating anti-symmetric vertical loads at the panel points, to anti-symmetric angles of attack and sideslip angles at the control point.

$\left[Q_Y \right] \rightarrow$ Theoretical aerodynamic induction matrix, relating lateral loads at the panel points, to anti-symmetric angles of attack and sideslip angles at the control points.

$\left\{ \alpha\beta \right\} \rightarrow$ Anti-symmetric angles of attack and sideslip angles at the control points.

The X,Y,and Z inertial loads are defined as follows:

$$\left\{ P_{X,Y,Z}^{INERTIA} \right\}_{RIGID} = \left[\left[P_X^{IN} \right] + \left[P_Y^{IN} \right] + \left[P_Z^{IN} \right] \right] \left\{ \begin{matrix} \ddot{Y} \\ \ddot{X} \\ \ddot{\phi} \end{matrix} \right\} \quad (3.98)$$

where:

$$\left[P_X^{IN} \right] = \left[\left\{ 0 \right\} \left\{ P_{X/\ddot{Y}} \right\} \left\{ 0 \right\} \right]$$

$$\left[P_Y^{IN} \right] = \left[\left\{ W \right\} \left\{ P_{Y/\ddot{Y}} \right\} \left\{ P_{Y/\ddot{\phi}} \right\} \right]$$

$$\left[P_Z^{IN} \right] = \left[\left\{ 0 \right\} \left\{ 0 \right\} \left\{ P_{Z/\ddot{\phi}} \right\} \right]$$

and

$$\left\{ W \right\}, \left\{ P_{Y/\ddot{\psi}} \right\}, \left\{ P_{Y/\ddot{\phi}} \right\} \rightarrow \text{Inertial Y loads due to a unit } n_Y, \ddot{\psi}, \text{ and } \ddot{\phi}, \text{ respectively.}$$

$$\left\{ P_{X/\ddot{\psi}} \right\} \rightarrow \text{Inertial X loads due to a unit } \ddot{\psi}$$

$$\left\{ P_{Z/\ddot{\phi}} \right\} \rightarrow \text{Inertial Z loads due to a unit } \ddot{\phi}$$

Thus, the net panel loads acting on the rigid airframe may be expressed as:

$$\left\{ P_{RIGID}^{NET} \right\} = \bar{q} \left[A_{Y,Z} \right] \left\{ \alpha\beta \right\} \beta + \left[P_{X,Y,Z}^{INERTIA} \right] \left\{ \begin{matrix} n_Y \\ \ddot{\psi} \\ \ddot{\phi} \end{matrix} \right\} \quad (3.99)$$

where:

$$\left[P_{X,Y,Z}^{INERTIA} \right] = \left[P_X^{IN} \right] + \left[P_Y^{IN} \right] + \left[P_Z^{IN} \right]$$

For a flexible structure, the net loads acting on the panel points may be expressed as follows:

$$\left\{ P_{flex}^{NET} \right\} = \left\{ P_{RIGID}^{NET} \right\} + \left\{ \Delta P_{Y,Z_{flex}}^{AIR} \right\} \quad (3.100)$$

and

$$\left\{ \Delta P_{Y,Z_{flex}}^{AIR} \right\} = \bar{q} \left[A_{Y,Z} \right] \left\{ \Delta\alpha\beta_e \right\} \quad (3.101)$$

The incremental change in local anti-symmetric angle of attack and sideslip angle due to airframe flexibility is :

$$\left\{ \Delta\alpha\beta_e \right\} = \left[D_{\alpha\beta} \right] \left[E^{AS} \right] \left\{ P_{flex}^{NET} \right\} \quad (3.102)$$

where

$[D_{\alpha\beta}] \rightarrow$ Differentiation matrix relating deflections at load points, to local angles of attack and sideslip angles at the control points.

$[E^{AS}] \rightarrow$ Anti-symmetric structural influence coefficient matrix.

From Equations (3.100) to (3.102), it can be seen that,

$$\{ P_{flex}^{NET} \} = \{ P_{RIGID}^{NET} \} + \bar{q} [A_{Y,Z}] [D_{\alpha\beta}] [E^{AS}] \{ P_{flex}^{NET} \} \quad (3.103)$$

or

$$\{ P_{flex}^{NET} \} = [D^{-1}] \{ P_{RIGID}^{NET} \} \quad (3.104)$$

where:

$$[D] = [I] - \bar{q} [A_{Y,Z}] [D_{\alpha\beta}] [E^{AS}] \quad (3.105)$$

Therefore, the solution to the three degree of freedom lateral/directional equations of motion may be solved using a summation of an anti-symmetric lateral and vertical panel point load system, that is,

$$\begin{Bmatrix} P_Y \\ N \\ L \end{Bmatrix} = \begin{Bmatrix} 0 \end{Bmatrix} = [E] \{ P_{flex}^{NET} \} \quad (3.106)$$

or

$$\begin{Bmatrix} 0 \end{Bmatrix} = [E] [D^{-1}] \{ P_{RIGID}^{NET} \} \quad (3.107)$$

It should be noted that the above solution reduces to the rigid case when $[D]$ is the identity matrix $[I]$. Equation (3.105) indicates that this is the case when the dynamic pressure equals zero, i.e. $\bar{q} = 0$, or when the structural influence coefficient matrix is null, i.e. $[E^{AS}] = [0]$. The equations of motion may be expanded by inserting Equations (3.99) and (3.104) into (3.106), as follows:

$$[\Sigma] \{ P_{flex}^{NET} \} = [\Sigma] \left\{ \bar{q} [D^{-1}] [A_{Y,Z}] \{ \alpha\beta \} \beta + [D^{-1}] [P_{X,Y,Z}^{INERTIA}] \begin{Bmatrix} n_Y \\ \psi \\ \phi \end{Bmatrix} \right\} = \{ 0 \} \quad (3.108)$$

$$\{ \Delta P_{Y,Z}^{AIR} \} = \left\{ [D^{-1}] - [I_{\setminus}] \right\} [P_{X,Y,Z}^{INERTIA}] \begin{Bmatrix} n_Y \\ \psi \\ \phi \end{Bmatrix} \quad (3.109)$$

$$\begin{Bmatrix} C_{Y\beta} \\ C_{n\beta} \\ C_{l\beta} \end{Bmatrix} = \left[\frac{1}{S/2} \right] [\Sigma] [D^{-1}] [A_{Y,Z}] \{ \alpha\beta \} \quad (3.110)$$

$$[C_{Y_{n_Y}}] = \left[\frac{1}{S/2} \right] [\Sigma] \left\{ [D^{-1}] - [I_{\setminus}] \right\} [P_{X,Y,Z}^{INERTIA}] \quad (3.111)$$

$$\begin{Bmatrix} W \\ S \end{Bmatrix} = \left[\frac{1}{S/2} \right] [\Sigma] [P_{X,Y,Z}^{INERTIA}] \quad (3.112)$$

Obviously, the above solutions for either fixed or free derivatives can be repeated for different types of $\{\alpha\beta\}$ distributions, such as for a rudder, ailerons, unit rolling velocity, or unit yawing velocity. The reader is referred to Subsections 3.7.3 and 3.7.4 for a description of the fixed and free airframe concepts of flexible stability derivatives.

3.7.3 Concept of Fixed Lateral/Directional Stability Derivatives

The stability derivatives derived in the previous paragraphs include the subscript "fixed" in their definition. Physically speaking, this designation implies that the airplane is constrained at two fixed points. These are the points in the $[E^{AS}]$ matrix which show zero deflection for all load conditions, and from which all elastic deflections are referenced.

By examining the individual stability derivatives of Equation (3.108) it is apparent that the force system represented in a series of airload distributions due to unit change in angles of attack is in balance with

concentrated loads at the constraint points. The entire system is in static balance.

Equation (3.108) may be used to generate a consistent set of "fixed" flexible stability derivatives suitable for use in time history balanced flight maneuver analysis. Specifically, two types of stability derivative output are required for a fixed airframe concept. The first type is the ratio of the flexible to rigid stability derivatives associated with the sideslip angle β . The second type consists of the inertia derivatives associated with n_Y , $\ddot{\Psi}$, and $\ddot{\Phi}$. The inertia derivatives represent the incremental airload of Equation (3.109).

The required flexible ratios and inertia increments may be obtained through the independent solution of the terms of Equation (3.94). The stability derivatives may be obtained by solution $\{C_{Y\beta}^{Fix}\}$ for a unit value of β . This solution is given by Equation (3.110). The inertia derivatives may be obtained by solution of $[C_{Yn_Y}]$ for unit values of n_Y , $\ddot{\Psi}$, and $\ddot{\Phi}$.

Equation (3.111) represents the required solution. The rigid values may be obtained by repeating the above solutions $[E^{AS}] = [0]$. Flexible/rigid ratios are obtained by element by element division of the above two equations.

Program DRSD solves the 3-DOF lateral/directional equations of motion for a "fixed" airframe using the above method. A description of this program is presented in Appendix D.3 of this report.

3.7.4 Concept of Free Lateral/Directional Stability Derivatives

The stability derivatives derived in the last section are for the so-called "fixed" airframe consideration. The following paragraphs present a method of generating stability derivatives for an unrestrained or "free" airplane force system. These stability derivatives reflect the effects of the simultaneous application of airload distribution, and the required balancing inertia load distributions. Thus they provide greater insight into the physical significance of each parameter.

The solution of the equations of motion for a "free" airframe may be illustrated by examining the "fixed" equations of motion. Thus Equation (3.94) may be rewritten as:

$$\begin{bmatrix} C_Y^{FIX} \\ \beta \end{bmatrix} + \begin{bmatrix} C_{Y_{n_Y}} \end{bmatrix} \begin{Bmatrix} n_Y \\ \ddot{\Psi} \\ \ddot{\Phi} \end{Bmatrix} = (1/\bar{q}) \begin{bmatrix} W \\ \bar{S} \end{bmatrix} \begin{Bmatrix} n_Y \\ \ddot{\Psi} \\ \ddot{\Phi} \end{Bmatrix} \quad (3.113)$$

The "free" stability derivatives incorporating both airload distributions due to the applied sideslip angle and the balancing inertia contributions may be expressed as follows:

$$\begin{Bmatrix} C_Y^{FREE} \\ \beta \end{Bmatrix} = \begin{Bmatrix} C_Y^{FIX} \\ \beta \end{Bmatrix} + \begin{bmatrix} C_{Y_{n_Y}} \end{bmatrix} \begin{Bmatrix} n_Y \\ \ddot{\Psi} \\ \ddot{\Phi} \end{Bmatrix}^{BALANCE} \quad (3.114)$$

For a unit value of β , Equation (3.113) becomes:

$$\begin{Bmatrix} C_Y^{FIX} \\ \beta \end{Bmatrix} = \left\{ -\begin{bmatrix} C_{Y_{n_Y}} \end{bmatrix} + (1/\bar{q}) \begin{bmatrix} W \\ \bar{S} \end{bmatrix} \right\} \begin{Bmatrix} n_Y \\ \ddot{\Psi} \\ \ddot{\Phi} \end{Bmatrix} \quad (3.115)$$

Therefore,

$$\begin{Bmatrix} n_Y \\ \ddot{\Psi} \\ \ddot{\Phi} \end{Bmatrix}^{BALANCE} = \left\{ -\begin{bmatrix} C_{Y_{n_Y}} \end{bmatrix} + (1/\bar{q}) \begin{bmatrix} W \\ \bar{S} \end{bmatrix} \right\}^{-1} \begin{Bmatrix} C_Y^{FIX} \\ \beta \end{Bmatrix} \quad (3.116)$$

Thus n_Y , $\ddot{\Psi}$, and $\ddot{\Phi}$ required to balance the "free" airframe may be obtained through the solution of Equation (3.116). The final value for the "free" derivative can be obtained from Equation (3.114). The elements of $\begin{bmatrix} C_{Y_{n_Y}} \end{bmatrix}$, $\begin{bmatrix} W \\ \bar{S} \end{bmatrix}$, and $\begin{Bmatrix} C_Y^{FIX} \\ \beta \end{Bmatrix}$ are the same as those in Subsection 3.7.3. and may be obtained from Equations (3.110) to (3.112).

It is obvious that the above solution can be repeated for other types of arbitrary anti-symmetric angles of attack and sideslip distribution.

Program DRSD solves the 3-DOF lateral/directional equations of motion for a "free" airframe using the above method of solution. A description of this program is presented in Appendix D.3 of this report.

SECTION 4
AERODYNAMICS FOR AEROSERVOELASTICITY

4.1 INTRODUCTION

The subdisciplines of aeroservoelasticity: aerodynamics, feedback servo control, and solid mechanics were developed, independently of each other over the course of aviation history. Interaction between these disciplines could be ignored roughly up to the 1950's. Modern fighters and transport airplanes operate at combinations of angle of attack (α) and dynamic pressure rendering the integration of these disciplines mandatory. The modern airplane design must ensure enhanced safety, reliability, operational life and unparalleled performance. In the following, a historical background relating to the evolution of these disciplines and the need for their subsequent integration into the new discipline of aeroservoelasticity is briefly outlined.

- Aerodynamics - Evolved from classical hydrodynamics and the empirical science of hydraulics. The former dealt with formal solutions to partial differential equations such as Laplace's equation and reached its zenith in the mid 1800s. The latter measured the flow of fluid in pipes, channels and wires and about bodies such as ship hulls and bridge piers. Scale ship models, for example, have been tow-tested for several hundred years. Aerodynamics as a subject emerged fewer than 100 years ago, and unsteady aerodynamics of lifting surfaces, about 60 years ago.
- Servo Control - Employment of measurements of the state of an object as a means of automatically changing that state to achieve a desired objective, defines feedback control. The device for amplifying the measurement signal to effect the change is the servomechanism. The steam engine with mechanical feedback of piston position for changing slide valve openings effecting steam delivery and exhaust, represented an application of this principal in the late 1700s. The coming of electric power in the late 1800s introduced and required the use of electrical feedback and electrical and electro-mechanical servos and began to lay the foundation of what was to become servo control theory. Modern evolution of the subject stems from chemical and petroleum process control that led to fully automated production plants as early as the 1920s. Modern servo control could thus be said to have a history of about 100 years.
- Solid Mechanics - The oldest of the three disciplines evolved through civil engineering from Roman times. Elasticity and maximum load

concepts gradually emerged through stone and concrete construction of in situ structures: bridges, aqueducts, dams, and buildings. Marine architecture extended the subject to vehicles. Wooden ship structural design evolved to steel within the last 150 years. Metal aircraft construction practice and theory followed that developed for steel ships. The study of elasticity thus has a history of over 2000 years and the theory employed in aircraft metal monocoque structures a history of over 100 years.

The three disciplines began interacting, two at a time, in aircraft analysis and design as early as the 1920s. A brief review of these sets the stage for the more complete discussion of aerodynamics and the part it plays in aeroservoelasticity, the subject of this report.

- **Aeroelasticity:** The first analyses of the interaction of unsteady aerodynamics and linear elastic structures were made in the early 1920s to gain an understanding of the previously unexplainable flutter of aircraft lifting surfaces. Design changes based on these analyses made the aeroelastic modes stable without the benefit of active servo control.

Static aeroelastic effects began to severely limit fighter aircraft maneuverability in WW II. Aileron reversal was the first example to appear. This combined discipline is approximately 70 years old, and is the oldest of the three.

- **Aeroservo Control:** The interaction of quasi-steady lifting surface aerodynamics, classical mechanics of rigid bodies (linearized) and servo control under gyroscope feedback acting through elevator, aileron, and rudder deflection began to be studied for the purpose of providing autopilots for commercial transport aircraft in the 1930s. The DC-3 could be flown "hands-off" for example.

This type of system was extended to high speed pilotless aircraft in WW II with the German V-1 pulsejet powered subsonic flying bomb and the supersonic V-2 rocket, a forerunner to today's space vehicle launch boosters.

- **Servoelastic Dynamics:** The third pair of disciplines - the interaction of the linear elastic modes of a flexible vehicle (with little aerodynamics influence) and servo control, under accelerometer feedback acting through swivelling main rocket thrusters, for example, began to be considered in earnest during the development of intercontinental ballistic missiles (ICBMs) and space vehicle launch boosters about 30 years ago.

It was necessary to stabilize not only the neutrally stable highly flexible body bending and axial modes and slosh modes of the fuel and

oxidizer in large diameter tanks but also the completely unstable vehicle "rigid" body modes.

The small damping of the elastic modes and fairly wide resonant frequency spacing often provided mode independence and permitted the separate stabilization of each.

As aircraft speeds increased in the 50s and 60s and wing thickness decreased, the effects of lifting surface elasticity became more pronounced - including the quasi-steady (or static) aeroelastic effects. These could usually be accounted for by modifying the aerodynamic stability and control derivatives of the rigid airplane. Thus the basic means of analyzing airplane stability and control did not have to change to accommodate static aeroelastic effects.

Dynamic effects at the structure mode frequencies could be neglected by designing the servo control to roll-off rapidly as these modal frequencies were approached. This permitted unsteady aerodynamics to also be neglected in stability and control analysis. This independence of the control system from rapid unsteady effects is still valid for many stability and control problems today. Dynamic aeroelastic modes are traditionally stabilized passively by aerodynamic, inertial, and structural design.

Static aeroelasticity very greatly affects servo control system design in typical fighter aircraft configurations. With increasing dynamic pressure, stability generally decreases (e.g., longitudinal static stability, $C_{M\alpha}$, decreases and lift curve slope $C_{L\alpha}$ increases with unswept wings due to leading-edge nose-up elastic twist) making the airplane more responsive to disturbances. At the same time controls become much less effective (e.g., positive elevator deflection bends the aft fuselage down causing stabilizer lift that acts to neutralize the elevator down force). Obviously, if the control aeroelastic derivative approaches zero, no control system will be able to stabilize and control the airplane.

When such behavior unexpectedly manifested itself in flight test, as it sometimes did in the 50s, the only recourse open to the operator was to

restrict flight operations to lower dynamic pressures (and sometimes to lower transonic Mach numbers). If such a problem were caught in the design phase, structural stiffness could sometimes be increased, though attendant weight increase would usually force a completely new structure to be designed that would produce a less severe deflection distribution.

Structural design began to be greatly affected by requirements for controls effectiveness, and the prevention of flutter and divergence. Required wing main box torsional stiffness increases resulted in skin and spar web thicknesses far beyond those required for optimum strength design. New and unorthodox controls configurations became necessary to save weight and retain aeroelastic controls effectiveness to high dynamic pressure.

It was into this atmosphere that the new discipline aeroservoelasticity was born.

4.2 EQUATIONS OF FLUID MOTION

The equations governing the aerodynamic forces employed in stability and control analyses are based on air considered as a continuum. The following equations are developed, in descending order of complexity:

- Navier-Stokes.
- Euler.
- Full Potential
- Prandtl-Glauert (Linearized Potential).
 - Hyperbolic (Supersonic).
 - Elliptic (Subsonic).
- Laplace (Incompressible).

Though it had been possible to develop the most comprehensive set of fluid motion equations (the Navier-Stokes) over a century ago they were of little use without the computer, except as the beginning of a path to simpler more restricted equations. The simpler equations were the first to yield technically useful results.

An example of simpler equations is provided by the Euler nonlinear partial differential equations, written in vector notation:

• Euler Equation

$$\frac{D\rho}{Dt} = -\rho \nabla \cdot \mathbf{u} \quad \text{Continuity}$$

$$\rho \frac{D\mathbf{u}}{Dt} = -\nabla p \quad \text{Momentum (Newton's Second Law)}$$

$$\rho \frac{De}{Dt} = -p \nabla \cdot \mathbf{u} \quad \text{Energy Balance}$$

Where:

$$\frac{D}{Dt} = \frac{\partial}{\partial t} + (\mathbf{u} \cdot \nabla) \quad \text{"Following the Motion" Operator}$$

These are usually written in divergence form to facilitate computation:

• Euler Equations in Divergence Form

$$\frac{\partial \rho}{\partial t} + \frac{\partial (\rho u)}{\partial x} + \frac{\partial (\rho v)}{\partial y} + \frac{\partial (\rho w)}{\partial z} = 0 \quad \text{Continuity}$$

$$\frac{\partial (\rho u)}{\partial t} + \frac{\partial (\rho u^2 + p)}{\partial x} + \frac{\partial (\rho uv)}{\partial y} + \frac{\partial (\rho uw)}{\partial z} = 0 \quad \text{Momentum, x component}$$

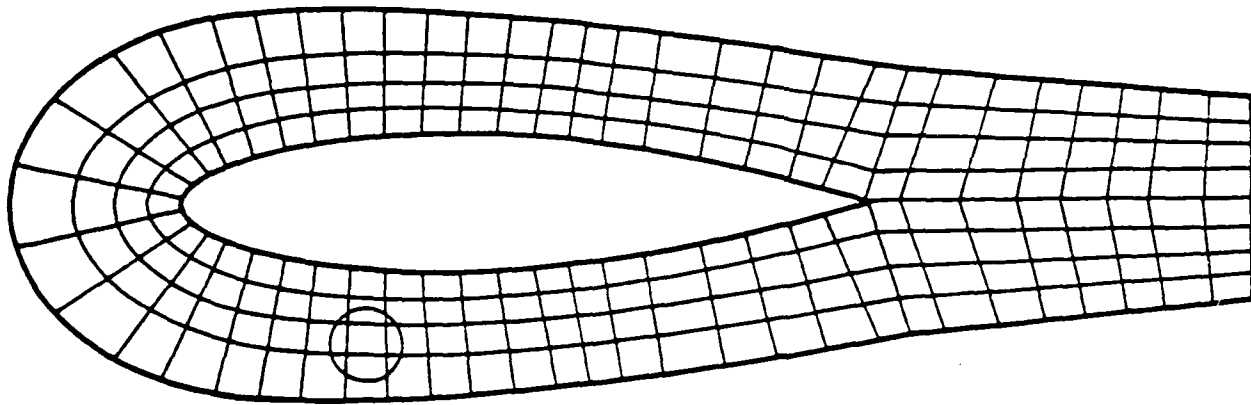
$$\frac{\partial (\rho v)}{\partial t} + \frac{\partial (\rho vu)}{\partial x} + \frac{\partial (\rho v^2 + p)}{\partial y} + \frac{\partial (\rho vw)}{\partial z} = 0 \quad \text{Momentum, y component}$$

$$\frac{\partial (\rho w)}{\partial t} + \frac{\partial (\rho wu)}{\partial x} + \frac{\partial (\rho wv)}{\partial y} + \frac{\partial (\rho w^2 + p)}{\partial z} = 0 \quad \text{Momentum, z component}$$

$$\frac{\partial}{\partial t} \left[\rho \left(e + \frac{q^2}{2} \right) \right] + \frac{\partial}{\partial x} \left[\left(\left(e + \frac{q^2}{2} \right) + \frac{p}{\rho} \right) \rho u \right] + \frac{\partial}{\partial y} \left[\left(\left(e + \frac{q^2}{2} \right) + \frac{p}{\rho} \right) \rho v \right]$$

$$+ \frac{\partial}{\partial z} \left[\left(\left(e + \frac{q^2}{2} \right) + \frac{p}{\rho} \right) \rho w \right] = 0 \quad \text{Energy}$$

Euler and Navier-Stokes nonlinear partial differential equations are solved by erecting a grid of volumetric elements that totally fills the space surrounding the object under study. The time rate of change of fluid density, momentum, or energy within an element is proportional to the net flux of the quantity into the element. A pseudo time-stepping procedure can find the no-flux condition that marks a steady-state solution (see Figure 4-1).



One dimensional continuity equation for typical volumetric element:

$$\begin{array}{c}
 \rho u \quad \boxed{} \quad \left(\rho u + \frac{\partial(\rho u)}{\partial x} \Delta x \right) \quad \frac{\partial \rho}{\partial t} = - \frac{\partial(\rho u)}{\partial x} \\
 \leftarrow \Delta x \rightarrow
 \end{array}$$

Figure 4-1. Euler Equation Solution Volumetric Element Grid

The potential equation of fluid motion may be obtained from the Euler equations as follows:

Full potential equation is based on:

$$\frac{D\rho}{Dt} = -\rho \nabla \cdot \mathbf{u} \quad \text{Conservation of Mass}$$

$$\rho \frac{Du}{Dt} = -\nabla p \quad \text{Newton's 2nd Law (F = ma)}$$

$$\frac{p}{\rho_0} = \left(\frac{\rho}{\rho_0} \right)^\gamma \quad \text{Isentropic Equation of State Substituted for the Energy Equation}$$

The potential equation applies to flows in which vorticity is null. It does not apply to:

- Boundary layers and wakes
- Separated regions
- Within shock thickness or behind curved shocks

If ϕ is the velocity potential, then the fluid velocity is given by

$$\mathbf{u} = \nabla\phi = i \frac{\partial\phi}{\partial x} + j \frac{\partial\phi}{\partial y} + k \frac{\partial\phi}{\partial z}$$

$$\text{Fluid Rotation } \omega = \nabla \times \mathbf{u} = \nabla \times \nabla \phi \equiv 0$$

First the Bernoulli equation is derived. the Momentum equation:

$$\frac{1}{\rho} \nabla p + \nabla \frac{\partial\phi}{\partial t} + (\nabla\phi \cdot \nabla) \nabla\phi = 0 \text{ with } \frac{\partial\nabla\phi}{\partial t} \equiv \nabla \frac{\partial\phi}{\partial t}$$

with $1/\rho$ substituted from the equation of state, may be integrated over any path through the fluid from point A to the point of interest.

$$\frac{p_0}{\rho_0} \frac{1}{\gamma} p^{-\frac{1}{\gamma}} \nabla p + \nabla \frac{\partial\phi}{\partial t} + (\nabla\phi \cdot \nabla) \nabla\phi = 0$$

$$\frac{p_0}{\rho_0} \frac{1}{\gamma} \int_A p^{-\frac{1}{\gamma}} \nabla p \cdot d\mathbf{r} + \int_A \nabla \frac{\partial\phi}{\partial t} \cdot d\mathbf{r} + \int_A (\nabla\phi \cdot \nabla) \nabla\phi \cdot d\mathbf{r} + C(A) = 0$$

The Bernoulli equation becomes:

$$\left(\frac{p_0}{\rho_0}\right)^{\frac{\gamma}{\gamma-1}} \left(\frac{p}{p_0}\right)^{\frac{\gamma-1}{\gamma}} + \frac{\partial\phi}{\partial t} + \frac{1}{2} \mathbf{u}^2 + C = 0$$

or equivalently:

$$\frac{1}{\gamma - 1} a^2 + \frac{\partial \phi}{\partial t} + \frac{1}{2}(\nabla \phi)^2 + C = 0$$

Now the conservation of mass equation may be written as follows:

$$\frac{1}{\rho} \frac{\partial \rho}{\partial t} + \nabla \cdot \nabla \phi + \nabla \phi \cdot \frac{\nabla \rho}{\rho} = 0$$

and from the Isentropic equation, may be substituted

$$\left(\frac{1}{\gamma - 1} \right) \frac{\partial a^2}{a^2} = \frac{\partial \rho}{\rho}$$

$$\left(\frac{1}{\gamma - 1} \right) \frac{\nabla a^2}{a^2} = \frac{\nabla \rho}{\rho}$$

to yield

$$\frac{1}{(\gamma - 1)a^2} \frac{\partial a^2}{\partial t} + \nabla \cdot \nabla \phi + \frac{1}{(\gamma - 1)a^2} \nabla \phi \cdot \nabla a^2 = 0$$

Differentiating Bernoulli's equation with respect to time gives:

$$\frac{\partial a^2}{\partial t} = -(\gamma - 1) \left(\frac{\partial^2 \phi}{\partial t^2} + (\nabla \phi \cdot \nabla) \frac{\partial \phi}{\partial t} \right)$$

and taking the gradient of Bernoulli's equation:

$$\nabla a^2 = -(\gamma - 1) \left(\nabla \frac{\partial \phi}{\partial t} + (\nabla \phi \cdot \nabla) \nabla \phi \right)$$

and substituting into the above equation yields:

$$a^2 \nabla^2 \phi - \frac{\partial^2 \phi}{\partial t^2} - 2 \nabla \phi \cdot \nabla \frac{\partial \phi}{\partial t} - \nabla \phi \cdot (\nabla \phi \cdot \nabla) \nabla \phi = 0$$

or more concisely:

$$a^2 \nabla^2 \phi = \frac{\partial^2 \phi}{\partial t^2} + \left[\frac{\partial}{\partial t} + \frac{1}{2} (\nabla \phi \cdot \nabla) \right] (\nabla \phi)^2$$

4.2.1 Linearized Potential Equation (Unsteady Prandtl-Glauert)

It applies to steady uniform free-stream flow. Body produces small perturbation unsteady velocities that decay rapidly with distance upstream.

$$U = \nabla \phi = \nabla \phi_\infty + \nabla \phi' = i(U + u) + jv + kw$$

Where: $\nabla \phi_\infty = iU$, and $\nabla \phi' = iu + jv + kw$

Thus:

$$\frac{\partial \phi}{\partial t} = \frac{\partial \phi'}{\partial t}, \quad \frac{\partial^2 \phi}{\partial t^2} = \frac{\partial^2 \phi'}{\partial t^2}, \quad \nabla^2 \phi = \nabla'^2 \phi' \quad \text{and}$$

$$(\nabla \phi)^2 = (\nabla \phi')^2 + 2U \frac{\partial \phi'}{\partial x} + U^2$$

Substituting these into the full potential equation yields:

$$a^2 \nabla'^2 \phi' = \frac{\partial^2 \phi'}{\partial t^2} + \left(\frac{\partial}{\partial t} + \frac{1}{2} (\nabla \phi' \cdot \nabla) \right) (\nabla \phi')^2 + 2U \frac{\partial \phi'}{\partial x} + U^2$$

Expanding the equation yields the nonlinear full potential equation in the perturbational potential:

$$a^2 \nabla'^2 \phi' - \frac{\partial^2 \phi'}{\partial t^2} = 2 \nabla \phi' \cdot \frac{\partial \nabla \phi'}{\partial t} + 2U \frac{\partial^2 \phi'}{\partial x \partial t} + 2U (\nabla \phi' \cdot \nabla) \frac{\partial \phi'}{\partial x} + \nabla \phi' \cdot (\nabla \phi' \cdot \nabla) \nabla \phi' + U^2 \frac{\partial^2 \phi'}{\partial x^2}$$

Discarding all nonlinear terms leads to:

$$\frac{\partial^2 \phi'}{\partial t^2} + 2U \frac{\partial^2 \phi'}{\partial x \partial t} + U^2 \frac{\partial^2 \phi'}{\partial x^2} = a^2 \nabla^2 \phi'$$

The equation is normally rewritten as follows:

$$(1 - M^2) \frac{\partial^2 \phi'}{\partial x^2} + \frac{\partial^2 \phi'}{\partial y^2} + \frac{\partial^2 \phi'}{\partial z^2} = \frac{1}{a^2} \left(\frac{\partial^2 \phi'}{\partial t^2} + 2U \frac{\partial^2 \phi'}{\partial x \partial t} \right)$$

which is the linearized unsteady Prandtl-Glauert equation.

Where $M = U/a$, the Mach number. For supersonic speeds, $M > 1.0$, the equation is elliptic in the spatial coordinate.

4.2.2 The Linearized Unsteady Bernoulli Equation

To go with the linear unsteady Prandtl-Glauert equation and to preserve linearity of the AIC matrix is the linearized unsteady Bernoulli equation:

$$\Delta p = p - p_s = -\rho_s \left(\frac{\partial \phi'}{\partial t} + U \frac{\partial \phi'}{\partial x} \right)$$

Before these equations can be solved the boundary, initial and uniqueness conditions must be specified.

4.3 BOUNDARY CONDITIONS

Boundary conditions on the surface of a moving body, see Figure 4-2, may be described by:

$$\frac{DF}{Dt} = 0$$

where:

$$F(r, t) = C$$

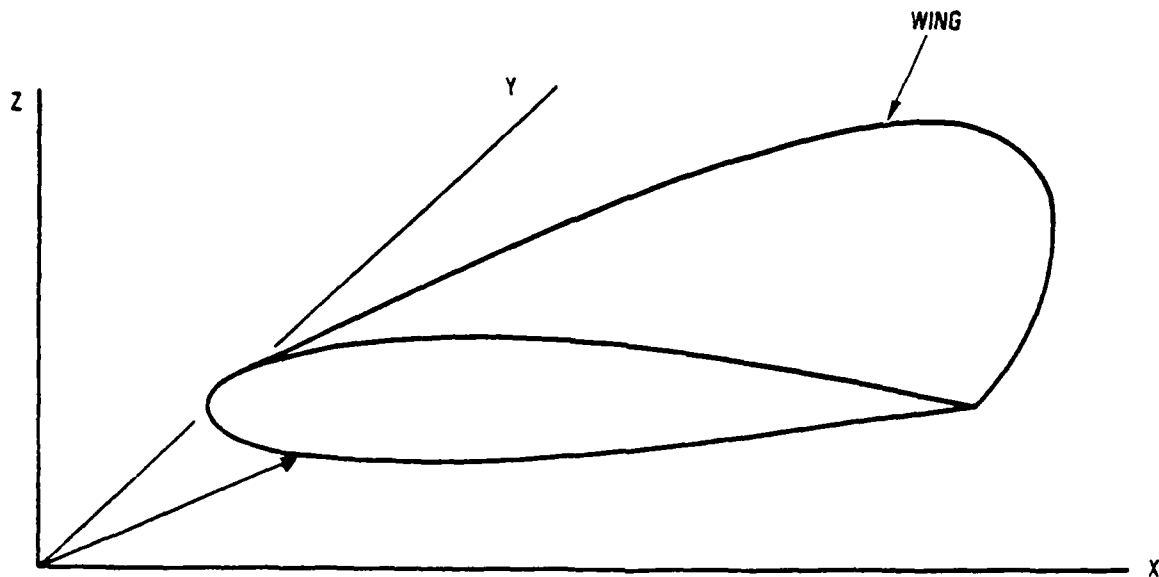


Figure 4-2. Body Defined by the Function $F(r,t) = 0$

is the function that describes the surface of the body and C may be zero or a constant.

Substituting F into the boundary condition equation and expanding yields:

$$\frac{\partial F}{\partial t} + \mathbf{u} \cdot \nabla F = 0$$

$$\frac{\partial F}{\partial t} + (U + u') \frac{\partial F}{\partial x} + v \frac{\partial F}{\partial y} + w \frac{\partial F}{\partial z} = 0$$

For example, with the body described by: $z = f(x,y,t)$, the function F becomes:

$$F(r,t) = z - f(x,y,t) = 0$$

The boundary condition becomes:

$$-\frac{\partial f}{\partial t} - (U + u') \frac{\partial f}{\partial x} - v \frac{\partial f}{\partial y} + w = 0$$

or

$$w = \frac{\partial f}{\partial t} + (U + u') \frac{\partial f}{\partial x} + v \frac{\partial f}{\partial y}$$

For a flat-plate lifting surface by linearized theory:

$$w = \frac{\partial z}{\partial t} + U \frac{\partial z}{\partial x} \quad \text{where } z \text{ is the structural deflection}$$

4.4 METHODS OF THE EQUATIONS SOLUTION

With a range of fluid motion equations available of varying capability and complexity, and with the principles for determining the boundary conditions understood, it becomes necessary to choose the equations that suit the problem. An appropriate analysis method is then found or created for that equation set.

The method of solution should be selected from the options listed in ascending order of complexity. These roughly parallel the original chronological development.

Methods for solving the simpler equations are listed first, thus laying a foundation for the more demanding methods needed by the more comprehensive equations. Some solution methods are as follows, each listed under its appropriate fluid motion equation:

- Incompressible Equation (Laplace).
 - Vortex Lattice (2-D Steady Lifting Surface).
 - IAMA (Incompressible Arbitrary Motions Aerodynamics).
- Linearized Potential Equation (Prandtl-Glauert).
 - Subsonic (Elliptical)
 - o USSAERO, DPM
 - o DOUBLET LATTICE METHOD (DLM) (unsteady).

- Supersonic (Hyperbolic).
 - o QUADPAN (Steady Panel).
 - o POTENTIAL GRADIENT (Unsteady Multiple Interfering Lifting Surfaces).
 - o MBOX, Harmonic Grad, DPM, Supersonic Kernel F.
- Full Potential Equation.
- Euler Equations.
- Navier-Stokes Equations.

4.4.1 Incompressible Equation (Laplace)

Introduction

Solutions of steady and unsteady lift distribution of surfaces may be expressed in terms of a number of elementary functions, that individually satisfy Laplace's equation. Each describes the spatial distribution of a scalar potential field. The corresponding gradient (or velocity) distributions approximate observable physical flows. Functions describing uniform flow and the flow fields resulting from the following elementary flow generating devices are described and discussed:

- Source (and Sink)
- Doublet
- Vortex

New functions formed by the superposition of elementary potential functions will also satisfy the linear Laplace equation and result in physically realizable flows. It is also permissible to construct solutions by superimposing elementary velocity fields and this is often more easily visualized.

In final combined solutions large velocities are admissible. If large, compared to the mean flow velocity, the "strong" Bernoulli's equation must be employed rather than the linearized version to obtain pressures in the flow.

Since Laplace's equation is time-independent, the gradient of the potential field at a point describes either a steady velocity or an instantaneous velocity changing with time. If the boundary and uniqueness conditions are satisfied and the resulting potential field satisfies Laplace's equation at that point in time the kinematics of the flow are valid independently of time.

Due to the discrete nature and finite strengths of the elementary flow generating devices - source, doublet and vortex - the corresponding functions are singular at the centers of their spatial location. As long as the devices can be employed as discrete elements and the boundary conditions met at points other than the points of origin, then the singularities cause no problem in numerical analysis. If, however, the devices are arranged in distributed fashion along filaments, in sheets, or throughout volumes, then integration may become singular and special means must be employed.

The devices are employed as discrete elements arranged in a pattern dictated by the geometry of the immersed lifting surface. The problem to be solved is the determination of the element strengths that satisfy the surface timewise varying boundary and uniqueness conditions. The timewise history of element strengths then defines the flow kinematic behavior. The forces acting on the body are determined from this by Bernoulli's equation.

Uniform Flow

If the coordinate axes are fixed near the immersed body and translate with it at a mean vehicle speed, U , the uniform flow potential function is:

$$\phi = Ux + C$$

The gradient of this scalar function

$$\nabla\phi = iU + j(o) + k(o)$$

is the freestream vector velocity.

4.4.1.1 Source (and Sink)

The potential function of a unit source, $m = 1.0$ (i.e., emitting a volume flow of 1.0 cubic ft/second), located at the origin is as follows:

$$\phi = -\frac{1}{4\pi r} ; r = \sqrt{x^2 + y^2 + z^2}$$

where r is the radial distance to any point.

The velocity vector from a source will always be directed radially, therefore, and is given by:

$$v_r = \frac{\partial \phi}{\partial r} = \frac{1}{4\pi r^2}$$

The flow velocity from a three-dimensional or spherical source, therefore, reduces as the reciprocal of square of the distance from its point of origin. It should be noted that the volume flow from the source must be equal to the product of flow velocity and surface area at any radial station.

$$\text{Volume flow} = v_r S = \frac{1}{4\pi r^2} \times 4\pi r^2 = 1.0 \text{ ft}^3/\text{sec}$$

Streamlines from a source radiate in straight lines from the point of origin, therefore, a source can induce no velocity in a plane passing through its origin. For this reason sources are not used for modeling lifting surfaces. The principal use of sources and sinks is to give thickness to bodies and wings. For example, a source in a uniform flow produces a flow about a shape resembling the front end of a body at zero angle-of-attack.

A sink is a negative source in which the flow velocity vector is directed toward the origin.

4.4.1.2 Doublet

A doublet may be formed by allowing a source and a sink of equal strength to approach one another with the strengths increasing as the distance between them decreases so that the product of strength and intervening distance remains constant.

Let a source of strength, m , be located a distance $\Delta z/2$ above the plane, $z = 0$, at the origin and a sink of equal magnitude be located the same distance below the plane. The strength of the doublet so formed is defined as

$$\mu = m \Delta z$$

and the units of μ is $\frac{\text{ft}^3}{\text{sec}} \times \text{ft} = \frac{\text{ft}^4}{\text{sec}}$

The equation of the potential function of the doublet may be obtained from that of the source and sink by combining them and finding the limit:

$$\phi_{\text{doublet}} = -\mu \frac{\partial \phi}{\partial z} \quad \text{unit source}$$

Therefore, the unit doublet potential function is:

$$\phi_d = \frac{\partial}{\partial z} \left(\frac{1}{4\pi r^2} \right)$$

$$\phi_d = \frac{-z}{4\pi r^3} ; r = \sqrt{x^2 + y^2 + z^2}$$

for z below the plane and $x = y = 0$, ϕ is positive, as z approaches the plane the function becomes infinite, switches to negative infinity above the plane and is negative above.

The velocity component normal to the plane is given by:

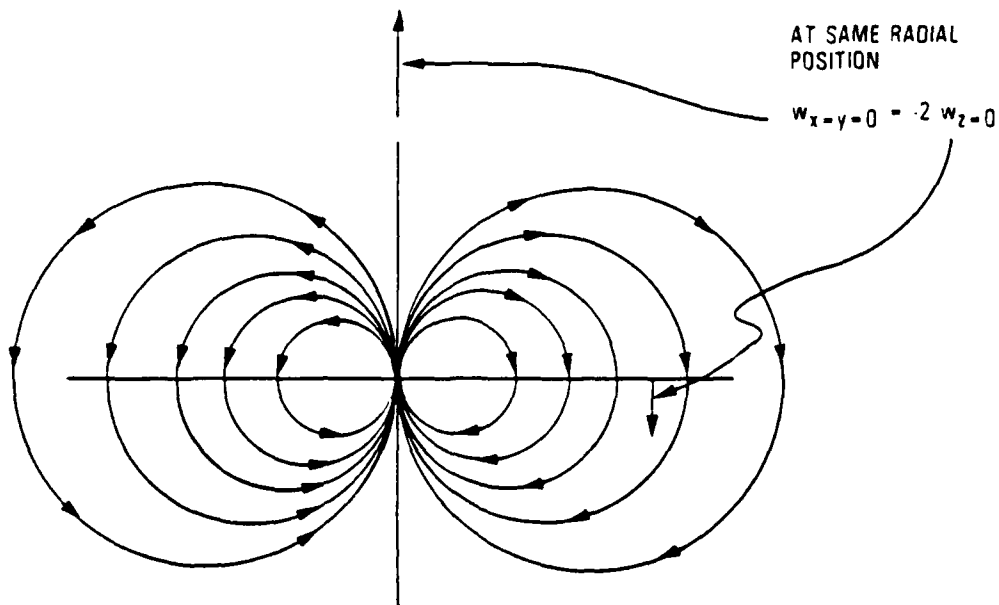
$$w = \frac{\partial \phi_d}{\partial z} = \frac{1}{4\pi r^3} \left(\frac{3z^2}{r^2} - 1 \right)$$

for $z = 0$ (i.e., velocity normal to x,y plan)

$$w = \frac{\partial \phi_d}{\partial z} = - \frac{1}{4\pi r^3}$$

for $x = y = 0$

$$w = \frac{\partial \phi_d}{\partial z} = + \frac{1}{2\pi r^3}$$



When $z = 0$ $\phi_d = 0$ so $\partial \phi_d / \partial x = \partial \phi_d / \partial y = 0$ and the map of streamlines is as shown above.

The doublet just described is physically like a tiny actuator disk (or propeller) that pulls in fluid from below the plane $z = 0$ and discharges into the region above. It neither adds nor subtracts fluid from the flow as do the source and sink.

Doublets are often distributed over lifting surface elements and are particularly useful for modeling thin surfaces of arbitrary planform.

Consider the characteristics of the uniform distribution of doublet strength over an area, Γ . The equivalent doublet on an increment of area is given by

$$\mu = \Gamma \, dx \, dy$$

and since μ has the dimensions ft^4/sec , Γ has the dimensions ft^2/sec .

A uniform distribution of doublet strength over an area is exactly equivalent to a ring of concentrated vorticity or a vortex encircling the region.

Some of the present applications employ concentrated, or discrete vortices running along lines, only. Any surface element of arbitrary shape lying in a plane, that supports a uniform distribution of doublet strength, Γ , may be replaced by a vortex of strength, Γ , running continuously about its periphery.

Remembering the equivalence between sheets of uniform doublet strength and circumscribing vortices permits the establishment of important laws governing discrete vortices.

4.4.1.3 Vortex

The vortex that occurs at the discontinuous edge of a constant doublet field is of a constant strength along its length. This is known as Helmholtz's first theorem.

Vortices often form closed endless filaments or rings. If the edge of the element of fluid supporting the doublet distribution was flowing past a wall, the mirror image of the flow on the other side of the wall would continue the vortex. The vortex then would appear to terminate at the wall. That the vortex filament must be endless or terminate at a wall is Helmholtz's second theorem.

In a vortex the tangential velocity is constant on a circle of radius r about an infinitely long two-dimensional vortex.

$$\text{Velocity} = \frac{\Gamma}{2\pi r}$$

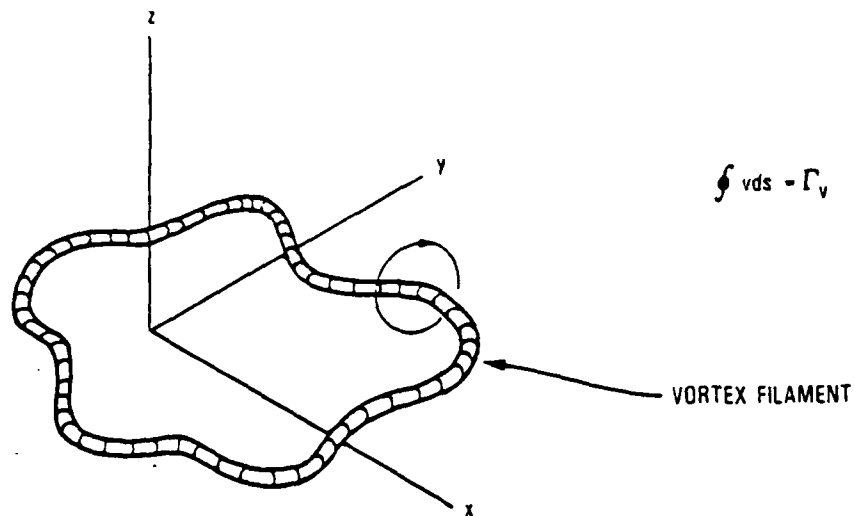
where Γ is the circulation of the vortex.

Any closed line integral of the velocity vector component, \bar{V} , along the line following any path that encloses the origin must equal, Γ .

$$\oint \bar{V} \cdot d\bar{s} = \Gamma$$

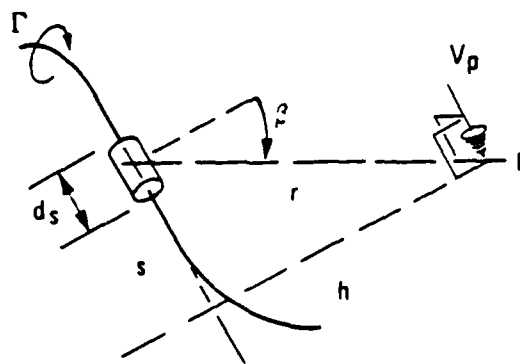
In general, a closed line integral of local fluid velocity component times line element length that encircles any closed vortex filament will yield the circulation of the filament.

Before leaving the vortex subject there is one last item of importance. To aid in the computation of the velocity field of complicated snakelike vortices, such as shown in the sketch below, the Biot-Savart Law may be employed. It is noted that a complicated vortex may be broken into a number of small equivalent elements and the flow fields of all pieces combined to yield the total complicated flow field.



An element of a vortex of strength, Γ , and length, ds , induces a velocity, dV_p , at Point p , normal to the plane formed by the radius, r , from the element to the Point p and the axis of the vortex element, according to the Biot-Savart Law:

$$d V_p = \frac{\Gamma}{4\pi} \frac{\cos\beta}{r^2} ds$$



where β is the angle between the radius to Point p and the normal to the vortex element in the above plane.

The Biot-Savart Law may be expressed in an alternative form by noting

$$\frac{s}{r} = \sin \beta; \quad \frac{h}{r} = \cos \beta$$

so that

$$\frac{s}{h} = \frac{\sin \beta}{\cos \beta}$$

and

$$\frac{ds}{h} = \frac{\cos^2 \beta + \sin^2 \beta}{\cos^2 \beta} d\beta = \frac{d\beta}{\cos^2 \beta}$$

Substituting the results

$$ds = \frac{h}{\cos^2 \beta} d\beta$$

and

$$r = \frac{h}{\cos \beta}$$

into the Biot-Savart equation gives

$$dV_p = \frac{\Gamma}{4\pi} \frac{\cos \beta}{h} d\beta$$

Example:

A straight line vortex is extending to infinity in both directions. The induced velocity at Point "p" a distance, h, from the vortex is:

$$V_p = \frac{\Gamma}{4\pi r} \int_{-\pi/2}^{\pi/2} \cos \beta d\beta$$

$$V_p = \frac{\Gamma}{2\pi h}$$

4.4.2 2-D Vortex Lattice Method

The 2-D Vortex Lattice method illustrates the means by which the chordwise distribution of lift is affected by the shape of the mean camber line, Figure 4-3, in incompressible flow:

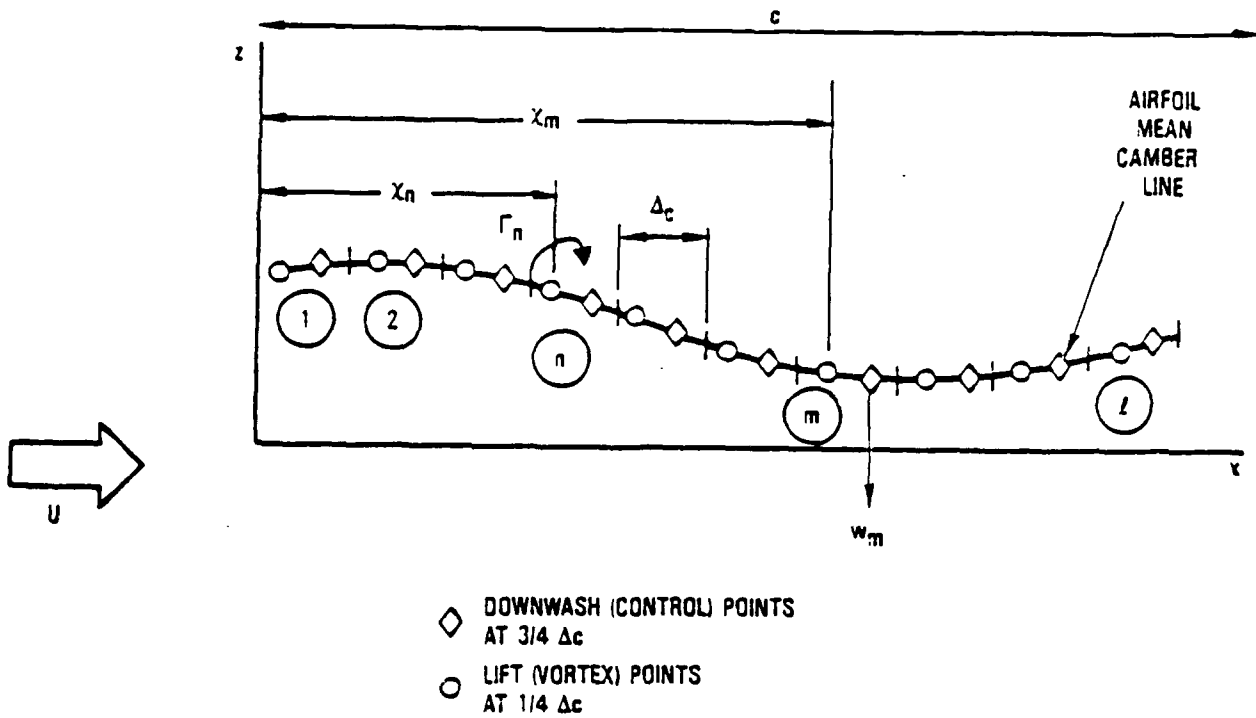


Figure 4-3. Incompressible, Steady, 2-D, Airfoil

Boundary Conditions at Control Points:

$$\begin{pmatrix} w_1 \\ w_2 \\ \vdots \\ w_k \end{pmatrix} = - \left[\begin{pmatrix} \frac{\partial z_1}{\partial t} \\ \frac{\partial z_2}{\partial t} \\ \vdots \\ \frac{\partial z_k}{\partial t} \end{pmatrix} + U \begin{pmatrix} \frac{\partial z_1}{\partial x} \\ \frac{\partial z_2}{\partial x} \\ \vdots \\ \frac{\partial z_k}{\partial x} \end{pmatrix} \right]$$

It should be noted that the first term in the R.H.S. of the above equation is zero for steady motion.

Aerodynamic Influence Coefficients (AIC):

$$W_m = \sum_{n=1}^k \frac{1}{2\pi(x_m + \frac{\Delta c}{2} - x_n)} \Gamma_n, \quad \text{i.e.,} \quad \begin{pmatrix} w_1 \\ w_2 \\ \vdots \\ w_k \end{pmatrix} = [\text{AIC}] \begin{pmatrix} \Gamma_1 \\ \Gamma_2 \\ \vdots \\ \Gamma_k \end{pmatrix}$$

This implies that

$$\text{AIC}_{mn} = \frac{1}{2\pi(x_m + \frac{\Delta c}{2} - x_n)}$$

Differential pressure coefficient across element n is given by

$$\Delta C_{p_n} = \frac{\rho \Gamma_n U}{\frac{\rho}{2} U^2}$$

$$\begin{pmatrix} \Delta C_{p_1} \\ \Delta C_{p_2} \\ \vdots \\ \Delta C_{p_k} \end{pmatrix} = \frac{\frac{\rho U}{\Delta c}}{\frac{\rho}{2} U^2} [\text{AIC}]^{-1} \begin{pmatrix} w_1 \\ w_2 \\ \vdots \\ w_k \end{pmatrix} = \frac{2}{\Delta c} [\text{AIC}]^{-1} \begin{pmatrix} \frac{\partial z_1}{\partial x} \\ \frac{\partial z_2}{\partial x} \\ \vdots \\ \frac{\partial z_k}{\partial x} \end{pmatrix}$$

EXAMPLE:

Let the airfoil experience a uniform unit angle-of-attack:

$$\frac{\partial z_1}{\partial x} = \frac{\partial z_2}{\partial x} = \dots = \frac{\partial z_k}{\partial x} = -1.0, \quad k = 20, \quad \Delta c = \frac{1}{20}, \quad c = 1.0$$

For this example, the pressure distribution is given by

$$\begin{pmatrix} \Delta C_{p_1} \\ \Delta C_{p_2} \\ \vdots \\ \vdots \\ \Delta C_{p_k} \end{pmatrix} = \frac{2}{\Delta c} [\text{AIC}]^{-1} \begin{pmatrix} 1.0 \\ 1.0 \\ \vdots \\ \vdots \\ 1.0 \end{pmatrix}$$

as shown in Figure 4-4.

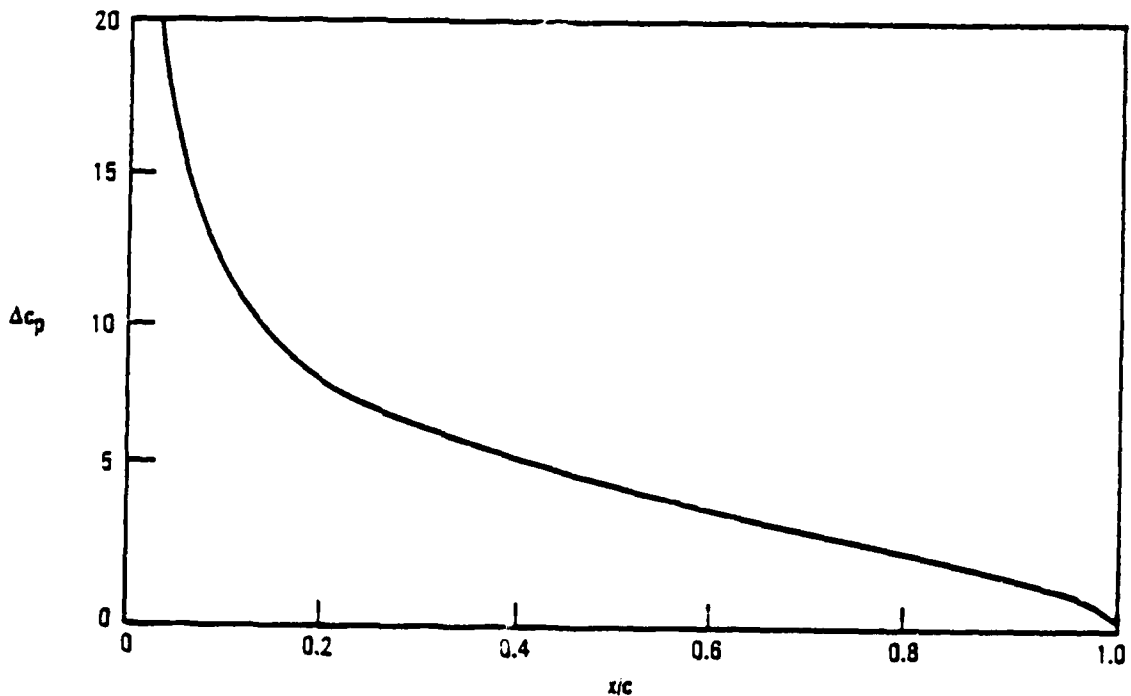


Figure 4-4. Chordwise Lift Distribution Due to Unit Angle-of-Attack

The Incompressible Arbitrary Motions Aerodynamics (IAMA) Method

This method illustrates the means by which a vortex lattice method may be employed to find the unsteady lift distribution on a low aspect ratio lifting surface. The surface may have any timewise and spatial distribution of slope and normal velocity. First the surface is divided into equal sized elements, as shown in Figure 4-5. A lift point is placed at the midpoint of each quarter chord line and a control point at each three-quarter chord line.

Ring vortices are placed on the surface and wake elements as shown in Figure 4-6.

A typical wing and wake is shown in Figure 4-7. A time-domain analysis yields the left distribution shown in Figure 4-8, and Figure 4-9 is the response to a step plunge velocity.

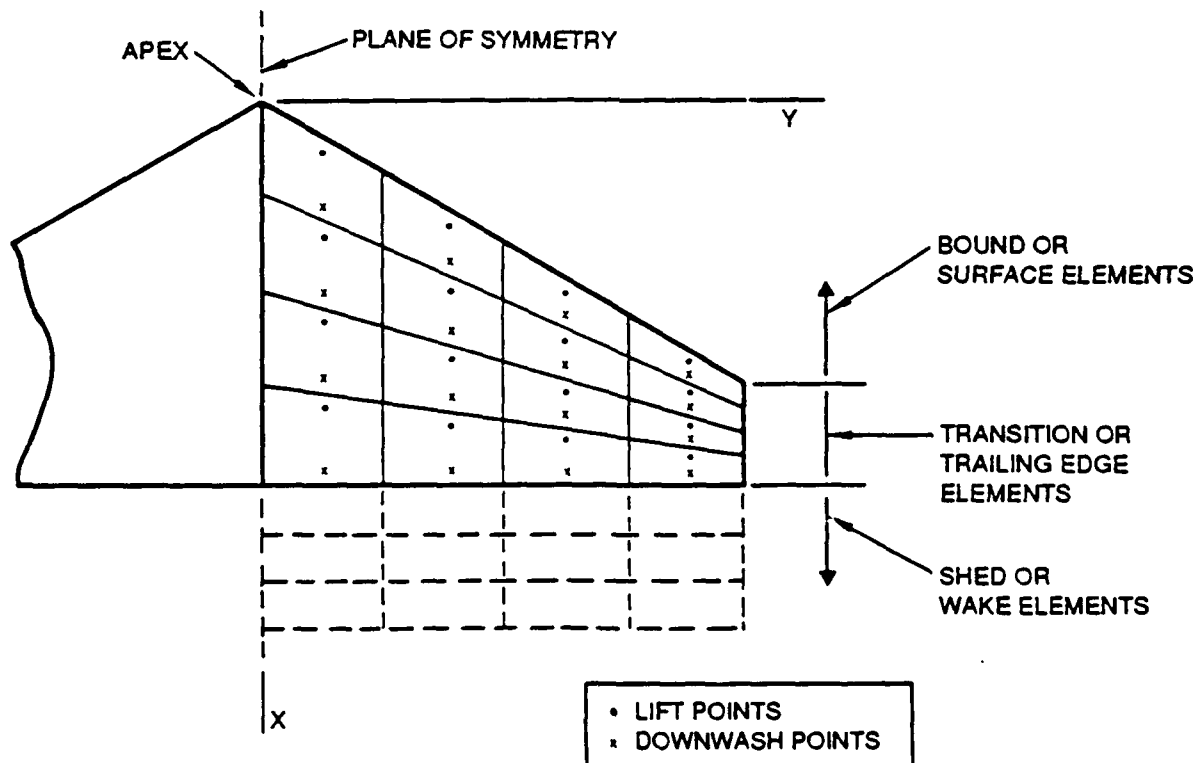


Figure 4-5. Surface and Wake Representation

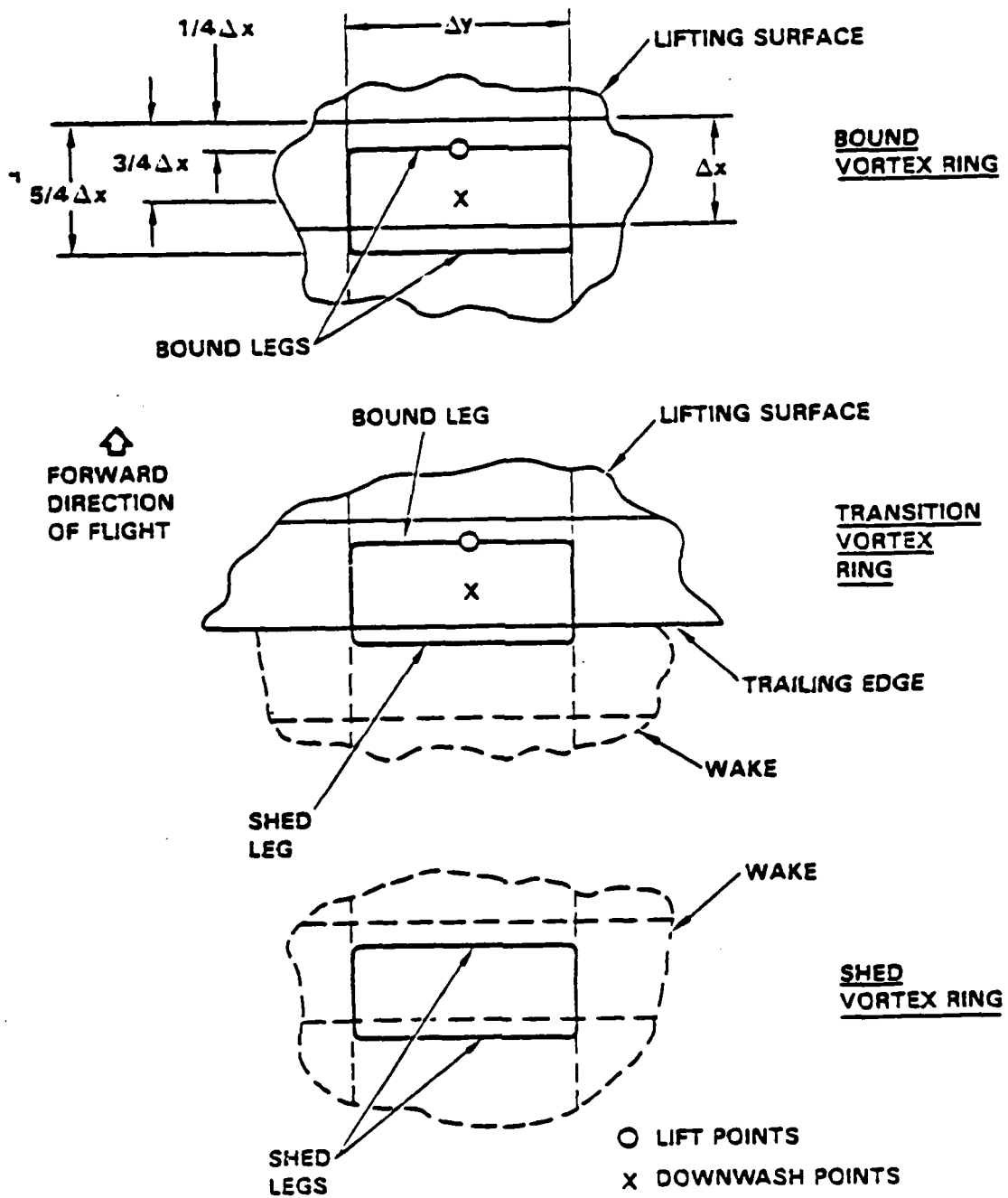


Figure 4-6. Ring Vortex Geometric Specification

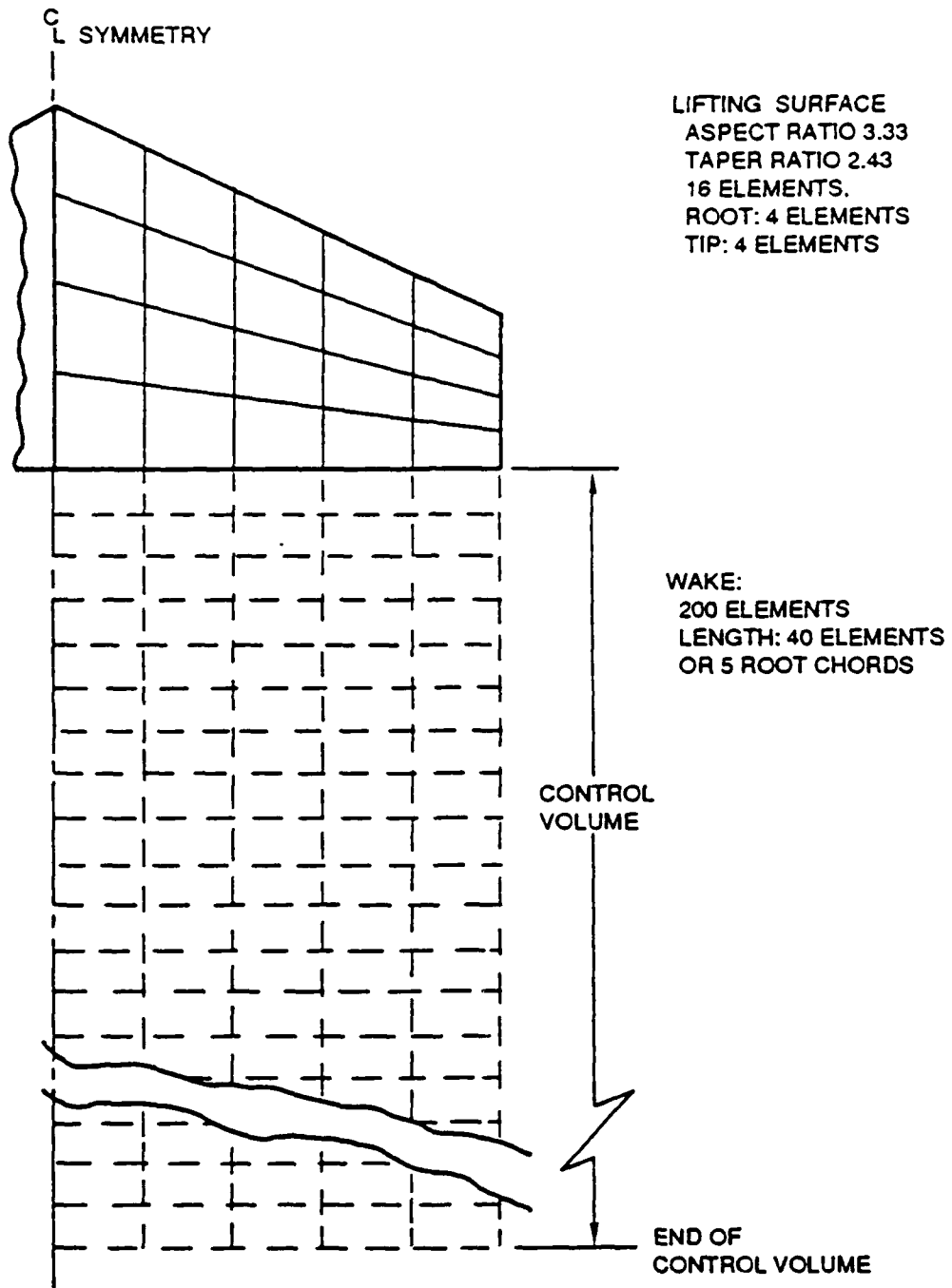


Figure 4-7. Typical Wing and Wake Model

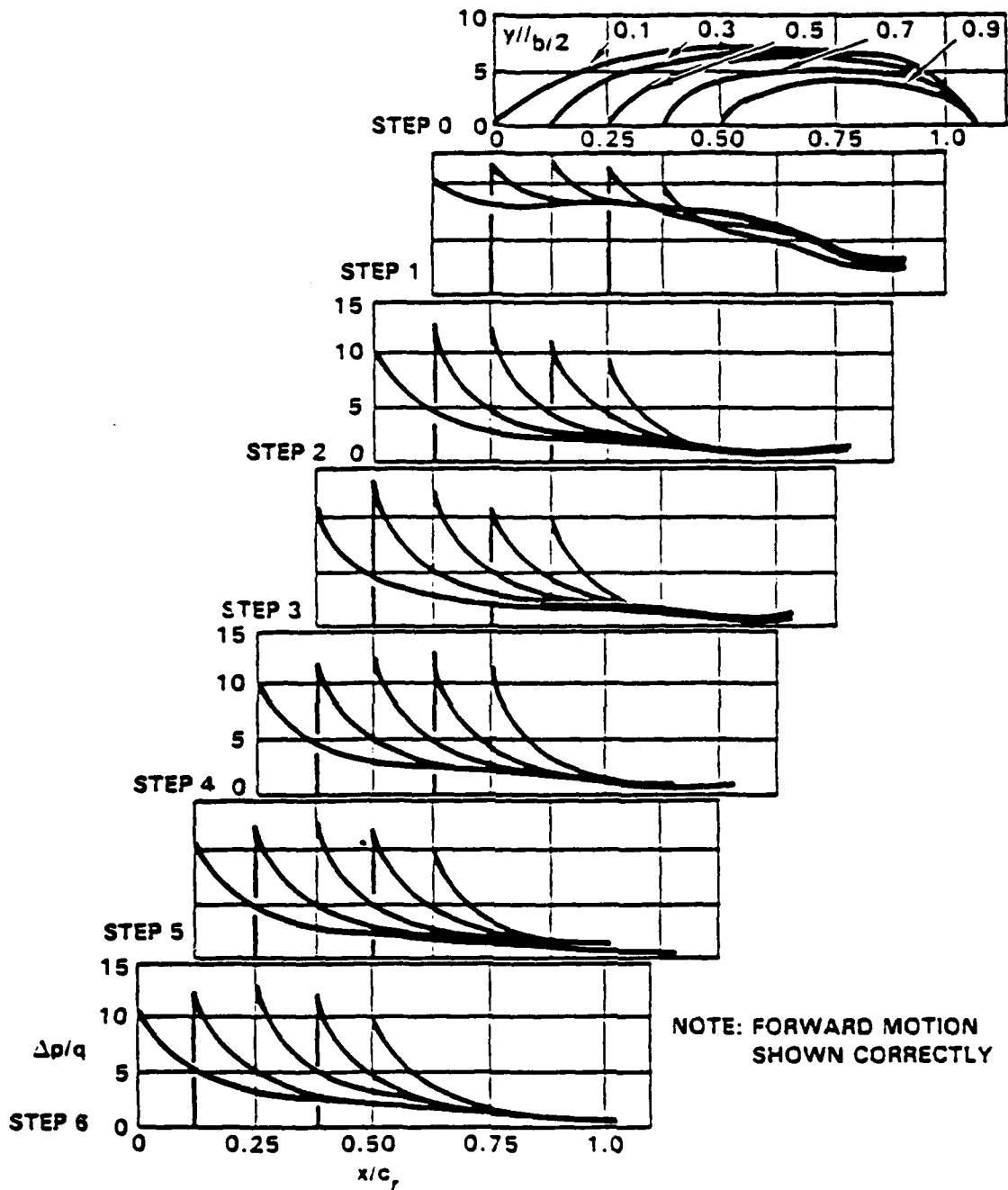


Figure 4-8. Pressure Distributions versus Time for the Indicial Response of a Wing of Aspect Ratio 3.33 and Taper Ratio 2.43

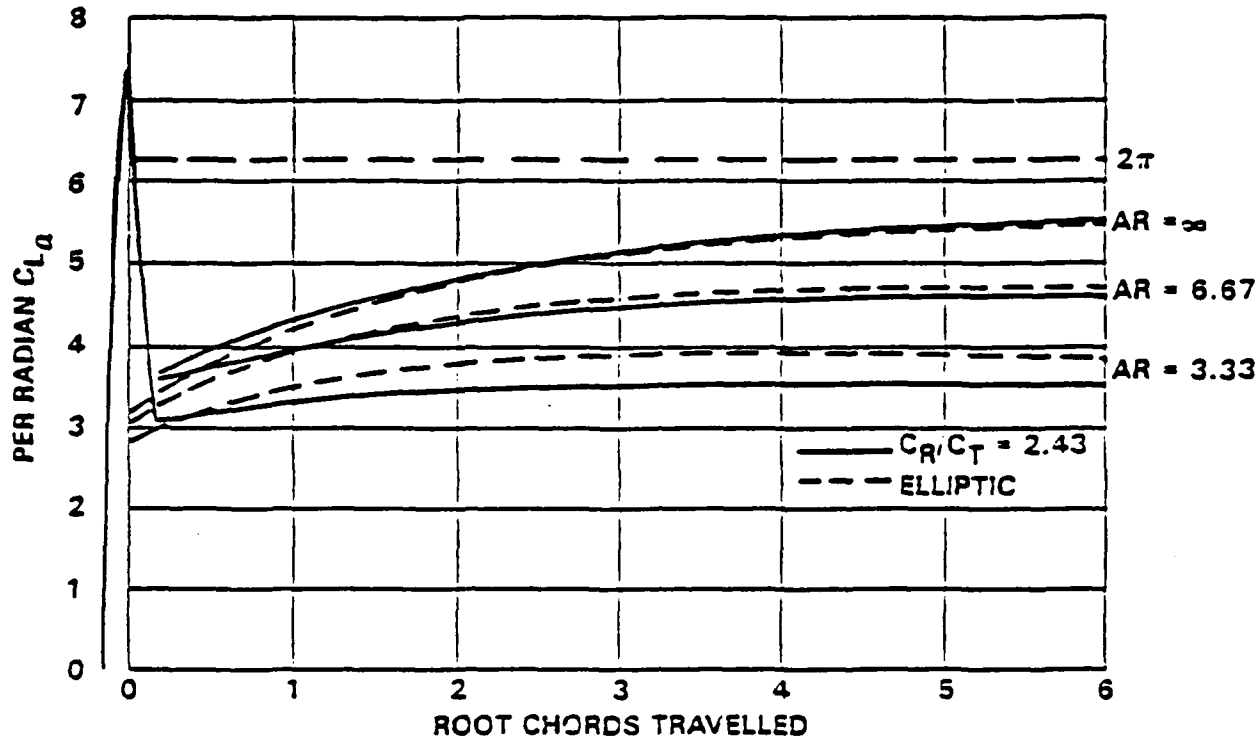


Figure 4-9. Indicial Lift versus Aspect Ratio

By use of the Biot-Savart relations given in previous section, the downwash, w , is related to the bound, transition and shed vortex strengths as follows:

$$\begin{matrix}
 \{w\} = \begin{pmatrix} w_{\Gamma_{b,t}} \\ \vdots \\ w_{\Gamma_s} \end{pmatrix} & \begin{pmatrix} \Gamma_{b,t} \\ \vdots \\ \Gamma_s \end{pmatrix} \\
 \text{nx1} & \begin{matrix} \text{nxn} & \text{nxm-n} \\ \text{mx1} \end{matrix}
 \end{matrix}$$

The downwash required at step, p , is given according to the boundary condition specification in Section 4.3 by:

$$\{w(p)\} = \{\partial z / \partial t(p)\} + U \{\partial z / \partial x(p)\}$$

Determination of ring vortex strengths, by satisfaction of boundary conditions at time step $p = 1$, is given by:

$t = x/U$ is the increment in the time between the points at which boundary conditions are satisfied.

$$\begin{pmatrix} \Gamma_{b,t}(1) \\ \vdots \\ \vdots \end{pmatrix}_{nx1} = \begin{pmatrix} w_{b,t} \\ \vdots \\ \vdots \end{pmatrix}_{nxn}^{-1} \{w(1)\}_{nx1}$$

p represents the p^{th} time step in a sequence.

Determination of strengths increments at time step $p = 2$.

$$\begin{pmatrix} \Delta\Gamma_{b,t}(2) \\ \vdots \\ \vdots \end{pmatrix}_{nx1} = \begin{pmatrix} \Gamma w_{b,t} \\ \vdots \\ \vdots \end{pmatrix}_{nxn}^{-1} \{w(2)\}_{nx1} - \{w(1)\}_{nx1} - w_{s_{nx(m-n)}} \begin{pmatrix} \Gamma_r(1) \\ 0 \\ 0 \\ \vdots \\ \vdots \end{pmatrix}_{m-nx1}$$

Total wing ring strength:

$$\{\Gamma_{b,t}(p)\} = \{\Gamma_{b,t}(p-1)\} + \{\Delta\Gamma_{b,t}(p)\}$$

Ring strength history is converted to differential pressure by the unsteady Bernoulli equation:

$$\Delta p = \rho[U\partial\Gamma/\partial x + \partial\Gamma/\partial t]$$

4.4.3 Linearized Potential Equation

Doublet Lattice Method

The DLM, see Reference [8], is employed in high subsonic speed flutter and atmospheric turbulence response.

Gridding

The method applies to wing, tail, control surfaces, flow-through nacelles, and body, if each can be represented as a combination of zero thickness flat panels (of any planform), that have no initial or steady-state inclination to the free-stream flow. The wire-frame geometry of the panels is such that it lies parallel to and does not deform the flow.

Flow inclinations are achieved solely by enforcing boundary conditions at one control point in each areal element into which the panels are divided. This has been called the "venetian blind" model. The major panels may have relative dihedral and vertical separation between them.

Panels are defined as lying in a single plane. The contiguous elements making up the panel must be arranged in chordwise strips, each of constant width, from leading edge to trailing edge, but elements in each strip may have varying leading- and trailing-edge sweep and chord length. Panels then are usually chosen to nest within the wing outline, with boundaries along control surface hinge lines. Control surface elements are treated the same way as other elements (these rules also apply to the Supersonic Potential Gradient Method (PGM) and ZONA 51).

Though no panels are required on lifting surface wakes (wake effects being included in the acceleration-potential methodology), two surfaces may not lie one-behind-the-other unless strips of elements have continuous width over the two surfaces. (This is because singularities stream behind the strip side edges and give spurious induced downwash on following-surface control points if they do not lie midway between edges.)

If it is not practical to keep strip widths continuous, the problem can be avoided by raising or lowering the second surface about one and one half strip widths relative to the forward surface. This small gap will usually not make a significant change to the results, since chordwise velocity perturbations are not employed in the method.

Bodies should be modeled as cruciform flat plates, looking forward. Some analysts have used a series of ring-wings of different radii fore and aft to represent tapering fuselages, but the calculated lifts on these elements must be reduced by a factor (usually 0.5), to account for the fact that the physical flow is not swallowed by these rings. This practice, however, is not recommended since in the event that the body cross-section is not circular, some other unknown factor would be more appropriate.

In the case of flow-through engine nacelles of any cross-section shape, however, no correction is needed and paneling that follows the shape is recommended.

The lift force on each panel element is assumed to be concentrated uniformly along a straight line across the quarter chord and is directed normal to the undeformed surface. The control points lie on element centerlines at the $3/4$ element chord position.

Method Description

The DLM is designed to treat discrete frequencies of oscillation, one at a time. The method assumes that all surface elements of the airplane are oscillating at this frequency, though not necessarily in phase. The frequency is non-dimensionalized so that model motions will synchronize with the drifting flow vorticity in the same way as they would on the full scale airplane regardless of scale or wind speed. The nondimensional frequency is called a "reduced frequency" or Strouhal number which is defined as the ratio of frequency in radians/second to numbers of passages of a reference length per second, i.e.:

$$k = \frac{\omega}{U/c} = \frac{\omega c}{U} \quad \text{radians/chord}$$

where c may be delta-wing root chord or conventional wing semi-chord at the 3/4 semi-span, and U is the flight speed.

Motions of the aircraft are specified at the control points, in matrix form, as

$$\begin{pmatrix} z_1 \\ z_2 \\ \vdots \\ z_k \end{pmatrix} = \begin{pmatrix} z_{10} \\ z_{20} \\ \vdots \\ z_{k0} \end{pmatrix} e^{i\omega t}$$

and are resolved into local angle of attack as discussed in the boundary conditions subsection:

$$\begin{aligned} \langle \alpha \rangle &= \frac{1}{U} \left\langle \frac{\partial z}{\partial t} \right\rangle + \left\langle \frac{\partial z}{\partial x} \right\rangle \\ &= \left(\frac{i\omega}{U} + \frac{\partial}{\partial x} \right) z \end{aligned}$$

The objective of the DLM is to find the matrix relationship between the induced velocities at each control point on the whole configuration and the sinusoidal oscillations of lift point on each element.

$$\begin{pmatrix} \alpha_1 \\ \alpha_2 \\ \vdots \\ \alpha_n \end{pmatrix} = \begin{bmatrix} a_{11} & a_{12} & \cdots & a_{1n} \\ a_{21} & a_{22} & \cdots & a_{2n} \\ \vdots & \vdots & \ddots & \vdots \\ a_{n1} & a_{n2} & \cdots & a_{nn} \end{bmatrix} \begin{pmatrix} l_1 \\ l_2 \\ \vdots \\ l_n \end{pmatrix}$$

where

$$d = \Delta p \Delta s$$

Δp is the differential pressure across the surface element, and Δs is the element area.

If the complex matrix $\begin{pmatrix} \alpha_1 \\ \alpha_2 \\ \cdot \\ \cdot \\ \cdot \\ \alpha_n \end{pmatrix}$ is known over the vehicle, then the complex

lift force is given by:

$$\begin{pmatrix} 1 \\ 2 \\ \cdot \\ \cdot \\ \cdot \\ n \end{pmatrix} = \underbrace{\begin{bmatrix} A_{11} & A_{12} & \dots & A_{1n} \\ A_{21} & A_{22} & \dots & A_{2n} \\ \cdot & & & \\ \cdot & & & \\ \cdot & & & \\ A_{n1} & A_{n2} & \dots & A_{nn} \end{bmatrix}}_{\text{[AIC]}} \begin{pmatrix} \alpha_1 \\ \alpha_2 \\ \cdot \\ \cdot \\ \cdot \\ \alpha_n \end{pmatrix}$$

[AIC] = Aerodynamic Influence Coefficients

and it fits into the linearized equations of aircraft motion, including structural motions as:

$$[M] \{\ddot{\alpha}\} + [K] \{\alpha\} - [AIC] \{\alpha\} = 0$$

The equation is usually written in terms of the structural modes (mass-stiffness). This causes the mass and stiffness matrices to become diagonals but leaves the [AIC] matrix full, (it is also complex).

Theory Discussion (Doublet Lattice Method)

The DLM is based on the acceleration potential rather than on the velocity potential discussed in the previous section. Other applications of the acceleration potential are discussed in Reference [5]. The relationship between the two is as follows. The acceleration potential is based on the momentum equation:

$$\rho \frac{Du}{Dt} = -\nabla p$$

Discussion of the DLM is simpler if the Eulerian axes are assumed to reside in the zero velocity fluid so that the aircraft, in passing, induces only small velocities and position changes to air particles. Thus:

$$\rho \frac{Du}{Dt} = \rho \frac{\partial u}{\partial t} + (u \cdot \nabla)u = -\nabla p$$

may be approximated to

$$\rho \frac{\partial u}{\partial t} = -\nabla p$$

This states that the instantaneous fluid acceleration is:

$$a = -\frac{1}{\rho} \nabla p$$

Because of the small translational displacements during acceleration to the distributed velocity, at time, t , the velocity may be obtained by:

$$u(t) = \int_{-\infty}^t a(\tau) d\tau$$

or

$$u(t) = \int_{-\infty}^t -\frac{1}{\rho} \nabla p(\tau) d\tau$$

By the velocity potential method, however, the velocity is given directly by the gradient of the scalar potential, ϕ .

$$\mathbf{u} = \nabla\phi$$

The relationship of the pressure p (a scalar) to the velocity potential is as follows:

$$-\frac{1}{\rho} \nabla p = \nabla \frac{\partial\phi}{\partial t}$$

The DLM employs lines of constant strength acceleration potential doublets along the quarter-chord loci of the panel elements. These are equivalent to lines of constant lifting force per unit span across element spans. (In the DLM these strengths vary sinusoidally in time at the specified reduced frequency.)

To illustrate the behavior of such aerodynamic devices a single point acceleration potential doublet, with axis normal to the plane (x, y) of the lifting surface and whose strength remains constant with time, will be discussed. It has the same form as the velocity point doublet of Section 4.4.1.2.

First the velocity potential doublet:

$$\phi_d = -\frac{z}{4\pi r^3} \mu \quad r = \sqrt{x^2 + y^2 + z^2}$$

where strength, μ , may be thought of in terms of distributed doublet strength per unit area, Γ , which is also the circumscribing vortex strength of an elemental area of constant doublet strength. Then

$$\mu = \Gamma \, dx dy \quad dx dy \text{ is element area.}$$

The velocity component, normal to the x, y plane at zero, then is given by

$$w = \frac{\partial \phi}{\partial z} = -\frac{1}{4\pi r^3} \Gamma \, dx dy$$

and the acceleration component normal to the surface:

$$\dot{w} = \frac{\partial}{\partial z} \frac{\partial \phi}{\partial t} = -\frac{1}{4\pi r^3} \frac{\partial \Gamma}{\partial t} \, dx dy$$

A pressure field due to a pressure difference across an elemental area may be assumed to be analogous to the velocity potential field due to a doublet. Hence, from the doublet equation, the pressure (or acceleration) potential is expressed as:

$$-\frac{1}{\rho} (p) = \frac{1}{\rho} \frac{-z}{4\pi r^3} \Delta p \, dx dy$$

where Δp is the differential pressure across the doublet origin and the acceleration normal to the x, y plane at r is then:

$$\dot{w} = -\frac{1}{\rho} \frac{\partial}{\partial z} p = \frac{1}{\rho} \frac{\partial}{\partial z} \frac{-z}{4\pi r^3} \Delta p \, dx dy$$

$$\dot{w} = -\frac{1}{\rho} \frac{1}{4\pi r^3} \Delta p \, dx dy$$

and the velocity component normal to x, y plane is given by:

$$w(x, y, t) = \int_{-\infty}^t \dot{w}(\tau) d\tau = \frac{dx dy}{\rho} \int_{-\infty}^t \frac{-1}{4\pi r^3} \Delta p(\tau) d\tau$$

Before moving on to discuss the acceleration potential doublet, as it acts in the DLM, it is instructive to equate the velocity and acceleration potential expressions for parcel acceleration, a , normal to the x, y plane.

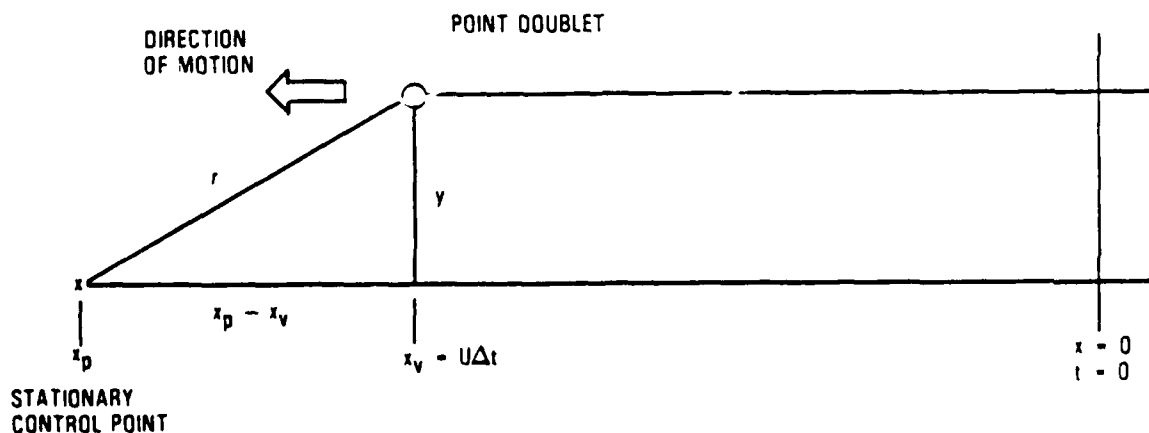
$$\begin{array}{ccc} \text{Velocity Potential} & & \text{Acceleration Potential} \\ \underbrace{\left(-\frac{1}{4\pi r^3} \frac{\partial \Gamma}{\partial t} dxdt \right)} & = & \underbrace{\left(-\frac{1}{\rho} \frac{1}{4\pi r^3} \Delta p dx dy \right)} \end{array}$$

Thus $\frac{\partial \Gamma}{\partial t} = \frac{\Delta p}{\rho}$

or $\Delta p = \rho \frac{\partial \Gamma}{\partial t}$

the well known result from compressible unsteady aerodynamics is the unsteady Bernoulli equation in stationary fluid.

It is now possible to determine the velocity, $w(x, y, t)$, at Point p , normal to the x, y plane in stationary air induced by a point doublet of constant strength moving past it at a constant speed and any subsonic Mach number. (In the DLM this point doublet would be spread out laterally across a strip width to form a finite width line doublet of the same total lift. The velocities induced by the line and point doublets would be approximately the same at control points several strip widths away. This illustrates the behavior of the DLM for steady nonoscillatory flow.)



The doublet will be assumed to come into existence at $x = 0$, $t = 0$ and to translate at speed, U , at a distance, y , laterally of Point, p . The problem is to deduce the time history of the development of normal velocity w . The doublet will be traveling at subsonic Mach number and compressibility effects are to be included.

The smooth motion of the doublet may be thought of as a series of closely spaced hops. At each point a frontal wave is sent out at the speed of sound, a , that produces a steady fluid acceleration pattern and centered at the position of the doublet. This pattern reaches Point p at a later time given by, $\frac{r}{a}$, where r is the radial distance, from the instantaneous position of the position of the doublet, to p .

It is clear that the time of arrival, τ , is given by

$$\tau = \frac{r}{a} + \frac{x_v}{U}$$

The velocity induced at Point p then is given by

$$w(x_p, t) = -\frac{\Delta p dx dy}{4\pi\rho} \int_0^t \frac{d\tau}{r^3}$$

where

$$r = \sqrt{(x_p - x_v)^2 + y^2}$$

$$x_v = U\Delta t$$

$$\tau = \frac{r}{a} + \Delta t$$

Δt and τ are dummy time measures.

Thus the two equations,

$$w(x, t) = -\frac{\Delta p dx dy}{4\pi\rho} \int_0^t \frac{1}{[(x_p - U\Delta t)^2 + y^2]^{\frac{3}{2}}} d\tau$$

$$\tau = \frac{1}{a} \sqrt{(x_p - U\Delta t)^2 + y^2} + \Delta t$$

will permit the problem to be solved.

Example:

The induced velocity, w , and acceleration, \dot{w} , are computed for $x_p = 10$, $y = 4$, and $u = 1.0$ for the three cases of $a = 5$ ($M = .2$), $a = 2$ ($M = 0.5$) and $a = 1.25$ ($M = 0.8$). The graphs for these cases for $\Delta p dx dy / 4\pi\rho = 1.0$ are shown in Figure 4-10.

In this example, it is important to note that the induced velocity increases to asymptotic level as the doublet passes by. This means that the doublet leaves a permanent wake behind it. A finite span line doublet, instead of a point, would leave a horseshoe vortex in steady flight. It should also be noted that the calculation procedure takes care of this wake automatically so that the wake need not be explicitly modeled.

An interpretation of this analysis is that, for a steady flow situation (not a sinusoidal variation of elemental lift force), we have calculated a number of elements in the reciprocal of the AIC or normalwash matrix. Suppose we consider a swept wing, flying at $M = 0.2$, $M = 0.5$ and $M = 0.8$. Its normal wash matrix was shown on Page 4-33, as

$$\{\alpha\} = [AIC]^{-1} \{l\}$$

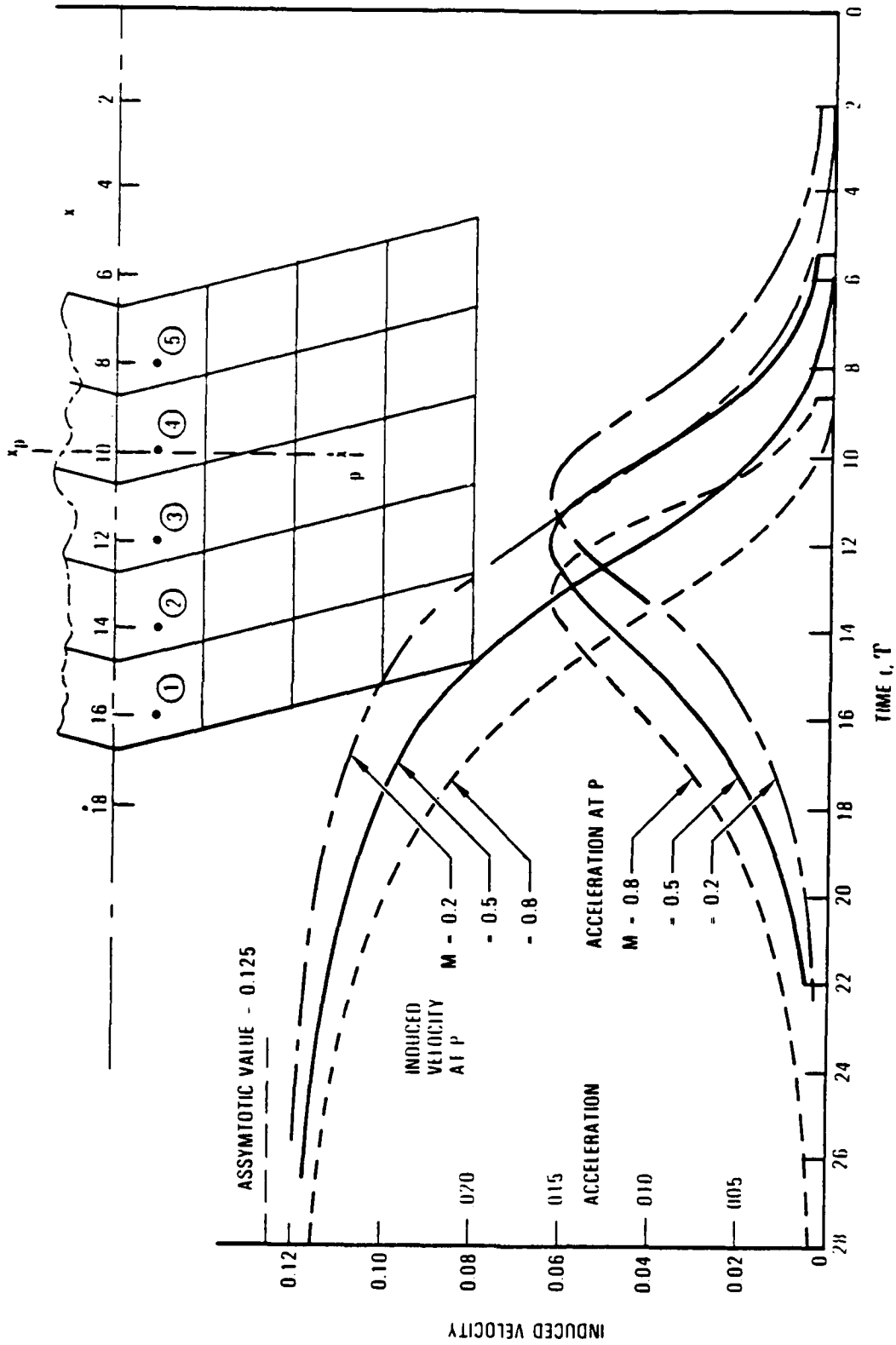


Figure 4-10. Upwash Induced at a Control Point by a Loaded Acceleration Potential Doublet Travelling at Subsonic Mach Numbers

Factoring it by the forward speed it gives the form just calculated:

$$\{w\} = [B] \{\ell\}$$

For example the matrix elements for element p due to the forces in elements 1 through 5 may be read from the plot, for M = 0.5

$$\begin{aligned} B_{p1} &= 0.09 \\ B_{p2} &= 0.072 \\ B_{p3} &= 0.042 \\ B_{p4} &= 0.017 \\ B_{p5} &= 0.002 \end{aligned}$$

This outlines the aerodynamic logic employed in the Doublet Lattice Method. The method is generally valid for attached leading edge flow at angles of attack from -5 to +10 degrees and to Mach numbers up to M = 0.8 for highly swept slender configurations or to slightly above the critical Mach number.

4.5 DERIVATION OF THE STATE-SPACE EQUATION

4.5.1 Introduction

The equations describing the dynamics of a flexible airplane in flight are usually written as a set of simultaneous second order differential equations. The aerodynamic forces are defined as functions of frequency and are, strictly, only valid for constant amplitude. The generally recognized form of the equation is:

$$\left[[M] s^2 + [D] s + [K] - \frac{1}{2} \rho V^2 [A(ik)] \right] \{z\} = 0 \quad (4.1)$$

where:

z degrees of freedom: discrete displacement at structural nodes
[M] mass matrix

[D]	viscous damping matrix
[K]	stiffness matrix
[A(ik)]	complex matrix of unsteady aerodynamic coefficients: a function of the reduced frequency $k = \omega c/V$
V	true airspeed
ρ	air density
s	Laplace transform parameter

Equation (4.1) is for free flight without excitation. Any excitation (e.g., through control surfaces) will add a right-hand side to Equation (4.1). Equation (4.1), therefore, is a stability equation and because it is for the flexible airplane, it is also called the flutter equation. Any instability associated with the structural modes of vibration is called flutter.

Stability of the system, defined by Equation (4.1), is defined by the roots of its characteristic equation: $s = (\gamma + i)\omega$, where ω is frequency in rad/sec and γ is the logarithmic increment. In solving the characteristic equation of Equation (4.1), the constraint $k = (c/V)IM(s)$ must be observed.

To take full advantage of the methodology developed under the discipline referred to as Modern Control Theory, it is necessary to reformulated Equation (4.1) in state-space format. The state-space format is set of simultaneous first order differential equations with constant coefficients:

$$s \{x\} = [A] \{x\} + [B] \{u\} \quad (4.2)$$

The degrees of freedom x are called state variables. For the second-order system, Equation (4.1), the state-space vector $\{x\}$ contains $\{z\}$ and $\{sz\}$. It may also contain higher derivatives, $\{s^2z\}$, etc., as well as lag functions such as $\{sz/(s+\beta)\}$. The additional state variables result from approximations of $[A(ik)]$ in terms of rational functions of s .

In the following, the state-space equation, corresponding to Equation (4.1) but with control added, is derived.

4.5.2 The Force Equation

The relation between the degrees of freedom $\{z\}$, the corresponding forces $\{Z\}$, and the elastic characteristics of the airplane is defined by:

$$[K] \{z\} = \{Z\} \quad (4.3)$$

The deflections $\{z\}$, most easily visualized as downward translations, may contain rotations as well as translations in other directions. Similarly, $\{z\}$ may contain moments.

The forces $\{Z\}$ are composed of inertia forces (d'Alambert's principle) viscous damping forces, and aerodynamic forces.

The inertia forces are:

$$\{Z_{inertia}\} = -[M] \{\ddot{z}\} \quad (4.4)$$

The viscous forces are:

$$\{Z_{viscous}\} = -[D] \{\dot{z}\} \quad (4.5)$$

The viscous forces may be associated with hydraulic dampers, or they may be used to approximately represent structural damping.

The aerodynamic forces are:

$$\{Z_{zero}\} = \frac{1}{2} \rho V^2 [A(ik)] \{z\} \quad (4.6)$$

The aerodynamics matrix $[A(ik)]$ is obtained from aerodynamic influence coefficients, a basic relation between the air aerodynamic force distribution

over a lifting surface and the angle-of-attack distribution. In some methods of computing unsteady aerodynamics a more basic relation is defined by a matrix of induced velocity coefficients, defining induced velocities in terms of a pressure distribution. In the following section, the more basic formulation leading to $[A(ik)]$ is presented, as well as the rational function approximation of $[A(ik)]$ needed for the state-space representation.

4.5.3 Formulation of the Aerodynamics

The formulation of the unsteady aerodynamics is based on the relation

$$\left\{ \frac{w}{V} \right\} = \frac{2}{\rho V^2} [NID] \{\Delta p\} \quad (4.7)$$

where $\{\Delta p\}$ represents the pressures at aerodynamic force nodes, $\{w\}$ is the velocities normal to the lifting surface, induced by $\{\Delta p\}$, and $[NID]$ is the induced normal downwash influence matrix. The induced velocities can be defined anywhere in the flow field. For the purpose of computing $\{\Delta p\}$ due to airplane motion, however, they are defined at so-called downwash collocation points.

Downwash collocation points are those points on a lifting surface at which the induced velocity normalized by the free stream velocity is equal to the local angle of attack $\{a\}$, i.e.,

$$\{a\} = \left\{ \frac{w}{V} \right\} \quad (4.8)$$

In the doublet lattice method of unsteady subsonic aerodynamics (Reference 25) there is a downwash collocation point associated with each aerodynamic force node point, although they don't coincide. The result is a square invertible matrix $[NID]$, and thus, from Equations (4.7) and (4.8):

$$\{\Delta p\} = \frac{1}{2} \rho V^2 [NID]^{-1} \{a\} \quad (4.9)$$

The inverse $[NID]^{-1}$ is the matrix of aerodynamic influence coefficients: [AIC]. Thus, Equation (4.9) is equivalent to:

$$\{\Delta p\} = \frac{1}{2} \rho V^2 [AIC] \{a\} \quad (4.10)$$

There are unsteady aerodynamic computer programs that compute [AIC] directly, some of them leading to a form consistent with the equation

$$\{Z_{aero}\} = \frac{1}{2} \rho V^2 [AICL] \{a\} \quad (4.11)$$

In this equation $\{Z_{aero}\}$ is defined at the structural nodes, in general different, and different in number, from the downwash collocation points. Thus, [AICL] is not necessarily a square matrix.

In the following derivation, Equation (4.9) is used as a starting point.

From $\{\Delta p\}$, by an integration or "lumping" process represented by [ZP], the aerodynamic forces are obtained:

$$\{Z_{aero}\} = [ZP] \{\Delta p\} \quad (4.12)$$

The local angle of attack, taken relative to the free stream velocity, V , is given by

$$\{a\} = \{a_{\theta}\} + \{a_z\} \quad (4.13)$$

The contribution a_{θ} is the instantaneous slope of the lifting surface, relative to V , in a plane through V perpendicular to the lifting surface:

$$\{a_{\theta}\} = [D_{\theta}] \{z\} \quad (4.14a)$$

where $[D_{\theta}]$ is a differentiating matrix.

The contribution a_z results from the rate of translation in a direction perpendicular to the lifting surface:

$$\{a_z\} = [D_z] \left\{ \frac{\dot{z}}{V} \right\} \quad (4.14b)$$

where $[D_z]$ is an interpolating matrix.

Note that to illustrate the principle, it is assumed that there are only z-type degrees of freedom and that all z's are defined perpendicular to the lifting surface.

Substituting Equation (4.14) into Equation (4.13) and replacing \dot{z} by sz yields:

$$\{a\} = \left[[D_\theta] + \frac{s}{V} [D_z] \right] \{z\} \quad (4.15)$$

Combining Equations (4.9), (4.12) and (4.15) leads to:

$$\{Z_{aero}\} = \frac{1}{2} \rho V^2 [ZP] [NID]^{-1} \left[[D_z] + \frac{s}{V} [D_z] \right] \{z\} \quad (4.16)$$

For constant amplitude oscillation $s = i\omega = i(Vk/c)$. The induced velocity matrix is a function of ik . It follows that Equation (4.16) can be written as:

$$\{Z_{aero}\} = \frac{1}{2} \rho V^2 [A(ik)] \{z\} \quad (4.17)$$

where $A(ik)$ is defined as in Equation (4.1) and is given by:

$$[A(ik)] = [ZP] [NID(ik)]^{-1} \left[[D_\theta] + \frac{ik}{c} [D_z] \right] \quad (4.18)$$

For developing the explicit function of s , $[A(s)]$, corresponding to $[A(ik)]$, the $[D_\theta]$ and $[D_z]$ contribution to $[A(ik)]$ are identified separately, and the explicit occurrence of s in Equation (4.16) is maintained.

$$[A(ik,s)] = [ZP] [NID(ik)]^{-1} [D_{\theta} + \frac{s}{V} [ZP] [NID(ik)]^{-1} [D_z] \quad (4.19)$$

Let:

$$[A_{\theta}(ik)] = [ZP] [NID(ik)]^{-1} [D_{\theta}] \quad (4.20)$$

and

$$[A_z(ik)] = [Zp] [NID(ik)]^{-1} [D_z] \quad (4.21)$$

Then:

$$[A(ik,s)] = [A_{\theta}(ik)] + \frac{s}{V} [A_z(ik)] \quad (4.22)$$

Preliminary to approximating $[A(ik,s)]$ by an explicit function of only s , $[A_{\theta}(ik)]$ and $[A_z(ik)]$ are approximated by $[A_{\theta}(p)]$ and $[A_z(p)]$, where p is the nondimensional form of s : $p = cs/V$.

Following Reference [26], the following terms are approximately,

$$[A_{\theta}(p)] = [B_{\theta 0}] + \sum_{j=1}^n \frac{[B_{\theta j}]p}{p + b_j} \quad (4.23)$$

$$[A_z(p)] = [B_{z0}] + \sum_{j=1}^n \frac{[B_{zj}]p}{p + b_j} \quad (4.24)$$

Because the state-space equation will be written in terms of s (see Equation (4.2)), Equations (4.23) and (4.24) are written in terms of s by letting $p = cs/V$:

$$[A_{\theta}(s)] = [B_{\theta 0}] + s \sum_{j=1}^n \frac{[B_{\theta j}]}{s + \beta_j} \quad (4.25)$$

$$[A_z(s)] = [B_{z0}] + s \sum_{j=1}^n \frac{[B_{zj}]}{s + \beta_j} \quad (4.26)$$

where

$$\beta_j = V b_j / c \quad (4.27)$$

Combination of Equations (4.17), (4.21), (4.22), (4.25), and (4.26) leads to the following approximate expressions for the aerodynamic forces:

$$\begin{aligned} \{Z_{aero}\} = & \frac{1}{2} \rho V^2 \left[[B_{\theta 0}] + s \sum_{j=1}^n \frac{[B_{\theta j}]}{s + \beta_j} \right] \{z\} \\ & + \frac{1}{2} \rho V^2 \left[\frac{s}{V} [B_{z0}] \frac{s^2}{V} + \sum_{j=1}^n \frac{[B_{zj}]}{s + \beta_j} \right] \{z\} \end{aligned} \quad (4.28)$$

With an obvious shortening of notation this is written as follows:

$$\{Z_{aero}\} = \frac{1}{2} \rho V^2 [A(s,V)] \{z\} \quad (4.29)$$

To clearly demonstrate how Equation (4.28) is used to develop the state-space equation, without using unnecessarily long algebraic expressions, it will be assumed that $n = 2$.

The following section deals with the incorporation of Equation (4.28) in the airplane dynamics equation, and the introduction of control surfaces.

4.5.4 The Dynamics Equation

The total force distribution on the airplane is given by the sum of the inertia forces, Equation (4.4), the viscous forces, Equation (4.5), and the aerodynamic forces, Equation (4.28) or (4.29). Replacing d/dt by s and d^2/dt^2 by s^2 , this leads to

$$\{Z\} = \left[-[M] s^2 - [D] s + \frac{1}{2} \rho V^2 [A(s,V)] \right] \{z\} \quad (4.30)$$

Combining Equation (4.30) with $[K]\{z\} = \{Z\}$, Equation (4.3), leads to the flutter equation, the equivalent of Equation (4.1).

To introduce the effect of a forced control surface deflection, a distinction must be made for z used in Equation (4.30). In Equation (4.3), z represents the sum of displacement due to rigid body motion and elastic deformations. The forces in Equation (4.30) are due to the sum of these displacements, and additional displacements, due to control surface deflection. To make the distinction, $\{z\}$ in Equation (4.30) is replaced by $\{\bar{z}\}$:

$$\{Z\} = \left[-[M] s^2 - [D] s + \frac{1}{2} \rho V^2 [A(s,V)] \right] \{\bar{z}\} \quad (4.31)$$

The relation between $\{z\}$ and $\{\bar{z}\}$ is given by

$$\{\bar{z}\} = [z_\delta] \{\delta\} + \{z\} \quad (4.32)$$

Each δ represents a forced control surface rotation, and each column in $[z_\delta]$ represents the z -type displacement due to the corresponding δ . Thus, $[z_\delta]$ contains nonzero elements only for nodes on control surfaces. Their values equal the distances from the nodes to the hingeline.

It should be understood that the forced displacements $[z_\delta] \{\delta\}$ are in addition to any displacements on the control surfaces included in $\{z\}$ that are part of the elastic or rigid body response. The actual control surface rotation, relative to the main surface, is the sum of δ and the rotation due to elastic response implied by Equation (4.3).

Equations (4.3), (4.31), and (4.32) are combined to

$$\begin{aligned} & \left[[M] s^2 + [D] s + [K] - \frac{1}{2} \rho V^2 [A(s,V)] \right] \{z\} \\ & = \left[-[M] s^2 - [D] s + \frac{1}{2} \rho V^2 [A(s,V)] \right] [z_\delta] \{\delta\} \end{aligned} \quad (4.33)$$

If $\{\delta\} = 0$, the right-hand side of Equation (4.33) is zero, and the equation corresponds to Equation (4.1), the flutter equation.

The number of discrete degrees of freedom $\{z\}$ may be large. For a typical airplane analysis it may range from 100 to 300. This is not an unreasonably high number for vibration analysis, but for flutter analysis and active control design it leads to higher-than-necessary computing costs.

The number of degrees of freedom is reduced by modalization, usually by means of natural vibration modes. The deflection $\{z\}$ is assumed to be a linear combination of lower-frequency, natural vibration modes, each of which is defined by a column in the modal matrix $[T]$:

$$\{z\} = [T] \{q\} \quad (4.34)$$

Elements of $\{q\}$ are the modal degrees of freedom, also called modal coefficients or participation coefficients. The modal matrix $[T]$, in general, also contains rigid body modes, if deemed necessary for description of the system under consideration. Typically, $\{q\}$ may have 2 to 50 elements.

Introducing Equation (4.34) into Equation (4.33) leads to more equations than there are degrees of freedom $\{q\}$. The number of equations is reduced to the number of degrees of freedom by premultiplication with the transpose of T : $[T^T]$.

The result is:

$$\begin{aligned} & [T^T] \left[[M] s^2 + [D] s + [K] - \frac{1}{2} \rho V^2 [A(s, V)] \right] [T] \{q\} \\ & = [T^T] \left[-[M] s^2 - [D] s + \frac{1}{2} \rho V^2 [A(s, V)] \right] [z_\delta] \{\delta\} \end{aligned} \quad (4.35)$$

Identifying $[T^T] [] [T]$ by an overbar $\bar{\quad}$ (e.g., $[T^T] [M] [T] = [\bar{M}]$) and $[T^T] [] [z_\delta]$ by a hat $\hat{\quad}$ (e.g., $[T^T] [M] [z_\delta] = [\hat{M}]$, Equation 4.35) is written as:

$$\begin{aligned} & \left[[\bar{M}] s^2 + [\bar{D}] s + [\bar{K}] - \frac{1}{2} \rho V^2 [\bar{A}(s,V)] \right] \{q\} \\ & = \left[-[\hat{M}] s^2 - [\hat{D}] s + \frac{1}{2} \rho V^2 [\hat{A}(s,V)] \right] \{\delta\} \end{aligned} \quad (4.36)$$

Introducing the detailed expression for the aerodynamic forces, Equation (4.28), with $n = 2$, into Equation (4.36), leads to:

$$\begin{aligned} & \left[[\bar{M}] s^2 + [\bar{D}] s + [\bar{K}] - \frac{1}{2} \rho V^2 [\bar{B}_{\theta 0}] - \frac{1}{2} \rho V^2 [\bar{B}_{z 0}] \frac{s}{V} \right. \\ & - \frac{1}{2} \rho V^2 [\bar{B}_{\theta 1}] \frac{s}{s+\beta_1} - \frac{1}{2} \rho V^2 [\bar{B}_{\theta 2}] \frac{s}{s+\beta_2} \\ & \left. - \frac{1}{2} \rho V^2 [\bar{B}_{z 1}] \frac{1}{V} \frac{s^2}{s+\beta_1} - \frac{1}{2} \rho V^2 [\bar{B}_{z 2}] \frac{1}{V} \frac{s^2}{s+\beta_2} \right] \{q\} \\ & = \left[-[\hat{M}] s^2 - [\hat{D}] s + \frac{1}{2} \rho V^2 [\hat{B}_{\theta 0}] + \frac{1}{2} \rho V^2 [\hat{B}_{z 0}] \frac{s}{V} \right. \\ & + \frac{1}{2} \rho V^2 [\hat{B}_{\theta 1}] \frac{s}{s+\beta_1} + \frac{1}{2} \rho V^2 [\hat{B}_{\theta 2}] \frac{s}{s+\beta_2} \\ & \left. + \frac{1}{2} \rho V^2 [\hat{B}_{z 1}] \frac{1}{V} \frac{s^2}{s+\beta_1} + \frac{1}{2} \rho V^2 [\hat{B}_{z 2}] \frac{1}{V} \frac{s^2}{s+\beta_2} \right] \{\delta\} \end{aligned} \quad (4.37)$$

The notation of the aerodynamics elements in Equation (4.37) is shortened: $[C_{\theta 0}] = 1/2 \rho V^2 [B_{\theta 0}]$, etc. The new symbols are defined below in terms of symbols without overbar or hat.

$$\begin{aligned}
[\bar{C}_{\theta j}] &= \frac{1}{2} \rho V^2 [T^T][B_{\theta j}][T] & \hat{C}_{\theta j} &= \frac{1}{2} \rho V^2 [T^T][B_{\theta j}][d_{\delta}] & j &= 0, 1, 2 \\
[\bar{C}_{zj}] &= \frac{1}{2} \rho V^2 [T^T][B_{zj}][T] \frac{1}{V} & \hat{C}_{zj} &= \frac{1}{2} \rho V^2 [T^T][B_{zj}][d_{\delta}] \frac{1}{V} & j &= 0, 1, 2
\end{aligned}
\tag{4.38}$$

With this notation, Equation (4.37) becomes:

$$\begin{aligned}
&\left[[\bar{M}] s^2 + [\bar{D}] s + [\bar{K}] - [\bar{C}_{\theta 0}] s - [\bar{C}_{\theta 0}] \frac{s}{s+\beta_1} - [\bar{C}_{\theta 0}] \frac{s}{s+\beta_2} + \right. \\
&- [C_{z1}] \frac{s^2}{s+\beta_1} - [C_{z2}] \frac{s^2}{s+\beta_2} \left. \right] \{q\} = \left[-[\hat{M}] s^2 - [\hat{D}] s + [\hat{C}_{\theta 0}] \right. \\
&+ [\hat{C}_{z0}] s + [\hat{C}_{\theta 1}] \frac{s}{s+\beta_1} + [\hat{C}_{\theta 2}] \frac{s}{s+\beta_2} + [\hat{C}_{z1}] \frac{s^2}{s+\beta_1} + [\hat{C}_{z2}] \frac{s^2}{s+\beta_2} \left. \right] \{\delta\}
\end{aligned}
\tag{4.39}$$

4.6 STATE SPACE EQUATIONS FOR AEROSERVOELASTICITY SYMMETRIC AIRPLANE

The development of the final state-space equations will be done in a manner similar to that of Section 4.5. However, gust equations will be included, and a more general form of the servoactuator will be used. At a later time, the equations for explicit force feedback may be added.

4.6.1 Gust Equations

The angle-of-attack due to penetration of a gust can be represented by

$$\{\alpha_G\} = \frac{i}{V} \left\{ e^{-\frac{i\omega\Delta x_i}{V}} \right\} = w \left\{ e^{-\frac{ik\Delta x_i}{c}} \right\}
\tag{4.40}$$

where

U = gust velocity

V = airplane true airspeed

c = reference length

$\Delta x_i = x_i - x_{CG}$ for each DOF

k = reduced frequency

w = u/V

The gust aerodynamic forces are then given by

$$\{F_G\} = \frac{1}{2} \rho V^2 [ZP] [A_\alpha(ik)] \{\alpha_G\} \quad (4.41)$$

After modalization

$$\{Q_G\} = [T]^T \{F_G\} = \frac{1}{2} \rho V^2 \{\bar{F}_G(ik)\} w \quad (4.42)$$

where

$$\{\bar{F}_G(ik)\} = [T]^T [ZP] [A_\alpha(ik)] \left\{ e^{\frac{-ik\Delta x_i}{c}} \right\} \quad (4.43)$$

Use the approximation from Reference [26]

$$\{F_G(p)\} = \{B_{G0}\} + \{B_{G1}\} p + \{B_{G2}\} p^2 + \sum_{j=3}^4 \frac{\{B_{Gj}\} p}{p+b_j} \quad (4.44)$$

Replace p with the generally used Laplace transform operator s :

$$p = \frac{c}{V} s \quad (4.45)$$

$$\begin{aligned} \{\bar{F}_G(s)\} &= \{B_{G0}\} + \{B_{G1}\} \frac{c}{V} s + \{B_{G2}\} \frac{c^2}{V^2} s^2 \\ &+ \{B_{G3}\} \frac{s}{s+\beta_3} + \{B_{G4}\} \frac{s}{s+\beta_4} \end{aligned} \quad (4.46)$$

and

$$\{Q_G(s)\} = \frac{1}{2} \rho V^2 \{\bar{F}_G(s)\} w \quad (4.47)$$

Equations (4.46) and (4.47) give the gust aerodynamic forces defined in terms of the state variables w , sw , s^2w , $sw/(s+\beta_3)$, and $sw/(s+\beta_4)$.

The basic gust input is taken to be white noise of level η . A filter is then defined which will convert this to the desired psd shape. The Dryden gust spectrum is generally used for control systems work, and will be employed here. A Dryden psd filter can be represented by

$$\begin{Bmatrix} \dot{w} \\ \dot{g} \end{Bmatrix} = \begin{bmatrix} a_1 & 1 \\ a_2 & 0 \end{bmatrix} \begin{Bmatrix} w \\ g \end{Bmatrix} + \begin{Bmatrix} c_1 \\ c_2 \end{Bmatrix} \eta \quad (4.48)$$

where g is a dummy variable, and

$$\begin{aligned} a_1 &= -\frac{2}{\tau} & c_1 &= \sqrt{\frac{3}{\pi\tau}} \\ a_2 &= -\frac{1}{\tau^2} & c_2 &= \sqrt{\frac{1}{\pi\tau^3}} \end{aligned} \quad (4.49)$$

and $\tau = L/V$, with $L =$ scale of turbulence.

Closer examination of Equations (4.46) and (4.48) reveal a singularity when combined with the identity equation $ws = ws$ (necessary because of the existence of both sw and w as states). These equations are

$$ws = ws \quad (4.50a)$$

$$ws = a_1 w + g + c_1 \eta \quad (4.50b)$$

$$gs = a_2 w + c_2 \eta \quad (4.50c)$$

Since w is a state variable, we need a derivative of this to put on the left side. Therefore, we will use a suggestion by Hassig and add $\epsilon_2 w s^2$ to Equation (4.50b). Thus, Equation (4.48) becomes

$$\begin{pmatrix} \dot{w} \\ s\dot{w} \\ \dot{g} \end{pmatrix} = \begin{bmatrix} 0 & 1 & 0 \\ a_1/\epsilon_2 & -1/\epsilon_2 & 1/\epsilon_2 \\ a_2 & 0 & 0 \end{bmatrix} \begin{pmatrix} w \\ sw \\ g \end{pmatrix} + \begin{pmatrix} 0 \\ C_1/\epsilon_2 \\ c_2 \end{pmatrix} \quad (4.51)$$

where ϵ_2 is a small quantity. Again care must be taken that this is chosen properly, i.e., small enough to be correct, but large enough to avoid ill-conditioning in the matrices.

4.6.2 Servoactuator Model

Assume a servoactuator which can be represented by a polynomial in s

$$\delta = \frac{N(s)}{D(s)} u = \frac{\sum_{i=0}^n a_i s^i}{\sum_{i=0}^m b_i s^i} u \quad ; m \geq n \quad (4.52)$$

where δ , the control surface rotation, is a response quantity, and u is the input command. Rewriting Equation (4.52),

$$(b_m s^m + b_{m-1} s^{m-1} + \dots + b_0) \delta = (a_n s^n + a_{n-1} s^{n-1} + \dots + a_0) u \quad (4.53)$$

Define additional state variables,

$$\begin{aligned} \delta_1 &= s \delta \\ \delta_2 &= s^2 \delta \\ &\vdots \\ &\vdots \\ \delta_{m-1} &= s^{m-1} \delta \end{aligned} \quad (4.54)$$

This takes care of the denominator, but the numerator requires an additional step. In order to achieve a state-space formulation we must change u and its derivatives into state variables. This can be done with the following equation:

$$(\epsilon_1 s^{n+1} + 1) u = u_c \quad (4.55)$$

Note that we must go to the $n+1$ power of s in this equation. This can be explained by examining Equation (4.53), where the term with the highest power of s on the right-hand side must represent a state variable - not the derivative of a state variable. In order to form the state-space equations, a derivative of this variable must appear - thus requiring the s^{n+1} term in Equation (4.55). Equation (4.55) allows the selection of small values for ϵ_1 , thus making u_c essentially equal to u for the problem at hand. Therefore, we can define the new "quasi-input" states

$$\begin{aligned} u_1 &= su \\ u_2 &= s^2u \\ &\vdots \\ &\vdots \\ u_n &= s^nu \end{aligned} \quad (4.56)$$

The complete state vector for the servoactuator is then $\delta, \delta_1, \delta_2, \dots, \delta_{m-1}, u, u_1, u_2, \dots, u_n$ - a total $m+n+1$ quantities.

Using Equations (4.53), (4.54), (4.55), and (4.56), we have the necessary $n+m+1$ equations to define the state-space model for the servoactuator. These are shown in complete form in Equation (4.57).

$$\begin{bmatrix} \dot{\delta} \\ \dot{\delta}_1 \\ \dot{\delta}_2 \\ \vdots \\ \dot{\delta}_{m-1} \\ \dot{u} \\ \dot{u}_1 \\ \dot{u}_2 \\ \vdots \\ \dot{u}_n \end{bmatrix} = \begin{bmatrix} \delta & \delta_1 & \delta_2 & \cdots & \delta_{m-1} & u & u_1 & u_2 & \cdots & u_n \\ 0 & 1 & 0 & \cdots & 0 & 0 & 0 & 0 & \cdots & 0 \\ 0 & 0 & 1 & \cdots & 0 & 0 & 0 & 0 & \cdots & 0 \\ 0 & 0 & 0 & \cdots & 0 & 0 & 0 & 0 & \cdots & 0 \\ \cdots & \cdots & \cdots & \cdots & \cdots & \cdots & \cdots & \cdots & \cdots & \cdots \\ -b_0 & -b_1 & -b_2 & \cdots & -b_{m-1} & a_0 & a_1 & a_2 & \cdots & a_n \\ \frac{b_0}{b_m} & \frac{b_1}{b_m} & \frac{b_2}{b_m} & \cdots & \frac{b_{m-1}}{b_m} & \frac{a_0}{b_m} & \frac{a_1}{b_m} & \frac{a_2}{b_m} & \cdots & \frac{a_n}{b_m} \\ 0 & 0 & 0 & \cdots & 0 & 0 & 1 & 0 & \cdots & 0 \\ 0 & 0 & 0 & \cdots & 0 & 0 & 0 & 1 & \cdots & 0 \\ 0 & 0 & 0 & \cdots & 0 & 0 & 0 & 0 & \cdots & 0 \\ \cdots & \cdots & \cdots & \cdots & \cdots & \cdots & \cdots & \cdots & \cdots & \cdots \\ 0 & 0 & 0 & \cdots & 0 & -1/\varepsilon_1 & 0 & 0 & \cdots & 0 \end{bmatrix} \begin{bmatrix} \delta \\ \delta_1 \\ \delta_2 \\ \vdots \\ \delta_{m-1} \\ u \\ u_1 \\ u_2 \\ \vdots \\ u_n \end{bmatrix} + \begin{bmatrix} 0 \\ 0 \\ 0 \\ \vdots \\ 0 \\ 0 \\ 0 \\ \vdots \\ 0 \\ 1/\varepsilon_1 \end{bmatrix} u_c \quad (4.57)$$

or

$$\begin{bmatrix} \delta \\ \dot{\delta}_1 \\ \vdots \\ \delta \end{bmatrix}_{m+n+1} = \begin{bmatrix} 0 & 1 & [0] \\ 0 & 0 & [y_1] \\ [B_\delta] & [B_{\delta_1}] & [B_{\delta_2}] \end{bmatrix} \begin{bmatrix} \delta \\ \delta_1 \\ \vdots \\ \delta \end{bmatrix} + \begin{bmatrix} 0 \\ 0 \\ B_u \end{bmatrix} u_c \quad (4.58)$$

where

$$y_1 = [1 \ 00 \ \cdots \ 0]_{1 \times m+n-1}; \quad \{B_\delta\}_{m+n-1} = \begin{bmatrix} 0 \\ 0 \\ -b_0 \\ \frac{b_0}{b_m} \\ 0 \end{bmatrix}; \quad \{B_{\delta_1}\} = \begin{bmatrix} 0 \\ 0 \\ -b_1 \\ \frac{b_1}{b_m} \\ 0 \end{bmatrix} \leftarrow \text{row } m$$

The requirements for choosing ε_1 will not be examined. Assume for low damping that:

$$s = i\omega = i 2 \pi f \quad (4.59)$$

where

ω = frequency in rad/sec

and f = frequency in Hertz

If ϵ_1 is chosen to make u and u_c differ by only a percent then

$$\epsilon_1 s^{n+1} \leq 0.01 \quad (4.60)$$

or

$$\epsilon_1 \leq \frac{0.01}{(2\pi f)^{n+1}} \quad (4.61)$$

Remembering that n is the order of the numerator in the polynomial expression for the servoactuator, we can see that for frequencies above 1 Hz, ϵ becomes a very tiny number quite rapidly, especially for complicated servos. For instance, let's compute it for $n=3$ and $f=1$ Hz:

$$\epsilon_1 \leq 0.01/(2\pi)^4$$

$$\epsilon_1 \leq 0.64 \times 10^{-5}$$

and

$$1/\epsilon_1 = 0.156 \times 10^6$$

This large number may make $[A]$ matrix somewhat ill-conditioned. Careful attention should, therefore, be paid to Equation (4.61).

4.6.3 Phugoid Mode

Equations for including the phugoid mode in the aeroservoelastic model will not be developed.

Assume a modal transformation such that:

$$\begin{Bmatrix} x \\ z \end{Bmatrix} = [T] \begin{Bmatrix} x_0 \\ z_0 \\ \theta_0 \\ q_f \end{Bmatrix} \quad (4.62)$$

where x and z are the deflection distribution, x_0 , z_0 and θ_0 are the rigid body degrees of freedom, and q_f is the flexible body degrees of freedom.

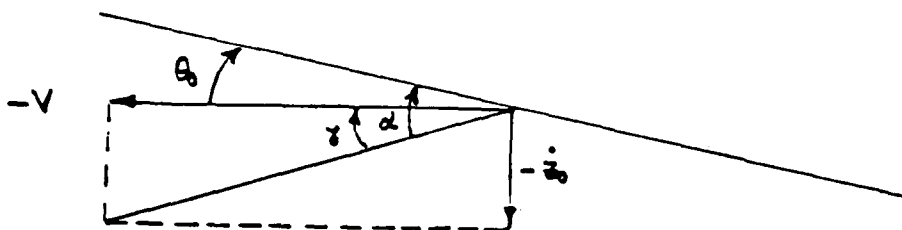
Keeping in mind that the flutter equation is a perturbation equation from an equilibrium state, let's look at the vertical force created by a small increment in forward velocity, ΔV . The aerodynamic forces are

$$\{Z_A\} = \frac{1}{2} \rho V^2 [AIC(0)] \{\alpha_{eq}\} \quad (4.63)$$

where $\{\alpha_{eq}\}$ is angle of attack at equilibrium.

The incremental increase in vertical forces is

$$\{\Delta Z_A\} = \rho V [AIC(0)] \{\alpha_{eq}\} \Delta V + \frac{1}{2} \rho V^2 [AIC(0)] \left\{ \frac{\partial \alpha_{eq}}{\partial V} \right\} \Delta V \quad (4.64)$$



$$\alpha = \theta_0 + \gamma \quad (4.65)$$

For

$$V \gg | \dot{z}_0 |, \quad \gamma = \tan \gamma$$

$$\tan \gamma = -\dot{z}_0/V \quad (4.46)$$

where the negative sign enters because of the definition of the direction of rotation of γ .

$$\alpha = \theta_0 - \frac{\dot{z}_0}{V} \quad (4.67)$$

$$\frac{\partial \alpha}{\partial V} = \frac{\dot{z}_0}{V^2} \quad (4.68)$$

Substituting this in the second term of Equation (4.64) gives an expression which is negligible because of the presence of both z_0 and ΔV as a product.

$$\frac{1}{2} \rho V^2 [\text{AIC}(0)] \left\{ \frac{\partial \alpha_{\text{eq}}}{\partial V} \right\} \Delta V = 0 \quad (4.69)$$

Thus, writing the perturbation in velocity as $-x_0$, since x is defined positive aft, Equation (4.64) becomes

$$\{\Delta Z_A\} = -\rho V [\text{AIC}(0)] \{\alpha_{\text{eq}}\} x_0 = -\frac{1}{2} \rho V p^2 \left(\frac{2}{V} \right) \{A_z\} \dot{x}_0 \quad (4.70)$$

Now consider the drag forces on the total airplane only,

$$D = 1/2 \rho V^2 C_D S \quad (4.71)$$

We are concerned with the incremental force due to x_0 , z_0 , and θ_0 .

$$\Delta D = \rho V C_D S \Delta V + 1/2 \rho V^2 S C_{D\alpha} \Delta \alpha$$

where $\alpha = \alpha(V, \dot{z}_0, \theta_0) \quad (4.72)$

$$\Delta \alpha = \frac{\partial \alpha}{\partial V} \Delta V + \frac{\partial \alpha}{\partial \dot{z}_0} \dot{z}_0 + \frac{\partial \alpha}{\partial \theta_0} \theta_0 \quad (4.73)$$

$$\Delta \alpha = \frac{\dot{z}_0}{V^2} \Delta V - \frac{1}{V} \dot{z}_0 + \theta_0 \quad (4.74)$$

The first term in Equation (4.74) can be neglected for the same reason as before in Equation (4.69).

$$\Delta D = - \rho V C_D S \dot{x}_0 + 1/2 \rho V^2 S C_{D\alpha} (\theta_0 - \dot{z}_0/V) \quad (4.75)$$

There is also a drag force due to the change in direction of total velocity due to an angle-of-attack change.

$$X_L = 1/2 \rho V^2 C_L S \dot{z}_0/V \quad (4.76)$$

The total force in the x-direction is

$$\Delta X_A = - \rho V C_D S \dot{x}_0 + \frac{1}{2} \rho V^2 S C_{D\alpha} \left(\theta_0 - \frac{\dot{z}_0}{V} \right) + \frac{1}{2} \rho V^2 C_L S \frac{\dot{z}_0}{V} \quad (4.77)$$

or

$$\Delta X_A = \frac{1}{2} \rho V^2 \left[\frac{-2}{V} C_D S x_0 + \frac{S}{V} (C_L - C_{D\alpha}) \dot{z}_0 + S C_{D\alpha} \theta_0 \right] \quad (4.78)$$

or

$$\Delta X_A = \frac{1}{2} \rho V^2 \begin{bmatrix} X_x & X_z & X_\theta \end{bmatrix} \begin{bmatrix} s x_0 \\ s z_0 \\ \theta_0 \end{bmatrix} \quad (4.79)$$

The total aerodynamic forces can then be written:

$$\begin{pmatrix} \Delta X_A \\ \Delta Z_A \end{pmatrix} = \frac{1}{2} \rho V^2 \begin{bmatrix} s X_x & s X_z & X_\theta & 0 \\ -\frac{2}{V} \{A_z\} s & \{AIC\} & & \end{bmatrix} \begin{pmatrix} x_0 \\ z_0 \\ \theta_0 \\ q \end{pmatrix} \quad (4.80)$$

where

$$\{AIC\} = \{AIC\} \{T_z\} \quad (4.81)$$

and

$$[T] = \begin{bmatrix} 1 & [0] \\ \{0\} & T_z \end{bmatrix} \quad (4.82)$$

Now define

$$[AIC] = [T_z]^T [AIC] [T_z] \quad (4.83)$$

If

$$\{a\} = \left[[D_\theta] + \frac{s}{V} [D_z] \right] [T_z] \{q_z\} \quad (4.84)$$

$$\{Q_z\} = \frac{1}{2} \rho V^2 [T_z]^T [ZP] [A_\alpha(ik)] \{a\} \quad (4.85)$$

This can be divided into pitch and plunge:

$$\{Q_z\} = \frac{1}{2} \rho V^2 \left[[A_\theta(s)] + \frac{s}{V} [A_z(s)] \right] \{q_z\} - \frac{2}{V} [T_z]^T \{A_z\} x_0 \quad (4.86)$$

where

$$[A_\theta(s)] = [T_z]^T [ZP] [A_\alpha(ik)] [D_\theta] [T_z] \quad (4.87)$$

and

$$[A_z(s)] = [T_z]^T [ZP] [A_\alpha(ik)] [D_z] [T_z] \quad (4.88)$$

Now using the rational function approximation,

$$[A_\theta(s)] = [A_\theta(0)] + \frac{s}{s+\beta_1} [B_{\theta 1}] + \frac{s}{s+\beta_2} [B_{\theta 2}] \quad (4.89a)$$

$$[A_z(s)] = [A_z(0)] + \frac{s}{s+\beta_1} [B_{z 1}] + \frac{s}{s+\beta_2} [B_{z 2}] \quad (4.89b)$$

where we use only two terms in the series. These matrices can be determined by a least square fit using two or more k -values. Note that the modal matrix $[T]$ is now of a predetermined form, i.e., the first 3 columns represent rigid body fore and aft, pitch, and plunge, in that order.

4.6.4 Equations of Motion

A control surface rotation, δ , gives the additional displacements.

$$\{z_c\} = [z_\delta] \{\delta\} \quad (4.90)$$

where the i th column of $[z_\delta]$ gives distances from a hinge line for the particular control surface corresponding to δ_i . The total deflection is

$$\{\bar{z}\} = \{z\} + \{z_c\} \quad (4.91)$$

The equations of motion are

$$\left[[M] s^2 + [D]s + [K] - \frac{1}{2} \rho V^2 [A(s,V)] \right] \{\bar{z}\} + [x] \{z\} = \{F_G(s,V)\} w \quad (4.92)$$

Substituting for \bar{z} from Equation (4.91) results in

$$\begin{aligned} & \left[[M] s^2 + [D] s + [K] - \frac{1}{2} \rho V^2 [A(s,V)] \right] \{z\} \\ & = \left[-[M] s^2 - [D] s + \frac{1}{2} \rho V^2 [A(s,V)] \right] [z_\delta] \{\delta\} \\ & + \{F_G(s,V)\} w \end{aligned} \quad (4.93)$$

Now,

$$\{z\} = [T] \{q\} \quad (4.94)$$

Note that, in order to incorporate the phugoid mode, we must modalize the aerodynamics first. This presents a possible problem for the aero forces on the right side of Equation (4.93). The contribution to X-forces due to rigid control surface motion should be zero since this side has not post-multiplying $[T]$. This requires that x_0 , z_0 , and θ_0 are not on a control surface. This seems to be acceptable. After modalizing, Equation (4.93) becomes

$$\begin{aligned}
& \left[[\tilde{M}] s^2 + [\tilde{D}] s + [\tilde{K}] - \frac{1}{2} \rho V^2 [\tilde{A}(s, V)] \right] \{q\} \\
& = \left[-[\hat{M}] s^2 - [\hat{D}] s + \frac{1}{2} \rho V^2 [\hat{A}(s, V)] \right] [z_\delta] \{\delta\} \\
& + \frac{1}{2} \rho V^2 \{\hat{F}_G(s, V)\} w
\end{aligned} \tag{4.95a}$$

where

$$[\tilde{\cdot}] = [T]^T [\cdot] [T] \tag{4.95b}$$

and

$$[\hat{\cdot}] = [T]^T [\cdot] \tag{4.95c}$$

Here

$$[\tilde{A}(s, V)] = \left[\begin{array}{c|c} \frac{sX_x}{-2s/V} & \begin{array}{c} sX_z \\ x_\theta \\ [0] \end{array} \\ \hline [T_z]^T [A_z] & \begin{array}{c} [T_z]^T [AIC] \\ [T_z] \end{array} \end{array} \right] \tag{4.96}$$

and

$$[\hat{A}(s, V)] = \begin{bmatrix} 0 & [0] \\ [0] & [T_z]^T [AIC] \end{bmatrix} \Delta = \begin{bmatrix} 0 & [0] \\ [0] & [AIC] \end{bmatrix} \tag{4.97}$$

Here $\{q\}$ also contains the rigid body DOF, i.e.,

$$\{q\} = \begin{pmatrix} x_0 \\ z_0 \\ \theta_0 \\ q_f \end{pmatrix} = \begin{pmatrix} x_0 \\ q_z \end{pmatrix} \tag{4.98}$$

where $\{q_f\}$ represents the flexible modes.

Redefine the parts of Equation (4.96):

$$[\tilde{A}(s, V)] = \left[\begin{array}{c|c} \frac{sX_x}{\{A_z\} s} & \begin{array}{c} sX_z \quad X_\theta \\ \{A\tilde{I}C\} \end{array} \\ \hline & [0] \end{array} \right] \quad (4.99)$$

where

$$\{A_z\} = -2/V [T_z]^T \{A_z\}$$

and

$$[A\tilde{I}C] = [T_z]^T [AIC] [T_z]$$

Leaving off the first row of each matrix in Equation (4.95), we have

$$\begin{aligned} & \left[[\tilde{M}_z] s^2 + [\tilde{D}_z] s + [\tilde{K}_z] - \frac{1}{2} \rho V^2 [A\tilde{I}C] \right] \{q_z\} \\ & = \left[-[\hat{M}_z] s^2 - [\hat{D}_z] s + \frac{1}{2} \rho V^2 [AIC] \right] \{z_\delta\} \{\delta\} \\ & + \frac{1}{2} \rho V^2 \{F_{Gz}(s, V)\} w + \frac{1}{2} \rho V^2 \{A_z\} s x_0 \end{aligned} \quad (4.10c)$$

Now,

$$[A\tilde{I}C] = [\tilde{A}_\theta(s, V)] + s/V [\tilde{A}_z(s, V)] \quad (4.101)$$

with

$$[\tilde{A}_\theta(s, V)] = [\tilde{A}_\theta(0)] + \frac{s}{s+\beta_1} [\tilde{B}_{\theta 1}] + \frac{s}{s+\beta_2} [\tilde{B}_{\theta 2}] \quad (4.102)$$

$$[\tilde{A}_z(s, V)] = [\tilde{A}_z(0)] + \frac{s}{s+\beta_1} [\tilde{B}_{z 1}] + \frac{s}{s+\beta_2} [\tilde{B}_{z 2}] \quad (4.103)$$

where

$$\beta_i = Vb_i/c$$

$$\begin{aligned} \{\hat{F}_{Gz}(s, V)\} &= \{\hat{B}_{G0}\} + \frac{cs}{V} \{\hat{B}_{G1}\} + \left\{\frac{cs}{V}\right\}^2 \{\hat{B}_{G2}\} \\ &+ \frac{s}{s+\beta_3} \{\hat{B}_{G3}\} + \frac{s}{s+\beta_4} \{\hat{B}_{G4}\} \end{aligned} \quad (4.104)$$

Let

$$\{C_{G0}\} = \frac{1}{2} \rho V^2 \{\hat{B}_{G0}\} \quad (4.105a)$$

$$\{C_{G1}\} = \frac{1}{2} \rho V^2 \{\hat{B}_{G1}\} \quad (4.105b)$$

$$\{C_{G2}\} = \frac{1}{2} \rho V^2 \{\hat{B}_{G2}\} \quad (4.105c)$$

$$\{C_{G3}\} = \frac{1}{2} \rho V^2 \{\hat{B}_{G3}\} \quad (4.105d)$$

$$\{C_{G4}\} = \frac{1}{2} \rho V^2 \{\hat{B}_{G4}\} \quad (4.105e)$$

$$\{C_x\} = \frac{1}{2} \rho V^2 \{\hat{A}_z\} \quad (4.106)$$

$$\{\bar{C}_{\theta 0}\} = \frac{1}{2} \rho V^2 \{\bar{A}_{\theta}(0)\} \quad (4.107a)$$

$$\{\bar{C}_{\theta 1}\} = \frac{1}{2} \rho V^2 \{\bar{B}_{\theta 1}\} \quad (4.107b)$$

$$\{\bar{C}_{\theta 2}\} = \frac{1}{2} \rho V^2 \{\bar{B}_{\theta 2}\} \quad (4.107c)$$

$$\{\bar{C}_{z0}\} = \frac{1}{2} \rho V \{\bar{A}_z(0)\} \quad (4.107d)$$

$$\{\bar{C}_{z1}\} = \frac{1}{2} \rho V \{\bar{B}_{z1}\} \quad (4.107e)$$

$$[\tilde{C}_{z2}] = \frac{1}{2} \rho V [\tilde{B}_{z2}] \quad (4.107f)$$

$$[\hat{C}_{\theta 0}] = \frac{1}{2} \rho V^2 [\hat{A}_{\theta}(0)] [z_{\delta}] \quad (4.107g)$$

$$[\hat{C}_{\theta 1}] = \frac{1}{2} \rho V^2 [\hat{B}_{\theta 1}] [z_{\delta}] \quad (4.107h)$$

$$[\hat{C}_{\theta 2}] = \frac{1}{2} \rho V^2 [\hat{B}_{\theta 2}] [z_{\delta}] \quad (4.107i)$$

$$[\hat{C}_{z0}] = \frac{1}{2} \rho V [\hat{A}_z(0)] [z_{\delta}] \quad (4.107j)$$

$$[\hat{C}_{z1}] = \frac{1}{2} \rho V [\hat{B}_{z1}] [z_{\delta}] \quad (4.107k)$$

$$[\hat{C}_{z2}] = \frac{1}{2} \rho V [\hat{B}_{z2}] [z_{\delta}] \quad (4.107l)$$

Note that the notation of Equations (4.95b) and 4.95c) still holds for these equations. Equation (4.100) becomes

$$\begin{aligned} & \left[[\tilde{M}_z] s^2 + [\tilde{D}_z] s + [\tilde{K}_z] - [\tilde{C}_{\theta 0}] - \frac{s}{s+\beta_1} [\tilde{C}_{\theta 1}] - \frac{s}{s+\beta_2} [\tilde{C}_{\theta 2}] \right. \\ & \quad \left. - s [\tilde{C}_{z0}] - \frac{s^2}{s+\beta_1} [\tilde{C}_{z1}] - \frac{s^2}{s+\beta_2} [\tilde{C}_{z2}] \right] \{q_z\} \\ & = \left[-[\hat{M}_z] s^2 - [\hat{D}_z] s + [\hat{C}_{\theta 0}] + \frac{s}{s+\beta_1} [\hat{C}_{\theta 1}] + \frac{s}{s+\beta_2} [\hat{C}_{\theta 2}] \right. \\ & \quad \left. + s [\hat{C}_{z0}] + \frac{s^2}{s+\beta_1} [\hat{C}_{z1}] + \frac{s^2}{s+\beta_2} [\hat{C}_{z2}] \right] \{\delta\} \\ & \quad + [C_{G0}] w + [C_{G1}] s w + [C_{G2}] s^2 w + [C_{G3}] \frac{s w}{s+\beta_3} \\ & \quad + [C_{G4}] \frac{s w}{s+\beta_4} + [C_x] s x_0 \end{aligned} \quad (4.108)$$

where

$$[\tilde{\cdot}] = [T_z]^T [\cdot] [T_z] \quad (4.109)$$

There is also an equation of motion for the fore and aft direction. Assuming x_0 to be uncoupled from the other DOF, for the free airplane we have

$$\begin{aligned} M_x s^2 x_0 + D_x s x_0 &= \frac{1}{2} \rho V^2 (X_x \dot{s} x_0 + X_z \dot{s} z_0 + X_\theta \theta_0) \\ &= \tilde{X}_x s x_0 + \left([\tilde{X}_z] s + [\tilde{X}_\theta] \right) \{q_z\} \end{aligned} \quad (4.110)$$

where

$$\tilde{X}_x = \frac{1}{2} \rho V^2 X_x \dot{s}, \quad (4.111a)$$

$$[\tilde{X}_z] = \frac{1}{2} \rho V^2 [X_z \ 0 \ 0 \ \cdots \ 0], \quad (4.111b)$$

and

$$[\tilde{X}_\theta] = \frac{1}{2} \rho V^2 [0 \ X_\theta \ 0 \ 0 \ \cdots \ 0] \quad (4.111c)$$

Now we are only lacking some identity relation in order to complete the state model. Some of these are:

$$s x_0 = s x_0 \quad (4.112)$$

$$s\{q_z\} = s\{q_z\} \quad (4.113)$$

For the others note the following:

$$\begin{aligned} \frac{s^2 q}{s + \beta_j} &= \frac{qs^2 + qs\beta_j - qs\beta_j}{s + \beta_j} \\ &= \frac{qs(s + \beta_j) - qs\beta_j}{s + \beta_j} \end{aligned}$$

Thus

$$\frac{s^2\{q\}}{s+\beta_j} = s\{q\} - \frac{s\{q\}\beta_j}{s+\beta_j} ; j=1,2 \quad (4.114)$$

This is also true for δ ,

$$\frac{s^2\{\delta\}}{s+\beta_j} = s\{\delta\} - \frac{s\{\delta\}\beta_j}{s+\beta_j} ; j=1,2 \quad (4.115)$$

likewise for the gust lag terms,

$$\frac{sw}{s+\beta_j} = \frac{ws + w\beta_j - w\beta_j}{s+\beta_j} = \frac{w(s+\beta_j) - w\beta_j}{s+\beta_j}$$
$$\frac{sw}{s+\beta_j} = w - \frac{w\beta_j}{s+\beta_j} ; j=3,4 \quad (4.116)$$

The complete equations for the state space model are found in Equations (4.60), (4.61), (4.108), (4.110), (4.112), (4.113), (4.114), (4.115), and (4.116). These are shown in full matrix form in Equation (4.121). This may be written:

$$[H] \{\dot{x}\} = [HA] \{x\} + [HB] \{u\} \quad (4.117)$$

Define

$$[A] = [H]^{-1} [HA] \quad (4.118)$$

$$[B] = [H]^{-1} [HB] \quad (4.119)$$

We then have the final state-space format:

$$\{\dot{x}\} = [A] \{x\} + [B] \{u\}$$

SECTION 5
MODEL-ORDER REDUCTION FOR LINEAR SYSTEMS

5.1 MODEL-ORDER REDUCTION FOR LINEAR SYSTEMS

5.1.1 Introduction

Model-order reduction makes application of modern control theory more practical. To include all of the huge number of modes of a structural dynamics model in the control-system plant of an active control system would not only strain the capability of the computer facility, but would lead to compensation transfer functions of much higher order than necessary.

A method of model-order reduction that Lockheed has successfully used in the past and some variations of a more general method, which are currently under study, will be discussed. These methods are: (1) spectral decomposition, and (2) balanced approximation. Spectral decomposition is the more direct method, but is limited to linear time-invariant (LTI) systems (the usual model for stability and control of airplanes). The balanced approximation method can be applied to time-variant models and, obviously, to their LTI extensions.

The main thrust of the model reduction problem, as reported here, will be limited to LTI systems denoted simply as (A,B,C) realizations. The corresponding state-space equations are:

$$\begin{aligned}\dot{\underline{x}}(t) &= A\underline{x}(t) + B\underline{u}(t) \\ \underline{y}(t) &= C\underline{x}(t)\end{aligned}\tag{5.1}$$

5.1.2 Background

Before the development of the jumbo air transports and other large aerospace vehicles, rigid-body equations were all that were needed for the mathematical description of an airframe in a control-system model. Except as needed for the judicious placement of sensors, concern with the structural

dynamics of the airframe was avoided. Structural paths affecting servo feedback signals were part of the control system technology, but any other aspects of structural dynamics were left to the dynamic loads and flutter disciplines.

With the advent of new technologies aimed at controlling the structural modes of large flexible bodies came the need to expand the control theory domain. The most obvious approach to these higher-order models was linear algebra, the basic analytical tool for structural dynamics, dealing with vectors and matrices. Adoption of these methods in control theory led naturally to the development of multi-loop optimization processes which utilize state-space models and which are covered under the broad discipline known as "modern control theory." Large scale digital computers were essential tools for this work because of the large matrix sizes.

Stability-and-control engineers have been working with vectors and matrices for decades. The state-space approach is little more than a method of accounting. It is equally applicable to time-domain (differential equation) or frequency domain (Fourier/Laplace transform) models of dynamic systems. There are several advantages to using state-space models, a few of which are:

- A large number of scalar equations can be expressed as a small number of vector-matrix equations.
- The linearization of aircraft equations, which are inherently nonlinear, is straightforward.
- Appropriate reduced-order models can be generated easily.

Of course, in order to apply the above conveniences, in addition to those of the previous classical methods, control theory applied to the design of airplanes is based primarily on linear analyses. Rigid-body data in the form of stability derivatives from the wind-tunnel curves are used to compute small perturbations and related output data characterizing the flight dynamics. A set of these linear models, each representing a particular flight condition is

used to study airplane control in the total flight envelope. The rigid body input data may also include stability derivative corrections to represent airframe flexure influences upon the aerodynamic forces. This is not sufficient, however, where the dynamics of the lowest structural mode couple with the short period of the rigid body model. Similarly, the lowest structural mode will couple with the next higher mode, ad infinitum; so that the correct model for some handling quality studies must include the dynamics of several modes. In case the original model (designed for flutter analysis) does not include accurate rigid-body characteristics, then a good representation can usually be obtained by inserting rigid-body coefficients in the appropriate matrix locations. This approach "estimates" the coupling between the short-period and the lowest structural mode. If this is not acceptable, then the original model must include accurate representation of the rigid-body modes. Lockheed is presently developing new flexible-modeling techniques that will yield large flexible models with accurate short-periods and phugoids.

Obviously, a large aeroelastic model of the type commonly used for loads or flutter analyses must be reduced to comparatively low order before it can be used in a practical setting for control system studies; e.g., a real-time flight simulator. Since structural-dynamics models are practically time invariant, the required simplifications can be done conveniently by exploiting the fundamental attributes of linear algebra: eigenvalues, eigenvectors, and superposition. After the aeroelastic model has been reduced to an appropriate order, it can then be superimposed upon a rigid-body, total-force model if desired. A comparatively simple alternative to the total-force model, sometimes used for take-off or landing, is one which utilizes time-variable interpolation of stability derivative increments between sets of stability derivatives. In most cases, however, linear models with constant coefficients are adequate for the study of stability and control characteristics, including handling qualities.

The eigenvalues are labelled such that λ_{s_i} is stable and λ_{u_j} is unstable.

Define

$$\bar{X} = P^{-1} X$$

$$\bar{B} = P^{-1} B$$

$$\bar{C} = C P$$

and partition \bar{B} and \bar{C} conformably with

$$\begin{pmatrix} \Lambda_s & 0 \\ 0 & \Lambda_u \end{pmatrix}$$

$$\text{i.e., } \bar{B} = \begin{pmatrix} \bar{B}_s \\ \bar{B}_u \end{pmatrix}, \quad \bar{C} = (\bar{C}_s \quad \bar{C}_u)$$

Combining the above yields the new state space model.

$$\dot{\bar{x}} = \begin{pmatrix} \Lambda_s & 0 \\ 0 & \Lambda_u \end{pmatrix} \bar{x} + \begin{pmatrix} \bar{B}_s \\ \bar{B}_u \end{pmatrix} u$$

$$y = (\bar{C}_s \quad \bar{C}_u) \bar{x}$$

It follows that

$$G(s) = \underbrace{\bar{C}_s (sI - \Lambda_s)^{-1} \bar{B}_s}_{G_s(s)} + \underbrace{\bar{C}_u (sI - \Lambda_u)^{-1} \bar{B}_u}_{G_u(s)}$$

The above is clearly the "stable + unstable" decomposition.

5.2 THE MATH MODEL - FROM FIRST PRINCIPLES

An airplane flying through changing flight conditions is described mathematically by a set of nonlinear aerodynamic curves from which stability derivatives are normally derived. A simulation of the exact equations would not include the stability derivatives per se; nevertheless, the derivatives would be represented in the simulation by the slopes of the aerodynamic curves. The resultant dynamics of the simulation will closely approximate those of a linear model as long as the motions are small perturbations.

The nonlinear equations of motion can be written as a single vector differential equation

$$\dot{\underline{x}}(t) = \underline{f}(\underline{x}(t), \underline{u}(t)) \quad (5.2)$$

where $\underline{x}(t)$ is the state vector, and $\underline{u}(t)$ is the control vector.

Output quantities are represented as

$$\underline{y}(t) = \underline{h}(\underline{x}(t), \underline{u}(t))$$

The aircraft is trimmed in unaccelerated flight if the system is at steady state, i.e., $\dot{\underline{x}}(t) = 0$. The states and controls for trim are defined by

$$0 = \underline{f}(\underline{x}_0(t), \underline{u}_0(t))$$

Perturbations from this trimmed condition can be characterized by a linear model, which is obtained by a Taylor series expansions of Equation (5.2) about \underline{x}_0 and \underline{u}_0 . The linearized dynamic equation is

$$\Delta \dot{\underline{x}}(t) = A \Delta \underline{x}(t) + B \Delta \underline{u}(t) \quad (5.3a)$$

and the linearized output is

$$\Delta \underline{y} = C \Delta \underline{x}(t) + D \Delta \underline{u}(t) \quad (5.3b)$$

where A,B,C, and D are Jacobian matrices of derivatives with respect to \underline{x} and \underline{u} evaluated at the trim condition. In this report, subsequent incremental equations of the above form will be written with the Δ 's deleted. All of the elements of these Jacobian matrices are real scalar variables. In general, the matrices are time-varying; but in keeping with the assumption that the aircraft is trimmed, it can usually be assumed that the matrices are constant. During flight maneuvers where the stability derivatives are changing rapidly, the linearized model must contain time-variant matrix coefficient; i.e.:

$$\dot{\underline{x}}(t) = A(t) \underline{x}(t) + B(t) \underline{u}(t) \quad (5.4a)$$

$$\underline{y}(t) = C(t) \underline{x}(t) + D(t) \underline{u}(t) \quad (5.4b)$$

where the state at time t, $\underline{x}(t)$, is an n-vector; the input at time t, $\underline{u}(t)$, is an m-vector and the output at time t, $\underline{y}(t)$, is an r-vector. A,B,C, and D are matrices of compatible size. We will refer to this model simply as (A,B,C,D).

The desired input from the aerodynamic and structural disciplines to the control system engineer are contributions to the A and B matrices for all trim conditions representative of the entire flight envelope. Selections of the C and D matrices depend upon the sensor locations. D is usually zero except for accelerometer outputs.

The elements of the state vector \underline{x} include all of the variables of the flexible model and of the control system, including the actuators and sensors. Those of the control vector \underline{u} contain all of the control commands. If the model is reduced from a larger one, then the negligible variables of the state vector are removed and the A,B, and C matrices are modified accordingly.

Figure 5-1 is a state-space block diagram of Equation (5.4) with no direct coupling from input to output ($D = 0$), but with anticipated feedback signals from output to input through the feedback matrix F. Although the

overall model-reduction problem is a function of the closed-loop system, the scope of this report is restricted to the open-loop realization (A,B,C).

5.2.1 Solutions of the State-Space Equation

The real-time solution of the state variable in Equation (5.4) is

$$\underline{x}(t) = \phi(t, t_0)\underline{x}(t_0) + \int_{t_0}^t \phi(t, \tau)B(\tau)\underline{u}(\tau)d\tau \quad (5.5)$$

where $\phi(t, t_0)$, known as the transition matrix, is defined by its time derivative:

$$\frac{d\phi}{dt}(t, t_0) = A(t)\phi(t, t_0); \phi(t_0, t_0) = I \quad (5.6)$$

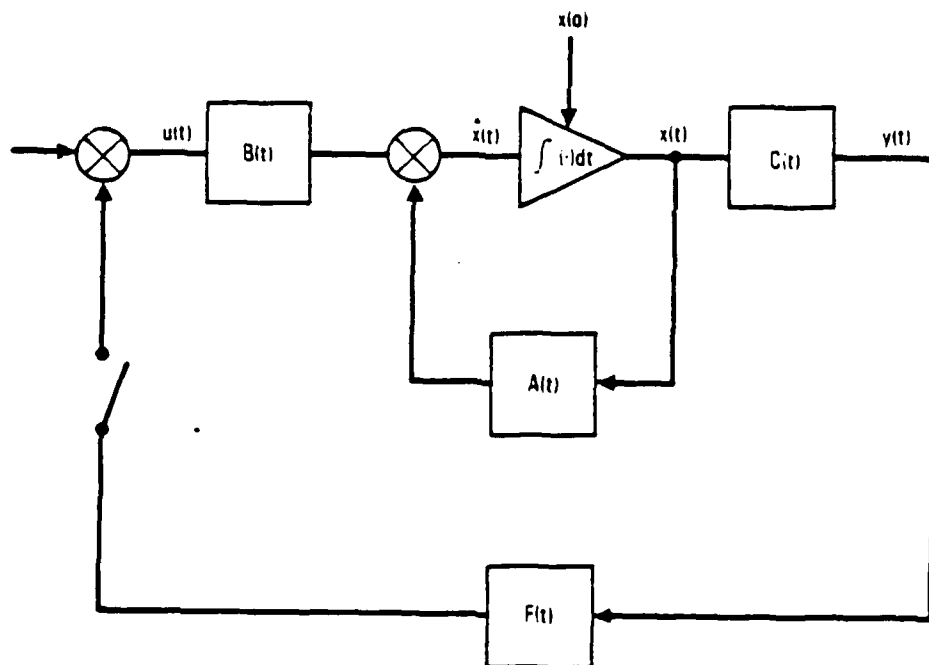


Figure 5-1. Time-Variant (A,B,C) Model With Anticipated Feedback

The transition matrix is exactly analogous to the integrating factor used in the classical solution of a single, first-order differential equation with variable coefficients.

If the matrix A is time invariant, then the transition matrix is

$$\phi(t, t_0) = e^{A(t-t_0)} = \phi(t-t_0) \quad (5.7)$$

Therefore, if the system, Equation (5.4) is time-invariant, the integral in Equation (5.5) becomes a convolution and the equation is simplified to:

$$\underline{x}(t) = \phi(t-t_0) \underline{x}(t_0) + \int_{t_0}^t \phi(t-\tau) B u(\tau) d \tau \quad (5.8)$$

Taylor's series expansion of the matrix exponential $e^{A(t-t_0)}$ provides a convenient computer implementation of the transition matrix of an LTI system, i.e:

$$\phi(t, t_0) = e^{A(t-t_0)} = \sum_{i=0}^{\infty} \frac{[A(t-t_0)]^i}{i!}$$

If the matrix A(t) is variable, then $\phi(t, t_0)$ is obtained by computer implementation of Equation (5.6).

Laplace transforms of the LTI systems with $t_0 = 0$, are:

$$L[\phi(t)] = (sI-A)^{-1}$$

$$\underline{X}(s) = (sI-A)^{-1} (\underline{x}(0) + B\underline{U}(s)) \quad (5.9)$$

The corresponding output, with the initial conditions at zero, is

$$Y(s) = C(sI-A)^{-1} B U(s) \quad (5.10)$$

The expression

$$G(s) = C(sI-A)^{-1}B$$

is the matrix transfer function of the (A,B,C) system.

5.3 MODEL-ORDER REDUCTION APPROACHES

Inspection of Equation (5.9) reveals a possible approach to the model-order reduction problem as follows:

1. With all initial conditions zero, consider all possible state responses to all possible unit impulses (one at a time) in the control vector.
2. With all input signals zero, consider all possible output transients due to each possible initial state (set at unit value, one at a time).
3. Weigh the above results by appropriate means; then eliminate the states that yield negligible results.

Clearly for this approach each of the matrices A, B and C contribute heavily in the evaluation. Controllability (state responses due to unit impulses at the input) and observability (output responses due to unit initial conditions) are the prime considerations. This is the basis for the method of "balanced realizations."

5.3.1 The Balanced Approximation Approach

As mentioned previously, inspection of Equation (5.9) suggests the steps for a balanced approximation of an LTI system. An intuitive application of each step would be as follows:

Step 1

As applied to the input of Equation (5.9) one at a time, the set of Laplace transforms of unit impulses could be represented by an identity matrix of order m ; i.e.:

$$[U_1(s) \ U_2(s) \ \dots \ U_m(s)] = I_m$$

The corresponding set of impulse response vectors in the time domain would be

$$[\underline{x}_1(t) \ \underline{x}_2(t) \ \dots \ \underline{x}_m(t)] = e^{At}B \quad (5.11)$$

If the system is stable, an appropriate measure of all possible impulse responses would be the time integral of a real symmetric non-negative definite nxn matrix reflecting $e^{At}B$; i.e.:

$$W = \int_0^{\infty} e^{At}BB'e^{A't}dt \quad (5.12)$$

A real symmetric matrix Q is non-negative definite if for all real nonzero vectors, the scalar $\underline{x}'Q\underline{x} \geq 0$.

Step 2

Similarly, with no input and with the initial conditions applied one at a time, the set of initial conditions could be represented by an identity matrix of order n ; i.e.:

$$[\underline{x}_1(0) \ \underline{x}_2(0) \ \dots \ \underline{x}_n(0)] = I_n$$

The corresponding set of output vectors (transient responses in the time domain) would be

$$[y_1(t) \ y_2(t) \ \dots \ y_r(t)] = Ce^{At} \quad (5.13)$$

Again, if the system is stable, an appropriate measure of all possible transient responses due to initial conditions would be the time integral of a real symmetric non-negative definite nxn matrix reflecting Ce^{At} ; i.e.:

$$M = \int_0^{\infty} e^{A't} C' C e^{At} dt \quad (5.14)$$

These matrices, W and M, are called the controllability and observability grammians respectively for an LTI system. Some of their properties are: They are symmetric; they are non-negative definite; and they satisfy the following time invariant Lyapunov equations, respectively:

$$AW + WA' + BB' = 0 \quad (5.15)$$

$$MA + A'M + C'C = 0 \quad (5.16)$$

If W (or M) is positive definite, then its eigenvectors are linearly independent, and each response vector in Equation (5.11) or (5.13) has a unique value other than zero.

The criterion for linear independence of vectors, called the Gram criterion, as presented in Reference [2], Chapter 2, is summarized below:

The criterion can be stated in terms of the positive definiteness of a grammian. A set of real vectors

$$\underline{x}_1, \underline{x}_2, \dots, \underline{x}_m$$

in a Euclidean space is called linearly independent if there exists no set of non-zero real numbers a_1, a_2, \dots, a_m such that

$$a_1 \underline{x}_1 + a_2 \underline{x}_2 + \dots + a_m \underline{x}_m = 0$$

To test a set of vectors for linear independence, a simple way is to form m equations by premultiplying the above equations by $\underline{x}_1', \underline{x}_2', \dots$ to obtain

$$\begin{bmatrix} \underline{x}_1' \underline{x}_1 & \underline{x}_1' \underline{x}_2 & \dots & \underline{x}_1' \underline{x}_m \\ \underline{x}_2' \underline{x}_1 & \underline{x}_2' \underline{x}_2 & \dots & \underline{x}_2' \underline{x}_m \\ \dots & \dots & \dots & \dots \\ \underline{x}_m' \underline{x}_1 & \underline{x}_m' \underline{x}_2 & \dots & \underline{x}_m' \underline{x}_m \end{bmatrix} \begin{bmatrix} a_1 \\ a_2 \\ \dots \\ a_m \end{bmatrix} = \begin{bmatrix} 0 \\ 0 \\ \dots \\ 0 \end{bmatrix}$$

The $m \times m$ matrix on the left is the gramian associated with the given set of vectors. It is clearly symmetric since $\underline{x}_i' \underline{x}_j = \underline{x}_j' \underline{x}_i$; moreover it is non-negative definite as shown by the easy calculation which follows:

$$\begin{bmatrix} a_1 & a_2 & \dots & a_m \end{bmatrix} \begin{bmatrix} \underline{x}_1' \underline{x}_1 & \underline{x}_1' \underline{x}_2 & \dots & \underline{x}_1' \underline{x}_m \\ \underline{x}_2' \underline{x}_1 & \underline{x}_2' \underline{x}_2 & \dots & \underline{x}_2' \underline{x}_m \\ \dots & \dots & \dots & \dots \\ \underline{x}_m' \underline{x}_1 & \underline{x}_m' \underline{x}_2 & \dots & \underline{x}_m' \underline{x}_m \end{bmatrix} \begin{bmatrix} a_1 \\ a_2 \\ \dots \\ a_m \end{bmatrix} = \left\| a_1 \underline{x}_1 + a_2 \underline{x}_2 + \dots + a_m \underline{x}_m \right\|^2$$

Clearly, if and only if (iff) the gramian is positive definite, there exists no nonzero set of a 's such that

$$a_1 \underline{x}_1 + a_2 \underline{x}_2 + \dots + a_m \underline{x}_m = 0$$

Therefore, if the vectors in Equations (5.11) and (5.13) are all shown to be independent by virtue of the positive definiteness of their gramians, then the corresponding (A,B,C) model is minimal; i.e., it cannot be reduced without introducing some error. However, if any of the vectors are dependent, then the corresponding gramian is not positive definite, and the system is not completely controllable or not completely observable, depending on which gramian is not positive definite. The corresponding model is not minimal and can be reduced without introducing error.

Beginning with a minimal system (both grammians positive definite) is a basic premise. Indeed, balancing cannot be extended to non-minimal systems without non-trivial modification, for balancing would attempt to equate a singular grammian to a non-singular one. Nevertheless, to view the system as if some of its states can be treated approximately as uncontrollable or unobservable is the key to model reduction by balancing. This concept is amplified in the next subsection, 5.3.1.1.

Step 3

The various singular values of W , relative to each other, represent the various degrees of input-state coupling in the (A,B,C) system. Likewise, the various singular values of M , relative to each other, represent the various degrees of state-output coupling.

As in the case of a scalar transfer function with its magnitude defined as the ratio of output to input, so might the magnitudes of a matrix transfer function be defined. This set of magnitudes comprises its "singular values". A squared singular value of any square matrix Q is an eigenvalue of $Q'Q$ explained as follows:

Denoting an eigenvalue of $Q'Q$ as σ^2 and its corresponding eigenvector as \underline{v} , then

$$Q'Q\underline{v} = \sigma^2\underline{v}$$

Premultiplying by \underline{v}' ,

$$\underline{v}'Q'Q\underline{v} = \sigma^2\underline{v}'\underline{v}$$

Therefore

$$\|Q\underline{v}\| / \|\underline{v}\| = \sigma$$

Thus, a singular value represents an output vector/input vector magnitude ratio.

Special coordinate transformations in the state space of the matrices W and M , called "balancing", result in identical sets of singular values for W and M . The balancing process will be explained in Paragraph 5.3.14.

In the following three subsections, excerpts from Reference (5.4) are presented as more rigorous background for the above statements. In Chapter 2 of the reference, it is shown how the input-output characteristics of two time-variant systems - even those of different order - can be exactly equivalent. This is true if the system of larger order is either uncontrollable or unobservable. The balanced realization approach is based on the principle that a system having a state which is comparatively uncontrollable and unobservable can be considered to be actually so without significant error in the approximation.

5.3.1.1 The Weighting Pattern

A relationship between an input \underline{u} and a response \underline{y} is commonly described by the triplet (A,B,C) which means

$$\dot{\underline{x}}(t) = A(t)\underline{x}(t) + B(t)\underline{u}(t), \quad \underline{y}(t) = C(t)\underline{x}(t) \quad (5.17)$$

In addition there exists, in accordance with Equation (5.5), a possibility of a description by an integral equation:

$$\underline{y}(t) = \underline{y}(t_0) + \int_{t_0}^t T(t,\sigma)\underline{u}(\sigma)d\sigma \quad (5.18)$$

where

$$\underline{y}(t_0) = C(t)\Phi(t,t_0)\underline{x}(t_0)$$

and

$$T(t, \sigma) = C(t)\Phi(t, \sigma)B(\sigma) \quad (5.19)$$

$T(t, \sigma)$ is called the weighting pattern. A given matrix $T(t, \sigma)$ is said to be realizable as the weighting pattern if there exist matrices A , B , and C such that Equation (5.17) holds for all pairs (t, σ) with $\dot{\Phi}(t, t_0) = A(t)\Phi(t, t_0)$ and $\Phi(t_0, t_0) = I$. The triplet (A, B, C) is then called a realization of $T(t, \sigma)$.

If a given weighting pattern has one realization, then it has many. For example if $P(t)$ is nonsingular and differentiable for all t and if system Equation (5.17) is one realization of $T(t, \sigma)$ then in terms of $\underline{z}(t) = P(t)\underline{x}(t)$, we have the alternative realization:

$$\dot{\underline{z}}(t) = (P(t)A(t)P^{-1}(t) + \dot{P}(t)P^{-1}(t))\underline{z}(t) + P(t)B(t)\underline{u}(t)$$

$$\underline{y}(t) = C(t)P^{-1}(t)\underline{z}(t)$$

By focusing on the weighting pattern, it is possible to define a type of equivalence between various systems with the same input-output characteristics when $\underline{x}(t_0) = 0$. Furthermore, with a given weighting pattern there exist realizations having state vectors of different dimension. If the system given by Equation (5.17) realizes the weighting pattern $T(t, \sigma)$ it will be called a minimal realization if there exists no other realization of $T(t, \sigma)$ having a lower dimensional state vector. This minimum dimension is called the order of the weighting pattern.

A lack of controllability indicates a deficiency in the coupling between input and state vector, and a lack of observability indicates a deficiency in the coupling between state and output; so it is reasonable to expect that minimality is related to these ideas. The following theorem states that this is indeed the case.

Theorem 1

The system Equation (5.17) is a minimal realization of Equation (5.19) if

$$W(t_0, t_1) = \int_{t_0}^{t_1} \Phi(t_0, \sigma) B(\sigma) B'(\sigma) \Phi'(t_0, \sigma) d\sigma$$

and

$$M(t_0, t_1) = \int_{t_0}^{t_1} \Phi'(t_0, \sigma) C'(\sigma) C(\sigma) \Phi(\sigma, t_0) d\sigma$$

are both positive definite for some pair (t_0, t_1) .

For the sake of brevity, lemmas and theorems from Reference [16] are stated here without proof. In the reference, the proof objectives are to show that: 1. For controllability, the state vector $\underline{x}(t)$ must lie within the range space of a prescribed linear mapping, and 2. For observability, the initial state vector $\underline{x}(t_0)$ must lie within the null space of another prescribed linear mapping. For example: \underline{z} belongs to the range space of A if there exists a \underline{y} such that $A\underline{y} = \underline{z}$; and \underline{y} belongs to the null space of A if $A\underline{y} = 0$.

The above matrices W and M are the controllability and observability grammians for time variant systems respectively. In the following two subsections some lemmas and theorems concerning controllability and observability will clarify the meaning of the above theorem.

5.3.1.2 Controllability

Problems associated with the controllability of time variant systems can be illustrated with a simple ballistic problem. Suppose the dynamics are given as

$$\dot{\underline{z}}(t) = B(t)\underline{u}(t)$$

Assume $B(t)$ and $\underline{z}(t_0)$ are known and let the problem be that of finding $\underline{u}(t)$ so as to insure that at $t = t_1 > t_0$, \underline{z} takes on a certain value.

Integrating yields

$$\underline{z}(t_1) = \underline{z}(t_0) + \int_{t_0}^{t_1} B(t)\underline{u}(t)dt$$

Hence, if $\underline{z}(t_1) - \underline{z}(t_0)$ lies in the range space of the linear mapping

$$L(\underline{u}) = \int_{t_0}^{t_1} B(t)\underline{u}(t)dt$$

then the desired transfer is possible; otherwise is it not. This statement is analogous to one which might say that a line and a plane in a three dimensional space can be expressed in terms of a two dimensional space if the line lies on the plane; otherwise it cannot.

Lemma 1

An n-tuple \underline{x}_1 lies in the range space of $L(\underline{u}) = \int_{t_0}^{t_1} B(t)\underline{u}(t)dt$ if it lies in the range space of the matrix

$$W(t_0, t_1) = \int_{t_0}^{t_1} B(t)B'(t)dt \quad (5.20)$$

Corollary

There exists a control \underline{u} which transfers the state of the system $\dot{\underline{z}}(t) = B(t)\underline{u}(t)$ from \underline{z}_0 at $t = t_0$ to \underline{z}_1 at $t = t_1$ iff $\underline{z}_1 - \underline{z}_0$ lies in the range space of $W(t_0, t_1)$ as defined in Equation (5.20).

The extension of these results to the (A,B,C) realization leads to

Theorem 2

There exists a \underline{u} which drives the state of the system

$$\dot{\underline{x}}(t) = A(t)\underline{x}(t) + B(t)\underline{u}(t)$$

from the value \underline{x}_0 at $t = t_0$ to the value \underline{x}_1 at $t = t_1 > t_0$ iff $\underline{x}_1 - \Phi(t_0, t_1)\underline{x}_0$ belongs to the range space of

$$W(t_0, t_1) = \int_{t_0}^{t_1} \Phi(t_0, t)B(t)B'(t)\Phi'(t_0, t)dt$$

The above controllability grammian plays an important role in the theory of forced linear systems. Some of its properties are: It is symmetric; it is non-negative definite $t_1 \geq t_0$; and it satisfies the linear matrix differential equation

$$\dot{W}(t, t_1) = A(t)W(t, t_1) + W(t, t_1)A'(t) + B(t)B'(t), \quad W(t_1, t_1) = 0$$

In the special case where A and B are time invariant it is possible to calculate the range space of W quite easily. Moreover, contrary to the general case, the range space does not depend on the arguments of W except in a trivial way.

The following theorem expresses the situation. Its proof is based on a Taylor series expansion of $B'\exp(A'(t_0 - \sigma))\underline{x}_1 = 0$. Note that

$$\underline{x}_1'W(t_0, t_1)\underline{x}_1 = \int_0^{t_1} \left\| B'\exp(A'(t_0 - \sigma))\underline{x}_1 \right\|^2 d\sigma$$

is equal to zero because \underline{x}_1 is in the null space of $W(t_0, t_1)$.

Theorem 3

For A and B constant and A nxn, the range space and the null space of $W(t_0, t)$ for $t > t_0$ coincide with the range space and null space of the nxn matrix

$$W_c = [B, AB, \dots, A^{n-1}B][B, AB, \dots, A^{n-1}B]'$$

Moreover, for any vector \underline{x}_0 and any $t > t_0$,

$$\text{Rank}[W(t_0, t), \underline{x}_0] = \text{Rank}[B, AB, \dots, A^{n-1}B, \underline{x}_0]$$

Therefore, an n-dimensional linear invariant system is controllable if $[B, AB, \dots, A^{n-1}B]$ is of rank n.

5.3.1.3 Observability

Observability questions relate to the problem of determining the value of the state vector \underline{x} , knowing only the output \underline{y} over some interval of time. Thus, consider the homogeneous system

$$\dot{\underline{x}}(t) = A(t)\underline{x}(t), \quad \underline{y}(t) = C(t)\underline{x}(t) \quad (5.21)$$

rather than to deal with the more complicated system Equation (5.17).

The homogeneous problem leads to the linear transformation

$$L(t) = C(t)\Phi(t, t_0)\underline{x}(t_0) = H(t)\underline{x}(t_0)$$

For these transformations we define the null space of this mapping as the set of all vectors \underline{x} such that $H(t)\underline{x}(t)$ is identically zero over the time interval $t_0 \leq t \leq t_1$. A characterization of the null space is given by the following lemma.

Lemma 2

Let C be an $m \times n$ matrix whose elements are continuous on the interval $t_0 \leq t \leq t_1$. The null space of the mapping $L(\underline{x}) = C\underline{x}$ coincides with the null space of

$$M(t_0, t_1) = \int_{t_0}^{t_1} C'(t)C(t)dt$$

The following theorem is closely related to Theorem 2.

Theorem 4

With A , C , and \underline{y} given on the interval $t_0 \leq t \leq t_1$, together with Equation (5.21), then it is possible to determine $\underline{x}(t_0)$ to within an additive constant vector which lies in the null space of $M(t_0, t_1)$, where

$$M(t_0, t_1) = \int_{t_0}^{t_1} \Phi'(t, t_0)C'(t)C(t)\Phi(t, t_0)dt$$

In particular, it is possible to determine $\underline{x}(t_0)$ uniquely if $M(t_0, t_1)$ is nonsingular. Moreover it is impossible to distinguish with a knowledge of \underline{y} , the starting state \underline{x}_1 from the starting state \underline{x}_2 if $\underline{x}_1 - \underline{x}_2$ lies in the null space of $M(t_0, t_1)$.

The above observability gramian plays a role analogous to that of $W(t_0, t_1)$ introduced in the previous section. As with $W(t_0, t_1)$, some of its properties are: It is symmetric; it is non-negative definite for $t_1 \geq t_0$; and it satisfies the linear matrix differential equation

$$-\dot{M}(t, t_1) = A'(t)M(t, t_1) + M(t, t_1)A(t) + C'(t)C(t), \quad M(t_1, t_1) = 0$$

Again, in the special case where A and B are time invariant it is possible to calculate the null space of M quite easily. Moreover, contrary to the general case, the null space does not depend on the arguments of M except in a trivial way. The following theorem expresses the situation

Theorem 5

For A and C constant and A nxn, the range space and the null space of $M(t_0, t)$ for $t > t_0$ coincide with the range space and null space of the nxn matrix

$$M_c = [C' \ A'C' \ \dots \ A'^{n-1}C']$$

As before, an n-dimensional linear constant system is observable if M_c is of rank n.

5.3.1.4 Balanced Approximations

Summaries relative to open-loop balancing in References [17] and [18] comprise most of this subsection. The basic idea is that the singular values of an appropriately defined matrix are system invariants which measure how strongly certain parts of a system enter into its input-output behavior in balanced coordinates. If some singular values are much smaller than the others, then a part of the system dynamics can be eliminated, resulting in a lower-order system approximation.

A disadvantage of open-loop balancing is that it requires that the original system be stable. Moreover, it is difficult to predict closed-loop stability of a control system based on an open-loop reduced model. Although the scope of this report does not include closed-loop balancing, such techniques have been developed (e.g., Equation (5.5)) and shown to guarantee closed-loop stability of reduced-order models.

As previously explained, the balancing approach to model reduction relies on measures of input-to-state and state-to-output coupling. These measures are based on the controllability and observability grammians which, for stable time-invariant systems, are defined by Equations (5.12) and (5.14) respectively. If (A,B,C) is uncontrollable or unobservable, then a lower-order model, having precisely the same impulse responses, can be found.

Two models are equivalent if they are related by a nonsingular transformation of coordinates. That is, if $\underline{x}(t) = T\underline{z}(t)$, then the model

$$\dot{\underline{z}} = T^{-1}A T \underline{z} + T^{-1} B \underline{u}, \underline{y} = CT\underline{z}$$

is equivalent to (A,B,C) . Letting

$$\bar{A} = T^{-1} A T, \quad \bar{B} = T^{-1} B, \quad \bar{C} = CT$$

then this equivalence is denoted as

$$(A,B,C) \stackrel{T}{\sim} (\bar{A},\bar{B},\bar{C}) \quad (5.22)$$

If Equation (5.22) holds, then it is easily shown by substitution into Equations (5.15) and (5.16) that the transformed controllability and observability matrices satisfy the relationships

$$\bar{W} = T^{-1} W T^{-1} \quad (5.23)$$

$$\dot{\bar{M}} = T' M T \quad (5.24)$$

A primary purpose for looking at equivalent systems is to discover what system properties are coordinate free; i.e., system invariant. A key element of the open-loop balancing theory is that while W and M do not have system invariant properties, the product of the two matrices does, and it provides a coordinate-free measure of state coupling. This fact follows directly from Equations (5.23) and (5.24).

$$\bar{W}\bar{M} = T^{-1} W M T \quad (5.25)$$

Equation (5.25) implies that the eigenvalues of the product matrix WM are system invariants. Since the matrices W and M are both positive definite if (A,B,C) is controllable and observable, the eigenvalues of WM will be strictly positive. Note that $WM = T\Lambda T^{-1}$ where $\Lambda = \bar{W}\bar{M}$. Denoting these eigenvalues as σ_i , they will be assumed to be ordered as

$$\sigma_1 \geq \sigma_2 \dots \geq \sigma_n > 0$$

If T is chosen to be the corresponding set of eigenvectors, then WM is the diagonal matrix of eigenvalues:

$$\bar{W}\bar{M} = \Lambda = \begin{bmatrix} \sigma_1 & & & 0 \\ & \sigma_2 & & \\ & & \ddots & \\ & & & \sigma_n \\ 0 & & & & 0 \end{bmatrix}$$

Corresponding reduced versions of \bar{W} and \bar{M} are

$$\hat{W} = \hat{M} = \Sigma_1$$

reduced from

$$\bar{W} = \begin{bmatrix} \Sigma_1 & 0 \\ 0 & \Sigma_w \end{bmatrix}, \quad \bar{M} = \begin{bmatrix} \Sigma_1 & 0 \\ 0 & \Sigma_m \end{bmatrix}$$

In balanced coordinates, each state component is as controllable as it is observable. Moreover, the σ_i 's give a measure of the degree of controllability and observability of each component.

Note that $\Sigma_w \Sigma_m = 0$ if the corresponding modes of the system are uncontrollable or unobservable, in which case the coordinate system is balanced:

$$\bar{M} = \bar{W} = \Sigma$$

Do these solutions satisfy Equations (5.23) and (5.24)? Yes; it can be shown in Equation (5.3) that specific eigenvectors can always be chosen such that

$$T^{-1}WT'^{-1} = \text{Block diag} (\Sigma_1, \Sigma_w)$$

$$T'MT = \text{Block diag} (\Sigma_1, \Sigma_m)$$

where

$$\Sigma = \text{diag} (\sigma_1, \sigma_2, \dots, \sigma_n)$$

$$\Sigma_w \Sigma_m = \text{diag} (\sigma_{k+1}, \sigma_{k+2}, \dots, \sigma_n)$$

with

$$\sigma_1 \geq \sigma_2 \geq \dots \geq \sigma_k > \sigma_{k+1} = \sigma_{k+2} = \dots = \sigma_n = 0$$

The system model is reduced from the n^{th} -order $(\bar{A}, \bar{B}, \bar{C})_n$ to the k^{th} -order $(\hat{A}, \hat{B}, \hat{C})_k$ by partitioning in accordance with the following rationale:

If for some k , $\sigma_{k+1} \ll \sigma_k$, then the first k state components represent the part of the system which carries most of the input/output information; i.e., the robustly controllable and observable part. Let Σ be partitioned as

$$\Sigma = \begin{bmatrix} \Sigma_1 & 0 \\ 0 & \Sigma_2 \end{bmatrix}$$

Let $(\bar{A}, \bar{B}, \bar{C})$ be partitioned conformably as

$$\bar{A} = \begin{bmatrix} \bar{A}_{11} & \bar{A}_{12} \\ \bar{A}_{21} & \bar{A}_{22} \end{bmatrix}, \quad \bar{B} = \begin{bmatrix} \bar{B}_1 \\ \bar{B}_2 \end{bmatrix}, \quad \bar{C} = [\bar{C}_1 \quad \bar{C}_2]$$

This implies that $(\bar{A}_{11}, \bar{B}_1, \bar{C}_1)$ is a good K^{th} -order approximation of the n^{th} -order system $(\bar{A}, \bar{B}, \bar{C})$. Indeed, letting T_{nk} represent the first k columns of T and letting S_{kn} represent the first k rows of T^{-1} , then

$$(\bar{A}_{11}, \bar{B}_1, \bar{C}_1) = (S_{kn}AT_{nk}, S_{kn}B, CT_{nk})$$

Fortunately, balanced realizations have some remarkable structural properties which make stability of the subsystems automatic.

Note that the reduced state variable is a part of the transformation \underline{z} , and not of the original \underline{x} . This is sufficient if the reduced model is to be used for control-law synthesis; but if it is required that all elements in the reduced state vector are to be observed (e.g., in an iron-bird simulation), then the original output matrix must be the identity matrix ($C = I_n$).

5.3.1.5 The Balancing Algorithm

Calculating the reduced order model using balancing requires computing the stable projection of the AST model from Figure 5-4. The steps for using the balanced approximation approach are as follows:

1. Compute the controllability matrix W and observability matrix M for (A, B, C) as solutions of the Lyapunov equations,

$$AW + WA' + BB' = 0$$

$$A'M + MA + C'C = 0$$

2. Compute a coordinate transformation matrix T to yield $(\bar{A}, \bar{B}, \bar{C})$. The system is balanced when T is chosen such that

$$WM = T\Lambda T^{-1}$$

where Λ is the diagonal matrix of eigenvalues of WM and where T is a corresponding matrix of eigenvectors. Then

$$\Lambda = \bar{W}\bar{M}$$

3. Organize the elements of Λ in descending order; i.e., arranged such that

$$\sigma_1 > \sigma_2 > \dots > \sigma_n$$

Then let $\Sigma (= \Lambda^{1/2})$ be partitioned as

$$\Sigma = \begin{bmatrix} \Sigma_1 & 0 \\ 0 & \Sigma_2 \end{bmatrix}$$

and let (A, B, C) be partitioned conformably as

$$\bar{A} = \begin{bmatrix} \bar{A}_{11} & \bar{A}_{12} \\ \bar{A}_{21} & \bar{A}_{22} \end{bmatrix}, \quad \bar{B} = \begin{bmatrix} \bar{B}_1 \\ \bar{B}_2 \end{bmatrix}, \quad \bar{C} = [\bar{C}_1 \quad \bar{C}_2]$$

4. Reduce the system model from n^{th} -order $(A, B, C)_n$ to k^{th} -order $(\hat{A}, \hat{B}, \hat{C})_k$ by letting T_{nk} represent the first k columns of T and letting S_{kn} represent the first k rows of T^{-1} ; then computing the reduced model.

$$(\bar{A}_{11}, \bar{B}_1, \bar{C}_1) = S_{kn} A T_{nk}, \quad S_{kn} B, C T_{nk}$$

5.3.1.6 Model Order Reduction Over a Disk

The error bound for the previous method, the balanced approximation approach, is,

$$\left\| \hat{G}(s) - G(s) \right\| \leq 2(\sigma_{r+1} + \dots + \sigma_n) \quad \forall s \in \text{RHP}$$

where \hat{G} is the reduced model of order r . n is the order of the full model. σ 's are singular values over the RHP. The proof is given in Reference [20].

It is more practical to minimize the error over the actuator bandwidth, i.e., a finite bandwidth, instead of over the entire bandwidth as done in the previous method. The problem of model reduction over a disk can be stated as, see Figure 5-2.

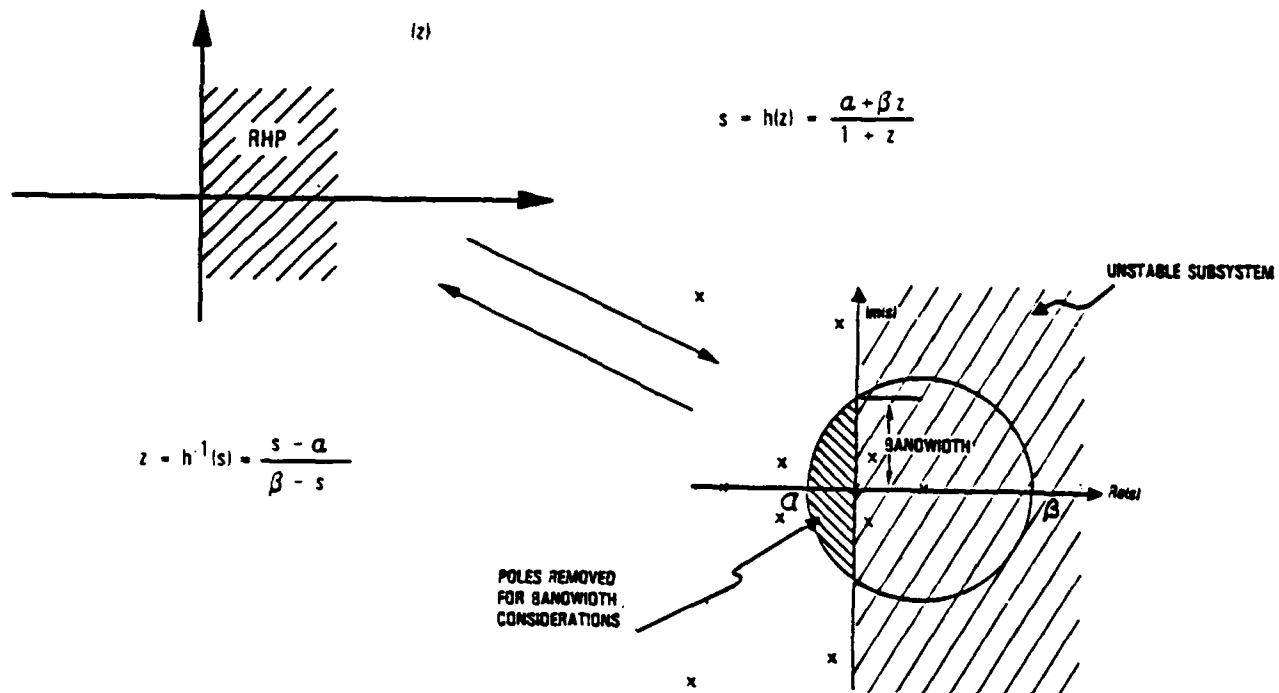


Figure 5-2. Bijective Mapping Between RHP and Disk D

$$\sup_{S \subset D} \left\| G(s) - \hat{G}(s) \right\| \leq \varepsilon$$

where ε is preferably smaller than the full RHP case, i.e.,

$$\varepsilon \leq 2(\sigma_{r+1} + \dots + \sigma_n).$$

Dr. Jonckheere and Li, Reference 20, have found a way to achieve the above objective. They use a bijective mapping which transforms the problem, and this new problem is solved using the balanced approximation method. But the error is found only over the disk which is less than or equal to the error over RHP. Their methodology follows.

The only known engineering solution to this general domain problem is to construct a conformal transformation h that establishes a bijective mapping between RHP and D ,

$$h: \text{RHP} \rightarrow D$$

and that hence reduces the problem to conventional balancing:

$$\sup_{S \subset D} \left\| G(s) - \hat{G}(s) \right\| = \sup_{Z \subset \text{RHP}} \left\| G(h(z)) - \hat{G}(h(z)) \right\|$$

The right half side of the above equation is a classical balancing problem provided the mapping $h: \text{RHP} \rightarrow D$ preserves the degree. The only case in which this happens is when D is a disk in which case h is a bilinear mapping, see Figure 5-2.

It remains to correctly place the disk in the complex plane. This is based on the following two considerations:

1. The full order model $G(s)$ must be analytic in disk. Therefore, the disk must not include any poles of G .

2. The disk must cover the interval $\{j\omega : -\Omega \leq \omega \leq \Omega\}$ of real frequencies not exceeding the bandwidth Ω of the actuators. This guarantees that the error bound is verified over this critical frequency range.

The bilinear mapping is, see Figure 5-2,

$$s=h(z)=\frac{\alpha + \beta z}{1 + z} \qquad z=h^{-1}(s)=\frac{s - \alpha}{\beta - s}$$

If $G(s) = C(sI-A)^{-1}B$, then $G(h(z))= J + H(zI-F)^{-1}G$ with

$$J=C(\beta I-A)^{-1}B$$

$$H=C(\beta I-A)^{-1}$$

$$F=-(\sigma I-A)(\beta I-A)^{-1}$$

$$G=(\beta - \sigma)(\beta I-A)^{-1}B$$

Using conventional balancing, a reduced model of order r , $\hat{G}(z)$ is obtained and it satisfies,

$$\left\| \left| G\left(\frac{\alpha + \beta z}{1 + z}\right) - \hat{G}(z) \right| \right\| \leq 2 (\sigma_{r+1}^D + \dots + \sigma_n^D), \quad \forall z \in \text{RHP}$$

where σ_D 's are the RHP singular values of $G(h(z))$.

The reduced model is recovered back by inverse mapping,

$$\hat{G}(s) = \hat{G}(h^{-1}(s))$$

Dr. Jonckheere and Li, Reference [20], have proven that for this mapping

$$2(\sigma_{r+1} + \dots + \sigma_n) \leq 2(\sigma_{r+1}^D + \dots + \sigma_n^D)$$

i.e., the error bound on the disk is smaller than the error bound over the RHP.

5.3.2 Model-Order Reduction by Spectral Decomposition

An appropriately reduced model, $(A, B, C)_k$ reduced from $(A, B, C)_n$, will describe the rigid-body dynamics and only that part of the structural dynamics necessary for the particular purpose at hand. A technique utilizing spectral decomposition provides a means for decoupling elements of the state variable of an LTI system into two or more models without serious degradation of the total results. For example, it permits model-order reduction of the decoupled parts of the original (A, B, C) triplet into $(\hat{A}, \hat{B}, \hat{C})_k$ and $(\hat{A}^*, \hat{B}^*, \hat{C}^*)_{n-k}$. The procedure begins with a truncated model of intermediate order, n , and uses spectral decomposition in the subsequent process. The intermediate model includes several structural modes couples by generalized, unsteady aerodynamic forces. Spectral decomposition leads to a singular matrix coefficient A_i for each eigenvalue λ_i in the intermediate model. Indeed, if spectral decomposition is used, these singular matrices are the n residues:

$$\begin{aligned} A_i &= \text{Res}_i (sI-A)^{-1}, \quad 1 \leq i \leq n \\ &= \lim_{s \rightarrow \lambda_i} (s - \lambda_i)(sI-A)^{-1} \end{aligned}$$

where A_i is in the i^{th} modal component of (A, B, C) , which means

$$\dot{\underline{x}}_i = A_i \underline{x}_i + B_i \underline{u}, \quad \underline{y}_i = C_i \underline{x}_i \quad (5.26)$$

with

$$A_i = E_i \lambda_i, \quad B_i = E_i B, \quad C_i = C E_i, \quad \underline{x}_i = E_i \underline{x}$$

The matrix E_i can be shown to be the outer product of \underline{e}_i and \underline{t}_i the normalized eigenvectors of A and A' , respectively, i.e., $E_i = \underline{e}_i \underline{t}_i'$. This matrix has one nonzero eigenvalue of 1, and its trace is also 1, because the trace of a matrix is equal to the sum of its eigenvalues.

In the application of classical control theory, which is devoted to LTI single-input, single-output (SISO) systems, it is common practice to ignore, in the transfer function, stable poles that are remotely located on the complex plane; because they are very lightly couples with the set of poles that are important to the analysis. The residue of any lightly coupled pole

is negligibly small; so the corresponding partial fraction can be dropped, thus reducing the order of the transfer function with negligible degradation. In other words, the residue is negligible and therefore comparatively "unobservable". It is the nature of partial fractions that a transfer function reduced in this manner preserves all of the residual influences of the deleted poles as reflected in the residue values of the important poles.

In addition to the remoteness of a pole as an indication that the pole is lightly coupled with the important part of the system, there is also the effect of the proximity of a zero to the pole. The residue of any pole is proportional to its proximity to a zero. Indeed, if a zero is superimposed onto a pole, it cancels the pole. In other words, if the pole is closed to a zero, it is nearly "uncontrollable" or "unobservable" because of its negligible residue.

The analogous situation with regard to a multi-input, multi-output (MIMO) system is that the matrix coefficient of any mode which is lightly coupled to the remaining part of the system is negligible and the mode can be dropped from the partial fraction representation. The corresponding rows and columns of the state space matrices can then be deleted, thus reducing the rank of the state variable matrix coefficient.

The roles of observability and controllability in LTI systems with unique eigenvalues can be made quite clear by substituting into Equation (5.10) the matrix TAT^{-1} in place of A . Then

$$\begin{aligned} Y(s) &= C(sI-A)^{-1}B U(s) \\ &= CT(sI-\lambda)^{-1}T^{-1}B U(s) \end{aligned}$$

CT and $T^{-1}B$ are the measurement and control influence matrices respectively. Denoting these in terms of their column or row vector respectively, as appropriate, then the $r \times m$ matrix transfer function is

$$G(s) = [g_1 \ g_2 \ \dots \ g_n] \begin{bmatrix} (s - r_1) & 0 & \dots & 0 \\ 0 & (s - r_2) & 0 & \dots & 0 \\ \dots & \dots & \dots & \dots & \dots \\ 0 & \dots & 0 & (s - r_n) & \dots \end{bmatrix}^{-1} \begin{bmatrix} \underline{h}_1' \\ \dots \\ \underline{h}_n' \end{bmatrix}$$

$$= \sum_{i=1}^n \frac{g_i h'_i}{(s - r_i)}$$

If, in $G(s)$, any pole $(s - r_i)$ is cancelled by a corresponding zero, then either g_i or h_i , is zero; i.e., this mode is either unobservable or uncontrollable.

Whether a particular mode of a MIMO system is lightly coupled with the remainder of the system is not immediately obvious, as it is in the case of a SISO system, because the "zeros" and residues of the transfer function are matrices rather than scalars; but, with inspection of A_i in Equation (5.26) above, it becomes obvious in view of a criterion for decoupling which is discussed in Paragraph 5.3.2.2.2.

5.3.2.1 Decoupling Rationale

Given a large system of simultaneous linear differential equations expressed in the state-space form Equation (5.1), a means of approximating the system by uncoupled models of lower order is explained below. Responses from the separate subsystems will combine to form a good approximation of the solution of the original set of simultaneous equations.

For simplicity, the present scope is limited to systems with distinct eigenvalues within well-separated groups of frequency ranges. The procedure decouples the frequency groups without producing significant departure in character from the corresponding components of the original model. Specifically, it is possible to write into a nearly equivalent partitioned form

$$\dot{\underline{x}}^{**} = A^{**}\underline{x}^{**} + B^{**}\underline{u}$$

in which the elements are decoupled subvectors and submatrices, i.e.:

$$\begin{bmatrix} \dot{\underline{x}}_1^{**} \\ \dot{\underline{x}}_2^{**} \\ \dots \\ \dot{\underline{x}}_v^{**} \end{bmatrix} = \begin{bmatrix} A_1^{**} & 0 & \dots & 0 \\ 0 & A_2^{**} & \dots & 0 \\ \dots & \dots & \dots & \dots \\ 0 & 0 & \dots & A_v^{**} \end{bmatrix} \begin{bmatrix} \underline{x}_1^{**} \\ \underline{x}_2^{**} \\ \dots \\ \underline{x}_v^{**} \end{bmatrix} + \begin{bmatrix} B_1^{**} \\ B_2^{**} \\ \dots \\ B_v^{**} \end{bmatrix} \underline{u}$$

Each decoupled subsystem

$$\dot{\underline{x}}_k^{**} = A_k^{**}\underline{x}_k^{**} + B_k^{**}\underline{u}, \quad 1 \leq k \leq v \quad (5.27)$$

represents a separate frequency range of the total system behavior.

The procedure begins with the spectral decomposition of the $n \times n$ matrix A into its special components corresponding to each of the n distinct eigenvalues:

$$A = \sum_{i=1}^n A_i \quad (5.28)$$

and with the corresponding decomposition of the other matrices in the triplet:

$$B = \sum_{i=1}^n B_i, \quad C = \sum_{i=1}^n C_i \quad (5.29)$$

where:

$$\begin{aligned} A_i &= \lambda_i E_i \\ B_i &= E_i B \\ C_i &= C E_i \end{aligned}$$

The A_i matrices corresponding to conjugate complex eigenvalues and other eigenvalues in the k^{th} frequency group are then combined into $n \times n$ A_k^* matrices such that

$$A = \sum_{k=1}^v A_k^* , B = \sum_{k=1}^v B_k^* , C = \sum_{k=1}^v C_k^* \quad (5.30)$$

Then, by selective nulling of rows and columns (setting all elements in selected row and column to zero), each triplet $(A_k^*, B_k^*, C_k^*)_n$ is decoupled to become $(A_k^{**}, B_k^{**}, C_k^{**})_n$.

It might be suspected that the same procedure can be centered about singular value decomposition (SVD), wherein the expansion of the square matrix is relative to its singular values instead of its eigenvalues. If practical, the SVD procedure would have certain advantages (e.g.: singular values are always non-negative real); but the SVD procedure is not practical because it can be applied only to symmetric A matrices as shown below.

5.3.2.2 Matrix Decomposition

As implied above, there are at least two basic approaches to decomposing a square matrix: 1. separation of eigenvalues in a spectral decomposition (SD), and 2. Separation of singular values in a singular value decomposition (SVD). The formulae for the two decompositions are of identical form:

$$A = EAR' \quad \text{for spectral decomposition} \quad (5.31)$$

$$A = U\Lambda V' \quad \text{for singular value decomposition} \quad (5.32)$$

where Λ and Σ are diagonal matrices of eigenvalues and singular values respectively; and E , R , U , and V are matrices of corresponding eigenvector sets as follows:

* This formula is true for rectangular matrices in general (not necessarily square) if the matrix is $m \times n$ with $m \leq n$.

E is the set of eigenvectors of A, normalized such that complex pairs are conjugate, and arranged according to the sequence of eigenvalues in A.

R is proportional to the corresponding set of normalized eigenvectors of A'. The proportionality constant is such that the corresponding vectors of E and R are orthonormal; i.e., $E'R = I$.

U is the set of normalized eigenvectors of AA' , arranged according to the sequence of singular values in Σ .

V is proportional to the corresponding set of normalized eigenvectors of $A'A$. The proportionality constant is ± 1 , with the sign selected such that $V\Sigma = A'U$.

Considering the similarities between the two matrix decompositions, why can't the SVD method be used for model-order reduction? The problem is that: $\dot{\underline{q}} = A\underline{q}$ is a valid transformation of $\dot{\underline{x}} = A\underline{x}$; but $\dot{\underline{q}} = \Sigma\underline{q}$ is valid only if A is symmetric. This is explained as follows:

Given that

$$\dot{\underline{x}} = A\underline{x} + B\underline{u} \quad (5.33)$$

and letting $\underline{x} = E\underline{q}$, then

$$\dot{\underline{q}} = R'AE\underline{q} + R'B\underline{u}, \quad R' = E^{-1}$$

with $R'AE = A$. On the other hand, substituting Equation (5.32) into Equation (5.33)

$$\dot{\underline{x}} = U\Sigma V'\underline{x} + B\underline{u}$$

Letting $\underline{x} = U\underline{q}$,

$$\dot{\underline{q}} = \Sigma V'U\underline{q} + U^{-1}B\underline{u}, \quad V' \neq U^{-1}$$

It should be noted that $V'U \neq I$ because $(AA')' \neq A'A$, except when A is symmetric.

Derivations of Equation (5.31) and Equation (5.32) are included in the following subsections. These include derivations of well known relationships that are commonplace; nevertheless they will be derived here to explain clearly their applications to the problems of model-order reduction.

5.3.2.2.1 Singular Value Decomposition - A left singular vector u_i of the matrix A is defined by

$$AA'u_i^2 = \sigma_i^2 u_i \quad (5.34)$$

where σ_i^2 and u_i are the i^{th} eigenvalue and eigenvector respectively of AA' . Assuming that $A'u_i$ is an eigenvector v_i of $A'A$ (right singular vector of A), then

$$A'A(A'u_i) = \sigma_i^2 (A'u_i) = A'\sigma_i^2 u_i \quad (5.35)$$

The above assumption is known to be true because of Equation (5.34); therefore

$$A'u_i = v_i \quad (5.36)$$

and

$$A'Av_i = \sigma_i^2 v_i \quad (5.37)$$

What is the length of v_i relative to that of u_i ? This can be computed as follows:

$$\|v_i\|^2 = v_i'v_i = (A'u_i)'(A'u_i) = u_i'AA'u_i = (AA'u_i)'u_i \quad (5.38)$$

Then substituting from Equation (5.34) into Equation (5.38):

$$\|v_i\|^2 = (\sigma_i^2 u_i)' u_i = \sigma_i^2 \|u_i\|^2$$

So,

$$\|v_i\| = \sigma_i \|u_i\| \quad (5.39)$$

From Equation 5.34) and Equation (5.36)

$$Av_i = \sigma_i^2 u_i \quad (5.40)$$

Dividing Equation (5.40) by Equation (5.39)

$$Av_i / \|v_i\| = \sigma_i^2 u_i / \sigma_i \|u_i\|$$

Then

$$Av_i = \sigma_i \underline{u}_i \quad (5.41)$$

In the above derivation, vectors in the equations preceding Equation (5.41) are intentionally not underlined. The underlined vectors in Equation (5.41) are normalized. The two sets of n vectors in Equation (5.41) can now be grouped into a matrix equation;

$$AV = U\Sigma \quad (5.42)$$

where

$$V = [\underline{v}_1 \ \underline{v}_2 \ \cdots \ \underline{v}_n] , \ U = [\underline{u}_1 \ \underline{u}_2 \ \cdots \ \underline{u}_n]$$

and where Σ is the diagonal matrix of singular values. Note that V is nonsingular and orthonormal. Therefore, this concludes the derivation of Equation (5.32), because Equation (5.42) and Equation (5.32) are equivalent.

5.3.2.2.2 Spectral Decomposition - From First Principles - The state vectors in Equation (5.1) can be resolved into a new set of coordinates, which is the set of eigenvectors corresponding to the matrix A; and then can be decomposed into separate equations describing the state of the system along each eigenvector coordinate. By a transformation of variables

$$\underline{x} = E\underline{q} \quad (5.43)$$

where E is the matrix of eigenvectors

$$E = [\underline{e}_1 \ \underline{e}_2 \ \cdots \ \underline{e}_n] \quad (5.44)$$

Then

$$\dot{\underline{q}} = \Lambda \underline{q} + E^{-1} B \underline{u}, \ \underline{y} = C E \underline{q} \quad (5.45)$$

where $\Lambda = E^{-1} A E$ is a diagonal matrix of the eigenvalues of A.

$$\Lambda = \text{Diag} (\lambda_1 \ \lambda_2 \ \cdots \ \lambda_n)$$

This means that the component equations in Equation (5.45) are decoupled. That Λ is a diagonal matrix of eigenvalues can be seen from the fundamental relationship for eigenvectors with respect to the matrix a and its transpose:

$$A \underline{e}_i = \lambda_i \underline{e}_i \quad (5.46)$$

$$A' \underline{r}_j = \lambda_j \underline{r}_j \quad (5.47)$$

Transposing Equation (5.47) and postmultiplying by \underline{e}_i

$$\underline{r}_j' A \underline{e}_i = \lambda_j \underline{r}_j' \underline{e}_i \quad (5.48)$$

Premultiplying Equation (5.46) by \underline{r}_j'

$$\underline{r}_j' A \underline{e}_i = \lambda_j \underline{r}_j' \underline{e}_i \quad (5.49)$$

Subtracting Equation (5.49) from Equation (5.48)

$$(\lambda_j - \lambda_i) \underline{r}_j' \underline{e}_i = 0$$

Then, if

$$\lambda_j \neq \lambda_i$$

$$\underline{r}_j' \underline{e}_i = 0 \quad (5.50)$$

showing that the vectors are orthogonal. Furthermore, if the eigenvectors are normalized such that,

$$\underline{r}_i' \underline{e}_i = 1 \quad i = 1, 2, \dots, n \quad (5.51)$$

then the vectors are orthonormal, and the product of the matrices

$$\begin{bmatrix} r_1 & r_2 & \cdots & r_n \end{bmatrix}' \begin{bmatrix} e_1 & e_2 & \cdots & e_n \end{bmatrix}$$

is a unit matrix, which is identical to the expression $R'E = I$.

Expanding

$$R'AE = \begin{bmatrix} r_1 & r_2 & \cdots & r_n \end{bmatrix}' A \begin{bmatrix} e_1 & e_2 & \cdots & e_n \end{bmatrix}$$

and substituting Equations (5.48), (5.50), and 5.51) yields the proof that

$R'AE = \Lambda$ is the diagonal matrix of eigenvalues.

Also, by pre- and post-multiplication

$$A = EAR' \quad (5.52)$$

Thus, eigenvalues and eigenvectors, although usually pictured only as functions associated with a matrix, can be regarded as basic elements from which the matrix is constructed. The spectral decomposition of a matrix into its basic elements can be observed from the above relationship, which when expanded is

$$A = \sum_{i=1}^n \underline{e}_i \lambda_i \underline{r}'_i = \sum_{i=1}^n A_i \quad (5.53a)$$

The spectral decomposition of B is, to a large extent, analogous to that above. $B = ER'B$ and, therefore, can be expressed as

$$B = \sum_{i=1}^n \underline{e}_i \underline{r}'_i B = \sum_{i=1}^n B_i \quad (5.53b)$$

Similarly

$$C = \sum_{i=1}^n C \underline{e}_i \underline{r}'_i = \sum_{i=1}^n C_i \quad (5.53c)$$

Writing the state-space Equation (5.1) as the sum of its spectrally resolved components yields:

$$\dot{\underline{x}} = \sum_{i=1}^n \dot{\underline{x}}_i = \sum_{i=1}^n (A_i \underline{x} + B_i \underline{u}) \quad (5.54)$$

In accordance with Equation (5.43)

$$\underline{x} = \underline{e}_1 q_1 + \underline{e}_2 q_2 + \dots + \underline{e}_n q_n = \sum_{k=1}^n \underline{e}_k q_k \quad (5.55)$$

showing the components of \underline{x} along the axes of the eigenvector coordinate system. The control vector \underline{u} and output vector \underline{y} also have components in this system as shown in Equation (5.45). This means that elements of the vector $R'B \underline{u}$ are in the system of eigenvector coordinates and are independent of each other. The matrix $R'B$ is called the control influence matrix. It should be noted that a row of zeros in this matrix means that the corresponding frequency mode cannot be influenced by the control vector, \underline{u} . Similarly CE is the measurement matrix.

Substituting from Equation (5.43) into the left-hand part of equation (5.45) and premultiplying by E

$$\dot{\underline{x}} = E (\Lambda \underline{q} + R'B \underline{u}) \quad (5.56)$$

The projection of the above derivative into the i th eigenvector is

$$\dot{\underline{x}}_i = \underline{e}_i (\lambda_i q_i + \underline{r}_i' B \underline{u}) \quad (5.57)$$

Now, from the definition of A_i in Equation (5.53) and from Equations (5.55) (5.50), and 5.51,

$$\begin{aligned} A_i \underline{x} &= \underline{e}_i \lambda_i \underline{r}_i' \sum_{k=1}^n \underline{e}_k q_k \\ &= \underline{e}_i \lambda_i q_i = \lambda_i \underline{x}_i \end{aligned} \quad (5.58)$$

Then, Equation (5.57) becomes

$$\dot{\underline{x}}_i = A_i \underline{x} + B_i \underline{u}, \quad (i = 1, 2, \dots, n) \quad (5.59)$$

or

$$\dot{\underline{x}}_i = \lambda_i \underline{x}_i + B_i \underline{u} \quad (5.60)$$

The Laplace transform solution of Equation 5.60) is

$$\underline{X}_i(s) = (\underline{x}_i(0) + B_i \underline{U}(s)) / (s - \lambda_i)$$

After summing all of the spectral components,

$$\underline{X}(s) = \Sigma \underline{X}_i(s) = \Sigma (\underline{x}_i(0) + B_i \underline{U}(s)) / (s - \lambda_i)$$

From Equation (5.58)

$$\underline{x}_i = A_i \underline{x} / \lambda_i$$

Then, denoting

$$A_i / \lambda_i = E_i$$

$$\underline{X}(s) = \Sigma (E_i \underline{x}(0) + B_i \underline{U}(s)) / (s - \lambda_i) \quad (5.61)$$

Therefore, the spectral components of the A and B matrices are exactly analogous to the coefficients of a partial fraction expansion. Clearly, from the development, each numerator in Equation (5.61) is a function of all modes, even though some of the modes in the "partial fraction expansion" are dropped.

5.3.2.3 Criterion for Decoupling with Spectral Decomposition

The degree of coupling which exists among the state vector elements can be determined by inspecting each of the E_i matrices. The E_i 's are all singular matrices, each having only one non-zero eigenvalue.

With spectral decomposition, the non-zero eigenvalue is always +1; and, because the trace of a matrix is equal to the sum of its eigenvalues, the trace of E_i is always unity. This provides the criterion for reducing the matrix. Any element in the diagonal of E_i with a modulus much less than unity can be deleted without significantly affecting the value of the trace, provided that the absolute sum of such elements is also much less than unity. The corresponding rows (and columns) in each of the equations represented by Equation (5.60) can be deleted. This can be easily justified as follows.

The transient solution of Equation (5.60) is

$$\underline{x}_i(t) = \underline{x}_i(0) \exp(\lambda_i t)$$

If all the elements in $\underline{x}_i(0)$ were identical, then all equations (rows) in

$$\underline{x}_i = A_i \underline{x}$$

would be duplicative. Clearly, the ones which are of no particular interest (the ones corresponding to negligible elements on the diagonal in A_i) can be deleted. The result of these deletions will be negligible if they do not significantly change the eigenvalue λ_i ; i.e., if they do not change the value of the trace of E_i significantly from its unit value.

Determination of what spectral components are combined into the corresponding A_k^* , B_k^* , and C_k^* matrices depends upon the overlaps of significant diagonal terms in the E_i 's. Then, after computation of each $A_i (= \lambda_i E_i)$ and each $B_i (= E_i B)$, and each $C_i (= C E_i)$, those which should be combined are added to yield the corresponding $(A_k^*, B_k^*, C_k^*)_n$. These in turn

are then decoupled to become the $(A_k^{**}, B_k^{**}, C_k^{**})_n$ triplet by appropriate nulling of rows and columns corresponding to the negligible diagonal elements in the selectively combined E_i 's.

The Algorithm for Spectral Decomposition

A summary of steps in the spectral decomposition approach is as follows:

1. Compute the eigenvalues and the corresponding eigenvectors of A and A' .
2. Compute the complete set of A_i matrices (n in number and $n \times n$ in dimension).
3. Null any row and corresponding column in each A_i where its diagonal element is negligible. Now it is apparent that, associated with each eigenvalue, there are certain components in the state vector which are thus identified as being insignificant.
4. Null the corresponding rows of B_i and the corresponding columns of C_i in Equation (5.53).
5. A new $(A, B, C)_n$ realization is formed by summing only those (A_i, B_i, C_i) 's which are associated with the eigenvalues in the frequency cluster of interest.
6. The $n-k$ insignificant states are then removed to form the minimal realization $(A, B, C)_k$.

5.3.2.3.1 Example: Rigid-Body Model

The following example will serve to illustrate the spectral decomposition and decoupling procedures. An intuitive approach for approximating the short period and phugoid modes of an airplane are presented in Sections 4 and 5 of Dynamics of the Airframe, Bu Aer Report AE-61-4II, Northrop Norair, September 1952 Reference [21]. Here the same airplane equations are used as a model for demonstrating the application of the spectral decomposition method.

Substituting the appropriate data into the corresponding longitudinal equations, then re-writing the equations in state-space form yields the following:

$$\begin{bmatrix} \dot{u} \\ \dot{\alpha} \\ \dot{\theta} \\ \dot{\theta} \end{bmatrix} = \begin{bmatrix} -.00970 & 1.0560 & 0 & -32.170 \\ -.00015 & -1.4300 & 1 & 0 \\ .00012 & -14.282 & -2.7780 & 0 \\ 0 & 0 & 1 & 0 \end{bmatrix} \begin{bmatrix} u \\ \alpha \\ \dot{\theta} \\ \theta \end{bmatrix} + \begin{bmatrix} 0 \\ .1058 \\ 26.01 \\ 0 \end{bmatrix} \delta_e \quad (5.62)$$

The eigenvalues of the square matrix, A, are $-2.1 \pm j 3.72$ and $-.00451 \pm j.0626$. Corresponding to the first eigenvalue, $-2.10 - j 3.72$, the matrix $e_1 r_1'$ is

$$E_1 = \begin{bmatrix} -.00003 & 2.8218 & .56345 & -.00079 \\ -j .00011 & -j 1.6526 & +j .65658 & -j .00023 \\ -.00001 & .50001 & -.00001 & -.00007 \\ -j .00002 & +j .09074 & +j .13445 & -j .00011 \\ -.00006 & .00062 & .50004 & -.00035 \\ -j .00002 & -j 1.9207 & -j .09052 & +j .00033 \\ .00001 & .39116 & -.03921 & -.00003 \\ -j .00001 & +j .22153 & +j .11229 & +j .00011 \end{bmatrix}$$

The diagonal elements of E_1 add to unity, and the first and fourth elements are negligible. E_2 , which corresponds to the second eigenvalue, is the conjugate of E_1 . Then $A_1 + A_2 = E_1 \lambda_1 + E_2 \lambda_2 =$

$$A_1^* = 2 \begin{bmatrix} -.00034 & -12.083 & 1.2557 & .00083 \\ -.00007 & -.71481 & .49998 & -.00025 \\ .00006 & -7.1431 & -1.3888 & .00198 \\ -.00006 & .00062 & .50004 & -.00035 \end{bmatrix}$$

and $B_1 + B_2 = (E_1 + E_2) B =$

$$B_1^* = 2 \begin{bmatrix} 14.95 \\ .05253 \\ 13.01 \\ -.978 \end{bmatrix}$$

Similarly, corresponding to the third eigenvalue, $- .00451 - j .0626$ the matrix $\underline{e}_3 \underline{r}'_3$, is

$$E_3 = \begin{bmatrix} .50003 & - 2.8218 & - .56345 & .00079 \\ - j .03599 & + j 201.11 & - j 20.086 & - j 256.78 \\ - .00001 & - .00001 & .00001 & .00007 \\ + j .00000 & - j .00311 & + j .00031 & + j .00396 \\ .00006 & - .00062 & - .00004 & .00035 \\ - j .00000 & + j .02468 & - j .00247 & - j .03151 \\ - .00001 & - .39116 & .03921 & .50003 \\ + j .00098 & - j .03845 & + j .00215 & + j .04156 \end{bmatrix}$$

Again, the diagonal elements add to 1, and the second and third elements are negligible. E_4 , which corresponds to the fourth eigenvalue, is the conjugate of E_3 . Then $A_3 + A_4 =$

$$A_2^* = 2 \begin{bmatrix} - .00451 & 12.611 & - 1.2557 & - 16.086 \\ 0 & - .00019 & .00002 & .00025 \\ 0 & .00155 & - .00015 & - .00198 \\ .0006 & - .00062 & - .00004 & .00035 \end{bmatrix}$$

and $B_3 + B_4 =$

$$B_2^* = 2 \begin{bmatrix} - 14.95 \\ .000368 \\ - .00115 \\ .978 \end{bmatrix}$$

Nulling the first and fourth rows and columns of A_1^* and the second and third rows and columns of A_2^* yields

$$A^{**} = \begin{bmatrix} -.00902 & 0 & 0 & -32.18 \\ 0 & -1.430 & 1 & 0 \\ 0 & -14.29 & -2.778 & 0 \\ .00012 & 0 & 0 & .00070 \end{bmatrix}$$

Similarly, nulling the first and fourth rows of B_1^* and the second and third rows of B_2^* yields

$$B^{**} = 2 \begin{bmatrix} -29.90 \\ .1051 \\ 26.01 \\ 1.956 \end{bmatrix}$$

The corresponding matrix equation is

$$\begin{bmatrix} \dot{u} \\ \dot{\alpha} \\ \dot{\theta} \\ \dot{\dot{\theta}} \end{bmatrix} = \begin{bmatrix} -.00902 & 0 & 0 & -32.18 \\ 0 & -1.320 & 1 & 0 \\ 0 & -14.29 & -2.778 & 0 \\ .00012 & 0 & 0 & .00070 \end{bmatrix} \begin{bmatrix} u \\ \alpha \\ \dot{\theta} \\ \theta \end{bmatrix} + \begin{bmatrix} -29.90 \\ .1051 \\ 26.01 \\ 1.956 \end{bmatrix} \delta_e$$

Writing the decoupled equations separately, the short period equation is

$$\begin{bmatrix} \dot{\alpha} \\ \dot{\theta} \end{bmatrix} = \begin{bmatrix} -1.430 & 1 \\ -14.29 & -2.778 \end{bmatrix} \begin{bmatrix} \alpha \\ \dot{\theta} \end{bmatrix} + \begin{bmatrix} .1051 \\ 26.01 \end{bmatrix} \delta_e \quad (5.63)$$

with eigenvalues: $-2.10 \pm j 3.72$; and the phugoid equation is

$$\begin{bmatrix} \dot{u} \\ \dot{\dot{\theta}} \end{bmatrix} = \begin{bmatrix} -.00902 & -32.18 \\ .00012 & .00070 \end{bmatrix} \begin{bmatrix} u \\ \theta \end{bmatrix} + \begin{bmatrix} -29.90 \\ 1.956 \end{bmatrix} \delta_e \quad (5.64)$$

with eigenvalues: $-.00416 \pm j .0620$

The state space equations corresponding to the approximations presented in the reference are, for the short period,

$$\begin{bmatrix} \dot{\alpha} \\ \ddot{\alpha} \\ \dot{\theta} \end{bmatrix} = \begin{bmatrix} -1.430 & 1 \\ -14.18 & -2.778 \end{bmatrix} \begin{bmatrix} \alpha \\ \dot{\theta} \end{bmatrix} + \begin{bmatrix} .1058 \\ -26.01 \end{bmatrix} \delta_e \quad (5.65)$$

with eigenvalues: $-2.10 \pm j 3.72$; and, for the phugoid,

$$\begin{bmatrix} \dot{u} \\ \dot{\theta} \end{bmatrix} = \begin{bmatrix} -.0097 & -32.17 \\ .000145 & 0 \end{bmatrix} \begin{bmatrix} u \\ \theta \end{bmatrix} + \begin{bmatrix} 0 \\ -.1058 \end{bmatrix} \delta_e \quad (5.66)$$

with eigenvalues: $-.00485 \pm j .0681$.

Comparison between the two short period approximations Equations (5.63) and (5.65) shows them to be almost identical; but comparison between the two phugoid approximations Equations (5.64) and (5.66) shows significant differences, although the eigenvalues are in fair agreement. The special decomposition method yields accurate results for both the short period and the phugoid. But, as pointed out in the reference, the phugoid approximation by the intuitive approach yields impulse responses with large amplitude and phase errors.

The transients responding to δ_e impulses of magnitude .02 for Equation (5.64) the reduced realization are easily computed to be

$$u = -20.3 e^{-.00416t} \sin .0620t$$

$$\theta = .0391 e^{-.00416t} \cos .0620t$$

The corresponding phugoid responses computed from the 4 x 4 system, Equation (5.62) are

$$u = -20.1 e^{-.00451t} \sin .0626t$$

$$\theta = .0393 e^{-.00451t} \cos .0626t$$

5.4 EXAMPLES

The two methods discussed in this report are: (1) balanced approximation, and (2) spectral decomposition. The balanced approximation approach is better known,, having been thoroughly developed and discussed in the technical literature since about 1979. The spectral decomposition approach was developed and used by Lockheed, beginning in 1974, during studies that led to the development of the L-1011 Active Control System.

More recently, Lockheed has been examining two forms of frequency compensation which supplement the balanced approximation approach: but these topics are beyond the scope of this report. The first of the frequency-compensation methods, developed by Honeywell, applies a balancing algorithm to a full model which includes frequency-dependent weighting. The second method, developed by the University of Southern California, truncates the model using approximate balancing; then applies the balancing algorithm to the truncated model after bilinear frequency weighting.

Comparison of results from the U.S.C. method and from the two methods which are the subject of this report are illustrated in this section. It comprises excerpts borrowed directly from Reference [22].

Two versions of the U.S.C. method are included in the Bode plots (Paragraph 5.4.4) which follows the numerical examples. They are labeled: "asymptotic balancing" and "pre-cleaned to 5th order."

5.4.1 Advanced Supersonic Transport Flexible-Body Model

The model used in this comparison is for the Advanced Supersonic Transport (AST) shown in Figure 5-3. It is a linear eighth order longitudinal system which includes the two lowest frequency structural modes: the first and second fuselage bending modes. The four inputs included in the control vector are the elevator, throttle, canard, and elevon. The state space model is given in Figure 5-4.

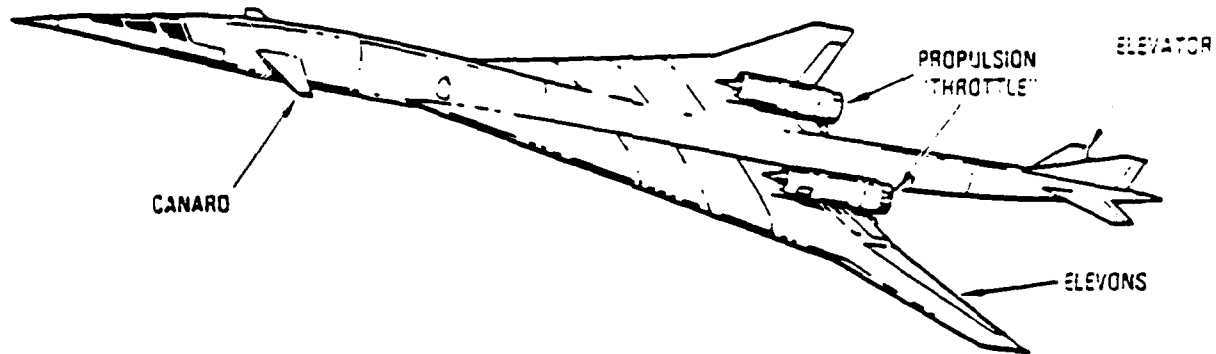


Figure 5-3. Advanced Supersonic Transport (AST)

$$\dot{x} = Ax + Bu$$

$$y = Cx$$

where:

\dot{u}	-	-0.0127	-0.0136	-0.0360	0.0000	0.0000	0.0000	0.0000	0.0000	0.0000	0.0000	0.0000	u
$\dot{\alpha}$	-	-0.0969	-0.4010	0.0000	0.9610	19.5900	-0.1185	-9.2000	-0.1326	0.0000	0.0000	0.0000	α
$\dot{\theta}$	-	0.0000	0.0000	0.0000	1.0000	0.0000	0.0000	0.0000	0.0000	0.0000	0.0000	0.0000	θ
\dot{q}	-	-0.2290	1.7260	0.0000	-0.7220	-12.0200	-0.3420	1.8420	0.8810	0.0000	0.0000	0.0000	q
\dot{x}_1	-	0.0000	0.0000	0.0000	0.0000	0.0000	1.0000	0.0000	0.0000	0.0000	0.0000	0.0000	x_1
\dot{x}_1	-	0.0000	0.1204	0.0000	0.0496	-44.0000	-1.2740	-4.0300	-0.5080	0.0000	0.0000	0.0000	\dot{x}_1
\dot{x}_2	-	0.0000	0.0000	0.0000	0.0000	0.0000	0.0000	0.0000	1.0000	0.0000	0.0000	0.0000	x_2
\dot{x}_2	-	0.0000	0.1473	0.0000	0.3010	-7.4900	-0.1257	-21.7000	-0.8030	0.0000	0.0000	0.0000	\dot{x}_2
+													
0.0000	0.0194	0.0000	0.0000	0.0000	0.0000	0.0000	0.0000	0.0000	0.0000	0.0000	0.0000	0.0000	δ_B
-0.0215	0.0000	-0.0040	-1.7860	0.0000	0.0000	0.0000	0.0000	0.0000	0.0000	0.0000	0.0000	0.0000	δ_t
0.0000	0.0000	0.0000	0.0000	0.0000	0.0000	0.0000	0.0000	0.0000	0.0000	0.0000	0.0000	0.0000	δ_c
-1.0970	0.0000	0.3660	-0.0569	0.0000	0.0000	0.0000	0.0000	0.0000	0.0000	0.0000	0.0000	0.0000	δ_a
0.0000	0.0000	0.0000	0.0000	0.0000	0.0000	0.0000	0.0000	0.0000	0.0000	0.0000	0.0000	0.0000	
-0.6400	0.0000	0.1625	-0.0370	0.0000	0.0000	0.0000	0.0000	0.0000	0.0000	0.0000	0.0000	0.0000	
0.0000	0.0000	0.0000	0.0000	0.0000	0.0000	0.0000	0.0000	0.0000	0.0000	0.0000	0.0000	0.0000	
-1.8820	0.0000	0.4720	-0.0145	0.0000	0.0000	0.0000	0.0000	0.0000	0.0000	0.0000	0.0000	0.0000	

and $C = I$ is the identity matrix.

Figure 5-4. AST Longitudinal Flexible-Body Model.

The eigenvalues of the unaugmented system show the short period to be statically unstable.

Short Period	0.6687	(Unstable)
	-1.7755	(Stable)
Phugoid	-0.0151	$\pm 0.0886i$
1st Fuselage Bending Mode (X_1)	-0.7257	$\pm 6.7017i$
2nd Fuselage Bending Mode	-0.3122	$\pm 4.4484i$

To illustrate these methods of model reduction, the original eighth order model will be reduced to a fourth order system. The eigenvalue matrix is a diagonal matrix with elements:

$$\begin{aligned}\lambda_1 &= -0.7257 + 6.7018i \\ \lambda_2 &= -0.3122 + 4.4485i \\ \lambda_3 &= -1.7756 \\ \lambda_4 &= 0.6687 \\ \lambda_5 &= -0.0151 + 0.0886i \\ \lambda_6 &= -0.0151 - 0.0886i \\ \lambda_7 &= -0.7257 - 6.7018i \\ \lambda_8 &= -0.3122 - 4.4485i\end{aligned}$$

The corresponding matrix of eigenvectors is:

$$V_{(1-8)} = \begin{bmatrix} \text{Columns 1 through 4} \\ \text{Columns 5 through 8} \end{bmatrix}$$

0.0002	+0.0006i	0.0001	+0.0008i	0.0017	-0.0142i	0.0357	+0.0345i
0.2694	-0.1506i	0.3879	-0.1877i	0.0659	-0.5390i	-0.2927	-0.2839i
0.0079	+0.0335i	-0.0504	+0.0671i	0.0597	-0.4888i	-0.5613	-0.5455i
-0.2306	+0.0288i	-0.2826	-0.2453i	-0.1059	+0.8679i	-0.3774	-0.3648i
0.0630	+0.1123i	0.0098	+0.0306i	0.0001	-0.0011i	-0.0005	-0.0005i
-0.7980	+0.3406i	-0.1390	+0.0339i	-0.0002	+0.0019i	-0.0004	-0.0004i
0.0236	+0.0341i	-0.1109	-0.1403i	-0.0010	+0.0081i	-0.0067	-0.0065i
-0.2460	+0.1335i	0.6586	-0.4497i	0.0018	-0.0144i	-0.0045	-0.0044i
-0.5991	+0.1935i	-0.5560	-0.3166i	0.0007	-0.0022i	-0.0020	+0.0012i
-0.1362	+0.0273i	-0.1299	-0.0553i	1.0180	+0.5465i	+0.2422	-1.2391i
0.4891	+1.4772i	0.7927	-1.3683i	0.0275	-0.1261i	-0.0681	+0.2361i
-0.1383	+0.0211i	-0.1332	-0.0497i	-0.8649	-0.0931i	1.0710	+0.2307i
-0.0003	+0.0001i	-0.0003	-0.0001i	0.2285	-0.4242i	0.0888	+0.0309i
0.0000	-0.0000i	0.0000	+0.0000i	-3.0085	-1.2237i	0.1650	+0.3852i
-0.0027	+0.0005i	-0.0026	-0.0010i	0.0862	-0.1293i	0.5238	+0.0133i
0.0000	-0.0003i	-0.0001	+0.0002i	-0.9291	-0.4838i	-0.1045	-2.3324i

5.4.2 Spectral Decomposition

Model reduction using spectral decomposition is accomplished by separating the rigid body motion from the structural dynamics.

Calculating the spectral decomposition $v_4(v^{-1})_4$ for the unstable short period of 0.668 gives:

$$v_4(v^{-1})_4 = \begin{bmatrix} 0.0357 & +0.0345i \\ -0.2937 & -0.2839i \\ -0.5643 & -0.5455i \\ -0.3774 & -0.3648i \\ -0.0005 & -0.0005i \\ -0.0004 & -0.0004i \\ -0.0067 & -0.0065i \\ -0.0045 & -0.0044i \end{bmatrix} \begin{bmatrix} 0.3338 & -0.3227i \\ -0.9445 & +0.9130i \\ -0.0180 & +0.0174i \\ -0.5937 & +0.5739i \\ -0.8696 & +0.8406i \\ -0.3103 & +0.2999i \\ 0.8037 & -0.7769i \\ 0.3829 & -0.3701i \end{bmatrix}^T$$

$$= \begin{bmatrix} 0.0230 & -0.0652 & -0.0012 & -0.0410 & -0.0600 & -0.0214 & 0.0555 & 0.0264 \\ -0.1897 & 0.5366 & 0.0102 & 0.3373 & 0.4941 & 0.1763 & -0.4566 & 0.2175 \\ -0.3644 & 1.0309 & 0.0196 & 0.6481 & 0.9492 & 0.3387 & -0.8773 & 0.4179 \\ -0.2437 & 0.6894 & 0.0131 & 0.4334 & 0.6348 & 0.2265 & -0.5867 & 0.2795 \\ -0.0004 & 0.0010 & 0.0000 & 0.0006 & 0.0009 & 0.0003 & -0.0008 & 0.0004 \\ -0.0002 & 0.0007 & 0.0000 & 0.0004 & 0.0006 & 0.0002 & -0.0006 & 0.0003 \\ -0.0043 & 0.0123 & 0.0002 & 0.0077 & 0.0113 & 0.0040 & -0.0105 & 0.0050 \\ -0.0029 & 0.0082 & 0.0002 & 0.0052 & 0.0076 & 0.0027 & -0.0070 & 0.0033 \end{bmatrix}$$

The diagonal of this matrix is used to identify the cross coupling between the states and the unstable short period. This diagonal is:

$$D_4 = \begin{bmatrix} 0.0230 \\ 0.5366 \\ 0.0196 \\ 0.4334 \\ 0.0009 \\ 0.0002 \\ -0.0105 \\ -0.0033 \end{bmatrix}$$

The sum of the diagonal terms $\sum_{i=1}^n d_i = 1$.

It is seen that the unstable short period is primarily described by the state of components α (angle-of-attack) and q (pitch rate).

Similarly, the spectral decomposition $v_3 (v^{-1})_3$ for the stable short period at -1.77 gives:

$$v_3 (v^{-1})_3 = \begin{bmatrix} -0.0006 & 0.0117 & 0.0000 & -0.0094 & -0.0068 & 0.0084 & 0.0197 & -0.0057 \\ -0.0221 & 0.4443 & -0.0004 & -0.3579 & -0.2586 & 0.3221 & 0.7491 & -0.2173 \\ -0.0200 & 0.4022 & -0.0004 & -0.3240 & -0.2341 & 0.2916 & 0.6782 & -0.1967 \\ 0.0355 & -0.7142 & 0.0007 & 0.5753 & 0.4157 & -0.5178 & -1.2043 & 0.3492 \\ 0.0000 & 0.0009 & 0.0000 & -0.0007 & -0.0005 & 0.0006 & 0.0015 & -0.0004 \\ 0.0001 & -0.0015 & 0.0000 & 0.0012 & 0.0009 & -0.0011 & -0.0026 & 0.0008 \\ 0.0003 & -0.0067 & 0.0000 & 0.0054 & 0.0039 & -0.0039 & -0.0112 & 0.0033 \\ -0.0006 & 0.0118 & 0.0000 & -0.0095 & -0.0069 & 0.0086 & 0.0199 & -0.0058 \end{bmatrix}$$

Identifying the cross coupling between the states and the stable short period, it is again seen that it is primarily described by the states α (angle-of-attack) and q (pitch rate).

$$D_3 = \begin{bmatrix} -0.0006 \\ 0.4443 \\ -0.0004 \\ 0.5753 \\ -0.0005 \\ -0.0011 \\ -0.0112 \\ -0.0058 \end{bmatrix}$$

Computing the spectral decomposition for the complex phugoid at -0.015

$\pm 0.088i$ gives:

$$E_5 = v_5(v^{-1})_5 =$$

Columns 1 through 4			
0.4888 + 0.0814i	0.0268 - 0.2901i	0.0006 + 0.1984i	0.0252 - 0.0656i
0.1051 + 0.0302i	0.0132 - 0.0629i	-0.0049 + 0.0435i	0.0072 - 0.0137i
0.1923 - 1.2095i	-0.7175 - 0.0609i	0.4904 - 0.0052i	0.1425 - 0.0610i
0.1043 + 0.0353i	-0.0162 - 0.0627i	-0.0069 + 0.0435i	0.0079 - 0.0135i
0.0002 + 0.0001i	0.0000 - 0.0001i	0.0000 + 0.0001i	0.0000 - 0.0000i
0.0000 + 0.0000i	0.0000 + 0.0000i	0.0000 - 0.0000i	0.0000 + 0.0000i
0.0021 + 0.0007i	0.0003 - 0.0013i	-0.0001 + 0.0009i	0.0002 - 0.0003i
Columns 5 through 8			
0.0305 - 0.2091i	0.0064 - 0.1357i	-0.0361 + 0.0620i	0.0102 + 0.1428i
0.0120 - 0.0451i	0.0048 - 0.0296i	-0.0095 + 0.0127i	0.0058 + 0.0310i
-0.5174 - 0.0717i	-0.3355 - 0.0132i	0.1539 + 0.0880i	0.3532 + 0.0225i
0.0141 - 0.0448i	0.0062 - 0.0295i	-0.0101 + 0.0123i	0.0073 + 0.0310i
0.0000 - 0.0001i	0.0000 - 0.0001i	0.0000 + 0.0000i	0.0000 + 0.0001i
0.0000 + 0.0000i	0.0000 + 0.0000i	0.0000 - 0.0000i	0.0000 - 0.0000i
0.0003 - 0.0009i	0.0001 - 0.0006i	-0.0002 + 0.0002i	0.0001 + 0.0006i
0.0001 + 0.0000i	0.0001 + 0.0000i	0.0000 - 0.0000i	0.0001 - 0.0000i

$$E_6 = v_6(v^{-1})_6 =$$

Columns 1 through 4			
0.4888 - 0.0814i	0.0268 + 0.2901i	0.0006 - 0.1984i	0.0252 + 0.0656i
0.1051 - 0.0302i	0.0132 + 0.0629i	-0.0049 - 0.0435i	0.0072 + 0.0137i
0.1923 + 1.2095i	-0.7175 + 0.0609i	0.4904 + 0.0052i	0.1425 + 0.0610i
0.1043 - 0.0343i	0.0162 + 0.0627i	-0.0069 - 0.0435i	0.0079 + 0.0135i
0.0002 - 0.0001i	0.0000 + 0.0001i	0.0000 - 0.0001i	0.0000 + 0.0000i
0.0000 - 0.0000i	0.0000 - 0.0000i	0.0000 + 0.0000i	0.0000 - 0.0000i
0.0021 - 0.0007i	0.0003 + 0.0013i	-0.0001 - 0.0009i	0.0002 + 0.0003i
-0.0001 - 0.0002i	0.0001 - 0.0000i	-0.0001 - 0.0009i	0.0000 - 0.0000i
Columns 5 through 8			
0.0305 + 0.2091i	0.0064 + 0.1357i	-0.0361 - 0.0620i	0.0102 - 0.1428i
0.0120 + 0.0451i	0.0048 + 0.0296i	-0.0095 - 0.0127i	0.0058 - 0.0310i
-0.5174 + 0.0717i	-0.3355 + 0.0132i	0.1539 - 0.0880i	0.3532 - 0.0225i
0.0141 + 0.0448i	0.0062 + 0.0295i	-0.0101 - 0.0123i	0.0073 - 0.0310i
0.0000 + 0.0001i	0.0000 + 0.0001i	0.0000 - 0.0000i	0.0000 - 0.0001i
0.0000 - 0.0000i	0.0000 - 0.0000i	0.0000 + 0.0000i	0.0000 + 0.0000i
0.0003 + 0.0009i	0.0001 + 0.0006i	-0.0002 - 0.0002i	0.0001 + 0.0006i
0.0001 - 0.0000i	0.0001 - 0.0000i	0.0000 + 0.0000i	0.0001 + 0.0000i

Eliminating the imaginary parts of the matrices by adding the complex conjugate pairs:

$$E_{56} = E_5 + E_6 = \begin{bmatrix} 0.9775 & 0.0535 & 0.0013 & 0.0503 & 0.0611 & 0.0127 & -0.0021 & -0.0203 \\ 0.2101 & 0.0264 & -0.0098 & 0.0144 & 0.0240 & 0.0097 & -0.0182 & -0.0117 \\ 0.3847 & -0.4351 & 0.9808 & -0.3251 & -1.0349 & -0.6710 & 0.0072 & 0.7064 \\ 0.2086 & 0.0324 & -0.0138 & 0.0157 & 0.0283 & 0.0125 & -0.0002 & -0.0146 \\ 0.0004 & 0.0001 & 0.0000 & 0.0000 & 0.0000 & 0.0000 & 0.0000 & 0.0000 \\ 0.0000 & 0.0000 & 0.0000 & 0.0000 & 0.0000 & 0.0000 & 0.0000 & 0.0000 \\ 0.0042 & 0.0006 & -0.0002 & 0.0003 & 0.0005 & 0.0002 & -0.0004 & -0.0003 \\ -0.0002 & 0.0002 & -0.0002 & 0.0000 & 0.0002 & 0.0001 & 0.0000 & 0.0001 \end{bmatrix}$$

Identifying the cross coupling between the states and the phugoid using the diagonal of this matrix,

$$D_{56} = \begin{bmatrix} -0.9775 \\ 0.0264 \\ 0.9808 \\ 0.0157 \\ 0.0000 \\ 0.0000 \\ -0.0004 \\ -0.0007 \end{bmatrix}$$

it is seen that the phugoid is primarily described by the states u (velocity) and θ (pitch attitude).

The transformed system is computed by taking each matrix $u_i (v^{-1})_i$ and multiplying each element by its associated eigenvalue λ_i . The sum $\Sigma (\lambda_i u_i (v^{-1})_i)$ is then computed, including each state which has a significant influence on the dynamics of the modes of interest. Thus, the transformed system becomes:

$$\tilde{A} = \tilde{A}_3 + \tilde{A}_4 + \tilde{A}_5 + \tilde{A}_6 = \sum_{i=3}^6 \lambda_i v_i (v^{-1})_i$$

$$\tilde{A} = \begin{bmatrix} -0.0127 & -0.0137 & -0.0360 & 0.0001 & 0.0080 & -0.0055 & -0.0077 & 0.0028 \\ -0.0962 & -0.4192 & 0.0001 & 0.8633 & 0.7972 & -0.4490 & -1.6375 & 0.2350 \\ 0.0004 & 0.0077 & 0.0000 & 1.0245 & 1.0788 & -0.2789 & -1.8112 & 0.0551 \\ -0.2353 & 1.7397 & 0.0000 & -0.7295 & -0.3062 & 1.0759 & 1.7440 & -0.8123 \\ -0.0002 & -0.0009 & 0.0000 & 0.0017 & 0.0015 & -0.0009 & -0.0032 & 0.0005 \\ -0.0003 & 0.0032 & 0.0000 & -0.0019 & -0.0012 & 0.0021 & 0.0042 & -0.0015 \\ -0.0037 & 0.0202 & 0.0000 & -0.0043 & 0.0008 & 0.0114 & 0.0129 & -0.0092 \\ -0.0009 & -0.0155 & 0.0001 & 0.0203 & 0.0173 & -0.0134 & -0.0400 & 0.0080 \end{bmatrix}$$

Computing the eigenvalues of this system as a computational check gives:

$$\Lambda = \begin{bmatrix} -1.7756 \\ 0.6687 \\ -0.0151 \pm 0.0886i \\ 0, 0, 0, 0 \end{bmatrix}$$

Note that the eigenvalues of interest have been preserved, while the other eigenvalues have been set to zero. From this analysis, it is seen that the important states to describe the rigid body dynamics are the first four state components (u, α, θ, q). Extracting the upper left 4 x 4 submatrix gives the reduced system \tilde{A}_{11} :

$$\tilde{A}_{11} = \begin{bmatrix} -0.0127 & -0.0137 & -0.0360 & 0.0001 \\ -0.0962 & -0.4192 & 0.0001 & 0.8633 \\ 0.0004 & 0.0077 & 0.0000 & 1.0245 \\ -0.2353 & 1.7397 & 0.0000 & -0.7295 \end{bmatrix}$$

The transformation from B to \tilde{B} is computed as $T' B$ as follows:

$$T = \sum_{i=3}^6 v_i (v^{-1})_i = \begin{bmatrix} 1.0000 & 0.0000 & 0.0000 & 0.0000 & -0.0057 & -0.0002 & 0.0030 & 0.0004 \\ -0.0016 & 1.0073 & 0.0000 & -0.0062 & 0.2594 & 0.5080 & 0.2736 & -0.4465 \\ 0.0003 & -0.0019 & 1.0000 & -0.0010 & -0.3198 & -0.0407 & 0.1088 & 0.0918 \\ 0.0004 & 0.0077 & 0.0000 & 1.0245 & 1.0788 & -0.2789 & 1.8112 & 0.0551 \\ 0.0000 & 0.0019 & 0.0000 & 0.0000 & 0.0005 & 0.0010 & 0.0006 & -0.0008 \\ -0.0002 & -0.0009 & 0.0000 & 0.0017 & 0.0015 & -0.0009 & -0.0032 & 0.0005 \\ 0.0002 & 0.0063 & 0.0000 & 0.0134 & 0.0157 & -0.0006 & 0.0221 & -0.0020 \\ -0.0037 & 0.0202 & 0.0000 & -0.0043 & 0.0008 & 0.0111 & 0.0129 & -0.0092 \end{bmatrix}$$

$$\bar{B} = T \cdot B = \begin{bmatrix} -0.0006 & 0.0194 & 0.0001 & 0.0000 \\ 0.5003 & 0.0000 & -0.1345 & -1.8110 \\ -0.1455 & 0.0000 & 0.0363 & 0.0037 \\ -1.0493 & 0.0000 & 0.3556 & -0.0625 \\ 0.0010 & 0.0000 & -0.0003 & -0.0034 \\ -0.0021 & 0.0000 & 0.0007 & 0.0015 \\ -0.0107 & 0.0000 & 0.0038 & -0.0119 \\ 0.0143 & -0.0001 & -0.0042 & -0.0362 \end{bmatrix}$$

Retaining the upper four rows of \bar{B} , which correspond to the state components of interest, gives:

$$\bar{B}_1 = \begin{bmatrix} -0.0006 & 0.0194 & 0.0001 & 0.0000 \\ 0.5003 & 0.0000 & -0.1345 & -1.8110 \\ -0.1455 & 0.0000 & 0.0363 & 0.0037 \\ -1.0493 & 0.0000 & 0.3556 & -0.0625 \end{bmatrix}$$

The final state equation describing the rigid body dynamics is thus:

$$\dot{\bar{x}} = \begin{bmatrix} -0.0127 & -0.0137 & -0.0360 & 0.0001 \\ -0.0962 & -0.4192 & 0.0001 & 0.8633 \\ 0.0004 & 0.0077 & 0.0000 & 1.0245 \\ -0.2353 & 1.7397 & 0.0000 & -0.7295 \end{bmatrix} \bar{x} + \begin{bmatrix} -0.0006 & 0.0194 & 0.1345 & 0.0000 \\ 0.5003 & 0.0000 & -0.1345 & 1.8110 \\ -0.1455 & 0.0000 & 0.0363 & 0.0037 \\ -1.0493 & 0.0000 & 0.3556 & -0.0625 \end{bmatrix} \begin{bmatrix} \delta e \\ \delta t \\ \delta c \\ \delta a \end{bmatrix}$$

where

$$\bar{x} = \begin{bmatrix} u \\ \alpha \\ \theta \\ q \end{bmatrix}$$

Similarly,

$$\tilde{C} = C \cdot T = \begin{bmatrix} 1.0000 & 0.0000 & 0.0000 & 0.0000 & -0.0057 & -0.0002 & 0.0030 & 0.0004 \\ -0.0016 & 1.0073 & 0.0000 & -0.0062 & 0.2594 & 0.5080 & 0.2736 & -0.4465 \\ 0.0003 & -0.0019 & 1.0000 & -0.0010 & -0.3198 & -0.0407 & 0.1088 & 0.0918 \\ 0.0004 & 0.0077 & 0.0000 & 1.0245 & 1.0788 & -0.2789 & 1.8112 & 0.0551 \\ 0.0000 & 0.0019 & 0.0000 & 0.0000 & 0.0005 & 0.0010 & 0.0006 & -0.0008 \\ -0.0002 & -0.0009 & 0.0000 & 0.0017 & 0.0015 & -0.0009 & -0.0032 & 0.0005 \\ 0.0002 & 0.0063 & 0.0000 & 0.0134 & 0.0157 & -0.0006 & -0.0221 & -0.0020 \\ -0.0037 & 0.0202 & 0.0000 & -0.0043 & 0.0008 & 0.0114 & 0.0129 & -0.0092 \end{bmatrix}$$

Retaining the first four columns of C gives the output equation:

$$y = \begin{bmatrix} u \\ \alpha \\ \theta \\ q \\ x_1 \\ \dot{x}_1 \\ x_2 \\ \dot{x}_2 \end{bmatrix} = \begin{bmatrix} 1.0000 & 0.0000 & 0.0000 & 0.0000 \\ -0.0016 & 1.0073 & 0.0000 & -0.0062 \\ 0.0003 & -0.0019 & 1.0000 & -0.0010 \\ 0.0004 & 0.0077 & 0.0000 & 1.0245 \\ 0.0000 & 0.0019 & 0.0000 & 0.0000 \\ -0.0002 & -0.0009 & 0.0000 & 0.0017 \\ 0.0002 & 0.0063 & 0.0000 & 0.0134 \\ -0.0037 & 0.0202 & 0.0000 & -0.0043 \end{bmatrix} \tilde{x}$$

5.4.3 Balancing

Calculating the reduced order model using balancing requires computing the stable projection of the AST model from Figure 5-4. Removing the unstable short period pole from the model results in the following first order unstable and seventh order stable models:

Unstable Projection $G(s)$:

$$A_U = [0.6687]$$

$$B_U = [-0.1634 \quad -0.0071 \quad 0.0908 \quad -1.8846]$$

$$C_U = \begin{bmatrix} -0.0633 \\ 0.5205 \\ 1.0000 \\ 0.6687 \\ 0.0010 \\ 0.0006 \\ 0.0119 \\ 0.0080 \end{bmatrix}$$

Stable Projection G_+ (s):

$$A_s = \begin{bmatrix} 0.0000 & 1.0000 & 0.0000 & 0.0000 & 0.0000 & 0.0000 & 0.0000 \\ -45.4405 & -1.4513 & 0.0000 & 0.0000 & 0.0000 & 0.0000 & 0.0000 \\ 0.0000 & 0.0000 & 0.0000 & 1.0000 & 0.0000 & 0.0000 & 0.0000 \\ 0.0000 & 0.0000 & -19.8865 & -0.6245 & 0.0000 & 0.0000 & 0.0000 \\ 0.0000 & 0.0000 & 0.0000 & 0.0000 & -1.7756 & 0.0000 & 0.0000 \\ 0.0000 & 0.0000 & 0.0000 & 0.0000 & 0.0000 & 0.0000 & 1.0000 \\ 0.0000 & 0.0000 & 0.0000 & 0.0000 & 0.0000 & -0.0081 & -0.0301 \end{bmatrix}$$

$$B_s = \begin{bmatrix} -0.9031 & 0.0000 & 0.2286 & -0.0360 \\ 2.2821 & 0.0000 & -0.5677 & -0.2025 \\ -1.5990 & 0.0001 & 0.4009 & 0.0323 \\ 0.7315 & 0.0000 & -0.1617 & -0.2178 \\ 0.9417 & 0.0007 & 0.2942 & 1.2568 \\ -0.5125 & 0.0075 & 0.1112 & 2.5962 \\ 0.0016 & 0.0040 & 0.0007 & -0.0590 \end{bmatrix}$$

$$C_s = \begin{bmatrix} 0.0000 & -0.0001 & -0.0004 & 0.0002 & -0.0163 & 0.0657 & 4.5647 \\ -0.3497 & 0.0056 & 0.5400 & 0.0180 & -0.6221 & 0.0042 & 0.9997 \\ 0.0025 & -0.0058 & -0.0973 & 0.0076 & -0.5632 & 1.0000 & 0.0000 \\ 0.2655 & 0.0110 & -0.1510 & -0.1020 & 1.0000 & 0.0000 & 1.0000 \\ -0.0319 & -0.0220 & -0.0088 & 0.0087 & -0.0012 & 0.0000 & 0.0020 \\ 1.0000 & 0.0000 & -0.1723 & -0.0142 & 0.0022 & 0.0000 & -0.0001 \\ -0.0147 & -0.0070 & -0.0314 & -0.0503 & 0.0093 & 0.0000 & 0.0200 \\ 0.3178 & -0.0045 & 1.0000 & 0.0000 & -0.0165 & -0.0002 & -0.0006 \end{bmatrix}$$

Using the AST model from Figure 5-4, the resulting balanced system is:

$$\hat{A} = \begin{bmatrix} -0.2036230E-01 & -0.7858880E-01 & -0.7396749E-02 & -0.2084407E-02 & -0.1557507E-01 & 0.2265723E-02 & 0.1889674E-02 \\ 0.1007108E+00 & -0.9248873E-02 & 0.2168032E-02 & 0.8971239E-03 & 0.8634662E-02 & -0.1086024E-02 & -0.7199143E-03 \\ 0.1065996E-01 & -0.8821540E-02 & -0.2255822E+00 & 0.4181750E+01 & -0.1347317E+00 & 0.4317310E-01 & 0.5369037E-02 \\ 0.5305186E-02 & -0.5965348E-02 & -0.4614011E+01 & -0.4391062E+00 & 0.7906792E+00 & 0.1029887E+00 & -0.6150533E-03 \\ 0.3492083E-01 & -0.2548000E-01 & -0.5439826E+00 & -0.8968613E+00 & -0.1866259E-01 & 0.2929760E+00 & -0.8364052E+00 \\ -0.6318043E-03 & -0.1368483E-02 & -0.4369408E+00 & -0.686701E+00 & -0.1408282E+01 & -0.1222905E+01 & -0.6684445E+01 \\ -0.6901658E-02 & 0.4934998E-02 & 0.9053631E-01 & 0.9063240E-01 & 0.1196825E+01 & 0.6535209E+01 & -0.9803707E-01 \end{bmatrix}$$

$$\hat{A} = \begin{bmatrix} 0.2323941E+00 & 0.1076423E-01 & -0.4590957E-01 & -0.1390776E+01 \\ -0.2356257E+00 & 0.2880195E-01 & 0.5724683E-01 & 0.8909944E-00 \\ -0.8289558E+00 & 0.8390716E-04 & 0.2126706E+00 & 0.2197501E+00 \\ -0.1171844E+01 & 0.8376537E-04 & 0.2947332E+00 & -0.2158914E-01 \\ -0.8687418E+00 & 0.4592771E-03 & 0.2709870E+00 & 0.1067235E+01 \\ -0.8848588E+00 & -0.5661499E-04 & 0.2171498E+00 & -0.1766557E+00 \\ 0.1216242E+00 & -0.1401305E-03 & -0.4328787E-01 & -0.2203461E+00 \end{bmatrix}$$

$$\hat{C} = \begin{bmatrix} 0.3936411E+00 & 0.5038438E+00 & -0.4706008E-02 & 0.5285127E-03 & -0.1779815E-01 & 0.2385362E-02 & 0.1191328E-02 \\ 0.1147306E+00 & 0.9297478E-01 & 0.1462935E+00 & 0.5397737E+00 & -0.7535492E+00 & -0.1919983E+00 & -0.9788920E-01 \\ -0.1347486E+01 & 0.7600453E+00 & -0.2096338E+00 & -0.4638257E-01 & -0.5585050E+00 & 0.7292331E-01 & 0.5712261E-01 \\ 0.8156066E-01 & 0.1154051E+00 & 0.5496500E+00 & -0.3964075E+01 & 0.1027327E+01 & 0.1044514E+00 & -0.3026464E-01 \\ 0.2310383E-03 & 0.1996241E-03 & -0.2306706E-01 & 0.3324961E-01 & 0.2696158E-01 & -0.3238327E-01 & 0.1214753E+00 \\ 0.4221588E-04 & -0.4880759E-04 & -0.1374297E+00 & -0.1012023E+00 & 0.1701929E+00 & 0.8440623E+00 & 0.1820389E+00 \\ 0.1402238E-02 & 0.2635938E-02 & 0.2172917E+00 & -0.1348816E+00 & -0.1757253E-01 & -0.3678231E-02 & 0.4792444E-01 \\ 0.9461917E-03 & -0.5863078E-03 & 0.5886990E+00 & 0.9901341E-01 & -0.4065918E-01 & 0.3077923E+00 & 0.3556501E-01 \end{bmatrix}$$

with transformation matrix T, obtained as eigenvectors of the (WM) where W and M, are controllability and observability grammian

$$T = \begin{bmatrix} -0.2082414E-03 & -0.8597499E-05 & 0.5010647E-03 & 0.2002548E-03 & 0.8635179E-02 & -0.4591832E-00 & 0.3550501E+01 \\ 0.6035055E-04 & -0.7355415E-06 & 0.5061510E-04 & -0.6234115E-04 & -0.5173666E-02 & 0.4885302E+00 & 0.6285399E+01 \\ -0.3883044E-01 & -0.3110237E-03 & 0.3827676E+00 & -0.1611084E+00 & 0.1438251E+00 & -0.3965853E-02 & -0.6325808E-02 \\ -0.5358829E-02 & -0.9387191E-02 & 0.7852067E+00 & 0.1083092E+00 & -0.2315098E-01 & -0.1461919E-02 & 0.2621500E-02 \\ 0.1607577E+00 & -0.1331345E-02 & -0.5543575E-01 & 0.3214354E-01 & 0.8928460E+00 & -0.1586629E-01 & -0.1029357E-01 \\ 0.1145134E+01 & 0.3550512E-01 & 0.6771160E-02 & -0.3542887E-01 & -0.1126888E+00 & 0.2131459E-02 & 0.1401021E-02 \\ 0.1081826E-02 & -0.1688358E+00 & -0.2005733E+00 & -0.5198703E-02 & 0.2044477E+00 & 0.3007044E-02 & 0.1218405E-03 \end{bmatrix}$$

The diagonal of the observability and controllability grammians are:

$$\Sigma = \text{Diag.} \quad \begin{bmatrix} 48.8769 & 46.1411 & 1.7304 & 1.6631 & 0.5272 & 0.3522 & 0.3326 \end{bmatrix}$$

It is desired to reduce the model to a third order system. Let T_{nk} comprises the first 3 columns of T, and S_{kn} comprises the first 3 rows of T^{-1} .

Then, the reduced order system

$$\hat{A}, \hat{B}, \hat{C} = (S_{kn} A T_{nk}, S_{kn} B, C T_{nk})$$

is given by

$$\begin{aligned} \dot{\vec{A}} &= \begin{bmatrix} -0.2036230E+01 & -0.7858880E-01 & -0.7396749E-02 \\ 0.1007108E+00 & -0.9248873E-02 & 0.2168032E-02 \\ 0.1065996E-01 & -0.8821540E-02 & -0.2255822E+00 \end{bmatrix} \\ \dot{\vec{B}} &= \begin{bmatrix} 0.2323941E+00 & 0.1076423E-01 & -0.4590957E-01 & -0.1390776E+01 \\ -0.2356257E+00 & 0.2880195E-01 & 0.5724683E-01 & 0.8909944E+00 \\ -0.8289558E+00 & 0.8390716E-04 & 0.2126706E+00 & 0.2197501E+00 \end{bmatrix} \\ \dot{\vec{C}} &= \begin{bmatrix} 0.3936411E+00 & 0.5038438E+00 & -0.4706008E-02 \\ 0.1147306E+00 & 0.9297478E-01 & 0.1462935E+00 \\ -0.1347486E+01 & 0.7600453E+00 & -0.2096338E+00 \\ 0.8156066E-01 & 0.1154051E+00 & 0.5496500E+00 \\ 0.2310383E-03 & 0.1996241E-03 & -0.2306706E-01 \\ 0.4221588E-04 & -0.4880759E-04 & -0.1374297E+00 \\ 0.1402238E-02 & 0.2635938E-02 & 0.2172917E+00 \\ 0.9461917E-03 & -0.5863078E-03 & 0.5886990E+00 \end{bmatrix} \end{aligned}$$

Appending the unstable short period results in the following fourth order system:

$$\begin{aligned} \dot{\vec{x}} &= \begin{bmatrix} -0.2036230E-01 & -0.7858880E-01 & -0.7396749E-02 & 0.0 \\ 0.1007108E+00 & -0.9248873E-02 & 0.2168032E-02 & 0.0 \\ 0.1065996E-01 & -0.8821540E-01 & -0.2255822E+00 & 0.0 \\ 0.0 & 0.0 & 0.0 & 0.6687 \end{bmatrix} \vec{x} \\ + & \begin{bmatrix} 0.2323941E+00 & 0.1076423E-01 & -0.4591226E-01 & -0.1390774E+01 \\ -0.2356257E+00 & 0.2880195E-01 & 0.5724683E-01 & 0.8909937E+00 \\ -0.8289558E+00 & 0.8390716E-04 & 0.2126706E+00 & 0.2197501E+00 \\ -0.1634 & -0.0071 & -0.0908 & -0.8846 \end{bmatrix} \begin{bmatrix} \delta e \\ \delta t \\ \delta c \\ \delta a \end{bmatrix} \end{aligned}$$

$$\mathbf{y} = \begin{bmatrix} u \\ \alpha \\ \theta \\ q \\ X_1 \\ \dot{X}_1 \\ X_2 \\ \dot{X}_2 \end{bmatrix} = \begin{bmatrix} 0.3936411E+00 & 0.5038438E+00 & -0.4706008E-02 & -0.0633 \\ 0.1147306E+00 & 0.9297478E-01 & 0.1462935E+00 & -0.5205 \\ -0.1347486E+01 & 0.7600453E+00 & -0.2096338E+00 & 1.0000 \\ 0.8156066E-01 & 0.1154051E+00 & 0.5496500E+00 & 0.6687 \\ 0.2310383E-03 & 0.1996241E-03 & -0.2306706E-01 & 0.0010 \\ 0.4221588E-04 & -0.4880759E-04 & -0.1374297E+00 & 0.0006 \\ 0.1402238E-02 & 0.2635938E-02 & 0.2172917E+00 & 0.0119 \\ 0.9461917E-03 & -0.5853078E-03 & 0.5886990E+00 & 0.0080 \end{bmatrix} \bar{x}$$

5.4.4 Comparison of Methods

The frequency responses generated using the fourth order models from the previous section are shown in Figures 5-5 through 5-8. The gradient fit method and the asymptotic balancing method are described in Reference [22]. These are the single-input single-output responses $u/\delta e$, $\alpha/\delta e$, $\theta/\delta e$, and $q/\delta e$.

As expected, the fuselage bending modes are excited by the elevator input, and thus are seen in those frequency responses. Because of the frequency separation between the rigid body modes and the fuselage bending modes, spectral decomposition provides a very good approximation to the high order system. For those "rigid-body" responses excited by an elevator input, spectral decomposition matches the high order system up to the fuselage bending modes. It does deviate from the high order system at low frequencies for $\alpha/\delta e$, although the amplitude is very low in this region.

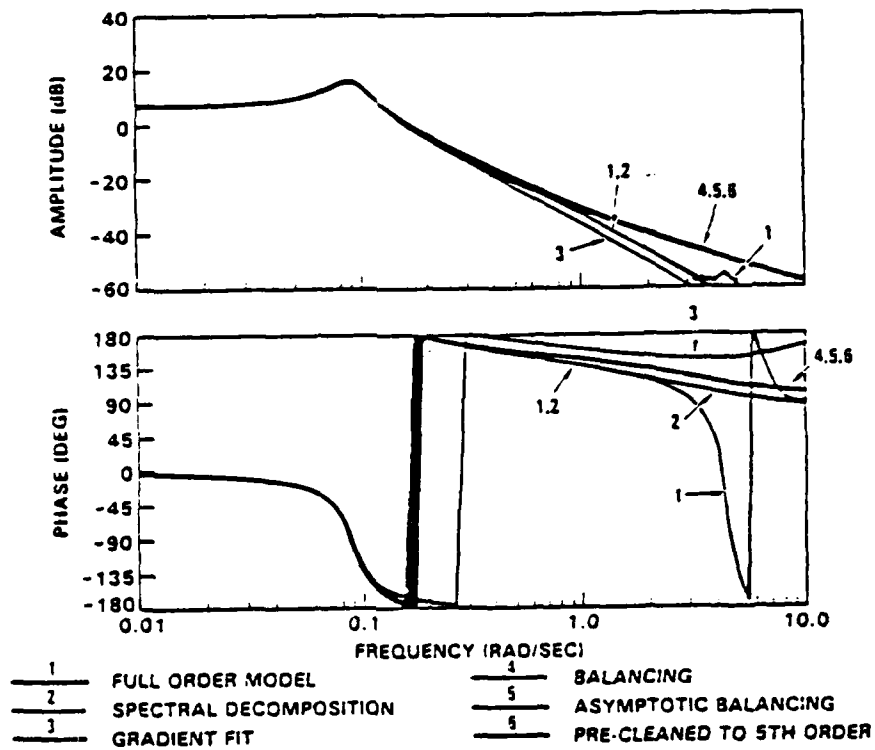


Figure 5-5. Frequency Response of $u/\delta e$

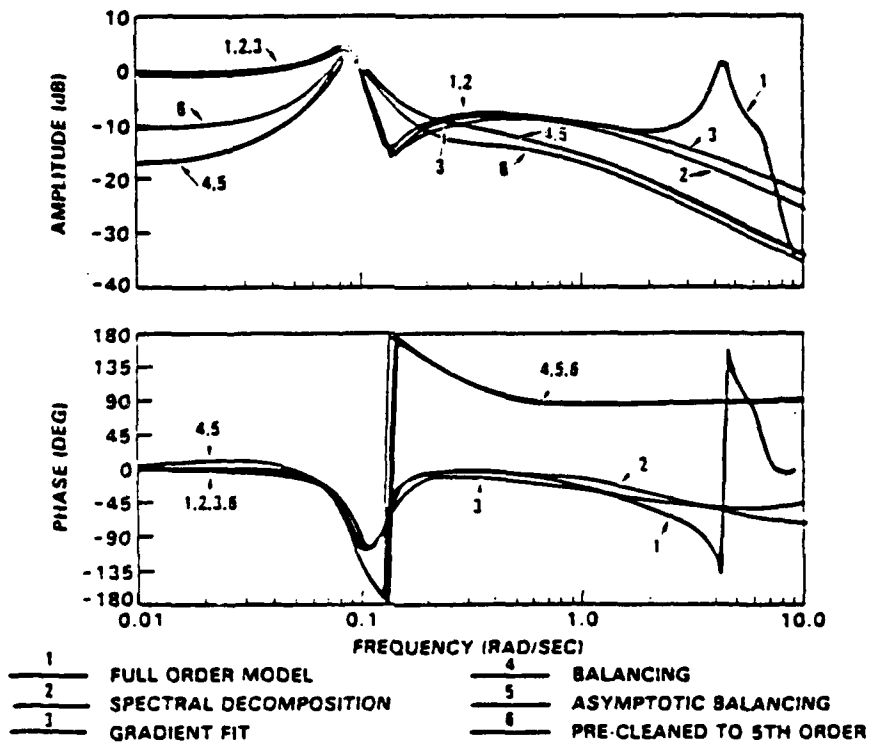


Figure 5-6. Frequency Response of $\alpha/\delta e$

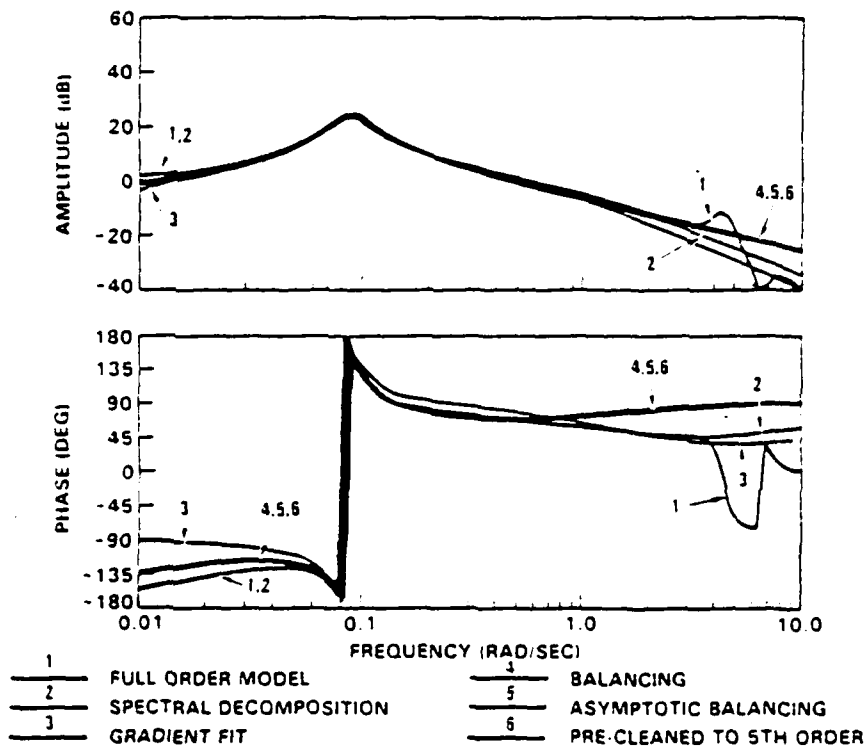


Figure 5-7. Frequency Response of $\theta/\delta\epsilon$

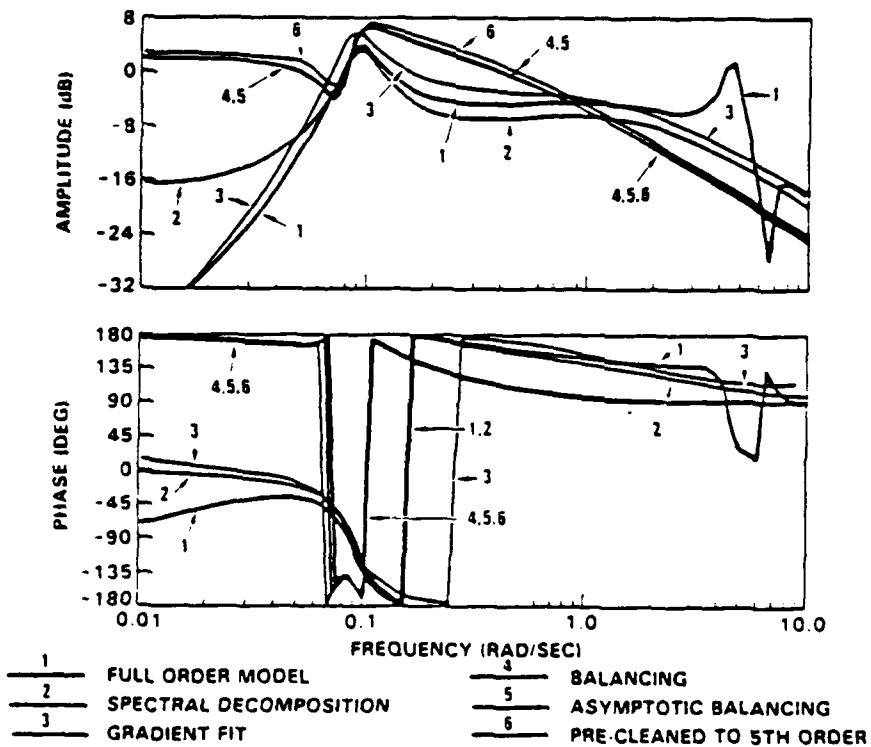


Figure 5-8. Frequency Response of $q/\delta\epsilon$

SECTION 6

HYDRAULIC ACTUATOR EQUATIONS FOR AEROSERVOELASTIC MODELING

6.1 INTRODUCTION

A fly-by-wire (FBW) actuation system has two major tasks: (1) to convert an electric command signal into a hydraulic command signal, and (2) to amplify that signal into a powerful output which can operate on the intended control-surface load. These tasks are performed by the "secondary" and "power" actuators respectively.

The secondary actuator drives the control valve in the power actuator system. Its power requirements are not very important, because the driver needs only to provide sufficient force to overcome friction, power valve flow forces, and emergency jam-breaking forces. Therefore, both hydraulic and electric drive actuator systems are candidate approaches.

On the other hand, in the case of power actuators, the hydraulic type is the accepted standard for flight control applications. Its advantages over a corresponding lightweight electric power actuator (designed with the new lightweight magnetic materials) are its high force gain and stiffness and its ease of configuring into redundant systems; e.g., no rotary gears which can be a single point failure.

The power actuator requirements depend on the characteristic of the load. As dynamic pressure increases, control-surface hinge moments increase. As vehicle size increases, control-surface areas increase. At low dynamic pressure the control surfaces must be capable of large deflections with relatively high angular velocities. At high dynamic pressure, corresponding small deflections and high stiffness are required.

The power actuator piston is sized by the maximum torque, which occurs during a high-speed run at sea level. Maximum actuator rate of travel is required at high speed at high altitude. Maximum actuator stroke is defined by a low-speed landing.

Aside from the usual specifics of maximum hinge moment and velocity, the requirements unique to actuation systems for large, high-speed aircraft are related to static and dynamic stiffness, frequency response, availability in redundant configurations, weight, and relative power consumption.

The ideal actuator characteristics would be linear, without offset, and having exactly the prescribed gain. This is a reasonable assumption for secondary actuators, but primary actuators under load are significantly nonlinear due to the square-law valve flow characteristic of a hydraulic orifice. The equations which yield the flow and pressure functions of the selected valve (four-way or three-way) should be included in a computer simulation for comparison with corresponding results for a linearized system.

Among the specifications for a linearized model of a power servo are pressure gain and flow gain. The pressure gain is specified on the basis of stiffness requirements and of the prescribed position error. The flow gain is specified on the basis of the prescribed actuator frequency response. Specifications relative to thresholds and hystereses are determined by computer simulation, such that their static and dynamic effects are negligible.

Input signals to the secondary servos originate at various sensors and are processed by a computer (analog or digital). The dynamic characteristics of most sensors are of sufficiently high frequency bandpass, that they can be neglected, except that typically in accelerometers, a first-order cut-off is designed for noise attenuation inside the force-balance servo loop. The effective transfer function of the accelerometer is

$$\frac{\Delta n}{\Delta n_c} = \frac{1}{\tau_n s + 1}$$

Although the resonant frequency mode of an accelerometer or rate gyro is typically neglected, the real transfer function includes second order poles. This factor

$$\frac{1}{\left(\frac{s}{\omega_0}\right)^2 + 2\zeta\left(\frac{s}{\omega_0}\right) + 1}$$

must be included when the sensor is used for controlling a structural mode, unless the natural frequency ω_0 is at least one decade above the frequency of the structural model.

To keep the natural frequency of the actuator spring-mass system above the aerodynamic flutter frequency requires that the "fluid spring" be as stiff as possible for a given surface inertia. The bulk modulus of the working fluid, in combination with associated structural compliances, defines the actuator stiffness.

As with sensors, the dynamic characteristics of secondary servos (series or parallel) are of sufficiently high bandpass that they usually can be neglected. If a structural mode is to be controlled, then the dynamics of the corresponding servo, up to one decade above the controlled structural mode, will be included in the model.

6.2 ACTUATOR SYSTEM MODEL

A mechanical schematic used for analysis of a particular single hydraulic actuator is shown in Figure 6-1. The indicated coordinates represent motion at (1) the servo input X_I , (2) the valve X_V , (3) the actuator X_P , and (4) the load X_L . The additional coordinates are: (5) X_S to represent the input system dynamics coupled from the pilot to the servo input through the cable, (6) X_O to represent motion of the feedback linkage pickoff point, and (7) X_C to represent the cylinder dynamics against the backup support. It is assumed that the valve module is at the reference position. All coordinates, except at the valve, are chosen conveniently to represent motion referenced with respect to the piston. Therefore $\delta X_I / \delta X_O = 1$ and $\delta X_V / \delta X_I = -\delta X_V / \delta X_O = G_I$, the feedback linkage ratio.

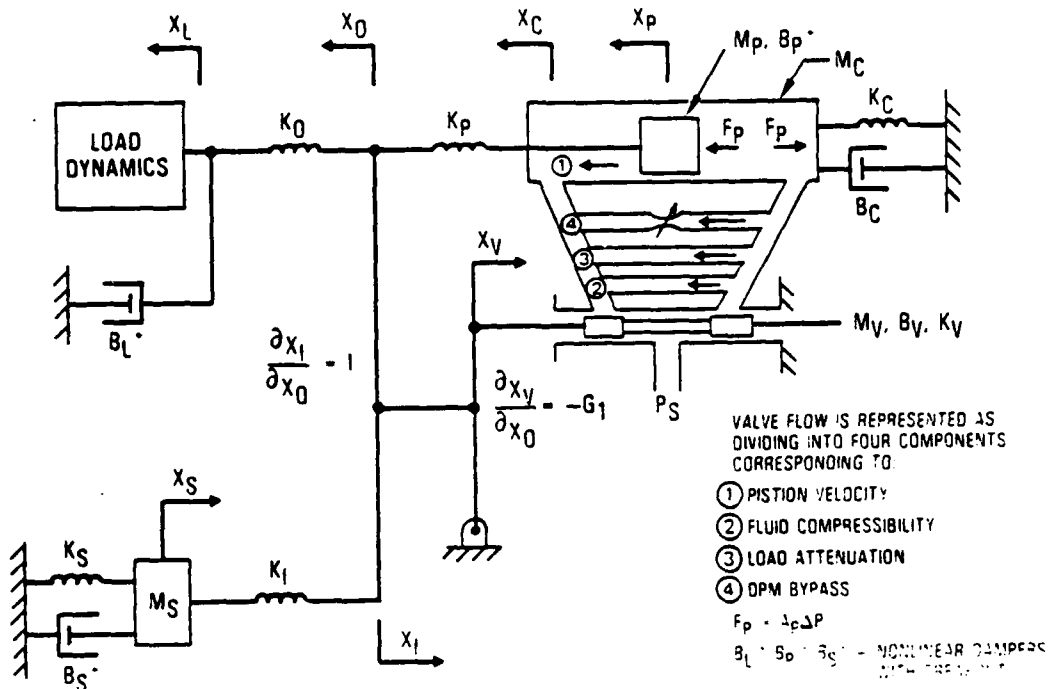


Figure 6-1. Hydraulic Servo-Dynamic Model

Hydraulic flow from the valve is shown divided into four components representing (1) piston velocity, (2) fluid compressibility, (3) load-pressure attenuation and leakage bypass due to load, and (4) bypass flow through the pressure modulated orifice for stability compensation.

6.2.1 Hydraulic Model

The schematic details of the hydraulic system are shown in Figure 6-2. It is represented as an equivalent electrical circuit in Figure 6-3. The pressure elements, analogous to voltage sources, are: (1) P_S , the pressure source, (2) ΔP , the load-induced pressure across the actuator piston, and (3) P_k and P_{FB} , the two differential pressures across two small pistons in the pressure modulating device. The impedance elements are: (1) R_1 and R_2 , orifice impedances of the four way control valve, assumed symmetrical, as sketched in Figure 6-2; (2) R_3 , the line and manifold impedances into the valve module, assumed to behave as if it were an equivalent orifice; and (3) R_0 and R_{BP} , the orifice impedances of the pressure modulating device.

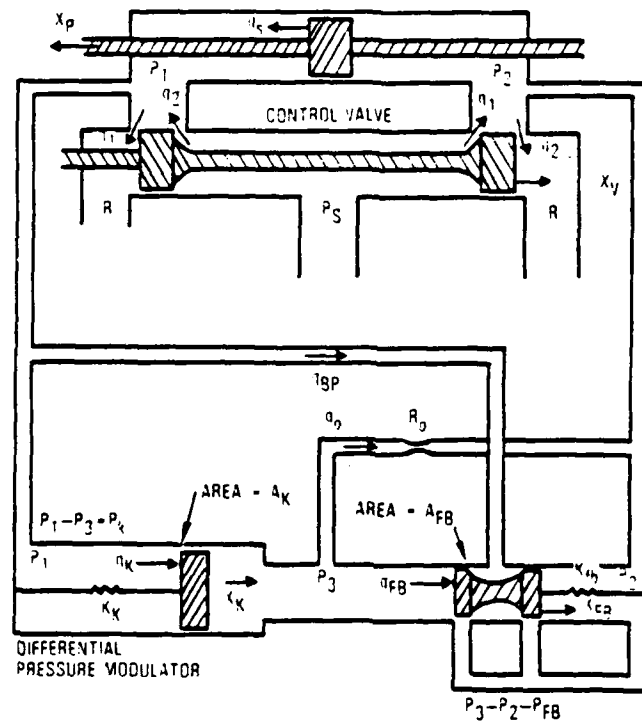


Figure 6-2. Hydraulic Component Interface

The flow variables are denoted by q as indicated. The diode in the pressure line represents the hydraulic check valve.

The equations of that part of the bridge network in Figure 6-3 comprising the valve impedances R_1 and R_2 , the pressure source P_S , and the load-induced pressure at the cylinder ΔP are:

$$P_S - \Delta P = R_1 q_1^2 \text{ Sgn } q_1$$

$$P_S + \Delta P = R_2 q_2^2 \text{ Sgn } q_2$$

$$q_a = q_1 - q_2$$

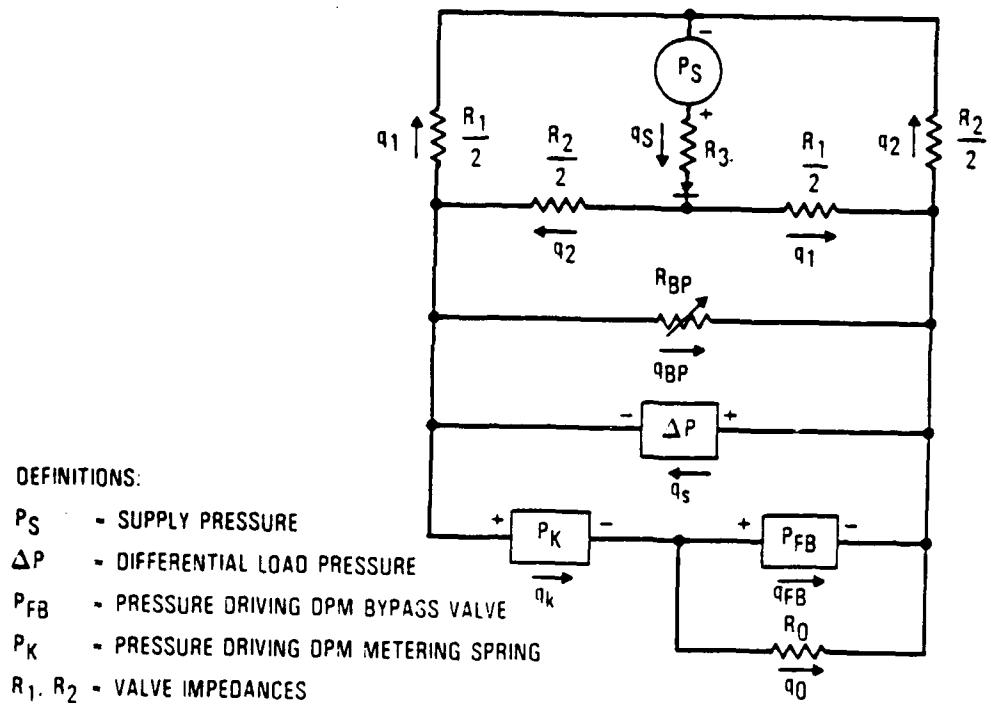


Figure 6-3. Hydraulic System Analog

Then the magnitude of flow through the cylinder is:

$$|q_a| = \left| \sqrt{\frac{P_S - \Delta P}{R_1}} - \sqrt{\frac{P_S + \Delta P}{R_2}} \right|$$

where R_1 and R_2 are functions of the valve stroke.

The quadratic flow characteristic is explained by the fact that the pressure drop corresponding to flow through an orifice is proportional to the square of the flow; i.e., $p = Rq^2$. Thus, the effect being similar to Ohm's law in electrical theory, Kirchoff's laws can be applied to yield the above set of nonlinear equations. For mathematical convenience, the square law can also be used as an approximation for high-velocity flow through tubes. (With Reynold's number above 3000 the relationship is $p = Rq^{1.75}$.)

6.2.1.1 Bernoulli's Equation

Bernoulli's equation simply states the conservation-of-energy principle as it pertains to hydraulic flow and pressure relationships. Expressing the total energy change in a mechanical system to be equal zero:

$$1/2 Mv^2 + Fd + Wh = 0$$

where the kinetic energy is one half mass times velocity squared ($1/2Mv^2$); the applied work is force times displacement (Fd); and the potential energy is weight times height (Wh).

The mechanical expression is converted to the hydraulic expression (Bernoulli's equation) by substitution and division as follows.

First, to convert the expression to a conventional form in terms of "head", divide by weight and substitute appropriate parameters which are:

mass density x volume:	$\rho V = M$
pressure x area:	$pA = F$
mass x gravity:	$Mg = W$

The total head (velocity head, pressure head, and elevation head) is thus shown to be:

$$v^2/2g + p/\rho g + h = 0$$

Then, for the more conventional Bernoulli form, multiply by weight density (ρg):

$$1/2 \rho v^2 + p + \rho g h = 0$$

The flow q through an orifice is derived from Bernoulli's equation by neglecting the velocity on the source-pressure side and equating the source energy to the energy on the load-pressure side. Then:

$$p_1 + \rho gh = 1/2 \rho v^2 + p_2 + \rho gh$$

Substituting flow in place of velocity ($v = q/a$), then the pressure drop is

$$\Delta p = 1/2 \rho v^2 \operatorname{sgn} v = 1/2 \rho (q/a)^2 \operatorname{sgn} q$$

where a is the cross-sectional area of the orifice.

Dropping the notations, sgn and Δ , except as needed:

$$q = a \sqrt{2p/\rho}$$

An "orifice loss" reduces the flow by a factor of C_d : so

$$q = C_d a \sqrt{2p/\rho}$$

If the area is variable (a function of valve stroke) and w is the width of the orifice, then

$$a = w x$$

and

$$q = C_d w x \sqrt{2p/\rho}$$

Therefore,

$$q^2 = p/R$$

where

$$R = \rho/2 (C_d wx)^2$$

6.3 FOUR-WAY HYDRAULIC VALVE

The control valve described here is a conventional four-way underlapped valve, which has well-defined flow and pressure characteristics around the null region.

The equations representing the orifice areas of an underlapped four-way valve are

$$a_1 = a_0 + w x \quad , \quad - a_0/w \leq x \leq x_{\max}$$

$$a_2 = a_0 - w x \quad , \quad x_{\min} \leq x \leq a_0/w$$

The valve orifice impedances are derived as follows

$$q_1^2 = (C_d a_1)^2 2p/\rho = p/(R_1/2)$$

Therefore

$$R_1/2 = \rho/2(C_d a_1)^2 = (C_o(a_0+wx))^{-2} \quad , \quad - a_0/w \leq x \leq x_{\max}$$

where

$$C_o = C_d \sqrt{2/\rho}$$

Similarly,

$$R_2/2 = (C_o(a_0-wx))^{-2} \quad , \quad -x_{\min} \leq x \leq a_0/w$$

If the operation were always within the underlap zone, then the constraining definitions could be ignored.

When the valve spool is fixed at a displacement in either direction beyond the underlap region, one of the two impedances approaches infinity, and the cylinder flow-pressure relationship is parabolic. When the valve stroke is within the underlap region, the relationship is the difference between two parabolas. The flow-pressure, flow-valve, and pressure valve characteristics are sometimes assumed to be linear, except in the regions approaching load stall or valve saturation.

Figures 6-4, 6-5, and 6-6 show these static characteristics as obtained from an analog simulation of the system represented in Figure 6-1. In Figure 6-4, the load pressure was varied while the valve position X_v was held at various constant values. In Figure 6-5, the valve stroke was varied with no load pressure; and in Figure 6-6, the valve stroke was varied with the actuator blocked (no cylinder flow). Corresponding hardware characteristics are routinely measured in the laboratory.

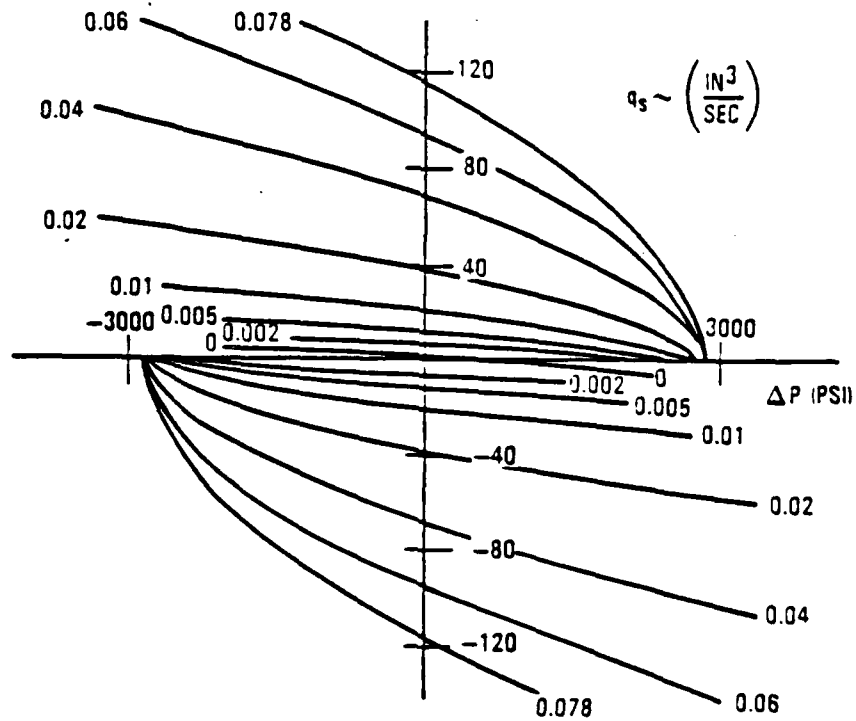


Figure 6-4. Valve Characteristics - Flow vs Load Pressure

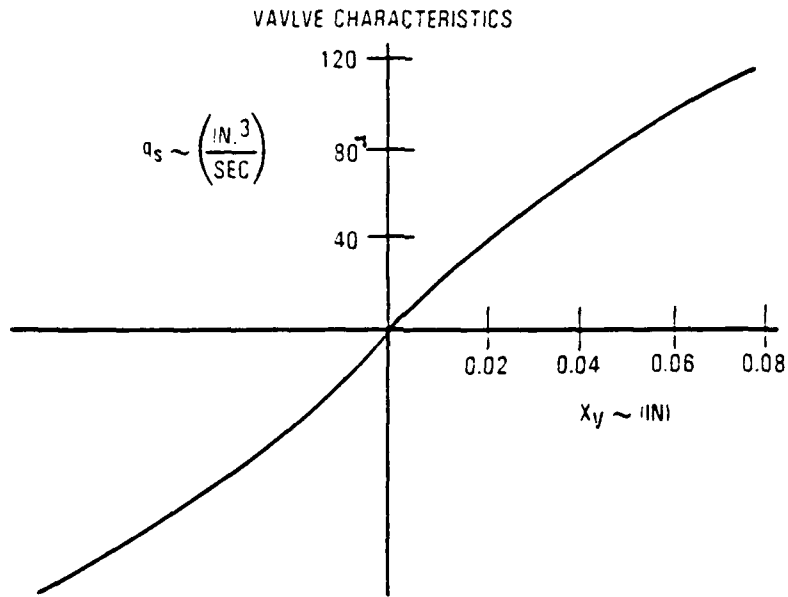


Figure 6-5. Flow vs Valve Stroke

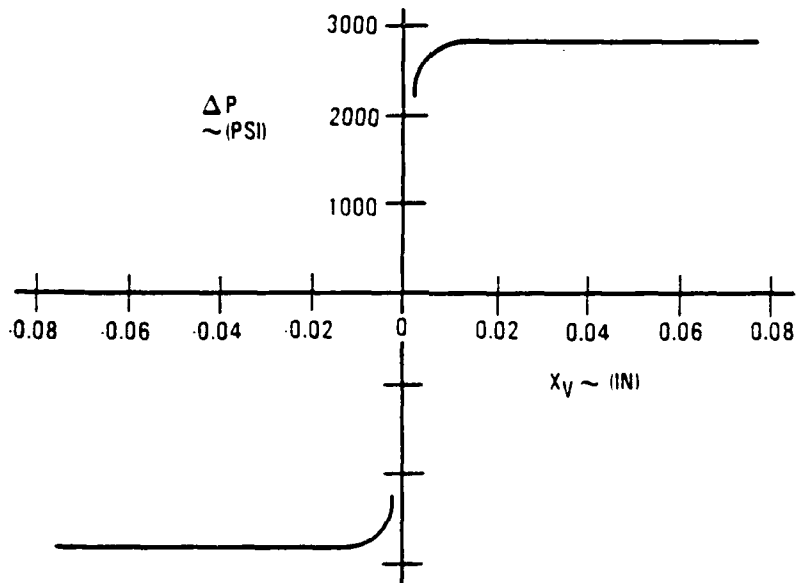


Figure 6-6. Load Pressure vs Valve Stroke

6.4 DIFFERENTIAL PRESSURE MODULATOR (DPM)

If stability compensation is required, a differential pressure modulator (DPM) can provide it by use of a frequency-variant bypass orifice across the piston, as shown schematically in Figure 6-2. Its operation is described as follows:

If the differential pressure, $(P_1 - P_2)$, is constant, the system establishes an equilibrium with $(P_3 = P_2)$, so that the piston of area A_{FB} is centered by the centering spring K_{FB} ; and the piston of area A_K is at an equilibrium position X_K .

Then, if the differential pressure is suddenly stepped, the A_K piston moves toward a new equilibrium, generating a change in the pressure P_3 , and driving the A_{FB} piston against its centering spring.

This opens the bypass between the two sides of the main actuator piston. Equilibrium, with the bypass valve centered, is reestablished as flow through the orifice R_0 is reduced to zero. The rate at which equilibrium is reestablished depends upon the size of the orifice R_0 and upon the size of the springs (K_K and K_{FB}) and pressure areas (A_K and A_{FB}). Thus the bypass remains closed with steady ΔP and responds to variations of ΔP as a function of frequency. Obviously, the DPM dynamic characteristics are nonlinear due to the orifice impedances.

The mathematical model for the differential pressure modulator is that part of the hydraulic network in Figure 6-2 comprising all except the control valve. The equations are:

$$A_K \dot{X}_K = q_K$$

$$A_K P_K = K_K X_K$$

$$P_K + P_{FB} = \Delta P$$

$$A_{FB} P_{FB} = K_{FB} X_{FB}$$

$$A_{FB} \dot{X}_{FB} = q_K - q_0$$

$$P_{FB} = R_o q_o^n$$

where $n = 2$ for nonlinear analysis

$n = 1$ for a linear approximation.

Combining the first three equations:

$$q_K = \frac{A_K^2}{K_K} \frac{d}{dt} (\Delta P - P_{FB})$$

Combining the last three equations with the linear approximation

$$\frac{dP_{FB}}{dt} = \frac{K_{FB}}{A_{FB}^2} \left(q_K - \frac{P_{FB}}{R_o} \right)$$

Let

$$\frac{K_K}{A_K^2} = C_K, \quad \frac{K_{FB}}{A_{FB}^2} = C_{FB}$$

Then from the above results:

$$\frac{dP_{FB}}{dt} = C_{FB} \left\{ \frac{1}{C_K} \frac{d}{dt} (\Delta P - P_{FB}) - \frac{P_{FB}}{R_o} \right\}$$

The corresponding transfer function is

$$\frac{P_{FB}}{\Delta P} = \frac{K_L \tau_L s}{\tau_L s + 1}$$

where

$$K_L = \frac{C_{FB}}{C_{FB} + C_K}, \quad \tau_L = \frac{R_o (C_{FB} + C_K)}{C_{FB} C_K}$$

A corresponding nonlinear analysis using the additional equations:

$$\begin{aligned} 1/R_0 &= (C_0 a_0)^2 \\ |\Delta P| &= R_{BP} q_{BP}^2 \\ 1/R_{BP} &= (C_0 w_{BP} x_{FB})^2 \end{aligned}$$

yields a nonlinear differential equation which can be solved by use of "separation of variables." This leads to a corresponding "pseudo transfer function":

$$\frac{P_{FB}}{\Delta P} = \frac{K_{NL} \tau_{NL}}{\tau_{NL} s + 1}$$

where

$$K_{NL} = \frac{C_0 w_{FB}}{A_{FB} C_{FB}} \sqrt{\Delta P} K_L$$

$$\tau_{NL} = \sqrt{\frac{C_{FB}}{C_{FB} + C_K} \frac{d\Delta P}{R_0}} \tau_L$$

Here $d\Delta P$ is a step-function change in ΔP which excites an exponential transient with an equivalent "time constant." The equivalent time constant produces the same initial-slope transient as that of the corresponding linear time constant.

6.5 DYNAMIC INERTIAL LOAD MODEL

A flexible control surface cannot be represented properly as a single lumped mass, because its fundamental bending mode is at a comparatively low frequency - lower than that due to the corresponding mass and actuator stiffness. In order to obtain a more accurate model, the surface is considered to be composed of several span-wise segments (say eight per side), arranged as shown in Figure 6-7. Each is represented by lumped elements with degrees of freedom corresponding to bending a torsion of a swept beam. The size and position of each element depends upon the true span-wise mass and stiffness distribution. The chordwise distribution determines the position of each element relative to the swept elastic axis.

A frequency analysis of this distributed-parameter model determines the resonant and anti-resonant frequencies. An equivalent model having only four lumped masses (two per side) is shown in Figure 6-7. It can be derived by neglecting all modes above a certain frequency and then matching the lower mode dynamics (position/force, function of frequency) as computed at the unrestrained actuator drive points when the model is driven symmetrically. The center spring shown in Figure 6-7 represents the stiffness of the center box between the two sides of the control surface. Its value is specified in accordance with servo tracking requirements. When the two sides are driven symmetrically ($F_1 = F_2$), the center spring has no influence. Therefore, the parameter values on each side (two masses and one spring) are determined by three known quantities: the first resonant frequency, the first anti-resonant frequency, and the sum of the two masses. When driven unsymmetrically, the antisymmetrical modes approximate those of the real system.

6.6 LINEARIZED SYSTEM MODEL

Figure 6-8 represents a linearized, simplified math model of the total actuator system (Figure 6-1). The load model in Figure 6-8 represents the symmetrically-driven structure in Figure 6-7. Any load model (e.g., a sophisticated state-space model) with correct force/position transfer functions at the points of actuation may be coupled into the math model in a manner similar to that shown in the block diagram (Figure 6-8).

The block diagram also shows how the flow gain and pressure gain are used in the linearized math model. In this model, the higher-frequency dynamics are assumed stable and are therefore neglected; i.e., M_p , B_p , M_v , B_v , K_v , M_c , B_c , and $1/K_c$ are assumed to be negligible. With the piston mass and friction are neglected, the hydraulic compressibility $1/K_B$ can be lumped together with the structural compliance inside the feedback loop, thus resulting in the effective compliance

$$1/C = 1/K_B + 1/K_p$$

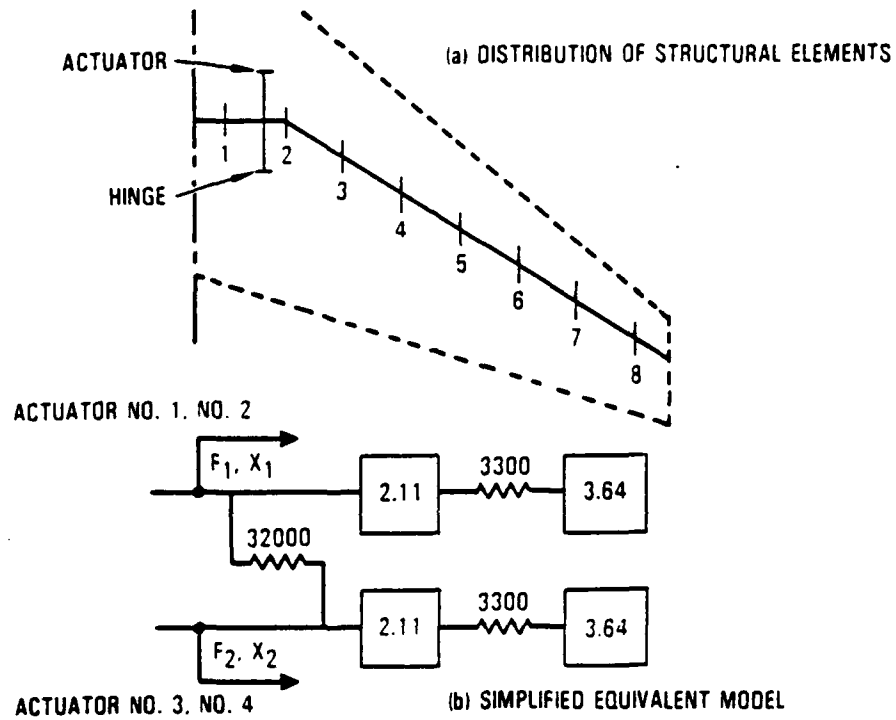


Figure 6-7. Load Dynamics - Flying Tail

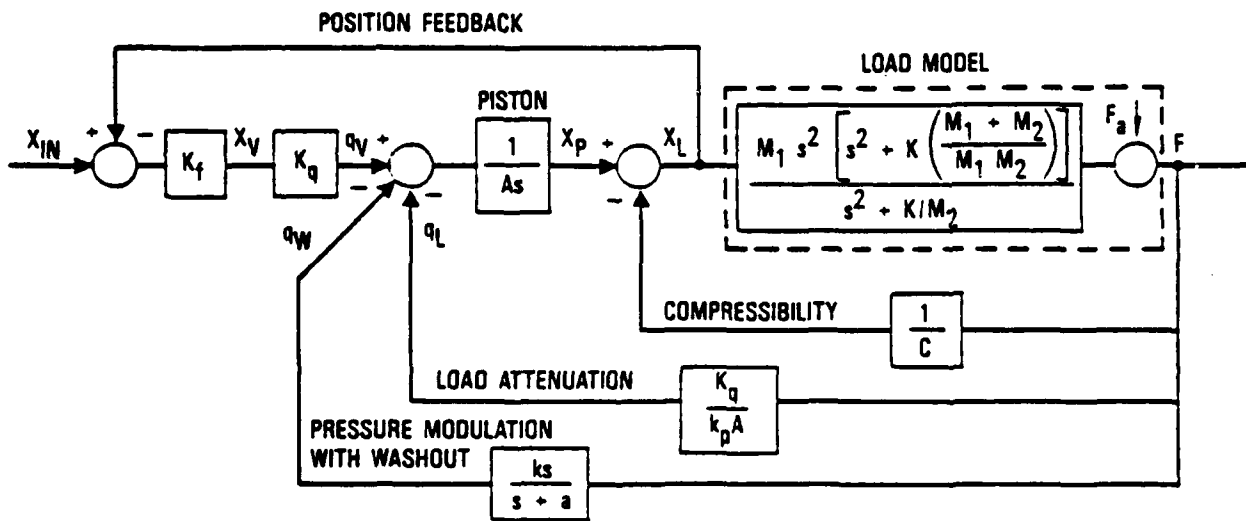


Figure 6-8. Hydraulic Servo System

The hydraulic compressibility is a nonlinear function of the piston position. Denoting the cylinder length as L , and the piston displacement from center as z , the volumes of the two hydraulic columns supporting the piston are $A(z + L/2)$ and $A(-z + L/2)$.

Fluid compressibility is defined (per unit volume) as the incremental volume change resulting from an incremental pressure change:

$$1/\beta = (dV/dp)/V$$

The reciprocal of fluid compressibility, β , is called the bulk modulus. The corresponding hydraulic "spring rate" of a fluid volume, $V_1 = AL_1$, is computed as follows. Since

$$\beta = V_1 (dF/dz)/A^2$$

then

$$K_{B1} = \beta A^2/V_1$$

Therefore, the sum of the two "spring rates" supporting the piston is

$$K_B = K_{B1} + K_{B2} = \beta A^2(1/V_1 + 1/V_2) = \beta AL/((L/2)^2 - z^2)$$

The compliance ($1/K_B$) is a parabolic function whose value is zero at each end of the piston stroke and whose maximum value is at the midstroke ($z = 0$).

It is usually acceptable to represent the hydraulic "spring rate" as a constant at its conservative (minimum) value. Then

$$K_B = 4\beta A^2/V$$

A linearized approximation of flow in the valve underlap is obtained by use of small-perturbation theory. The differential flow

$$dq = \frac{\delta q}{\delta X_v} dX_v + \frac{\delta q}{\delta \Delta P} d\Delta P$$

Let the flow gain $\delta q/\delta X_v$ be denoted as a constant K_q ; and let the pressure gain $-\delta \Delta P/\delta X_v$ be denoted as a constant, K_p . Then

$$dq = K_q dX_v - (K_q/K_p) d\Delta P$$

Recognizing that the differential symbols are replaced by the corresponding symbols which denote small perturbations:

$$q_v = K_q X_v - (K_q/K_p) \Delta P$$

A normalized form of the flow-pressure equation in subsection 6.2.1 is:

$$q = (1+y) \sqrt{(1-p)} - (1-y) \sqrt{(1+p)}$$

where the normalized flow is

$$q = q_a/a_0 C_0 \sqrt{P_S/2}$$

and where p is the normalized pressure $\Delta P/P_S$ and $y = wx/a_0$ is the ratio of the valve stroke to its corresponding maximum; i.e., in the underlap region, the maximum stroke is the magnitude of the underlap. The corresponding normalized partial derivatives, which represent flow gain, flow attenuation due to load, and pressure gain are:

$$\delta q/\delta y = \sqrt{(1-p)} + \sqrt{(1+p)}$$

$$\delta q/\delta p = -.5 \left(\frac{(1+y)}{\sqrt{(1-p)}} + \frac{(1-y)}{\sqrt{(1+p)}} \right)$$

$$\delta p / \delta y = \frac{2[(1-p) \sqrt{1+p} + (1+p) \sqrt{1-p}]}{(1+y) \sqrt{1+p} + (1-y) \sqrt{1-p}}$$

Note that if the normalized load pressure is relatively small such that $\sqrt{1+p} \approx \sqrt{1-p}$ then each of the derivatives would be nearly constant, thus supporting the linear approximations within the underlap region.

6.6.1 Dynamic Stability

In order to understand the stabilizing influence of the pressure modulating device, consider a single mass with light damping as the load. Beyond a certain loop gain to establish the hydraulic servo frequency bandwidth the quadratic roots will become unstable. A common method of damping such roots in electrically driven servos is to use velocity feedback, as shown in the feedback path of Figure 6-9.

The inner loops of Figure 6-8 reduce to the models of Figure 6-9 as follows: letting $K = 0$ and $F_a = 0$, the load model of Figure 4-8 reduces to $M_1 s^2$. Moving the load attenuation summing point to the right of the piston block and closing the compressibility and load attenuation loops, the inner loop transfer function becomes

$$\frac{X_L}{\bar{X}_2} = \frac{C/M_1}{s^2 + C/B_q s + C/M_1}$$

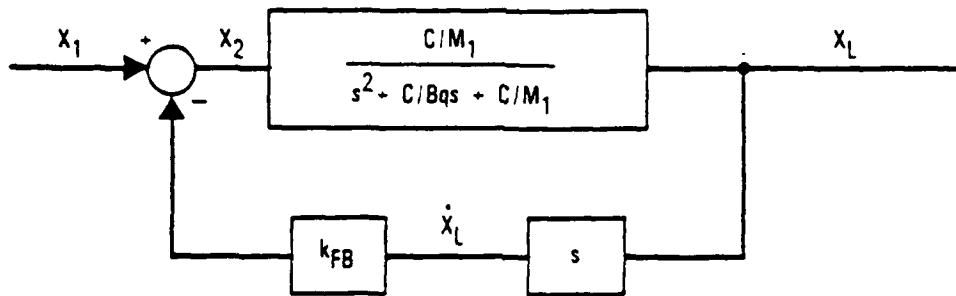
where

$$B_q = K_p A^2 / K_q$$

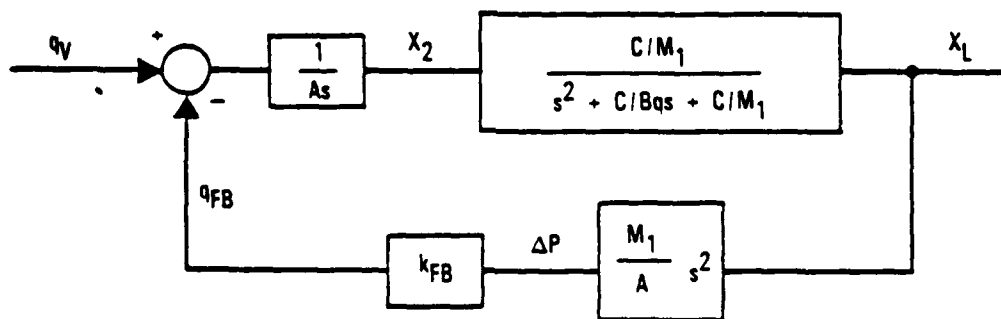
Closing the velocity feedback loop of Figure 6-9.

$$\frac{X_L}{\bar{X}_1} = \frac{C/M_1}{s^2 + (C/B_q + K_{FB} C/M_1) s + C/M_1}$$

The damping coefficient has been increased by $\frac{K_{FB} C}{M_1}$ over what it would have been without the feedback path.



(a) TYPICAL SERVO MODEL WITH VELOCITY FEEDBACK



(b) CORRESPONDING HYDRAULIC MODEL

Figure 6-9. Velocity Feedback Models

A possible method of implementing this effect in hydraulic servos is to use hydraulic flow bypass through an orifice. As seen in the block diagram of Figure 6-9, q_{fb} is produced by the load acceleration X_L , which is then

integrated through the piston to appear as velocity feedback. This is the linear equivalent to placing a hole through the actuator piston. The feedback flow in Figure 6-9 corresponds to the washed-out feedback flow in Figure 6-8. The washout (provided by the DPM) maintains "stiffness" of the actuator fluid column during static conditions.

6.7 STATIC STIFFNESS

The purpose of the servo is to drive a load which is both dynamic and static. A static load driven by the compensated servo will require additional flow through the control valve to supply the leakage through the bypass orifice. Furthermore, the static stiffness might be degraded, as will be shown. These objections can be avoided by the addition of a device which makes the size of the bypass orifice variable with the frequency of the dynamic load force. A practical transfer function to produce this effect, called a "washout," is $s/(s+a)$.

The operation of the washout can be explained as follows. Consider the system (Figure 6-8) to be inertially unloaded ($M_1 = M_2 = 0$). The compliance transfer function (output position response to aerodynamic force on the piston rod) is

$$\frac{X_L}{F_a} = \frac{1}{C} \frac{s^2 + (a + C/B_q + Ck/A) s + Ca/B_q}{s^2 + (\frac{K_f K_q}{A} + a) s + \frac{K_f K_q a}{A}}$$

Note that the output compliance in response to a high frequency force is independent of the compensation device and depends only upon the inherent servo compliance. This fact can be seen by

$$\left. \frac{X_L}{F_a} \right|_{s \rightarrow \infty} = 1/C$$

Note also that the static compliance with the washout ($a \neq 0$) is dependent only upon the pressure gain of the valve as operated through the feedback path.

$$\left. \left(\frac{X_L}{F_a} \right) \right|_{s \rightarrow 0} = \frac{1}{K_p K_f A}$$

However, when the washout is removed ($a = 0$) the static compliance looking back into the servo is increased, thus allowing appreciable position error due to static load.

$$\left. \left(\frac{X_L}{F_a} \right) \right|_{\substack{a = 0 \\ s = 0}} = \frac{1}{K_f K_p A} + \frac{k}{K_f K_q}$$

Thus, it is seen that the washout negates the increased static stiffness caused by the pressure feedback. The value of the washout pole, a , must be chosen carefully, because intermediate frequency compliance can be degraded by an improper choice.

6.8 AEROSERVOELASTIC INTEGRATION

The structural dynamics of a control surface couples into the main structure as a function of the applied actuator forces. If the surface is comparatively flexible, then special equations which reflect the servo load must be represented as

$$F = H_i (s) X_{jn} - H_p (s) X_L$$

where F is the actuator force; X_L is the elongation of the actuator; and X_{jn} is the commanded elongation. The above expression takes into account all static and dynamic loads applied by the actuator to the connecting points between the airframe and the control surface. These points are included in the state vector of the structural model.

The computation of the above force includes effects due to the hydraulic flow and pressure characteristics of the control valve and of any load compensating device.

Again considering Figure 6-8, a more useful model for aeroservoelastic integration of the actuator system is obtained by inverting the load model and "sensing" F through the compressibility spring, i.e.,

$$F = C (X_p - X_L)$$

Denoting the existing load model (with no F_a) and $F/X_L = 1/G(s)$, the inverted load model is $X_L/(X_p - X_L) = CG(s)$; and the variable F is found between blocks C and $G(s)$ in the revised model. Now an expression for F , independent of $G(s)$, can be derived from this revised version of Figure 6-8.

$$F = \frac{(a_1 s + b_1) X_c - (s^2 + a_2 s + b_2) X_L}{d_2 s^2 + d_1 s + d_0}$$

where

$$\begin{aligned} a_1 &= K_f K_q / A \\ b_1 &= a_1 a \\ a_2 &= a_1 + a \\ b_2 &= a_1 a \\ d_0 &= 1/B_q a \\ d_1 &= a/C + k/A + 1/B_q \\ d_2 &= 1/C \end{aligned}$$

6.8.1 Required Representation of Servo Nonlinearities

As described previously, the hydraulic servos can usually be represented with linear models. In order for the assumptions to be acceptable, however, care must be taken that excessive flow rates not be commanded such as to exceed the saturation level corresponding to the maximum valve stroke. If rate saturation does occur, it sharply lowers the cutoff frequency of the linearized first-order model.

Other important nonlinear effects might be due to DPM effects or to the parabolic characteristic (flow versus pressure) of the valve. A trim condition with the quiescent design load near stall is unusual. It occurs only in cases where load limiting is required, such as for spoiler or rudder blowback, or in cases where parallel systems have failed. If operation requires high inertial loads at high frequencies, then the valve's parabolic characteristic becomes very significant; and the model must include some linear representation, such as a describing function, whereby frequency and phase characteristics are functions of actuator displacement amplitudes.

REFERENCES

1. Likins, P. W., "Dynamics and Control of Flexible Space Vehicles." Technical Report 32-1329, Jet Propulsion Laboratory, Pasadena, California, 15 January 1970.
2. Beer, Ferdinand P. and E. Russel Johnston, Jr., Vector Mechanics for Engineers, Dynamics, (3rd. ed.), McGraw-Hill, Inc., New York, New York, 1977.
3. Hurty, Walter C. and Moshe F. Rubinstein, Dynamics of Structures. Prentice-Hall, Englewood Cliffs, New Jersey, 1964.
4. Kane, Thomas R., Dynamics, Holt, Rinehart and Winston, Inc., New York, New York, 1968.
5. Tuma, Jan J., Engineering Mathematics Handbook, McGraw-Hill, Inc., New York, New York, 1979.
6. Etkin, Bernard, Dynamics of Flight, Stability and Control. John Wiley and Sons, Inc., New York, New York, 1959.
7. Nelson, F. R., et al, "Dynamics of the Airframe," A-E-61-4 II. Northrop Aircraft, Inc., Hawthorne, California, 1952.
8. Albano, Edward and William P. Rodden, "A Double-Lattice Method for Calculating Lift Distribution on Oscillating Surfaces in Subsonic Flow," AIAA paper No. 68-73 presented at 6th Aerospace Sciences Meeting, New York, New York, 22-24 January 1968 submitted February 1968. Revision received 20 August 1968, Northrop Corporation, Norcour Division. Hawthorne, California, AIAA Journal Vol. 7, No. 2, February 1969.
9. Jones, William P. and Kari Appa, "Unsteady Supersonic Aerodynamic Theory for Interfacing Surfaces by the Method of Potential Gradient." NASA CR-2898 Bell Aerospace Textron. Buffalo, New York, October 1977.
10. Lyle N. Long and George A. Watts, "A General Theory of Arbitrary Motion Aerodynamics Using an Aeroacoustic Approach," 55th Fluid Dynamics Panel Meeting, Toronto, Canada, October 1984.
11. Goforth, E. A., working paper, "Approximation for Gust Aerodynamics," October 1986.
12. Goforth, E. A., working paper titled, "Rational Function Approximation of Aerodynamics," September 12, 1986.
13. Silverman, L. M., "Model Reduction in Optimal Control System Design." Lockheed-California Company, Project No. 80011119, LR29364. 1980.

REFERENCES (Continued)

14. Davis, W. J., and Chiodi, O. A., A Method for Decoupling of Equations by Spectral Decomposition, Lockheed-California Company, LR 27470, December 19, 1975.
15. Davis, W. J., Analytical Basis for Linear Synthesis and Nonlinear Simulation of a Flexible-Airplane Control System, Lockheed-California Company, LR 30070, May 21, 1982.
16. Brockett, R. W., Finite Dimensional Linear Systems, John Wiley and Sons, 1970.
17. Enns, D., Model Reduction for Control System Design, Ph. D. Dissertation, Department of Aeronautics and Astronautics, Stanford University, 1984.
18. Silverman, L. M., Balanced Approximations, Lockheed-California Company, LR30360, December 17, 1982.
19. Jonckheere, E. A., and Silverman, L. M., "A New Set of Invariants for Linear Systems - Application to Reduced Order Compensator Design," IEEE Transactions on Automatic Control, Vol. AC-28, No. 10, October 1983.
20. Jonckheere, E., and Rongsheng, L., "Generalization of Optimal Henkelnorm and Balanced Model Reduction by Bilinear Mapping," Int. J. Control, 1987, Vol. 45, No. 5, 1751-1769.
21. Dynamics of the Airframe, Bu Aer Report, AE-61-4II, Northrop Navair, September 1952.
22. Colgren, R. D., "Methods for Model Reduction," to be presented at the AIAA Guidance, Navigation and Control Conference, Minneapolis, 15-17 August 1988.
23. Blackburn, J. F., Reethof, G., and Shearer, J. L., Fluid Power Control, The M. I. T. Press, 1960.
24. Davis, W. J., and Levi, R. W., "Preliminary Stability Analysis of the L-1011 Horizontal Stabilizer Servos," FGC/1011-7, Lockheed-California Company, August 15, 1969.
25. Albano, Edward and William P. Rodden, "A Doublet-Lattice Method for Calculating Lift Distribution on Oscillating Surfaces in Subsonic Flow," AIAA paper No. 68-73 presented at 6th Aerospace Sciences Meeting, New York, New York, 22-24 January 1968, submitted February 1968. Revision received 20 August 1968, Northrop Corporation, Norcour Division. Hawthorne, California, AIAA Journal Vol. 7, No. 2, February 1969.

REFERENCES (Continued)

26. Roger, K. L.. "Airplane Math Modeling Methods for Active Control Design," in AGARD Structures and Materials Panel, 44th Meeting, Lisbon, Portugal, April 1977.

GLOSSARY

Dextral:

Right handed.

Elastic structure:

Assumed linear. This implies that the elastic limit of the material is not exceeded. This also implies that as the component of the j^{th} restoring force is proportional only to the corresponding component of the j^{th} component of deformation: that is, $[K]$ is constant (with respect to $\{q\}$).

Inertial reference frame:

That reference frame of the vector space for which the second time derivative relative to this reference frame of a point mass is proportional to the net force applied to the point mass.

Sub-body:

A finite rigid structural member of the airframe.

Panel:

A linearly-varying member of the aircraft surface.

Element:

A member of a matrix or a differential member of a rigid sub-body.

ACRONYMS

ASE	Aeroservoelastic Modeling
MFA	Modeling Flexible Aircraft
f_{grav}	Forces Due to Gravitation Acceleration
T_{grav}	Gravitational Force Matrix
GAM	General Aerodynamic Matrix
t_{aero}	Aerodynamic Torque Equal to Sum of Rolling, Pitching and Yawing Moments.
F_{aero}	Aerodynamic Loads
C_{shuf}	Shuffle Matrix
SSMP	Simplified Structural Modeling Program
ASTROS	Automated Structures Optimization System
FEM	Finite Element Method
CDMS	Configuration Data Management System
CADS	Computer Aided Design System
MFAAP	Modeling Flexible Aircraft Program

SYMBOLS

UPPER CASE

A	Aircraft.
A	Flexible vehicle skew-symmetric stiffness matrix.
A	n-1 flexible vehicle apparent stiffness matrix.
A_S	Rigid sub-body of A.
A_V	Reduced variable total vehicle apparent stiffness matrix.
A_{VR}	Total vehicle apparent translational stiffness matrix.
A_{VT}	Total vehicle apparent rotational stiffness matrix.
A_{Vjk}	Partition of flexible vehicle mass matrix: $(j=\bar{u}, u_n; k=\bar{u}, u_n).$ $(j=\bar{\beta}, \beta_n; k=\bar{\beta}, \beta_n).$
A_{jk}	Partition of flexible vehicle apparent stiffness matrix: $(j=\bar{u}, u_n; k=\bar{u}, u_n).$ $(J=\bar{u}, u_n; k=\bar{\beta}, \beta_n).$ $(j=\bar{\beta}, \beta_n; k=\bar{u}, u_n).$ $(j=\bar{\beta}, \beta_n; k=\bar{\beta}, \beta_n).$
A'	Arbitrary skew-symmetric stiffness matrix.
A'_R	Skew-symmetric torque stiffness matrix.
A'_T	Skew-symmetric force stiffness matrix.
B	Rigid massless body.
C	Direction cosine matrix relating $\{a\}$ relative to $\{b\}$.
C_S	Direction cosine matrix relating $\{a_S\}$ relative to $\{a\}$.
C_{Sj}	Euler angle relating $\{a_S\}$ relative to $\{a\}$ ($j=1$ to 3).
CM	Vehicle mass center.
\underline{D}	Arbitrary dyadic.
D	Flexible vehicle symmetric damping matrix.
D	n-1 flexible vehicle damping matrix.
D_R	Internal torque damping matrix.
D_T	Internal force damping matrix.

SYMBOLS (Continued)

D_{jk}	Partition of flexible vehicle damping mass matrix: $(j=\bar{u}, u_n; k=\bar{u}, u_n).$ $(j=\bar{u}, u_n; k=\bar{\beta}, \beta_n).$ $(j=\bar{\beta}, \beta_n; k=\bar{u}, u_n).$ $(j=\bar{\beta}, \beta_n; k=\bar{\beta}, \beta_n).$
D'	Arbitrary symmetric damping matrix.
D'_R	Symmetric torque damping matrix.
D'_{RT}	Rotation on force damping matrix.
D'_T	Symmetric force damping matrix.
D'_{TR}	Translation on torque damping matrix.
\underline{E}	Unit dyadic.
E	Matrix of unit dyadic magnitudes.
$E(j)$	Unit matrix of dimension $j \times j$.
\underline{F}	External vehicle force.
F_B	Column matrix of stiffness forces on B.
\underline{F}_S	Force acting on A_S at P_S .
F_S	Column matrix of \underline{F}_S magnitudes.
G	Flexible vehicle skew-symmetric damping matrix.
G	$n-1$ flexible vehicle apparent damping matrix.
G_V	Reduced variable total vehicle apparent damping matrix.
G_{VR}	Total vehicle apparent rotational damping matrix.
G_{VT}	Total vehicle apparent translational damping matrix.
G_{Vjk}	Partition of flexible vehicle mass matrix: $(j=\bar{u}, u_n; k=\bar{u}, u_n).$ $(j=\bar{\beta}, \beta_n; k=\bar{\beta}, \beta_n).$
G_{jk}	Partition of flexible vehicle apparent damping matrix: $(j=\bar{u}, u_n; k=\bar{u}, u_n).$ $(j=\bar{u}, u_n; k=\bar{\beta}, \beta_n).$ $(j=\bar{\beta}, \beta_n; k=\bar{u}, u_n).$ $(j=\bar{\beta}, \beta_n; k=\bar{\beta}, \beta_n).$

SYMBOLS (Continued)

G'	Arbitrary skew-symmetric damping matrix.
G'_R	Skew-symmetric torque damping matrix.
G'_T	Skew-symmetric force damping matrix.
\underline{H}_S	Inertial angular momentum of A_S about P_S .
\underline{I}	Inertial dyadic of A.
I	Matrix of A inertia dyadic magnitudes.
I_{ij}	Element (i,j) of I (i,j=1 to 3).
\underline{I}_S	Inertial dyadic of A_S about P_S .
I_S	Matrix of A_S inertia dyadic magnitudes.
I_{Sij}	Element (i,j) of I_S (i,j=1 to 3, α, β).
K	Flexible vehicle symmetric stiffness matrix.
\bar{K}	n-1 flexible vehicle stiffness matrix.
K_A	Stiffness matrix of flexible aircraft.
K_{PBq}	Stiffness sub-matrix of forces on B due to q.
K_{PBu_S}	Stiffness sub-matrix of forces on B due to u_S (s=1 to n.B).
$K_{PB\beta_S}$	Stiffness sub-matrix of forces on B due to β_S (s=1 to n.B).
K_{LqQ}	Stiffness sub-matrix of loads on A_S due to q.
K_{LqUB}	Stiffness sub-matrix of loads on A_S due to u_B .
$K_{Lq\beta_B}$	Stiffness sub-matrix of loads on A_S due to β_B .
K_R	Internal torque stiffness matrix.
\bar{K}_T	Internal force stiffness matrix.
K_{TBq}	Stiffness sub-matrix of torques on B due to q.
K_{TBu_S}	Stiffness sub-matrix of torques on B due to u_S (s=1 to n.B).
$K_{TB\beta_S}$	Stiffness sub-matrix of torques on B due to β_S (s=1 to n.B).
K_{qBq}	q_B due to q via the vehicle stiffness.

SYMBOLS (Continued)

$K_{q_B \bar{q}}$	q_B due to \bar{q} via the vehicle stiffness.
$K_{q_B q_n}$	q_B due to q_n via the vehicle stiffness.
$K_{u_n \bar{u}}$	u_n due to \bar{u} via the vehicle stiffness.
$K_{u_n \bar{\beta}}$	u_n due to $\bar{\beta}$ via the vehicle stiffness.
$K_{\beta_n \bar{u}}$	β_n due to \bar{u} via the vehicle stiffness.
$K_{\beta_n \bar{\beta}}$	β_n due to $\bar{\beta}$ via the vehicle stiffness.
K_{jk}	Partition of flexible vehicle stiffness matrix: $(j=\bar{u}, u_n; k=\bar{u}, u_n)$. $(j=\bar{u}, u_n; k=\bar{\beta}, \beta_n)$. $(j=\bar{\beta}, \beta_n; k=\bar{u}, u_n)$. $(j=\bar{\beta}, \beta_n; k=\bar{\beta}, \beta_n)$.
K'	Arbitrary symmetric stiffness matrix.
K'_R	Symmetric torque stiffness matrix.
K'_{RT}	Rotation on force stiffness matrix.
K'_T	Arbitrary symmetric force stiffness matrix.
K'_{TR}	Translation on torque stiffness matrix.
L_A	Internal stiffness loads.
L	Flexible vehicle load matrix (column).
\bar{L}	$n-1$ flexible vehicle apparent load matrix.
L_q	Column matrix of sub-body stiffness loads.
\bar{L}_V	Total vehicle apparent load matrix.
L_{VR}	Total vehicle apparent torque matrix.
L_{VT}	Total vehicle apparent force matrix.
L_j	Partitioned column matrix apparent sub-body load ($j=\bar{u}, u_n, \bar{\beta}, \beta_n$).
L'	Arbitrary load matrix (column).
L'_R	Torsion matrix (column).
L'_T	Force matrix (column).

SYMBOLS (Continued)

M	Flexible vehicle mass matrix.
\bar{M}	n-1 flexible vehicle apparent mass matrix.
M_A	Total vehicle mass.
M_R	Sub-body inertial distribution matrix.
M_T	Sub-body mass distribution matrix.
\bar{M}_T	n-1 sub-body mass distribution matrix.
\bar{M}_V	Reduced variable total vehicle apparent mass matrix.
M_{VR}	Total vehicle apparent inertia matrix.
M_{VT}	Total vehicle apparent mass matrix.
M_{Vjk}	Partition of flexible vehicle mass matrix: $(j=\bar{u}, u_n; k=\bar{u}, u_n)$. $(j=\bar{\beta}, \beta_n; k=\bar{\beta}, \beta_n)$.
M_{jk}	Partition of flexible vehicle mass matrix: $(j=\bar{u}, u_n; k=\bar{u}, u_n)$. $(j=\bar{u}, u_n; k=\bar{\beta}, \beta_n)$. $(j=\bar{\beta}, \beta_n; k=\bar{u}, u_n)$. $(j=\bar{\beta}, \beta_n; k=\bar{\beta}, \beta_n)$.
M'	Arbitrary mass matrix.
M'_R	Torque mass matrix.
M'_T	Force mass matrix.
O	origin of B.
O'	Inertial origin.
P_S	Mass center of A_S .
\underline{P}_S	Inertial location of P_S .
Q	Point at which A is attached to B.
\underline{R}	Location of Q relative to O.
R	Column matrix of \underline{R} component magnitudes.
R_j	Element j of R (j=1 to 3).

SYMBOLS (Continued)

R'	Column matrix of R .
\bar{R}'	$n-1$ column matrix of R .
\underline{T}	External vehicle torque.
T_B	Column matrix of stiffness torques on B .
\underline{T}_S	Torque acting on A_S at P_S .
T_S	Column matrix of \underline{T}_S component magnitudes.
$\underline{V}, \underline{W}$	Arbitrary vectors.
V, W	Column matrix of $\underline{V}, \underline{W}$ Component magnitudes.
V_j, W_j	Element j of V, W ($j=1$ to 3).
\underline{X}	Inertial location of CM.
X	Column matrix of \underline{X} component magnitudes.
X_j	Element j of X ($j=1$ to 3).
X'	Column matrix of X .
\bar{X}'	$n-1$ column matrix of X .

LOWER CASE

\underline{a}	Rigid body acceleration.
$\{a\}$	Orthogonal unit vector base fixed to A (undeformed).
\underline{a}_j	Unit vector j component of $\{a\}$ ($j=1$ to 3).
$\{a_S\}$	Orthogonal unit vector base fixed to A_S .
\underline{a}_{Sj}	Element j component magnitude of $\{a_S\}$ ($j=1$ to $3, \alpha, \beta$).
$\{b\}$	Orthogonal unit vector base fixed to B .
\underline{b}_j	Unit vector j component of $\{b\}$ ($j=1$ to 3).
\underline{c}	Location of O relative to CM.
c	Column matrix of \underline{c} component magnitudes.
c_j	Element j of c ($j=1$ to 3).

SYMBOLS (Continued)

dm	Differential mass element of A.
$\{e\}$	Arbitrary unit vector base.
f	Column matrix of external force magnitudes.
\bar{f}	$n-1$ column matrix of external force magnitudes.
f_n	n^{th} column matrix of external force magnitudes.
f_1, f_2	Arbitrary reference frames.
$\{i\}$	Inertial orthogonal unit vectors.
\underline{i}_j	Unit vector j component of $\{i\}$ ($j=1$ to 3).
m_s	Total mass of A_s .
m_s	Mass matrix of A_s .
m_j	Diagonal element j of m_s .
n	Total number of A_s elements.
p	Location of dm relative to O .
p_j	Element j component magnitude of p ($j=1$ to 3).
q	Column matrix of scalar unknowns.
q	Column matrix of $6n-6$ independent unknowns.
q_n	Column matrix of 6 dependent unknowns.
q_A	Flexible vehicle deformations.
q'	Arbitrary column matrix of unknowns.
\underline{r}_s	Location of P_s relative to Q (undeformed).
r_s	Column matrix of \underline{r}_s component magnitudes.
r_{sj}	Element j of r_s ($j=1$ to 3).
r'	Column matrix of r_s .
\bar{r}'	$n-1$ column matrix of r_s .
t	Column matrix of external torque magnitudes.

SYMBOLS (Continued)

τ	n-1 column matrix of external torque magnitudes.
τ_n	n th column matrix of external torque magnitudes.
u_B	Column matrix of components of translational deformation of { <u>b</u> } relative to { <u>a</u> }.
u_n	Column matrix of dependent u_S .
\underline{u}_S	Translational deformation of A_S .
u_S	Column matrix of \underline{u}_S component magnitudes.
u_{Sj}	Element j of u_S (j=1 to 3).
u'	Column matrix of u_S .
\underline{v}	Rigid body velocity.

GREEK

β_B	Rotational deformation of { <u>b</u> } relative to { <u>a</u> }.
β_B	Column matrix of β_B component magnitudes.
β_{Bj}	Element j of β_B (j=1 to 3).
β_S	Column matrix of dependent β_S .
$\underline{\beta}_S$	Rotational deformation of A_S .
β_S	Column matrix of $\underline{\beta}_S$ component magnitudes.
β_{Sj}	Element j of β_S (j=1 to 3).
β'	Column matrix of β_S .
$\underline{\Gamma}$	Rotational deformation of { <u>i</u> } relative to { <u>b</u> }.
Γ	Column matrix of $\underline{\Gamma}$ component magnitudes.
Γ_j	Element j of Γ (j=1 to 3).
Γ^*	Column matrix components of { <u>i</u> } relative to { <u>b</u> }, initially.
θ	Direction cosine matrix of { <u>b</u> } relative to { <u>i</u> }.

SYMBOLS (Continued)

μ_S	Ratio of m_S to M_A .
$\underline{\rho}$	Location of dm relative to CM.
$\underline{\rho}_S$	Location of dm relative to P_S .
$\underline{\Omega}^a$	Angular velocity of A relative to B.
$\underline{\Omega}^a$	Column matrix of $\underline{\Omega}^a$ component magnitudes.
$\underline{\Omega}^{a'}$	Column matrix of $\underline{\Omega}^a$.
$\underline{\Omega}^S$	Angular velocity of A_S relative to A.
$\underline{\Omega}^S$	Column matrix of $\underline{\Omega}^S$ component magnitudes.
$\underline{\omega}$	Inertial angular velocity of B.
$\underline{\omega}$	Column matrix of $\underline{\omega}$ component magnitudes.
$\underline{\omega}_S$	Inertial angular velocity of A_S .
$\underline{\omega}'$	Column matrix of $\underline{\omega}$.
$\underline{\omega}'$	n-1 column matrix of $\underline{\omega}$.
$\underline{\omega}_{f2 f1}$	Angular velocity of f2 relative to f1.

OPERATORS

$c(*)$	Cosine(*).
$s(*)$	Sine(*).
$[\]^T$	Matrix transpose.
$[\]^{-1}$	Matrix inverse.
$[\]^2$	Square.
$[\]'$	Matrix expanded to j partitions of \otimes (j=n,n-1).
$[\]_R$	Identifies torque variable or coefficient.
$[\]_T$	Identifies force variable or coefficient.
$[\]_{jk}$	Matrix representing result on j due to input k.
$[\]_k$	Element summation index (k=1 to n).

SYMBOLS (Concluded)

$\{ \}_s$	Element index (s=1 to n)
$(\dot{ })$	First inertial time derivative.
$(\ddot{ })$	Second inertial time derivative.
$\tilde{[]}$	Skew-symmetric matrix of column elements.
$\bar{[]}$	Matrix associated with reduced variable.
$\{ \}$	Column matrix or extra parentheses.
$[]$	Square matrix or extra parentheses.
\times	Vector cross product.
\cdot	Vector inner product.
Σ	Summation.
\int	Integration.
$k_d \frac{d}{dt}$	First time derivative relative to k reference frame (k=i,b,,s,f1,f2).
$k_d^2 \frac{d^2}{dt^2}$	Second time derivative relative to k reference frame (k=i,b,a,s,f1,f2).
$[]^{\wedge n}$	Matrix constant multiplier.
$[]^{\Sigma_n}$	$n \times n$ matrix summation.
$[]^{\Pi_n}$	$n \times 1$ column summation.

APPENDIX A - SIGN CONVENTION AND DEFINITIONS

AERODYNAMIC SIGN CONVENTION

<u>ITEM</u>	<u>POSITIVE WHEN</u>
Lift, L	Up
Drag, D	Aft
Pitching Moment, M	Nose Up
Side Force, Y	Right
Yawing Moment, N	Nose Right
Rolling Moment, L	Right Wing Down
Angle of Attack, α_{FRL}	Nose Up From Relative Wind Velocity
Angle of Yaw, Ψ	Nose Right of Relative Wind Velocity
Angle of Sideslip, β	Nose Left of Relative Wind Velocity
Stabilizer Angle, δ_H	Trailing Edge Down
Elevator Angle, δ_e	Trailing Edge Down
Rudder Angle, δ_r	Trailing Edge to Left
Total Aileron Angle: $\delta_a = \delta_{a_{Left}} + \delta_{a_{Right}}$	Trailing Edge Down on Left Aileron
Spoiler Angle, δ_{sp}	Trailing Edge Down
C_{L_T}	Lift Coefficient, $\frac{Lift}{q_0 S_w}$: principally affects the phugoid mode, with both damping and the period are decreasing with an increase in C_L . In addition, because many of the lateral derivatives are functions of C_L , the lateral dynamics are affected. The main effect is a decrease in Dutch roll damping with an increase in C_L .

STABILITY DERIVATIVEMEANINGS $C_{L_{\delta H_M}}$ Lift Coefficient Measured in Wind Tunnel @ δH_M C_{D_T} Drag Coefficient, $\frac{\text{Drag}}{q_0 S_w}$; main contributor to the damping of the phugoid moment. C_m Pitching Moment Coefficient, Pitching Moment;

$q_0 \bar{c}_w S_w$

the aerodynamic pitching moment coefficient about the center of gravity required to balance the moment coefficient due to thrust, when the aircraft is in equilibrium flight. The major contributions are from a trim elevator deflection. It principally affects the longitudinal phugoid mode, where positive values will tend to decrease the period of oscillation.

 C_{m_0}

Pitching Moment Coefficient at Zero Lift

 C_l Rolling Moment Coefficient, Rolling Moment
 $q_0 b_w S_w$ C_n Yawing Moment Coefficient, Yawing Moment
 $q_0 b_w S_w$ C_y Sideforce Coefficient, Sideforce
 $q_0 S_w$ $C_{n_\beta} = \partial C_n / \partial \beta$

Directional Stability Derivative, 1/Deg.: the change in yawing moment coefficient with variation in sideslip angle. It is usually referred to as the static directional derivative, or the "weathercock" derivative. It is very important in determining lateral dynamic stability and control characteristics. A high value aids the pilot in executing coordinated turns, and prevents excessive sideslip and yawing moments in extreme flight maneuvers and in rough air. It primarily determines the natural frequency of the Dutch roll mode, and is also a factor in determining the spiral stability characteristics.

STABILITY DERIVATIVEMEANINGS

$$C_{y\beta} = \partial C_y / \partial \beta$$

Sideforce Derivative, 1/Deg.: the change in sideforce coefficient with changing sideslip angle. It can be referred to as the sideforce damping derivative. The major portion usually comes from the vertical tail. It is fairly important to lateral dynamics because it contributes to the damping of the Dutch roll mode. A large negative value would be desirable, however, a large value may create an undesirable lag effect in the airplanes response when an attempt is made to hold the wings level in rough air, or to perform aileron maneuvers.

$$C_{l\beta} = \partial C_l / \partial \beta$$

Dihedral Effect, 1/Deg.: the change in rolling moment coefficient with variation in sideslip angle, usually referred to as the "effective dihedral derivative." It is very important in lateral stability and control. To improve the Dutch roll damping characteristics, small negative values are desired, but to improve spiral stability, large negative values are desired. Since at least some "positive dihedral effect" is necessary for good maneuvering qualities, the design value must be a compromise between the static lateral requirements of "positive dihedral effect", and the dynamic lateral requirement of satisfying Dutch roll damping and spiral stability.

$$C_{n\delta_a} = \partial C_n / \partial \delta_a$$

Adverse Yaw Due to Aileron, 1/Deg.: the change in yawing moment coefficient with change in aileron deflection. It is quite important in determining the lateral control qualities of an airframe; for good response to aileron deflection, it should be zero or a very small positive value.

$$C_{l\delta_a} = \partial C_l / \partial \delta_a$$

Rolling Moment Due to Aileron, 1/Deg.: the change in rolling moment coefficient with change in aileron deflection, it is commonly referred to as aileron effectiveness or aileron power. In lateral dynamics, this is the most important of the control surface derivatives. The aileron effectiveness in conjunction with the damping in roll (C_{lp}) establishes the maximum available rate of roll, which is a very important consideration in fighter combat tactics at high speed. The aileron effectiveness is also very important at low-speed flight (take-offs and landings) where adequate lateral control is necessary to counteract asymmetric gusts which tend to roll the aircraft. Desirable values for a particular fighter can be obtained by the Navy and Air Force specification that the value of the wing tip helix angle during a rolling maneuver for full aileron deflection should be at least $pb/2U = .09$.

STABILITY DERIVATIVEMEANINGS

$$C_{y\delta_a} = \partial C_y / \partial \delta_a$$

Sideforce Due to Aileron, 1/Deg.: the change in sideforce coefficient with aileron deflection. For most conventional aircraft, the magnitude of this is zero; however, for certain aircraft (highly swept wings of low aspect ratio) a value may be obtained. The effect on lateral stability is of second order.

$$C_{n\delta_r} = \partial C_n / \partial \delta_r$$

Rudder Directional Control Parameter, 1/Deg.: the change in yawing moment coefficient with variation in rudder deflection, commonly known as rudder effectiveness, or rudder power. The design value for a jet-powered airframe is usually determined by considering such requirements as counteracting adverse yaw in rolling maneuvers, directional control in crosswind take-offs and landings, antisymmetric power, and spin recovery control. An additional factor which can be influential in determining a design value is introduced when an automatic pilot operates the rudder.

$$C_{l\delta_r} = \partial C_l / \partial \delta_r$$

Rolling Moment Due to Rudder, 1/Deg.: the change in rolling moment coefficient with variation in rudder deflection. In lateral control, its effects are of second order.

$$C_{y\delta_r} = \partial C_y / \partial \delta_r$$

Sideforce Due to Rudder, 1/Deg.: the change in sideforce coefficient with variation in rudder deflection. If the airframe alone is considered, the effect on lateral stability is of second order. However, when an autopilot is considered, it should not be neglected in the design analyses because its influence on the combined airframe plus autopilot may not be negligible.

$$C_{L\alpha}$$

Lift Due to Angle of Attack (α): the change in lift coefficient with varying angles of attack, commonly known as the "lift-curve slope." Important contributor to the damping of the longitudinal short period mode.

$$C_{L\delta_H} = \partial C_L / \partial \delta_H$$

Lift Control Due to Stabilizer, 1/Deg.

$$C_{L\delta_e} = \partial C_L / \partial \delta_e$$

Lift Control Due to Elevator, 1/Deg.: the change in the lift coefficient with changes in elevator deflection. On conventional aircraft, the horizontal tail is an appreciable distance from the center of gravity thus its effects are of second order. However, on tailless aircraft, it can be comparatively large and cannot be neglected.

STABILITY DERIVATIVEMEANINGS

$$C_{L\delta_{SP}} = \partial C_L / \partial \delta_{SP}$$

Lift Control Due to Spoiler, 1/Deg.

$$C_{m\alpha}$$

Pitching Moment Due to Angle of Attack (α): the change in pitching moment coefficient with varying angle of attack, commonly referred to as the longitudinal static stability derivative. The magnitude and sign are a function of the center of gravity. It is very important in longitudinal stability and control. If the center of gravity is ahead of the aerodynamic center the value of $C_{m\alpha}$ is negative, and the airframe is said to possess static longitudinal stability. Conversely, if the center of gravity is aft of the aerodynamic center, the $C_{m\alpha}$ value is positive, and the airframe is statically unstable. It is perhaps the most important derivative as far as longitudinal stability and control are concerned. It establishes the natural frequency of the short period mode.

$$C_{m\delta_H} = \partial C_m / \partial \delta_H$$

Pitching Moment Due to Stabilizer, 1/Deg.

$$C_{m\delta_e} = \partial C_m / \partial \delta_e$$

Pitching Moment Due to Elevator, 1/Deg.: the change in pitching moment coefficient with changes in elevator deflection, commonly known as the elevator effectiveness or elevator power. The design value is essentially determined by the anticipated fore and aft center of gravity travel of an airframe.

$$C_{m\delta_{SP}} = \partial C_m / \partial \delta_{SP}$$

Pitching Moment Due to Spoiler, 1/Deg.

$$C_{D_{cg}}$$

Trim Drag Correction for Center of Gravity Change from $.25\bar{c}_w$

$$C_{D\delta_{SP}} = \partial C_D / \partial \delta_{SP}$$

Drag Due to Spoiler

$$C_{L_q} = \partial C / \partial \left\{ \frac{qc}{2V} \right\}$$

Lift Due to Pitch Rate, 1/Rad.: the change in the lift coefficient, with no change in angle of attack of the airplane as a whole with varying pitch velocity. In longitudinal stability, it has a second order effect.

STABILITY DERIVATIVEMEANINGS

$$C_{m_q} = \partial C_m / \partial \left\{ \frac{q\bar{c}}{2V} \right\}$$

Moment Due to Pitch Rate, 1/Rad.: the change in pitching moment coefficient due to varying pitch velocity, commonly referred to as the pitch damping derivative. It is very important in longitudinal dynamics, because it contributes a major portion of the damping of the short period mode in conventional aircraft.

$$C_{L_{\dot{\alpha}}} = \partial C_L / \partial \left\{ \frac{\dot{\alpha}\bar{c}}{2V} \right\}$$

Lift Due to Plunge, 1/Rad.: the change in lift coefficient with variation in rate of change of the angle of attack. It is sometimes referred to as $C_{L\dot{\omega}}$ the change in lift coefficient with vertical acceleration. In longitudinal dynamics, it's effects are of second order.

$$C_{m_{\dot{\alpha}}} = \partial C_m / \partial \left\{ \frac{\dot{\alpha}\bar{c}}{2V} \right\}$$

Moment Due to Plunge, 1/Rad.: the change in pitching moment coefficient with variation in the rate of change of angle of attack. It is sometimes referred to as $C_{m\dot{\omega}}$, the change in pitching moment coefficient with change in vertical acceleration. It is quite important in longitudinal dynamics because it is involved in the damping of the short period mode. A negative value increases this mode, and consequently, high negative values of this derivative are desirable.

$$C_{n_p} = \partial C_n / \partial \left\{ \frac{p\bar{b}}{2V} \right\}$$

Yawing Moment Due to Roll Rate, 1/Rad.: the change in yawing moment coefficient with varying rolling velocity, arises from two main sources, the wing and the vertical tail. It is fairly important in lateral dynamics because of its influence on the Dutch roll mode.

$$C_{l_p} = \partial C_l / \partial \left\{ \frac{p\bar{b}}{2V} \right\}$$

Rolling Moment Due to Roll Rate, 1/Rad.: the change in rolling moment coefficient with change in rolling velocity, usually known as the roll damping derivative. It is quite important in lateral dynamics because it alone, essentially, determines the damping of roll characteristics of the aircraft. Normally, small values are more desirable than large ones because the airframe will respond better to a given aileron input, and will suffer fewer flight perturbations due to gust inputs.

STABILITY DERIVATIVEMEANINGS

$$C_{y_p} = \partial C_y / \partial \left\{ \frac{pb}{2V} \right\}$$

Sideforce Due to Roll Rate, 1/Rad.: the change in sideforce coefficient with variation in rolling velocity. In lateral dynamics, its effect is of second order, therefore, it is common practice to neglect this derivative in lateral calculations.

$$C_{n_r} = \partial C_n / \partial \left\{ \frac{rb}{2V} \right\}$$

Yawing Moment Due to Yawing Rate, 1/Rad.: the change in yawing moment coefficient with change in yawing velocity, also known as the yaw damping derivative. The main contribution is made by the vertical tail (80-90%). It is very important in lateral dynamics because it is the main contributor to the damping of the Dutch roll oscillatory mode (large negative values are desirable).

$$C_{l_r} = \partial C_l / \partial \left\{ \frac{rb}{2V} \right\}$$

Rolling Moment Due to Yawing Rate, 1/Rad.: the change in rolling moment coefficient with change in yawing velocity. In lateral dynamics, its effects are of second order, since it has only a slight effect on the Dutch roll damping characteristics. In the spiral mode, however, it is desirable that the value be small and positive. It is not usually considered a preliminary design parameter.

$$C_{y_r} = \partial C_y / \partial \left\{ \frac{rb}{2V} \right\}$$

Sideforce Due to Yawing Rate, 1/Rad.: the change in sideforce coefficient with variation in yawing velocity. In lateral dynamics, its effect is of second order and, therefore, it is common practice to neglect this derivative in lateral calculations.

$$C_{n_{\dot{\beta}}} = \partial C_n / \partial \left\{ \frac{\dot{\beta}b}{2V} \right\}$$

Yawing Moment Due to Rate of Change of Sideslip Angle. the change in yawing moment coefficient with variations in rate of change of the sideslip angle. Its effect on lateral dynamics is mainly in the Dutch roll mode; to increase damping, positive values are desirable.

$$C_{y_{\dot{\beta}}} = \partial C_y / \partial \left\{ \frac{\dot{\beta}b}{2V} \right\}$$

Sideforce Due to Rate of Change of Sideslip Angle

APPENDIX B
DEFINITION OF AXES SYSTEMS

B.1 STABILITY COORDINATES

The equations of motion commonly used for analysis of transient maneuvers involving all six degrees of freedom of the rigid airplane employ four different axes systems; these axes systems are designated ground axes, body axes, stability axes and wind axes. The definition of these axes and their functions are as follows:

- Ground Axes - Ground axes are a set of orthogonal axes fixed with respect to the ground. The z axis is coincident with the weight vector. The x and y axes are arbitrary but the equations are simplified if either the x and y axis is chosen to coincide with the horizontal component of the wind relative to the ground. Ground axes are required to define components of weight and ground winds in the other axes systems.
- Body Axes - Body axes are a set of orthogonal axes through the airplane c.g. which remain fixed relative to the body. The y axis is chosen normal to the plane of symmetry (for most airplanes there is a plane of symmetry and this plane is designated the xz plane). The x axis is usually the horizontal reference axis. The moment equations are in the body axes system because inertia properties remain fixed with respect to these axes.
- Stability Axes - Stability axes are a set of orthogonal axes through the airplane c.g., the y axis of which is coincident with the body y axis. The x axis is coincident with the velocity component in the xz plane. The velocity is defined as the velocity of the airplane relative to the air surrounding it. Aerodynamic forces and moments are usually defined in the stability axes system.
- Wind Axes - Wind axes are a set of orthogonal axes through the airplane c.g., the z axis of which is coincident with the z-axis of the stability axis system. The x axis is coincident with the resultant airplane velocity vector. Again, the velocity is the airplane velocity relative to the air. The force equations are simplest when written in the wind axes system.

The relationships between ground, body, stability, and wind axes, are shown in Figure 1-2.

APPENDIX C
AERODYNAMIC EQUATIONS

This section presents the aerodynamic equations in the three degree-of-freedom longitudinal maneuver.

The equations presented for lift, pitching and moment and drag include rigid airplane component contributions and the corresponding flexibility correction factors.

The equations are developed in the stability axis system. Provisions are included for transferring the forces and moments to the airplane center of gravity.

C.1 AIRPLANE RIGID ANGLE OF ATTACK

The solution of the equation of motion provide a value for a flexible airplane angle of attack, α_f , at every discrete time t . Before α_f can be used to determine rigid airplane aerodynamics coefficients, it must be converted to a rigid value. This is accomplished by subtracting a theoretical flexible increment at the zero lift angle.

The aerodynamic coefficients were measured on a wind tunnel model built to a mid-cruise shape. Theoretical airplane flexibility correction factors were calculated based on a jig wing shape. Therefore, an additional increment must be subtracted to account for the above shape difference. Thus the rigid airplane angle of attack is defined as follows:

$$\Delta\alpha_R = \alpha_f - (\Delta\alpha)_F - (\Delta\alpha)_{jig} \quad (1)$$

C.2 AIRPLANE LIFT CHARACTERISTICS

The total flexible airplane lift equation related to the stability axis system may be expressed as follows,

$$LIFT = \bar{q}S C_{L_T} \quad (2)$$

where the total lift coefficient is,

$$C_{L_T} = (C_L)_\alpha + (C_L)_{\delta_H} + (C_L)_{\delta_e} + (C_L)_q + (C_L)_{\dot{\alpha}} + (\Delta C_L)_{\delta_{SP}} + (C_L)_{\dot{q}} + (C_L)_{n_z} \quad (3)$$

The individual flexible components are defined as follows:

Lift coefficient due to angle of attack at $\delta_H = \delta_e = 0^\circ$

$$(C_L)_\alpha = \left[\left(C_{L_{\alpha_{HM}}} \right)_R - \left(C_{L_{\delta_H}} \right)_R * \delta_{HM} \right] * \left(C_{L_{\alpha_F}} / C_{L_{\alpha_R}} \right) \quad (4)$$

where

$$\left(C_{L_{\delta_H}} \right)_R = \left(\frac{\bar{c}}{t} \right) * \left(C_{M_{\delta_H}} \right)_R$$

Lift coefficient due to horizontal stabilizer deflection

$$\left(C_L \right)_{\delta_H} = \left(\frac{\bar{c}}{t} \right) \left(C_{M_{\delta_H}} \right)_R * \left(C_{L_{\delta_H_F}} / C_{L_{\delta_H_R}} \right) * \delta_H \quad (5)$$

Lift coefficient due to elevator deflection

$$\left(C_L \right)_{\delta_e} = \frac{\bar{c}}{t} \left(C_{M_{\delta_e}} \right)_R * \left(C_{L_{\delta_e_F}} / C_{L_{\delta_e_R}} \right) * \delta_e \quad (6)$$

Lift coefficient due to pitching velocity

$$\left(C_L \right)_q = \left(C_{L_q} \right)_R * \left(C_{L_{q_F}} / C_{L_{q_R}} \right) * \left(\frac{\bar{c}}{2v} \right) * q \quad (7)$$

Lift due to plunging velocity

$$\left(C_L \right)_{\dot{\alpha}} = \left(C_L \right)_{\dot{\alpha}_R} * \left(C_{L_{\dot{\alpha}_F}} / C_{L_{\dot{\alpha}_R}} \right) * \left(\frac{\bar{c}}{2v} \right) * \dot{\alpha} \quad (8)$$

Lift due to spoiler deflection

$$\left(\Delta C_L \right)_{\delta_{SP}} = \sum_{i=1}^n \left[\left(\Delta C_L \right)_{\delta_{SP}_R} * \left(C_{L_{\delta_{SP}_F}} / C_{L_{\delta_{SP}_R}} \right) * \delta_{SP} \right]_i \quad (9)$$

where n = number of spoilers

Lift due to angular acceleration

$$\left(C_L \right)_{\dot{q}} = \left(C_L \right)_{\dot{q}} * \dot{q} \quad (10)$$

Lift due to normal load factor

$$\left(C_L \right)_{n_z} = - \left(C_L \right)_{n_z} * n_{z_a} \quad (11)$$

If Equations (3) through (11) are substituted into Equation (2), and the terms rearranged, the lift may be expressed as follows:

$$\text{LIFT} = \bar{q}S \left[C_{L_1} + (\bar{c}/2v) * C_{L_2} \dot{\alpha} + C_{L_3} \dot{q} - C_{L_4} * n_{z_a} \right] \quad (12)$$

where

$$\begin{aligned}
 C_{L1} = & \left(C_{L\theta_{\delta_{H_M}}} \right)_R * \left(C_{L_{\alpha_F}} / C_{L_{\alpha_R}} \right) + \left(C_{L_{q_R}} \right) * \left(C_{L_{q_F}} / C_{L_{q_R}} \right) * \left(\frac{\bar{c}}{2v} \right) * q \\
 & + \left(\frac{\bar{c}}{t} \right) \left(C_{M_{\delta_H}} \right)_R \left[\left(C_{L_{\delta_{H_F}}} / C_{L_{\delta_{H_R}}} \right) * \delta_H - \left(C_{L_{\alpha_F}} / C_{L_{\alpha_R}} \right) * \delta_{H_M} \right] \\
 & + \left(\frac{\bar{c}}{t} \right) \left(C_{M_{\delta_e}} \right)_R * \left(C_{L_{\delta_{e_F}}} / C_{L_{\delta_{e_R}}} \right) * \delta_e \\
 & + \sum_{i=1}^n \left[\left(\Delta C_{L_{\delta_{SP}}} \right)_R * \left(C_{L_{\delta_{SP_F}}} / C_{L_{\delta_{SP_R}}} \right) * \delta_{SP} \right]_i \\
 \\
 C_{L2} = & \left(C_{L_{\dot{\alpha}}} \right)_R * \left(C_{L_{\dot{\alpha}_F}} / C_{L_{\dot{\alpha}_R}} \right) \\
 \\
 C_{L3} = & C_{L_{\dot{q}}} \\
 \\
 C_{L4} = & C_{L_{n_z}}
 \end{aligned}$$

Equation (12) is used in the solution of the equations of motion as F_k . Since the sign convention for the equations of motion defines F_k as positive downward, the final expression for the lift is:

$$F_k = - \text{LIFT} \quad (13)$$

C.4 AIRPLANE DRAG CHARACTERISTICS

The total airplane drag equation related to the stability axis system may be expressed as follows:

$$\text{DRAG} = \bar{q} S C_{D_T} \quad (14)$$

where the total drag coefficient is

$$C_{D_T} = (C_D)_\alpha + (\Delta C_D)_{cg} + (\Delta C_D)_{\delta_{SP}} + (\Delta C_D)_h \quad (15)$$

The individual components are defined as follows:

Trim drag due to basic lift

$$(C_D)_\alpha = C_D @ C_{L_{BASIC}} \quad (16)$$

where

$$C_{L_{BASIC}} = (C_L)_\alpha + (C_L)_{\delta_H} + (C_L)_{\delta_e} \quad (17)$$

Drag due to spoiler deflection

$$\left(\Delta C_D \right)_{\delta_{SP}} = \sum_{i=1}^n \left(C_{D_{\delta_{SP}}} \right)_i * \left(\delta_{SP_i} \right) \quad (18)$$

when n = number of spoilers

Reynold number correction for profile drag.

$$(\Delta C_D)_h = (30,000 - h) (4.5) \times 10^{-8} \quad (19)$$

and $(\Delta C_D)_{cg}$ = trim drag correction for center of gravity shift from $\bar{c}/4$

Equation (14) is used in the solution of the equations of motion as F_i . Since the sign convention for the stability axis defines F_i as positive forward, the final expression for drag is:

$$F_i = - \text{DRAG} \quad (20)$$

C.3.1 Airplane Pitching Moment Characteristics

The rigid pitching moment data are referred to the $c_w/4$ and $WL = 200$ in the stability axis system. The total flexible airplane pitching moment equation about any center of gravity may be expressed as follows:

$$M_{CG} = \bar{q}S\bar{c}C_{M_{c/4}} + \bar{q}S \left(C_{L_T} \cos \alpha_F + C_{D_T} \sin \alpha_F \right) \left(X_{cg} - X_{REF} \right) + \bar{q}S \left(C_{L_T} \sin \delta_F - C_{D_T} \cos \delta_F \right) \left(WL_{cg} - WL_{REF} \right) \quad (21)$$

where the pitching moment coefficient at $\bar{c}/4$ is,

$$C_{M_{CG}} = (C_M)_\alpha + (C_M)_{\delta_H} + (C_M)_{\delta_e} + (C_M)_q + (C_M)\dot{\alpha} + (\Delta C_M)_{\delta_{SP}} + (C_M)\dot{q} + (C_M)n_z \quad (22)$$

The individual flexible components are defined as follows:

Pitching moment due to angle of attack at $\delta_H = \delta_e = 0$

$$(C_M)_\alpha = \left[\left(C_{M_{\delta_{H_M}}} \right)_R - \left(C_{M_{\delta_H}} \right)_R * \delta_{H_M} \right] + \Delta (C_M/C_L)_F * (C_L)_\alpha + (\Delta C_{M_0})_F + (\Delta C_{M_0})_{JIG} \quad (23)$$

Pitching moment due to horizontal stabilizer

$$(C_M)_{\delta_H} = \left(C_{M_{\delta_H}} \right)_R * \left(C_{M_{\delta_{H_F}}} / C_{M_{\delta_{H_R}}} \right) * \delta_H \quad (24)$$

Pitching moment due to elevator deflection

$$(C_M)_{\delta_e} = \left(C_{M_{\delta_e}} \right)_R * \left(C_{M_{\delta_{e_F}}} / C_{M_{\delta_{e_R}}} \right) * \delta_e \quad (25)$$

Pitching moment due to pitching velocity

$$(C_M)_q = (C_{M_q})_R * (C_{M_{q_F}} / C_{M_{q_R}}) * \left(\frac{\bar{c}}{2v}\right) * q \quad (26)$$

Pitching moment due to plunging velocity

$$(C_M)_{\dot{\alpha}} = (C_{M_{\dot{\alpha}}})_R * (C_{M_{\dot{\alpha}_F}} / C_{M_{\dot{\alpha}_R}}) * \left(\frac{\bar{c}}{2v}\right) * \dot{\alpha} \quad (27)$$

Pitching moment due to spoiler deflection

$$(\Delta C_{M_{\delta_{SP}}}) = \sum_{i=1}^n \left[\left(\Delta C_{M_{\delta_{SP}}} \right)_R - \left(C_{M_{\delta_{SP}_F}} / C_{M_{\delta_{SP}_R}} \right) * \delta_{SP} \right]_i \quad (28)$$

where n = number of spoilers

Pitching moment due to angular acceleration

$$(C_M)_{\dot{q}} = (C_{M_{\dot{q}}}) * \dot{q} \quad (29)$$

Pitching moment due to normal airplane load factor

$$(C_M)_{n_z} = - (C_{M_{n_z}}) * n_{z_a} \quad (30)$$

If Equations (22) through (30) are substituted into Equation (21), and terms rearranged, the pitching moment may be expressed as follows:

$$M_{CG} = \bar{q} S \bar{c} \left[C_{M_1} + \left(\frac{\bar{c}}{2v}\right) * C_{M_2} * \dot{\alpha} + C_{M_3} * \dot{q} - C_{M_4} * n_{z_a} \right] - F_K * \bar{c} * (XZCG1) - F_i * \bar{c} * (CXCG2) \quad (31)$$

where

$$\begin{aligned}
 C_{M_1} = & \left(C_{M_{e\delta_{H_M}}} \right)_R + \left(\Delta C_M / C_L \right)_F * (C_L)_\alpha + \left(\Delta C_{M_0} \right)_F + \left(\Delta C_{M_0} \right)_{jig} \\
 & + \left(C_{M_{\delta_H}} \right)_R \left[\left(C_{M_{\delta_{H_F}}} / C_{M_{\delta_{H_R}}} \right) * \delta_H - \delta_{H_M} \right] \\
 & + \left(C_{M_{\delta_e}} \right)_R * \left(C_{M_{\delta_{e_F}}} / C_{M_{\delta_{e_R}}} \right) * \delta_e + \left(C_{M_q} \right)_R * \left(\frac{C_{M_{q_F}}}{C_{M_{q_2}}} \right) * \left(\frac{c}{2v} \right) + q \\
 & + \sum_{i=1}^n \left[\left(\Delta C_{M_{\delta_{SP}}} \right)_R * \left(C_{M_{\delta_{SP_F}}} / C_{M_{\delta_{SP_R}}} \right) * \delta_{SP} \right]_i
 \end{aligned}$$

$$C_{M_2} = \left(C_{M_\alpha} \right)_R * \left(C_{M_{\alpha_F}} / C_{M_{\alpha_R}} \right)$$

$$C_{M_3} = C_{M_q}$$

$$C_{M_4} = C_{M_{n_z}}$$

$$XZCG1 = \left[\cos \alpha (X_{cg} - X_{REF}) + \sin \alpha (WL_{cg} - WL_{REF}) \right] / \bar{c}$$

$$XZCG2 = \left[\sin \alpha (X_{cg} - X_{REF}) - \cos \alpha (WL_{cg} - WL_{REF}) \right] / \bar{c}$$

$$F_K = - \bar{q} S C_{L_T}$$

$$F_i = - \bar{q} S C_{D_T}$$

APPENDIX D

FIXED LONGITUDINAL FLEXIBLE STABILITY DERIVATIVE PROGRAM P-107

This program generates rigid stability derivatives, flexible stability derivatives, flexible/rigid ratios, incremental flexible stability derivatives and flexible inertia derivatives for a fixed airplane, airplane less tail and tail only configuration.

The stability derivatives generated by this program consist of two distinct sets. One set, referred to as fixed stability derivatives, reflects the effects due to the application of airload distributions only. The second set, referred to as fixed inertia derivatives, reflects the effects due to the application of unit inertia distributions only.

Rigid and flexible derivatives are calculated for up to five altitudes per Mach number for up to five Machs. Appropriate flexible/rigid ratios, flexible increments and inertia derivatives are inserted into output matrices compatible with the automatic plotting routine of Program P-115.

The following sections present a description of the above procedures.

D.1 FIXED STABILITY DERIVATIVES DUE TO AIRLOAD ONLY

The rigid and flexible fixed stability derivatives are a function of theoretical airload distributions only, and may be generated for up to nine separate angle distributions, as listed below:

<u>Unit Angle Distributions</u>	<u>Input Symbol</u>
1) Unit angle of attack for the complete airplane	FORMED INTERNALLY
2) Angles of attack due to a unit pitching velocity	$\dot{\theta}_z$
3) Reference airplane camber and twist angles of attack	$^{\circ}C\&T$

- | | |
|---|------------|
| 4) Unit angles of attack for the tail plane only | α_T |
| 5) Unit deflection angles for the horizontal stabilizer | δ_H |
| 6 Unit deflection angles for the elevator | δ_e |
| 7, 8 & 9) Arbitrary unit angle distributions for user
specified component; $i = 1,2,3$ | α_i |

The input order of θ_z , $\alpha_{C\&T}$ and α_T must be as listed above at all times. If this order is not followed, all output parameters for α_o , C_{m0} , ϵ_o , $d\epsilon/d\alpha$ and α will be incorrect.

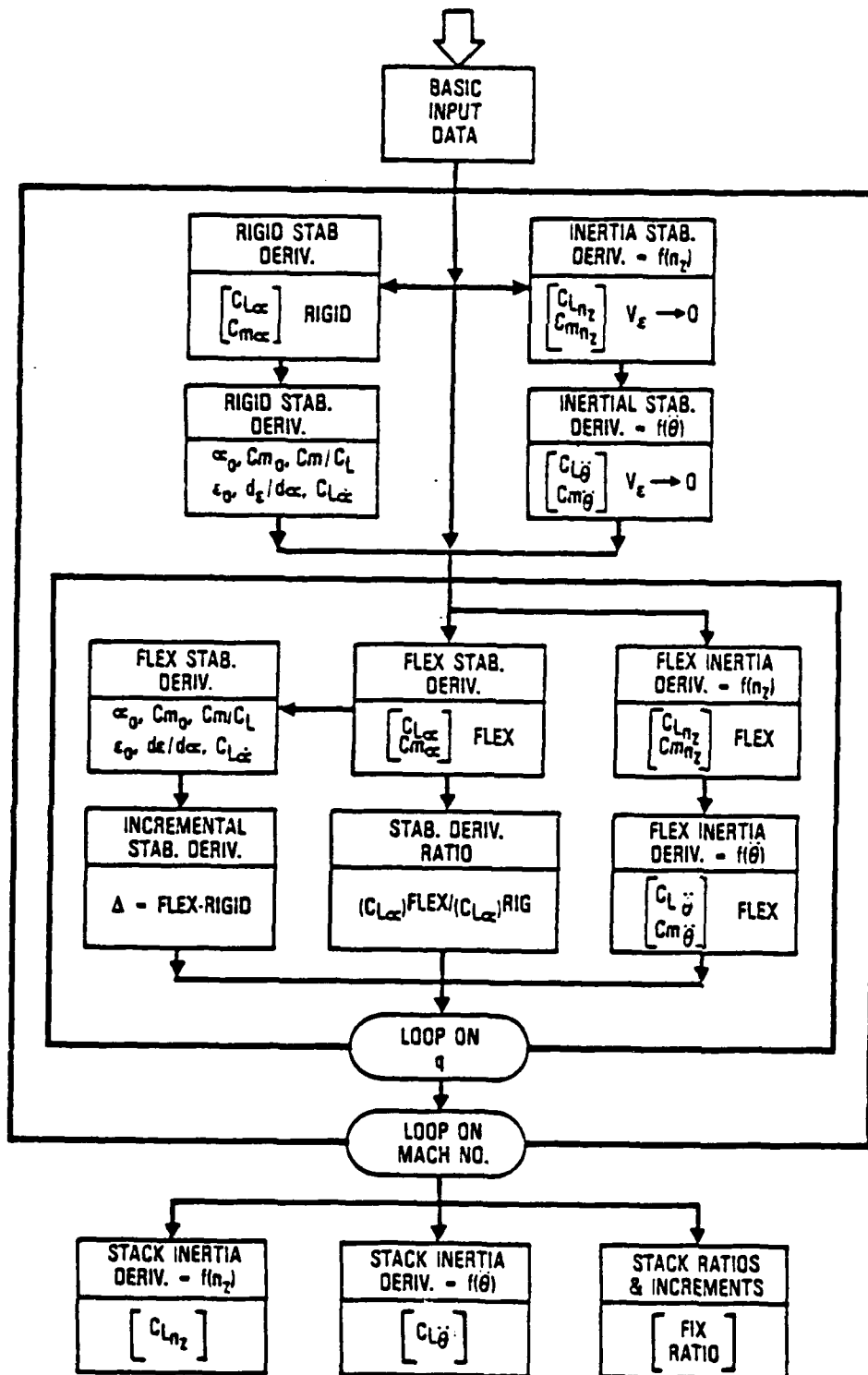


Figure D.1. Fixed Longitudinal Stability Derivative Program


```

      CMOAP := TMP6 - TMP5 * TMP4;
      CMCLAP := TMP4;
S
      CALL MXELOP ( [A],3,3,[A],1,3,4,TMP7);
S
      AOAT := -TMP7;
S
      CALL MXELOP ( [A],1,4,[A],1,3,4,TMP8);
      CALL EXREAL ( , [A],3,3,TMP9);
      CALL EXREAL ( , [A],3,4,TMPA);
S
      CMOAT := TMPA - TMP9 * TMP8;
S
      CALL MXELOP ( [A],1,4,[A],1,3,4,CMCLAT);
S
      PRINT ( "(1X,'*** *** *** *** *** *** *** *** ***')");
      PRINT ( "(1X,'EPS-0',10X,'DEPS/DALP',10X,'CLAC',10X,'CMAC')");
      PRINT ( "(1X, 4F13.6),'EO,DTDA,CLAD,CMAD);
      PRINT ( "(1X,'ALPHA-0 A/P',4X,'CM-0 A/P',10X,'CM/CL A/P')");
      PRINT ( "(1X, 3F13.6),'AOAP,CMOAP,CMCLAP);
      PRINT ( "(1X,'ALPHA-0 A-T',3X,'CM-0 A-T',10X,'CM/CL A-T')");
      PRINT ( "(1X, 3F13.6),'AOAT,CMOAT,CMCLAT);
S
      IF INT = 0 THEN
S
          DEO1 := EO;
          DEA1 := DTDA;
          DAO1 := AOAP;
          DCA1 := CMOAP;
          DMA1 := CMCLAP;
          DAT1 := AOAT;
          DCT1 := CMOAT;
          DMT1 := CMCLAT;
          RCD1 := CLAD;
          RCM1 := CMAD;
S
          CALL MXONE ( , [DXT], 1, 6, 2 );
          CALL MXONE ( , [DYT], 1, 6, 2 );
          CALL MXONE ( , [DZT], 1, 6, 2 );
          CALL PKREAL ( [DZT], 1, 1, MQ );
          ENDIF;
S
      IF INT = 1 THEN
          DEO := EO - DEO1;
          DEA := DTDA - DEA1;
          DAO := AOAP - DAO1;
          DCA := CMOAP - DCA1;
          DMA := CMCLAP - DMA1;
          DAT := AOAT - DAT1;
          DCT := CMOAT - DCT1;
          DMT := CMCLAT - DMT1;
          RCD := CLAD / RCD1;
          RCM := CMAD / RCM1;
S
          CALL PKREAL ( [DXT], 1, 5, DEO );
          CALL PKREAL ( [DXT], 1, 6, DEA );
          CALL PKREAL ( [DXT], 1, 1, DAO );
          CALL PKREAL ( [DXT], 1, 2, DCA );
          CALL PKREAL ( [DYT], 1, 2, DMA );
          CALL PKREAL ( [DXT], 1, 3, DAT );
          CALL PKREAL ( [DXT], 1, 4, DCT );
          CALL PKREAL ( [DYT], 1, 4, DMT );
          CALL PKREAL ( [DYT], 1, 5, RCD );
          CALL PKREAL ( [DYT], 1, 6, RCM );
          CALL PKREAL ( [DZT], 1, 2, MQ );
S

```



```

NQ := 5;           $ NUMBER OF Q'S FOR EACH MACH      $
KNT := 1;         $ INITIALIZE COUNTER OF TOTAL LOOPS $
ITST := 0;        $ INTEGER TEST IF Q = 0            $
NTST := 1.;       $ REAL TEST IF Q = 0              $
$                                                         $
C1 := 3456.0;     $ C1 = S (FTxFT)                  $
C2 := 1014336.0; $ C2 = S x CBAR (FTxFTxIN)         $
$                                                         $
$ Initialize Matrices:                                     $
$                                                         $
CALL IFP( GSIZE );                                       $
$                                                         $
$ *** MACH LOOP ***                                       $
$                                                         $
FOR IMACH = 1 TO NMCH DO                                  $
$                                                         $
. CALL EXREAL ( , [MCH], 1, IMACH, MACH );              $
  [QLDS100] := [Q(IMACH)];                               $
$                                                         $
PRINT ( "(IX,'*** *** *** *** *** *** *** *** *** ***')");
PRINT ( "(IX,'*** MACH CASE #',I4),'IMACH)");
PRINT ( "(IX,'*** MACH = ',F6.3),'MACH)");
$                                                         $
$ Matrix Calculations:                                     $
$                                                         $
[OSIC] := [DZ114] * [QLDS100];                          $
$                                                         $
$ Stack of Alpha Matrices:                               $
$                                                         $
CALL MXONE ( , [ON1], 1, 152, 2 );
CALL COLMERGE( [AT1], [ON1], [THZ], [CP1] );
CALL COLMERGE( [AT2], [AT1], [ACT110], [CP2] );
CALL COLMERGE( [AT3], [AT2], [AD1115], [CP3] );
CALL COLMERGE( [AT4], [AT3], [AD2116], [CP4] );
CALL COLMERGE( [AT5], [AT4], [AD3117], [CP5] );
CALL COLMERGE( [AT6], [AT5], [AD4118], [CP6] );
CALL COLMERGE( [AT7], [AT6], [A5], [CP7] );
CALL COLMERGE( [ADST],[AT7], [A6], [CP8] );
$                                                         $
IFLG := 0;           $ FLAG = 0 FOR RIGID DERIVATIVES $
[PZRG] := [OSIC] * [ADST];
[CLRG] := [CLCM] * [PZRG];
CALL FLEX ( [CLRG], [DCX], [DCY], [DCZ], MACH, IFLG );
$                                                         $
$ Stack of Weight Matrices:                             $
$                                                         $
CALL COLMERGE( [VT1], [V1], [W1101], [CP1] );
CALL COLMERGE( [VT2], [VT1], [W2102], [CP2] );
CALL COLMERGE( [VT3], [VT2], [W4], [CP3] );
CALL COLMERGE( [VT4], [VT3], [W5], [CP4] );
CALL COLMERGE( [VT5], [VT4], [W3103], [CP5] );
CALL COLMERGE( [VT6], [VT5], [W7], [CP6] );
CALL COLMERGE( [VT7], [VT6], [W8], [CP7] );
CALL COLMERGE( [VT8], [VT7], [W9], [CP8] );
CALL COLMERGE( [VT9], [VT8], [W10], [CP9] );
CALL COLMERGE( [VT10], [VT9], [W11], [CP10] );
CALL COLMERGE( [VT11], [VT10], [W12], [CP11] );
CALL COLMERGE( [VT12], [VT11], [W13], [CP12] );
CALL COLMERGE( [VT13], [VT12], [W14], [CP13] );
CALL COLMERGE( [VN], [VT13], [W15], [CP14] );
$                                                         $
$ Stack of PzTheta Matrices:                             $
$                                                         $
CALL COLMERGE( [PT1], [P1], [PZTH1104], [CP1] );
CALL COLMERGE( [PT2], [PT1], [PZTH2105], [CP2] );

```

```

CALL COLMERGE( [PT3], [PT2], [P4], [CP3] );
CALL COLMERGE( [PT4], [PT3], [P5], [CP4] );
CALL COLMERGE( [PT5], [PT4], [PZTH3106], [CP5] );
CALL COLMERGE( [PT6], [PT5], [P7], [CP6] );
CALL COLMERGE( [PT7], [PT6], [P8], [CP7] );
CALL COLMERGE( [PT8], [PT7], [P9], [CP8] );
CALL COLMERGE( [PT9], [PT8], [P10], [CP9] );
CALL COLMERGE( [PT10], [PT9], [P11], [CP10] );
CALL COLMERGE( [PT11], [PT10], [P12], [CP11] );
CALL COLMERGE( [PT12], [PT11], [P13], [CP12] );
CALL COLMERGE( [PT13], [PT12], [P14], [CP13] );
CALL COLMERGE( [PN], [PT13], [P15], [CP14] );
S
[WSIC] := [DZ114] * [VN];
[PSIC] := [DZ114] * [PN];
S
[SUMW] := (C1) [CLCM] * [WSIC];
[SIYY] := (C2) [CLCM] * [PSIC];
[QDE] := [QSIC] * [DTH108] * [E107];
S
[CLNR(KNT)] := [CLCM] * [QDE] * [WSIC];
[CLNT(KNT)] := [CLCM] * [QDE] * [PSIC];
S
CALL MXIDENT ( , [I], 156, 2 );
S
S *** Q LOOP ***
S
FOR IQ = 1 TO NQ DO
S
CALL EXREAL ( , [QREAL], IMACH, IQ, QS1 );
CALL RLCNPR ( QS1, NTST, 6, IRES );
S
IF IRES > ITST THEN
QI1 := 1./QS1;
ELSE
QI1 := 100000.;
PRINT ( "(IX,'*** Q OUT OF BOUNDS ***',FB.3),'QS1);
PRINT ( "(IX,'*** INVERSE OF Q ***',F12.3),'QI1);
ENDIF;
S
PRINT ( "(IX,'*** *** *** *** *** *** *** *** *** ***')");
PRINT ( "(IX,'*** Q CASE #',I4,'IQ);
PRINT ( "(IX,'*** Q = ',FB.3),'QS1);
PRINT ( "(IX,'*** INV Q = ',F12.3),'QI1);
S
[D] := [I] - [(QS1) [QDE]];
S
[DINV] := INV( [D] );
S
[CLF] := [CLCM] * [DINV];
S
[CLI] := (QI1) [(CLF) - [CLCM]];
S
[CLNZ(KNT)] := [CLI] * [WSIC];
[CLTB(KNT)] := [CLI] * [PSIC];
S
[CLNF] := [CLF] * [PZRG];
S
IFLG := 1; S FLAG = 1 FOR FLEXIBLE DERIVATIVES
CALL FLEX ( [CLNF], [DCX], [DCY], [DCZ], QS1, IFLG );
CALL MXDVD ( , [CLNF], [CLRG], [RTIO(KNT)] );
S
CALL COLMERGE( [RTMP1], [RTIO(KNT)], [DCX], [CP9] );
CALL COLMERGE( [RTMP2], [RTMP1], [DCY], [CP10] );
CALL COLMERGE( [RATIO(KNT)], [RTMP2], [DCZ], [CP11] );
S

```

```

S   Print Matrices:
S
CALL UTMPT( , [CLRG], [CLNR(KNT)], [CLNT(KNT)] );
CALL UTMPT( , [CLNF], [CLNZ(KNT)], [CLTH(KNT)] );
CALL UTMPT( , [RATIO(KNT)] );
S
KNT := KNT + 1;
S
ENDDO;
ENDDO;
S
END;
BEGIN BULK
S
S Direct Matrix Input:
S
DMI, CP1, RSP, REC, 2, 1, ..., -DMI
+DMI, 1, 1, 0.0, 1.0
DMI, CP2, RSP, REC, 3, 1, ..., -DMI
+DMI, 1, 1, 0., 0., 1.
DMI, CP3, RSP, REC, 4, 1, ..., -DMI
+DMI, 1, 1, 0., 0., 0., 1.
DMI, CP4, RSP, REC, 5, 1, ..., -DMI
+DMI, 1, 1, 0., 0., 0., 0., 1.
+DMI, 1, 5, 1.
DMI, CP5, RSP, REC, 6, 1, ..., -DMI
+DMI, 1, 1, 0., 0., 0., 0., 1.
+DMI, 1, 5, 0., 1.
DMI, CP6, RSP, REC, 7, 1, ..., -DMI
+DMI, 1, 1, 0., 0., 0., 0., 1.
+DMI, 1, 5, 0., 0., 1.
DMI, CP7, RSP, REC, 8, 1, ..., -DMI
+DMI, 1, 1, 0., 0., 0., 0., 1.
+DMI, 1, 5, 0., 0., 0., 1.
DMI, CP8, RSP, REC, 9, 1, ..., -DMI
+DMI, 1, 1, 0., 0., 0., 0., 1.
+DMI, 1, 5, 0., 0., 0., 0., 1.
+DMI, 1, 9, 1.
DMI, CP9, RSP, REC, 10, 1, ..., -DMI
+DMI, 1, 1, 0., 0., 0., 0., 1.
+DMI, 1, 5, 0., 0., 0., 0., 1.
+DMI, 1, 9, 0., 1.
DMI, CP10, RSP, REC, 11, 1, ..., -DMI
+DMI, 1, 1, 0., 0., 0., 0., 1.
+DMI, 1, 5, 0., 0., 0., 0., 1.
+DMI, 1, 9, 0., 0., 1.
DMI, CP11, RSP, REC, 12, 1, ..., -DMI
+DMI, 1, 1, 0., 0., 0., 0., 1.
+DMI, 1, 5, 0., 0., 0., 0., 1.
+DMI, 1, 9, 0., 0., 0., 1.
DMI, CP12, RSP, REC, 13, 1, ..., -DMI
+DMI, 1, 1, 0., 0., 0., 0., 1.
+DMI, 1, 5, 0., 0., 0., 0., 1.
+DMI, 1, 9, 0., 0., 0., 0., 1.
+DMI, 1, 13, 1.
DMI, CP13, RSP, REC, 14, 1, ..., -DMI
+DMI, 1, 1, 0., 0., 0., 0., 1.
+DMI, 1, 5, 0., 0., 0., 0., 1.
+DMI, 1, 9, 0., 0., 0., 0., 1.
+DMI, 1, 13, 0., 1.
DMI, CP14, RSP, REC, 15, 1, ..., -DMI
+DMI, 1, 1, 0., 0., 0., 0., 1.
+DMI, 1, 5, 0., 0., 0., 0., 1.
+DMI, 1, 9, 0., 0., 0., 0., 1.
+DMI, 1, 13, 0., 0., 1.
DMI, QREAL, RSP, REC, 5, 7, ..., -DMI

```

```

+DMI, 1, 1, 133.5, 91.8, 61.4, 39.7 , , , +DMI
+DMI, 1, 5, 24.8, , , , , , +DMI
+DMI, 2, 1, 370.8, 255.1, 170.5, 110.3 , , , +DMI
+DMI, 2, 5, 68.9, , , , , , +DMI
+DMI, 3, 1, 646.1, 444.4, 297.2, 192.2 , , , +DMI
+DMI, 3, 5, 120. , , , , , +DMI
+DMI, 4, 1, 834.3, 573.9, 383.7, 248.2 , , , +DMI
+DMI, 4, 5, 155. , , , , , +DMI
+DMI, 5, 1, 0. , 719.9, 481.3, 311.4 , , , +DMI
+DMI, 5, 5, 194.4, , , , , , +DMI
+DMI, 6, 1, 0. , 826.4, 552.6, 357.5 , , , +DMI
+DMI, 6, 5, 223.2, , , , , , +DMI
+DMI, 7, 1, 0. , 920.7, 615.7, 398.3 , , , +DMI
+DMI, 7, 5, 248.7, , , , , ,
DMI, MCH, RSP, REC, 7, 1, , , , +DMI
+DMI, 1, 1, .3, .5, .66, .75, , , +DMI
+DMI, 1, 5, .84, .9, .95,
ENDDATA

```

D.2 FREE LONGITUDINAL FLEXIBLE STABILITY DERIVATIVE PROGRAM P-137

MADOL Program P-137 generates rigid stability derivatives, flexible stability derivatives, flexible/rigid ratios and incremental flexible stability derivatives for a free airplane, airplane less tail and tail only configuration.

The stability derivatives generated by this program reflect the effects of the application of airload and inertia load distributions to an unrestrained, or free, balanced airplane.

Rigid and flexible stability derivatives are calculated for up to five altitudes per Mach number for up to ten Machs. Appropriate flexible/rigid ratios and flexible increments are inserted into output matrices compatible with the automatic plotting routine of program P-115.

The following sections present a description of the above procedures.

D.2.1 Free Stability Derivatives

The rigid and flexible stability derivatives are a function of theoretical airload distributions, inertia load distributions and applied external load distribution for a balanced airplane. Stability derivatives are generated for the following independent distributions:

<u>Type of Distribution</u>	<u>Input Symbol</u>
1) Unit angle of attack for the complete airplane	FORMED INTERNALLY
2) Fuselage station of control points	X_{CP}
3) Reference airplane camber and twist angle of attack	$\alpha_{C\&T}$
4) Unit angle of attack for the tail plane only	α_T
5) Unit deflection angles for the horizontal stabilizer	δ_H
6) Unit deflection angles for the elevator	δ_e

- | | |
|--|---------------|
| 7) Arbitrary unit angle distribution | α_4 |
| 8) External applied load distribution at load points | ΔPZ_1 |
| 9) External applied load distribution at load points | ΔPZ_2 |

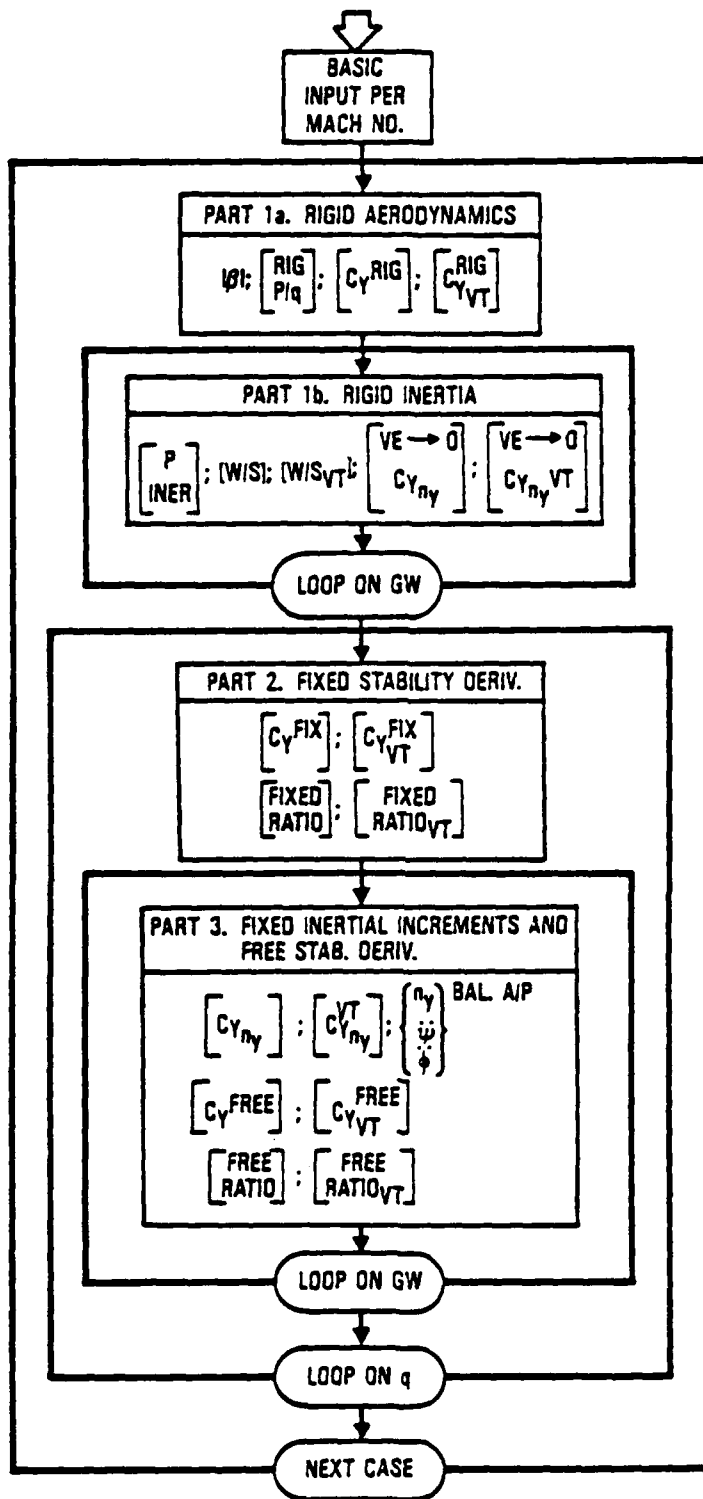


Figure D.2. Flow Chart for Lateral/Directional Stability Derivative Programs


```

MATRIX [RT5],      [RT6];
$
MATRIX [CP1],      [CP2],      [CP3],      [CP4];
MATRIX [CP5],      [CP6],      [CP7],      [CP8];
$
$ Initialize Scalars:
$
$ INT := 1;          $ FLAG TO PERFORM COMPONENT INTEGRATIONS
$                   $ INT = 0    NO COMPONENT INTEGRATION $
$                   $ INT = 1    COMPONENT INTEGRATION   $
$ NMCH := 6;        $ NUMBER OF MACH'S                     $
$ NQ := 5;          $ NUMBER OF Q'S FOR EACH MACH         $
$ NVT := 1;         $ INITIALIZE COUNTER OF TOTAL LOOPS   $
$ ITST := 0;        $ INTEGER TEST IF Q = 0              $
$ NTST := 1.;       $ REAL TEST IF Q = 0                 $
$ NWT := 1;         $ NUMBER OF WEIGHT CASES             $
$
$ Initialize Matrices:
$
$ CALL MXIDENT ( , [I], 146, 2 );
$ CALL MXIDENT ( , [T], 3, 2 );
$
$ IF INT = 1 THEN
$   CALL MXNULL ( , [SYVT136], 337, 1, 2 );
$   CALL MXNULL ( , [SSYF137], 337, 1, 2 );
$   CALL MXNULL ( , [SMXY138], 337, 1, 2 );
$   CALL MXNULL ( , [SMXZ139], 337, 1, 2 );
$ ENDIF;
$
$ CALL IFF( GSIZE );
$
$ Matrix Calculations: Part Ia. (Computed once per mach)
$
$ *** MACH LOOP ***
$
$ FOR IMACH = 1 TO NMCH DO
$
$   CALL EXREAL ( , [MCH], 1, IMACH, MACH );
$
$   PRINT ( "(IX,'*** *** *** *** *** *** *** *** *** ***')");
$   PRINT ( "(IX,'*** MACH CASE #',I4),'IMACH);");
$   PRINT ( "(IX,'*** MACH = ',F6.3),'MACH);");
$
$   [Q201] := [[DZ107] * [QZ(IMACH)]] + [[DY108] * [QY(IMACH)]];
$
$ Stack of Beta Matrices:
$
$ CALL COLMERGE( [RT1], [B111], [BR112], [CP1] );
$ CALL COLMERGE( [RT2], [RT1], [BDR113], [CP2] );
$ CALL COLMERGE( [RT3], [RT2], [AD1114], [CP3] );
$ CALL COLMERGE( [RT4], [RT3], [AD2115], [CP4] );
$ CALL COLMERGE( [RT5], [RT4], [PB2V116], [CP5] );
$ CALL COLMERGE( [B202], [RT5], [AV117], [CP6] );
$
$ [PYQ203] := [Q201] * [B202];
$ [CTR204] := [SAP105] * [PYQ203];
$
$ [CTVT205] := [SVT106] * [PYQ203];
$ [QDE206] := [Q201] * [DB104] * [E103];
$
$ IF INT = 1 THEN
$
$   [SUM1207] := [SYVT136] * [QY(IMACH)];
$   [SUM2208] := [SSYF137] * [QY(IMACH)];
$
$   [SUM3209] := [SMXY138] * [QY(IMACH)];

```

```

$ [SUM4210] := [SMXZ139] * [OZ(IMACH)];
$
$ [DBE211] := [DB104] * [E103];
$
$ [SY1221] := [SUM1207] * [B202];
$ [SY2222] := [SUM2208] * [B202];
$
$ [MXY223] := [SUM3209] * [B202];
$ [MXZ224] := [SUM4210] * [B202];
$ ENDIF;
$
$ Matrix Calculations: Part 1b. (Computed once per mach)
$
$ FOR IWT = 1 TO NWT DO
$
$ CALL COLMERGE( [RT6], [PYNV(IWT)], [PYEP(IWT)], [CP1] );
$ CALL COLMERGE( [PXI301], [RT6], [PYTH(IWT)], [CP2] );
$
$ [PYI302] := [DY108] * [PXI301];
$ [PZ303] := [DZ107] * [PZTH(IWT)] * [CP7];
$ [PX304] := [DX109] * [PXTH(IWT)] * [CP8];
$
$ [P305(IWT)] := [PYI302] + [PZ303] + [PX304];
$
$ [VS306(IWT)] := [SAP105] * [P305(IWT)];
$ [SVT307] := [SVT106] * [P305(IWT)];
$
$ [DPY308] := [ODE206] * [P305(IWT)];
$
$ [CYNV309] := [SAP105] * [DPY308];
$ [CYVT310] := [SVT106] * [DPY308];
$
$ IF INT = 1 THEN
$ [SY1350] := [SYVT136] * [PXI301];
$ [SY2351] := [SSYF137] * [PXI301];
$
$ [MXY352] := [SMXY138] * [PXI301];
$ [MXZ353] := [SMXZ139] * [PZTH(IWT)];
$
$ [DB354] := [DBE211] * [P305(IWT)];
$
$ [SY10355] := [SUM1207] * [DB354];
$ [SY20356] := [SUM2208] * [DB354];
$
$ [MXY0357] := [SUM3209] * [DB354];
$ [MXZ0358] := [SUM4210] * [DB354];
$ ENDIF;
$ ENDDO;
$
$ Matrix Calculations: Part 2. (Computed once per mach and q)
$
$ *** Q LOOP ***
$
$ FOR IQ = 1 TO NQ DO
$
$ CALL EXREAL ( , [OREAL], IMACH, IQ, QX );
$ CALL RLCMPR ( QX, NTST, 6, IRES );
$
$ IF IRES > ITST THEN
$ K1 := 1./QX;
$ ELSE
$ K1 := 100000.;
$ PRINT ( "(1X, '*** Q OUT OF BOUNDS ***', F8.3), "QX);
$ PRINT ( "(1X, '*** INVERSE OF Q ***', F12.3), "K1);
$ ENDIF;
$

```

```

PRINT ( "(1X,'*** *** *** *** *** *** *** *** *** ***')");
PRINT ( "(1X,'***          Q CASE #',I4),'IQ)");
PRINT ( "(1X,'***          Q =      ',F8.3), 'QX)");
PRINT ( "(1X,'***          INV Q =    ',F12.3),'K1)");
S
[D213] := [I] - (QX)[QDE206];
S
[DINV214] := INV ( [D213] );
[PYQ215] := [DINV214] * [PYQ203];
S
[CY216] := [SAP105] * [PYQ215];
[CVT217] := [SVT106] * [PYQ215];
S
[DDI218] := [DINV214] - [I];
S
CALL MXDVD ( , [CY216], [CYR204], [FRX(KNT)] );
CALL MXDVD ( , [CVT217], [CVT205], [FRXV(KNT)] );
S
IF INT = 1 THEN
[ BFF250 ] := [B202] + (QX) [DBE211] * [PYQ215];
S
[SY1F251] := [SUM1207] * [BFF250];
[SY2F252] := [SUM2208] * [BFF250];
S
[MX1F253] := [SUM3209] * [BFF250];
[MX2F254] := [SUM4210] * [BFF250];
ENDIF;
S
S Matrix Calculations: Part 3. (Computed once per mach and q)
S
FOR IWT = 1 TO NWT DO
[DPYQ226] := (K1) [DDI218] * [P305(IWT)];
S
[CYNY(KNT)] := [SAP105] * [DPYQ226];
[CYFV(KNT)] := [SVT106] * [DPYQ226];
S
[VQS229] := [T] * [[CYNY(KNT)] + (K1) [WS306(IWT)]];
[BINV230] := INV ( [VQS229] );
S
[NY231] := (-1) [BINV230] * [T] * [CY216];
S
[PYFR232] := [DPYQ226] * [NY231] + [PYQ215];
[CYFR(KNT)] := [SAP105] * [PYFR232];
S
CALL MXDVD ( , [CYFR(KNT)], [CYR204], [FR(KNT)] );
[FRCY(KNT)] := [SVT106] * [PYFR232];
CALL MXDVD ( , [FRCY(KNT)], [CVT205], [VTR(KNT)] );
S
IF INT = 1 THEN
[DBNY260] := [DBE211] * [DINV214] * [P305(IWT)];
S
[SY1N261] := [SUM1207] * [DBNY260];
[SY2N262] := [SUM2208] * [DBNY260];
S
[MX1N263] := [SUM3209] * [DBNY260];
[MX2N264] := [SUM4210] * [DBNY260];
S
[BFF265] := [B202] + [[DBE211] * ((QX)[PYFR232] + [P305(IWT)] * [NY231])];
S
[SY1F266] := [SUM1207] * [BFF265];
[SY2F267] := [SUM2208] * [BFF265];
S
[MX1F268] := [SUM3209] * [BFF265];
[MX2F269] := [SUM4210] * [BFF265];
ENDIF;
KNT := KNT + 1;

```


D.3 FIXED AND FREE LATERAL/DIRECTIONAL FLEXIBLE STABILITY DERIVATIVE PROGRAM DRSD

Master Deck program DRSD F-72 generates lateral-directional stability derivatives for a fixed and free airplane.

The stability derivatives generated by this program consist of two distinct sets. One set, referred to as fixed stability derivatives, reflects the effects due to independent application of airload distributions and inertia distributions on a restrained, or fixed, airplane. The second set, referred to as free stability derivatives, reflects the effects of a simultaneous application of airload distributions and inertia distributions on an unrestrained, or free, balanced airplane.

Rigid and flexible derivatives are calculated for up to six altitudes per Mach number. Appropriate flex/rigid ratios are inserted into output matrices compatible with the automatic plot routine of program P-115. The following sections present a description of the above procedures:

D.3.1 Fixed Lateral-Directional Stability Derivatives

The fixed stability derivatives generated by this program consist of two distinct subsets. One subset, referred to as fixed stability derivatives, reflects the effects of the application of asymmetric vertical and lateral airload distributions only. The second subset, referred to as fixed inertia derivatives, reflects the effects due to the application of inertia distributions only.

Appropriate flexible/rigid ratios of the fixed derivatives and flexible inertia derivatives are inserted into output matrices compatible with the automatic plotting routine of program P-115.

The following sections present a description of the above procedures.

D.3.1.1 Fixed Stability Derivatives Due to Airload Only

The rigid and flexible fixed stability derivatives are a function of theoretical asymmetric vertical and lateral airload distribution only, and may be generated for up to seven independent unit angle distributions, as listed below:

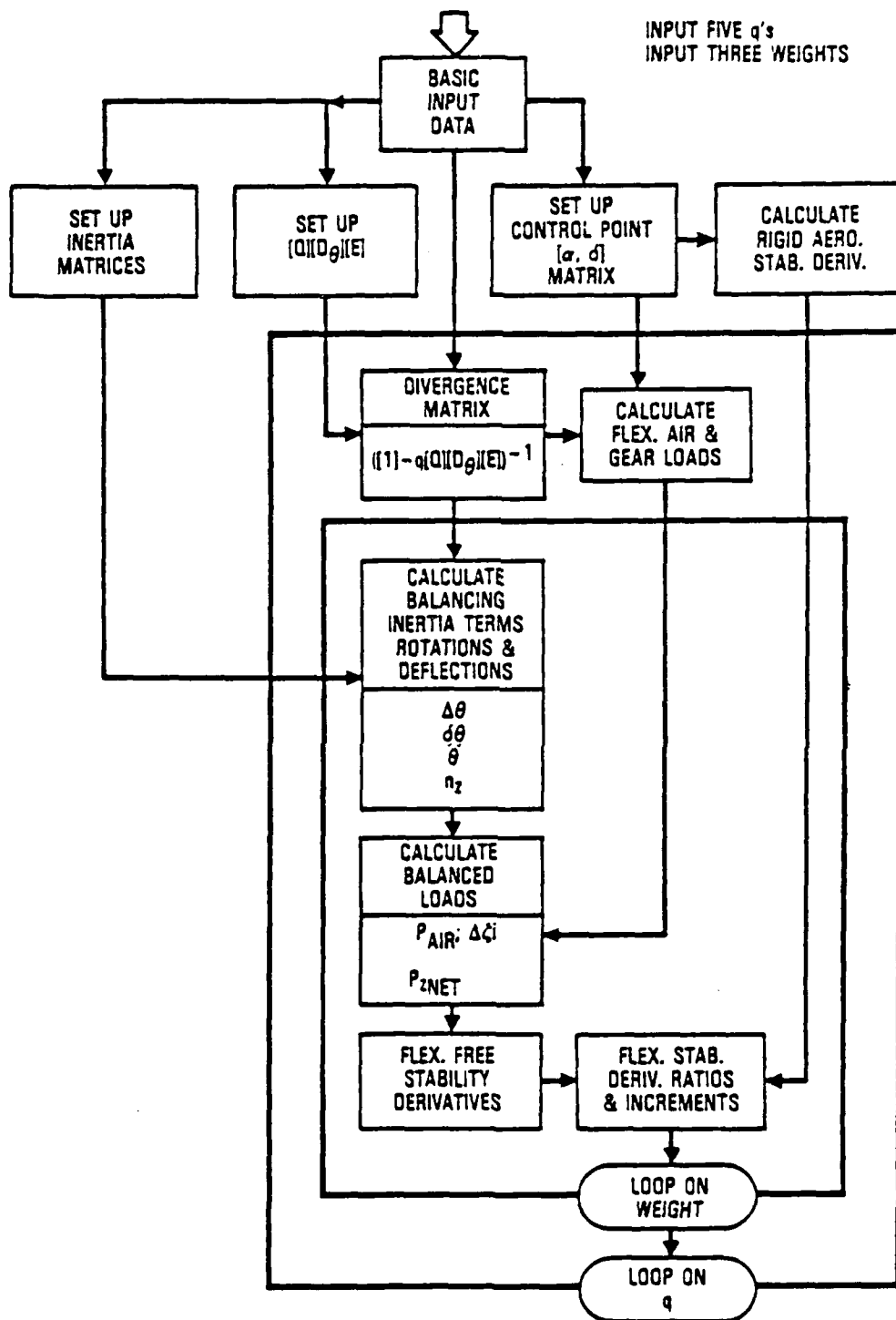


Figure D.3. Flow Chart for Longitudinal Free Stability Derivative Program


```

CALL EXREAL ( , [A],3,2,TMP6);
S
CHOAP := TMP6 - TMP5 * TMP4;
CNCLAP := TMP4;
S
CALL MXELOP ( [A],3,3,[A],1,3,4,TMP7);
S
AOAT := -TMP7;
S
CALL MXELOP ( [A],1,4,[A],1,3,4,TMP8);
CALL EXREAL ( , [A],3,3,TMP9);
CALL EXREAL ( , [A],3,4,TMPA);
S
CHOAT := TMPA - TMP9 * TMP8;
S
CALL MXELOP ( [A],1,4,[A],1,3,4,CNCLAT);
S
PRINT ( "(1X,'*** ***)");
PRINT ( "(1X,'EPS-0',10X,'DEPS/DALP',10X,'CLAC',10X,'CMAC')");
PRINT ( "(1X, 4F13.6),'EO,DTDA,CLAD,CMAD);
PRINT ( "(1X,'ALPHA-0 A/P',4X,'CM-0 A/P',10X,'CM/CL A/P')");
PRINT ( "(1X, 3F13.6),'AOAP,CHOAP,CNCLAP);
PRINT ( "(1X,'ALPHA-0 A-T',3X,'CM-0 A-T',10X,'CM/CL A-T')");
PRINT ( "(1X, 3F13.6),'AOAT,CHOAT,CNCLAT);
S
IF INT = 0 THEN
S
DEO1 := EO;
DEA1 := DTDA;
DAO1 := AOAP;
DCA1 := CHOAP;
DMA1 := CNCLAP;
DAT1 := AOAT;
DCT1 := CHOAT;
DMT1 := CNCLAT;
RCD1 := CLAD;
RCH1 := CMAD;
S
CALL MXONE ( , [DXT], 1, 6, 2 );
CALL MXONE ( , [DYT], 1, 6, 2 );
CALL MXONE ( , [DZT], 1, 6, 2 );
S
CALL PKREAL ( [DZT], 1, 1, MQ );
ENDIF;
S
IF INT = 1 THEN
DEO := EO - DEO1;
DEA := DTDA - DEA1;
DAO := AOAP - DAO1;
DCA := CHOAP - DCA1;
DMA := CNCLAP - DMA1;
DAT := AOAT - DAT1;
DCT := CHOAT - DCT1;
DMT := CNCLAT - DMT1;
RCD := CLAD / RCD1;
RCH := CMAD / RCH1;
S
CALL PKREAL ( [DXT], 1, 5, DEO );
CALL PKREAL ( [DXT], 1, 6, DEA );
CALL PKREAL ( [DXT], 1, 1, DAO );
CALL PKREAL ( [DXT], 1, 2, DCA );
CALL PKREAL ( [DYT], 1, 2, DMA );
CALL PKREAL ( [DXT], 1, 3, DAT );
CALL PKREAL ( [DXT], 1, 4, DCT );
CALL PKREAL ( [DYT], 1, 4, DMT );
CALL PKREAL ( [DYT], 1, 5, RCD );

```



```

S MATRIX [DZ1274], [CFCR275(35)], [C275(35)]; S
S MATRIX [VM01], [VM02], [VM03], [VM04], [VM05];
S MATRIX [VM06], [VM07], [VM08], [VM09], [VM10];
S MATRIX [VM11], [VM12], [VM13], [VM14], [VM15]; S
S MATRIX [VM16], [VM17], [VM18], [VM19], [VM20];
S MATRIX [VM21], [VM22], [VM23], [VM24], [VM25];
S MATRIX [VM26]; S
S MATRIX [CP9], [CP10], [CP11];
S MATRIX [RTMP1], [RTMP2]; S
S Initialize Scalars: S
S K2 := 1216.375;
S K3 := 0.0005787;
S K4 := 0.0006814;
S K5 := 0.000001972;
S K6 := 987.0;
S K7 := 726.9; S
S NMCH := 7;
S NQ := 5;
S KNT := 1;
S ITST := 1;
S NTST := 1.; S
S Initialize Matrices: S
S CALL IFP( GSIZE ); S
S *** MACH LOOP *** S
S FOR IMACH = 1 TO NMCH DO S
S CALL EXREAL ( , [MCH], 1, IMACH, MACH );
S [QLDS100] := [Q(IMACH)]; S
S PRINT ( "(1X,'*** *** *** *** *** *** *** *** *** ***')");
S PRINT ( "(1X,'*** MACH CASE #',I4),'IMACH);
S PRINT ( "(1X,'*** MACH = ',F6.3),'MACH); S
S S Matrix Calculations: Part 1 S
S [W1P201] := [DZ114] * [W1101];
S [W2P202] := [DZ114] * [W2102];
S [W3P203] := [DZ114] * [W3103]; S
S [PZ1P204] := [DZ114] * [PZTH1104];
S [PZ2P205] := [DZ114] * [PZTH2105];
S [PZ3P206] := [DZ114] * [PZTH3106]; S
S [WIP207] := [[W1P201] * [VM01]] + [[W2P202] * [VM02]] +
[[W3P203] * [VM03]]; S
S CALL MXONE ( , [Z111], 1, 152, 2 );
S CALL MXONE ( , [Z113], 156, 1, 2 ); S
S [VTOT208] := [Z113] * [WIP207];
S [XVI209] := [XSIC112] * [WIP207]; S
S CALL MXDVD ( , [XVI209], [VTOT208], [XTOT210] ); S
S [TMP1] := (K2) [Z111];

```

```

[XCPR212] := (K4) [[XCP109] - [TMP1]];
S
[AI213] := [[Z111] * [VMO4]] + [[XCPR212] * [VMO5]] +
[[ACT110] * [VMO6]] + [[AD1115] * [VMO7]] +
[[AD2116] * [VMO8]] + [[AD3117] * [VMO9]] +
[[AD4118] * [VM10]];
S
[QSCP214] := [DZ114] * [OLDS100];
[POI215] := [QSCP214] * [AI213];
[XSXR216] := (K2) [Z113] - [XSIC112];
S
[S2217] := (K3) [Z113];
[XS2218] := (K5) [XSXR216];
[XINV219] := [VM11] * [Z113] + [VM12] * [XSXR216];
S
S
CALL MXMULT ( [Z123], [S2217], [S2I280] );
CALL MXMULT ( [Z123], [XS2218], [XS2I281] );
S
[S2AT282] := [S2217] - [S2I280];
[XS2R283] := [XS2218] - [XS2I281];
S
S
[XSUM220] := [VM13] * [S2217] + [VM14] * [XS2218] +
[VM15] * [S2AT282] + [VM16] * [XS2R283] +
[VM17] * [S2I280] + [VM18] * [XS2I281];
S
[CLRG221] := [XSUM220] * [POI215];
IFLG := 0;
CALL FLEX ( [CLRG221], [DCX], [DCY], [DCZ], MACH, IFLG );
S
CALL MXNULL ( , [DPZM121], 1, 251, 2 );
CALL MXNULL ( , [DPZM122], 1, 251, 2 );
[PZM222] := [[DPZM121] * [VM19]] + [[DPZM122] * [VM20]];
S
[PZM223] := [DZ114] * [PZM222];
[PZX224] := [XINV219] * [PZM223];
S
CALL MYR2D ( [XSIC112], [XSD225] );
CALL MXIDENT ( , [Z119], 156, 2 );
[XD1F226] := [XSD225] - (K6) [Z119];
S
CALL TRANSPOSE( [XSIC112], [XST227] );
CALL MXONE ( , [Z120], 1, 156, 2 );
S
[XRD228] := [XST227] - (K6) [Z120];
[QDE229] := [QSCP214] * [DTB108] * [E107];
S
S
S Matrix Calculations: Part 2 (cyclic for each q)
S Portion of flexible airplane stability derivative calculation
S independent of gross weight.
S
S
S *** Q LOOP ***
S
FOR IQ = 1 TO NQ DO
S
CALL EXREAL ( , [QREAL], IMACH, IQ, K1 );
CALL BLCMPR ( K1, NTST, 6, IRES );
S
IF IRES < ITST THEN
PRINT ( "(IX,*** Q OUT OF BOUNDS ***',PB.3),"K1);
CALL MXNULL ( , [C275(KNT)], 12, 6, 2 );
CALL MXNULL ( , [CPCR275(KNT)], 9, 6, 2 );
ELSE

```



```

- [[DIAZ249] * [DTH267]];
$
[PAIR272] := [PIA235] + [[ADE231] * [PNET271]]
- [[ASIC234] * [Z111] * [DTH267]];
$
[CL273] := (K8) [[XSUM220] * [PAIR272]];
IFLG := 1;
$
CALL FLEX ( [CL273], [DCX], [DCY], [DCZ], K1, IFLG );
$
[DZI274] := [[E107] * [PNET271]]
- [[Z120] * [DZ268]]
+ [[XRD228] * [DTH267]];
$
CALL MXDVD ( , [CL273], [CLRG221], [CFGR275(KNT)] );
$
CALL COLMERGE( [RTMP1], [CFGR275(KNT)], [DCX], [CP9] );
CALL COLMERGE( [RTMP2], [RTMP1], [DCY], [CP10] );
CALL COLMERGE( [C275(KNT)], [RTMP2], [DCZ], [CP11] );
$
CALL UTMFRT ( , [CLRG221], [CL273], [CFGR275(KNT)] );
ENDIF;
$
KNT := KNT + 1;
$
ENDDO;
ENDDO;
$
END;
$
$ Vector Matrix Input:
$
BEGIN BULK
DMI, VMO1, RDP, REC, 1, 3, ..., +DMI
+DMI, 1, 1, 1.0, , , ... +DMI
+DMI, 2, 1, 0.0, , , ... +DMI
+DMI, 3, 1, 0.0, , , ... +DMI
DMI, VMO2, RDP, REC, 1, 3, ..., +DMI
+DMI, 1, 1, 0.0, , , ... +DMI
+DMI, 2, 1, 1.0, , , ... +DMI
+DMI, 3, 1, 0.0, , , ... +DMI
DMI, VMO3, RDP, REC, 1, 3, ..., +DMI
+DMI, 1, 1, 0.0, , , ... +DMI
+DMI, 2, 1, 0.0, , , ... +DMI
+DMI, 3, 1, 1.0, , , ... +DMI
DMI, VMO4, RDP, REC, 1, 9, ..., +DMI
+DMI, 1, 1, 1.0, , , ... +DMI
+DMI, 2, 1, 0.0, , , ... +DMI
+DMI, 3, 1, 0.0, , , ... +DMI
+DMI, 4, 1, 0.0, , , ... +DMI
+DMI, 5, 1, 0.0, , , ... +DMI
+DMI, 6, 1, 0.0, , , ... +DMI
+DMI, 7, 1, 0.0, , , ... +DMI
+DMI, 8, 1, 0.0, , , ... +DMI
+DMI, 9, 1, 0.0, , , ... +DMI
DMI, VMO5, RDP, REC, 1, 9, ..., +DMI
+DMI, 1, 1, 0.0, , , ... +DMI
+DMI, 2, 1, 1.0, , , ... +DMI
+DMI, 3, 1, 0.0, , , ... +DMI
+DMI, 4, 1, 0.0, , , ... +DMI
+DMI, 5, 1, 0.0, , , ... +DMI
+DMI, 6, 1, 0.0, , , ... +DMI
+DMI, 7, 1, 0.0, , , ... +DMI
+DMI, 8, 1, 0.0, , , ... +DMI
+DMI, 9, 1, 0.0, , , ... +DMI
DMI, VMO6, RDP, REC, 1, 9, ..., +DMI

```

```

+DMI, 1, 1, 0.0, , , , , +DMI
+DMI, 2, 1, 0.0, , , , , +DMI
+DMI, 3, 1, 1.0, , , , , +DMI
+DMI, 4, 1, 0.0, , , , , +DMI
+DMI, 5, 1, 0.0, , , , , +DMI
+DMI, 6, 1, 0.0, , , , , +DMI
+DMI, 7, 1, 0.0, , , , , +DMI
+DMI, 8, 1, 0.0, , , , , +DMI
+DMI, 9, 1, 0.0, , , , , +DMI
DMI, VM07, RDP, REC, 1, 9, , , , +DMI
+DMI, 1, 1, 0.0, , , , , +DMI
+DMI, 2, 1, 0.0, , , , , +DMI
+DMI, 3, 1, 0.0, , , , , +DMI
+DMI, 4, 1, 1.0, , , , , +DMI
+DMI, 5, 1, 0.0, , , , , +DMI
+DMI, 6, 1, 0.0, , , , , +DMI
+DMI, 7, 1, 0.0, , , , , +DMI
+DMI, 8, 1, 0.0, , , , , +DMI
+DMI, 9, 1, 0.0, , , , , +DMI
DMI, VM08, RDP, REC, 1, 9, , , , +DMI
+DMI, 1, 1, 0.0, , , , , +DMI
+DMI, 2, 1, 0.0, , , , , +DMI
+DMI, 3, 1, 0.0, , , , , +DMI
+DMI, 4, 1, 0.0, , , , , +DMI
+DMI, 5, 1, 1.0, , , , , +DMI
+DMI, 6, 1, 0.0, , , , , +DMI
+DMI, 7, 1, 0.0, , , , , +DMI
+DMI, 8, 1, 0.0, , , , , +DMI
+DMI, 9, 1, 0.0, , , , , +DMI
DMI, VM09, RDP, REC, 1, 9, , , , +DMI
+DMI, 1, 1, 0.0, , , , , +DMI
+DMI, 2, 1, 0.0, , , , , +DMI
+DMI, 3, 1, 0.0, , , , , +DMI
+DMI, 4, 1, 0.0, , , , , +DMI
+DMI, 5, 1, 0.0, , , , , +DMI
+DMI, 6, 1, 1.0, , , , , +DMI
+DMI, 7, 1, 0.0, , , , , +DMI
+DMI, 8, 1, 0.0, , , , , +DMI
+DMI, 9, 1, 0.0, , , , , +DMI
DMI, VM10, RDP, REC, 1, 9, , , , +DMI
+DMI, 1, 1, 0.0, , , , , +DMI
+DMI, 2, 1, 0.0, , , , , +DMI
+DMI, 3, 1, 0.0, , , , , +DMI
+DMI, 4, 1, 0.0, , , , , +DMI
+DMI, 5, 1, 0.0, , , , , +DMI
+DMI, 6, 1, 0.0, , , , , +DMI
+DMI, 7, 1, 1.0, , , , , +DMI
+DMI, 8, 1, 0.0, , , , , +DMI
+DMI, 9, 1, 0.0, , , , , +DMI
DMI, VM11, RDP, REC, 2, 1, , , , +DMI
+DMI, 1, 1, 1.0, 0.0, , , , +DMI
DMI, VM12, RDP, REC, 2, 1, , , , +DMI
+DMI, 1, 1, 0.0, 1.0, , , , +DMI
DMI, VM13, RDP, REC, 6, 1, , , , +DMI
+DMI, 1, 1, 1.0, 0.0, 0.0, 0.0, , +DMI
+DMI, 1, 5, 0.0, 0.0, , , , +DMI
DMI, VM14, RDP, REC, 6, 1, , , , +DMI
+DMI, 1, 1, 0.0, 1.0, 0.0, 0.0, , +DMI
+DMI, 1, 5, 0.0, 0.0, , , , +DMI
DMI, VM15, RDP, REC, 6, 1, , , , +DMI
+DMI, 1, 1, 0.0, 0.0, 1.0, 0.0, , +DMI
+DMI, 1, 5, 0.0, 0.0, , , , +DMI
DMI, VM16, RDP, REC, 6, 1, , , , +DMI
+DMI, 1, 1, 0.0, 0.0, 0.0, 1.0, , +DMI
+DMI, 1, 5, 0.0, 0.0, , , , +DMI
DMI, VM17, RDP, REC, 6, 1, , , , +DMI

```



```

+DMI, 1, 1, 0.0, 0.0, 0.0, 0.0,,, +DMI
+DMI, 1, 5, 1.0, 0.0
DMI, VM18, RDP, REC, 6, 1, , , , +DMI
+DMI, 1, 1, 0.0, 0.0, 0.0, 0.0,,, +DMI
+DMI, 1, 5, 0.0, 1.0
DMI, VM19, RDP, REC, 1, 9, , , , +DMI
+DMI, 1, 1, 0.0, , , , , +DMI
+DMI, 2, 1, 0.0, , , , , +DMI
+DMI, 3, 1, 0.0, , , , , +DMI
+DMI, 4, 1, 0.0, , , , , +DMI
+DMI, 5, 1, 0.0, , , , , +DMI
+DMI, 6, 1, 0.0, , , , , +DMI
+DMI, 7, 1, 0.0, , , , , +DMI
+DMI, 8, 1, 1.0, , , , , +DMI
+DMI, 9, 1, 0.0
DMI, VM20, RDP, REC, 1, 9, , , , +DMI
+DMI, 1, 1, 0.0, , , , , +DMI
+DMI, 2, 1, 0.0, , , , , +DMI
+DMI, 3, 1, 0.0, , , , , +DMI
+DMI, 4, 1, 0.0, , , , , +DMI
+DMI, 5, 1, 0.0, , , , , +DMI
+DMI, 6, 1, 0.0, , , , , +DMI
+DMI, 7, 1, 0.0, , , , , +DMI
+DMI, 8, 1, 0.0, , , , , +DMI
+DMI, 9, 1, 1.0
DMI, VM21, RDP, REC, 1, 4, , , , +DMI
+DMI, 1, 1, 1.0, , , , , +DMI
+DMI, 2, 1, 0.0, , , , , +DMI
+DMI, 3, 1, 0.0, , , , , +DMI
+DMI, 4, 1, 0.0
DMI, VM22, RDP, REC, 1, 4, , , , +DMI
+DMI, 1, 1, 0.0, , , , , +DMI
+DMI, 2, 1, 1.0, , , , , +DMI
+DMI, 3, 1, 0.0, , , , , +DMI
+DMI, 4, 1, 0.0
DMI, VM23, RDP, REC, 1, 4, , , , +DMI
+DMI, 1, 1, 0.0, , , , , +DMI
+DMI, 2, 1, 0.0, , , , , +DMI
+DMI, 3, 1, 1.0, , , , , +DMI
+DMI, 4, 1, 0.0
DMI, VM24, RDP, REC, 1, 4, , , , +DMI
+DMI, 1, 1, 0.0, , , , , +DMI
+DMI, 2, 1, 0.0, , , , , +DMI
+DMI, 3, 1, 0.0, , , , , +DMI
+DMI, 4, 1, 1.0
DMI, VM25, RDP, REC, 4, 2, , , , +DMI
+DMI, 1, 1, 1.0, 0.0, 0.0, 0.0,,, +DMI
+DMI, 2, 1, 0.0, 1.0, 0.0, 0.0
DMI, VM26, RDP, REC, 4, 2, , , , +DMI
+DMI, 1, 1, 0.0, 0.0, 1.0, 0.0,,, +DMI
+DMI, 2, 1, 0.0, 0.0, 0.0, 1.0
DMI, CP9, RSP, REC, 10, 1, , , , +DMI
+DMI, 1, 1, 0., 0., 0., 0., , , , +DMI
+DMI, 1, 5, 0., 0., 0., 0., , , , +DMI
+DMI, 1, 9, 0., 1.
DMI, CP10, RSP, REC, 11, 1, , , , +DMI
+DMI, 1, 1, 0., 0., 0., 0., , , , +DMI
+DMI, 1, 5, 0., 0., 0., 0., , , , +DMI
+DMI, 1, 9, 0., 0., 1.
DMI, CP11, RSP, REC, 12, 1, , , , +DMI
+DMI, 1, 1, 0., 0., 0., 0., , , , +DMI
+DMI, 1, 5, 0., 0., 0., 0., , , , +DMI
+DMI, 1, 9, 0., 0., 0., 1.
DMI, QREAL, RSP, REC, 5, 7, , , , +DMI
+DMI, 1, 1, 133.5, 91.8, 61.4, 39.7 , , , +DMI
+DMI, 1, 5, 24.8, , , , , , , +DMI

```

```

+DMI, 2, 1, 370.8, 255.1, 170.5, 110.3 ,,, +DMI
+DMI, 2, 5, 68.9, , , ,,, +DMI
+DMI, 3, 1, 646.1, 444.4, 297.2, 192.2 ,,, +DMI
+DMI, 3, 5, 120. , , ,,, +DMI
+DMI, 4, 1, 834.3, 573.9, 383.7, 248.2 ,,, +DMI
+DMI, 4, 5, 155. , , ,,, +DMI
+DMI, 5, 1, 0. , 719.9, 481.3, 311.4 ,,, +DMI
+DMI, 5, 5, 194.4, , , ,,, +DMI
+DMI, 6, 1, 0. , 826.4, 552.6, 357.5 ,,, +DMI
+DMI, 6, 5, 223.2, , , ,,, +DMI
+DMI, 7, 1, 0. , 920.7, 615.7, 398.3 ,,, +DMI
+DMI, 7, 5, 248.7, , , ,,, +DMI
DMI, MCH, RSP, REC, 7, 1, ,,, +DMI
+DMI, 1, 1, .3, .5, .66, .75,,, +DMI
+DMI, 1, 5, .84, .9, .95,
ENDDATA

```